Piotr Migoń
(Ed.)

Geomorphological Landscapes of the World

Springer

Geomorphological Landscapes of the World

Piotr Migoń
Editor

Geomorphological Landscapes of the World

Springer

Editor
Piotr Migoń
Department of Geography and Regional Development
University of Wrocław
Poland
migon@geogr.uni.wroc.pl

ISBN 978-90-481-3054-2 e-ISBN 978-90-481-3055-9
DOI 10.1007/978-90-481-3055-9
Springer Dordrecht Heidelberg London New York

Library of Congress Control Number: 2009941466

Cover images: background image, Durdle Door in the Purbeck, photo R. Edmonds; images from left to right: Nærøyfjorden, photo A. Nesje; Uluru (Ayers Rock), Central Australia, photo C. R. Twidale; the Pokhara valley, Nepal, photo M. Fort; the Dead Sea area in the Middle East, photo D. Bowman.

Printed on acid-free paper

Springer is part of Springer Science+Business Media (www.springer.com)

Contents

Introduction

Geomorphology, a part of Earth Sciences, is the scientific study of landforms, their assemblages, and processes that molded them in the past and that change them today. Geomorphologists study shapes of landforms and regularities of their spatial distribution, decipher their origin and evolution, and try to establish their ages. Geomorphology is also a science of considerable practical importance since many geomorphic processes occur so suddenly and unexpectedly and with such a force that they pose significant hazards to human populations.

But geomorphology has also been named "the Science of Scenery." And the natural scenery, which is essentially a combination of landforms of different sizes, shapes, origins, and ages, can be captivating. You do not need to be a geomorphologist to marvel at the Grand Canyon of Colorado, the fjords of Norway, or the lofty peaks of the Himalayas, to name just a few great landscapes on Earth. However, where an untrained eye sees mainly the beauty of a physical landscape, geomorphologists go a step further, trying to answer how and why such a natural beauty has come into being. Many of the great landscapes are unique by global standards and a question inevitably arises what is the reason for this uniqueness. What are the fundamental controls on the evolution of landscape? Tectonics, rocks, changing climates, or humans? In short, each geomorphological landscape tells a story and unravels pages from the history of the Earth. Yet, deciphering a complete story is not always easy and many striking landscapes still remain somewhat mysterious.

This book aims to tell some of these stories, hidden behind the marvelous sceneries. It does so in the hope that better scientific understanding will not deprive the world's iconic landscapes of their magic, but may help us to appreciate their beauty even more than before. It is a joint endeavor of nearly 50 geomorphologists from more than 20 countries, who for many years have researched some of the most fascinating sceneries on Earth and are willing to share their knowledge. The scientific patronage for the book is provided by the International Association of Geomorphologists. Among its statutory aims are promotion of geomorphology and fostering international cooperation, and this is precisely the idea of the presented volume. The International Association of Geomorphologists, which now has more than 60 member states, was founded 20 years ago, in 1989, and so with this book we also salute its 20th anniversary and its overall success.

Altogether, there are 36 individual stories told. Selecting the landscapes to write about was an arduous task and I am fully aware of themes which some readers may miss. However, each continent is present, and the most splendid sceneries have their chapters. It was intended to present landscapes of different origin, so that the reader can learn about the complexity of processes behind the sceneries and discover that the

sadly too often used phrase "the action of water and wind" does not do justice to the geomorphological wonders of our Planet.

The primary control on the evolution of landscapes is tectonics – the movement of the Earth's crust – but in some places its influence is clearer than in others. Landforms offer unparalleled insights into the nature of tectonic processes, and plate boundaries in particular host spectacular tectonic landscapes, however, constantly modified by erosion. A few such stories, from different tectonic and climatic settings, can be found in this volume. T. Waltham tells a geomorphic story from diverging plates in *Afar* in northeast Africa, D. Bowman presents the great strike-slip structure of the *Dead Sea Graben*, whereas a story of uplift and erosion can be read from the landscape of *Wellington* in New Zealand (M. Crozier and N. Preston). Finally, M. Fort, using the *Pokhara Valley* in the Nepal Himalaya as an example, introduces processes shaping the highest mountains on Earth, situated at a convergent plate boundary. Among the most intriguing gross geomorphic features of the world are Great Escarpments, which border ancient landmasses, particularly in the southern hemisphere. Their complex evolution is presented through the examples of the *Drakensberg* in South Africa (S. Grab) and the *Western Ghats* of India (V. Kale). In many places tectonics goes side by side with volcanism, which is one of the great sculptors of the Earth surface. Two famous volcanoes are presented in detail, the archetypal stratovolcano of *Mt. Fuji* (T. Oguchi and C. Oguchi) and the 1943-born *Parícutin* in Mexico (I. Alcántara-Ayala). However, on a larger scale, the magnificent scenery of *Iceland* is very much a product of volcanism, in addition to glacial and fluvial processes (B. Whalley).

Many great landscapes of the world are those of karst and these feature extensively in this volume. Examples of limestone scenery include the cold-climate karst of *South Nahanni* in Canada (D. Ford), the cockpit karst of *Jamaica* (P. Lyew-Ayee), the famous tower karst of *Guangxi* in south China (T. Waltham), and the big cave-riddled tropical karst of *Mulu* in Borneo (D. Gillieson and B. Clark). However, karst is not necessarily confined to carbonate rocks and this volume contains two fascinating stories of karst on quartzite and sandstone, of *Gran Sabana* in Venezuela (R. Wray) and *Bungle Bungle* in Australia (R. Young), respectively. Another rock which supports distinctive morphology is granite and no volume about the greatest world's landscapes would go without stories from granite terrains. Yet these can be strikingly different as can be seen comparing ones from the wider surroundings of *Rio de Janeiro* (N. Fernandes et al.), *Sanqing Mountains* of east China (M. Thomas), and the *Spitzkoppe massif* in the Namib Desert (P. Migoń). Sandstones have a decisive influence on landforms too, as explored by R. Twidale who reads the story behind one of the truly iconic landforms worldwide, *Uluru* in Australia. No less impressive are the sandstone "rock cities" of the *Saxon-Bohemian Switzerland* in Central Europe (V. Cílek) and the multitude of arches and deep canyons in the *Canyonland – Arches* area of Utah, USA (J. Dixon). Finally, the *Dolomites* of Italy (M. Soldati) tell a complex story of how rocks, glaciers, and landslides created one of the most attractive and unique mountain sceneries.

Deserts have long conquered the minds of many geomorphologists, attracted by their unusual scenery and the power of wind in shaping the surface. One of greatest sand seas on Earth, the *Namib Sand Sea*, is presented by A. Goudie, whereas D. Busche unravels the complex story behind the Saharan landscape of *northeast Niger*, which can be traced back to much wetter periods of the distant past. Wherever it is more humid, rivers assume the role of a key modeler of any scenery. However, before rainwater reaches large permanent rivers, it can do marvels on unconsolidated deposits,

creating some of the most striking erosional landscapes on the world, among which the *badlands of the Great Plains* of North America are the most famous (M. Gonzalez). The great efficiency of erosion can also be admired in the *Loess Plateau* of China, as presented by X. Yang et al. Riverine landscapes can be subtle and subdued, but can also be awe-inspiring. Such are the great waterfalls and associated canyons, including two featuring in this volume, the *Iguazu Falls* in South America (J. Stevaux and E. Latrubesse) and the *Victoria Falls* in Africa (A. Moore and F. Cotterill). A very different type of landscape is associated with great deltas, and the *Mackenzie Delta*, introduced by C. Burn, is of particular interest because much of the ground there is frozen. But perhaps *the* most famous geomorphological landscape of the world is one created by the Colorado River where it cuts through the Colorado Plateau and forms the *Grand Canyon*. Surprisingly, or maybe not, its history is still open to debate as reviewed by L. Dexter.

Rivers have great power, but even greater landscape effects are associated with megafloods, which typified the period of decay of huge Pleistocene ice sheets. The *Channeled Scablands* of the northwest USA, presented by V. Baker, is the area where this sheer power was appreciated for the first time. Megafloods occurred in Antarctica too, forming a page in the complex story of inheritance and glacial erosion deciphered in the *Dry Valleys of Antarctica* (D. Sugden). Glaciers have been of fundamental importance in morphological evolution of the *Southern Patagonian Andes* (E. Mazzoni et al.), whereas in a different location they remodeled the preexisting fluvial landscape to create another wonder of the world – the *fjords of Norway* (A. Nesje). The fjords are not the only landscape where the meeting of land and sea produces spectacular scenery. Two other coastal sceneries are explained in the volume. The *Dorset and East Devon Coast* of southern England (D. Brunsden and R. Edmonds) is a natural laboratory for coastal geomorphology, whereas the remote *atolls of the Pacific* (P. Nunn) show how living organisms, adapting to changing conditions at the sea floor, contribute to the evolution of the Earth's surface.

The beauty of many geomorphological landscapes has long been recognized, starting from travelogues of ancient travelers and scientists. Today, many such landscapes, if easily accessible, are top tourist destinations, accommodating millions of visitors annually. They come to see the scenery, which in their eyes has outstanding universal value. However, this phrase has also a more formal meaning. Places, whose outstanding universal value can be demonstrated beyond doubt, fulfill one of the criteria to be inscribed on the prestigious list of UNESCO World Heritage properties. Among 36 landscapes presented in this volume, nearly half have already received this distinction, whereas others are protected and cherished at a national level, as national parks, reserves, and areas of outstanding beauty. The closing chapter in this volume, written by T. Badman, reviews the position of geomorphological landscapes in the World Heritage initiative and indicates the way forward.

The volume could not have been completed without the help and assistance of various individuals. First and foremost, I would like to thank the contributors themselves who enthusiastically responded to the invitation, added this one more task to their busy agendas, and came up with texts which required very limited further work. Particular thanks go to Professor Andrew Goudie, who came with the original idea of this volume, helped to select chapters and authors, and then kindly reviewed many individual chapters and corrected English of non-native authors. At the early stage of preparation I also enjoyed the assistance of Professor Denys Brunsden, Professor Michael Crozier, and Professor Carol Harden. Dr Wolfgang Eder, the former Director

of Earth Science Division of UNESCO, provided a vital link to the Springer Verlag, for which I am immensely grateful. My very special words of thanks are to Ms Joanna Remisz who expertly drew most of the figures for this volume. Ms Monika Krawczyńska helped with editorial work in the closing stages, when it was all too easy to get lost. Finally, I thank my wife Edyta for the constant encouragement and the brave decision to accept living with yet another book.

Wrocław, June 2009 Piotr Migoń

Chapter 1
The Mackenzie Delta: An Archetypal Permafrost Landscape

Christopher R. Burn

Abstract The Mackenzie Delta, in Canada's western Arctic, is North America's largest arctic delta. For over half the year the rivers and lakes of this vast alluvial plain are ice covered. Permafrost is ubiquitous in the delta and the surrounding landscape. Treeline traverses the delta, separating closed-canopy white spruce forests in southern parts from low shrub tundra and sedge wetlands at the Beaufort Sea coast. The extension of the delta northwards into the ocean is the net result of 128 Mt of sediment brought annually to the delta by Mackenzie and Peel Rivers, of which about two thirds are deposited offshore. The permafrost of the uplands adjacent to the delta is ice-rich, with numerous tabular bodies of almost pure ice that formed when the ground originally froze. Throughout the region the terrain surface is criss-crossed by networks of ice-wedge polygons, formed by water freezing in cracks opened by ground contraction during winter cooling. The world's largest population of pingos – ice-cored, conical hills up to 50 m high – has developed in the sandy sediments of drained lakes in the area. These features form as permafrost aggrades in saturated lake sediments, and continual uplift of these little hills demonstrates the enormous forces that can be generated by ground freezing.

Keywords Ground ice • ice-wedge polygons • Mackenzie Delta • permafrost • pingos

1.1 Introduction

Mackenzie River's delta is North America's largest arctic delta, and, with an area of 13,000 km^2, the world's second largest arctic delta, smaller than only the delta of the Lena River in Russia. The Mackenzie Delta is a maze of lakes and sinuous channels, carrying the discharge of Mackenzie and Peel Rivers to the Beaufort Sea (Fig. 1.1). For over half the year the rivers and lakes are ice covered, and in this period roads and trails can be constructed to connect points accessible in summer only by boat or aircraft (Fig. 1.2). Treeline crosses the delta, with spruce forest covering the southern portions, and willow bushes and sedge wetlands and marshes to the north. The Delta is an alluvial plain with lakes occupying up to half of the total area (Mackay 1963). It is 210 km long and on average 62 km wide. The elevation at Point Separation, at its apex (Fig. 1.1), is only about 15 m above mean sea level (Mackay 1963). A few bedrock "islands" are exposed in the southeast portion of the Delta, the highest being about 30 m above the delta plain.

The northern portion of the delta, adjacent to the Beaufort Sea, and the area to the east form the Tuktoyaktuk Coastlands, a rolling, lake-rich plain, only a few tens of meters above sea level. The area is a treasure trove of landforms created by the ubiquitous presence of permafrost, ground that remains at or below 0°C for 2 or more years. The world's largest population of pingos – small, conical, ice-cored hills – is found here (Fig. 1.3), and over vast swaths of the terrain the ground surface is dissected by networks of ice-wedge polygons (Fig. 1.4). Landforms caused by the melting of permafrost are also abundantly distributed over the landscape, especially where wave erosion along lake shores or at the coast has exposed ice-rich ground (Fig. 1.5).

Mackenzie Delta is a post-glacial feature, building out into the southeastern Beaufort Sea (Fig. 1.1). Most of the ground in the delta is underlain by permafrost, but there are patches, or taliks, of unfrozen ground due to the influence of shifting river channels on ground temperatures (Smith 1976). The Beaufort Delta region

P. Migoń (ed.), *Geomorphological Landscapes of the World*,
DOI 10.1007/978-90-481-3055-9_1, © Springer Science+Business Media B.V. 2010

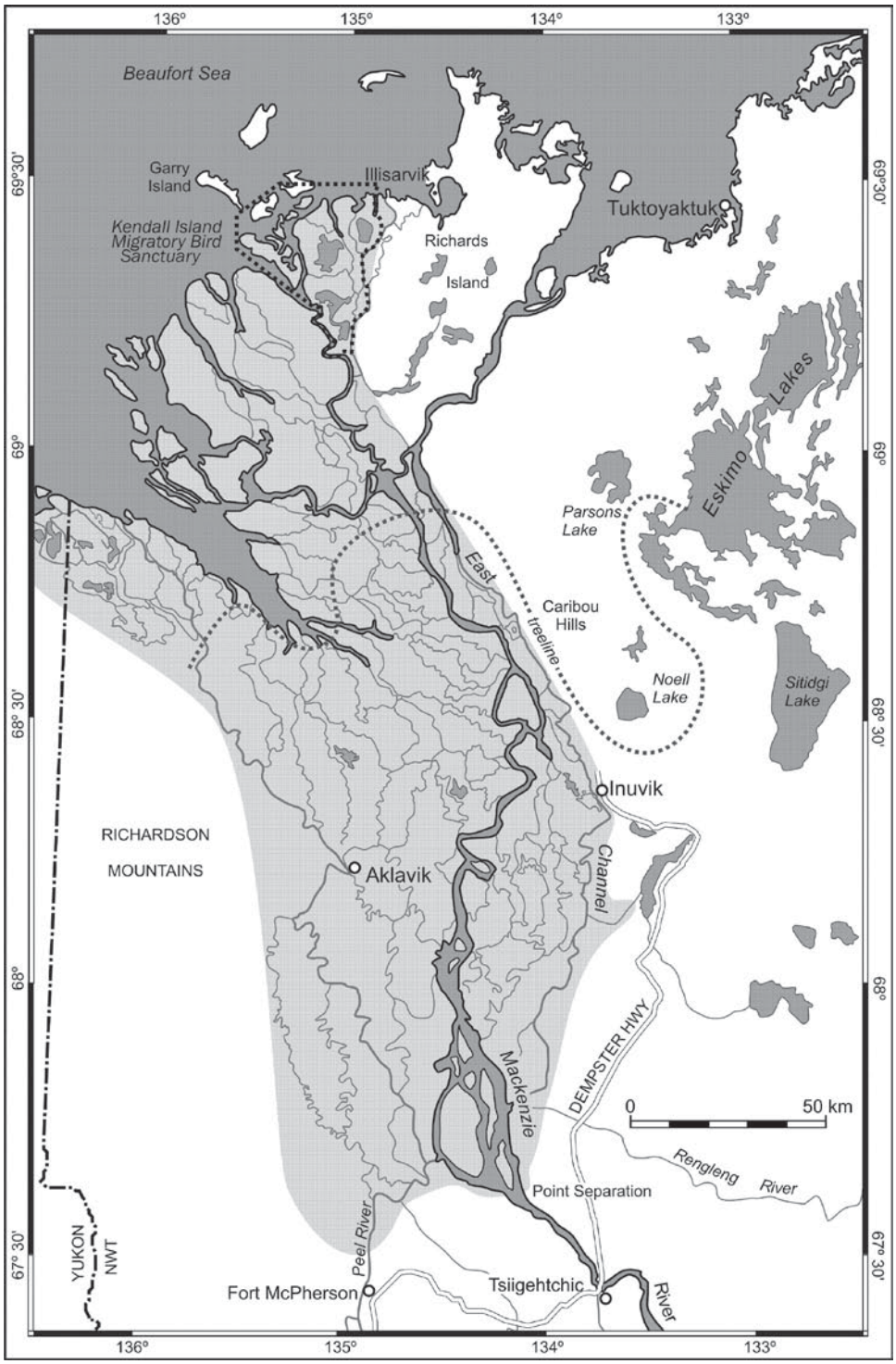

Fig. 1.1 Location map of the Mackenzie Delta area. Treeline is from Mackay (1963; Fig. 70)

Fig. 1.2 The Mackenzie Delta in winter, showing an ice road built on a river channel (Photo C.R. Burn)

is the northernmost extent of the Western Canada Sedimentary Basin, and contains considerable discovered and anticipated reserves of oil and gas (Dixon et al. 1994). The delta is an arctic wetland of international significance, providing critical habitat for numerous fish and mammals, and for thousands of migratory birds, as recognized through establishment of the Kendall Island Bird Sanctuary in 1960 (Fig. 1.1). Each summer, hundreds of beluga whales use the warm water in the near offshore for calving. Inuvik is the principal settlement in the region, established in 1958 as an alternative to Aklavik, which is flooded about once in every 10 years.

1.2 Geographical Setting

The Mackenzie Delta lies at the northern margin of North America. The land to the east and south of the Delta is the northwest corner of the Interior Plains of Canada, a sedimentary basin between the Western Cordillera and the Canadian Shield. The hilly uplands east of the delta are generally less than 60 m above sea level. The western side of the delta is bounded by Richardson Mountains, which rise to over 1,500 m and are part of the northernmost ranges in the Western Cordillera. At the foot of Richardson Mountains, the Delta fills part of Mackenzie Trough, which trends northwest into the Beaufort Sea (Rampton 1988). The most northern portion of the delta, around the Kendall Island Bird Sanctuary, lies north of Mackenzie Trough. In this area, the hilly uplands have been partially eroded by sea-level rise and degradation of the ice-rich permafrost that underlies the upland terrain. In the last 1,500 years the area between the remaining hills has become incorporated into the distributary system of the delta.

The climate of the region is bounded by conditions at Fort McPherson and Tuktoyaktuk, where the mean annual air temperatures and total precipitation are −7.3 and −9.8°C and 310 and 151 mm, respectively. The ecological gradient evident across the treeline is associated with the climatic gradient through the region,

Fig. 1.3 Ibyuk Pingo near Tuktoyaktuk. Ibyuk at 50 m height is the tallest pingo in Canada, and is currently growing higher at about 2 cm/year. Ice-wedge polygons are visible in drained-lake basins in the lower right of the photograph (Photo C.R. Burn)

controlled by latitude and proximity to the Beaufort Sea (Burn 1997). A snow cover is established throughout the region by early October, but while it melts at Fort McPherson before the end of May, it remains into June at Tuktoyaktuk, where the presence of sea-ice offshore in early summer lowers coastal temperatures during on-shore winds. Mean annual air temperatures have increased recently throughout northwest Canada, and the rate of change is relatively high in the Delta area. The regional temperature was relatively stationary between 1926 and 1969, but subsequently the annual mean temperature at Inuvik has increased at a rate of 0.77°C per decade, with the warming primarily in winter. These observations are consistent with projections for climate warming in northern Canada being greatest in winter and least in summer.

1.3 Glaciation and Sedimentation

Most of the bedrock beneath the delta is sandstone and shale, and in the middle of the Delta lies approximately 80 m below the ground surface (Johnston and Brown 1965). The area was entirely covered by the northwest corner of the Laurentide ice sheet for several thousand years during the last glaciation, with the maximum extent perhaps reached about 30,000 years ago (Duk-Rodkin and Lemmen 2000). Portions of the outer delta area and Richards Island were ice-free for much of the glaciation, but the Inuvik area was not deglaciated until about 14,500 years ago (Ritchie 1985). The delta has been building seaward for about the last 14,000 years. It is a result of drainage diversion, for before glaciation, most of Mackenzie River basin

Fig. 1.4 Ice-wedge polygons in the outer Mackenzie Delta. The growth of ice wedges deforms the adjacent ground, raising the soil on either side of the wedge. The vegetation on these ridges is modified from the plant community that grows in the saturated ground in the middle of the polygons (Photo C.R. Burn)

drained eastwards and emptied into the Atlantic Ocean (Duk-Rodkin and Lemmen 2000). At present, the Mackenzie Delta receives about 128 Mt of sediment each year, with 83% supplied by Mackenzie River and the remainder by Peel River (Carson et al. 1998). About two thirds of the sediment load are deposited in the ocean and the balance is added to the delta, mostly in the outer margins. The sediment is dominantly silt.

Sea level has risen since glaciation (Hill et al. 1985), and there has been considerable inundation of low-lying areas, erosion of ice-rich ground, and, in total, coastal retreat of about 100 km. As a result, there are four depositional histories for terrestrial sites in the area. First, there is upland terrain that has remained above water level since glaciation. In these areas the ground is characteristically covered by sand or glacial till. Several hills in the Kendall Island Bird Sanctuary represent such terrain. Second, parts of the outer delta have been submerged by sea-level rise, but have emerged as a result of sedimentation (Taylor et al. 1996). Third, in most of the delta the surface has built up over time, emerged from the ocean, and ground level has kept pace with sea level. Finally, in some parts of the hilly terrain, peat deposits have accumulated in low-lying ground.

1.4 Hydrology

The flooding hydrology of the Mackenzie Delta creates the stark contrast between the wetlands of the delta plain and the dry terrain of the surrounding uplands. Peak water levels occur in late May or early June, as snow melt from the Mackenzie basin, which extends southwards to Alberta and British Columbia, reaches the coast. There is relatively modest precipitation

Fig. 1.5 Two retrogressive thaw slumps on the coast of Kendall Island. Ice wedges are exposed in the thaw slumps, and their polygons are visible in the adjacent ground (Photo C.R. Burn)

locally during summer, and discharge into the delta responds to frontal precipitation in Mackenzie River valley and the Peel River basin. Great Slave and Great Bear lakes are permanent reservoirs for Mackenzie River, so there is a constant discharge into the delta in winter, and the water level in the Delta rises as distal channels freeze through.

In late summer, when water levels in the delta are low, storm surges may advance upstream to Point Separation and beyond (Marsh and Schmidt 1993). These surges may inundate the outer delta, but they are rarely sufficient to flood areas south of treeline. Instead, the principal flood hazard occurs in late May and early June when ice jamming may raise water levels to flood much of the delta. The frequency and duration of flooding has systematic effects on vegetation development, so that specific forest communities in the delta are associated with flooding regimes, in addition to the vegetation succession that may be anticipated on aggrading point bars (Pearce et al. 1988). The hydrology of lakes in the delta is closely associated with the hydrograph, for the annual water balance of the area is negative, and over time water bodies will dry up, unless refilled by flooding (Marsh and Hey 1989).

1.5 Channel Migration

Mackenzie Delta is a maze of shifting channels and lakes (Fig. 1.2). Channel migration can be inferred from the vegetation succession on the edges of channels, especially at point bars, which are commonly opposite cut banks. The vegetation succession in the forested areas of the delta follows a path from horsetail (*Equisetum* spp.) in newly emerged river bars, through willow and alder associations (*Salix* spp., *Alnus crispa*), to white spruce forest (*Picea glauca*) (Pearce et al. 1988). Channel migration undercuts the surface vegetation, which then floats away. Flooding commonly

leads to sediment deposition on the forest floor, and over time adventitious roots may extend out from tree trunks. However, the aggradation of the delta is primarily by infilling of channels, because forest vegetation, particularly logs, are rarely encountered while drilling.

1.6 Permafrost and Ground Ice

Perennially frozen ground is ubiquitous north of treeline and beneath forested surfaces in the middle and upper delta. Permafrost is absent beneath lakes and river channels that do not freeze to the bottom, where the water maintains a mean annual temperature above 0°C (Smith 1976). Along the edges of channels permafrost may not be formed where willows capture snow blown off river or lake ice in winter to create deep snow banks that keep summer heat in the ground. In forested terrain the mean annual ground temperature is about −2°C. This is considerably higher than the mean annual air temperature, due to the proximity of "warm" water bodies, and because snow in the forest does not drift, but accumulates steadily through the winter. In contrast, in the tundra of the outer delta, where the snow depth is reduced by wind scour, the mean annual ground temperature is about −6°C (Kokelj et al. 2007).

Permafrost thicknesses in the Delta may be divided into three categories. First, in places that were unglaciated for much of the last 100,000 years, the thickness is on the order of 500 m or more. These environments include parts of the outer delta that were submerged relatively recently, and have now emerged due to sedimentation (Taylor et al. 1996). Second, in much of the delta itself, the thickness is less than 100 m, as a result of relatively warm ground at depth, due to the abundance of water bodies (Smith 1976). Third, permafrost is thin in the emerging sedimentary environments of Mackenzie Trough, where it is beginning to develop.

Although the permafrost in the delta contains ice throughout its depth, most of the sediments, having been laid down in river channels, were not exposed at the ground surface. As a result, the majority of the permafrost contains ice in the sediment pore spaces only. However, high ice contents develop beneath exposed surfaces, as water is drawn into permafrost from thawed, saturated soil near the ground surface at the end of summer. Characteristically, the uppermost 2–3 m of permafrost are ice-rich and release water upon thawing, but below this the soil ice content is close to the pore volume only (Williams 1968).

In the glacial outwash sediments of the outer delta area and Tuktoyaktuk Coastlands, there are extensive bodies of massive ground ice (Fig. 1.6) that formed after glaciation as permafrost grew in the exposed ground. In some places glacier ice may lie buried under a veneer of till. Retrogressive thaw slumps, up to 200 m wide, commonly form where such ground ice is exposed by erosion (Fig. 1.5), and the warmth of summer conditions begins to thaw the permafrost.

Ice wedges develop under contemporary conditions in the outer delta, where the winter cold is sufficient to lead to ground contraction and cracking. These linear cracks are filled with snow melt water, leading to veins of ice in the ground. After many years of repeated cracking, the veins develop into wedge-shaped bodies of almost pure ice (Fig. 1.7). Characteristically, these wedges form polygonal networks, with a distance across each polygon of about 10 m. Ice-wedge polygons are visible in much of the outer delta, but there are also similar features in the forest. In tundra lowlands, these networks are readily visible (Fig. 1.4), but in uplands the appearance is less common, because slope movement obscures their surface expression on hillsides. Ice-wedge polygons are best developed in drained-lake basins, which may cover several square kilometers (Fig. 1.3). Ice wedges in the forests of the delta do not crack under the present ground climate, although they were active until early in the twentieth century (Kokelj et al. 2007).

1.7 Pingos

The landforms of the Mackenzie Delta area have stimulated a considerable amount of the geocryological research in the region, because they are natural indicators of the geotechnical behavior of permafrost. The most well known are the closed-system pingos of the Tuktoyaktuk Coastlands (Fig. 1.3), which demonstrate the efficacy of pore-water expulsion during ground freezing to deform permafrost (Mackay 1998).

Pingos – the name is derived from the Inuvialuktun word for a hill – are generally conical, ice-cored hills, which reach up to the heights of 50 m, and are up to >100 m in basal diameter. In the Mackenzie Delta area,

Fig. 1.6 Massive ground ice exposed near Tuktoyaktuk. This ice was formed after melting of glacial ice from the landscape, as permafrost developed in the exposed sediments. The ice grew from water injected under pressure toward the growing permafrost. Sand below the ice was the conduit through which a water supply was maintained to feed the ice body as it grew (Photo C.R. Burn)

most of the pingos occur in drained lake basins (Fig. 1.3). There are about 1,350 pingos in the region, with the largest being Ibyuk Pingo, a few kilometers south of Tuktoyaktuk. These landforms grow because of the ubiquitous permafrost, the sandy sediments, and the presence of about 5,000 lakes in the Tuktoyaktuk Coastlands.

Each year one or two of the lakes drain as the permafrost retaining the water is eroded (Fig. 1.8a). Usually drainage occurs in a matter of hours, and commonly small ponds are left in depressions on the drained-lake bottom. Prior to drainage, permafrost is absent beneath the lake if the water depth is sufficient to prevent freezing of the lake-bottom sediments. But after drainage, permafrost invades the talik and the saturated lake-bottom sediments freeze. During freezing, water expands as it turns to ice, leading to a greater volume of pore contents than pore space in the unfrozen, saturated sediments. The excess volume is accommodated by expelling water from the location of freezing, and this builds up a pressure inside the talik, because the excess water is confined by the surrounding permafrost. In some cases, pore water has been ejected from the ground along fractures, but in others sufficient pressure develops to deform the aggrading permafrost, leading to heave of the ground surface (Fig. 1.8b). The ground is domed up by a lens of water, which freezes over time to form the pingo's core of ice (Fig. 1.9). Pingos may keep growing while the talik continues to freeze, and Ibyuk Pingo (Fig. 1.3), which is over 1,200 years old, is still growing. In some cases more than one pingo may form in a drained-lake basin (Fig. 1.9). The pressures involved in lifting a pingo the size of Ibyuk are remarkable, for the weight of this 50 m high hill is equivalent to that of a 50-story building, and demonstrates the forces generated by permafrost aggradation.

The first scientific reports on pingos were provided by Sir John Franklin and Sir John Richardson during their journeys to the Mackenzie Delta area in 1825–1826 and in 1848, but the vast majority of our knowledge of these features and of permafrost in the Mackenzie Delta area

Fig. 1.7 An ice wedge exposed near Tuktoyaktuk. The wedge is about 3 m tall. A thermal contraction crack penetrates the wedge. The growth of the wedge, by repeated thermal contraction cracking and infilling with snow melt water, has deformed the sediments on each side of the wedge (Photo C.R. Burn)

comes from the pioneering field research of Professor J.R. Mackay, which began in 1951 and continues to this day (2009) (e.g., Mackay 1963, 1997; Mackay and Burn 2002).

1.8 Conclusion

The Mackenzie Delta is ecologically the most productive landscape in arctic Canada, fundamentally nourished by the annual flood of the Mackenzie River. For millennia it has provided nesting and staging grounds for thousands of migratory birds and calving grounds for beluga whales. It has sustained a population of indigenous people, hunting and trapping for food and clothing. Analysis of the development of landforms in the region has contributed a large portion of our knowledge concerning the behavior of freezing ground and permafrost. For the last 50 years, there has been considerable interest in the energy resources of the region, especially the significant reservoirs of natural gas, held both in conventional reservoirs and as hydrates. Exploitation of these resources poses substantial engineering challenges, principally due to the presence of permafrost and ground ice in a deltaic setting. These issues are perhaps matched in difficulty by the


a
b

Fig. 1.9 A collapsing pingo on Richards Island in the outer Mackenzie Delta area, showing the interior core of ice in the pingo. A second pingo in the same drained-lake basin is to the right (Photo C.R. Burn)

challenges of managing industrial development in a remote but ecologically critical environment.

The Author

Chris Burn is Professor of Geography and NSERC Northern Research Chair at Carleton University in Ottawa, Canada. His research concerns the permafrost environments of northwest Canada, especially central Yukon and the Mackenzie Delta area. He has published over 30 chapters in books and more than 50 peer-reviewed papers, all concerning northern Canada, and recently concentrating on the impact of climate change on permafrost conditions. He is Vice President of the Royal Canadian Geographical Society.

Fig. 1.8 (**a**) The Illisarvik drained-lake experiment, Richards Island. Illisarvik – an Inuvialuktun word meaning "a place of learning" – is a full-scale field experiment initiated by Professor J. Ross Mackay of the University of British Columbia, when he drained this lake in 1978 by digging a small trench between the lake and the coast (Mackay 1997). The trench was eroded by the flowing water to form the ditch visible on the left foreground of the photograph, as the water flow accelerated from a trickle to a torrent. A residual pond remains in the center of the lake, and a small pingo has grown in the middle of the lake bed. This photograph was taken in July 2008, almost 30 years after drainage, and shows the considerable development of vegetation in the lake basin. Illisarvik is the location of continuing research into the geomorphological effects of permafrost aggradation. (**b**) A profile of the small pingo that has developed in the center of Illisarvik since winter 1994–1995. The people in the photograph are approximately of the same height. The pingo is about 1 m tall and 50 m in diameter (Photos C.R. Burn)

Acknowledgments Our research on permafrost in the Mackenzie Delta area is supported by the Natural Sciences and Engineering Research Council of Canada, Indian Affairs and Northern Development Canada, the Polar Continental Shelf Project, Natural Resources Canada, and the Aurora Research Institute.

References

Burn CR (1997) Cryostratigraphy, paleogeography, and climate change during the early Holocene warm interval, Western Arctic coast, Canada. Can J Earth Sci 34:912–925

Carson MA, Jasper JN, Conly FM (1998) Magnitude and sources of sediment input to the Mackenzie Delta, Northwest Territories, 1974–1994. Arctic 51:116–124

Dixon J, Morrell GR, Dietrich JR (1994) Petroleum resources of the Mackenzie Delta and Beaufort Sea. Part 1: Basin analysis. Geol Surv Can Bull 474

Duk-Rodkin A, Lemmen DS (2000) Glacial history of the Mackenzie region. In: Dyke LD, Brooks GR (eds) The physical environment of the Mackenzie valley, Northwest Territories: a base line for the assessment of environmental change. Geol Surv Can Bull 547:11–20

Hill PR, Mudie PJ, Moran K, Blasco SM (1985) A sea-level curve for the Canadian Beaufort Shelf. Can J Earth Sci 22:1383–1393

Johnston GH, Brown RJE (1965) Stratigraphy of the Mackenzie River Delta, Northwest Territories, Canada. Geol Soc Am Bull 76:103–112

Kokelj SV, Pisaric MFJ, Burn CR (2007) Cessation of ice-wedge development during the 20th century in spruce forests of eastern Mackenzie Delta, Northwest Territories, Canada. Can J Earth Sci 44:1503–1515

Mackay JR (1963) The Mackenzie Delta area, N. W. T. Dep Mines Tech Surv, Geogr Branch, Mem 8

Mackay JR (1997) A full-scale field experiment (1978–1995) on the growth of permafrost by means of lake drainage, western Arctic coast: a discussion of the method and some results. Can J Earth Sci 34:17–33

Mackay JR (1998) Pingo growth and collapse, Tuktoyaktuk Peninsula area, western Arctic coast, Canada: A long-term field study. Géogr phys Quat 52:271–323

Mackay JR, Burn CR (2002) The first 20 years (1978/79 to 1998/99) of ice-wedge growth at the Illisarvik experimental drained lake site, western Arctic coast, Canada. Can J Earth Sci 39:95–111

Marsh P, Hey M (1989) The flooding hydrology of Mackenzie Delta lakes near Inuvik, N. W. T., Canada. Arctic 42:41–49

Marsh P, Schmidt T (1993) Influence of a Beaufort Sea storm surge on channel levels in the Mackenzie Delta. Arctic 46:35–41

Pearce CM, McLennan D, Cordes LD (1988) The evolution and maintenance of white spruce woodlands on the Mackenzie Delta, N. W. T., Canada. Holarctic Ecol 11:248–258

Rampton VN (1988) Quaternary geology of the Tuktoyaktuk Coastlands, Northwest Territories. Geol Surv Canada, Mem 423

Ritchie JC (1985) Late-Quaternary climatic and vegetational change in the Lower Mackenzie Basin, Northwest Canada. Ecology 66:612–621

Smith MW (1976) Permafrost in the Mackenzie Delta, Northwest Territories. Geol Surv Canada, Pap 75–28

Taylor AE, Dallimore SR, Judge AS (1996) Late Quaternary history of the Mackenzie-Beaufort region, Arctic Canada, from modeling of permafrost temperatures. 2. The Mackenzie Delta – Tuktoyaktuk Coastlands. Can J Earth Sci 33:62–71

Williams PJ (1968) Ice distribution in permafrost profiles. Can J Earth Sci 5:1381–1386

Chapter 2
The South Nahanni: High-Latitude Limestone Landscapes

Derek Ford

Abstract South Nahanni River drains a basin of ~34,000 km^2 at 61°N in the remote Mackenzie Mountains of the Northwest Territories, Canada. In its central sector it flows through a never-glaciated zone where resistant limestones, dolomites, and sandstones are folded into regular anticline and overthrust topography rising to 2,000 m a.s.l. Permafrost is widespread below 1,200 m, technically continuous above. The river has carved three magnificent antecedent meandering canyons through the anticlines. The Nahanni Formation (Devonian) is an ideal platformal karstic limestone 180 m thick, resting on 800 m of karstifiable dolomites in the First Canyon. Relict caves in the canyon contain ancient phases of speleothem growth that were investigated in some of the pioneer applications of U series dating to geomorphic questions, such as rates of canyon entrenchment. The most accentuated surface karst landforms known in any arctic or sub-arctic region extend as a belt for 40 km north of First Canyon. A natural labyrinth of solutional corridors, plus sinkholes and small poljes has developed in the limestone there, modified by scabland glacial outbursts when water was impounded by Laurentide Glacier ice from the east. Modern drainage is all underground, over distances up to 25 km and rates >3,500 m/day in both limestones and dolomites. Northwest of the main belt an ancient upland karst has been gutted by canyon recession and periglacial action. In contrast, most of a younger anticline to the northeast was not stripped of shale cover strata until the regional permafrost was well established: there are deeply entrenched canyons but little karst in either limestone or dolomite as a consequence.

Keywords Antecedent river canyons • aquifers • caves • karst • neotectonics • permafrost • periglacial processes

2.1 Introduction

The Mackenzie Mountains are a chain of ranges extending between latitudes 60° and 67°N, dividing Pacific drainage (Yukon Territory) from that to the Mackenzie River and Arctic Ocean (Northwest Territories; Fig. 2.1). They are scarcely peopled. Along the spine, batholithic rocks of Cretaceous age are carved into typical alpine topography – the "Ragged Ranges." They supported extensive Cordilleran valley glaciers during the ice ages and preserve a few extant glaciers and ice caps today. To the east, thick sequences of Paleozoic sedimentary rocks were deformed by the plutonic injections into fold and overthrust topographies, with rivers flowing eastwards across them – the "Canyon Ranges." Their western parts were invaded by the Cordilleran valley glaciers, while the Laurentide Continental Ice Sheet was able to override the most easterly sectors: in between there is a never-glaciated corridor in which magnificent river canyon landscapes are preserved. Limestone, dolomite, and gypsum are prominent amongst the sedimentary rocks and there is salt at depth. As a result, karst landforms are frequent, exhibiting many different morphologic styles as consequences of their differing composition, lithology, geologic structure, and glacial or periglacial history. This account focuses on the most spectacular of the limestone landscapes, which are found in the eastern sector of the South Nahanni River basin and the smaller Ram River basin to the north of it, as shown in Fig. 2.1.

P. Migoń (ed.), *Geomorphological Landscapes of the World*,
DOI 10.1007/978-90-481-3055-9_2,

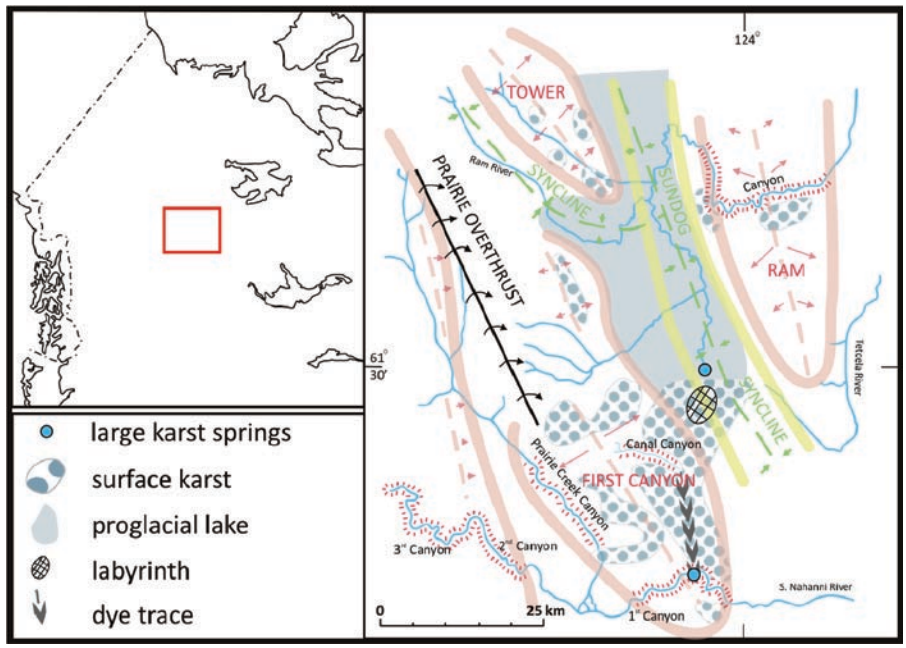

Fig. 2.1 The location and principal topographic and geologic structural features of the South Nahanni karst lands, Northwest Territories, Canada; see the text for details

2.2 The Geologic and Physiographic Settings

The principal karst stratum is the Nahanni Formation of Devonian age, 180–220 m of thick to massive, regularly bedded, platformal limestones. They are chemically pure and mechanically resistant, very like such well-known karstic limestones as those of the Yorkshire Dales in England or the Burren in Ireland. They are overlain by mechanically weak shales that are readily stripped off. The underlying facies are more complex. Broadly, underneath the First Canyon and Ram Plateau anticlines (Fig. 2.1) there are medium-to-thick bedded, mechanically strong, dolomites >800 m in total thickness. They display a few scattered dolines and other karst forms at the surface and may channel groundwater flow in solution conduits. Underneath the Tower anticline, the dolomites are replaced by much weaker shales, calcareous shales and thin dolomites that together function as an aquitard in which groundwater flow is greatly inhibited.

The structural features (Fig. 2.1) are bold and simple. The three anticlines are each broad, symmetrical domal forms with gentle stratal dips. Ram Plateau (the Ram anticline) retains a nearly complete cover of Nahanni Limestone, and even of the overlying shales around its southern margins and north of the river canyon. The limestone is removed from the crest of the First Canyon anticline, exposing the dolomites there. The Tower anticline has been gutted by dozens of canyons entrenched in the underlying shales; the limestone is preserved only on its eastern flank and at scattered localities along ridge crests.

It is most important to appreciate that these structures have been active during neotectonic times. The epicenter of the strongest earthquake experienced anywhere in continental Canada during the past 50 years (Richter 6.9) was at shallow depth on the Ram anticlinal trend 40 km further north; it triggered a major landslide in the limestone there. As consequences of this continuing activity, the trunk rivers have carved antecedent, meandering canyons 300–1,000 m in depth across the up-domings in their paths, and tributary Prairie Creek cut a comparably deep canyon along the strike in the flank of the First Canyon anticline (Fig. 2.1; Ford 1991).

At its greatest extent the Laurentide Ice Sheet buried Ram Plateau and the Sundog Syncline and extended

up to elevations of ~1,400 m above sea level on the eastern flanks of the First Canyon and Tower anticlines (Ford 1974; Brook 1976). Land to the west was not glaciated. In the last glaciation, ice advanced up the Syncline to a terminus just south of the northern springs marked on Fig. 2.1, impounding proglacial "Lake Sundog" at ~900 m a.s.l. to the north. Deposition of ~100 m of lacustrine silts buried much preexisting karst there. The Lake drained abruptly at some time after 40,000 years ago (based on a ^{14}C date of tree wood in the silts – A. Duk-Rodkin, personal communication, 2006): it cut a broad spillway through the silts and into the top of the karst beneath it.

Today, karst features extend from 240 m a.s.l. (the springs in First Canyon, Fig. 2.1) to ~1,900 m a.s.l. on the crest of the First Canyon dome. The climate is sub-arctic to arctic. Mean annual temperatures range from −3°C on the low ground to −10°C or below on the crests. Treeline marking the limit of the Northern Boreal Forest is at ~1,200 m a.s.l. Permafrost is widespread but discontinuous below that elevation, technically continuous above it. Annual precipitation ranges 400–800 mm or more across the elevations, about half of it falling as snow. Summer rains can be intensive when systems from the northeast Pacific and the Beaufort Sea (Arctic Ocean) clash (Brook and Ford 1980). There is some evidence to suggest that the frequency and intensity of these storms is increasing as a consequence of the general summer melt of sea ice over the Beaufort Sea; this is suggested by a great increase in the number of landslides over permafrost on steep shale slopes in the region.

2.3 The Relict Caves of First Canyon

More than 200 relict karst solution caves (i.e., caves drained of their formative waters) have been found in the region but most are sealed off by ground ice or frozen lacustrine silts within a few meters of their entrances. The lengthiest open systems are preserved along the North (updip) wall of First Canyon, near its mouth. Their form is of dendritic drainage, from the sinkpoints of allogenic streams flowing from a shale cover that is now largely or entirely removed. Flow was downdip into the river at and just below the contemporary water tables. A first example, Grotte Valerie, has 2 km of passages now stranded in cliffs 450 m above the river. It has partial fillings of lacustrine silts, and winnowings of an older till cemented by calcite (Fig. 2.2). Its modern entrances (former downstream galleries now truncated by cliff recession) are south-facing. In the summer cold air drains from a low exit, drawing warm air to replace it through an entry that is 40 m higher. This creates (1) a "warm entrance cave" (+6 to +1°C) where there is active deposition of small speleothems today, supplying moist air to (2) a "cool exit cave" (0 to −1.5°C) that is covered with ice and hoar frost: behind and below both is (3) a "permafrost cave" receiving only the cold air of winter, dry and dusty, without speleothems or ice and preserving the remains of 80 or more wild sheep. It is a spectacular example of cave climate zonation (see Ford and Williams 2007: 294–298 for details).

Nearby, Grotte Mickey has more than 3 km of galleries at several different levels between 250 m and 400 m above the river. This multilevel, multiphase pattern points to extended development that kept pace with the entrenchment of First Canyon for a while (Schroeder 1977, 1979).

An important feature of these caves and some in the Labyrinth (discussed below) is the occurrence of large, highly ornamented, stalagmites, columns, and flowstones of calcite. They are no longer growing (modern growth is limited to very small deposits) and most are weathered, partly eroded by invading streams or shattered by freezing (Fig. 2.2). They are indicative of much warmer conditions in the past which (allowing for truncation of the caves by cliff recession since) extended much further into cave interiors than today. There is an abundance of uranium in the cover shales which, re-precipitated in the calcite, has made the speleothems particularly suitable for U series dating. This region saw much of the pioneer speleothem dating work as a consequence (e.g., Harmon et al. 1977). The large majority of samples proved to be >350,000 years in age (the limit of the dating method using 1970s α spectrometric technology), although they were younger than 1.25 million years. The first application of U series speleothem dating to a geomorphic problem was by the author, who showed that the mean rate of South Nahanni River entrenchment below Grotte Valerie could not be more than 0.8 m/ka and that there had been possibly as much as 350 m of uplift on the First Canyon anticlinal axis since 1.5 million years ago (Ford 1973).

Fig. 2.2 Scenes from Grotte Mickey and Grotte Valerie in the First Canyon, South Nahanni River, Northwest Territories. These are relict stream caves now raised high above the River in the canyon walls. *Upper center*: glaciolacustrine silts on the floor of a large stream cave passage. *Upper right*: modern speleothem deposition in the warm sector of Grotte Valerie. The stalactites and stalagmites are typically small. Their bright red coloration is due to contained organics. *Lower left*: above the figure is a typical relict stalagmite and flowstone of the warm period >400 ka BP; only stalagmites of ice grow in this gallery today. *Lower center and right*: ice stalagmites and hoarfrost in the cool sector, Grotte Valerie. The base of the hoarfrost in the center frame marks the surface of a lake of very cold air that is trapped behind the ice dam; it is renewed only by winter inflow (Photos D.C. Ford and J. Schroeder)

2.4 Springs

The main belt of karst terrain between First Canyon and the Sundog Syncline (Fig. 2.1) drains to just two sets of springs. At the north end, "Bubbling Springs" (700 m a.s.l.) rise where the stratigraphic top of the limestone dips under impermeable cover shales in the Syncline. They drain perhaps the northern one-third of the belt, with discharges >10 m^3/s during wet summer spells. In contrast, "White Spray," the southern spring, discharges at 240 m a.s.l. in First Canyon from dolomites that are stratigraphically ~580 m below the base of the Nahanni Limestone. Most of their discharge is into the river bed and is strong enough to keep this stretch of the river free of ice throughout the winter, a unique feature; "White Spray" itself is the summer overflow spring. These springs must drain much of the First Canyon dome, including Canal Canyon (30 km in length, up to 1,000 m in depth) which drains underground where it is blocked by a Last Glacial terminal moraine at its mouth. Dye traces from there (Fig. 2.1) and a lake further north proved the existence of underground flow of 21+ km at mean rates >3,500 m/day on hydraulic gradients of 0.03 or lower. Although no enterable caves have been found in them yet, the dolomites thus can rapidly develop efficient, well-integrated systems of underground solutional conduits.

2.5 The Nahanni Labyrinth

Between Canal Canyon and Bubbling Springs the Nahanni Labyrinth is developed in the limestone. It is the largest example of karstic labyrinth morphology reported in the Northern Hemisphere. The outstanding landforms are dissolutional corridors ("streets") that follow major vertical fractures created by the doming (Brook 1976; Brook and Ford 1978). Individual corridors are 10–100 m wide and deep, and up to 6 km in length. For a distance of 13 km they intersect one another to form a natural labyrinth. The walls recede from frost shattering, causing some parallel corridors to amalgamate into broader closed depressions, like squares in a pattern of city streets; the greatest of these measures 800 × 400 m. Towers isolated by cliff recession are preserved within them. The floor profiles of the corridors and squares are highly irregular, with local streams sinking into depressions between talus accumulations or into bedrock shafts. In the labyrinth and elsewhere on the limestone are large, vertical-walled sinkholes and smaller, elliptical solutional shafts (Fig. 2.3). Many can trap water for a succession of melt seasons: its depth increases slowly until pressure bursts an ice plug below and the feature drains with catastrophic rapidity. Raven Lake, an unusually large doline within a corridor, is 300 m in length and 180 m deep; under flood conditions waters rise >75 m in it, at rates up to 3 m/day.

At the north end of the labyrinth the shale cover and glaciolacustrine silts encroach to reduce the limestone outcrop to a narrow spillway with three small (<2.5 km^2) but elegant poljes developed in it. There are many collapse and suffosion dolines in the flanking shale and silt terraces, pointing to the existence of mature karst drainage in the past that is now largely clogged by the proglacial injecta.

Although all of the labyrinth is drained by mature karst groundwater systems that existed before the last glacial invasion and formation of glacial Lake Sundog,

Fig. 2.3 In the heart of the Nahanni Labyrinth. Helicopter view of large solutional corridors to left, right, and in rear. In center, "Cenote Col" is a cluster of cenote-form shafts 40 m or more in depth; some are filled with water ponded above ground ice plugs, others are dry (Photo P. Sanborn)

Fig. 2.4 Three scenes on the Tower Anticline. *Upper*: looking down into the Sundog Syncline across glaciated pavement with dolines on the well-preserved southeast end of the structure. *Lower left*: relict limestone pavement at the gutted center of the anticline; *lower right*: final remnants at the western end (Photos D.C. Ford)

the extent to which the surface karst landforms were modified by scablands melt flood processes during their reexcavation remains undetermined.

2.6 Tower Anticline Contrasted with Tower Syncline and Ram Plateau

To conclude this review of a great limestone karst that has experienced vigorous neotectonism, Quaternary cold with the ingrowth of permafrost, and partial, sporadic glacial invasions, it is interesting to compare the limestone morphology on the northern structures shown in Fig. 2.1. Tower Anticline was upraised and stripped of its shale cover at broadly the same time as the First Canyon anticline, probably late Miocene-Pliocene. But it did not have the strong, karstifiable dolomites of First Canyon beneath the limestone. Instead there were weak, shaley strata. In both the sector that was glaciated and further west in the never-glaciated zone, Tower Anticline first developed an extensive plateau epikarst with limestone pavement and dolines (Fig. 2.4) but this has since been almost entirely destroyed by

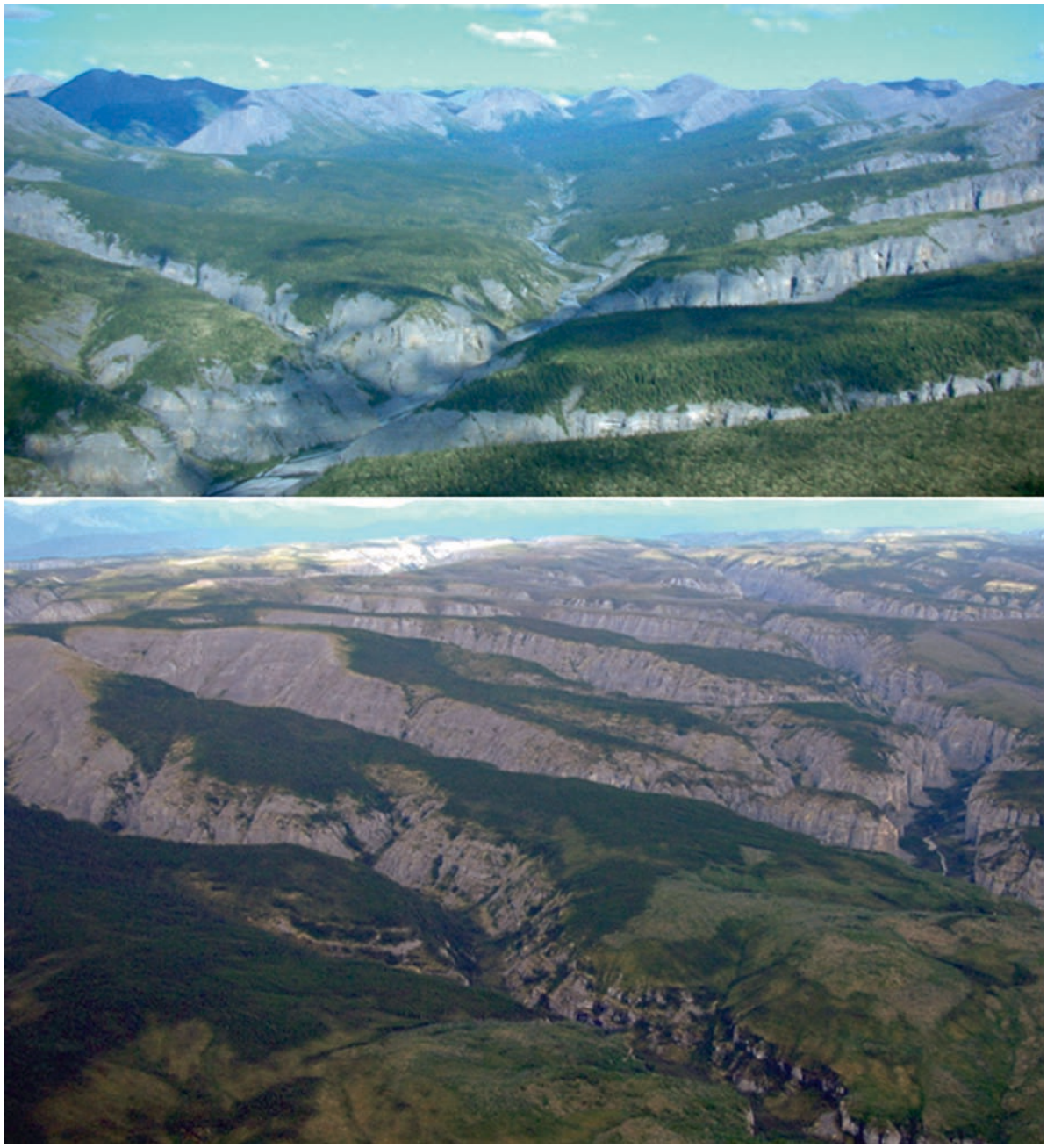

Fig. 2.5 *Upper*: the Nahanni Limestone formation, stripped of its shale cover and dissected by consequent canyons at the head of the Tower syncline. *Lower*: the same situation is seen in the southern half of the Ram Plateau anticline; some last vestiges of the shale cover are seen in the foreground (Photos S. Worthington and P. Sanborn)

growth of permafrost that impeded the groundwater circulation which, as a consequence, has been replaced by the headward and lateral enlargement of flashflood canyons in the shales.

In contrast, stripping of the shales overlying the limestone was later in the adjoining Tower Syncline because of its lower elevation, and on Ram Plateau because (renewed?) tectonic uplift there came later

due to its more easterly location. The consequences were that exposure of the limestone largely occurred after the permafrost had arrived. Except in few places of early stripping, karst groundwater circulation systems could not be established before the rock froze. Instead of karst, classical consequent river drainage patterns with canyons were carved into the limestone, as shown in Fig. 2.5.

The Author

Derek Ford is Professor Emeritus of Geography and Earth Sciences, McMaster University, Canada. His main interests are in karst processes and landforms, cave genesis and karst aquifers, and paleoclimate studies of speloethems. These days he is most interested in applied consulting, and advising on UNESCO World Heritage site applications. He is author/co-author of ~200 journal papers, many reports, co-author or -editor of ten scientific books, one coffee table book, and the producer of one movie for the National Film Board of Canada. He is a former president of the Canadian Association of Geographers and of the International Union of Speleology, a Fellow of the Royal Society of Canada, and Gold Medalist of the Royal Canadian Geographical Society.

Acknowledgments Field research in the magnificent but remote Nahanni country has relied upon the vigorous support of geomorphology students and cave enthusiasts for many years. Particular thanks to Steve Catto, Marcel Cholo, and Dana Haggarty of Parks Canada for their company and logistic support in 2006 and 2007. Paul Sanborn, Jacques Schroeder, and Steve Worthington have freely made their photographs available. The Natural Sciences and Engineering Research Council of Canada and Parks Canada are thanked for financial aid.

References

Brook GA (1976) Karst terrains of the South Nahanni area, Mackenzie Mountains. N.W.T. Ph.D. thesis, McMaster University

Brook GA, Ford DC (1978) The nature of labyrinth karst and its implications for climaspecific models of tower karst. Nature 275:493–496

Brook GA, Ford DC (1980) Hydrology of the Nahanni Karst, northern Canada, and the importance of extreme summer storms. J Hydrol 46:103–121

Ford DC (1973) Development of the canyons of the South Nahanni River, N.W.T. Can J Earth Sci 10:366–378

Ford DC (1974) Evidences of multiple glaciation in South Nahanni National Park, Mackenzie Mountains, N.W.T. Can J Earth Sci 13:1433–1445

Ford DC (1991) Antecedent canyons of the South Nahanni River. Can Geogr 35:426–431

Ford DC, Williams PW (2007) Karst Hydrogeology and Geomorphology. Wiley, Chichester

Harmon RS, Ford DC, Schwarcz HP (1977) Interglacial chronology of the Rocky and Mackenzie Mountains based upon $^{230}/Th^{234}$ U dating of calcite speleothems. Can J Earth Sci 14:2543–2552

Schroeder J (1977) Les formes de glaces des grottes de la Nahanni, T.N.O. Can J Earth Sci 14:1179–1185

Schroeder J (1979). Le développement des grottes dans la région du Premier Canyon de la rivière Nahanni Sud. T.N.-O. Ph.D. thesis, University of Ottawa

Chapter 3
Channeled Scablands: A Megaflood Landscape

Victor R. Baker

Abstract The Channeled Scabland of east-central Washington in the USA is a complex of anastomosing, rock-cut fluvial channels, rock basins, cataracts, streamlined loess hills, and immense gravel bars. It was all produced by cataclysmic erosion and deposition from Pleistocene megaflooding derived from the margins of the Cordilleran Ice Sheet that covered much of the mountainous northwestern part of North America.

Keywords coulees • fluvial erosion • megaflooding • scabland

3.1 Introduction

The Channeled Scabland is a spectacular complex of anastomosing channels, cataracts, loess "islands," rock basins, broad gravel deposits, and immense gravel bars in east-central Washington state, first described in a series of papers during the 1920s and 1930s by J Harlen Bretz. Field relations among many of these features, most notably the multiple levels of divide crossings, the cataracts, gravel bars, and rock basins led Bretz to propose that an immense cataclysmic flood had swept across the Columbia Plateau in late Pleistocene time (Bretz 1923; Bretz et al. 1956). So much floodwater crossed the plateau that it completely filled the preexisting valleys, allowing water to spill across the intervening divides. In this way the pre-flood valleys were transformed into a complex of dividing and rejoining channelways, which Bretz (1923) named the Channeled Scabland. The source for the immense scabland flooding was eventually established to be glacier lake Missoula (Pardee 1942), which had been impounded over a large region of western Montana because of a lobe of the Cordilleran Ice Sheet that extended into northern Idaho (Fig. 3.1). More recent work (Baker 1973) has shown that the outburst floods were indeed megafloods (flows with peak discharges of at least 1×10^6 m^3s^{-1}), and that they occurred repeatedly (Baker and Bunker 1985; Waitt 1985; Benito and O'Connor 2003).

3.2 Geographical Setting

The Channeled Scabland is developed on a gently warped plateau-like surface of predominantly basalt bedrock, the northern and western margins of which are marked by a great arc of the Columbia River. Though it is commonly known as the Columbia Plateau, this region is structurally a large basin that was downwarped to the southwest after the Miocene emplacement of the flood basalt. The margins of this warp rise to elevations of 800 m in the north, where local knobs of older crystalline rock poke through the basalt, reaching elevations of greater than 1,000 m just south of the city of Spokane, Washington, which is located at the northeastern end of the "plateau." The surface progressively slopes to the southwest, reaching near sea level at its southeast corner, near Pasco, Washington. A series of generally east–west anticlinal ridges, with relief of up to 600 m, occur in the southwestern portion of the region. These have prominent water gaps and breaches that carried the cataclysmic flood flows.

Prevailing westerly winds control the climate of the region, which is dominated by the rain shadow effect of the Cascade Mountain range to the west. Mean annual precipitation varies from about 150 mm in the low-lying southwest corner to over 1,000 mm in the high elevations

P. Migoń (ed.), *Geomorphological Landscapes of the World*,
DOI 10.1007/978-90-481-3055-9_3,

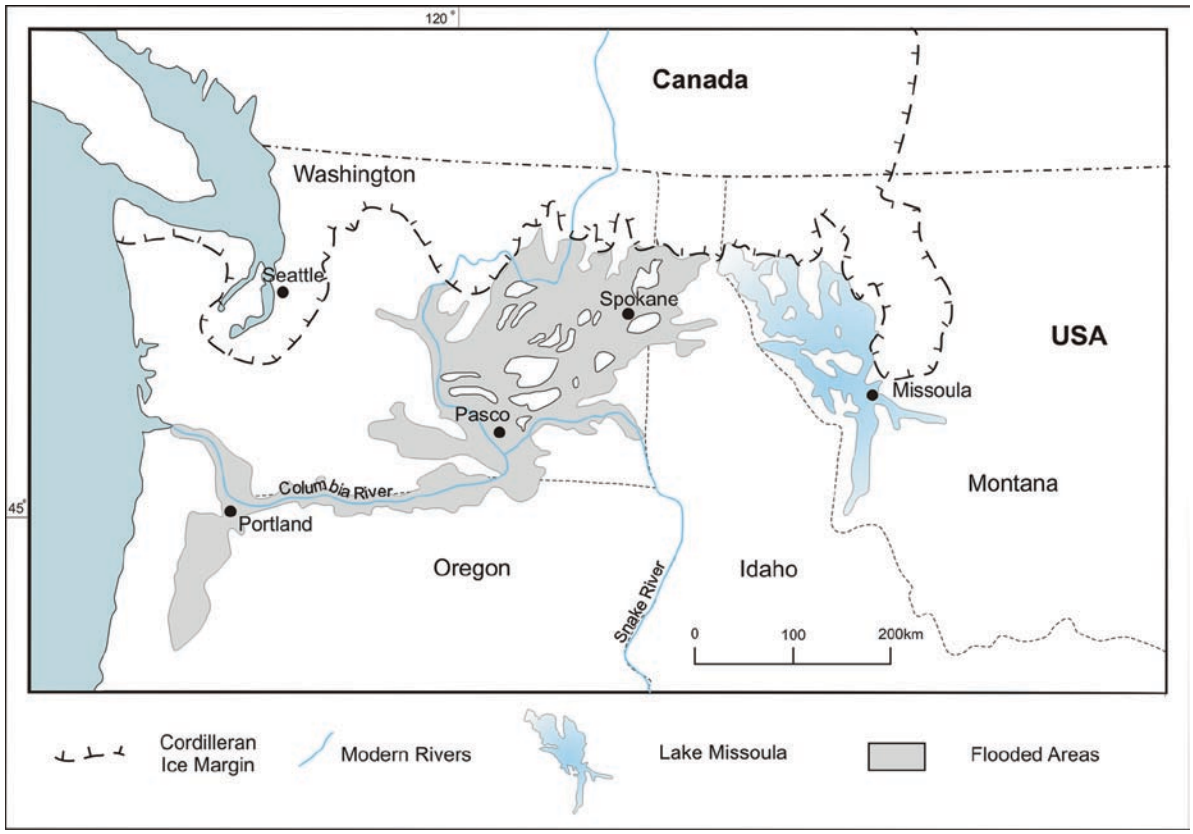

Fig. 3.1 Location map showing glacial Lake Missoula and the extent of late-glacial flooding in the channeled Scabland and adjacent areas of the northwestern USA

to northeast and east of the plateau. Much of the precipitation falls from October to late May. Afternoon temperatures in summer range from the 20s to 40°C or more.

The predominant Miocene-aged basalt bedrock is locally overlain by a thick cover of Pleistocene loess upon which a series of soils developed, sustaining a rich wheat-growing economy. Aridisols occur in the drier central and southwestern areas, but these transition to Molisols and Alfisols to the north and the east. Similarly, vegetation in drier areas is dominated by xerophytic shrubs, such as sagebrush (*Artemisia tridentata*), and grasses. Coniferous forests encroach upon the region from the north and the east.

3.3 Landforms

3.3.1 Scablands

Bretz defined "scablands" as lowlands diversified by a multiplicity of irregular channels and rock basins eroded into basalt. The term was in local use in reference to chaotically eroded tracts of bare basalt that occur in relatively large channels that the floods cut through the loess cover on the plateau. The most common landform in eroded rock of scabland tracts is butte-and-basin topography (Fig. 3.2). The usual development is small anastomosing channels and rock

Fig. 3.2 Oblique aerial view of butte-and-basin Scabland topography near Lenore Canyon, lower Grand Coulee, Washington. Individual basins are up to 100 m in diameter (Photo V.R. Baker)

basins surrounding buttes and mesas with a typical relief of 30–100 m. The rock basins range in scale from shallow saucers or deep potholes, 10–100 m in width, to Rock Lake, a huge inner channel 11 km long and 30 m deep. Bretz (1932: 26–28) described this combination of features as follows: "The channels run uphill and downhill, they unite and they divide, they head on the back-slopes and curt through the summit; they could not be more erratically and impossibly designed."

3.3.2 Coulees and Dry Falls

In the northwestern USA, the term "coulee" is applied to very large steep-walled, trench-like troughs that commonly contain no stream along the valley floor. These are commonly the spillways and flood channels of the overall scabland plexus, and many were parts of pre-flood fluvial valleys that formerly were more shallowly incised into the basalt plateau. Hanging valleys occur where the tributaries to these valleys are no longer graded to the main valley floor because of its deepening and widening by the cataclysmic flood scour. Examples occur in Moses Coulee and Lenore Canyon, where the pre-flood tributaries enter cliff faces on the coulee margins at elevations of 100 or more meters above the coulee floor.

The most famous of the cataract complexes of the Channeled Scabland is located near Coulee City, about 30 km north of Soap Lake, Washington. Named Dry Falls, it consists of four major alcoves extending over a width of 5.5 km, each with a vertical drop of about 120 m (Fig. 3.3). It occurs at the northern end of Lenore Canyon, which was excavated by cataclysmic flood water from a zone of fractured basalt along the axis of the Coulee Monocline (Bretz 1932). It is also at the upstream terminus of an inner channel that receded headward into the Hartline Basin, near Coulee City, Washington.

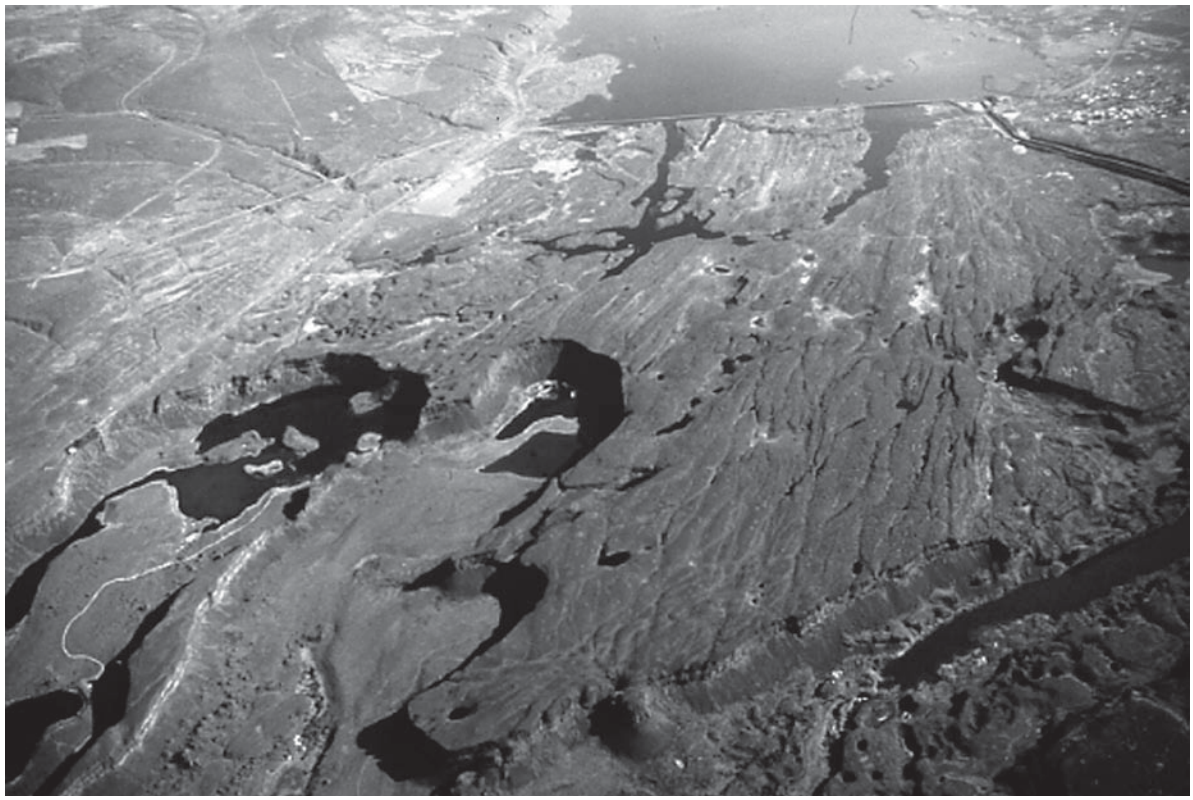

Fig. 3.3 Oblique aerial view of the Dry Falls complex (foreground). The complex has a width of about 5 km. Note the two prominent horseshoe-shaped cataracts at the left center of the image and the striking longitudinal groove topography immediately upstream of the cataract cliffs (Photo V.R. Baker)

3.3.3 Streamlined Hills and Islands

The eastern portions of the Channeled Scabland contain spectacular examples of kilometer-scale hills that show distinctive flow streamlining of the edges ("islands") and, in some cases, tops. These generally occur in local clusters, organized in a braid-like pattern within the overall scabland complex. The hills are composed predominantly of remnant loess that was not stripped from the underlying basalt by the floodwaters. They generally rise up to 50 m above the surrounding scabland areas, and they are commonly 1–4 km long and 0.5 km wide. Bretz (1923) first recognized their remarkable shape, with steep, ungullied bounding hillslopes that converge upstream to prow-like terminations and downstream to tapering tails. This streamlining serves to reduce the drag or resistance to a flowing fluid, resulting in distinctive relationships among lengths, widths, and areas for the landforms (Baker 1979). In general, the lengths of the streamlined hills are about three times their widths in the plan view, widths are about two-thirds the square root of the planimetric area, and lengths are about two times the planimetric area.

3.3.4 Gravel Fans and Bars

Bretz (1923) provided the first interpretation of the Channeled Scabland's large mounded scabland gravel deposits as subfluvially emplaced gravel bars. Great depths of water were required to submerge these bars, an interpretation that was also consistent with the indicated crossings of divide areas by the floodwaters. It was this combined evidence that led Bretz (1923: 649)

to conclude: "It was a debacle which swept the Columbia Plateau." Bretz later recognized that large fan complexes occur where constricted cataclysmic flood channel ways debouched their water and sediment into large structural basins. A well-developed example occurs at the Ephrata Fan, where the floodwaters from the lower Grand Coulee expanded into the wide Quincy Basin in the west-central part of the Channeled Scabland.

3.3.5 Giant Current Ripples (Dunes)

Bretz et al. (1956) applied the name "giant current ripples" to the mesoscale transverse gravel depositional forms of the Channeled Scabland. Following Pardee's (1942) discovery of similar features in the basin of Glacial Lake Missoula, Bretz et al. (1956) identified about a dozen examples. Subsequently, Baker (1973) documented 60 of the most prominent sets of "giant current ripple" (GCR) forms. The striking appearance of the scabland GCR forms on aerial photographs arises from local post-depositional factors. Deposition of aeolian silt in the swales that occur between the ripple crests locally results in differences in vegetation cover. In drier regions, the gravelly GCR summits are covered by sagebrush (*Artemisia tridentata*), and the adjacent swales are covered by cheat grass (*Bromus tectorum*). In contrast, a prominent GCR occurrence in the wetter region near Spirit Lake, Idaho, has a second-growth forest cover in which the larger pine trees (*Pinus ponderosa*) occupy the relative wet swales, but not the drier surface form summits (Fig. 3.4).

Fig 3.4 Giant current ripples (dunes) near Spirit Lake, northern Idaho. Ponderosa Pine (Pinus ponderosa) occupies the ripple swales, which are spaced up to 100 m apart (Photo V.R. Baker)

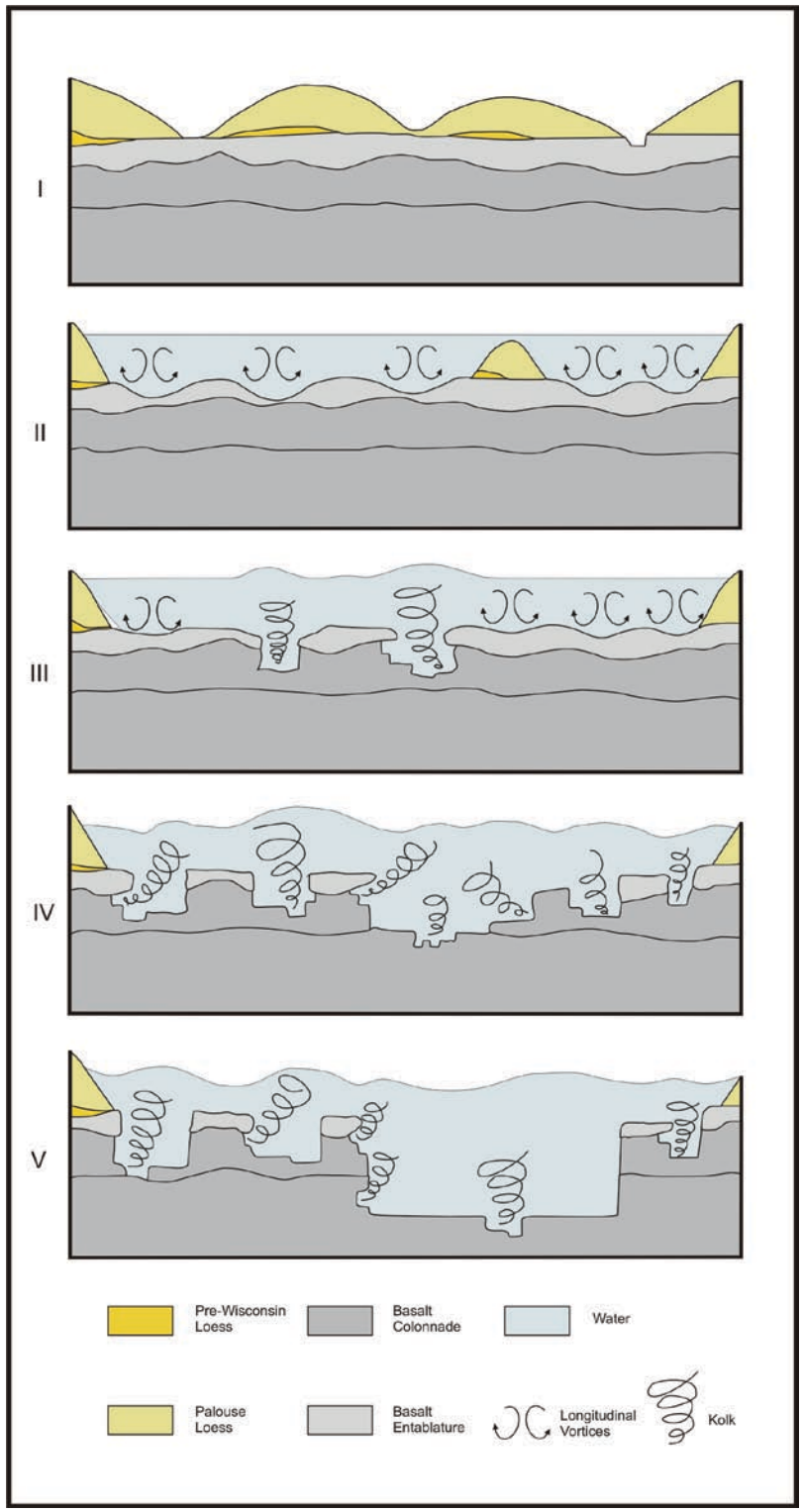

Fig 3.5 Hypothetical evolutionary sequence of flood erosion (top to bottom) showing the action of turbulent cataclysmic flood flows, which eroded into the basalt by the hydraulic plucking action of both longitudinal and vertical vortices. Different phases (I–V) of the evolution are described in the text

3.4 Evolution

The erosion by Missoula Flood waters into the Columbia Plateau surface probably occurred in an organized sequence of stages (Fig. 3.5), examples of which can be found throughout the Channeled Scabland. The first floodwater encountered a plateau surface capped by loess that had been shaped into hills by the gentle dissection of streams fed by rainfall and runoff on the plateau itself (Phase I). The high-velocity water quickly filled the relatively small pre-flood valleys, shaping the remnant of loess divides between them into streamlined loess hills (Phase II). The entablature of the uppermost underlying basalt flow was next encountered by the incising floodwater. The resistant entablature surface was probably initially scoured by longitudinal grooves, similar to those observed near Dry Falls (Fig. 3.3). As the scour cut deeper into a basalt flow, it would next encounter the well-developed columnar jointing that occurs in the flow interiors. The joint-bounded columns were very susceptible to plucking-type erosion (Phase III) in which the pressure fluctuations associated with vertical vortices (kolks) lifted sections of column and entrained them into the floodwater. The resulting potholes would then enlarge and coalesce (Phase IV), comprising the common butte-and-basin scabland topography of the region (Fig. 3.2). Eventually, a prominent inner channel (Phase V) would develop, probably by the initiation and headward migration of a cataract, such as Dry Falls (Fig. 3.3).

3.5 Discussion

Bretz once considered the landforms of the Channeled Scabland to be unique in the world. In being so, he reasoned, their cataclysmic origin might be more acceptable to his contemporary geologists who held to an overly rigid form of uniformitarianism (Baker 1978). In contrast to these views, however, cataclysmic flood landscapes have now been documented in many parts of the world, including central Asia and the margins of the former Laurentide Ice Sheet in North America (Baker 2002, 2007). Spectacular examples of giant current ripples occur in central Asia (Baker et al. 1993), along with immense gravel bars and scour marks (Herget 2005). Streamlined hill and bar morphologies occur in the glacial lake spillway channels of central North America (Kehew and Lord 1986). Nevertheless, because of their spectacular preservation and relative accessibility, the patterns, forms, and processes evident in the Channeled Scabland have helped inform understanding of processes that occur at various scales in bedrock channels that are highly influenced by extreme flood processes.

The Author

Dr **Victor R. Baker** is Regents' Professor of Hydrology and Water Resources, The University of Arizona, Tucson, AZ, USA. He has authored or co-authored more than 350 research papers and chapters on topics including fluvial palaeohydrology and geomorphology, geomorphic features on Mars and Venus, and history and philosophy of the Earth Sciences. He was the 1998 President of the Geological Society of America and the 1995–1999 President of the International Union for Quaternary Research (INQUA), Commission on Global Continental Paleohydrology. He is a Fellow of the American Geophysical Union, the Geological Society of America, and the American Association for the Advancement of Science, as well as an Honorary Fellow of the European Union of Geosciences, and a Foreign Member of the Polish Academy of Sciences.

References

Baker VR (1973) Paleohydrology and sedimentology of Lake Missoula flooding in Eastern Washington. Geol Soc Amer Spec Pap 144:1–79

Baker VR (1978) The spokane flood controversy and the Martian outflow channels. Science 202:1249–1256

Baker VR (1979) Erosional processes in channelized water flows on Mars. J Geophys Res 84:7985–7993

Baker VR (2002) High-energy megafloods: Planetary settings and sedimentary Dynamics. In: Martini IP, Baker VR, Garzon G (eds) Flood and megaflood deposits: Recent and ancient examples. Int Assoc Sediment Spec Publ 32:3–15

Baker VR (2007) Greatest floods–largest rivers. In: Gupta A (ed) Large rivers: Geomorphology and management. Wiley, New York, pp 65–74

Baker VR, Bunker RC (1985) Cataclysmic late Pleistocene flooding from glacial Lake Missoula: A review. Quat Sci Rev 4:1–41

Baker VR, Benito G, Rudoy AN (1993) Paleohydrology of Late Pleistocene superflooding, Altay Mountains, Siberia. Science 259:348–350

Benito G, O'Connor JE (2003) Number and size of last-glacial Missoula floods in the Columbia River valley between the Pasco Basin, Washington, and Portland, Oregon. Geol Soc Amer Bull 115:624–638

Bretz JH (1923) The Channeled Scabland of the Columbia Plateau. J Geol 31:617–649

Bretz JH (1932) The Grand Coulee. Amer Geogr Soc Spec Publ 15:89

Bretz JH, Smith HTU, Neff GE (1956) Channeled Scabland of Washington: New data and interpretations. Geol Soc Amer Bull 67:957–1049

Herget J (2005) Reconstruction of Pleistocene Ice-dammed Lake Outburst floods in the Altai Mountains. Siberia Geol Soc Amer Spec Pap 386:118

Kehew AE, Lord ML (1986) Origin of large-scale erosional features of glacial-lake spillways in the northern Great Plains. Geol Soc Amer Bull 97:162–177

Pardee JT (1942) Unusual currents in glacial Lake Missoula. Geol Soc Amer Bull 53:1569–1600

Waitt RB Jr (1985) Case for periodic, colossal jokulhlaups from Pleistocene glacial Lake Missoula. Geol Soc Amer Bull 96:1271–1286

Chapter 4
Badlands of the Northern Great Plains: Hell with the Fires Out

Mark A. Gonzalez

Abstract Badlands occur worldwide and are especially common in the Northern Great Plains of North America. Badlands form where the erosive power of slopewash reaches its maximum expression and is optimized by the combination of steep, local topography; weakly indurated, readily eroded bedrock; and sparsely vegetated hillslopes. Erosional landforms include finely rilled hillslopes, pipes, gullies, pedestals, and hoodoos. Landslides modify many slopes. Depositional and transportational landforms include pediments, fans, and terraces. Clinker is common; it forms when seams of lignite burn subterraneously and bake overlying rock into a naturally fired brick. Badlands of the Northern Great Plains contain paleontological records of the final days of dinosaurs and the emergence of mammals. Badlands capture the imagination with its geologic wonders, paleontological treasures, and spellbinding vistas.

Keywords Badlands • clinker • geomorphology • Great Plains • landforms

4.1 Introduction

For Native Americans and early Euro-American explorers, few landscapes stirred the imagination more or created more trepidation than the badlands. The indigenous population of Dakotahs, or Sioux Indians, referred to the badlands as "*makó shika*" ("land bad"), French fur-trappers referred to the badlands as "*Les mauvaises terres a' traverser*" (bad lands to cross), later shortened to "*les mauvaises terres*." In 1864 Alfred Sully, General of the US Cavalry, encountered the Little Missouri Badlands in the Dakota Territory (present day North Dakota). Perhaps awed by the stark landscape or recognizing the challenges posed in trying to traverse this rugged landscape with a heavily laden military party, he described these badlands as, "hell with the fires out" (Schoch 1974).

Badlands worldwide are formed by the forces of gravity and running water, especially by the process of slopewash erosion, which reaches its maximum potential under the combination of: (1) steep local topography; (2) weakly cemented, poorly indurated, readily eroded bedrock; and (3) a semiarid continental climate that supports a sparse vegetation cover, yet delivers precipitation in relatively high-magnitude, short-lived convective storms. This combination ensures that hillslopes are highly vulnerable to erosion, and erosive forces of running water reach their maximum expression on Earth.

4.2 Geographical Setting

Badlands occur throughout Earth and are especially common in the Northern Great Plains in the north-central part of the USA and the adjacent part of Canada (Fig. 4.1). Badlands most commonly occur within major river valleys that are entrenched 100–250 m below the general elevation of the surrounding plains, which are typified by flat, gently dipping, and/or gently undulating landscapes of low relief. The Great Plains lie east of the Rocky Mountains. Formation of the Rocky Mountains during the Laramide Orogeny in the Late Cretaceous and Palaeogene periods created sources of sediment that were transported eastward toward depocenters in the interior of North America, such as the Williston Basin. These sediments formed the bedrock that eventually would be exposed again and carved into badlands during Neogene and Quaternary time.

P. Migoń (ed.), *Geomorphological Landscapes of the World*,
DOI 10.1007/978-90-481-3055-9_4, © Springer Science+Business Media B.V. 2010

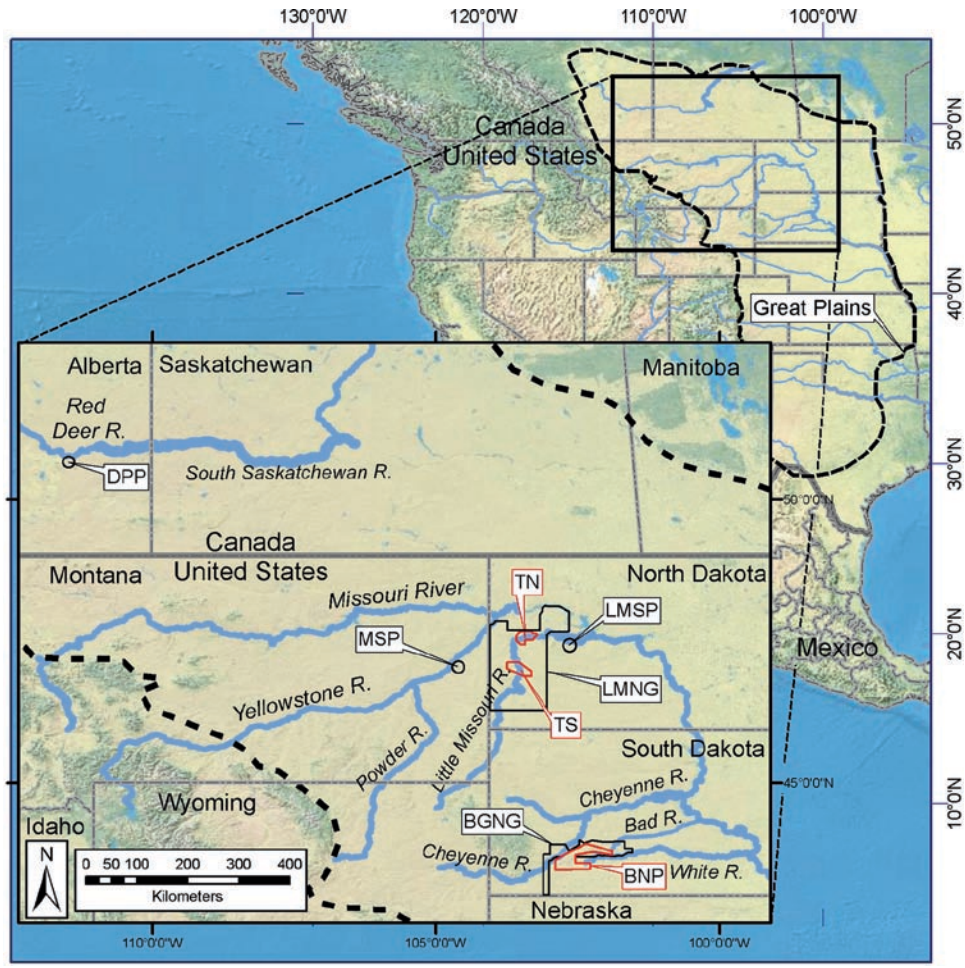

Fig. 4.1 The Great Plains of North America are located east of the Rocky Mountains and extend from Alberta, Canada, through the central United States and into northern Mexico. Federal, state, and provincial parks and grasslands provide outstanding opportunities to explore and experience badlands. These public lands include Badlands National Park (BNP), parts of the Buffalo Gap National Grassland (BGNG), Theodore Roosevelt National Park (TN, North Unit; and TS, South Unit), Little Missouri National Grassland (LMNG), Dinosaur Provincial Park (DPP), Makóshika State Park (MSP), and Little Missouri State Park (LMSP)

Badlands topography occurs within many stream valleys in the Northern Great Plains such as the Little Missouri River, Yellowstone River, Powder River, Missouri River, White River, Cheyenne River, and Red Deer River in the states of North Dakota, South Dakota, Montana, and Wyoming, and the Canadian province of Alberta (Fig. 4.1). The Little Missouri Badlands is representative of many badlands in the Northern Great Plains and has been selected here to discuss specific information, such as its climate, landforms, strata, and geologic evolution.

The Little Missouri Badlands occurs in a belt that is from 15 to 40 km wide along the lower 300 km of the Little Missouri River (Fig. 4.1). The climate of the Little Missouri Badlands is continental and semiarid. Mean annual precipitation averages 390 mm per year, with nearly three-fourths of this falling from April through August (Gonzalez 2001). Much of the summer precipitation is delivered in powerful convective thunderstorms. Mean monthly temperatures range from 21°C in July to −2°C in January; extreme temperatures range from −40°C to 40°C (Gonzalez 2001). Native vegetation includes mixed-grass prairies on level ground with good soil development, plains cottonwood along watercourses, small shrubs on thin soils, and near absence of all vegetation on steep, bedrock hillslopes (Fig. 4.2).

Fig. 4.2 The Little Missouri Badlands are formed in the Late Cretaceous Hell Creek Formation and the Paleocene Bullion Creek and Sentinel Butte formations. The Sentinel Butte Formation (shown here) typically has sparsely vegetated hillslopes. The base of the Sentinel Butte Formation is demarcated locally by a discontinuous bed of lignite, which has burned underground in many places to produce clinker (Photo: M.A. Gonzalez)

The Little Missouri Badlands is among the least populated landscapes in the contiguous USA, owing to its remoteness from major markets and the challenges of installing and maintaining infrastructure in this highly erosive landscape.

4.3 Landforms

4.3.1 Erosional Landforms of Hillslopes and Escarpments

Escarpments commonly rise 100–200 m or more from the axial streams that drain badlands to the flat-lying terrain that makes up the undulating topography of the Northern Great Plains. Escarpments are steep and nearly devoid of vegetation, especially on south-facing slopes (Fig. 4.3). Beautiful exposures of the bedrock create remarkable glimpses into the geologic history of the continent's interior over the last 20–70 million years.

High local relief and presence of structurally weak strata, especially lignite seams and bentonite beds, create conditions where slope failure is especially prevalent. Along some segments of the Little Missouri River valley, 40% of the valley margin is modified by landslides (Murphy 2000). The flanks of many buttes (isolated, commonly flat-topped hills that are several hectares to a few hundred hectares in size) are modified by landslides and slumps too.

Two types of landslides are particularly common in the Little Missouri Badlands, slumps and earthflows. Slumps are characterized by rotation and downslope translocation of fairly intact, coherent blocks along a

Fig. 4.3 The Late Cretaceous and Palaeogene sedimentary strata in the Northern Great Plains are nearly horizontal and form so-called "pancake" stratigraphy – note such in the hillslope. A large rotational slump block on the valley floor (right-center portion of view) has internally coherent beds that dip about 35° toward the hillslope, where in situ bedrock is flat-lying. The yellow bed near the top of the slump block was part of the yellow bed that extends at or near the top of the hillslope (Photo: M.A. Gonzalez)

concave-upward failure surface (Figs. 4.3 and 4.7, inset A). The horizontal to gently dipping Palaeogene beds are tilted 25°–50° into the hillslope within rotational slumps. The bases of many landslides are characterized by earthflows. Earthflows are incoherent; their internal strata are completely distorted and show evidence of turbulent flow. Landslides vary from a fraction of a hectare to nearly 100 ha in area. Most are a few to a few tens of hectares in size.

Hillslopes of 25° to greater than 60° typify badlands (Fig. 4.4). Weakly lithified Late Cretaceous- through Miocene-age strata are readily eroded by slopewash. Running water creates finely dissected rills on many hillslopes and castellated weathering patterns on nearly vertical cliffs. Erosion-resistant concretions, channel sandstones, and stumps of petrified trees serve as cap rocks to create pedestals and hoodoos.

Sodic soils are quite abundant in the Little Missouri Badlands. When sodic soil and weakly lithified bedrock are wetted, sodium ions disperse clay particles. The dispersive process can be so strong that some claystones appear to dissolve like granules of sugar in water. When clay particles are dispersed, subterranean pipes may form. These can grow into conduits that are a few meters in diameter. Roofs over shallow pipes commonly collapse to form steep-walled gullies. Pipes and gullies may pose hazards to travel and infrastructure.

Creep processes gradually move unconsolidated soil and sediment down hillslopes, particularly on north-facing slopes, which typically contain more moisture, deeper soils, and more vegetation than south-facing slopes, which are modified more by slopewash processes.

Fig. 4.4 Slopewash erosion sculpts badlands hillslopes with a dense network of rills. Resistant lithologies and rocks, such as stumps of petrified trees, iron and manganese concretions, or well-cemented channel sandstones, create pedestals and hoodoos (Photo: M.A. Gonzalez)

4.3.2 Transportational and Depositional Landforms – Pediments, Fans, and Terraces

Pediments typically form below badlands hillslopes. The transition from sparsely vegetated badlands hillslope to pediment is commonly abrupt (Fig. 4.5) The slope above the hillslope–pediment junction ranges from 5° to 60°, whereas the pediments have an average slope of less than 2° (Schumm 1962).

Schumm's (1962) seminal work was confined to miniature pediments (ones measuring a few meters in length). Observation of pediments formed beneath badland escarpments that are 100 or more meters tall, shows that pediments may be a few hundred meters to more than a kilometer long. Many of these large, well-developed pediments are commonly overlain by one to several meters of alluvium (primarily slopewash deposits) and possibly aeolian deposits, indicating that the erosive conditions that form pediments may eventually give way to a period of alluvial fan formation and pedogenesis (Biek and Gonzalez 2001; Gries 2005). In subsequent periods of incision, channels have cut down through pediments, leaving them elevated as a "sod table." Once channels have incised a pediment surface, runoff and sediment from overlying hillslopes bypass the pediment. Soil development occurs on the inactive pediment. Eventually the soils on pediments, or sod tables, evolve to support a grass and/or shrub plant communities.

4.3.3 Clinker Fields

Beds of lignite are especially common in the Paleocene-age strata of the Little Missouri Badlands of North Dakota and the Powder River Basin of Wyoming and Montana (Coates 1980). Where lignite is exposed at the surface, it is susceptible to ignition from wildfires

Fig. 4.5 The base of many badlands hillslopes coincides with an abrupt change in slope. Many hillslopes transition into pediment surfaces – flat, gently sloping, erosional surfaces with little to no accumulation of sediment (Photo: M.A. Gonzalez)

or spontaneous combustion. Once ignited, the lignite burns underground so long as ground fractures provide conduits for oxygen to fuel the fire. Heat released from coal-seam fires metamorphoses overlying rocks into naturally fired bricks. Clinker is a general term for the heat-baked rock. Clinker varies in color depending on the chemistry of the rock, but an abundance of iron in many Paleocene strata typically leads to the formation of bright orange-, rust-, and red-colored clinkers (Fig. 4.6).

Clinker is generally far more resistant to erosion than surrounding, unbaked sediments. Consequently, clinker serves as a caprock on many hills, ridges, knobs, buttes, and plateaux. Overlying clinker and overburden collapse into the void created by the burned lignite to create a highly irregular, jumbled landscape. In addition, chimneys form where hot gases escaped to the surface; they commonly stand as small conical hills or spires above undulating clinker fields. Well-developed clinker fields have an irregular and undulatory surface as chaotic as a storm-driven sea (Fig. 4.2).

4.4 Paleontology

Although the focus of this volume is geomorphology, no visitor to the badlands can fail to notice the abundance of fossils. Fossil preservation is especially high for terrestrial deposits, owing to the low-energy of the depositional environment, which in many respects was quite similar to the coastal zone surrounding the modern-day Gulf of Mexico. In addition to the abundance of fine-textured sandstone, siltstone, and mudstones, lignite beds are ubiquitous. Plant fossils are especially well preserved in lignite, which formed in anaerobic swamps. Finally, beds of bentonite, derived from Cainozoic volcanism in western North America,

Fig. 4.6 Clinker forms when underground seams of burning coal or lignite metamorphose overlying rock into a natural brick. Clinker is highly variable. Hot spots, such as the roof of a burning coal seam, or the wall of a chimney, may melt and form glass-like rocks. The loss of gases and steam from lignite can form highly vesicular rocks, which have enough void space to float in water. Columnar joints, as commonly found in basalt flows, also occur in clinker. Columnar joints form when hot clinker cools and contracts (Photo: M.A. Gonzalez)

repeatedly blanketed the region, smothered life, and preserved it in incredible detail.

Badlands have long been a treasure chest for paleontologists. Sparse vegetation cover and phenomenal bedrock exposures reveal myriad details of ancient life. An extensive petrified forest is found in the lower strata of the Paleocene-age Sentinel Butte Formation in the Little Missouri Badlands (Biek and Gonzalez 2001). Much of our understanding of the end days of the dinosaurs and the ascent of mammals comes from fossils found in the badlands of the Northern Great Plains.

4.5 Evolution

The bedrock now exposed at the surface in the Northern Great Plains was deposited originally from the Late Cretaceous Period through the Miocene Epoch of the Neogene Period. In Late Cretaceous time, an epicontinental seaway extended across the interior of North America, linking the Gulf of Mexico with the Arctic Ocean (Roberts and Kirschbaum 1995). Fine-textured deposits (Pierre Formation) accumulated in this shallow, inland sea, and terrestrial sediments (Fox Hills and Hell Creek formations) were deposited on the margin of the sea in a low-lying coastal environment that probably most closely resembled the estuaries, deltas, shorelines, bayous, floodplains, coastal plains, and everglades that compose the coastal environment of the modern-day Gulf of Mexico (Bluemle 2000: 155; Hoganson and Murphy 2003: 60).

By the Paleocene Epoch, the last vestige of the inland sea (the Cannonball Sea) had retreated from the Northern Great Plains. Rivers carried sediment from the Rocky Mountains, and winds bore volcanic ash from volcanic centers in the western United States and deposited these sediments (Fort Union Group)

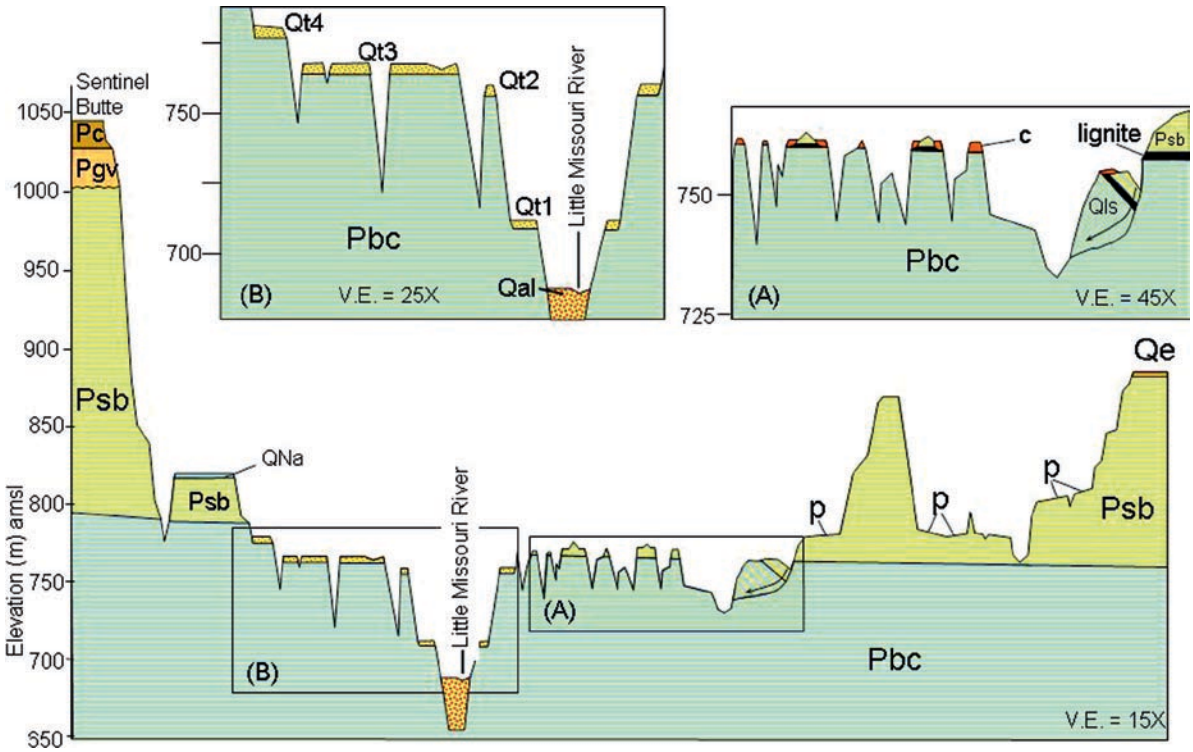

Fig. 4.7 Landscape schematic of the Little Missouri Badlands illustrates the accumulation of swamp, floodplain, and coastal terrestrial deposits (Pbc: Bullion Creek Formation; and Psb: Sentinel Butte Formation) during the Paleocene Epoch. Eocene (Pgv: Golden Valley Formation and Pc: Chadron Formation), Oligocene, and Miocene rocks underlie prominent buttes and mesas in the Northern Great Plains. (**A**) The contact between Pbc and Psb is locally marked by either the HT Butte lignite bed or the HT Butte clinker (**c**), where the lignite has burned underground and baked overlying rock. Pleistocene- and Holocene-age landslides (Qls) are common on steep badlands slopes. The base of many slumps transition into mud- or earthflows. Though fan deposits occur at the mouth of canyons, many hillslopes transition to erosional surfaces or pediments (**p**) where there is surprisingly little storage of slopewash sediment (see Fig. 4.5). (**B**) Plio-Pleistocene erosion has created topographic inversion with ancestral stream deposits now forming prominent topographic highs (e.g., QNa is an ancestral stream deposit of the Little Missouri River that is more than 600,000 years old). Pleistocene diversion of drainages, including the Little Missouri River, led to a powerful cycle of incision that has carved the Little Missouri Badlands in the last 600,000 years. Episodic base-level stability led to the development of four prominent cut-and-fill terraces (Qt1-Qt4: youngest to oldest) during the mid- to late Quaternary Period. Three to four cut-and-fill terraces have formed within 15 m height above modern alluvial deposits (Qal) during the Holocene Epoch (not shown due to scale) along many tributary streams. Late Pleistocene and Holocene aeolian deposits (Qe) have accumulated on broad, stable surfaces above large river valleys (Schematic diagram modified from Biek and Gonzalez 2001)

throughout the Northern Great Plains. Regional deposition of Rocky Mountain-derived sediment continued across the Northern Great Plains into the Miocene. In the Little Missouri Badlands, most of the exposed strata are the lignite-bearing Bullion Creek and the Sentinel Butte formations (Fig. 4.7). These formations comprise intercalated layers of lignite, sandstone, siltstone, mudstone, and bentonite. They formed in large coastal swamps and meandering floodplains (Bluemle 2000; Hoganson and Murphy 2003: 112).

Eocene- (Pgv and Pc; Fig. 4.7) and Oligocene-age strata lie unconformably over the Fort Union Group. These strata are not well preserved in North Dakota and are found near the top of scattered buttes and mesas (Murphy et al. 1993). The rapid rates of deposition that characterized the Palaeogene declined and alternated with intervals of regional erosion during Neogene times. These erosion intervals are observed as major unconformities or disconformities.

Erosion has been the primary landscape-forming process over the past 5 million years during Plio-Pleistocene time (Bluemle 2000). Naturally, this erosion was not uniform. Well-indurated, freshwater limestone (lake) deposits and coarse-caliber, gravel (stream) deposits served as resistant caprocks on low-lying parts of the Miocene landscape. As the overall landscape was eroded, these former low spots (lakes and rivers) were more resistant to erosion and became isolated as topographic high spots – modern-day buttes and mesas (e.g., Sentinel Butte and the QNa deposit in Fig. 4.7). This process of creating high topographic points from formerly low points is known as topographic inversion.

During the Pleistocene Epoch, the ancestral drainage of the Little Missouri River, Yellowstone River, Missouri River, and other major drainages of the Northern Great Plains were diverted from their ancestral course to Hudson Bay by the growth and southward expansion of continental ice sheets (Howard 1960; Bluemle 1972). The Missouri River became an ice-marginal drainage bound for the Gulf of Mexico. It in turn diverted the drainage of the Little Missouri River. This diversion is believed to have occurred approximately 600,000 years ago, based on the stratigraphy of valley-fill deposits in the pre-diversion, ancestral Little Missouri River valley (Bluemle 1972, 2000).

The diverted course of the Little Missouri River was shorter and steeper than its ancestral drainage; consequently, the stage was set for a period of powerful stream incision to commence, continuing today with more than 200 m of channel incision over the past 600,000 years. A series of mid- to late-Quaternary terraces are preserved as inset valley-side benches or mid-valley buttes in the Little Missouri Badlands (Fig. 4.7B).

In the Little Missouri Badlands, there are five prominent terraces that record the history of stream incision over the past few million years. The age of the oldest ancestral terrace of the Little Missouri River is poorly constrained. A tentative Plio-Pleistocene age is assigned to this oldest and highest terrace and its associated alluvium (QNa; Fig. 4.7; Biek and Gonzalez 2001). Four younger inset terraces (Qt1–Qt4) were likely formed in the past 600,000 years; the interval when most of the badlands was carved. All terraces in the Little Missouri Badlands are fill terraces. Stream deposits of gravel, sand, and silt, are typically overlain by aeolian deposits of fine sand and silt.

Drill-hole data indicate that the lower reach of the Little Missouri Badlands is filled with as much as 60 m of alluvium (Qal). Apparently, the badlands were more deeply incised at some point in the early or pre-Wisconsinan before the Little Missouri River partially back-filled its valley during Wisconsinan time. Tributaries to the Little Missouri River contain a higher resolution record of Holocene- and settlement-age cut-and-fill terraces (Gonzalez 2001). These terraces record a dynamic fluvial history apparently tied to climatic conditions during the mid- to late Holocene.

During the past half-million or more years, the Little Missouri Badlands has enlarged by headward incision. Also tributaries have adjusted to falling base level along the axial Little Missouri River by downcutting and headward incision. Consequently, the Little Missouri Badlands has become longer, deeper, and wider through time.

4.6 Summary

Badlands are landscapes where the erosive power of slopewash reaches its maximum expression on Earth. The slopewash process is optimized because of the combination of steep local topography; weakly indurated, readily eroded bedrock; and sparsely vegetated hillslopes due to the semiarid climate and the paucity of soil development.

Slopewash and landslides create myriad sculptures that frustrate travel and dazzle the imagination. A labyrinth of twisted gullies, streams valleys, and box canyons provides an unparalleled opportunity for modern humans to explore the natural world and disappear into a fantastical realm. The naked hillslopes divulge countless secrets of the past 20–70 million years. The rich paleontological treasures of these badlands record the final days of the dinosaurs and the emergence of mammals. Nestled in the interior of North America, badlands carve a deep fissure into the Earth's dermis, from which we learn much about the formation of the Rocky Mountains, the pulses of North American volcanism, and the rise and fall of the epicontinental seas.

Despite its austere-sounding name, the Badlands beckon the intrepid geologist and explorer like few places on Earth. Opportunities to see and experience the rugged landscapes of badlands are plentiful. Federal, state, and provincial governments have created several public parks in the

Northern Great Plains including Theodore Roosevelt National Park and Little Missouri State Park in North Dakota, Badlands National Park in South Dakota, Makoshika State Park in Montana, and Dinosaur Provincial Park in Alberta, Canada. The United States Forest Service also oversees more than 500,000 ha in the Little Missouri National Grassland and Buffalo Gap National Grassland, which includes the largest tracts of publicly accessible badlands in the United States. Badlands enchant the mind with geologic and paleontological wonders, myriad wildlife, and spellbinding vistas.

The Author

Mark Gonzalez is a geoscientist with the Dakota Prairie Grasslands of the United States Department of Agriculture-Forest Service, Bismarck, North Dakota. He has studied the ecology, hydrology, pedology, and geomorphology of badlands over the past 26 years. Previously he was a geologist with the North Dakota Geological Survey, and a professor in the Department of Geography, University of Denver, Denver, Colorado.

References

Biek RF, Gonzalez MA (2001) The geology of Theodore Roosevelt National Park: Billings and McKenzie counties, North Dakota. North Dakota Geol Surv Misc Series No 86. Bismarck, North Dakota

Bluemle JP (1972) Pleistocene drainage development in North Dakota. Geol Soc Amer Bull 83:2189–2193

Bluemle JP (2000) The face of North Dakota, 3rd edn. North Dakota Geol Surv Educational Series 26. Bismarck, North Dakota

Coates DA (1980) Formation of clinker by natural burning of coal beds in the Powder River Basin, Wyoming. In: Carter LM (ed) Proceedings of the fourth symposium on the Geology of Rocky Mountain Coal. Colorado Geol Surv Resource Series No 10:37–40

Gonzalez MA (2001) Recent formation of arroyos in the Little Missouri Badlands of southwestern North Dakota. Geomorphology 38:63–84

Gries JP (2005) Roadside geology of South Dakota. Mountain Press, Missoula, Montana (4th printing)

Hoganson JW, Murphy EC (2003) Geology of the Lewis and Clark Trail in North Dakota. Mountain Press, Missoula, Montana

Howard AD (1960) Cenozoic history of Northeastern Montana and Northwestern North Dakota with emphasis on the Pleistocene. US Geol Surv Prof Pap 326:107

Murphy EC (2000) Landslides in Western North Dakota. Geol Soc Amer Abstracts with Programs 32(7):57

Murphy EC, Hoganson JW, Forsman NF (1993) The Chadron, Brule, and Arikaree Formations in North Dakota: The Buttes of Southwestern North Dakota. North Dakota Geol Surv Report of Investigations No 96

Roberts LNR, Kirschbaum MA (1995) Paleogeography of the Late Cretaceous of the Western Interior of middle North America: Coal distribution and sediment accumulation. US Geol Surv Prof Pap 1561:115

Schoch HA (1974) Theodore Roosevelt: The story behind the scenery. KC Publications, Las Vegas, Nevada

Schumm SA (1962) Erosion on miniature pediments in Badlands National Monument, South Dakota. Geol Soc Amer Bull 73:719–724

Chapter 5
Canyonlands and Arches: Windows on Landscapes in the American Southwest

John C. Dixon

Abstract The southwestern United States is characterized by dramatic canyon-dominated sandstone landscapes. The canyons are typically steep-sided and display segmented valley walls reflecting the variable resistance of the rocks into which they are cut. Three broad sets of geomorphic processes are principally responsible for canyon formation: groundwater sapping, fluvial erosion, and salt tectonics. Extensively associated with the sandstone landscapes of the American southwest is the development of spectacular arches and natural bridges. These forms are the result of the structurally controlled dissolution of calcite cements, and subsequent enlargement by removal of loosened grains, boulders, and slabs by wind, gravity, and water.

Keywords Arches • Canyonlands • dissolution • natural bridges • salt tectonics • sapping

5.1 Introduction

The southwestern United States is characterized by dramatic canyon-dominated sandstone landscapes. Perhaps the most well-known are those of the Colorado Plateau. The canyons are typically steep-sided, often displaying segmented valley walls in response to the variable resistance of the rocks through which the canyons are cut (Nicholas and Dixon 1986; Howard and Kochel 1988). Canyon morphology varies depending on the processes responsible for their formation. While many have perennially flowing streams in their bottoms, many only carry water after rain events, and some are essentially perennially dry. The bold cliffs of the canyon country are to a large extent the result of the combined effects of the prevailing arid climate and the resistance of the sandstone. Yet many of these apparently strong sandstones are cemented by weak minerals and are susceptible to weathering and erosion that results in the formation of spectacular natural arches and bridges. In addition, a wide variety of minor landforms also occur on the sandstone surfaces (Howard and Kochel 1988).

5.2 Geographical Setting

The Colorado Plateau covers some 400,000 km^2 at the intersection of the American states of Colorado, Arizona, Utah, and New Mexico. It lies to the west of the Rocky Mountains and to the east of the Basin and Range geomorphic regions and is drained by the Colorado River and its tributaries. It is these tributaries that are fundamentally responsible for carving the distinguishing canyons. The Colorado Plateau is subdivided into six distinctive sections and the Canyonlands Section covers approximately one-third of the northern part of the Colorado Plateau (Thornbury 1965) (Fig. 5.1).

The Colorado plateau rises to an elevation of approximately 1600 m with high peaks in mountain massifs attaining elevations of 3500 m. Consequently, there is a strong precipitation gradient ranging from 100 mm to 400 mm; however, mean annual precipitation is only 220 mm. The overall aridity is largely due to the rain shadow effect of the plateau edge to the west as well as its overall distance from moisture sources. Effective moisture is generally lower however, except for high-intensity, short-duration thunderstorms and spring snowmelt which are significant geomorphic agents. Strong temperature contrasts also characterize the region with hot summers and cold winters. Frost-free days range from 100 days or less at the highest elevations to as many as 200 days in many canyon bottoms (Hunt 1974). The region also exhibits

P. Migoń (ed.), *Geomorphological Landscapes of the World*,
DOI 10.1007/978-90-481-3055-9_5, © Springer Science+Business Media B.V. 2010

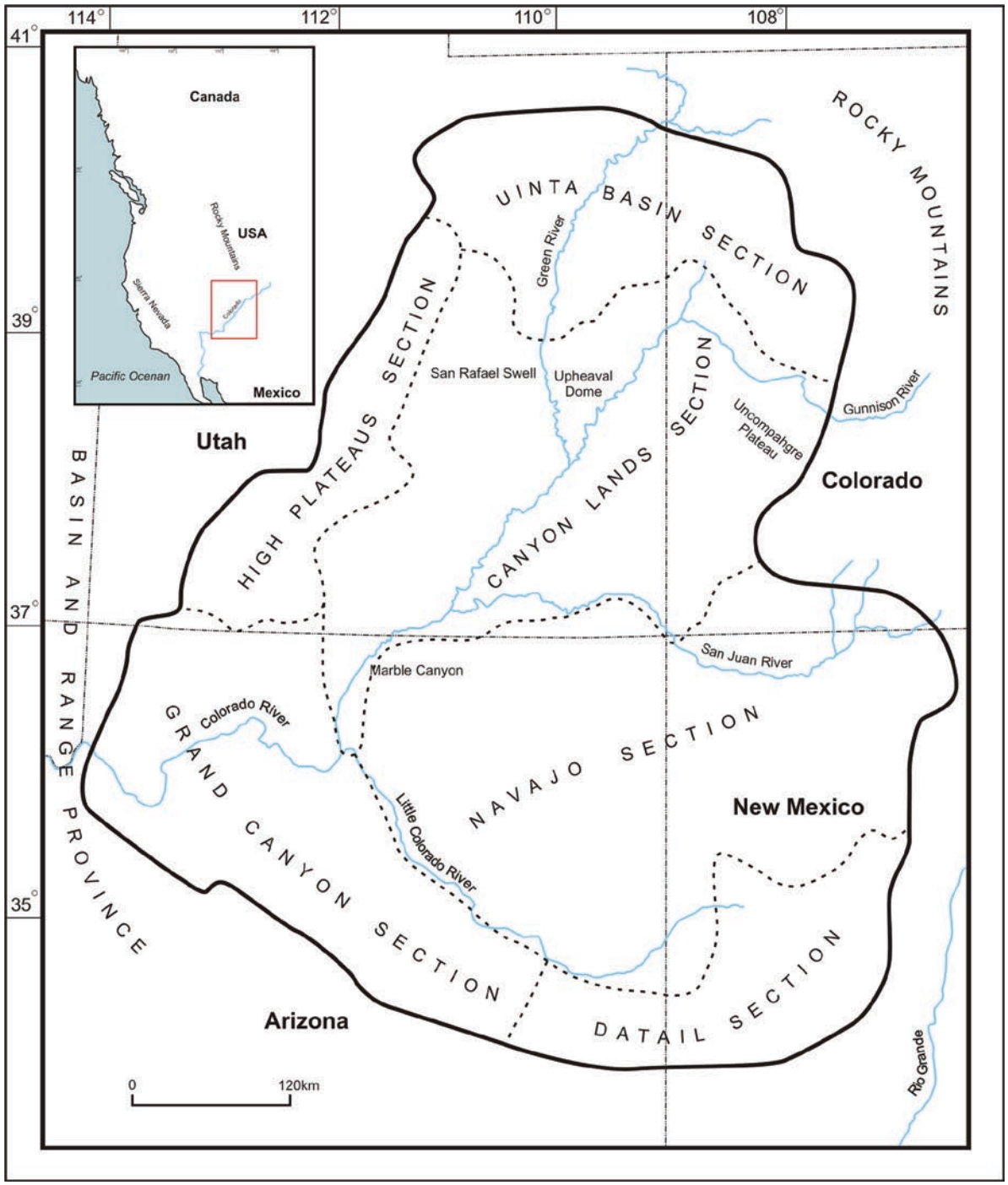

Fig. 5.1 Location and major geomorphic sections of the Colorado plateau (Thornbury 1965)

the influence of alternating humid and arid episodes during the Quaternary (Goudie 2002).

Vegetation on the Plateau is strongly vertically zoned in response to the strong precipitation and temperature gradients imposed by the overall saucer shape and deep incision of the plateau. Plateau rims and mountain massifs are forested and the interior is dominated by desert shrubs and grasslands. Canyon bottoms support a diversity of hydrophytic vegetation (Hunt 1974).

5.3 Geomorphic and Geological Setting

Deep canyons are cut into pre-Cainozoic age sedimentary rocks that have been uplifted into a broad saucer-shaped plateau by epeirogenic processes with numerous laccolith-dominated mountains. The dominant canyons of the region include those of the Colorado River and its tributaries including Marble Canyon, Glen Canyon, and Cataract Canyon. Other significant canyons include those of the Green, San Juan, Gunnison, Dolores, San Rafael, Dirty Devil, and Escalante Rivers. In addition, many ephemeral, "box canyons" contribute to the dissected nature of this part of the Colorado Plateau (Thornbury 1965).

The Canyonlands section of the Colorado Plateau displays the presence of four broad upwarps which exert strong controls on regional landscape development. These include the Uncompahgre Upwarp, the Circle Cliffs Upwarp, Monument Upwarp, and the San Rafael Swell. These swells are unfaulted.

The canyons and associated landform elements have been eroded primarily into sandstones and shales of upper Paleozoic and lower Mesozoic age. The most significant formations in the evolution of the Canyonlands landscape include the Jurassic age Entrada Sandstone which is the dominant cliff-forming unit and host to all of the arches in Arches and Natural Bridges National Parks. This unit consists of three members deposited in marginal marine environments with associated sand dunes. Below the Entrada is the late Triassic to early Jurassic Glen Canyon Group which consists of the major canyon-forming units of the aeolian Navajo Sandstone, fluvial Kayenta Formation, and aeolian Wingate Sandstone. The late Triassic age fluvial Chinle Formation lies beneath the Glen Canyon Group and is dominated by siltstones, mudstones, and sandstones. Beneath the Chinle Formation is the marine Moenkopie Formation of Early/Middle Triassic age which consists of mudstones, sandstones, and some conglomerates. Below the Moenkopie Formation is the fluvial Cutler Formation. The upper part of the formation consists of the Organ Rock unit which is another major cliff-forming unit (Nicholas and Dixon 1986), while the lower part of the formation consists of the Cedar Mesa Sandstone which is a calcareous cemented unit supporting the slot-canyon dominated landscape of The Maze as well as being the unit in which most of the arches in Canyonlands National Park are developed. The lowermost unit in the Canyonlands section of the Colorado Plateau is the Permian age marine Hermosa Formation which consists primarily of limestone, sandstone, and shale and at its base, salt, gypsum, and anhydrite dominate (Lohman 1974).

Mountain massifs, comprising principally the Henry Mountains and the La Sal Mountains, represent structural domes formed by the intrusion of stocks into sedimentary rock units. As the stocks grew in size the overlying beds were deformed into steep-sided anticlines. Where the magma in the stocks encountered shales it flowed laterally and formed the laccoliths which dominate the structure of these mountains (Hunt 1974).

In addition to the deep, steep-sided canyons developed in the thick, essentially horizontal massive sandstones which characterize the canyonlands, the landscape also displays a variety of other forms. Where the thick resistant sandstone units have been upturned along the flanks of the anticlinal upwarps and along the flanks of the mountain massifs, hogbacks are extensively developed along the anticlinal ridges. These sandstones also erode into dome-like forms (Bradley 1963), along with buttes, mesas, and spires with steep bedrock bounding escarpments (Nicholas and Dixon 1986). Within the Colorado Plateau/Four Corners area of the United States we see some of the most outstanding examples of the relationships between structure-lithology and relief to be observed anywhere in the world. It is no accident that the foundations of modern geomorphology formulated by Gilbert, Powell, and Dutton were based on observations from the Colorado Plateau.

5.4 The Canyons

The Canyonlands section of the Colorado Plateau is dominated by deep, steep-sided canyons cut into massive sandstones, especially the Entrada Sandstone and those of the Cutler and Glen Canyon Formations. Three specific sets of geomorphic processes are largely responsible for landform evolution: groundwater sapping, fluvial erosion, and salt tectonic processes. The spectacular amphitheaters and alcoves, fluvially eroded canyons, and graben canyons are the respective outcomes of these processes.

5.4.1 Sapping

Sapping is the geomorphic process resulting in the undermining and collapse of valley head and side

Fig. 5.2 Looking north along Millard Canyon, Canyonlands National Park, a straight, sheer-walled canyon formed principally by groundwater sapping (Photo J.C. Dixon)

walls by weakening and/or removal of basal support as a result of enhanced weathering and erosion by concentrated fluid flow at the site of seepage from the wall usually at a lithologic contact with marked permeability contrast (Laity and Malin 1985). Canyons and canyon networks formed predominantly by sapping display a set of distinctive forms. These canyons display steep, cuspate "theater" (U-shaped) headwalls, constant valley widths, and linear longitudinal profiles that approximate the angle of the dipslope of the rock units in which they develop (Fig. 5.2). Runoff from plateau surfaces is insufficient to account for the retreat of large-scale headwalls by waterfall erosion. Sapped valleys typically extend headward slowly to gradually occupy an ever-increasing proportion of the drainage basin. There is a wide variation in the drainage basin area occupied by such valley forms depending on age. Canyons grow in response to the hydraulic gradient of groundwater flow and reflect the regional joint pattern even in debris-mantled basins. Stream flow derived from groundwater discharge increases steadily from canyon headwall to valley midsection and then increases only slightly to valley outlet. Canyon development is strongly controlled by lithology, structure, and groundwater hydrology (Laity and Malin 1985; Howard and Kochel 1988; Laity 1988).

5.4.2 Fluvially Eroded Canyons

The role of fluvial erosion in the evolution of canyons of the Colorado Plateau has long been recognized (Powell 1875; Gilbert 1877; Dutton 1882). Fluvially eroded canyons result principally from overland flow and to a more limited extent from infiltration and groundwater flow (Ahnert 1960; Laity and Malin 1985) (Fig. 5.3). The distinguishing characteristics of fluvially eroded canyons include valley widths that increase with distance from the headwall and with increasing stream order, tapered or V-shaped valley heads in planform, longitudinal profiles that are concave,

Fig. 5.3 View from Dead Horse Point, Utah, looking southwest across Islands in the Sky section of Canyonlands National Park. Goose Necks Canyon, carved by the Colorado River is in the foreground (Photo J.C. Dixon)

and knickpoints in the profile that fit well to drainage. Branched networks dominate the drainage basin at all stages of its evolution, evolving rapidly in its early stages and slowing thereafter. Direction of growth of the drainage network is affected primarily by surface topography and exposed fractures. The drainage network may be joint-controlled where fractures are exposed on the surface but show no control when joints are buried beneath regolith. Stream flow increases downstream in perennial streams (Laity and Malin 1985).

5.4.3 Graben Canyons

In the vicinity of the confluence of the Green and Colorado Rivers there occurs an area characterized by the development of numerous canyons associated with extensive graben development (Fig. 5.4). The canyons are downdropped blocks of crust with wall heights that approximate the amount of vertical displacement of the fault planes, approximately 90 m. The canyons vary in width from as little as 2–3 m to as much as 600 m, but average 150 m and several kilometers in length. The canyons are flat-floored and sediment-covered with little in the way of through-flowing drainage, rather they consist of a series of small basins. The graben canyons are the result of sagging associated with the solution of salt and gypsum in the Hermosa formation or collapse due to the weight of the overlying pile of sediment or a combination of both (Lohman 1974).

5.5 Arches

Natural arches and bridges are common landforms associated with the sandstones of the Canyonlands. Natural bridges are stone arches that span a water course while natural arches do not span valleys (Lohman 1975). Arches are typically formed in sandstones cemented by calcium carbonate and in which the abundance of carbonate

Fig. 5.4 Needles section of Canyonlands National Park, looking toward the Fins. Narrow walls of sandstone are separated by narrow graben canyons resulting from salt tectonics in the underlying Hermosa Formation (Photo J.C. Dixon)

is unevenly distributed. In the Canyonlands section of the Colorado Plateau the two dominant rock units in which arches are found are the Entrada Sandstone and the Cedar Mesa Sandstone. Arches may be vertical (Fig. 5.5) or horizontal in form (Fig. 5.6) and occur in both flat-lying sandstone beds as well as on vertical thin walls or fins of sandstone (Lohman 1975). The arches form as a result of dissolution of calcite cements and subsequent enlargement by removal of loosened grains, boulders, and slabs by wind, gravity, and water (Lohman 1975; Young and Young 1992) (Fig. 5.7). Patterns of cement dissolution are strongly influenced by the pattern of distribution of both horizontal and vertical fractures developed in response to regional tectonic history (Cruikshank and Aydin 1994).

The largest concentration of sandstone arches in the southwestern United States occurs in Arches National Park near Moab, Utah. Here, in excess of 700 arches ranging in widths from 1 m to 93 m and as much as 34 m high are to be found in an area of approximately 300 km^2 (Stevens and McCarrick 1988). The arches are formed principally in the Entrada Sandstone which consists of marine and windblown sands. These sands, and subsequent rock units, were originally deposited atop thick accumulations of salt. As the weight of the sands increased through Miocene time, the ability of the underlying salt to support the ever-increasing weight of rock diminished and the salts eventually began to deform and flow. As the salt flowed, the overlying sandstone was deformed into the Salt Valley Anticline. Over time the salts began to dissolve and the overlying sandstones failed and fractured (Doelling 1985) (Fig. 5.8). The pattern of fracturing was predominantly vertical, forming vertically oriented slabs of sandstone a few meters apart resulting in the fins described above. The extensive development of fins and associated fracture zones fundamentally explains why so many arches are developed over such a restricted area in Arches National park (Cruikshank and Aydin 1994).

Fig. 5.5 Vertical Wall Arch developed on a sandstone fin in Arches National Park (Photo J.C. Dixon)

Fig. 5.6 Landscape Arch, a horizontal arch 60 m long and 40 m high in Arches National Park is reputed to be the longest arch on Earth (Photo J.C. Dixon)

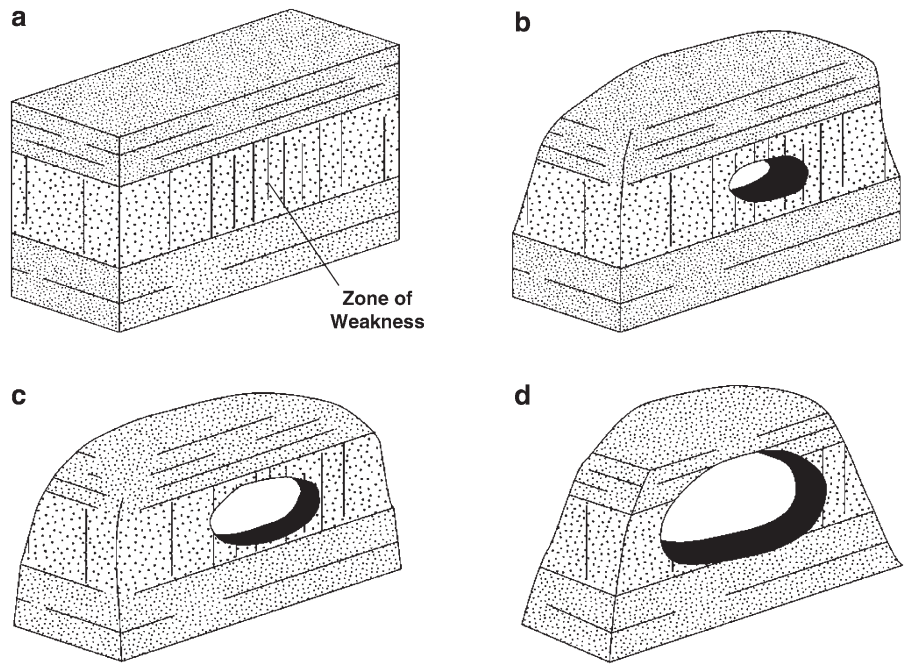

Fig. 5.7 Model of arch evolution illustrating role of weak layer distributions in determining location of arches within overall resistant sandstones (Adapted from Orndorff et al. 2006)

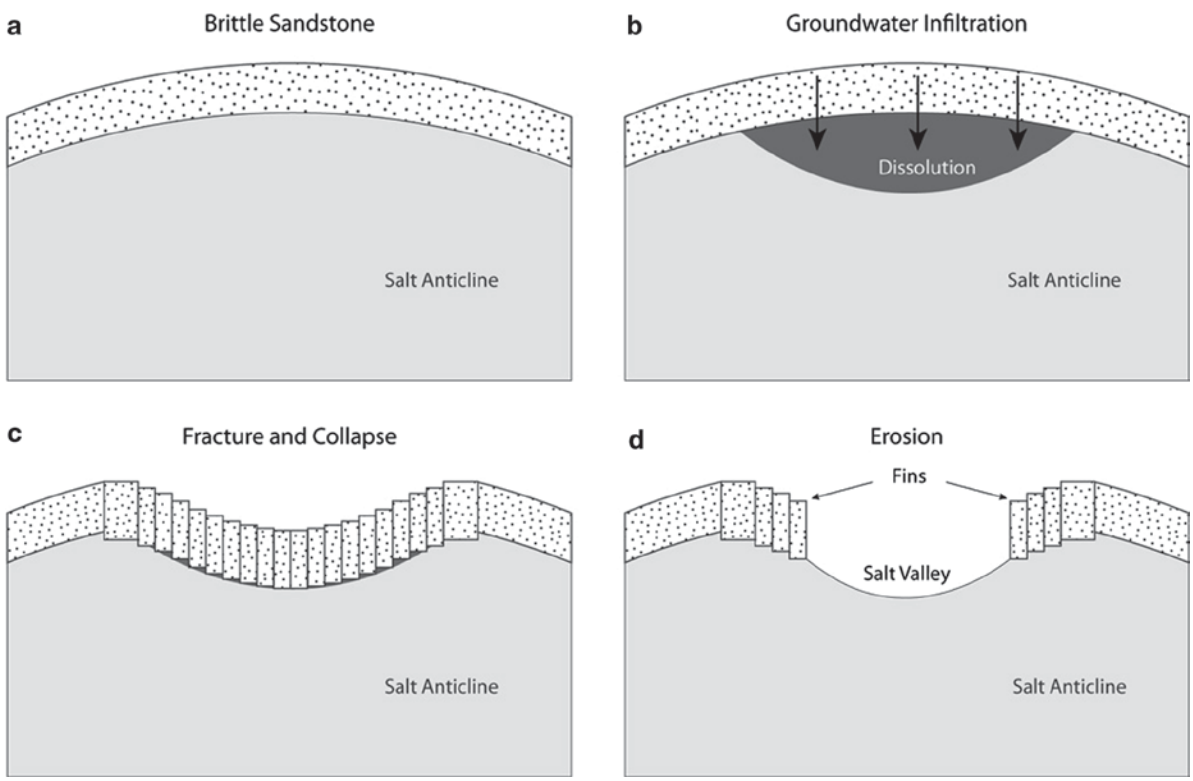

Fig. 5.8 Formation of fins associated with salt deformation and faulting of overlying sediments. (**a**) Deposition of sediments over salt and associated deformation. (**b**) Groundwater infiltration through sediments and associated underlying salt dissolution. (**c**) Fracturing of sediments over dissolved salt and subsequent collapse. (**d**) Formation of salt valley and gliding of faulted bedrock across underlying salts to form grabens and expose fins (Adapted from Orndorff et al. 2006)

5.6 Conclusions

The spectacular canyons and arches of the landscapes of the Colorado Plateau result from the weathering and erosion of resistant sandstones in an arid environment. They are a reflection of the interaction of resistant rocks and the effects of surface and groundwater and internal earth processes, with subsequent modification by weathering processes. The geomorphological significance of the canyons and arches of the Colorado Plateau region of the United States is enhanced by their relative ease of access. Many of the best examples are protected within major national parks including Canyonlands and Arches National Parks in the state of Utah. Additionally, these parks provide excellent visitor centers and accompanying explanations of landform and landscape evolution.

The Author

John Dixon is a professor in the Department of Geosciences at the University of Arkansas, Fayetteville, in the United States. His research interests are broadly focused on the role of weathering processes in landscape evolution in cold and warm climates. He has published over 50 papers and book chapters in international journals of geomorphology and monographs on various geomorphic subjects.

References

Ahnert F (1960) The influence of Pleistocene climates upon the morphology of cuesta scarps on the Colorado Plateau. Ann Assoc Amer Geogr 50:139–156

Bradley WC (1963) Large-scale exfoliation in massive sandstone of the Colorado Plateau. Geol Soc Amer Bull 74:519–527

Cruikshank KM, Aydin A (1994) Role of fracture localization in arch formation, Arches National Park, Utah. Geol Soc Amer Bull 106:879–891

Doelling HH (1985) Geology of Arches National Park. Utah Geological and Mineral Survey. Map 74, Accompanying notes

Dutton CE (1882) Tertiary history of the Grand Canyon District, with atlas. US Geol Surv Monograph 2

Gilbert GK (1877) Report on the Geology of the Henry Mountains. US Geogr Geol Surv, Rocky Mountain Region 1170.

Goudie AS (2002) Great warm deserts of the world. Oxford University Press, Oxford

Howard AD, Kochel RC (1988) Introduction to cuesta landforms and sapping processes on the Colorado Plateau. In: Howard AD, Kochel RC, Holt HE (eds) Sapping features of the Colorado Plateau: A comparative planetary Geology field guide. NASA, Washington DC, pp 6–59

Hunt CB (1974) Natural regions of the United States and Canada. Freeman, New York

Laity J (1988) The role of groundwater sapping in valley evolution on the Colorado Plateau. In: Howard AD, Kochel RC, Holt HE (eds) Sapping features of the Colorado Plateau: A comparative planetary Geology field guide. NASA, Washington DC, pp 63–70

Laity JE, Malin MC (1985) Sapping processes and the development of theater-headed valley networks of the Colorado Plateau. Geol Soc Amer Bull 96:203–217

Lohman SW (1974) The Geologic story of Canyonlands National Park. US Geol Surv Bull 1327

Lohman SW (1975) The Geologic story of Arches National Park. US Geol Surv Bull 1393

Nicholas RM, Dixon JC (1986) Sandstone scarp form and retreat in the land of standing Rocks, Canyonlands National Park. Z Geomorph NF 30:167–187

Orndorff RL, Wieder RW, Futey DG (2006) Geology underfoot in Southern Utah. Mountain Press, Missoula

Powell JW (1875) Exploration of the Colorado River of the west and its tributaries 1869–1872. US Gov Printing Office, Washington DC

Stevens DJ, McCarrick JE (1988) The arches of Arches National Park, a comprehensive study: Moab, Utah. Mainstay Publishing, Salt Lake City, Utah

Thornbury WD (1965) Regional Geomorphology of the United States. Wiley, New York

Young RW, Young A (1992) Sandstone landforms. Springer, Berlin

Chapter 6
Grand Canyon: The Puzzle of the Colorado River

Leland R. Dexter

Abstract The Grand Canyon of the Colorado is the best-known example of fluvial canyon erosion on Planet Earth. It is carved into the southwestern edge of the Colorado Plateau physiographic region. The Grand Canyon displays impressive arid land cliff-and-slope topography over its 360 km length, 30 km maximum width and 1,830 m maximum depth. While it is apparent that the Canyon was carved by the Colorado River, the exact sequence of events and timing of the erosion are open to debate. Many hypotheses, grouped here simplistically into one of three general viewpoints, have evolved over the last 150 years: (1) the mono-river or "old river" view, (2) the headward eroding poly-phase river or "integrated river" view, and (3) the ponding, spillover, and pro-elongating river or "new river" view. The puzzle of the formation of the Grand Canyon has not yet been completely solved.

Keywords Colorado River • fluvial erosion • Grand Canyon • landscape evolution

6.1 Geomorphology of Modern Grand Canyon

6.1.1 Overview

The Grand Canyon of the Colorado, located in northern Arizona, USA (Fig. 6.1), is the best-known example of fluvial canyon erosion on Planet Earth (Fig. 6.2). It is the largest of several major canyons traversed by the Colorado River on a course from its headwaters in the Rocky Mountains to its delta at Sea of Cortez. The Grand Canyon receives water from Glen and Marble Canyons immediately upstream (Fig. 6.3); and empties into Iceberg and Boulder Canyons downstream from the Grand Wash Cliffs (Fig. 6.4). Grand Canyon proper is about 360 river kilometer long and up to 30 km wide. Along this course, the Colorado River has cut into, and exposed up to, 1,830 vertical meters of sedimentary and metamorphic rocks of the adjacent Hualapai, Coconino, Kaibab, Uinkaret, Kanab, and Shivwits Plateaus (Figs. 6.1 and 6.2).

6.1.2 General Lithological History

Two episodes of Proterozoic Era orogeny left behind highly deformed mountain roots as the basement rocks for today's Grand Canyon. These metamorphosed rocks are found within the Canyon's "Inner Gorge" (Fig. 6.5). Prolonged erosion beveled these ancestral mountains leaving behind the "Great Unconformity," a relatively flat erosional surface upon which younger sedimentary rocks have been deposited. Successive oceanic transgressions and regressions lapped onto, and off of, the edge of the developing North American proto-continent during the Paleozoic and Mesozoic Eras. These seas deposited thousands of vertical meters of sandstones, shales, and limestones over the Great Unconformity (Breed and Roat 1974; Beus and Morales 1990).

6.1.3 The Laramide Orogeny and the Basin and Range Extension

Beginning about 70–75 million years ago the thick rock sequences described above were uplifted during the Laramide Orogeny, a largely compressional tectonic event that elevated the present Kaibab Plateau along

P. Migoń (ed.), *Geomorphological Landscapes of the World*,
DOI 10.1007/978-90-481-3055-9_6, © Springer Science+Business Media B.V. 2010

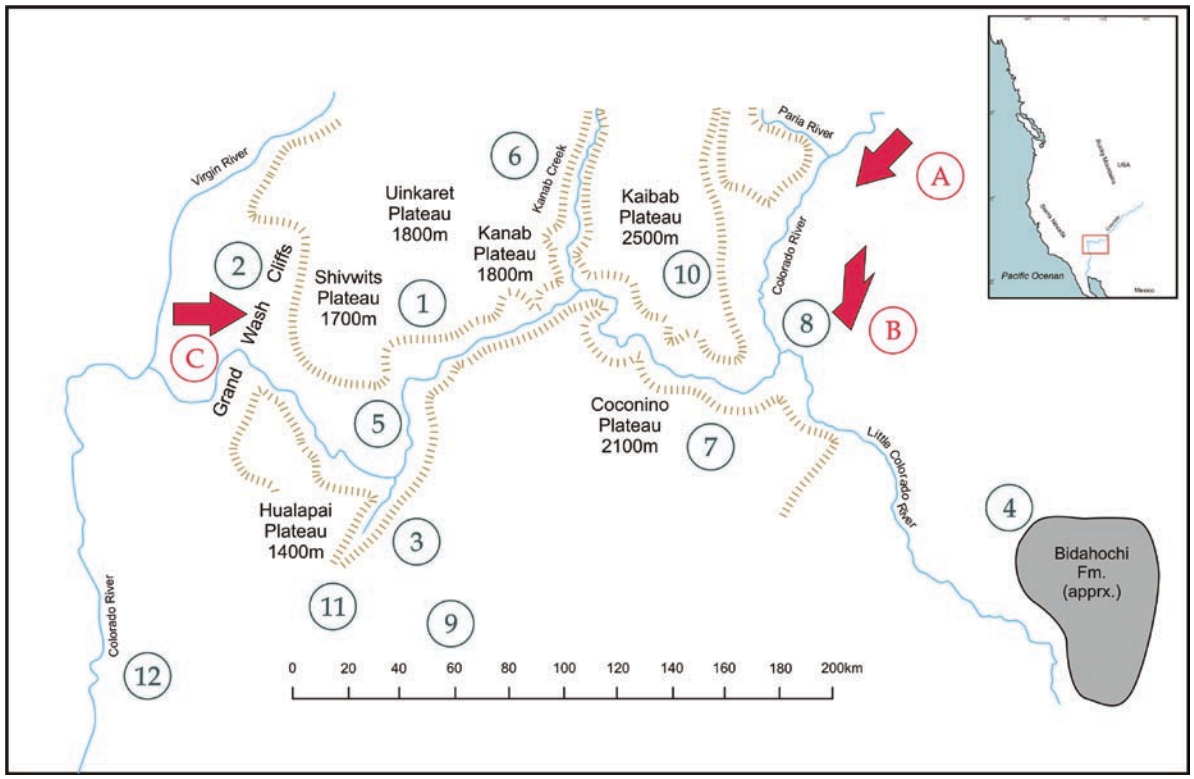

Fig. 6.1 Map of the Grand Canyon illustrating the location of key features pertaining to theories about the evolution of the Canyon. (**a**) The "old river" proponents would have the Colorado River following its modern course even before the Laramide Orogeny which subsequently uplifted the plateaus leaving the Canyon to be cut by antecedence. The "new river" proponents would have the Colorado pro-elongating down this course also; however, due to the blocking plateaus, a lake would form immediately upstream. The lake would ultimately overtop the Kaibab Plateau and drain rapidly to the west eroding the Grand Canyon in a very short period of time. (**b**) Shows the course of the "Hopi Lake alternative" as proposed at the 1964 Museum of Northern Arizona symposium. According to this view, the ancestral Colorado, flowing into Hopi Lake, would have been captured by the Hualapai Drainage System eroding from the west. (**c**) The direction of headward erosion by the younger Hualapai Drainage System as envisioned by proponents of the "integrated river" view. The circled numbers are keyed to more detailed descriptions of features found within the text. Elevations are the approximate mean value for the plateau (Map compiled by L.R. Dexter)

with many other structures now found in the western USA. Recent studies of fish suggest that the Continental Divide was located far to the west of its current position during Laramide times (Spencer et al. 2008). About 10–25 million years ago the stress field reversed (House et al. 2005) creating numerous north–south trending block-faulted mountains and valleys throughout the interior West called the Basin and Range Province. In the Grand Canyon area, extension and subsidence of the Basin and Range occurred to the west and uplift of the Colorado Plateau occurred to the east about 16 million years ago. This major tectonic reversal left a number of regional-scale high plateaus on the southwestern edge of the greater Colorado Plateau Province. These regional-scale plateaus sit adjacent to spectacular faulted Basin and Range topography along a line marked by the modern Grand Wash Cliffs (Figs. 6.1 and 6.4). For a Geomorphologist, one of the most dramatic vistas in the western USA is the panorama of the Colorado Plateau–Basin and Range boundary as seen from Grapevine Mesa (a small portion of which is shown in Fig. 6.4).

Fig. 6.2 The main section of Grand Canyon in the vicinity of Grand Canyon village as seen looking from the South Rim toward the North Rim. The South Rim is about 2,130 m a.s.l. here and the North Rim is about 2,440 m a.s.l. and 17 km distant. The Colorado River is at about 760 m elevation (Photo L.R. Dexter)

6.1.4 The Incision of the Colorado River

Sometime during or after these tectonic events, the Colorado River carved the Grand Canyon into these regional plateaus. Vast amounts of rock overlaying the region were also eroded away during this time in what Clarence Dutton (1882) termed "The Great Denudation." The Colorado River dissected the regional plateaus asymmetrically by cutting into the side-slopes rather than directly into the summits. The North Rim at 2,440 m is about 300 m higher than the South Rim. As a result, long consequent side-canyons and large temples (buttes) are found on the north side of the river. Short, steep obsequent side-canyons and smaller temples (buttes) are found on the south side of the river (Fig. 6.5). As Grand Canyon formed, several volcanic eruptions spilled lava around and into the Canyon. Some of the flows completely dammed the Colorado River forming lakes within Grand Canyon. Once filled, the lakes overtopped and breached the lava dams (Hamblin 1994; Fenton et al. 2004). Vulcan's Throne, a volcanic cone on the rim of the Canyon, and Lava Falls Rapid at the river level immediately below, are the remnants of such a process (Fig. 6.1 – 1).

6.1.5 Slope and Cliff Topography

Given that the rocks of the Grand Canyon were formed under such a wide variety of processes, environmental conditions, and over an immense length of time, it is not surprising that the various layers are of greatly differing composition, hardness, and erosional resistance.

Fig. 6.3 The eastern Grand Canyon as seen looking northeast from Desert View. The upwarp of the Kaibab Plateau can be seen within the layers of the Canyon walls. The Colorado River is visible at the bottom of the Canyon a few kilometers below its exit from Marble Canyon (appearing faintly in the distance) (Photo L.R. Dexter)

When exposed to weathering and subsequent erosional removal, rock layers with different resistances tend to produce the characteristic cliff-and-slope topography found inside the Grand Canyon today (Figs. 6.2, 6.3, and 6.5). Rocks with great resistance to weathering and erosion (e.g., the schists of the inner gorge near the River or the Coconino Sandstone found a 100 m or so below the Canyon rim) form striking cliff bands. Rocks that are less resistant to weathering and erosion (e.g., the shales of the Hermit and Bright Angle formations) wear away quickly, often undercutting the resistant layers above, leaving broad lower-angle slopes or terraces behind. The very prominent wide bench seen near the bottom of the Canyon is called the Tonto Platform (Fig. 6.5). The Tonto Platform was created by rapid backwearing of the Bright Angle Shale which lies directly over the highly resistant Tapeats Sandstone. One interesting rock type with respect to weathering resistance is limestone. In many humid regions of the world limestone is very prone to chemical attack. But in arid landscapes, limestone is quite resistant to weathering and the well-known Redwall Limestone creates one of the most prominent cliffbands in the Grand Canyon.

Widening of the Canyon continues to occur by various hillslope processes such as rockfall and landslides (Hereford and Huntoon 1990), along with flood-induced debris flows from tributary side-canyons occurring mostly during intense monsoonal summer thunderstorms (Webb et al. 1987). Debris flows carry hillslope detritus to the river level very efficiently while the river needs additional time to transport the material further downstream. As a result, debris flows issuing from the side canyons form shallow dams

Fig. 6.4 The Colorado River (*left* side of the photo) exits western Grand Canyon here at the Grand Wash Cliffs. The view is northeast from the northern tip of Grapevine Mesa toward the Shivwits Plateau on the far skyline. The Muddy Creek Formation is created from colluvium shed from these cliffs. Pearce Canyon and its alluvial fan cut by the Colorado can be seen downstream (*left*) of the river's exit (Photo T. Paradis)

which impede the river's flow producing the famous pools and rapids of Grand Canyon (Webb et al. 1987).

6.2 Geomorphological Evolution of Grand Canyon

6.2.1 Overview

Conceptually, the formation of Grand Canyon should be very simple to explain. The Colorado River floods annually in the spring from snowmelt in the Rocky Mountains. These floods exert large tractive (erosional) forces against the bed of the river. Over many millions of years the river cut the magnificent canyon into the adjacent plateaus. In actuality, the processes are far more complicated and have not been completely explained. Two fundamental problems exist with the simplified origin of the Grand Canyon described above. The first problem stems from the substantial elevated topographic barrier that the combined Hualapai, Coconino, Kaibab, Uinkaret, Kanab, and Shivwits Plateaus present to the course of the Colorado River (Figs. 6.1 and 6.6). The Colorado, following its present course, could not have flowed uphill over these elevated barriers. The second problem is that the time over which the Grand Canyon could have been carved is constrained by several lines of evidence to a remarkably short 5–6 million years (Lucchitta 1988, 1989; Young and Spamer 2001).

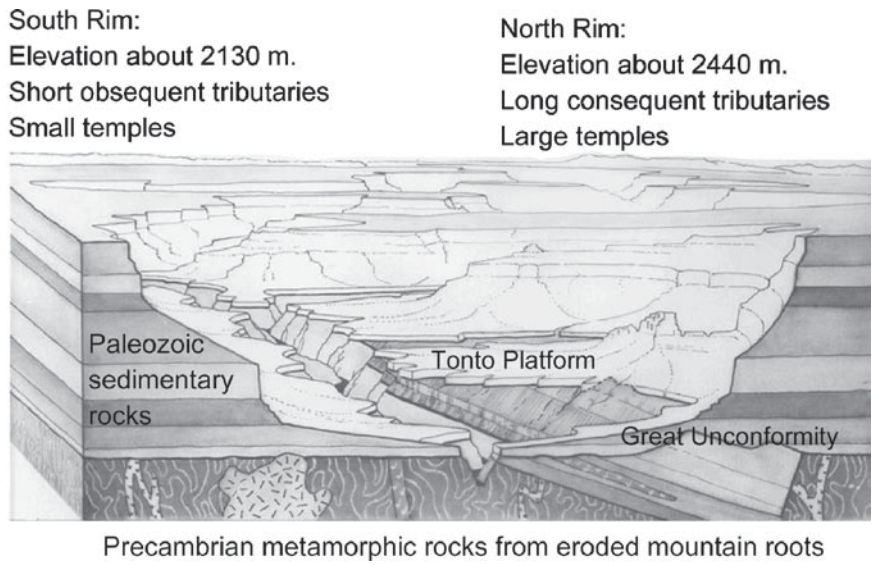

Fig. 6.5 A drawing illustrating the principal geomorphic features of modern Grand Canyon, including the narrow Inner Gorge cut into resistant Precambrian rock, the Great Unconformity, the Tonto Platform adjacent to the rim of the Inner Gorge, the cliff-and-slope topography of the Paleozoic Rocks, the vertically offset rims, the short obsequent drainages from the South Rim to the Colorado River, and the longer consequent drainages from the North Rim to the River (Modified from H. Shelton in Shelton 1966: 250)

In 1857 John Newberry became the first trained geologist to view the Grand Canyon and he proposed that the Canyon was carved by the Colorado River. Since then numerous complications to this simple explanation have fostered the development of well over a dozen unique theories on how the Canyon was actually carved (Ranny 2005; Powell 2006). The various major hypotheses on the formation of the Grand Canyon can be simplistically grouped into three basic viewpoints:

1. The mono-river or "old river" view
2. The headward eroding poly-phase river or "integrated river" view
3. The ponding, spillover, and pro-elongating river or "new river" view

The details of each viewpoint are presented in the following historical framework.

6.2.2 The Mono-River or "Old River" View

Powell (1875) attributes several canyons along the Colorado River (including Grand Canyon) to antecedence where an old river cuts through more recently uplifted surrounding rock. Powell applies this concept to fit observations he collects during his two historic Colorado River expeditions in 1869 and 1871–1872. Powell's influence makes this the "hypothesis of choice" in the late nineteenth century and it is still often used today as a simple (although not well-supported) explanation for the formation of the Canyon. Dutton (1882) defers to Powell, agreeing that antecedence is the most likely explanation for the origin of the Grand Canyon. But Dutton hints at the possibility of "superimposition" since the concept fits so well with his Great Denudation hypothesis. Superimposition means that the ancestral Colorado River would have started out flowing on top of the younger Mesozoic layers and, during the course of the Great Denudation, would have slowly eroded down into the older Paleozoic and Precambrian rocks to cut the Canyon. The famous geologist G. K. Gilbert, friend and colleague of both Powell and Dutton, expresses reservations about the antecedence hypothesis but he never develops a strong alternative explanation (Gilbert 1876).

As the nineteenth century comes to a close a number of problems begin to surface with the antecedence hypothesis. Wallcott (1890) studies the Mesa Butte Fault and East Kaibab Monocline in the eastern Grand

Fig. 6.6 The Coconino Plateau (left and center skyline) and the Kaibab Plateau (right-most distant skyline) with the Grand Canyon in between the two as seen from the east near the Little Colorado River Gorge (immediate foreground). These plateaus were once connected and thus formed a substantial (at least 1,000 m high) barrier across the course of the modern Colorado River (Photo L.R. Dexter)

Canyon region and he determines the structures are surprisingly old. For antecedence to work, the Colorado River would have to be older than these structures. Wallcott leans toward the superimposition hypothesis because it allows for the possibility of a young river cutting into a buried structure formed at some earlier time. Emmons (1897) also finds a major flaw in the antecedence hypothesis when he shows that, in the Uinta Mountains region, the Colorado River is actually cutting through young lake deposits adjacent to the uplifted areas that had shed them. This observation produces a serious dilemma to Powell's line of reasoning. Then in 1946, Longwell shows that very young (5–8 million years old) locally derived hillslope colluvium (the Muddy Creek Formation) eroded from the Grand Wash Cliffs at the west end of Grand Canyon is also cut by the Colorado River (Figs. 6.1 – 2 and 6.4) (Longwell 1946). This mounting evidence almost completely negates Powell's old river idea.

Hunt (1956, 1969, 1974), grasping onto the mono-river view with hypotheses even he considers "outrageous," tries to bypass the "Muddy Creek problem" by suggesting that either Peach Springs Canyon (Fig. 6.1 – 3) carried the river around the Muddy Creek Formation, or an extensive karst (cave) network in the thick limestone layers "piped" water under the Muddy Creek Formation. According to Hunt, the western Grand Canyon formed following collapse of the cave system. Analogs to this piping process exist today in the form of widespread underground water delivery systems to Blue Springs, Thunder River, and the numerous springs in Havasupai Canyon.

6.2.3 The Headward Eroding Poly-Phase River or "Integrated River" View

In the first few years of the twentieth century, William Morris Davis turns his attention to Grand Canyon. Davis is famous for developing a landscape evolution theory that features river valleys transforming from youthful to mature to old age as they wear away the land. Thus Davis is attracted to Dutton and Wollcott's superimposition ideas over Powell's antecedence hypothesis. Importantly, Davis also realizes that even higher barriers than exist today had blocked the course of the modern Colorado River. The ancestral Mogollon (pronounced Mowg-ee-own) Highlands ringed the southwestern edge of the present-day Colorado Plateau before it existed as an elevated surface. This configuration forced a northeast flowing drainage pattern on the entire region. Davis (1901) postulates that a flow reversal to the southwest occurred when the more recent Basin and Range faulted down to the southwest and the Colorado Plateau uplifted to the northeast.

In 1945, Babenroth and Strahler refine Dutton and Wollcott's superimposition hypothesis suggesting that the ancestral Colorado River, flowing on top of Mesozoic sedimentary rocks, had cut down into the Paleozoic rocks at the toe of the Kaibab Plateau to form the broad curve in the Colorado River in the eastern Grand Canyon (Fig. 6.1–7) (Babenroth and Strahler 1945). Finally, they suggest an aggressive stream flowing from the west captured the ancestral Colorado. This stream piracy is a key notion that has been invoked by many subsequent investigators to tie together the relatively "old-appearing" upper River to the relatively "young-appearing" lower River.

The integrated river view gets a large boost in 1964 when the first major collective effort is made to pool data and explain the evolution of the Grand Canyon and a symposium on "Evolution of the Colorado River in Arizona" is convened at the Museum of Northern Arizona (McKee et al. 1967). The members of the symposium introduce the "Hopi Lake alternative" which integrates the large but vaguely bounded area of extensive freshwater deposits called the Bidahochi Formation found southeast of Grand Canyon (Fig. 6.1 – 4). The symposium group proposes that a large lake (called Hopi Lake or Lake Bidahochi) formed from Colorado River water ponded during the time that the Mogollon Rim was uplifting to the south. Coincidentally, as proposed earlier by Babenroth and Strahler, a young stream rapidly eroding from the west (called the Hualapai Drainage System) (Fig. 6.1 – 5) captures the main ancestral Colorado River by headward erosion and stream piracy thus draining Hopi Lake.

Later, Young and McKee (1978), noting that some sections of the Grand Canyon seem morphologically older than others, posit that the modern river has come together from the integration of three separate drainage systems. They keep the ancestral Colorado and the eastward eroding Hualapai Drainage System in the same locations proposed by the symposium group, but insert a third drainage flowing north along the current trend of Kanab Creek (Fig. 6.1–6) in between the other two. Kanab Creek is a large tributary to the modern Colorado presently draining to the south. They suggest the modern Grand Canyon is an integration of the three.

Finally, Lucchitta (1988, 1989) combines the Babenroth and Strahler hypothesis with the Young and McKee hypothesis. Like Babenroth and Strahler, Lucchitta uses the superimposition concept to construct a "racetrack-like" annular drainage over the present-day Kaibab Plateau. As the river cut down guided by this racetrack, it entrenched to form the broad curved valley we see today in the eastern half of the Grand Canyon (Fig. 6.1 – 7). This older river drained to the northwest out Kanab Creek to some unknown destination but was ultimately captured by the younger eastward-eroding Hualapai Drainage System.

The most recent support for a headward-eroding river comes from investigations using uranium-lead dating of cave mammillaries (speleothems) associated with a preexisting local water table. Dates of such speleothems taken from nine sites in the western Grand Canyon indicate that the apparent local water table declined at a rate of 55–123 m per 1 million years. If the water table drawdown is assumed to be the same as the incision rate of the Colorado River then the chronology and inferred incision rates suggest that the Grand Canyon evolved via headward erosion over the past 17 million years (Polyak et al. 2008).

Many detractors to these stream capture hypotheses remark on the unusual amount of erosion required of the small and somewhat localized Hualapai Drainage System. They sometimes cynically call these ideas "the precocious gully" hypotheses.

6.2.4 The Ponding, Spillover, and Pro-Elongating River or "New River" View

It is rather interesting to read Newberry's (1861: 19–20) impression of the lower Colorado River basin:

> Doubtless in earlier times [the Colorado River] filled these basins to the brim, thus irrigating and enriching all its course. In the lapse of ages, however, its accumulated waters, pouring over the lowest points in the barriers which opposed their progress towards the sea, have cut them down from summit to base forming that remarkable series of deep and narrow cañons through which its turbid waters now flow, with rapid and almost unobstructed current, from source to mouth.

It thus appears that the very first geologist ever to visit the Grand Canyon in the mid-1800s attributes its creation to a river system growing downstream from the headwaters by ponding and spillover (pro-elongation)! In the early 1930s Blackwelder (1934), aware of the problems with Powell's "old river" view, dismisses the common geologic convention of headward erosion and presents arguments for a Grand Canyon that has been cut by a young pro-elongating river.

Newberry and Blackwelder's unique ideas are largely ignored until 2000 when another symposium on the evolution of Grand Canyon is held at Grand Canyon National Park under the auspices of the US National Park Service (Young and Spamer 2001). At that conference Meek and Douglass (2001) present an independently rediscovered version of Newberry and Blackwelder's hypothesis. Meek had studied the Pleistocene development of the Mojave River system in neighboring California. He demonstrated that the Mojave River, flowing northeast from its source in the San Bernardino Mountains, developed from lakes that successively overtopped a series of closed basins. Meek and Douglass use the evolution of the Mojave River as an analog for the development of the Colorado River. Afton Canyon, along the Mojave River, was cut following the overtopping of paleo-Lake Manix and they propose it is an analog to the incision of Grand Canyon.

Several other presentations delivered at the 2000 symposium also support the notion of lake overtopping. Scarborough (2001) finds evidence of late Neogene sediments and spillover stripping in the area immediately east of Grand Canyon where lake ponding should be most noticeable if the hypothesis is correct (Fig. 6.1 – 8). No other major pluvial deposits from such a lake have yet been found however. Spencer and Pearthree (2001, 2005) summarize recent work with the basin deposits of the Bouse Formation along the Colorado River below the Grand Canyon. Their conclusion is that the Bouse deposits are not of seawater origin but rather originate in a series of small basins filled by fresh water from a pro-elongating river system related to the opening of the Grand Canyon, probably by lake overtopping. Recent detailed studies of Tertiary alluvium in the lower Colorado River valley (House et al. 2005) and of fish fossils and fish mitochondrial DNA (Spencer et al. 2008) seem to support the spillover and pro-elongation hypothesis.

6.3 Conclusion

The Grand Canyon of the Colorado is the best-known example of fluvial canyon erosion on Planet Earth. Grand Canyon proper is about 360 river kilometer long and up to 30 km wide. Along this course, the Colorado River has cut into, and exposed up to, 1,830 vertical meters of sedimentary and metamorphic rocks. A combination of arid hillslope erosion and fluvial erosion acting on rock layers of differing resistance has produced the dramatic multi-colored cliff and slope topography for which the Canyon is famous. While the Grand Canyon is clearly a product of the Colorado River, its evolution over the last few million years is not exactly known and a number of theories exist attempting to explain how the Canyon came to be. The theories can be roughly grouped into three major viewpoints: (1) the mono-river or "old river" view, (2) the headward eroding poly-phase river or "integrated river" view, and (3) the ponding, spillover, and pro-elongating river or "new river" view. It is exciting to realize that such a well-known landform like the Grand Canyon still holds an element of mystery!

The Author

Leland R. Dexter is an Emeritus Professor of Geography recently retired from Northern Arizona University, Flagstaff and now living in Cloudcroft, New Mexico. During his career he taught numerous classes in mountain geography, physical geography, geomorphology, climatology, and geographic information systems (GIS). His research interests include snow and ice processes in high mountain environments

(especially avalanches and snow sublimation), sandbar morphology and evolution in the Grand Canyon, microclimate energy balance studies, and GIS analyses of various environmental issues.

References

Babenroth DL, Strahler AN (1945) Geomorphology and structure of the East Kaibab Monocline, Arizona and Utah. Geol Soc Am Bull 56:107–150

Beus SS, Morales M (eds) (1990) Grand Canyon Geology. Oxford University Press, New York

Blackwelder E (1934) Origin of the Colorado River. Geol Soc Am Bull 45:551–566

Breed WJ, Roat EC (eds) (1974) Geology of the Grand Canyon Museum of Northern Arizona, Flagstaff. Grand Canyon Natural History Association, Flagstaff

Davis WM (1901) An excursion to the Grand Canyon of the Colorado. Bull Mus Comp Zool (Harvard College) 38, Geol Series 5:107–201

Dutton CE (1882) Tertiary history of the Grand Cañon District. U. S. Geol Surv Monograph 2

Emmons SF (1897) The origin of the Green River. Science 131:20–21

Fenton CR, Poreda RJ, Nash BP, Webb RH, Cerling TE (2004) Geochemical discrimination of five Pleistocene lava-dam outburst-flood deposits, western Grand Canyon, Arizona. J Geol 112:91–110

Gilbert GK (1876) The Colorado Plateau as a field for geological study. Amer J Sci, 3rd Series 12:101–102

Hamblin WK (1994) Late Cenozoic lava dams in the Western Grand Canyon. Geol Soc Am Mem 183

Hereford R, Huntoon PW (1990) Rock movement and mass wastage in the Grand Canyon. In: Beus SS, Morales M (eds) Grand Canyon Geology. Oxford University Press, New York, pp. 433–459

House PK, Pearthree PA, Howard KA, Bell JW, Perkins ME, Faulds JE, Brock AL (2005) Birth of the lower Colorado River – Stratigraphic and geomorphic evidence for its inception near the conjunction of Nevada, Arizona, and California. Geol Soc Am Field Guide 6:357–387

Hunt CB (1956) Cenozoic Geology of the Colorado Plateau. US Geol Surv Prof Pap 279

Hunt CB (1969) Geologic history of the Colorado River. US Geol Surv Prof Pap 669-C:59–130

Hunt CB (1974) Grand Canyon and the Colorado River, their geologic history. In: Breed WJ, Roat EC (eds) Geology of the Grand Canyon, Museum of Northern Arizona, Flagstaff and Grand Canyon Natural History Association, Flagstaff, pp 129–141

Longwell CR (1946) How old is the Colorado River? Am J Sci 244:817–835

Lucchitta I (1988) Canyon maker. Plateau 59(2):1–32

Lucchitta I (1989) History of the Grand Canyon and of the Colorado River in Arizona. In: Jenny JP, Reynolds SR (eds) Geologic evolution in Arizona. Arizona Geol Soc Digest, vol 17, pp. 701–716

McKee ED, Wilson RF, Breed WJ, Breed CS (eds) (1967) Evolution of the Colorado River in Arizona. Museum of Northern Arizona Bull vol 44, pp. 1–68

Meek N, Douglass J (2001) Lake overflow: An alternative hypothesis for Grand Canyon incision and development of the Colorado River. In: Young RA, Spamer EE (eds) (2001) Colorado River Origin and Evolution: Proceedings of a Symposium Held at Grand Canyon National Park in June, 2000. Grand Canyon Association Monograph 12, pp. 199–204

Newberry JS (1861) Part 3: Geological Report. In: Ives JC (ed) Report upon the Colorado River of the West, Explored in 1857 and 1858. US Government Printing Office, Washington, DC, pp 19–20

Polyak V, Hill C, Asmerom Y (2008) Age and evolution of the Grand Canyon revealed by U-Pb dating of water table-type speleothems. Science 319:1377–1380

Powell JL (2006) Grand Canyon: Solving earth's grandest puzzle. Plume – Penguin Group, New York

Powell JW (1875) Exploration of the Colorado River of the West and its tributaries. Smithson Inst Annu Rep, Washington, DC

Ranny W (2005) Carving Grand Canyon, evidence, theories, and mystery. Grand Canyon Association, Grand Canyon

Scarborough R (2001) Neogene development of the Little Colorado River Valley and Eastern Grand Canyon: Field evidence for an overtopping hypothesis. In: Young RA, Spamer EE (eds) Colorado River origin and evolution: Proceedings of a symposium held at Grand Canyon National Park in June, 2000. Grand Canyon Association Monograph 12, pp. 207–212.

Shelton JS (1966) Geology Illustrated. W. H. Freeman, San Francisco, CA

Spencer JE, Pearthree PA (2005) Abrupt initiation of the Colorado River and initial incision of the Grand Canyon. Arizona Geol Surv 35(4):1–4

Spencer JE, Pearthree PA (2001) Headward erosion versus closed-basin spillover as alternative causes of Neogene capture of the ancestral Colorado River by the Gulf of California. In: Young RA, Spamer EE (eds) Colorado River origin and evolution: Proceedings of a symposium held at Grand Canyon National Park in June, 2000. Grand Canyon Association Monograph 12, pp. 215–219.

Spencer JE, Smith GR, Dowling TE (2008) Middle and late Cenozoic geology, hydrography, and fish evolution in the American Southwest. In: Reheis M et al (eds) Late Cenozoic drainage history of the Southwestern Great Basin and lower Colorado River region: Geologic and biotic perspectives. Geol Soc Am Spec Pap 439

Walcott CD (1890) Study of a line of displacement in Grand Cañon of the Colorado, in Northern Arizona. Geol Soc Am Bull 1:49–64

Webb RH, Pringle PT, Rink GR (1987) Debris flows from tributaries of the Colorado River in Grand Canyon National Park, Arizona. US Geol Surv Open-File Report 87–118

Young RA, McKee ED (1978) Early and middle Cenozoic drainage and erosion in west-central Arizona. Geol Soc Am Bull 89:1745–1750

Young RA, Spamer EE (eds) (2001) Colorado River origin and evolution: Proceedings of a symposium held at Grand Canyon National Park in June, 2000. Grand Canyon Association Monograph 12

Chapter 7
Parícutin Volcano: To the Other Side

Irasema Alcántara-Ayala

Abstract Landscapes are wonders of the Earth, and undoubtedly, due to its magnificence and extraordinary story, Parícutin volcano has called the attention of the whole world. The birth of Parícutin in 1943 on a Mexican cornfield has been recognized as one of the most remarkable examples for the understanding of volcanic landforms in terms of genesis, dynamic processes, and evolution in recent times. Therefore, besides the historical account of the series of events associated with the activity of Parícutin and a general view of its societal impact, the chapter reviews the geomorphological evolution of the volcanic cone and associated landforms.

Keywords Cinder cone • landform evolution • lava flows • Mexico • Parícutin volcano

7.1 Introduction

There are very rare occasions when people can see a new volcano emerging from virtually nowhere. Considered by some as one of the Seven Wonders of the Natural World, Parícutin (pronounced Pah-ree-koo-teen) volcano is undoubtedly one of the wonderful geomorphological landscapes of the Globe. Deriving its name from the Purepecha or Tarascan language *Parhikutini*, which means "to the other side," the birth of this volcano in the twentieth century revealed the amazing secrets of the deep Earth.

Since landforms are dynamic elements resulting from the interaction between endogenic and exogenic forces that evolve through time, on very rare occasions humankind has been able and fortunate to witness and enjoy their creation. In historical times, the story of Parícutin volcano has been recognized as one of the most remarkable scientific examples for the understanding of landforms in terms of genesis, dynamical processes, and evolution.

Monogenetic volcanoes, usually scoria or cinder cones of mafic composition, such as Parícutin, are characterized by single eruptive episodes or cycles, in other words, brief time intervals of activity ranging from weeks to centuries. The activity of this volcano began on 20 February 1943 and ended 9 years and 11 days later, on 4 March 1952 (Yokoyama and De la Cruz-Reyna 1990).

Parícutin volcano was born on a Mexican cornfield owned by Dionisio Pulido, the farmer who saw vapor emanating from a hollow and shortly afterwards, witnessed the beginning of a unique event of a volcano being created. The ejection of pyroclastic material with an average of 6 million m^3/day, along with a total volume of 700 millions m^3 of lava flows that covered an area of 24.8 km^2, strongly and rapidly transformed a piece of the Tarascan landscape. Sixty five years after the event, Parícutin remains a scientific challenge that shall continue to capture human curiosity.

7.2 Geographical Setting

Parícutin volcano rises up to 2,820 m a.s.l. at 19°29′32″N and 102°15′03″W, ~330 km to the west of Mexico City, and 20 km NW of the town of Uruapan (Fig. 7.1). It is situated near the former town of San Salvador Parícutin, municipality of Parangaricuturo, in the Michoacan Province, Mexico. As part of Michoacan-Guanajuato monogenetic volcanic field, it belongs to the Quaternary Trans-Mexican Volcanic Belt (TMVB). This area is located within the Apatzingan Sierra; the Angaguan hill (3,292 m) lies to

P. Migoń (ed.), *Geomorphological Landscapes of the World*,
DOI 10.1007/978-90-481-3055-9_7,

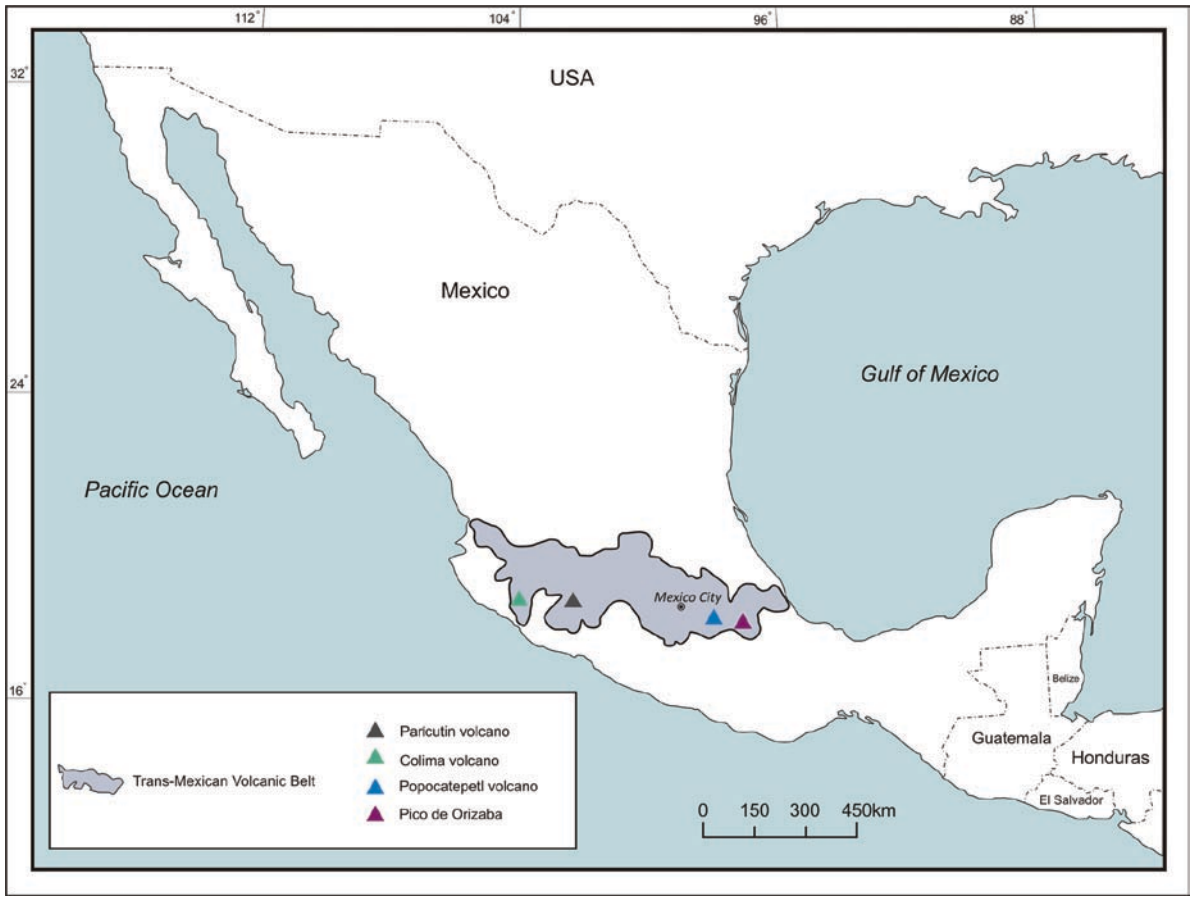

Fig. 7.1 Location of Parícutin and its position within the Trans-Mexican Volcanic Belt

the north, and the northern sector of the Pico de Tancítaro volcano (3,860 m) to the south. According to Inbar et al. (1994), the local landscape prior to the eruption of Parícutin volcano consisted of a small Pleistocene volcanic plateau located at a height of ~2,400 m a.s.l. Both the Apatzingan Sierra and the plateau were the main geomorphological features of the region before the appearance of this magnificent volcano.

The climate is humid subtropical, including heavy rain in summer time; February, March, and April are the driest months, while June, July, and September are the wettest. The mean annual temperature ranges from 12 to 18°C, whereas during winter it is between 4 and 20°C, and in summer it varies from 13 to 22°C. The area is located in the Itzícuaro river watershed. During the eruption, hydrographic conditions were significantly modified; two outer marginal basins at the lava front were developed, but superficial and subterranean flow continued draining westwards.

7.3 Genesis and Evolution

The first morphological feature associated with the birth of Parícutin volcano was perhaps the formation of a small depression around a preexisting pit of 5 m diameter and 1.5 depth in Dionisio Pulido's cornfield in August 1942. Fifteen days before the actual birth of the volcano on 20 February 1943, high seismic activity, subterranean noise, and tremors were registered in the San Juan Parangaricutiro area. At approximately 4 p.m., Mr Pulido observed a new fissure from where soon afterwards ash began to be ejected; a 6 m high cone was formed just before midnight. According to Ordoñez (1943), on 23 February Parícutin's cone height was 60 m and lava flows advanced at a rate of 6–12 m/h to the north and north-east.

Parícutin volcano involved a strombolian-type eruption, although sporadically the volcano presented a vulcanian-type. The former consists of intermittent

explosions or fountaining of basaltic lava from a single vent or crater, originated by the release of volcanic gases, while the latter is a type of moderate-sized explosive eruption that emits a vast amount of volcanic ash, bombs, and blocks. The chronology of its main development can be divided into three stages: *Quitzocho*, *Sapichu*, and *Taquí* (Foshag and González-Reyna 1956). Subsequently, the final period included a small reactivation and afterwards the activity came to an end (Corona-Chávez 2002) (Table 7.1).

The *Quitzocho* period occurred from 20 February to 18 October 1943, and was characterized by the construction of the cone, lava flows, and pyroclastic airfall deposits such as lapilli and volcanic bombs. During this phase the cone reached a little more than 300 m in height. Violent explosive paroxysmal activity comprising fumaroles, ash fall, and lava flows of basaltic and andesitic chemical composition took place. Specifically, it included an early explosive phase, heavy cineritic activity (significant damage of house-roofs occurred by that time), recurrent lava flows, formation of the Quitzocho ridge at the north-west base of the cone, and two slumps on the north flank.

Between 18 October 1943 and 8 January 1944, the *Sapichu* or middle stage took place. Abundant lava flows occurred and particular volcanic conduits were formed along a line of weakness, among which *Mesa del Corral*, *Sapichu*, and *Ahuan* stood out. This period is named after the parasitic volcanic cone called *Sapichu*, meaning "child" or "youth" in Tarascan language, and yielded a nearly 2 km long flow to the NE of Parícutin in November–December 1943. During its two-and-half-month life, *Sapichu* was characterized by strombolian activity and the relatively small diameter of the vent. Blocks of diorite and granite xenolites came into sight and clearly expressed the basement lithology underlying the newly formed volcano. Fed by pyroclastic deposits, the cone reached 350 m at the end of this stage. Lava flows were continuous in this period, whereas in the previous one they were intermittent.

In the *Taquí* stage, from 8 January 1944 to 12 January 1945, a series of volcanic conduits known as *Taquí* and *Ahuan* were formed to the south and east of the main cone. Parícutin was reactivated and lava flows up to 60 m thick traveled up to 10 km (*Taquí* flow), covering an area of more than 17 km^2 of arable land. Mesa de los Hornitos, a small volcano, appeared in the southern sector of the main cone. Parícutin grew up to 355 m, had a basal diameter of 1 km, and the diameter of the crater was about 400 m. Its activity was higher during this period than in the previous stage, although it was not as intense as during the Quitzocho era. Ash deposition diminished considerably, but lava flows reached and overwhelmed the town of San Juan Parangaricutiro, which had been previously evacuated. Moreover, and quite interestingly, the growth of *volcancitos* and *hornitos* on the surface of the Taquí and the Ahuán flows took place at this time, presumably as a result of emanations from the subcrustal lava through several canals in the crust itself. Parícutin was in the mature stage, and since its activity reduced, substantial morphological changes came to an end.

Lastly, the phase between January 1945 and February1952 is considered as the ending period and the final reactivation. Irregular and low intensity eruptions comprising pyroclastic material and lava took place. Morphological changes due to volcanic activity were limited, except those derived from significant mass movement processes occurring on the flanks of the main cone between 1946 and 1948. In January 1952, a reactivation of the volcano was registered, including, besides few minor eruptions of short duration and low intensity, a single event that produced a 3 km

Table 7.1 Summary of eruptive history of Parícutin volcano (After Foshag and González-Reyna 1956)

Stage	Duration	Ejected solid material (average per day)	Nature of volcanic activity
Quitzocho	21 February–19 October 1943	315,000 t	Heavy ash laden eruptive column; moderate lava flows
Sapichu	19 October 1943–8 January 1944	350,000 t	Large lava flow; moderate but constant vapor emission from adventitious vent
Taquí	8 January 1944–12 January 1945	100,000 t	Large lava flows, slight ash fall, variable vapor emission
Final	January 1945–February 1952	N.A.	Irregular and low intensity eruptions, mass movement processes in the flanks

high column of vapor and ash. It meant that after 3 years of virtual calm, the final reactivation was produced. From 4 March 1952 onwards, fumarolic activity has remained as the only evidence of Parícutin's activity.

7.4 Landforms

As a result of the eruption, lava flows ranging from 3 to more than 254 m thick at the cone base covered a total area of 24.8 km^2; a few isolated areas such as the Tipacua, Capatzun, and Kipuca Eastern and Western plains (llanos) remained within. Ash-fall impact was much higher: the 1 m isopach covered an area of 61 km^2, while the 25 cm isopach had an envelope of 233 km^2, and the 1 mm isopach up to 60,000 km^2 (Bullard 1956; Rees 1979). Original landforms suffered dramatic changes and as a consequence, the main geomorphological units of the area since the eruption of Parícutin volcano can be identified as follows: main cone, crater, ash deposit terrain, lava flows, and plains.

7.4.1 Parícutin Cone and Crater

Shaped by a number of layers of pyroclastic material, a cinder cone, like Parícutin, can be considered as the most basic volcanic structure (Fig. 7.2). Ever since Parícutin was born, different researchers have attempted to determine its significant morphometric parameters (Table 7.2). Based on recent topographic maps, air photos, and field measurements, Inbar et al. (1994) estimated the cone height to be 280 m above the ground (western side); 2,820 m of altitude on the NW point of the crater rim; an elliptical basal cone with a NW–SE axis of 965 m, and a NE–SE axis of 620 m length; crater outer diameter of 262 m; and the volume of the cone equal to 0.14 km^3. Moreover, as a result of active slumps, rock falls, and slides, the crater maximum depth was reduced, from 50 m (as calculated in 1957) to 42 m, and the gradient of its walls ranged from 32° to 40°. Weathering, landsliding, and revegetation can be considered as the main mechanisms of change (Fig. 7.3).

Due to the effects of wind erosion, the cone is not covered by fine ash any longer, but by coarse ash and lapilli deposits, allowing for infiltration on the undissected 31–32° slopes. According to its internal structure and associated surface processes, Legorreta-Paulín (1999) categorized Parícutin's flanks as follows: (1) SW slope (volcanic scoria and rocks); (2) NE slope (lapilli, scoria, and solid rock: this sector is stable due to the presence of plants and moss); (3) ESE slope (partially stable lapilli strips); and (4) WNW slope (moderately stable lapilli and scoria corridors).

7.4.2 Ash Deposit Terrain

Ash deposits are formed by particles with a diameter equal to or smaller than 2 mm. According to one of the most recent studies concerning the geomorphological evolution of Parícutin (Inbar et al. 1994), all ash deposits derived from its activity have been subjected to wind and water erosion; thanks to fluvial processes fine material is redeposited in the llanos or incorporated into the soil profiles as they are covered by vegetation, while coarse material fills up stream channels and supports small sand dunes in flat areas. The extent of ash stripping has largely been determined by the original thickness of the deposit, material size, revegetation processes, morphological characteristics, and anthropic influence.

7.4.3 Lava Flows

Since the lava type of Parícutin volcano was of basaltic to basaltic andesite composition, lava flows are blocky and vesicular, of a type. The main feature of a lava is a rough, jagged, bumpy, rugose, and clinker-like rubble surface, often overlaying a more massive core; scoria and angular fragments are common (Fig. 7.4). Lava flows initiated 3 days after Parícutin started its activity, mainly at the base of the cone. They were named after the mouths from which material was ejected, such as Quitzocho, Pastory, Mesa el Corral, Quiquicho, La Lagunilla flows. Parícutin issued an estimated 24.8 km^2 of mafic lava over a 9-year period (Fries 1953; Wood 1980; Foshag and González-Reyna 1956). The widespread occurrence of lava flows in time and space makes it difficult to generate exact maps of individual flows since lava flow fields are usually generated by

Fig. 7.2 Parícutin volcano as seen from the west, ash fall terrain in the foreground. Note widespread occurrence of dry lapilli avalanches on the slopes of the cone (Photo R. Garnica Peña)

Table 7.2 Geomorphic change of the volcanic cone of Parícutin through time

	6 March 1943[a]	3 November 1943[b]	31 March 1945[c]	27 July 1946[d]	31 December 1947[e]
Maximum height of crater rim (m)	137	282	342	354	385
Average height of crater rim (m)	110	255	315	327	376
Average diameter of crater rim (m)	216	260	280	320	240
Average height of volcanic cone base above the ground (m)	12	40	96	153	212
Calculated average diameter of the base (m)	520	900	980	890	770
Average depth of crater (m)	70	85	85	70	60
Total volume of the cone (10^6 m^3)	11	73	124	141	157

[a]Fries (1953); [b]Flores-Covarrubias (1945); [c]Segerstrom (1950) in Fries (1953); [d]Segerstrom and Gutierrez (1947) in Fries (1953); [e]Wilcox (1948) in Fries (1953)

Fig. 7.3 Crater of the Parícutin volcano (Photo R. Garnica Peña)

Fig. 7.4 Lava flow morphology, with blocky lava dominating (Photo P. Migoń)

superposition of various individual flow units; nonetheless, it can be said that the San Juan lava flow was the most significant as it produced a path of 10 km length in June 1943 (Fig. 7.5).

There are four key units in this flow (Inbar et al. 1994): (a) rough terrain with large blocks; (b) blocky lava terrain; (c) crevices or trenches in the lava fields; and (d) front of lava flow. Approximately two-thirds of the lava flow is formed by blocks bigger than 1 m across, arranged in ridges with quite abrupt walls. Blocky lava terrains are composed by blocks smaller than 1 m, with deep crevices between them. Depressions

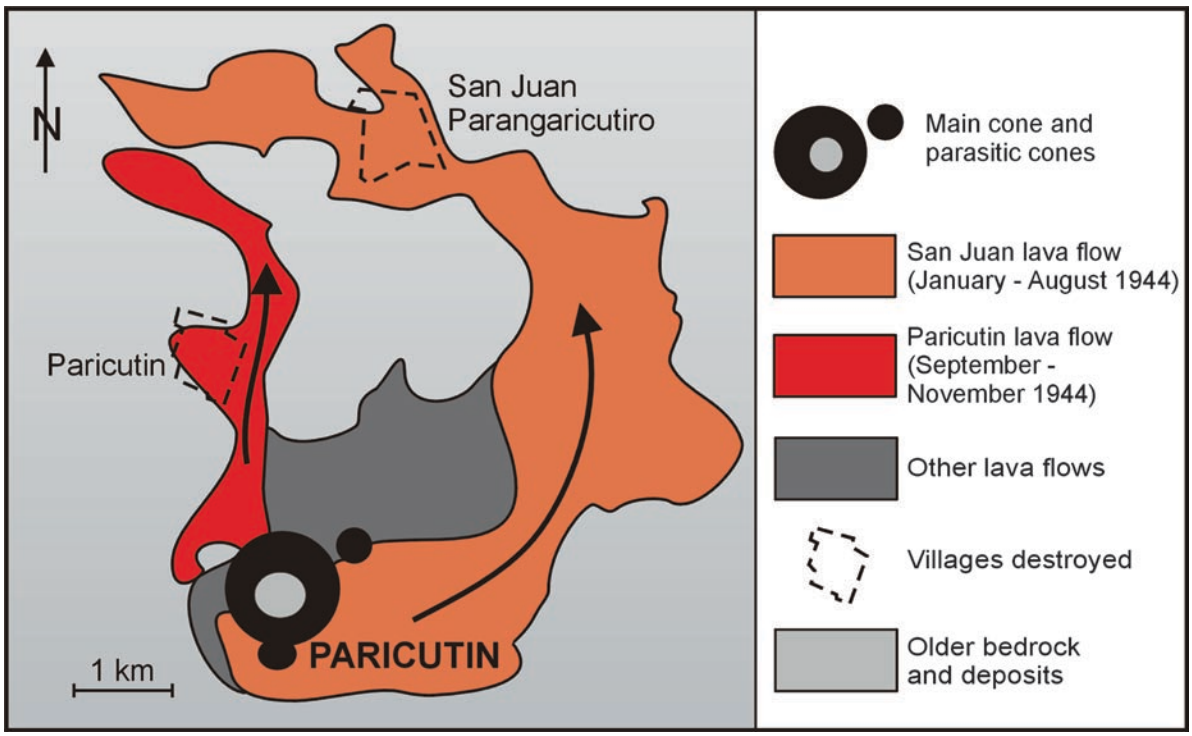

Fig. 7.5 The extent of lava flows issued by the Parícutin volcano

do not follow an apparent array and their depth is less than 5 m. The arrangement of large crevices, 4–5 m deep, is irregular, either parallel or perpendicular to the main flow, and cavities up to 6.5 m deep occur. Drainage systems are autonomous, and sediment accumulation supports vegetation succession. Although several posterior lava flows covered to a great extent the San Juan lava flow, the lava front remained exposed at the northern edge (Segerstrom 1950; Inbar et al. 1994).

7.4.4 Plains

Lava-dammed plains, referred to as *llanos* by native farm workers, act as storage space or sediment sinks for volcanic pyroclastic deposits. Defined as ponded areas associated with the lava field and called *playas* by Eggler (1948) and Segerstrom (1966), these volcanic plains covered an area of 5.06 km^2 and were mainly distributed in the eastern sector of the lava field. Detailed field investigations carried out by Inbar and coworkers (Inbar et al. 1994) estimated the area of the nine plains or *llanos* located in the Parícutin region as follows: Grande – 2.48 km^2; Chorotiro – 0.43 km^2; Terupicua – 0.08 km^2; Capatzun – 0.06 km^2; Tipacua – 0.06 km^2; Curupichu north – 0.31 km^2; Curupichu south – 0.57 km^2; Loma Larga – 0.62 km^2; Tiporacuaru – 0.44 km^2.

Notwithstanding that after 50 years of activity natural vegetation has established itself in areas with high moisture content, such as those around the edges of the lava front in some *llanos*, detailed studies suggest that few species colonized the *llanos* and the total plant cover remains low (<10%) and patchy (Lindig-Cisneros et al. 2006).

7.5 Hazards

The eighteenth-century church of the Lord of the Miracles, partially covered by the San Juan lava flow which emanated from Parícutin volcano (Fig. 7.6), is certainly one of the most vivid pictures representing the hazards associated with volcanic eruptions.

Fig. 7.6 The eighteenth-century church of the Lord of the Miracles partially covered by the San Juan lava flow, Parícutin volcano in the background (Photo R. Garnica Peña)

Watched by peasants from neighboring communities, scientists, tourists, and reporters, five villages were dramatically affected in terms of land devastation. Fields were buried to considerable depths under ash and lava flows, in addition to the impact of pyroclastic falls, which involved a radius of ~25 km. The latter were associated with the constant presence of black clouds, cold rain of sand and mud, vapor, and sulfur smell conditions. Evacuation of villagers took place by their own will and in some cases by force. Consequently and fortunately, human losses due to the eruption of Parícutin did not occur.

7.6 Conclusions

Undoubtedly, Parícutin volcano has been and will remain the most amazing natural geomorphological laboratory Earth scientists could have dreamt of. The birth of Parícutin volcano in a Mexican-Tarascan cornfield a little more than 60 years ago has offered to native people and academicians the possibility to observe, study, and enjoy, in a very short time interval, a wonderful piece of the volcanic earth surface, as well as its associated processes and landforms.

The Author

Irasema Alcántara-Ayala is Director and Professor of the Institute of Geography, National Autonomous University of Mexico (UNAM), in Mexico City. Her research concerns mass movement processes, natural hazards, vulnerability, risk, and disaster prevention. Publication record includes more than 20 peer-reviewed papers, several book chapters, and numerous documents on landslide disaster prevention. Currently she serves as President of the Mexican Society of Geomorphology, Chair of the Geomorphological Hazards Working Group of the International Association of Geomorphologists (IAG) and Vice-President of the International Geographical Union (IGU).

References

Bullard FM (1956) Resumen de la historia del volcán Parícutin, Michoacán, México. In: Congreso Geológico Internacional, XX, México. Excursiones A-15, pp. 61–74

Corona-Chávez P (2002) Parícutin: una de las doce maravillas naturales del mundo. Universidad de Michoacán, México. http://www.umich.mx/mich/volcan-paricutin/Paricu22.pdf

Eggler WA (1948) Plant communities in the vicinity of the volcano El Paricutín, México, after two and a half years of eruption. Ecology 29:415–436

Flores-Covarrubias L (1945) Cálculos para la determinación de la altura del cono del volcán del Parícutin. In: El Paricutín: México, D.F., Universidad Nacional Autónoma de México, 19–20.

Foshag WF, González-Reyna JR (1956) Birth and development of Paricutín volcano, México. US Geol Surv Bull 965D:355–489

Fries C Jr (1953) Volumes and weights of phyroclastic material, lava and water erupted by Paricutín volcano, Michoacán, México. Eos, Trans Amer Geophys Union 34(4):603–616

Inbar M, Lugo J, Villers L (1994) The geomorphological evolution of the Paricutín cone and lava flows, México, 1943–1990. Geomorphology 9:57–76

Legorreta-Paulín G (1999) Geomorphological processes in the Parícutin volcano. M.Sc. thesis, Faculty of Philosophy and Letters, UNAM (in Spanish)

Lindig-Cisneros R, Galindo-Vallejo S, Lara-Cabrera S (2006) Vegetation of tephra deposits 50 years after the end of the eruption of the Paricutin Volcano, Mexico. Southwestern Naturalist 51:455–461

Ordoñez E (1943) El volcán de Parícutin. Irrigación en México 24(4):5–36

Rees JD (1979) Effects of the eruption of Parícutin volcano on landforms, vegetation, and human occupancy. In: Sheets PD, Grayson DK (eds) Volcanic activity and human ecology. Academic Press, New York, pp 249–292

Segerstrom K (1950) Erosion studies at the Paricutín, state of Michoacan, Mexico. US Geol Surv Bull 965A:1–164

Segerstrom K (1966) Paricutin, 1965; aftermath of eruption. U S Geol Surv Prof Pap 550C:93–101

Segerstrom K, Gutierrez C (1947) Activity of Paricutin Volcano from May 4 to September 8, 1946. Eos, Trans Amer Geophys Union 28:559–566

Wilcox RE (1948) Activity of Paricutin volcano from December 1, 1947 to March 31, 1948. Eos, Trans Amer Geophys Union 29:355–360

Wood CA (1980) Morphometric evolution of cinder cones. J Volcanol Geotherm Res 7:387–413

Yokoyama I, De la Cruz-Reyna S (1990) Precursory earthquakes of the 1943 eruption of Parícutin Volcano, Michoacan, Mexico. J Volcanol Geotherm Res 44:265–281

Chapter 8
The Cockpit Country of Jamaica: An Island Within an Island

Parris Lyew-Ayee

Abstract Cockpit karst landscapes are among the most distinctive and unique landscapes in the world, and have attracted attention from scientists and tourists alike from across the world and throughout recorded history. So named because of the bowl-shaped depressions resembling cock fighting arenas, its "*type area*" is the Cockpit Country in Jamaica, a rugged area dubbed "*terra incognita*" by early colonial settlers. A dramatic example of tropical karst topography, of which there are several, the Cockpit Country displays the best-developed type of cockpit karst in the world, a function of the material properties of the underlying limestone, water table depth, and tectonic setting as much as the climate in which it was formed.

Keywords Cockpit country • Cockpit karst • Jamaica • tropical karst evolution

8.1 Introduction

Cockpit karst landscapes are among the most distinctive landscapes in the world, and have been the focus of much scientific study over the past half century. A dramatic example of tropical karst topography, the terrain and its constituent landforms are the products of the unique properties of the limestones in which they form, climatic influences, and the tectonic setting of the karst region. The cockpit type of karst landscapes has its best expression in Jamaica, where the type area for this landscape – the Cockpit Country – is found.

Cockpit karst refers to an assemblage of enclosed cockpit depressions and residual hills (Sweeting 1972). Cockpits themselves are deep, irregularly shaped depressions in the landscape through which water is conducted underground; residual hills surround these depressions. However, there has been some disagreement over the past century as to the nature of cockpit karst. This is reflected in the confusing terminologies derived for areas with similar landforms, with names ranging from *Kegelkarst* to cone karst, all purportedly describing similar landscapes. Recent studies have added further quantitative descriptions of cockpit karst landscapes, showing that cockpit karst areas have pronounced vertical relief development over a relatively short horizontal space, with significant topographic roughness (Lyew-Ayee et al. 2007), distinguishing these areas from other landscapes, karst or otherwise.

Cockpit karst areas are typically found in areas with high rainfall. Sweeting (1972) mentioned that both high amounts and high intensities of rainfall are required for the development of cockpit karst, because high rates of solution would be required to sculpt the landscape. But high levels of rainfall alone would not result in the development of a cockpit karst landscape. It would require the limestone to be hard and compact, with marked development of fracture systems through which water would be vertically redirected to begin and continue sculpting the terrain. It is the combination of these factors that would result in the development of a cockpit karst landscape.

It is the geology of the limestone – its lithology and structure – that plays an important role as a control on cockpit karst development. Monroe (1966) commented, from his observations in Puerto Rico, that different lithologic units gave rise to different types of karst phenomena, while Day (1978), in his study of tropical karst landscapes across the Caribbean, looked at the material properties of the limestone – hardness, purity, petrology, and porosity – as well as the structural patterns of joints and faults. One of his key findings was that high limestone purity and high mechanical strength were the main controls

P. Migoń (ed.), *Geomorphological Landscapes of the World*,
DOI 10.1007/978-90-481-3055-9_8,

on cockpit karst development, a fact confirmed by more recent research (Lyew-Ayee 2004). In addition to these lithological controls, structure also plays a very important role. Fractures, joints, bedding planes, and faults all serve to redirect and control the movement of water through the karst terrain, resulting in preferential solution occurring. As a result, certain areas in the limestone landscape are dissolved at a faster rate than others.

Another important control is the karst base level, where water draining vertically through the limestone meets an impermeable stratum or the water table, at which point the water begins to flow laterally underground. Where the base level is at great depth, the dissolution of the limestone can continue vertically, and surface landforms have pronounced vertical development. These factors – geological and hydro-meteorological – operating in tandem, result in the development of cockpit karst landscapes.

8.2 Geographic Setting

Cockpit karst landscapes are not limited to Jamaica. Other areas in the Caribbean have them too – those in Belize and Puerto Rico have been well-documented (Day 1978, 1982; Monroe 1966) – and other areas around the world have been described as having similar landscapes with alternating hills and depressions. While other places in Jamaica also have cockpit karst topography, the region known as the Cockpit Country has the most dramatic and extensive cockpit karst development on the island.

Jamaica is the third largest island in the Greater Antilles, in the western part of the Caribbean Sea, located roughly 18°N and 77°W. The island lies on the eastern end of the Nicaragua Rise, a topographic extension of northern Central America, and is separated from Cuba to the north by the 7,200 m deep Cayman Trough.

The island is essentially divided into two broad physiographic units: the Eastern Mountain Mass, with Cretaceous and Eocene clastic rocks, and the Main Block, which consists of dissected limestone plateaux, in which karst features have their best expression. Tectonic displacement in the early Cenozoic had the effect of "breaking up hard limestone beds and increasing its permeability" (Versey 1972: 450). He also added that this block was uplifted in the Miocene in a manner similar to that of a large calcareous shoal, with no drainage superimposed upon it. The future karst landscape would depend on the character of the newly exposed limestone, as well as the amount of uplift (which influences the karst base level) and fracturing. The tectonic activity also resulted in the exposure of Cretaceous-age volcaniclastic rocks beneath the limestone, which led to allogenic runoff on to the surface of the adjacent limestone beds, contributing to both chemical and mechanical erosion from the sediment-laden waters.

It is in this environment and system that the Cockpit Country developed. Situated on the Main Block, it makes up part of a limestone plateau, reaching altitudes of more than 900 m a.s.l., developing on the hard and pure White Limestone Group found in this area. Other spectacular karst features are found along this plateau, for example, the degraded karst of the Dry Harbour Mountains (Sweeting 1958; Day 1978) and the interior valley (polje) at Lluidas Vale (Landmann 1990), although none as spectacular as the Cockpit Country. First described in 1869 by Sawkins, for whom the ruggedness of the terrain was "well deserving of the appellation *terra incognita*," the Cockpit Country remains to this day an area of undisturbed natural beauty of immense interest to scientific study (Figs. 8.1–8.3).

The Cockpit Country is defined to the north and east by major fault systems, with a significant lithological change in the limestones to the east as well. The southeastern and western boundaries are defined by outcrops of volcaniclastic material, which also result in a very different topographic character in these places. These areas also have surface drainage which contributes allogenic material into the karst hydrosystem of the Cockpit Country. The southern boundary is defined by interior valleys, with extensive areas of gentle relief development (Fig. 8.4).

The region has strong historical significance, with many pre-Columbian Taino Indian artifacts found in the caves within the Cockpit Country, as well as Maroon settlements with the descendants of runaway slaves from the sugarcane plantations that surround the region, who used the rugged terrain to escape and evade colonial soldiers.

Fig. 8.1 The Cockpit Country from the air (Photo P. Lyew-Ayee)

8.3 Landforms

It is the assemblage of the different landforms that comprise the overall landscape. While cockpit karst landscapes are invariably described as having alternating residual hills and enclosed depressions, these often have very different forms.

Cockpit depressions average more than 50 m in depth, and are distinct from dolines, "the diagnostic karst feature" (Ford and Williams 2007), in both the depths of the cockpits as well as in planar complexity (dolines tend to have simpler planar forms). Cockpits often occur with multiple sinks per depression through which surface water is redirected downward. While some researchers (Sweeting 1972; Miller 1998; Mitchell et al. 2003) have described cockpit depressions as being star-shaped in plan, this is a very qualitative generalization. Depressions have various shapes and forms, ranging from simple circular cockpits (different from dolines and other karst depressions because of their depths) to very irregular depressions. Elongated glades form when depressions develop along a fault or major joint set, which controls the orientation of the landforms, while uvalas are formed when cockpits coalesce. While cockpits have been described as having steep slopes (Sweeting 1958, 1972), a depression may have very steep slopes along parts of its sides, with gentler slopes on other sides; in both plan and profile, depressions are highly irregular.

Cockpit depressions are formed at the intersection of major joint sets, where dissolution of limestone by water traveling along these is greatest. It is along such lines of secondary porosity that much of the surface water is redirected into the rock, resulting in preferential dissolution of the limestone in these areas. The limestones found in the Cockpit Country already have fairly low primary porosities due to recrystallization and case-hardening. Where the limestone stratum is thick, and the karst base level at great depth, the vertical flow of water (and its solutional effects) along the fractures continues to sculpt the landscape and maintain the characteristic relief of the cockpits.

The surrounding residual hills are (broadly) relicts of the original limestone plateau. They generally have

Fig. 8.2 Another view of the Cockpit Country from the air. Non-cockpit karst landforms are in the background (Photo P. Lyew-Ayee)

concordant summits, with vertical dissolution of the limestone largely concentrated in the depressions. Hills are generally more interconnected than the isolated cockpits, with "saddles" connecting individual hills and separating cockpits. The hills may have undercut notches at their bases, where lateral dissolution may occur from the ponding of water in depressions following heavy rainfall. Caves may also be associated with the sides of hills, these being remnants of former underground water channels that have been uplifted and subsequently exposed. It is in these caves that there have been archaeological discoveries associated with Taino settlements.

Both depressions and residual hills show a narrow horizontal spacing; these features are generally close to each other, with sinks and summits roughly 100 m apart from each other on average. The resulting density of features, coupled with the high range in elevation (between 50 m and 100 m) between these features, give the Cockpit Country its characteristic rugged landscape.

8.4 Landscape

Ultimately, as the type area for cockpit karst, all descriptions of the cockpit karst of Jamaica refer to the Cockpit Country. The region is not homogeneous; cockpit karst dominates the Cockpit Country, but does not compose the entire region: elongated glades (described later) and localized areas of lateral corrosion result in some areas not attaining the same vertical development of the landscape as other places. On the

Fig. 8.3 Inside a cockpit surrounded by residual hills (Photo P. Lyew-Ayee)

whole, however, the landscape shows very pronounced vertical relief development, especially when compared to the landscapes which surround the Cockpit Country, as well as a greater degree of topographic roughness (Lyew-Ayee et al. 2007). These surrounding regions show a mix of tower karst topography (in areas where the karst base level is near the surface, which promotes lateral dissolution of the landscape) and doline karst (in areas of more impure limestone), as well as entirely non-limestone regions devoid of karst. In all these landscapes, however, the level of vertical terrain development, as well as the narrow horizontal spacing of features, attained in the Cockpit Country is not present.

Other karst landscapes surround the Cockpit Country. There are interior valleys (poljes) to the north and south of the region, with portions of tower karst contained therein, as well as pockets of doline karst areas. To the east lies an area of degraded karst, described by Sweeting (1958) and Day (1982) as a modification of existing cockpit karst, where deepening of cockpits has ceased, resulting in the sides of the depressions slumping in, reducing slope angles. The cockpits, as a result, become less deep (from the slumping of the sides as well as accumulation of talus deposits and bauxite deposits in these depressions) and morphologically distinct from the cockpit karst in the Cockpit Country. Here, there are large elongated glades where cockpits coalesce and develop parallel to the existing fracture orientations. The limestone in this region is lithologically different from that found in the Cockpit Country, but the area is found on the same limestone plateau as the Cockpit Country, with similar karst base level depths and local climate, and, as such, illustrates nicely the lithological controls on cockpit karst development.

Ultimately, the cockpit karst of the Cockpit Country is distinct from other similarly described landscapes with alternating series of karst depressions and residual hills. Cockpit karst is not cone karst; the former describes negative relief landforms in the landscape, while the latter describes positive relief features.

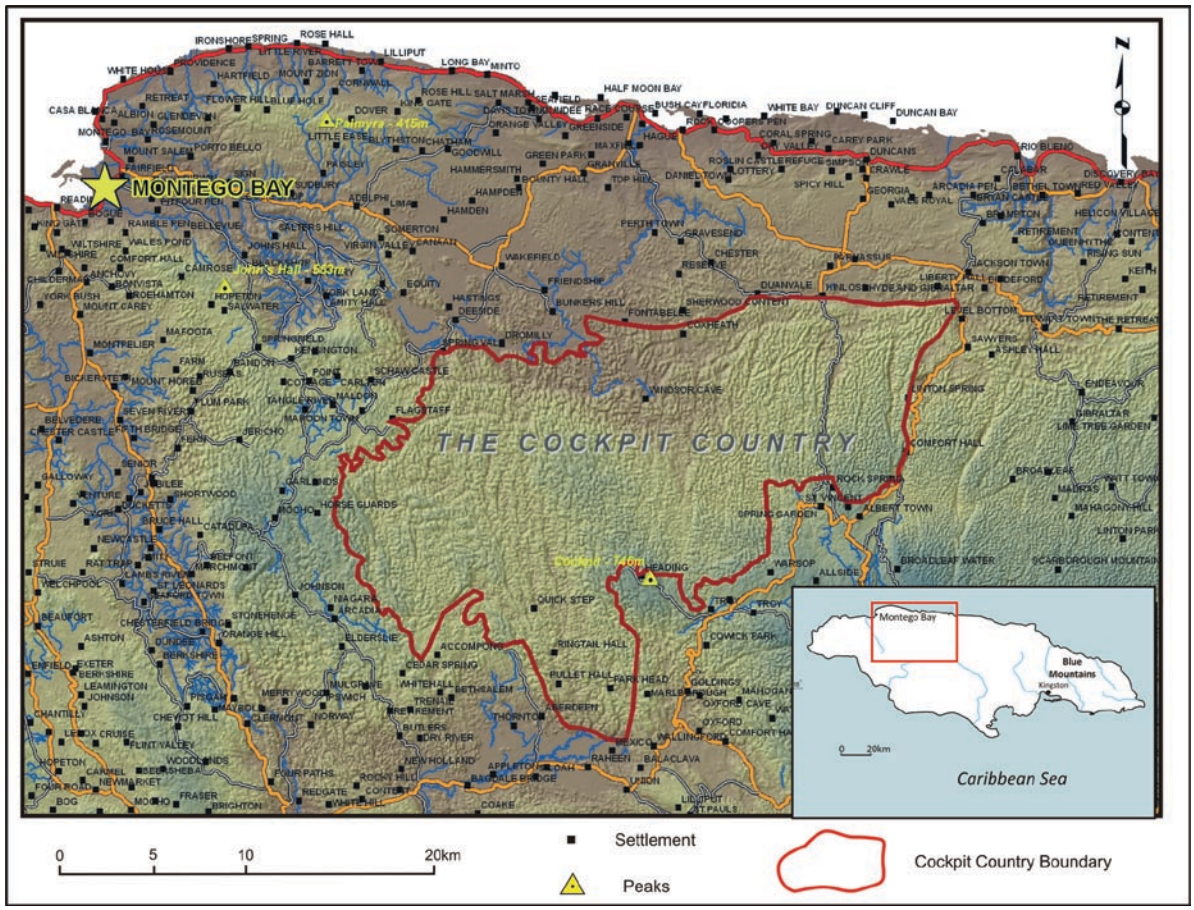

Fig. 8.4 Cockpit Country location map

Cone karst areas were described in the Far East by Lehmann (1936), and Jennings (1972) noted the full, rounded shapes of the hills, while Sawkins commented in 1869 on the cockpit depressions in Jamaica resembling arenas used for cockfighting. The cone karst of Gunung Sewu (whose name means "thousand hills" in Javanese) in Java, Indonesia, was described in 1845 by Junghuhn, who noted the extensive series of hills there. These (qualitative) perceptions of scientists and observers over the past century and a half seem to describe two very different landscapes. There is no such thing as cockpit cone karst.

8.5 Morphogenesis

Hill's (1899) model of karst landform development in Jamaica (Fig. 8.5) was largely simplistic, but correctly considered both rock type and the karst base level as important controls in landscape evolution, and is still relevant more than a century later. This model predated hypotheses on karst landscape evolution by Grund in 1914 and Cvijić in 1918, yet all maintained that an initial limestone surface was sufficiently weathered, producing karst landforms, and, over time, an impermeable rock stratum is exposed which does not support further karst development.

The limestone plateau upon which the Cockpit Country developed would have had no drainage superimposed on it. This corresponds to Hill's Stage I of karst development. The exposed limestone was then subjected to surface weathering, and karstification began. Local conditions, however, would determine the extent of karstfication and the variety of landforms produced. The Cockpit Country would represent Stage II of Hill's model.

However, the simple linear progression of karst development, from uplifted shoal to cockpit karst

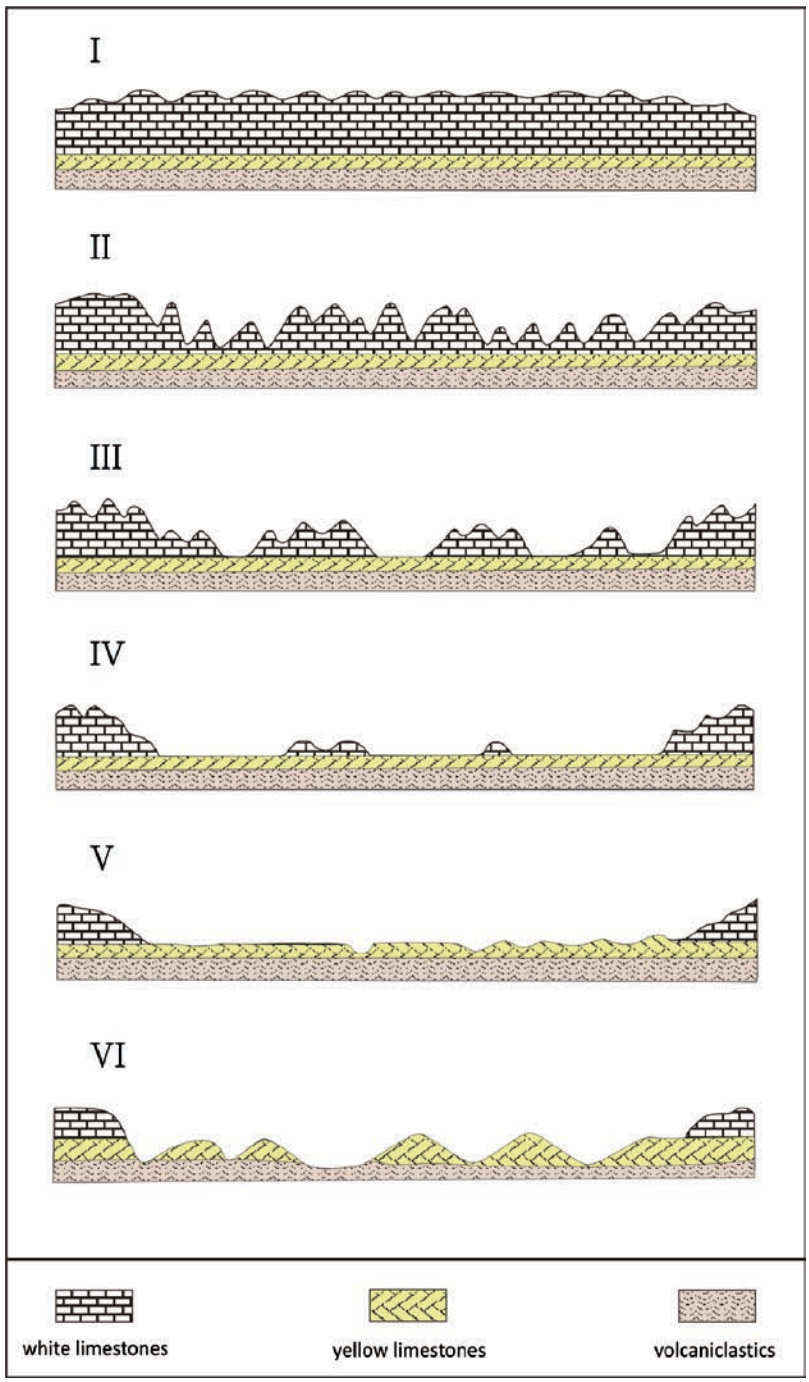

Fig. 8.5 Hill's evolutionary model for karst morphogenesis in Jamaica

landscape, to the complete removal of limestone cover and destruction of the karst environment, may be incorrect. The generalized models by Hill (1899) and Smith et al. (1972), both of which were based on research done in Jamaica, did not consider the effect of the allogenic contribution of low-permeability material which would form a superficial karst base level and accelerate the destruction of the karst surface.

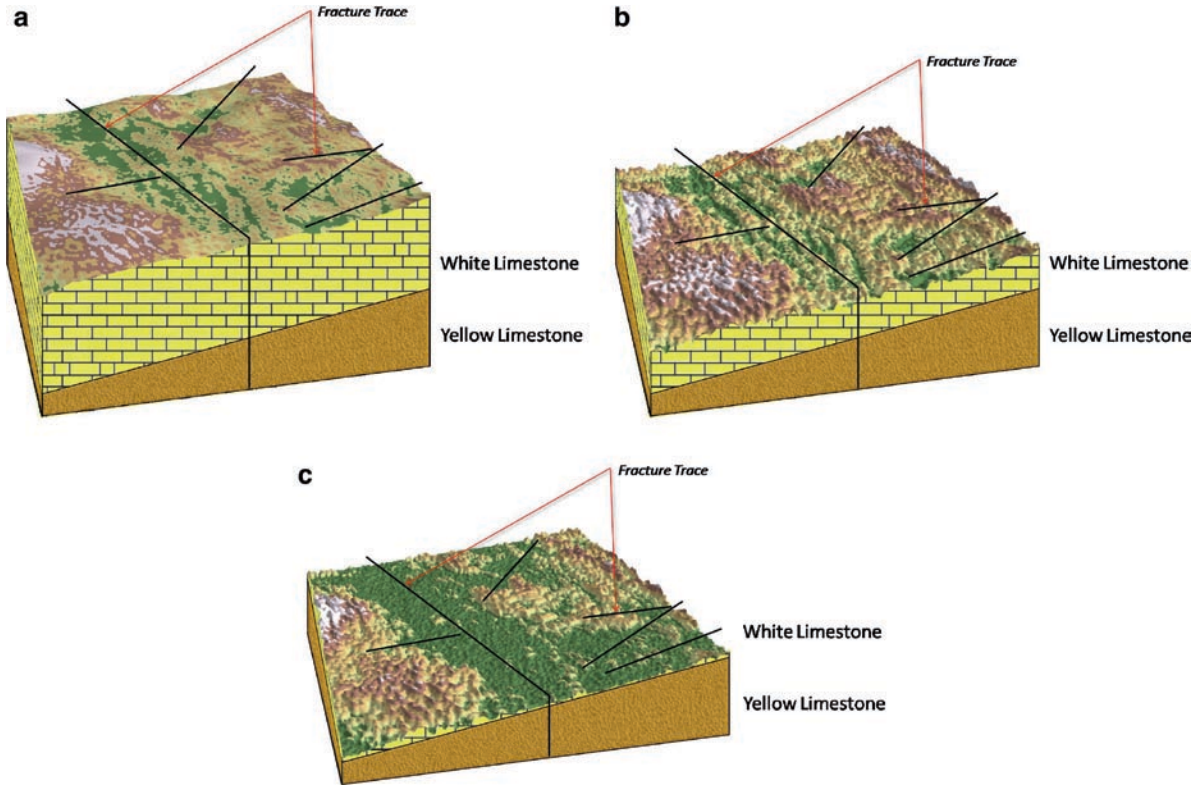

Fig. 8.6 Revised evolutionary model for karst morphogenesis in Jamaica. Stage B is a DEM of an actual part of the Cockpit Country. Evolution is controlled by the lithology of the White Limestone, the height above the karst base level at the Yellow Limestone contact, and the fractures in the landscape which influence the vertical transmission of water

These models, which generally describe a progression from doline karst to cockpit karst to tower karst before the removal of the limestone cover, also do not account for the evolution and existence of degraded karst, found to the east of the Cockpit Country.

Figure 8.6 revisits Hill's model, as well as that developed by Smith et al. (1972), using a contemporary model of the landscape. Figure 8.6a portrays the landscape as an uplifted shoal, while Fig. 8.6b shows the current landscape, and Fig. 8.6c the landscape as it would look after continued development through to its destruction on encountering the karst base level at the White Limestone–Yellow Limestone contact. The actual fracture traces in the landscape are shown, and erosion tends to be focused along these. As such, the models show the effects of both lithological and structural controls, as well as the nature of the karst base level, in the evolution (and destruction) of the cockpit karst landscape.

The Main Block, upon which the Cockpit Country developed, was uplifted in the Miocene (Versey 1972; Mitchell 2004), and has had continuous exposure to surface weathering since. However, the fact that not all features contained in the region are uniform, even in areas with similar lithology, suggests that different processes are at work. While solution is the main process at work in sculpting the Cockpit Country, local hydrological and geological conditions dictate the effectiveness of this. The alignments of fractures, as well as the effect of allogenic drainage, all served to influence how the region developed. As a result, while still composed of alternating cockpits and residual hills, these landforms do not necessarily have uniform characteristics.

8.6 Conclusions

The unique landscape of the Cockpit Country is certainly one of the most interesting places in the Caribbean. The rugged landscape there also supports one of the highest densities of endemic species of flora and fauna in Jamaica, resulting in a great deal of ecological

interest in the region in recent times. Certainly, over the past few years, the bulk of Cockpit Country research has focused on this aspect of the region. Studies have also focused on the historical aspect of the Cockpit Country region (Lyew-Ayee and Conolley 2008), with the recent discoveries of significant Taino artifacts in the area.

However, it is the geomorphology of the place that resulted in the Cockpit Country supporting such species endemism, with the ruggedness of the terrain deterring human encroachments; its cave systems attracted Taino ceremonial burials. This combination of scenic value, historical interest, and biodiversity has resulted in the Cockpit Country becoming worthy of local, regional, and international interest, scientifically, culturally, and otherwise. After all, it is one of the most exciting karst landscapes on Earth.

The Author

Dr **Parris Lyew-Ayee** is the Director of the Mona GeoInformatics Institute at the Mona (Jamaica) campus of the University of the West Indies. His doctoral dissertation at the University of Oxford was on "Digital Topographic Analysis of Cockpit Karst: A Morpho-Geological Study of the Cockpit Country Region, Jamaica." His research has focused on Geographic Information Systems; digital topographic analysis, and topographic signature identification, including geocomputational and mathematical analyses of land surfaces; and natural hazards simulation and disaster response coordination.

References

Day MJ (1978) The morphology of tropical humid karst with particular reference to the Caribbean and Central America. D.Phil. thesis, University of Oxford, U.K.

Day MJ (1982) The influence of some material properties on the development of tropical karst terrain. Trans British Cave Res Assoc 9:27–37

Ford DC, Williams PW (2007) Karst Hydrogeology and Geomorphology. Wiley, Chichester

Hill RT (1899) The geology and physical geography of Jamaica: A study of a type of Antillean development. Bull Mus Comp Zool 34:1–226

Jennings JN (1972) The character of tropical humid karst. Z Geomorph NF 16:336–341

Landmann M (1990) Reliefgenesis in the Lluidas Vale area of central Jamaica. Z Geomorph NF Suppl 77:67–84

Lehmann H (1936) Morphologische Studien auf Java. Geogr Abh 3(9):1–114

Lyew-Ayee P (2004) Digital topographic analysis of cockpit karst: A morpho-geological study of the Cockpit Country region, Jamaica. D.Phil. thesis, University of Oxford, U.K.

Lyew-Ayee P, Viles HA, Tucker GE (2007) The use of GIS-based digital morphometric techniques in the study of cockpit karst. Earth Surf Proc Landf 32:165–179

Lyew-Ayee P, Conolley I (2008) The use of imagery to locate Taino sites in a GIS environment. In: Reid B (ed) Archaeology and Geoinformatics: Case Studies from the Caribbean. University of Alabama Press, Tuscaloosa, pp 137–152

Miller DJ (1998) Invasion of the cockpits: Patterns of encroachment into the wet limestone rainforest of Cockpit Country, Jamaica. In: McGregor DFM, Barker D, Evans SL (eds) Resource Sustainability and Caribbean Development. The Press, University of the West Indies, Kingston, Jamaica, pp 373–389

Mitchell SF (2004) Lithostratigraphy and palaeogeography of the White Limestone Group. In: Donovan SK (ed) The White Limestone Group of Jamaica. Cainozoic Res 3:5–9

Mitchell SF, Miller DJ, Maharaj R (2003) Field guide to the geology and geomorphology of the Tertiary limestones of the Central Inlier and Cockpit Country. Carib J Earth Sci 37:39–48

Monroe WH (1966) Formation of tropical karst topography by limestone solution and reprecipitation. Carib J Sci 6:1–7

Smith DI, Drew DP, Atkinson TC (1972) Hypotheses of karst landform development in Jamaica. In Trans Cave Research Group of Great Britain, 14(2):159–173

Sweeting MM (1958) The karstlands of Jamaica. Geogr J 124:184–199

Sweeting MM (1972) Karst Landforms. MacMillan, London

Versey HR (1972) Karst in Jamaica. In: Herak M, Springfield VT (eds) Important Karst Regions of the Northern Hemisphere. Elsevier, New York, pp 445–466

Chapter 9
The Gran Sabana: The World's Finest Quartzite Karst?

Robert A.L. Wray

Abstract The Gran Sabana in tropical Venezuela, with its huge mist shrouded, mesa or *tepui* that tower over 1,000 m above the lowlands, undoubtedly form one of the world's more spectacular landscapes. These vertically walled quartzite table mountains are composed of Pre-Cambrian Roraima Group quartzites and sandstones, and crest a series of regional planation surfaces. Because of their isolation the summits are often biologically unique. Extremely long periods of geologic stability and weathering have produced a vast range of karstic forms in the quartzites, such as caves, towers, grikes, and smaller *karren*. Quartzite is not a rock usually associated with karst forms, but here they are expressed better than anywhere else in the world. Sections of the Gran Sabana and its *tepui* are listed as World Heritage, and its remoteness and often-poor accessibility possibly make it the most poorly explored of the great geomorphological landscapes.

Keywords karst • quartzite • solutional weathering • table mountain • Venezuela

9.1 Introduction

Amongst the most impressive of the world's great scenic landscapes is the Gran Sabana of the humid tropical borders of Venezuela, Guyana, and Brazil. The most impressive feature of the Gran Sabana is its spectacular quartzite mesa and butte topography and highly developed quartzite karst formed in the Pre-Cambrian igneous and metamorphic rocks of the Guyana Shield. More than a hundred sandstone and quartzite mesas (George 1989), or table mountains, ranging in size from a fraction of a km^2 to perhaps 15 km^2 (White et al. 1966) stand above the surrounding lowlands, each ringed by massive near-vertical cliffs often 1,000 m or more in height (Fig. 9.1). The Pemón Indian word for these table mountains is *tepui*.

Biologically the tepui summits are virtually unique ecosystems, cloud-shrouded much of the time – so isolated they are said to have inspired Conan Doyle's "Lost World." All the tepui are remote, only about half have been extensively explored, and virtually unbroken cliffs mean that almost all tepui summits are only accessible by helicopter.

But it is not just the scale of the massive cliffs that make these tepui so impressive. A high rainfall, long geologic stability, and a vast time of exposure have given rise to a widespread and extremely impressive range of solutional landforms – karst – within the quartzites. The Gran Sabana tepui have probably been the most intensively studied quartzite landscapes in the last 30 years (Chalcraft and Pye 1984; Pouyllau and Seurin 1985; Briceño and Schubert 1990; Briceño et al. 1990; Wray 1997a, b; Doerr 1999). If any place could be considered a "type" area for quartzite karst, the tepui of the Gran Sabana is certainly that place. These quartzite karst forms are comparable to those developed within many limestones, and include tower fields, ruiniform assemblages, corridors and grikes, sinkholes, polje, collapse shafts and caves, and smaller *lapiés* such as runnels and basins. The solubility of the quartzite is however very much lower than that of limestone.

These characteristics together mean that the Gran Sabana and its tepui are the most remarkable and well-developed quartzite karst areas in the world. It is certainly one of the more spectacular landscapes, and one of the lesser accessible and most poorly explored of the great geomorphological landscapes.

P. Migoń (ed.), *Geomorphological Landscapes of the World*,
DOI 10.1007/978-90-481-3055-9_9,

Fig. 9.1 The massive 700 m high cliffs of Kukenhan Tepui rising above the Wonkén Surface of the surrounding Gran Sabana. The mist-shrouded summit is the Auyán-Tepui Surface, and the cliffs and summit plateau are cut in the quartzite of the Matauí Formation. Note the high waterfall cascading down the cliffs from the summit plateau (Photo S.H. Doerr)

9.2 Geographical Setting

The Gran Sabana is an immense upland formed on the Pre-Cambrian rocks of the Guyana Shield in the south-eastern part of Venezuela, close to the borders of Guyana and Brazil (Fig. 9.2). The climate of the area is humid tropical, precipitation maxima are in May–June and December–February (White et al. 1966), but the alternating rainy and dry seasons are not well-marked (Briceño et al. 1990).

Tepui summits are typically between 1,900 m to 2,700 m elevation, and stand between 900 to 1,600 m above the surrounding lowlands (Briceño and Schubert 1990) (Fig. 9.1). The highest summit, Mount Roraima, attains 2,810 m (Chalcraft and Pye 1984). The tepui summits are generally cloud-covered and the precipitation is very high; exact values have not been accurately measured, but estimates range from 3,800 mm to as much as 7,500 mm per annum (Chalcraft and Pye 1984; George 1989). This extremely high precipitation supports rudimentary, cool temperate vegetation; forests, sedges, grasses, and bromeliads grow in the sheltered locations, peat swamps are well-developed and often extensive, and large areas of the summits are bare of vegetation except for mosses, lichens, and algae.

The surrounding Gran Sabana is generally between 400 m and 1,000 m elevation, with an annual rainfall typically around 1,000 mm (White et al. 1966). Much of it is vegetated by savanna grassland with rainforest along water courses and in the pediment zones around the tepui (Chalcraft and Pye 1984; Briceño and Schubert 1990; Briceño et al. 1990).

9.3 Geology

The clastic sediments of the Pre-Cambrian Roraima Group (generally quartz sandstones, quartzites, and conglomerates) (Briceño et al. 1990) form the bedrock of

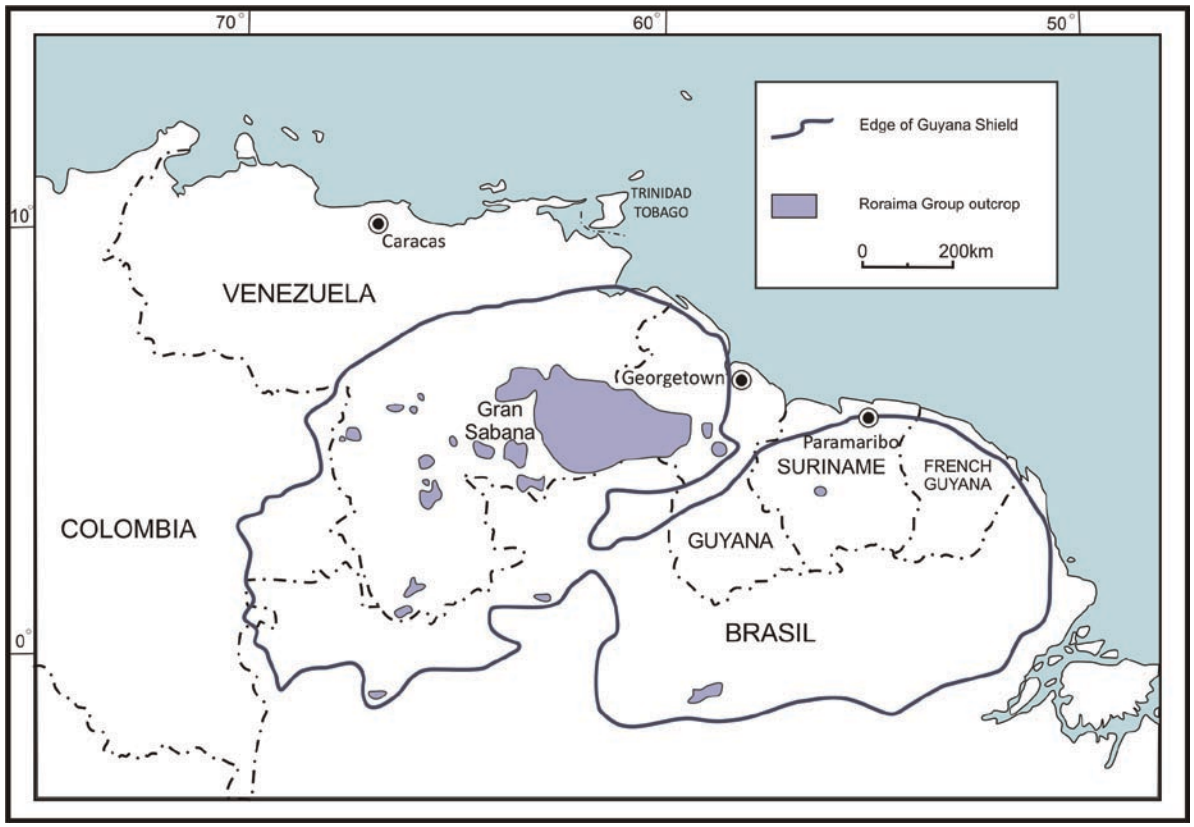

Fig. 9.2 Map showing the location of the Gran Sabana, the outcrop of the Roraima Group rocks and the Guyana Shield

the Gran Sabana. The age of these rocks is controversial, but presumed to be around 1.8–1.4 Ga (Briceño et al. 1990); there are no fossils, and they are intruded by numerous diabase sills and dykes with ages of 1.6 and 1.5 Ga (Briceño and Schubert 1990). The Roraima Group was also intruded by Mesozoic diabase dykes with ages of around 200 million years, associated with the opening of the Atlantic Ocean (Briceño et al. 1990). The Group type section near Mt Roraima is 1,800 m thick, but near the middle the formation is estimated to be 3,000–4,000 m thick (Briceño and Schubert 1990).

The principal structures of the Roraima Group are large radius anticlinoria and synclinoria that have given rise to cuestas and large areas of nearly horizontal strata. These relatively horizontal beds and nearly vertical jointing have promoted erosion around the edges of the tepui being dominated by collapse of bedding and joint defined blocks. Such collapse has led to the maintenance of the table-mountain topography (Briceño and Schubert 1990).

The most resistant unit of the Group is the uppermost Matauí Formation, which forms the tepui cliffs and summits, the most conspicuous landscape elements. It consists of 600–900 m of quartzite and dominantly quartzitic arenites, with some wackes, lithic wackes, and subarkoses with abundant cross-bedding (Briceño et al. 1990).

White et al. (1966) described the quartzite as haematite-stained, medium-grained orthoquartzite sandstone, which is often deeply weathered on the surface. The unweathered rock is nearly white and very well-cemented. The grains are well-rounded, interlocking, and cemented with quartz overgrowths. More than 95–98% of the clastic grains are quartz, with minor feldspar, mica, and heavy minerals (White et al. 1966; Chalcraft and Pye 1984; Doerr 1999). It breaks with a conchoidal fracture across the grains (White et al. 1966; Chalcraft and Pye 1984).

The Guyana Shield has been geologically very stable for an extremely long period of time, and tepui summits

are believed to have been exposed and weathering for more than 70 million years (Briceño and Schubert 1990; Briceño et al. 1990).

9.4 Landforms

The geography of the Gran Sabana region was first described by Tate (1938), but the fullest descriptions of the regional geomorphology were by Briceño and Schubert (1990) and Briceño et al. (1990).

9.4.1 Planation Surfaces

One of the most dominant landscape features in the Gran Sabana is a flight of planation surfaces rising from modern sea level to the summits of the high tepui (Briceño and Schubert 1990). Six planation surfaces of more or less flat areas of regional extent and accordant summit elevations have been recognized on the Guyana Shield, most being correlated with similar surfaces in surrounding regions. Although the influence of tectonic uplift has been difficult to determine, Briceño and Schubert (1990) believe uplift was involved in the formation of large differences in elevation, particularly between the two highest surfaces.

The ages of the planation surfaces are also controversial. Planation probably began during the Pre-Cambrian, and continued through an unknown number of Palaeozoic erosion cycles in rocks above the Roraima Group. Remnants of these ancient surfaces no longer exist. The youngest surface is the Holocene alluvial plain of the Orinoco River (0–50 m a.s.l.), above which is the Llanos Surface (80–150 m), a Plio-Pleisticene depositional surface lying on either basement rocks or Pleistocene sediments. The 200–450 m a.s.l. erosional Caroní-Aro Surface has formed on the basement rocks of the Shield or very locally the Roraima Group, and is characterized by bornhardts with beveled summits surrounded by weathered rocks and thin alluvial cover. Regional correlations with Brazil and Surinam suggest it is of Oligo-Miocene (?) age. The last surface for which any reasonable age criterion exists is the Early Tertiary (?) Imataca Surface (600–700 m), which cuts the igneous basement and the lower formations of the Roraima Group.

Briceño and Schubert (1990) speculate that the two highest and best-developed planation surfaces, the Wonkén and Auyán-Tepui Surfaces, are presumably Mesozoic in age. The Wonkén Surface truncates rocks of the lower Roraima Group and at elevations of 900–1,200 m forms the main surface of the Gran Sabana (the low area surrounding the table mountains) (Fig. 9.1).

The highest surviving planation level is the Auyán-Tepui Surface that forms the quartzite tepui summits (2,000–2,900 m). The age of initiation of this surface is not known with certainty, but Briceño and Schubert (1990) proposed that considering the rock thickness that must have existed above it, the main part of the Shield may have been exposed since the Pre-Cambrian, and that as Cretaceous sediments are found on a younger surface in Surinam, a speculative Mesozoic (Jurassic?) or older age is likely.

9.4.2 Table Mountains – Tepui

The most impressive landscapes of the Gran Sabana are the numerous tepui rising abruptly above of the surrounding plains. They are generally composed of up to five elements or zones (Briceño and Schubert 1990) (Fig. 9.3). These include: the surrounding pediment and alluvial surfaces (Zone 1), the foothills (Zone 2), the vertical scarps (Zone 3), the rim zone (Zone 4), and the tepui summit (Zone 5).

The pediment area (Zone 1) is formed on quartzitic and volcaniclastic sandstones of the middle to upper-middle Roraima Group. It is of low relief and rises at slopes of 5°–15° into the tepui foothills, and degrades down into the surrounding herbaceous or forested savannas. The pediment zone is formed by scarp retreat across bedrock and then covered by alluvial-colluvial fan material derived from the upper parts of the tepui. The hilly and densely forested foothills (Zone 2) are formed on similar rocks of the upper-mid Roraima Group and thick diabase sills. Large fallen quartzite blocks mantle the upper sections of the pediment.

The impressive and sometimes overhanging cliffs (Zone 3) up to 1,000 m high are formed in the quartzites of the upper Roraima Group. In many places water movement down joint and bedding planes has formed caverns in the cliffs. Groundwater often resurges from these caverns, with waterfalls cascading hundreds of

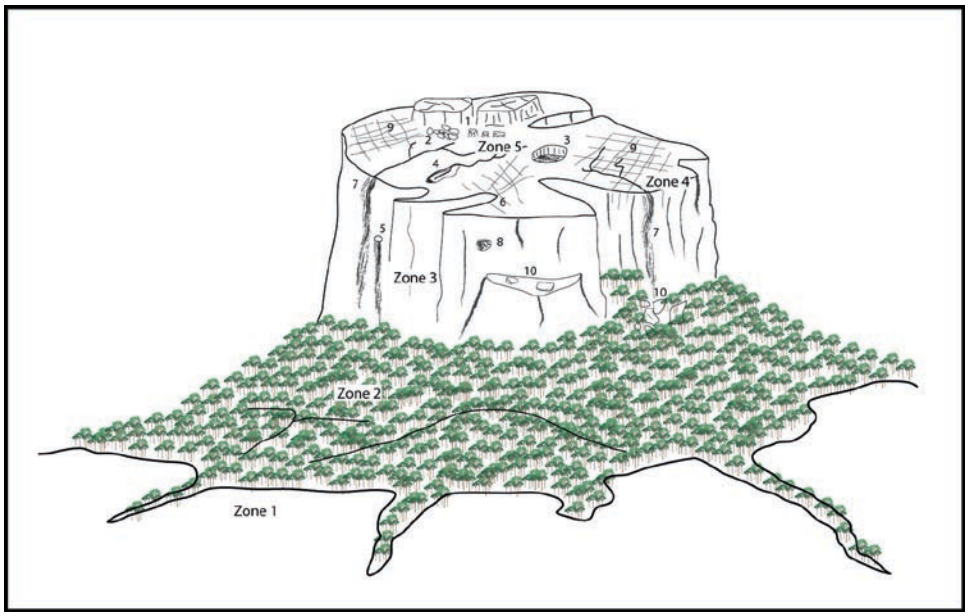

Fig. 9.3 Diagrammatic representation of a typical tepui. Zone 1: pediment, Zone 2: foothills, Zone 3: cliff, Zone 4: tepui rim, Zone 5: tepui summit. 1: Residual summit towers, 2: Chaotic block accumulations, 3: Collapse shaft, 4: Stream sink or polje, 5: Cliff resergence waterfall, 6: Embayed tepui rim, 7: Waterfall, 8: Cliff caverns, 9: Joint systems and grikes, 10: Fallen blocks (Modified after Pouyllau and Seurin (1985); Briceño and Schubert (1990))

meters to the pediment below. These outlets are often amplified by collapse of quartzite blocks from the walls, or the collapse of cavern roofs, and they themselves promote collapse and the perseverance of the vertical cliffs.

The area of the tepui rims (Zone 4) is highly irregular and embayed by deep gorges controlled by joint systems (Briceño and Schubert 1990; Briceño et al. 1990). Fracture systems are the dominant control on tepui rim geomorphology. One of the most important dynamic processes is the widening of the fractures within the quartzite by solutional weathering leading to collapse and fall of large blocks to the scarp base (Pouyllau and Seurin 1985). A large part of the runoff is channeled through these weathered fissures and caves before resurging at the cliff faces.

The summit areas (Zone 5) are a more regular, smoother topography than the rims. Gentle rounded hills covered by low forest often form on diabase dikes or sills (Briceño and Schubert 1990). Wide areas of the plateau surface are covered with deposits of peat or fields of residual quartzite and sandstone towers. Vegetation is often very sparse and simple; often the only covering of the rock are a thin algal film, moss, or lichens.

Deep joint-controlled gorges also cut back deeply into many tepui summits. Small variations in resistance to solutional weathering between the individual layers within the quartzites and sandstones impart a slightly stepped topography, with more resistant quartzite towers and blocks towering a few meters above the more weathered rocks.

9.4.3 Drainage

The joint systems play a major role in channeling rainwater flow on the tepui summits. The extensive peat deposits store and slowly release large volumes of water, presumably charged with organic acids that further enhance chemical weathering of the quartzose rocks (see Young et al. 2009). The stream beds are cut into the base rock, but clastic bedloads of sand and gravel are mostly absent, which Briceño and Schubert (1990) argued provides good evidence for high stream competence.

Principal drainage directions are controlled by fracture systems and lithological contacts. The longitudinal profiles of the drainage systems, both on the surface

and underground, are quite irregular, with many rapids and waterfalls separating relatively flat sections (Briceño and Schubert 1990). Drainage proceeds either directly over the tepui rims in high waterfalls (Angel Falls cascading 979 m down the face of Auyan-Tepui is the world's highest waterfall) (see a similar 700 m high waterfall on Fig. 9.1), or very commonly, into deep fissures, canyons, sinkholes, cave systems to later resurge as waterfalls below the tepui rims.

9.4.4 *Karst Forms*

The large-scale forms of the tepui are indeed impressive, but superimposed on these are smaller weathering forms *par excellence*. These tepui are home to the world's best quartzite and sandstone karst; the high precipitation and long weathering has led to the formation of an impressive range of karstic forms.

Although the tepui quartzites are of very low solubility, they abound with a vast range of karstic surface and underground forms which conform to the definition of karst morphology. These include arches, towers and tower fields, depressions (including dolines, collapse shafts and even large polje), corridors, grikes, and large and extensive caves. Study of these karstic forms and processes during the last 3 decades has spearheaded a worldwide recognition of true karst forms on relatively "insoluble" sandstones and quartzites (Wray 1997a, b; see also Young et al. 2009).

The summits of the tepuis (where not covered by peat bogs) consist of bare, relatively smooth, sandstone and quartzite pavements. However, between the scarps and the areas of smoother topography, the summit plateaus are normally dissected along vertical joints into a chaotic labyrinth of walls, arches, towers, and pinnacles. "Ruiniform" is a term often applied to such landscapes for they resemble ancient, collapsing ruins (Fig. 9.4). Along some of the major joints, chasms, corridors and grikes have developed, 50 m or more deep. Extensive fields of small joint-bound towers (averaging 1–2 m wide at the base and 1.5–2 m or higher) are common (Briceño and Schubert 1990).

Fig. 9.4 Highly joint-controlled "ruiniform" tower fields on the summit plateau of Kukenhan Tepui. Individual towers range from 3 m to 10 m in height (Photo S.H. Doerr)

Their widths are controlled by the distance between the joints and fractures, and their heights by the thickness of the bedding. Many of these towers are extensively perforated by tafoni, and undercut "mushroom-like" rocks are widespread.

A whole variety of smaller minor features are superimposed on these larger forms, including weathering pits and pans, rills and fluted surfaces, case-hardened crusts, and other residual erosion forms (White et al. 1966; Urbani and Szczerban 1974; Chalcraft and Pye 1984; Pouyllau and Seurin 1985; Briceño and Schubert 1990; Briceño et al. 1990; Doerr 1999).

9.4.5 Caves

The existence of extensive quartzite caves and huge collapse shafts over 300 m deep (Fig. 9.5) within the tepui has been known for a long time, with rivers disappearing into sinkholes, caves (Fig. 9.6), and depressions so large that they resemble poljes. The water reappears on the cliff walls hundreds of meters below the summit plateaus.

Systematic exploration and documentation began in the mid-1970s (Urbani and Szczerban 1974; Pouyllau and Seurin 1985), and recent explorations have revealed extensive caves many kilometers in length; the Roraima Sur – Los Ojos de Cristal cave system, for example, in the western part of Roraima is 10.8 km long with passages up to 20 m in diameter (Galán et al. 2004). Other long and deep Gran Sabana quartzite caves are listed in Table 9.1. Cave planforms are controlled by joints, and bedding influences horizontal development. Within many of these caves are extensive speleothem deposits of silica and other minerals (Urbani 1976; Aubrecht et al. 2008).

9.5 Evolution

The evolution of the quartzite landscape of the Gran Sabana has been a very long-term process. The rocks are very ancient, the region geologically stable, and the highest planation surfaces, forming the tepui summits and the plains of the surrounding Gran Sabana have been exposed for more than 70 million years, probably

Fig. 9.5 Joint-controlled collapse shaft more than 50 m deep on the summit plateau of Kukenhan Tepui (Photo S.H. Doerr)

Fig. 9.6 Entrance to *Cueva Kukenhan*. Note the stream flowing into the cave and the rounded quartzite columns 2–3 m in height that continue along much of the underground cave passage (Photo S.H. Doerr)

since the mid-Mezozoic (Jurassic?) (Briceño and Schubert 1990; Briceño et al. 1990). It is this aspect of very, very, long periods of time for weathering, longer than most places on Earth, which is probably critical for the development of the striking landscapes of the Gran Sabana.

Climate is also important on the erosional processes. The high rainfall contributes to the chemical solution of these highly quartzose rocks, and the large volumes of flowing water rapidly remove dissolved silica and weathered clastic material.

However the origin of the caves and other karst forms is a little problematic. The solubility of quartz is quite low, and field measurements suggest that dissolved silica concentrations in surface waters on the tepui summits are very low (generally less than 1 mg/l) (Pouyllau and Seurin 1985; Briceño et al. 1990; Piccini 1995; Mecchia and Piccini 1999), surprising given the widespread occurrence of solutional forms. Although silica concentrations are low, rates of silica removal may nevertheless be quite considerable because of the very high rainfall and rapid runoff of large volumes of

Table 9.1 The longest and deepest quartzite caves and shafts of the Gran Sabana Roraima Group, Guyana Shield (Carreño and Blanco 2004; Galán et al. 2004, Audy and Šmída n.d.)

Cave system	Length (km)	Depth (m)
Sistema Roraima Sur	10.8	72
Cueva Ojos de Cristal	5.3	72
Cueva Charles Brewer	4.8	110
Sima Auyán-*tepui* Noroeste	2.9	370
Cueva del Diabolo	2.3	–
Sima Aonda Superior	2.13	320
Sima Aonda	1.88	383
Sima Acopán 1	1.38	90
Sima de la Lluvia	1.35	202
Sima Menor	1.16	248
Sima Aonda 2	1.05	325

water from the tepuis' summits (Chalcraft and Pye 1984; Piccini 1995; Mecchia and Piccini 1999). Multiply this by the extremely long periods of time involved, and the amount of silica actually removed may be quite high (Doerr 1999).

White et al. (1966) suggested that the rate of weathering of the Roraima quartzites might be enhanced by the conversion of the low-solubility quartz cement to far more soluble opal. However, most authors now agree (Chalcraft and Pye 1984; Briceño and Schubert 1990; Briceño et al. 1990; Yanes and Briceño 1993; Piccini 1995; Doerr 1999; Mecchia and Piccini 1999; Galán et al. 2004) that the process responsible for karst development is the intergranular corrosion (solution) of quartz cement and grain surfaces with the subsequent mechanical removal of loose weathered grains by flowing water, "arenisation" in the terms of Martini (2000). Arenised rock breaks down to sand and is easily removed by flowing water. However, on the surface runoff waters do not have enough time to dissolve the silica cement of the arenite, and the alternation of wet and dry conditions actually leads to the formation of hard crusts of silica cement and iron oxides which protect the rock surface. Arenisation acts most effectively along the joints in the subsurface, where circulating water has a greater time of reaction between water and rock than water flowing over the surface.

Briceño and Schubert (1990) have also argued that the Roraima cliffs and other landforms are essentially fossil, and attribute them to arid conditions during Pleistocene glacial periods. Young and Young (1992) and Young et al. (2009), however, believe this explanation raises more problems than it solves. They note that Briceño and Schubert (1990) compared the Roraima with the cliffed landscape of the arid southwest of the United States, but suggested that the similarity is mainly due to lithological and structural constraints, rather than to climatic control. The massively bedded and jointed Roraima quartzites and sandstones have a very high mass strength rating, and can therefore be expected to form extremely steep slopes. Moreover, appeals to arid climates to explain the cliffs are difficult to reconcile with the widespread and well-developed karst features on the tepui summits and on the faces of the cliffs themselves. Young and Young (1992) and Young et al. (2009) believe that such solutional features would not be expected within a morphoclimatic zone characterized by minimal chemical weathering.

The formation of a well-developed karst landscape on these tepui has therefore been possible because the environmental conditions have limited the effects of mechanical weathering, allowing – over a very long time – the strong development of solution forms. Mechanical processes are active, but their effects are mostly concentrated along the streams and fracture zones, especially near the border of the plateau, and inside the active caves. A combination of factors has therefore allowed the intense karstification in these quartzites (Doerr 1999):

- Although the unweathered rock may be of very low porosity, a dense network of joints and microfissures has allowed water to infiltrate and initiate corrosion.
- The arenite is very pure. In rocks of a more heterogeneous mineralogy, fissures enlarged by corrosion may become clogged by weathering residue.
- High precipitation has countered the low total solubility of silica.
- There is little soil or other sediment to block passages and prevent further karstification.
- No other geomorphic processes such as glaciation, periglaciation, submergence under the sea, or frost weathering have interfered with karstification.
- Very long periods of sub-aerial exposure to weathering with stable geomorphic processes have been available for karstic development, for at least several tens of millions of years.

It is the relatively uncommon combination of these factors in the Gran Sabana, which has led to the spectacular tepui and their highly developed quartzose karst landscapes.

9.6 Conclusions

The quartzite table-mountain landscape of the Gran Sabana is one of the best examples of its kind in the world. Its outstanding value stems from two circumstances. First, it is the size of individual landforms present here. The tepui are among the tallest and visually most striking known, the landscapes are among the oldest, the quartzite karst the best-developed and the caves some of the largest and deepest. Second is the geomorphological diversity. Examples of virtually any karst landforms described from limestone terrains can be found here, in quartzite – one of the least soluble of rocks, in a close coexistence with each other. Finally, the Gran Sabana and particularly its tepui, has a superlative scenic and aesthetic beauty, and has been recognized by UNESCO as a World Heritage site since 1994; its remoteness and often-poor accessibility possibly make it the most poorly explored of the great geomorphological landscapes.

The Author

Dr **Robert Wray** is a Fellow in the School of Earth and Environmental Sciences, University of Wollongong, in Australia. His research concerns long-term landform evolution, sandstone geomorphology, sandstone and quartzite karst geomorphology, and conservation of geomorphological heritage. His previous publications include coauthoring of *Sandstone Landforms* (2009), an entry in the *Encyclopaedia of Geomorphology* (2004), and more than 20 peer-reviewed papers.

References

Aubrecht R, Brewer-Carías C, Šmída B, Audy M, Kovácik L (2008) Anatomy of biologically mediated opal speleothems in the world's largest sandstone cave Cueva Charles Brewer, Chimantá Plateau, Venezuela. Sediment Geol 203:181–195

Audy M, Šmída B (n.d.) Speleologie v kvarcitových masivech. Retrieved 4 September 2007, from http://audy.speleo.cz/quarzit/index.html

Briceño HO, Schubert C (1990) Geomorphology of the Gran Sabana, Guyana Shield, Southeastern Venezuela. Geomorphology 3:125–141

Briceño HO, Schubert C, Paolini J (1990) Table-mountain geology and surficial geochemistry: Chimantá Massif Venezuelan Guyana Shield. J S Amer Earth Sci 3: 179–194

Carreño R, Blanco F (2004) Notas sobre la exploración del sistema kárstico de Roraima Sur, Estado Bolívar. Bol Soc Venezolana Espeleología 38:45–52

Chalcraft D, Pye K (1984) Humid tropical weathering of quartzite in southeastern Venezuela. Z Geomorph NF 28:321–332

Doerr SH (1999) Karst-like landforms and hydrology in quartzites of the Venezuelan Guyana shield: Pseudokarst or real karst? Z Geomorph NF 43:1–17

Galán C, Herrera F, Carreño R, Pérez MA (2004) Roraima Sur System, Venezuela: 10.8km, World's longest quartzite cave. Bol Soc Venezolana Espeleología 38:53–60

George U (1989) Venezuela's islands in time. Nat Geogr 175:526–561

Martini JEJ (2000) Dissolution of Quartz and Silicate minerals. In: Klimchouk A, Ford DC, Palmer AN, Dreybrodt W (eds) Speleogenesis – evolution of karst aquifers. NSS, Huntsville, pp 171–174

Mecchia M, Piccini L (1999) Hydrogeology and SiO_2 geochemistry of the Aonda cave system, Auyán-Tepui, Boívar, Venezuela. Bol Soc Venezolana Espeleología 33:1–18

Piccini L (1995) Karst in siliceous rocks: Karst landforms and caves in the Auyán-tepui massif, Bolivar, Venezuela. Int J Speleol 24:2–13

Pouyllau M, Seurin M (1985) Pseudo-karst dans des roches gréso-quartzitiques de la formation Roraima. Karstologia 5:45–52

Tate GHH (1938) Notes on the Phelps Venezuelan expedition. Geogr Rev 28:452–474

Urbani F (1976) Opalo, Calcedonia y Calcita en la Cueva del Cerro Autano (Am 11), Territorio Federal Amazonas, Venezuela (in Spanish, English summary). Bol Soc Venezuela Espeleologia 7(14):129–145

Urbani F, Szczerban E (1974) Venezuelan caves in non-carbonate rocks: a new field in karst research. NSS News 32:233–235

White WB, Jefferson GL, Haman JF (1966) Quartzite karst in southeastern Venezuela. Int J Speleol 2:309–316

Wray RAL (1997a) A global review of solutional weathering forms on quartz sandstone. Earth Sci Rev 42:137–160

Wray RAL (1997b) Quartzite dissolution: Karst or pseudokarst? Cave Karst Sci, Trans Brit Cave Res Assoc 24(2):81–86

Yanes CE, Briceño HO (1993) Chemical weathering and the formation of pseudo-karst topography in the Roraima Group, Gran Sabana, Venezuela. Chem Geol 107:341–343

Young RW, Young ARM (1992) Sandstone landforms. Springer, Berlin

Young RW, Wray RAL, Young ARM (2009) Sandstone landforms. Cambridge University Press, Cambridge

Chapter 10
Rio de Janeiro: A Metropolis Between Granite-Gneiss Massifs

Nelson F. Fernandes, Miguel Tupinambá, Claudio L. Mello, and Maria Naíse de O. Peixoto

Abstract The city of Rio de Janeiro is well-known for its outstanding landscape, particularly the several steep rocky domes that emerge close to the coast. Such a wonderful scene results from a combination of differential weathering controlled by the presence of a variety of Neoproterozoic gneisses and Cambrian granites and strong valley incision along subvertical faults and fractures. In this chapter we present the geological and geomorphological aspects that influence the daily life of more than 12 million inhabitants of the Rio de Janeiro metropolitan region, in two areas around Guanabara Bay: Coastal Massifs and the Serra dos Órgãos escarpment. The combination of such topographic constraints, intense summer rainstorms, and dense occupation frequently creates a scenario with a high potential for landslide-derived hazards.

Keywords Differential weathering • Guanabara Bay • landscape evolution • landslides • Sugar Loaf

10.1 Introduction

The city of Rio de Janeiro, located in southeastern Brazil, is known as the "Wonderful City," largely due to its outstanding geomorphological landscape. This scene is basically characterized by the majestic Guanabara Bay surrounded by stepped mountains, many of them consisting of steep rocky walls (Fig. 10.1), resulting from differential landscape dissection controlled by the presence of a variety of Neoproterozoic gneisses and granites, crossed by many faults and fractures, mostly subvertical. The magnificence of such topography impressed the first Portuguese sailors who navigated through the entrance of Guanabara Bay in January of 1502, passing just around the nowadays famous Pão de Açúcar (Sugar Loaf) hill. In fact, because they thought that the bay was the mouth of a large river (rio), they called the city Rio de Janeiro.

More than 12 million people live today in the Rio de Janeiro metropolitan area. Situated mostly on a coastal plain, this heavily urbanized area spreads around Guanabara Bay, between isolated granitic and gneissic massifs and toward a 2,000 m high escarpment separating the coastal plain and the interior plateau (Fig. 10.2). For people living at the foothills of these granitic domes and peaks, geological and geomorphological local conditions are vital for their safety and health. In this chapter, we present some impressive examples to show the importance of geoscience in the daily life of the urban area, introducing also some of the most spectacular geomorphological elements of the landscape. At the same time that these natural monuments are fascinating, their high suitability to trigger catastrophic mass movements must be understood and respected.

10.2 Geological and Geomorphological Evolution

The geological history of Rio de Janeiro and adjacent areas is related to the evolution of a tectono-metamorphic belt (Ribeira Belt) that covers a large area along the South Atlantic Brazilian coast (Fig. 10.2a). This belt originated during the Neoproterozoic-Ordovician collision and terrain accretion of the Western Gondwana Supercontinent (see review in Heilbron et al. 2008). In the vicinity of Rio de Janeiro (Fig. 10.2b and 10.2c), the oldest outcropping rocks are Meso- to Neoproterozoic garnet-cordierite metapelitic gneisses and calc-silicate rocks. Several metamorphosed Neoproterozoic syn- to

P. Migoń (ed.), *Geomorphological Landscapes of the World*,
DOI 10.1007/978-90-481-3055-9_10,

Fig. 10.1 General view of the steep rock walls around the southern part of Rio de Janeiro city. In this view, taken from the entrance of the Guanabara Bay looking towards the west one can observe the Sugar Loaf in the foreground, Copacabana Beach on the left side, and the Gávea Rock with its flat granitic top on the upper right corner (Photo R. Azoury)

late-tectonic plutonites (orthogneisses) crosscut the metasedimentary sequence. Cambrian to Ordovician post-tectonic granite plutons, dikes, and sills are related to the tectonic collapse of the Ribeira Orogen (Tupinambá et al. 2003; Valeriano et al. 2003).

The area was later subjected to tectonic reactivation during the Cretaceous and the Palaeogene, associated with the Gondwana fragmentation and the opening of the South Atlantic Ocean (Ferrari 2001; Riccomini et al. 2004). This tectonism was followed by tholeiitic magmatism, characterized by NE trending diabase dikes, dated from 138 to 135 Ma[1] (Guedes et al. 2005). The alkaline magmatism is represented by several plutonic bodies dated from Late Cretaceous to Palaeogene and numerous dikes, with the main intrusions basically constituted by syenite and nepheline-syenite (Ferrari 2001). The resulting ensemble of tectonic valleys, sedimentary basins, and mountains was called by Riccomini et al. (2004) the Continental Rift of Southeastern Brazil. This geotectonic entity shows a NE–SW strike, is transversely segmented and, according to these authors, originated through crustal stretching during the Palaeogene, associated with tectonic tilting of the adjacent oceanic Santos basin.

The normal faults of Meso-Cenozoic age are responsible for the topographic partitioning of the area (Fig. 10.2b) that has led to the raising and lowering of adjacent crustal blocks. One tectonic block raised high is represented by the Serra dos Órgãos (the local name of the Serra do Mar) escarpment. This regional structure may represent the retreat of the Cretaceous South Atlantic rift border (e.g., Gallagher et al. 1995; Almeida and Carneiro 1998) or the dissected front of a Cenozoic fault (e.g., Asmus and Ferrari 1978). Coastal massifs, as the Sugar Loaf that will be discussed later, are located along smaller and less elevated blocks.

The Guanabara Graben (Almeida 1976; Ferrari 2001), one of the segments of the Continental Rift of Southeastern Brazil, is situated at a NE trending lower

[1] Ma stands for "million years ago"

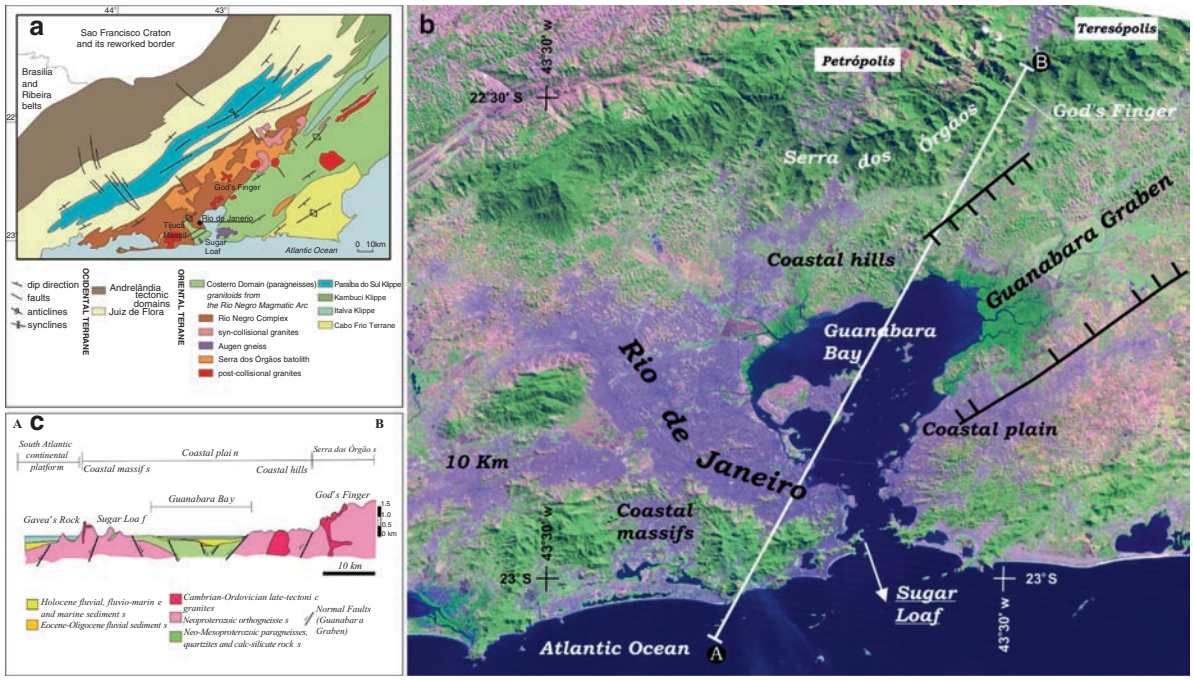

Fig. 10.2 Geological setting of Rio de Janeiro. (**a**) Tectonic map of part of southeastern Brazil showing the main divisions of the Central Ribeira Belt (Modified from Heilbron and Machado 2003). (**b**) LANDSAT image of the Rio de Janeiro metropolitan area with Rio de Janeiro urban area in light violet, geomorphological domains indicated as coastal massifs, hills and plains, and the Serra dos Órgãos escarpment, main normal faults of the Guanabara Graben (indentation in the lower block), location of the God's Finger and Sugar Loaf (see text), and location of cross-section profile. (**c**) Geological-geomorphological cross section: normal faults along the section taken from the geological map by Ferrari (2001); Holocene sediments, granites, and gneiss distributions taken from the map of Silva and Cunha (2001); Eocene-Oligocene sediments below the Holocene sediments at the bottom of the Guanabara Bay are extrapolated from northern outcropping similar sediments from the Macacu Basin (Ferrari 2001); granitic dikes and sills at the Gávea Rock (Modified from Motoki 1991)

block partially covered by the Guanabara Bay (Fig. 10.2b). Inside the graben, coastal hills and some isolated massifs were developed by partial denudation processes over tectonic blocks, and Eocene-Oligocene fluvial sediments spread along flattened areas. Marine and alluvial sediments of Holocene age cover the coastal plains, which are now almost completely urbanized. Proximal alluvial fans at the foothills of the Coastal Massifs are also densely populated.

10.3 The Coastal Massifs

Such a complex geologic background controlled subsequent erosion and landscape dissection, leading to an impressive agglomeration of steep rock escarpments and domes, generally called sugar loaves, throughout the Coastal Massifs (Fig. 10.1). The Sugar Loaf is certainly the most famous postcard of Brazil, well-known worldwide (Fig. 10.3). The typical view of this monument shows two hills side by side: Sugar Loaf Hill (392 m) on the left and Urca Hill (222 m) on the right. It is this scene that astonished Charles Darwin, who wrote in 1832 that "nothing can be more striking than the effect of these huge rounded masses of naked rock rising out of the most luxuriant vegetation." In 2000, during the 31st International Geological Congress, a memorial tablet with its geochronological dating was installed there (Silva and Ramos 2002), recognizing it as one of the main sites of geological interest around the world.

The Sugar Loaf has an intimate relationship with the history of the city of Rio de Janeiro. The city was initially established by a Portuguese exploratory mission in 1565 at the entrance of Guanabara Bay, in an area between the Sugar Loaf and the Cara de Cão Hill

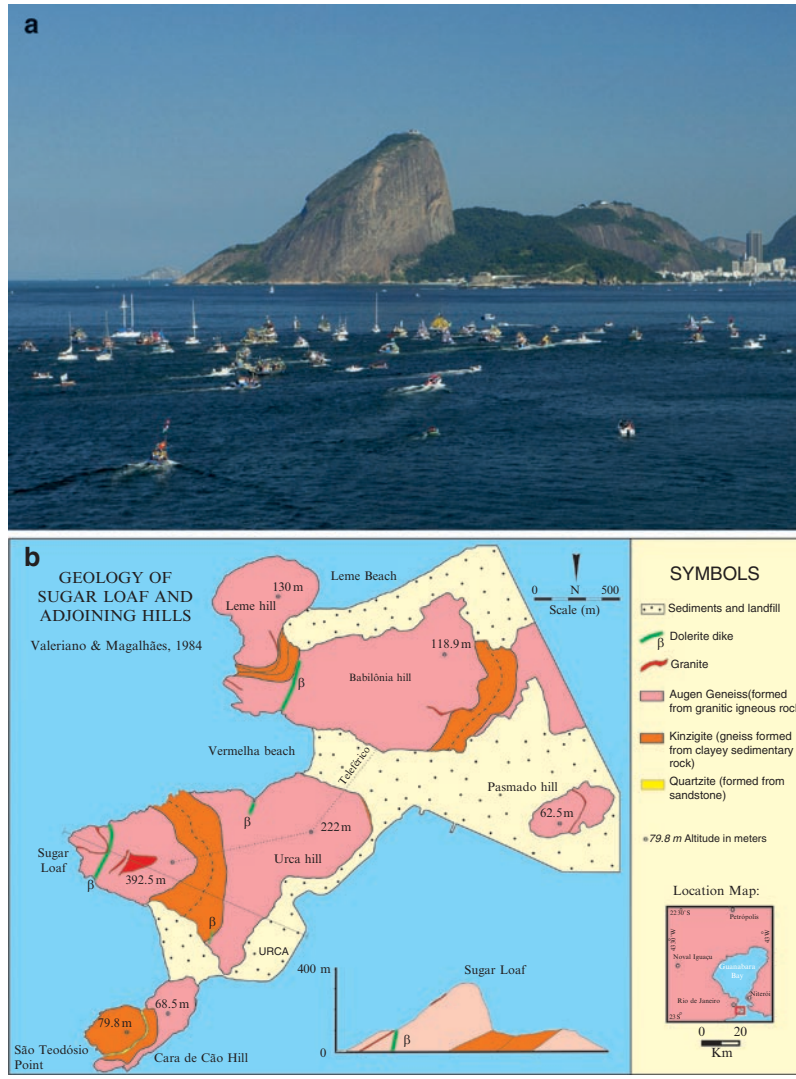

Fig. 10.3 (**a**) General view of the Sugar Loaf and (**b**) a simplified geologic map of the area presented by Valeriano and Koga (2006). The picture on the top shows the Sugar Loaf (*left*) and the Urca Hill (*right*) close to the entrance of the Guanabara Bay (Photo A. Teixeira)

(Fig. 10.3). In fact, viewing from the sea, one can say that the Rio de Janeiro city really starts at the Sugar Loaf (see Fig. 10.1). Since 1913, a cable car system connects Urca Hill and the Sugar Loaf, allowing visitors to have a wonderful 360° panoramic view of the city and the bay. Although there is some controversy concerning the origin of the name, the official version considers that it was derived from the similarity of the topography with the conical form of sugar cones, known as sugar loaves, used to preserve sugar during transport from Madeira Island to Europe in the sixteenth century, and later from Brazil.

In basic terms, the geology at the western part of the entrance of the Guanabara Bay, including the Sugar Loaf and its vicinity, is represented by Meso-Neoproterozoic high grade metasedimentary rocks intruded by Neoproterozoic syn- to post-tectonic granitoid rocks and thin Cretaceous diabase dikes (Silva and Ramos 2002; Valeriano et al. 2003). Unloading fractures are usually present in these rocks and play a major role in controlling hillslope evolution. The main outcropping rocks at the Sugar Loaf are metapelitic gneiss (kinzigite) and augen gneiss, a deformed and recrystallized porphyritic granite that intruded the

kinzigite (Silva et al. 2003; Valeriano et al. 2003). Because the kinzigite is less resistant to weathering and erosion than the augen gneiss, the former usually forms topographic depressions if they occur side by side. This is exactly the case in the typical picture of the Sugar Loaf postcard, where the kinzigite gneiss is present in the depression between Urca Hill and the Sugar Loaf, which is composed of more resistant granitoid rocks (Fig. 10.3). A thin dike of post-tectonic granite controls the angle of the eastern hillslope of the Sugar Loaf, as depicted in the geological cross section of Fig. 10.3.

The two famous peaks, the Sugar Loaf and Urca Hill, represent typical outcrops of augen gneiss, the most important lithology in the southern part of the city. This syn-tectonic granitoid controls most of the steep buttress-like rock walls of the city (Fig. 10.1). The post-tectonic granite that outcrops in the Sugar Loaf also forms granitic caps that are well-preserved at the top of some hills and distinctly influence their geometry, like in the Gávea Rock (Figs. 10.4 and 10.5). This impressive geomorphological feature is basically constituted at the base by augen gneiss and is capped by about 150 m of granite (Motoki 1991).

Geomorphology has played a major role in controlling the spatial and temporal patterns of human occupation in the city of Rio de Janeiro, especially during the past few centuries. Although the city initially spread out across the coastal plains and interior lowlands, later it extended its limits toward the steep hillslopes of the so-called Coastal Massifs, characterized by thin soils, highly heterogeneous slope deposits

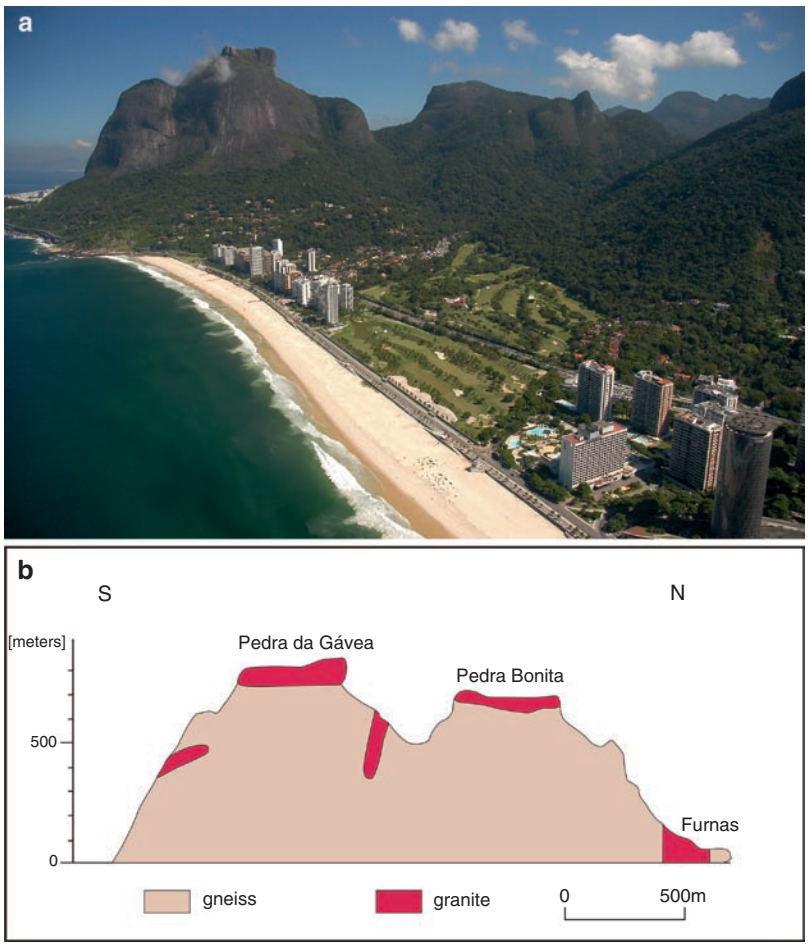

Fig. 10.4 General view of São Conrado beach (**a**) with the Gávea Rock (Pedra da Gávea) in the left corner (Photo A. Valentim). The simplified geologic profile (**b**) shows the granitic cap overlaying the gneiss (Motoki 1991)

Fig. 10.5 Detailed view of the contact at the top of the Gávea Rock (looking toward south) shown in Fig. 10.4b. The "face" results from differential weathering, with the "eyes" situated close to the contact between granite (*top*) and gneiss (Photo W. de Moura)

(talus), and granite gneiss domes. This is the case of many impressive slums that were established in these massifs, especially after the 1950s, without the minimum required infrastructure, like the Vidigal slum close to Ipanema beach (Fig. 10.6), where more than 10,000 people live today.

Today, such topographic constraints combined with a continuously growing dense occupation lead to a variety of environmental problems including catastrophic landslides. Although the oldest records of deaths associated with landslides and flooding in the city can be traced back to the early 1700s, it was only in 1966 and 1967 that the city was intensively affected by catastrophic mass movements for the first time (Jones 1973). Since then, major landsliding events have become more frequent (e.g., in 1987, 1988, 1996, 2002) causing considerable economic losses and many fatalities. According to Amaral (2004), since 1930 more than 500 people have been killed by different types of landslides in the city. On February 1996, during an intense summer rainstorm, hundreds of shallow landslides were triggered in the upper portions of the

Fig. 10.6 Aerial view of the Vidigal slum that expanded over the hillslopes of the Dois Irmãos (Two Brothers) Hill, located between Ipanema/ Leblon and São Conrado beaches. This view is toward the west and the Gávea Rock can be seen at the top left corner (Photo J.R. Couto)

steep soil-mantled hillslopes, most of them under natural forest. These shallow translational landslides had a strong topographic control (Fernandes et al. 2004) and converged downhill toward the valleys, initiating huge debris flows that produced catastrophic consequences in the densely occupied lowlands at the base of the escarpments (Fig. 10.7).

10.4 The Serra Dos Órgãos Escarpment

As previously discussed, the northern limit of the Guanabara Graben is defined by the Serra do Órgãos, a local name for the Serra do Mar between the cities of Petrópolis and Teresópolis in the highlands of Rio de Janeiro state (Fig. 10.2). It is believed that this name derives from the similarity of its vertically elongated topographic forms with the tubes of an organ, typical of the churches at the time of Portuguese colonization. Along the Serra dos Órgãos escarpment (Fig. 10.8), over about 4 km of horizontal distance, the elevation varies from 2,260 m a.s.l. at the top of the plateau to about sea level in the coastal plain.

Among the several steep rock walls formed in this escarpment, the Dedo de Deus (God's Finger) and its adjacent peaks are by far the most striking, representing one of the most impressive geomorphological feature of southeastern Brazil (Fig. 10.9). On a clear day, the God's Finger (1,692 m) and the Escalavrado (1,490 m) peaks can be seen from many distant places in Rio de Janeiro city, like the Sugar Loaf (about 50 km away). In the same way, they can usually be seen just after taking off from Rio de Janeiro International Airport, since the airport was built inside the Guanabara Graben not far from this area.

The unique geomorphic situation of the God's Finger geological monument is due to the combination of structural and lithological constraints, as initially proposed by Junho and Penha (1985) and later popularized

Fig. 10.7 Upper portion of a valley affected by debris flows in the Tijuca Massif (one of the Coastal Massifs) that occurred in 1996. Shallow landslides were triggered under forest and converged in the main valley initiating a huge debris flow that led to great destruction downslope (Photo N. Fernandes)

by Tupinambá and Medeiros (2005). A NW fracture set observed at the exposed rock surfaces of the plateau controls the direction of valleys and ridges in the river basins along the Serra dos Órgãos escarpment. One of these NW trending ridges is fully ornamented with granitic peaks, among them being the God's Finger (Fig. 10.9). Additionally, the NW structures are cut at right angles by regularly spaced (about 500 m) NE vertical fractures. Strong erosional incision along these fractures dissected the topography and lowered the summit line of the NW trending ridges, leaving elevated massive rock blocks between eroded fractured zones (Figs. 10.8 and 10.9).

Although the interplay between the two sets of vertical fractures occurs in many other drainage basins at the Serra dos Órgãos escarpment, the rocky towers of the God's Finger occurs in only one ridge. In this case, differential erosion plays the complementary role since a thick dike of Cambrian equigranular to porphyritic post-tectonic granite sustains the ridge (Fig. 10.9).

Fig. 10.8 Aerial view of the Serra dos Órgãos Escarpment close to Teresópolis city (see Fig. 10.2). In the foreground one can observe the BR-116 road passing through the huge barrier imposed by the Escalavrado and Dedo de Deus peaks while the 2,000 m high plateau is in the background. A geological cross section along this escarpment is presented in Fig. 10.9 (Photo by L.C. Marigo)

This granite is more resistant to weathering than the country rocks, two types of Neoproterozoic orthogneisses.

As presented in the geological cross section of Fig. 10.9, leucogranitic gneiss dips at 80° to the SE at the foothills of the Serra dos Órgãos escarpment. To the interior of the range, the foliation changes to a gentle NW dipping structure. In the higher parts of the escarpment, there is a concordant contact between the leucogranitic gneiss and hornblende biotite gneiss from the Serra do Órgãos Batholith (see Tupinambá et al. 2003 for more details). The granite structure is discordant to the gneissic foliation and contacts. At the base of the Escalavrado Peak, the post-tectonic granite presents a vertical contact at the SE part of the ridge, probably a feeder dike, as denoted by the presence of numerous angular dioritic autholiths. Along the ridge, the granite dike dips to the SE, outcropping as erosional relicts at the summit of God's Finger and higher peaks. The contact of the granite dike does not fit along the ridge since the southeastern portion is less elevated than the northeastern end. The apparent offset suggests that at least some of the NE trending fractures may be normal faults. Unfortunately, the steepness of the terrain as well as the presence of a dense tropical forest did not allow further detailed fieldwork along the granite contact.

Landscape evolution in this area, including the development of granitic towers, was mainly controlled by intensive mass movement processes, especially rock falls along the fractured walls, as denoted by the presence at the base of the escarpment of thousands of angular boulders some tens of meters across. Besides, intensive valley incision by debris flows has taken place in the drainage basins in the long term, as indicated by well-preserved huge debris flow deposits. Recently, in November 1981, hundreds of shallow landslides and many debris flows were triggered in this escarpment after an intensive rainy period (more than 300 mm in a

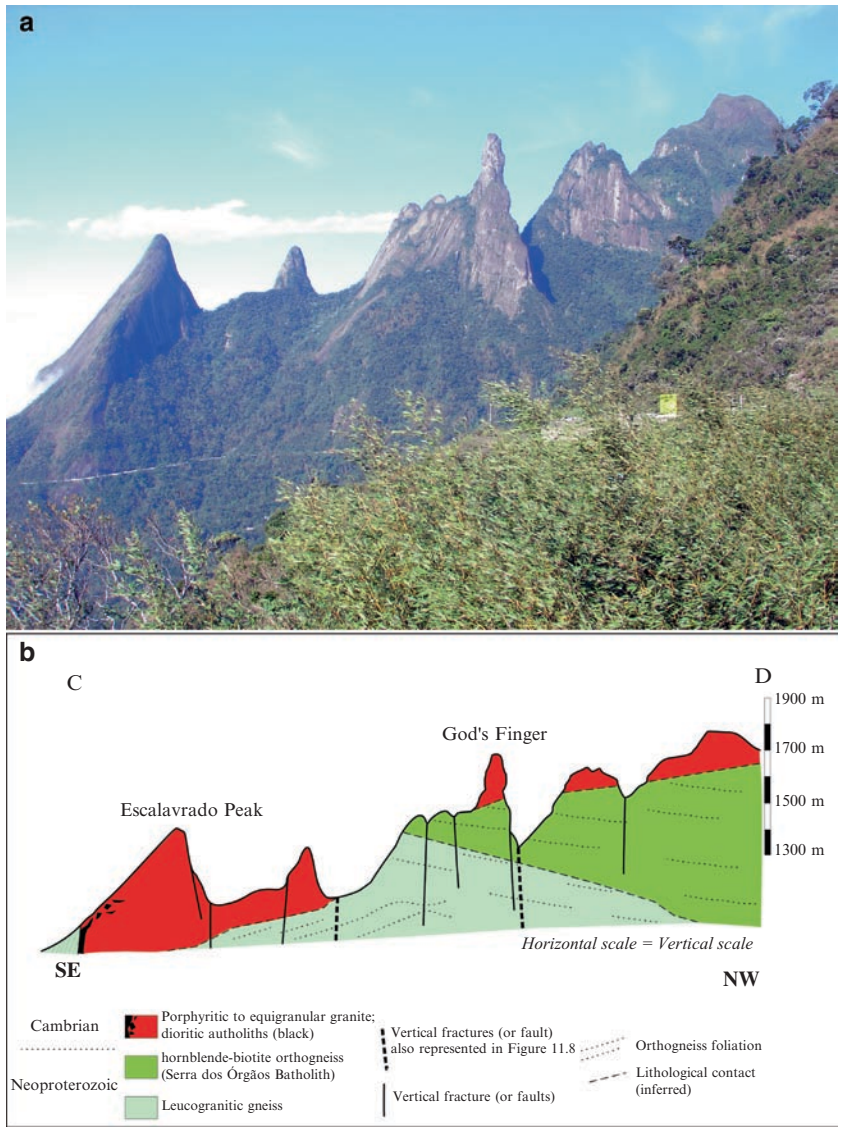

Fig. 10.9 (**a**) Detailed view of the Serra dos Órgãos escarpment with the Dedo de Deus (God's Finger) Peak at the center (Photo M Tupinambá). The picture was taken from the Soberbo viewpoint at the entrance of Teresópolis city (see Fig. 10.2b). (**b**) Geologic profile showing the main lithologies and structures observed. Neoproterozoic orthogneisses are intruded by Cambrian post-tectonic discordant granite which caps most of the peaks of the ridge (Modified from Junho and Penha 1985 and Tupinambá et al. 2003)

few hours), killing about 20 people along the BR-116 road and leading to a complete traffic interruption for some weeks (Fernandes and Meis 1982). As in many other places around the world, there is here an intrinsic relationship between natural splendor and danger. The BR-116 road along the Serra dos Órgãos Escarpment, as presented in Fig. 10.8, crosses one of the most beautiful natural sceneries in Brazil, which in turn has a high potential for landslide-derived hazards.

The Authors

Nelson Fernandes is Professor in the Department of Geography in the Geosciences Institute, Federal University of Rio de Janeiro, Brazil. His main research topics are landscape evolution, soil hydrology, soil erosion, and landslide prediction. He has published more than 30 peer-reviewed papers and supervised more than 25 graduate students. During the period 2003–2004

he served as the President of UGB (Brazilian Geomorphological Union).

Miguel Tupinambá is Professor in the Department of Regional Geology and Geotectonics in the Faculty of Geology at the Rio de Janeiro State University, Brazil. His research deals with plutonic and high-grade metamorphic rocks from the Ribeira Belt, in southeastern Brazil. At present he is working on granite emplacement and granite geomorphology, with the support of field mapping, petrography, lithogeochemistry, geophysics, and geochronology.

Claudio Limeira Mello is Professor in the Department of Geology in the Geosciences Institute, Federal University of Rio de Janeiro, Brazil. His main research topics are the Cenozoic evolution of southeastern Brazil, including the relationship between Neotectonics and landscape evolution. He has published more than 15 peer-reviewed papers and counseled more than 20 graduate students. During the period 1997–1998 he served as a Director of ABEQUA (Brazilian Association of Quaternary Research).

Maria Naíse de O. Peixoto is Professor in the Department of Geography in the Geosciences Institute, Federal University of Rio de Janeiro, Brazil. Her research deals with Quaternary geomorphology in southeastern Brazil, focusing on slope and valley evolution, soil erosion, and Quaternary mapping. She has published about ten peer-reviewed papers and supervised 8 graduate students.

Acknowledgments The authors would like to thank Katia Mansur and DRM-Departamento de Recursos Minerais/RJ (Department of Mineral Resources of Rio de Janeiro State) for allowing the use of material from posters (Tupinambá and Medeiros 2005, Valeriano and Koga 2006) of the Geological Trails Project. The main objective of this project is to popularize geological science by implementation of interpretative posters in the main geological monuments of the state (see http://www.drm.rj.gov.br). We also thank Ricardo Azoury, Carla Madureira Cruz, André Teixeira, William de Moura, J. R. Couto and Luiz Claudio Marigo who allowed us to use their photographs and images in this chapter.

References

Almeida FFM (1976) The system of continental rifts bordering the Santos Basin. An Acad Bras Ciências 48(Suppl.):15–26

Almeida FFM, Carneiro CDR (1998) Origem e evolução da Serra do Mar. Rev Brasil Geociências 28(2):135–150

Amaral C (2004) Geological factors triggering landslides in Rio de Janeiro: basic criteria for landslide risk assessment. In: Lacerda WA, Ehrlich M, Fontoura SAB, Sayão ASF (eds) Landslides: Evaluation and stabilization, vol 1. Taylor and Francis Group, London, pp 419–423

Asmus HE, Ferrari AL (1978) Hipótese sobre a causa do tectonismo cenozóico na região Sudeste do Brasil. In: Aspectos Estruturais da Margem Continental Leste e Sudeste do Brasil. Petrobrás**,** Rio de Janeiro, pp 75–88

Fernandes NF, Meis MRM (1982) Mass movements in the Serra do Mar, Teresópolis (RJ). In: Proceedings of the V International Geographical Union, Commission on Field Experiments in Geomorphology, Rio de Janeiro, Brazil

Fernandes NF, Guimarães RF, Gomes RAT, Vieira BC, Montgomery DR, Greenberg HM (2004) Topographic controls of landslides in Rio de Janeiro: Field evidence and modeling. Catena 55:163–181

Ferrari AL (2001) Evolução tectônica do Graben da Guanabara. Ph.D. thesis, Instituto de Geociências, Universidade de São Paulo

Gallagher K, Hawkesworth CJ, Mantovani MSM (1995) Denudation, fission track analysis and the long-term evolution of passive margin topography: Application to the southeast Brazilian margin. J S Amer Earth Sci 8:65–77

Guedes E, Heilbron M, Vasconcelos PM, Valeriano CM, Almeida JCH, Teixeira W, Thomaz Filho A (2005) K-Ar and $^{40}Ar/^{39}Ar$ ages of dikes emplaced in the onshore basement of the Santos Basin, Resende area, SE Brazil: implications for the south Atlantic opening and Tertiary reactivation. J S Amer Earth Sci 18:371–382

Heilbron M, Machado N (2003) Timing of terrane accretion in the Neoproterozoic-Eopaleozoic Ribeira Orogen (SE Brazil). Precambrian Res 125:87–112

Heilbron M, Valeriano CM, Tassinari CCG, Almeida JCH, Tupinambá M, Siga Jr. O, Trouw RJA (2008) Correlation of Neoproterozoic terranes between the Ribeira Belt, SE Brazil and its African counterpart: Comparative tectonic evolution and open questions. In: Pankhurst RJ, Trouw RAJ, Brito Neves BB, De Wit MJ (eds) West Gondwana pre-Cenozoic correlations across the south Atlantic Region. Geol Soc London Spec Publ 294: 211–237

Jones FO (1973) Landslides of Rio de Janeiro and the Serra das Araras Escarpment, Brazil. US Geol Surv Prof Paper 697:1–42

Junho MCB, Penha HM (1985) Geologia e geoquímica preliminar dos granitos de Teresópolis, RJ. An. Acad. Bras. Ciências 57:53–62

Motoki, A. (1991). Granito da Pedra da Gávea, Sheet Subhorizontal ou Base de Plutão? In: 2º Simpósio de Geologia do Sudeste, São Paulo, SBG, pp. 155–160

Riccomini C, Sant'Anna LG, Ferrari AL (2004) Evolução geológica do Rift Continental do Sudeste do Brasil. In: Mantesso-Neto V, Bartorelli A, Carneiro CDR, Brito Neves BB (eds) Geologia do Continente Sul-americano: Evolução da Obra de Fernando Flávio Marques de Almeida. Beca, São Paulo, pp 383–405

Silva LC, Cunha HCS (coord) (2001) Geologia do Estado do Rio de Janeiro: texto explicativo do mapa geológico do Estado do Rio de Janeiro. CPRM, Brasília. CD-ROM

Silva LC, Ramos AJA (2002) Pão de Açúcar, RJ – Cartão Postal Geológico do Brasil. In: Schobbenhaus C, Campos DA, Queiroz ET, Winge M, Berbert-Born M (eds) Sítios Geológicos e Paleontológicos do Brasil. DNPM/CPRM, Comissão Brasileira de Sítios Geológicos e Paleobiológicos (SIGEP), Brasília, pp 263–268

Silva LC, McNaughton NJ, Hartmann LA, Fletcher IR (2003) Zircon U-Pb SHRIMP dating of the Serra dos Órgãos and Rio de Janeiro gneissic granitic suites: Implications for the (560 Ma) Brasiliano/Pan-African Collage. Rev Brasil Geociências 33:237–244

Tupinambá M, Medeiros F (2005) Teresópolis – The Serra dos Órgãos and the Dedo de Deus Peak. Geological Trails Project. DRM – Department of Mineral Resources, Rio de Janeiro State [online]. Available at: http://www.drm.rj.gov.br [retrieved Sept. 20, 2008]

Tupinambá M, Penha HM, Junho MCB (2003) Arc-related to post-collisional magmatism at Serra dos Órgãos region, Rio de Janeiro State, Brazil: Products of Gondwana assembly during the Brasiliano-Pan African Orogeny. In: Chaves H, Camozzato E, Loguercio S, Campos DA (eds) Field Trips of the 31st International Geological Congress. SBG/CPRM**,** Rio de Janeiro

Valeriano CM, Koga FH (2006) The Sugar Loaf Odyssey – Rocks tell their story. Geological Trails Project. DRM – Department of Mineral Resources, Rio de Janeiro State [online]. Available at: http://www.drm.rj.gov.br [retrieved Sept. 20, 2008]

Valeriano CM, Almeida JCH, Heilbron M (2003). Precambrian gneisses in Rio de Janeiro: from the Sugar Loaf to the Arpoador outcrops. In: Chaves H, Camozzato E, Loguercio S, Campos DA (eds) Field Trips of the 31st International Geological Congress. SBG/CPRM**,** Rio de Janeiro

Chapter 11
Iguazu Falls: A History of Differential Fluvial Incision

José C. Stevaux and Edgardo M. Latrubesse

Abstract The Iguazu Falls are one of the most beautiful in the world because of the combination of a high and wide structural step across a fluvial system with large water discharge and the tropical environmental location that sustains an exuberant forest and high biodiversity. The geology of the area consists of three layers of basalts that give a staircase-type shape to the falls. The Iguazu River is about 1,500 m wide above the falls and forms many rapids between rock outcrops and small islands. The falls have a sinuous arch-like head 2.7 km long, and part of water volume enters a canyon 80–90 m wide and 70–80 m deep, forming the spectacular "Garganta do Diabo" (Devil's Gorge). Part of river water enters the canyon by its left side and generates a front with 160–200 individual falls that form a unique wall of water during floods. Although no absolute ages exist on the evolution of the fluvial system, it has been suggested that the falls have been continuously wandering upstream to its present position by progressive headwater erosion at a rate of 1.4–2.1 cm/year in the last 1.5–2.0 million years. The falls are recognized as UNESCO World Heritage property and regarded as a Geomorphological Site by the Brazilian Commission of Geologic and Paleobiological Sites – SIGEP.

Keywords Iguazu falls • basalts • Paraná basin • World Heritage • Geomorphological Site

11.1 Introduction

Waterfalls are impressive geomorphological features with strong scenic value. Considering that South America is drained by huge and complex drainage systems, especially in tropical areas, and that the largest South American rivers contribute to 28% of the total fresh water to the oceans, waterfalls and long series of rapids are common features in South American landscapes. The continent hosts the highest fall on Earth, Angel Falls in the Gran Sabana of Venezuela, and the mightiest one – according to many – the Iguazu Falls (Fig. 11.1). The name Iguazu comes from the Tupi-Guarani native language and means Great (*guassu*) Water (*y*).

Without any doubt, the world famous Iguazu Falls are the most spectacular waterfall of South America and one of the most beautiful worldwide due to a combination of remarkable factors: the existence of a high and wide structural step across a fluvial system with large water discharge and the tropical environmental location that sustains an exuberant forest and high biodiversity.

The falls developed across the Iguazu River and are located at the border of Argentina and Brazil (Figs. 11.2, 11.3). The area is covered by tropical forest and the mean annual rainfall is 1,712 mm. The relief oscillates between 100 and 300 m a.s.l. The falls are part of the Bi-National Park of Iguazu (Argentina and Brazil). The Argentinean park was created in 1934 and the Brazilian park in 1939 and both spread on near 2,500 km^2. The Argentinean area was recognized as UNESCO World Heritage in 1984 and 2 years later, in 1986, the site was extended to include the Brazilian side as well. Iguazu Falls are regarded as a Geomorphological Site by the Brazilian Commission of Geologic and Paleobiological Sites – SIGEP (Salamuni et al. 2002). With an annual mean of 1.5 million visitors, the falls are among the main tourist spots for both countries.

The Iguazu River rises near the Atlantic Ocean in the Serra do Mar range (c 900 m a.s.l.) and drains a basin of 78,800 km^2. It runs for 1,300 km (1,205 km in Brazilian territory and 105 km along the Argentinean–Brazilian border) and joins the Paraná River as its left

P. Migoń (ed.), *Geomorphological Landscapes of the World*,
DOI 10.1007/978-90-481-3055-9_11,

Fig. 11.1 General view of the Iguazu Falls (central part of left side). Water runs over basalt rocks forming impressive stair-step waterfalls. Reddish color of water results from erosion of basaltic soil during rainy season

tributary at an altitude of 170 m a.s.l. Upstream of the Iguazu Falls the river generates several minor falls and rapids in the Brazilian territory. The Upper Paraná Basin is the most dammed fluvial basin for hydroelectrical energy generation in South America. For that reason, many falls in the Brazilian territory have disappeared under large reservoirs.

The mean annual discharge of the Iguazu River at the falls is 1,413 $m^3.s^{-1}$, but discharges as high as 27,500 $m^3.s^{-1}$ can be found in historical records, for example during the 1982–1983 ENSO (PACI 2002, Canstanharo and Buba 2008) (Table 11.1). During the dry season the Iguazu River transports a low quantity of suspended load and for that reason its waters are clear with a slightly greenish hue. Its color changes to strongly reddish during the summer rainy season due to the suspended sediment eroded from the basaltic red soils (Fig. 11.1). Incidentally, the falls may dry up almost totally, as in 1978.

11.2 Structural and Geological Setting of the Paraná River Basin and Iguazu Falls

The Upper Paraná River basin is developed almost completely on sedimentary and volcanic rocks of the Paleozoic-Mesozoic Paraná Sedimentary Basin (Fig. 11.2). The drainage network is asymmetrical compared to the length of its eastern and western tributaries. Main left-hand (eastern) tributaries have their sources near the Atlantic Ocean and run approximately E–W for 600–800 km to reach the Paraná River in the center of the basin. They cross the cuesta escarpments of the Serra de São Luiz and Serra Geral Mountains built by sedimentary rocks and plateau basalt through narrow gaps ("percées") (Fig. 11.5). Right-hand tributaries are shorter (c 350 km), with headwaters located in the western cuestas of Maracaju-Amambaí Mountains formed by Cretaceous sandstone of the Bauru Group.

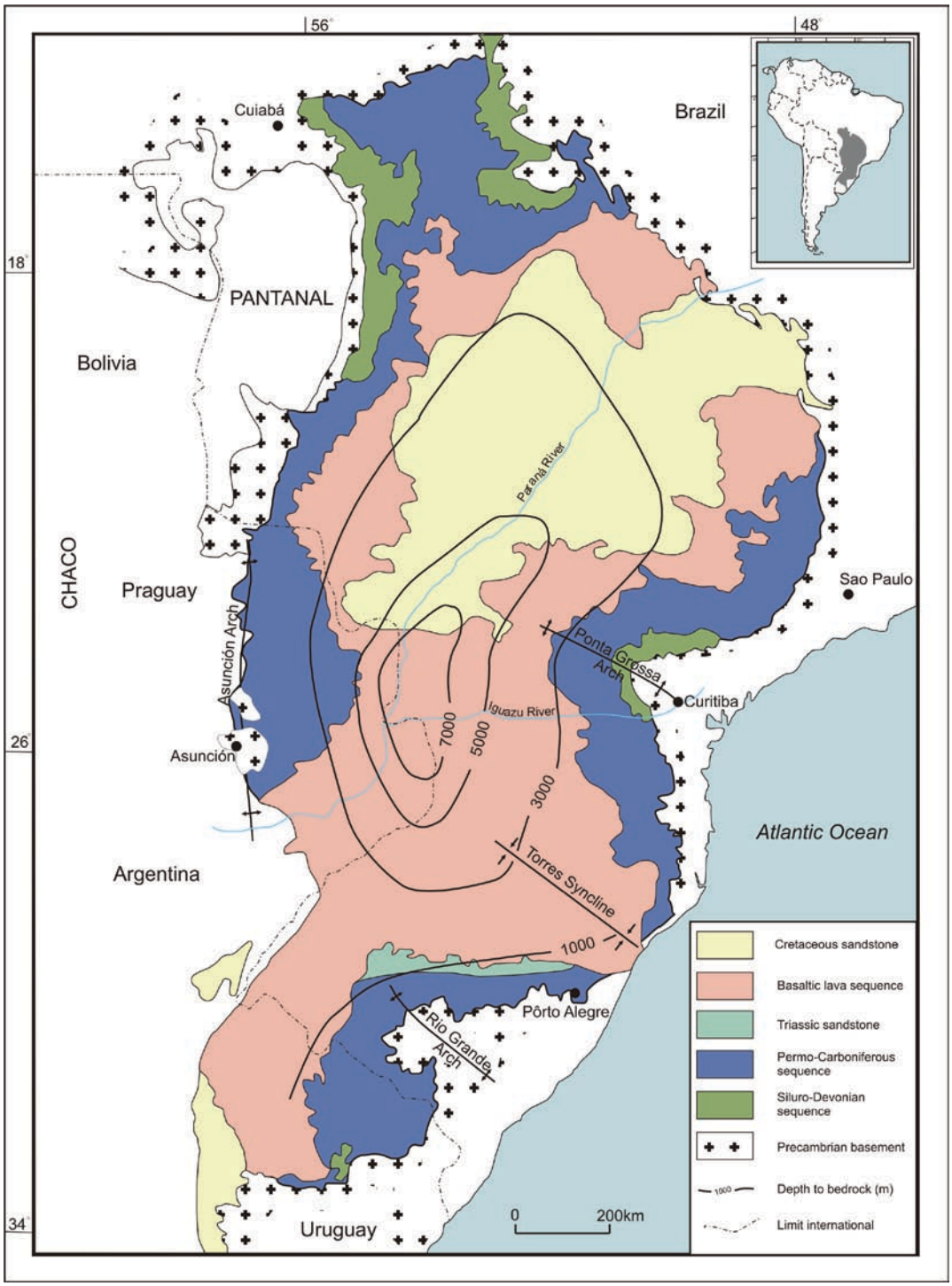

Fig. 11.2 Geological map of the Paraná Sedimentary Basin with the main tributaries of the upper Paraná River. Iguazu Falls developed on a thick basaltic plateau formed by the Serra Geral Formation (J-K) (Modified from Milani 2004)

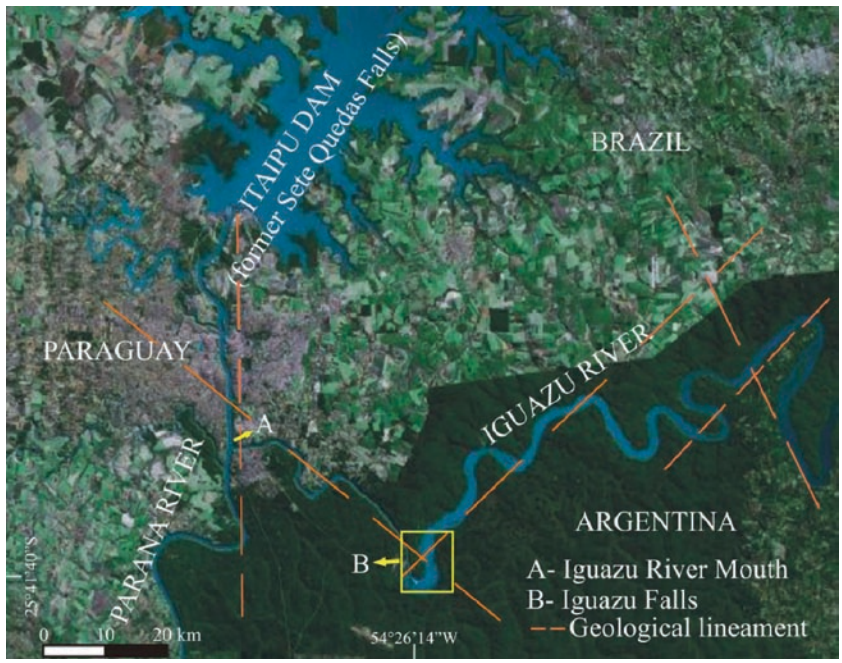

Fig. 11.3 Confluence of the Iguazu and Paraná Rivers. The Iguazu River presents a structurally controlled meander pattern beyond the falls. A-B (21 km) is the canyon excavated by headwater retraction from the mouth of the Iguazu River at the Paraná up to the present location of the Igauzu Falls (Yellow square – see Fig. 11.4). The end portion of this canyon is the impressive Garganta do Diabo. At the top, a partial view of the Itaipu Reservoir covering the ancient Sete Quedas Falls, the main knickpoint of the Paraná River

Table 11.1 Discharge at the Igauzu Falls gauging station (in $m^3.s^{-1}$) for a basin area of 78,800 km^2

Q_{mean}	Q_{max} average	Q_{min} average	Q_{max} (1983)	Q_{min} (1978)
1,413	2,506	1,326	27,500	90

The sedimentary basin of Paraná is crisscrossed by a complex net of structural lineaments, episodically active since the beginning of its history (Silurian-Devonian) with main NW–SE, E–W, and NE–SW patterns. These lineaments were intensively reactivated during the Gondwana breakup initiated in the Early Jurassic period (Bartorelli 2004). A large amount of lava was extruded along the NW–SE fractures during the Early Cretaceous, 132–133 million years ago (Saadi 1993; Marques and Ernesto 2004), forming a Basalt Plateau with a 1 km thick layer of successive basaltic lava flows (stair-step type) and frequent occurrence of dikes and sills of diabase.

The Paraná River basin started to develop concurrently with the rifting processes, related to the opening of the South Atlantic, when Gondwanaland was dismembered. River valley formation surely started after the prevailing desert conditions during part of the Cretaceous age, when a big sand sea spread along a large part of southeastern Brazil (Caiua Group). During this time the development of endorreic drainage under arid to semi-arid conditions could be the first evidence of a fluvial system being present in the former Paraná Basin after the immense basaltic extrusion event linked to the Gondwana partition. Despite its long history, the Paraná fluvial system is not well-understood. Geological evidence from Cenozoic sediments studied in southeast Brazil, particularly in the state of São Paulo, suggests that the Paraná fluvial basins were acquiring their present-day shape because of tectonic movements during the Neogene period. During the Miocene, the littoral area of the south-southeastern Brazil was uplifted, forming the Serra do Mar Mountains, a 1,500 km long chain of mountains parallel to the coast (Figs. 11.2 and 11.5). It is probable that this uplift reorganized the fluvial basin toward the shape we see today: a huge area that collects water from 980,000 km^2 of Brazilian territory up to the confluence with the Iguazu River.

The majority of the left-hand tributaries of the Paraná River Basin run over the Basaltic Plateau along

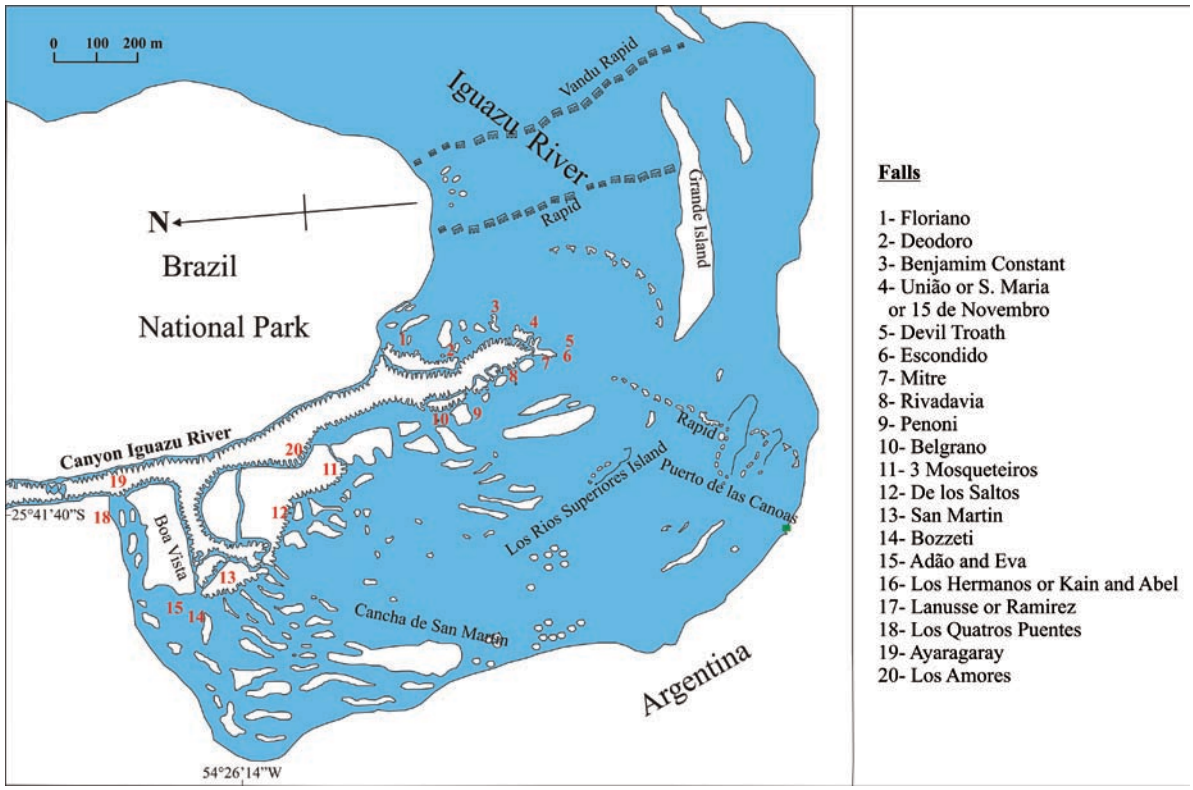

Fig. 11.4 Detailed map of the Iguazu Falls with main geomorphic features (see Fig. 11.3 for location). Beyond the falls river has small islands with little alluvial deposition and many rock exposition at the middle-level water (Modified from Maack 1968)

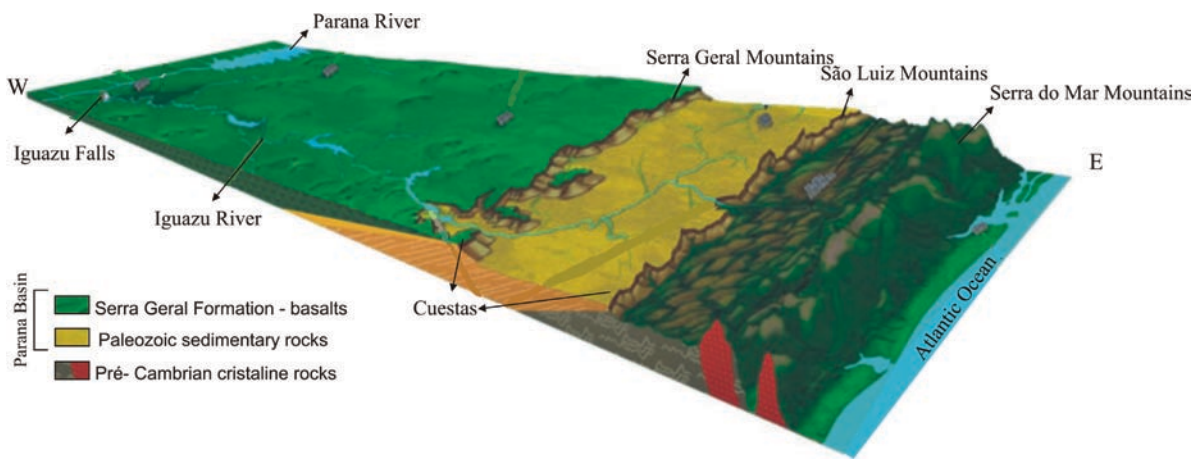

Fig. 11.5 Schematic model of the Iguazu River from its source at the Serra do Mar Mountains near the Atlantic Ocean (East) up to the mouth at the Paraná River (West). Channel cuts the cuesta escarpments of the São Luiz do Purunã and Cadeado Ranges and runs in its middle and lower reach over basalts of the Serra Geral Formation (Modified from Marini and Xisto in MINEROPAR 2006)

the NW–SE lineaments, forming hundreds of falls developed over basaltic rocks. As discussed above, there are strong controversies about the age of the present Paraná River system. Soares and Landim (1976) mentioned that the rocks of the Paraná basin suffered regional planation processes during the Tertiary period

(Oligocene-Miocene limit) and correlated this surface (incised by the Iguazu Falls) with the South American Regional Planation Surface (in the sense of King 1950). The Paraná marine transgression of the middle Miocene period invaded the Chaco-Pampa area across the Paraná River valley but did not reach the Brazilian territory. Fluvial sediments are characteristic along the Paraná River starting from the Late Miocene, as recorded in Argentina. In Brazil, alluvial sedimentary records related to the main valley of the Paraná Rivers are scarce and incomplete, restricted only to the Pleistocene-Holocene period (Stevaux 1994).

11.3 Description and Origin of the Iguazu Falls

The Iguazu Falls are the largest of the Paraná River Basin in relation to their height and water volume, except for Sete Quedas Falls (see comments ahead). The Iguazu River is about 1,500 m wide above the falls and there are many rapids between rock outcrops and small islands (Fig. 11.4). Then the river channel changes abruptly its direction from south to N-NW and its water falls down from a height of 80 m. The falls have a sinuous arch-like head some 2.7 km in length where part of the water volume enters a canyon 80–90 m wide and 70–80 m deep, excavated within plateau basalts for 21 km upstream of the confluence of the Iguazu and Paraná rivers. This forms the spectacular Garganta do Diabo (Devil's Gorge) (Figs. 11.4, 11.6). Another part of the river water enters the canyon by its left side and generates a front with 160–200 individual falls (depending on available discharge) that during floods forms a single front. The falls of San Martin, Adam and Eva, Penoni, and Bergano are the largest of these isolated water falls (Fig. 11.4). In the central portion of the front the falls are formed by two steps, 35 and 40 m high, defined by a highly resistant layer of vesicular basalt (Figs. 11.1, 11.7).

The geological structure of the falls is simple and consists of three layers of lava that give a staircase-type shape to the falls. These steps are formed by massive black basalt in the central part of the former flow, with an impressive system of prismatic columnar jointing, and a 8–10 m layer of vesicular basalt at the top. This situation produces a two-step waterfall controlled by the contact between the two basaltic traps (Fig. 11.7). In the upper portion of the basaltic flow the occurrence

Fig. 11.6 Garganta do Diabo (Devil's Gorge) at the beginning of the Iguazu River's canyon, 21 km upstream of its mouth (Photo Z. Koch, in Salamuni et al. 2002)

Fig. 11.7 *Left*: Schematic profile of the Iguazu Falls: two basaltic trapps control the falls' staircase. *Right*: General view of the falls with evidence of lithological and structural control of waterfalls (Modified from Martini and Xisto in MINEROPAR 2006)

of geodes of zeolites, agate, amethyst, and chalcedony is common and these are economically exploited elsewhere in the region. Normally, basalt in this portion is reddish-grey due to weathering of iron-rich minerals. A dense system of vertical fractures formed during solidification of lava, producing a columnar jointing pattern. This repetitive jointing pattern within the trap sequence, supplemented by horizontal fractures, produced a peculiar structural design for the development of the falls. Vertical fractures developed further under more recent unloading conditions and became more important while the canyon was excavated. The basal portion of a lava layer develops a system of vertical fractures by the contact of hot lava with the preexisting surface (MINEROPAR 2006). Two other systems of fractures (N 80° and N 170°) occur in the area; those are generated by tectonic activity and contribute for block formation.

The structural base level of the Upper Paraná River Basin is controlled by the formation of the canyon of the Paraná River and a sequence of falls named Sete Quedas Falls: 19 falls developed along 3 km of a 200 m wide straight channel (Fig. 11.4). These falls are covered today by the Itaipu Reservoir. Sete Quedas Falls also constitute a main river's knickpoint that separates the Upper and the Medium Paraná River (Stevaux 1994; Orfeo and Stevaux 2002). Bartorelli (1997) suggested that NW–SE and SW–NW lineaments controlled the development of the Sete Quedas Falls (The Upper Paraná River Basin base level) and many falls over basalt in practically all left-hand tributaries. In the proximity of the Iguazu Falls, both the Paraná and Iguazu Rivers run over the basaltic sequence of the Serra Geral Formation formed by 1,000 m of volcanic rocks intercalated with thin layers of sandstone. The differential erosion rates between the Paraná and Iguazu rivers created an 80–70 m initial fall at their confluence, the proto-Iguazu Falls. Although no absolute ages exist as well as no good knowledge of the evolution of the fluvial system since the Pliocene period, it has been suggested that the falls were continuously wandering upstream to their present position by progressive headwater erosion (Fig. 11.6) at a rate of 1.4–2.1 cm/year over the last 1.5–2.0 million years (Bartorelli 1997). In spite of the speculation on the age of the Iguazu Falls and the rates of headwater erosion, the falls remain a spectacular example of long-term knickpoint retreat from a tributary/trunk stream confluence.

There are few studies about the formation processes of the Sete Quedas Falls. Bed quarrying and hydraulic wedging are probably the more efficient processes in this case. Miller (1991) emphasized the importance of quarrying as the most rapid means of eroding a bedrock channel floor, especially in this case, where a dense system of joints and fractures improves block formation. In a previous phase joint surfaces are weathered and wedged apart and bashed by bedload (Hancock et al. 1998). However, Bartorelli (1997) attributes the evolution of Sete Quedas Falls and consequently the retreat of the Iguazu River canyon to 'rapid geological

processes'. Evidence of slackwater deposits interpreted as extreme flood events were observed by Stevaux (1993) in the Iguazu River mouth area. However, the author did not mention any relationship between big or megaflood events and the evolution of the falls.

11.4 Conclusion and Final Remarks

The Iguazu Falls, as the other waterfalls of the Paraná River Basin, have a strong structural control imposed by NW and WNW lineaments. The formation of the falls is also associated with the neotectonic reactivation of the ancient 'megastrutural' lineaments of the Brazilian Platform (Almeida 1967) under the influence of intensive epeirogenesis (upwarping) since the Pliocene-Pleistocene (Bartorelli 1997; 2004; Marques and Ernesto 2004). The differential mobilization of tectonic blocks by general epeirogenesis generated the present-day basin topography. Unfortunately, with the intensive program of hydroelectric dam construction initiated during the 1970s dozens of wonderful falls like Sete Quedas, São Simão, Avanhandava, and São Luiz disappeared together with their luxurious forest and amazing fauna. In this sense, the Iguazu Falls are a precious last example of the spectacular falls of the Paraná River Basin.

The Authors

José C. Stevaux is Professor of Geomorphology and Quaternary of the Maringa State University and Researcher of the National Council of Research-CNPQ, Brazil. He is coleader of the IGCP 582 project "Tropical Rivers" and cochair of the Working Group on Large Rivers of GLOCOPH (Global Commission on Continental Paleohydrology). His research interests include geomorphology, hydrology of large rivers, and the impacts of human activities on large fluvial systems, as well as Quaternary paleohydrology. He has been researching several regions of South America such as the Paraná basin, the Araguaia, the Orinoco Llanos, and the Bolivian Chaco. He has published more than 50 scientific papers in peer-reviewed periodicals and edited volumes.

Edgardo Latrubesse is Associate Professor in the Department of Geography and the Environment of the University of Texas at Austin, USA. He was professor at different Argentinean and Brazilian universities, Director of the Laboratory of Tritium and Radiocarbon-LATYR-CONICET, Argentina and honored as T.W. Rivers Distinguished Professor in International Affairs at East Carolina University, USA. He was member of the Executive Committee of the International Association of Geomorphologist (2001–2005) and is currently the chair of the GLOCOPH (Global Commission on Continental Paleohydrology) Working Group on Large Rivers and leader of IGCP 582 project "Tropical Rivers". His research interests include geomorphology, hydrology of large rivers, and the impacts of human activities on large fluvial systems and tropical biomass, as well as Quaternary paleohydrology. He worked extensively on some of the largest rivers of South America, such as the Amazon, Negro, Madeira, Purús, Araguaia, Paraná, and Sao Francisco. He has published more than 50 scientific papers and book chapters.

References

Almeida FFM (1967) Origem e evolução da Plataforma Brasileira. Departamento Nacional da Produção Mineral/DGM Bull. 241, Rio de Janeiro, Brasil

Bartorelli A (1997) As principais cachoeiras da Bacia do Paraná e sua relação com alinhamentos tectônicos. Doctoral thesis, IGCE-UNESP, Rio Claro

Bartorelli A (2004) Origem das grandes cachoeiras do planalto basático da Bacia do Paraná: Evolução quaternária e geomorfologia. In: Mantesso-Neto V, Bartorelli A, Carneiro CDR, Brito-Neves BB (eds) Gelogia do Continente Americano: Evolução da Obra de Fernando Flávio Marques de Almeida. Becca Produções Culturais, São Paulo, Brazil, pp 95–111

Canstanharo G, Buba H (2008) Review of hydraulic behavior of the Igauçu River in the region of União da Vitória and its impacts on operation of the Foz do Areia and Segrado Reservoir. Espaço Energia 6:28–39

Hancock GS, Anderson RS, Whipple KX (1998) Beyond power: bedrock river incision process and form. In: Tinkler KJ, Wohl EE (eds) Rivers over rock: fluvial processes in bedrock channels, Amer Geophys Union, Washington, DC. Geophys Monograph 107:35–60

King LC (1950) The study of the world's plain lands. Quart J Geol Soc 106:101–131

Maack R (1968) Geografia Física do Estado do Paraná. UFPR/IBPT, Curitiba, Brazil

Marques LS, Ernesto M (2004) O magamatismo toleítico da Baia do Paraná. In: Mantesso-Neto V, Bartorelli A, Carneiro CDR, Brito-Neves BB (eds) Gelogia do Continente Americano: Evolução da Obra de Fernando Flávio Marques de Almeida. Becca Produções Culturais, São Paulo, Brazil, pp 246–263

Milani EJ (2004) Comentários sobre a origem e a evolução tectônica da Bacia do Paraná. In: Mantesso-Neto V, Bartorelli A, Carneiro CDR, Brito-Neves BB (eds) Gelogia do Continente Americano: Evolução da Obra de Fernando Flávio Marques de Almeida. Becca Produções Culturais, São Paulo, Brazil, pp 265–291

Miller JR (1991) The influence of bedrock geology on knickpoint development and channel-bed degradation along downcutting stream in south-central Indiana. J Geol 99:591–605

MINEROPAR (2006) Minerais do Paraná S.A. http://www.pr.gov.br/mineropar/geoturismo_iguacu.html

Orfeo O, Stevaux JC (2002) Hydraulic and morphological characteristics of middle and upper reaches of the Paraná River (Argentina and Brazil). Geomorphology 44:309–322

Saadi A (1993) Neotectônica da Plataforma Brasileira: esboço e interpretações preliminares. Geonomos 1(1):1–15

Salamuni R, Salamuni E, Rocha A, Rocha A (2002) Parque Nacional do Iguaçu, PR. In: Schobbenhaus C et al (eds) Sitios Geológicos e Paleontológicos do Brasil I. DNPM-SIGEP, Brasilia, pp 1–9

Soares PC, Landim PMB (1976) Depósitos cenozóicos da região Centro-Sul do Brasil. Notícias Geomorfológicas, Campinas 16(31):17–39

Stevaux JC (1993) O rio Paraná superior: gemorfologia, sedimentação e evolução quaternária. Doctoral Thesis, Intitute of Geosciences, University of São Paulo, Brazil

Stevaux JC (1994) The Upper Paraná River (Brazil): geomorphology, sedimentology and paleoclimatology. Quat Int 21:143–161

Chapter 12
The Southern Patagonian Andes: The Largest Mountain Ice Cap of the Southern Hemisphere

Elizabeth Mazzoni, Andrea Coronato, and Jorge Rabassa

Abstract This chapter describes physiographic characteristics and geomorphological processes of the southernmost portion of the Andean Cordillera. This sector of the Andean Ranges includes the only two mountain ice fields of South America which represent the largest freshwater reserve of southern Patagonia. Discharge glaciers flow out of the ice fields on both sides, modeling the landscape in the past and present times. As a product of intense glacial action, the mountain ranges show steep slopes and rugged summits with cirque glaciers. The valleys are partially occupied by lakes, some of them of large size (over 1,000 km^2). These basins are surrounded by basaltic tablelands, complex moraine systems, and glaciofluvial plains. The dominant geomorphological processes are glacial and fluvial, besides mass movements and cryogenic activity in the highest zone. The landscape is covered by several vegetation formations, adapted to the very important W–E rainfall gradient. This orographic system offers a landscape of great beauty and high biodiversity, protected within large national parks both in Argentina and Chile.

Keywords Andean Cordillera • Patagonia • glaciers • climatic gradient

12.1 Introduction

The Patagonian region occupies the southern end of the South American continent, extending between latitudes 37° and 56°S. Along its western portion the Andean Cordillera is located, being the result of Cenozoic orogenic processes and intense plutonic and volcanic activity. This section of the Cordillera is known as the *Cordillera Patagónica* or Patagonian Andes. The *Cordillera Principal*, where Mount Aconcagua (6,900 m a.s.l; the highest peak in the Southern Hemisphere) is located, is found northwards, in central Argentina and northernmost Patagonia. This mountain range is the backbone of South America, being the most important positive relief element at the continental scale.

The Southern Patagonian Andes (Ramos 1999) extend from the latitude of Lago Fontana (44º58´S) until the Seno Otway (53º55´S) in the Magellan Straits region. At latitude 46º30´S it is divided in two segments whose structure, geological composition, topography, and geological history are significantly different. This boundary is coincident with the Aysén Triple Junction, which in the Pacific Ocean sector separates the Nazca and the Antarctic plates (Ramos 1989). The northern area, though it exposes a volcanic arc, has lower relative relief than the southern sector. The latter is described below in greater detail due to the large variability of its geomorphological features, typical of high mountain environments modeled by past and present glacial processes.

12.2 Geology

The southern portion of the Southern Patagonian Andes (Fig. 12.1) is composed of a fold-and-thrust belt, generated by the collision of the Pacific tectonic plates, which caused shortening and uplifting of the mountain ranges (Ramos 1989). It includes many granitic peaks such as San Valentín, San Lorenzo, the famous Fitz Roy or Chaltén, Murallón, Stockes, and the spectacular Torres del Paine, whose elevations range between 2,000 and 3,400 m above present sea level. All these features have impressive, almost vertical

P. Migoń (ed.), *Geomorphological Landscapes of the World*,
DOI 10.1007/978-90-481-3055-9_12,

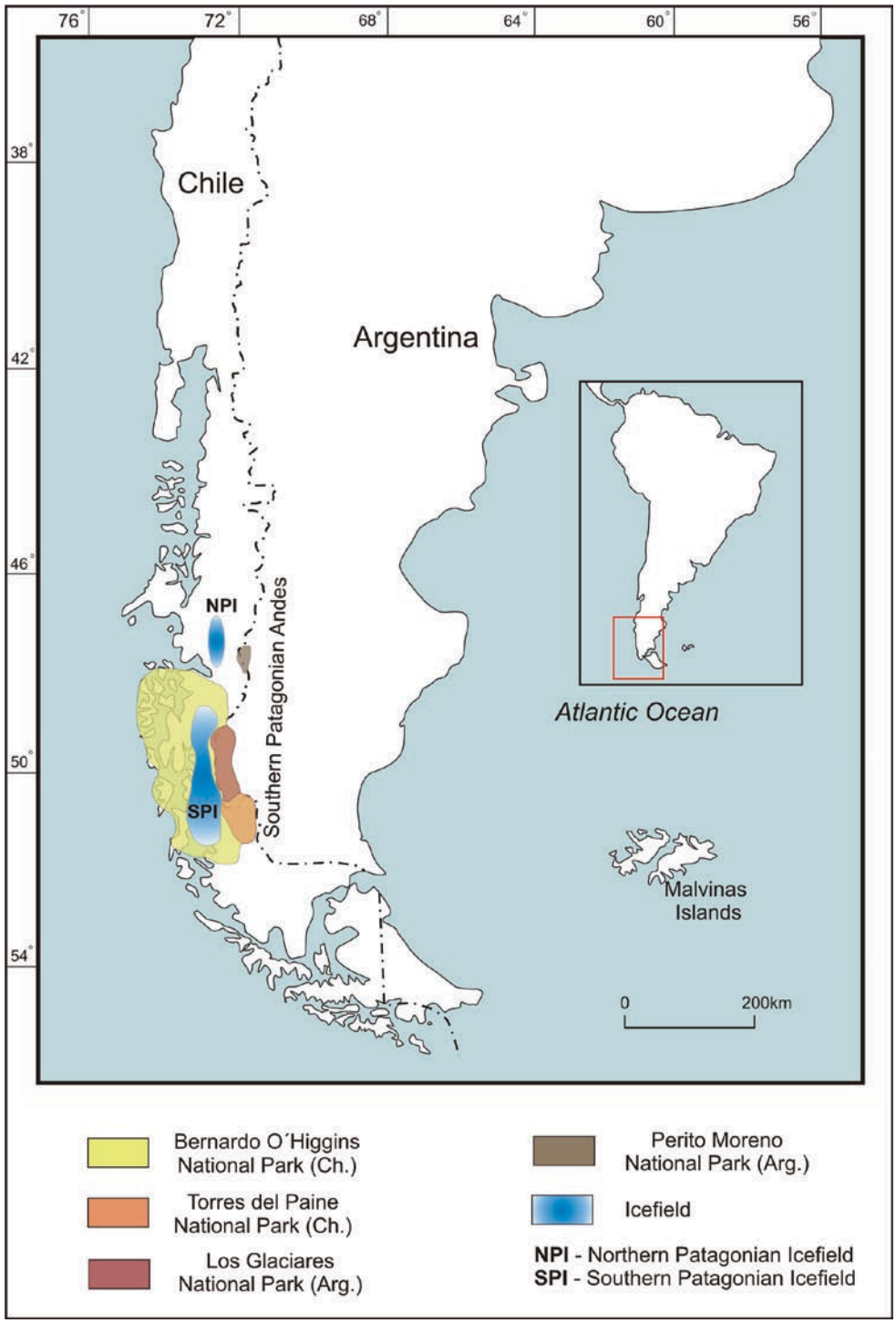

Fig. 12.1 Location map (Modified from Coronato et al. 2008), indicating the position of the Southern Patagonian Andes

sideslopes modeled by glacial erosion, of great interest to expert climbers and mountaineers.

This portion of the Cordillera has a few small volcanic cones, which are found south of 48°S along the Andean Volcanic Zone (AVZ) (Stern 2007), coinciding with the segment of the Antarctic oceanic plate which is subducting underneath the South American continental platform. In the AVZ only six small stratovolcanoes are

found, largely separated from each other, located in the westernmost portion of the Cordillera. Some of them, as the Lautaro and Viedma volcanoes, occur amidst the Patagonian Ice Cap. Volcán Lautaro is the most active, with many historical records of activity (Martinic 1988). Other volcanoes, such as Aguilera, Reclus, and Mount Burney have had eruptions during Late Glacial and Holocene times (Stern 2007).

12.3 Climate and Vegetation

The regional climatic conditions show strong gradients both from W–E and N–S and also in altitude, allowing one to distinguish different climate types. The W–E gradient is determined by the action of the South Pacific Anticyclone, which sends winds that discharge most of their moisture on the western side of the Patagonian Andes. Thus, total rainfall reaches 4,000 mm per year along the Pacific Ocean coast (hyperoceanic and oceanic climates) and then diminishes to values between 1,200 and 730 mm per year at the western side of the Andes, at the meteorological stations of Coyhaique (45.6ºS, 72.1ºW; 310 m a.s.l.) and Cochrane (47.23ºS, 72.55ºW; 182 m a.s.l.), respectively (Servicio Meteorológico de Chile, http://www.meteochile.cl/climas/climas_undecima_region.html). Along the eastern slope and piedmont area precipitation varies between approximately 400 and 200 mm per year, defining sub-humid to semiarid climate types. At the El Calafate meteorological station (50.4ºS, 72ºW; 204 m a.s.l.; Estación Meteorológica El Calafate, Servicio Meteorológico Argentino) only 123 mm of annual rainfall was recorded in the 1981–1990 decade.

The N–S gradient is related to latitudinal position and generates progressive temperature lowering southwards. The topographic effect is also shown in the thermal gradient. Starting from 800 m a.s.l., temperatures are low enough to maintain ice fields. There are no reliable meteorological records in this sector, but it may be estimated that the mean annual temperature may be slightly below 0°C. The mean maximum temperatures rise above 0°C only in summer time, whereas the mean minimum temperatures are likely to be below 0°C all year around and are extremely low in winter, thus generating almost exclusively snowfall (www.meteochile.cl). Under these conditions, there are no permanent human settlements in this area.

This climatic gradient has a great influence on the geomorphological and ecological processes, which produce contrasting landscapes as the observer moves from west to east. In this sense, and over a distance of approximately 50 km, the environment changes from very humid to semiarid climates and from rugged mountain landscapes to horizontal or sub-horizontal surfaces, accompanied by ecosystems ranging from evergreen forests composed mainly of *Nothofagus betuloides* (‘guindo’) in the western portion, to mesophyllic forests, formed basically by deciduous trees such as *Nothofagus pumilio* (‘lenga’) and *Nothofagus antarctica* (‘ñire’). Forests occupy mainly the mountain slopes whereas natural pastures occur in the valley floors. Toward the eastern margin of the Southern Patagonian Andes, grassy and xeric steppes are found in contact with the forest (Roig 1998).

Above the upper tree limit, approximately located at 1,500 m a.s.l., high altitude tundra is developed, with different types such as Magellanic tundra, Andean tundra, high altitude prairies with cushion plants and stony surfaces, showing sparse vegetation (Roig 1998, Fig. 12.2).

12.4 Glaciers and Lakes

Snow precipitation feeds the accumulation zones of the mountain ice sheet and other glaciers, known as a whole as the Northern and Southern Patagonian Icefield (*Hielo Patagónico Norte* and *Hielo Patagónico Sur*, NPI and SPI, respectively). These ice fields, which together cover up to 17,200 km^2 (Skvarca 2002), are the most important ones in South America and form a very significant freshwater reserve for Southern Patagonia. Discharge outlet glaciers descend from the ice fields along both eastern and western slopes (see Table 12.1; Figs. 12.3 and 12.4).

The SPI is the more extended icefield, being the largest mass of ice in the Southern Hemisphere outside of Antarctica (Aniya et al. 1996). It has mean width of 35 km and minimum width of 9 km, and is composed of 48 major outlet glaciers and over 100 small cirque and valley glaciers (Casassa et al. 2002). Glaciers on the western slopes end in deep fjords, whereas those in the eastern slope do so into relict glacial lakes located in ecotone areas. The largest glacier is the Pio XI Glacier on the western slope, followed by the Viedma and Uppsala glaciers, which flow toward the eastern Andean slope.

In the Glaciares National Park of Argentina, close to the town of El Calafate, the Perito Moreno Glacier

Fig. 12.2 Typical landscape of the Southern Patagonian Andes, where the amplitude of its relative relief may be observed, as well as the presence of forest ecosystems occupying the slopes almost up to the permanent snowline. In the foreground, a detail of several *Nothofagus* individuals. In the center of the picture is the Río de las Vueltas (49º07'S; 72º55'W) (Photo E. Mazzoni)

is noteworthy as one of the most accessible glacier tongues in temperate regions of the world, very well known for its peculiar glaciological dynamics, characterized by repeated advance of its front and subsequent damming of the southernmost branch of Lago Argentino, known as Brazo Rico. This glacier has a length of 30 km and an ice surface of 258 km^2, distributed from an elevation of 2,950 m a.s.l. to its terminal front into the aforementioned lake at an elevation of only 175 m a.s.l.

The glacier has not shown significant thickness changes in recent decades (Rignot et al. 2003) suggesting that its mass balance is in equilibrium (Rott et al. 1998) due to, among other factors, the fact that its hypsometric distribution presents a strong slope in the zone around its equilibrium line altitude (ELA). Thus the temperature increase that took place in Patagonia between 1960 and 1990 (Rosenblüth et al. 1997) has not forced any significant reduction of its accumulation zone (Naruse et al. 1995). This glacier has one of the highest net annual accumulation rates on the planet (5,250 ± 474 kg m^{-2}) and a very high rate of ice loss due to calving (that is, iceberg formation), which also explains the ice front stability of recent decades (Stuefer 1999). Table 12.1 shows the main characteristics of the outlet glaciers of the Patagonian Ice Cap.

The lakes of this region are amongst the largest freshwater bodies in the South American continent, among which the Buenos Aires, Viedma, and Argentino lakes are the largest, each of them with surface areas above 1,000 km^2. Table 12.2 provides the basic characteristics of the major Southern Patagonian lakes.

The drainage system is well-integrated and includes the upper reaches of allochtonous streams that drain

Table 12.1 Physical characteristics of several outlet glaciers from the Southern Patagonian Icefield (From Casassa et al. 2002). Information is only partially available for most glaciers

Glacier name	Location	Length (km)	Total area (km^2)	Maximum elevation (m)	Minimum elevation (m)	Equilibrium Line Altitude (m)	Orientation
Jorge Montt	48º 04´ S, 73º 30´ W	42	464	2,640	0	950	N
Greve	48º 58´ S, 73º 55´ W	51	438	3,607	–	1,000	NW-W
HPS8	49º 02´ S 73º 47´W	11	38	–	–	–	SE
Pío XI	49º 13´ S 74º W	64	1,265	3,607	0		W
Amalia	50º 57´ S 73º 45´ W	21	158	–	0	900	W
Tyndall	51º 15´ S 71º 15´W	32	331	–	50	900	E
Perito Moreno	50º 30´ S 73º W	30	258	2,950	175	1,150	NE
Uppsala	49º 59´ S 73º 17´ W	60	902	3,180	175	1,150	SE
Viedma	49º 31´ S 73º 01´ W	71	945	–	250	1,250	E-S
O'Higgins	48º 55´ S 73º 08´W	46	810	3,607	285	1,300	N-S-E

toward the Atlantic Ocean and smaller basins which cross the Andean ranges toward the Pacific Ocean.

12.5 Landforms and Geomorphological Processes

The mountain ranges that form the Southern Patagonian Andes have, in general, very abrupt slopes and summits, with cirque glaciers and glacial troughs occupied by many lake basins (Fig. 12.4). The relative local relief is very significant, sometimes over 2,000–2,500 m. The bottoms of the larger glacial valleys are located around 200 m a.s.l. These valleys are bounded by basaltic tablelands, complex moraine systems, and glaciofluvial plains that originated either during the Last Glacial Maximum (LGM), which took place around 25,000 years ago (Singer et al. 2004; Kaplan et al. 2004; Rabassa 2008) or during Early and Middle Pleistocene glaciations (Rabassa et al. 2005; Rabassa 2008).

This orographic system, modeled by past and present glacial action, covered by dense, pristine forests and drained by mountains creeks and lacustrine basins, offers a magnificent landscape of noted beauty and rich biodiversity which is protected by the Los Glaciares and Perito Moreno national parks in Argentina and the Bernardo O'Higgins and Torres del Paine national parks in Chile, several of them having been inscribed as UNESCO World Heritage monuments (see Fig. 12.1 for location).

The geomorphic processes that have modeled these landscapes are diverse and complex, including endogenous and exogenous agents, whose relative participation varies according to the analyzed geographical areas. The orogenic and volcanic processes had their maximum expression during earlier periods of the Cenozoic, but are still very active, being associated with the subduction of the Pacific oceanic plates such as the Nazca and the Antarctic plates underneath the South American continent. The intense eruption of Volcán Hudson (45º55'S, 72º58'W) in 1991 covered thousands of square kilometers in the Province of Santa Cruz (Argentina) with volcanic ashes that reached as far as Tierra del Fuego. As a noted testimony of the present volcanic activity, while a first draft of this chapter was being completed, Volcán Chaitén (43º30'S) was erupting in Chile, throwing its ashes on to the Argentinean city of Esquel, located 100 km eastwards, to the entire piedmont area of the Northern Patagonian Andes in Argentina and even to the Atlantic coast of Buenos Aires province (38°S).

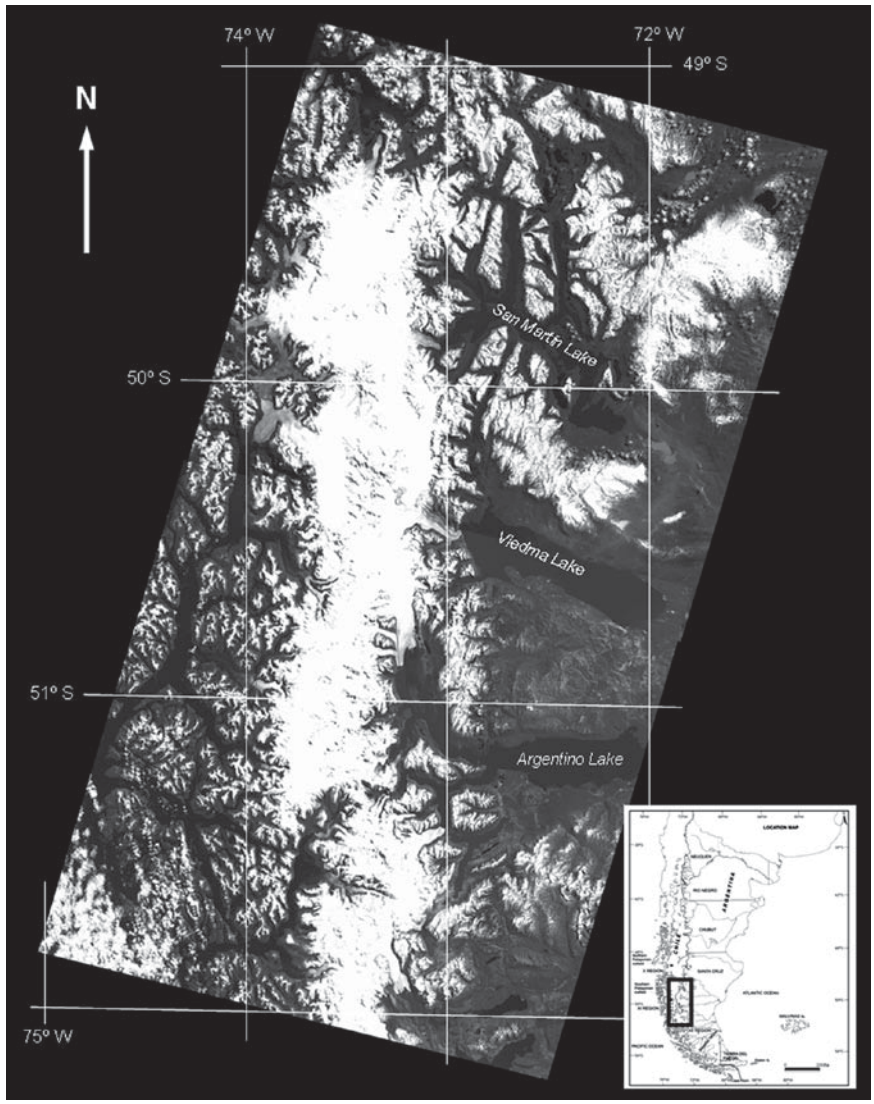

Fig. 12.3 Satellite mosaic in which the Southern Patagonian Ice Cap and its discharge glaciers are shown (the images are Landsat 7, Band 8). In whitish, shiny tones the fresh snow is distinguished from the icefields, where the highest peaks of the mountain ranges are found. The glaciers appear in greyish tones, draining toward large Patagonian lakes of the eastern slopes or to the Pacific coastal fjords

Cryogenic and glacial processes are still active above the tree limit, at the summits and within upper slopes (Fig. 12.5). Glacier action is evident in the lowlands, where the large lakes of the eastern piedmont area are located, but also down to present sea level at the western margin, where an intricate network of glacial troughs, fjords, and channels was excavated by the Pleistocene glaciers during the LGM, when sea level was at least 120 m lower than today. Mass movement processes shaped the slopes, leading to the origin of stony surfaces in the higher zones of bare rocks, whereas landslides affected the forested slopes during periods of exceptionally high precipitation. Debris flows are concentrated in channels and ephemeral stream beds, transporting big glacial boulders and tree trunks, which usually generate drainage obstruction or diversion, and block roads in the piedmont or lowland areas.

Fluvial action appears to be dominant at present, basically due to the high erosive power of mountain streams. The high availability of water in the system, provided by ice and snow melt and abundant orographic precipitation, is shown by a very high drainage

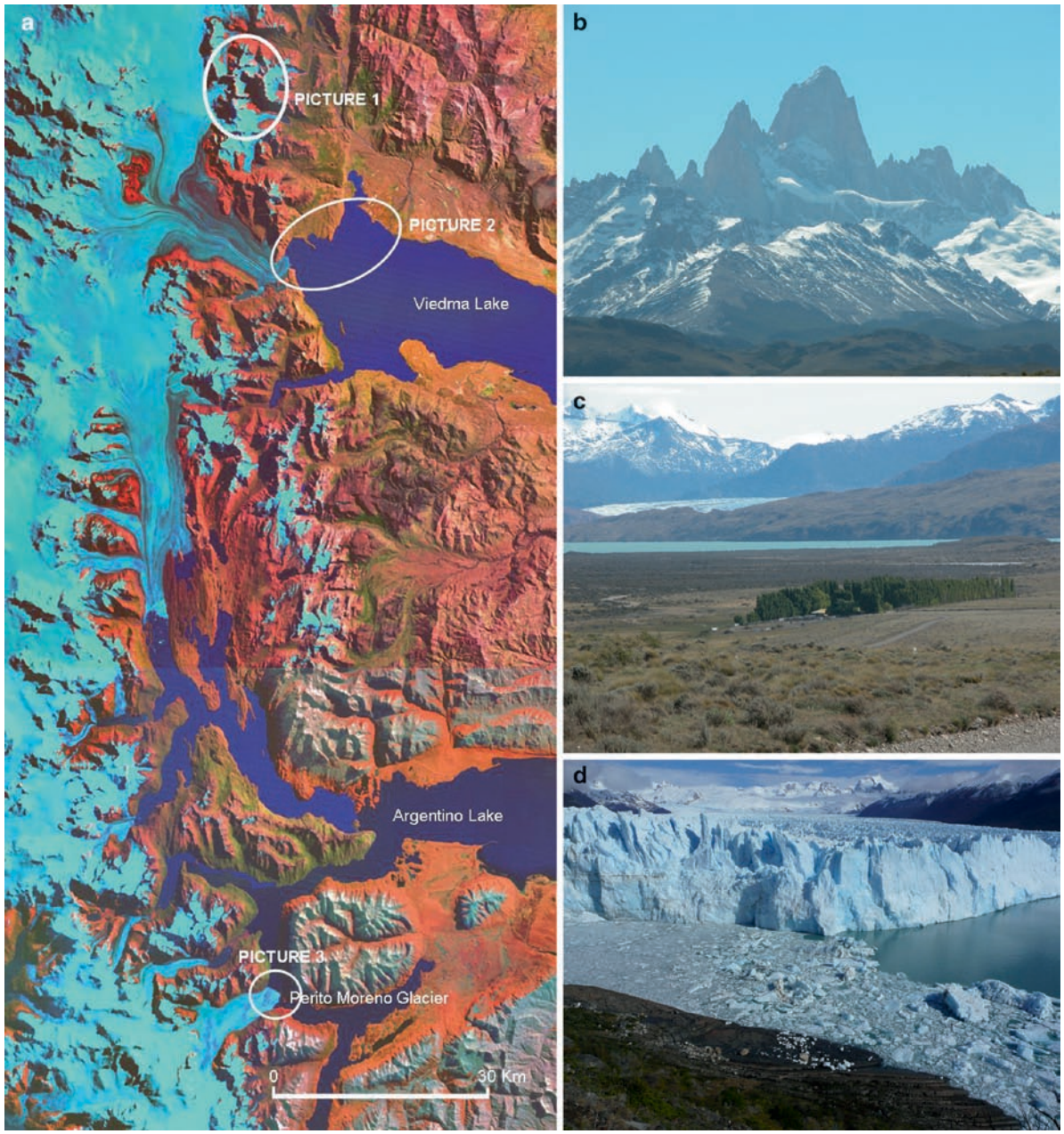

Fig. 12.4 A view of the Southern Patagonian Ice Cap, between 49º07' and 50º34'S. The Landsat image (**a**) shows the main discharge glaciers coming from this icefield, which reach different fjord-like branches of the Viedma (*upper*) and Argentino (*lower*) lakes along the eastern slopes. The southernmost glacier that appears in the image is the Perito Moreno Glacier, whose details are shown in the lower picture (**d-picture 3**). Photograph **b-picture 1** exposes the granitic arête in which the famous peaks Cerro Fitz Roy and Cerro Torre are found, as well as the cirque and valley glaciers of the area. In the central photography (**c-picture 2**) the transitional tablelands/Cordillera landscape and the immense amplitude of the Patagonian landscape may be observed. There, the main housing facilities of the "estancias" are the only expressions of human activity, detected by implanted European trees (mostly poplars), which provide some shelter from the roaring westerlies. In the central section of the photograph the Viedma Glacier and Lago Viedma are found (Photos E. Mazzoni)

density of fluvial networks composed of permanent and ephemeral streams. The trunk streams reach the lower portions of the landscape where they flow in the main, flat-bottomed, ancient glacial valleys with braided channel patterns. In these conditions, streams lose energy and increase alluvial deposition.

Table 12.2 Physical characteristics of the most important lakes located along the Southern Patagonian Andes. In italics, the Chilean name of the lakes if they extend both in Argentina and Chile. Location was measured in the central point of the lake; the absolute maximum depth of many of these lakes is still unknown

Lake name	Location	m a.s.l.	Surface (km^2)	Maximum depth (m)	Mean depth (m)	Length of the shoreline (km)	Slope
Buenos Aires	46º 29´S	217	1,850	590	No data	422.1	Pacific
General Carreras	71º 26' W						
Pueyrredón	47º 20´S		320	No data	No data	171.5	Pacific
Cochrane	71º 56´W						
Posadas	47º 30´S	112	45.3	No data	31.2	26.6	Endorreic
	71º 50´W						
Belgrano	47º 47´S	919	42.8	No data	No data	1.4	Atlantic
	72º 14´W						
Burminster	47º 51´S	931	14	No data	No data	68	Atlantic
	72º 08´W						
San Martín	49º 08´S	285	1,013	836	No data	571	Pacific
O'Higgins	72º40´W						
Del Desierto	49º 02´S		12	No data	70	22.7	Atlantic
	72º 52´W						
Viedma	49º37´S	250	1,100	No data	No data	234	Atlantic
	72º30´W						
Argentino	50º 13´S	187	1,466	500	150	558.2	Atlantic
	72º 30´O						

Fig. 12.5 At elevations above 1,500 m a.s.l. tundra and stony surfaces with sparse vegetation are found. In these high portions of the landscape, glacial and cryogenic processes are particularly active (Photo A. Coronato)

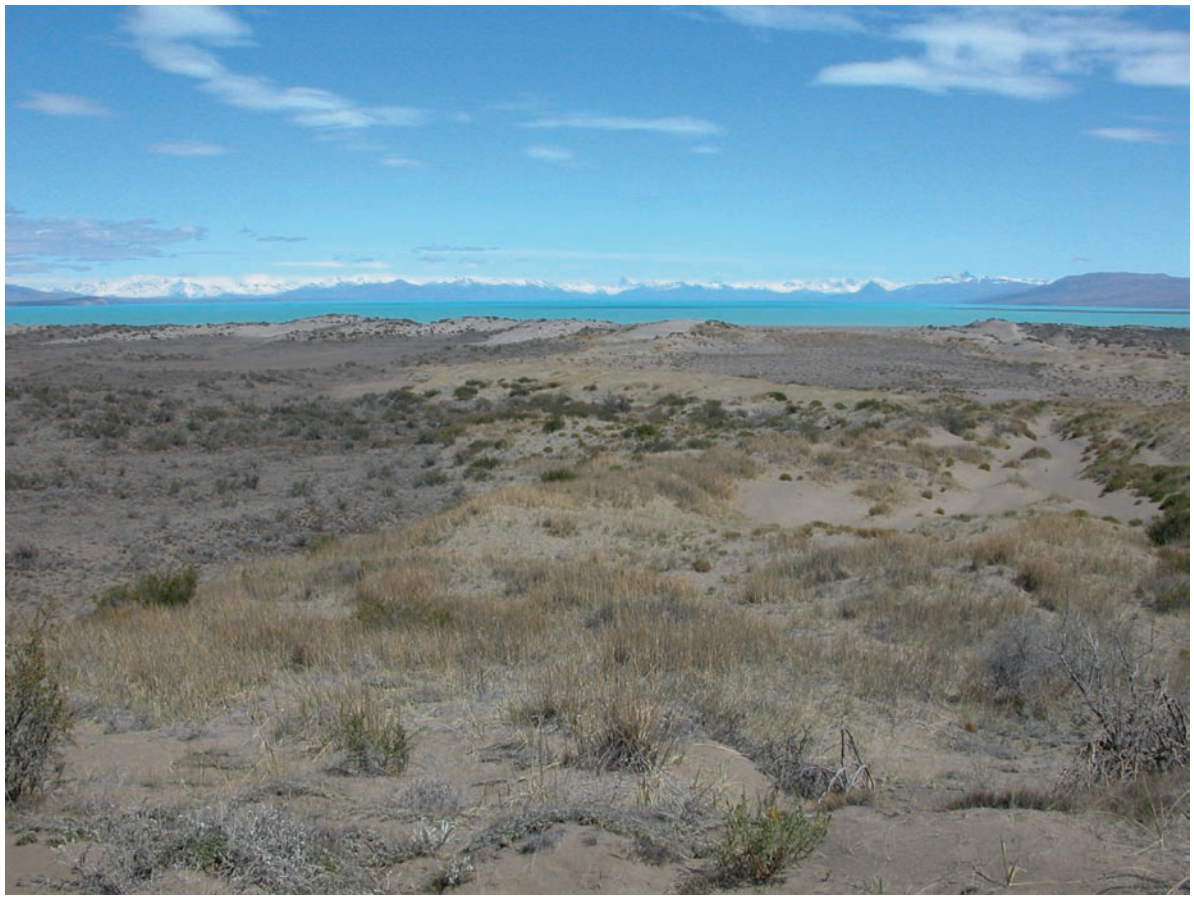

Fig. 12.6 A view of dune fields, partially covered by vegetation, extending along the eastern margins of large lakes (Photo E. Mazzoni)

At the eastern piedmont of the Andes, where the large relict glacial lakes are found, coastal processes have modeled their shores by intense wave action, forced by the permanent action of the westerlies. In these open spaces, parabolic and longitudinal dunes are found, as well as aeolian pavements. These mostly occur along ancient shorelines lacking vegetation or in deforested areas or those with vegetation degraded by desertification processes (Fig. 12.6).

12.6 Final Remarks

The Southern Patagonian Andes is one of the regions with the highest landscape diversity of the austral end of the South American continent. This geomorphological diversity, due to the regional geological and climate characteristics, offers a variety of natural resources, particularly those of a scenic nature which have determined that a large portion of these territories is protected as national parks and natural reserves, including the declaration of the Los Glaciares National Park, among others, as a UNESCO World Heritage site in 1981.

This mountain environment has a wet, cold climate that allows for the development of dense forest cover on its slopes and the survival of one of the most important icefields of the temperate regions on Earth. The availability of water resources is also shown in a very dense drainage network composed of many streams and large lakes of glacial origin. The rugged relief and the abundance of ice and water have favored the development of active geomorphological processes that are accompanied by very strong wind action, particularly in the eastern piedmont.

Some of the most beautiful and spectacular landscapes in the Southern Hemisphere are found in the Southern Patagonian Andes. The combination of lively Cenozoic tectonics, powerful volcanic activity, vigorous glacial action, abundant meltwater runoff, a harsh climate, and pristine ecosystems has created the geomorphological conditions for the development of such a magnificent landscape.

The Authors

Elizabeth Mazzoni is Professor of Geomorphology and Remote Sensing at the Universidad Nacional de la Patagonia Austral (UNPA), Río Gallegos, Argentina. She is a member of the Laboratorio de Teledetección and GIS, Unidad Académica Río Gallegos, UNPA, working on projects in physical geography and remote sensing. In recent years she has worked on geomorphology and hydrology of Patagonian volcanic landscapes, desertification, and continental wetlands in arid environments.

Andrea Coronato is Professor of Physical Geography at the Universidad Nacional de la Patagonia-San Juan Bosco in Ushuaia, Tierra del Fuego, Argentina, and researcher of the Laboratorio de Cuaternario, Centro Austral de Investigaciones Científicas (CADIC), Consejo Nacional de Investigaciones Científicas y Tecnológicas (CONICET) at Ushuaia, with emphasis on the physical geography, geomorphology, and paleoenvironments of Southern Patagonia and Tierra del Fuego. In the last years she has worked on the study of glacial, fluvial, and aeolian geomorphology, Quaternary glaciations and environmental impact of Canadian beavers on fluvial systems of Tierra del Fuego.

Jorge Rabassa is Professor of Geography at the Universidad Nacional de la Patagonia-San Juan Bosco, Ushuaia, Tierra del Fuego, Argentina, and researcher of the Laboratorio de Cuaternario, Centro Austral de Investigaciones Científicas (CADIC), Consejo Nacional de Investigaciones Científicas y Tecnológicas (CONICET) at Ushuaia, working on Late Cenozoic geology, geomorphology, and paleoenvironments. During the past years he has studied glacial geology and geomorphology of Southern Patagonia and Tierra del Fuego, Late Cenozoic glaciations, and the impact of global climate change on Patagonian glaciers. His recent publications include the book *The Late Cenozoic of Patagonia and Tierra del Fuego* (2008).

References

Aniya M, Sato H, Naruse R, Skvarca P, Cassasa G (1996) The use of satellite and airborne imagery to inventory outlet glaciers of the Southern Patagonian Icefield, South America. Photogramm Eng Remote Sens 62:1361–1369

Casassa G, Rivera A, Aniya M, Naruse R (2002) Current knowledge of the Southern Patagonian Icefield. In: Casassa G, Sepúlveda F, Sinclair R (eds) The Patagonian Icefields: a Unique Natural Laboratory for Environmental and Climate Change Studies, CECS Series of the Centro de Estudios Científicos. Kluwer/Plenum, New York, pp 67–83

Coronato A, Coronato F, Mazzoni E, Vázquez M (2008) Physical Geography of Patagonia and Tierra del Fuego. In: Rabassa J (ed) Late Cenozoic of Patagonia and Tierra del Fuego. Development in Quaternary Sciences, vol 11. Elsevier, Amsterdam, pp 13–56

Kaplan M, Douglass D, Singer B, Ackert R, Mc Caffee M (2004) Cosmogenic nuclide chronology of pre-last glacial maximum moraines at Lago Buenos Aires, 46ºS, Argentina. Quat Res 63:301–315

Martinic M (1988) Actividad volcánica histórica en la región de Magallanes. Rev Geol Chile 16(2):181–186

Naruse R, Aniya M, Skvarca P, Casassa G (1995) Recent variations of calving glaciers in Patagonia, South America, revealed by ground surveys, satellite-data analyses and numerical experiments. Ann Glaciol 21:297–303

Rabassa J (ed) (2008) Late Cenozoic glaciations in Patagonia and Tierra del Fuego. In: Late Cenozoic of Patagonia and Tierra del Fuego. Development in Quaternary Sciences, vol 11. Elsevier, Amsterdam, pp 151–204

Rabassa J, Coronato AM, Salemme M (2005) Chronology of the Late Cenozoic Patagonian glaciations and their correlation with biostratigraphic units of the Pampean region (Argentina). J South Amer Earth Sci 20:81–104

Ramos V (1989) Foothills structure in Northern Magallanes Basin, Argentina. Amer Assoc Petrol Geol Bull 73:887–903

Ramos V (1999) Las provincias geológicas del territorio argentino. Geología Argentina, Anales 29(3):41–96. Instituto de Geología y Recursos Minerales, Buenos Aires.

Rignot E, Rivera A, Casassa G (2003) Contribution of the Patagonia Icefields of South America to global sea level rise. Science 302:434–437

Roig F (1998) Vegetación de la Patagonia. In: Correa M (ed) Flora Patagónica, vol 1. INTA, Buenos Aires, pp 48–391

Rosenblüth B, Fuenzalida H, Aceituno P (1997) Recent temperature variations in southern South America. Int J Climatol 17:67–85

Rott H, Stuefer M, Siegel A, Skvarca P, Eckstaller A (1998) Mass fluxes and dynamics of Moreno Glacier, Southern Patagonia Icefield. Geophys Res Lett 25:1407–1410

Singer B, Ackert R, Guillou H (2004) $^{40}Ar/^{39}Ar$ and K-Ar chronology of Pleistocene glaciations in Patagonia. Geol Soc Amer Bull 116:434–450

Skvarca P (2002) Importancia de los glaciares del Hielo Patagónico Sur para el desarrollo regional. In: Haller M (ed) Geología y Recursos Naturales de Santa Cruz. Relatorio del XV Congreso Geológico Argentino, El Calafate 5(1):785–798. Buenos Aires

Stern C (2007) Holocene tephrochronology record of large explosive eruptions in the southernmost Patagonian Andes. Bull Volcanol 70:435–454

Stuefer M (1999) Investigations on mass balance and dynamics of Moreno Glacier based on field measurements and satellite imagery. PhD dissertation, Leopold-Franzens-Universität, Innsbruck

Chapter 13
The Dry Valleys: An Ancient and Cold Desert in Antarctica

David Sugden

Abstract The Dry Valleys comprise an ice-free part of the Transantarctic Mountains in Antarctica, bounded by the East Antarctic Ice Sheet on the landward side and a coastal ice dome at the coast. Weathering rates are among the lowest on Earth and reflect the persistent hyper-arid, cold polar desert climate. Some buried ice has survived for over 8 million years. The main escarpments and valleys were created on a passive continental margin as Antarctica split from Australia some 55 million years ago. Ice sheet glaciations covered the area some 14 million years ago, deepening some valleys. Sub-glacial lake outbursts, possibly from Lake Vostok, cut the spectacular Labyrinth, a network of vast channels. During Pleistocene glacial periods grounded ice in the Ross Sea dammed large lakes in the lower reaches of the valleys.

Keywords Antarctic • geomorphology • ice sheets • Dry Valleys

13.1 Introduction

Taylor Valley, one of the Dry Valleys, was discovered by accident by Robert Scott and sledging companions in the early years of the twentieth century. Remarkably, Wright and Victoria Valleys were discovered only during the International Polar Year activities of 1957. The valleys are well-hidden from travellers by the gentle rise of a coastal ice rise which blocks the exit to the sea and by a high escarpment which bounds them on their inland end. A first-time visitor to the valleys is struck by the barren, rock-strewn landscape, the scale of valley sides that sweep upwards 1,000 m, the cliffed glacier lobes standing proud of the valley sides, and the many spectacular landforms. The latter include the ice-covered and salty Lake Vanda, the sand dunes of Lower Victoria Valley, the rock glaciers and ancient buried ice in Beacon Valley, and the spectacular canyons and potholes of the Labyrinth in Upper Wright Valley. In recent years it has become clear that this remarkable landscape bears witness to a long and varied history of landscape evolution over the course of tens of millions of years and is in many ways unique in the world.

13.2 Geographical Context

The Dry Valleys are part of the Transantarctic Mountains which extend 3,000 km across Antarctica. These mountains form the faulted and uplifted shoulder of the West Antarctic rift system (Kerr et al. 2000). In the Dry Valleys area they comprise gently tilted sedimentary rocks (Devonian-Triassic Beacon Supergroup) overlying Precambrian-Devonian basement, intruded and capped by dolerites and basalts of Jurassic age (Ferrar Supergroup). The Dry Valleys comprise one tectonic block with summit elevations of up to ~2,400 m in the Asgard and Olympus ranges that lie on either side of Wright valley (Fig. 13.1). The Royal Society block immediately to the south rises above 4,000 m and the Convoy block to the north has summits with elevations of ~2,400 m. Outlet glaciers from the East Antarctic Ice Sheet flow in troughs that cut across the Transantarctic Mountains for much of their length. What marks out the Dry Valleys is that the valleys are only partially filled with ice overspilling from the ice sheet and remain ice-free except for local glaciers on the higher bounding mountains and the coastal piedmont. The ice-free length of Wright Valley is 55 km. In the vicinity of Lake Vanda the valley sides are over 1,000 m high (Fig. 13.2).

P. Migoń (ed.), *Geomorphological Landscapes of the World*,
DOI 10.1007/978-90-481-3055-9_13,

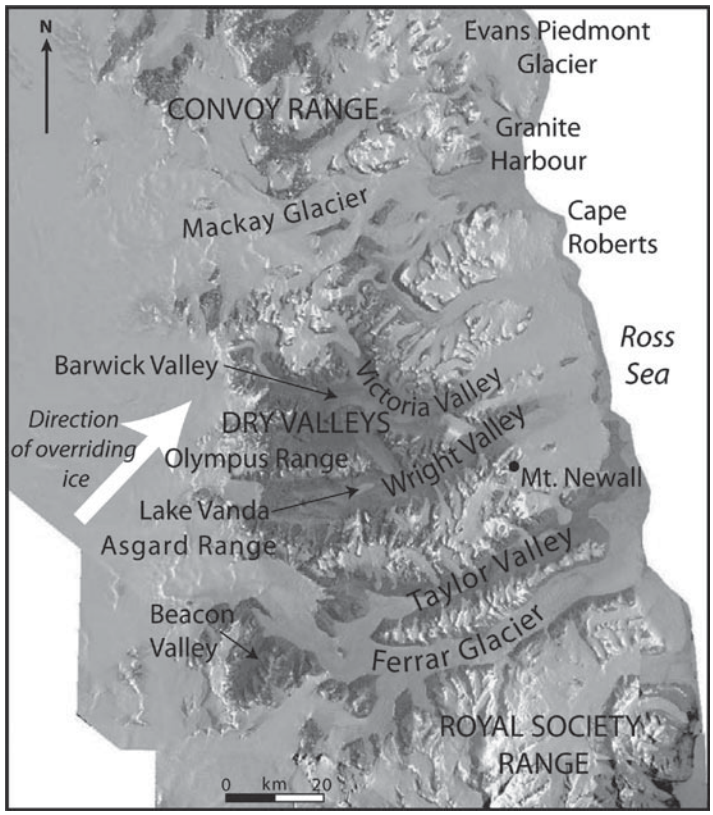

Fig. 13.1 Satellite image showing the Dry Valleys and their geographical context. The East Antarctic ice sheet is to the west and the Ross Sea to the east. The Dry Valleys block is bounded by Ferrar Glacier to the south and Mackay to the north. Figure prepared by Anthony Newton

The climate of the valleys is dominated by the East Antarctic Ice Sheet and is subject to frequent katabatic winds. Mean annual temperatures are close to −20°C on the valley floors and range from −30°C to −40°C at higher elevations. Melting can occur on the lower valley floors for a few days in midsummer. Precipitation falls from the coast, where it approximates 100 mm per year, to inland locations where annual totals are less than 10 mm.

13.3 Landforms

The main landscape features of the Dry Valleys are those of a passive continental margin, similar in many ways to the fluvial landscape of southern Africa. There is a main escarpment up to 1,200 m high separating an undulating upland from a series of lower planation surfaces often, but not always, coinciding with near-horizontal sills of dolerite. Inselbergs often rise cleanly above such lower surfaces (Fig. 13.3). A further escarpment overlooks the coastal lowland piedmont. The latter surface is eroded into basement rocks. This staircase of surface remnants has been dissected by the valleys which retain many features indicative of fluvial action. These include graded long profiles, dendritic and sinuous patterns, straight slope profiles commonly at angles of 26–37° that are at the angle of rest of weathered bedrock material, and lower gradient valley-foot slopes of around 18°, as in upper Victoria Valley. The mountains are similar to areas of mid-western USA with a sharp break between the weathering-limited slopes of the inselbergs or valley sides and the transport-dominated gentle slopes of the plain or valley floor.

A suite of glacial landforms tells of thicker ice overriding the Dry Valleys and associated mountains in a SSW to NNE direction as it flowed towards the offshore continental shelf. The clearest effect is the trough head and over-deepening of Wright Valley in the vicinity

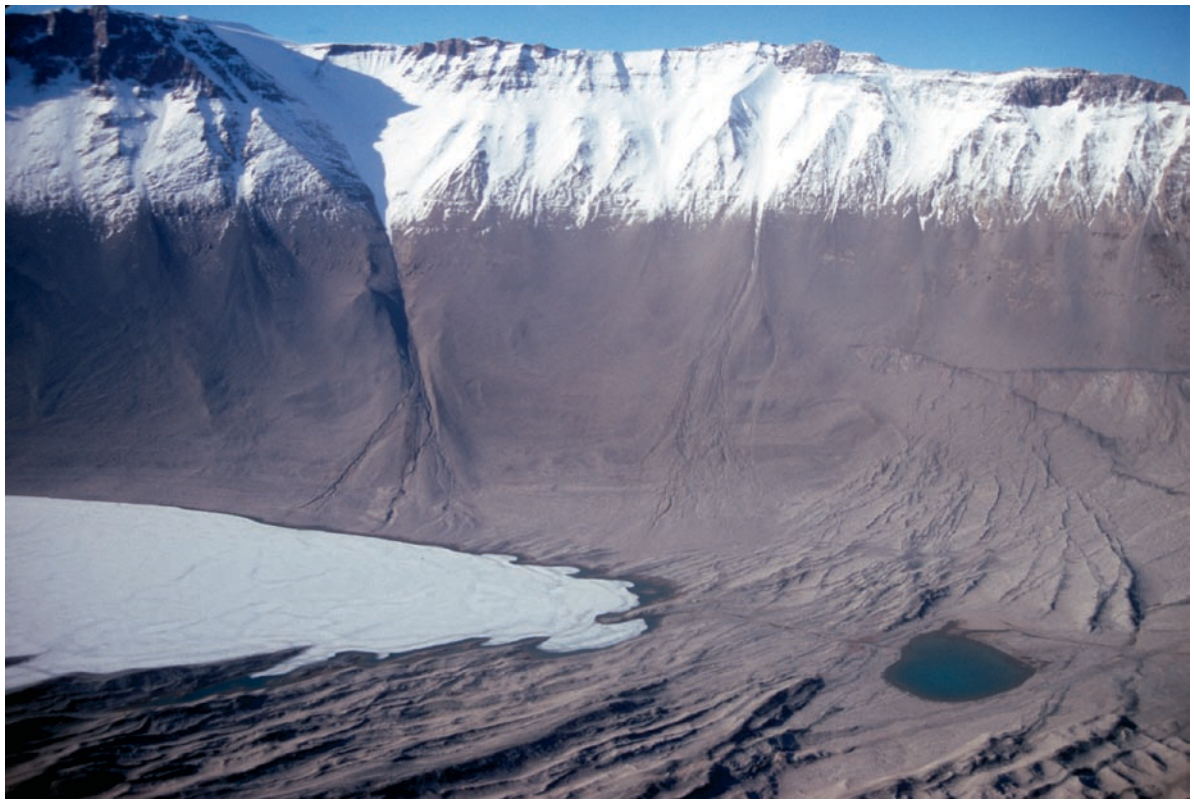

Fig. 13.2 View across Lake Vanda towards the north flank of Wright Valley, following a summer snow storm, showing the ice-covered saline lake, the corrugated bedrock floor cut by ancient sub-glacial meltwater outbursts and the presence of water influenced gullies near the valley floor (Photo D.E. Sugden)

of what is now the site of Lake Vanda. Thicker ice is also demonstrated by ice-scoured bedrock landscapes along the coastal margins up to altitudes of 1,400 m and by ice-moulded saddles, sometimes with roche moutonnée forms, in the interior mountains.

There are also meltwater landforms at all altitudes. The Labyrinth is one of the most remarkable features on Earth (Fig. 13.4). It covers an area of some 40 km^2 and consists of an anastomosing pattern of channels, some of which are over 300 m deep (Lewis et al. 2006). The amplitude of the forms tells of catastrophic sub-glacial meltwater flow on a scale equivalent to the sudden drainage of large lakes, as for example in the case of the Missoula floods of northwest USA (Baker 1978). The orientation of smaller meltwater channels and corrugated bedrock surfaces in Wright Valley demonstrate sub-glacial meltwater flow crossing the mountains from SSW to NNE (Denton and Sugden 2005). One point of interest is the observation that present-day local glaciers flowing down the flanks of Wright and Upper Taylor Valley do not occupy troughs but are superimposed on the overall valley side.

Glacial deposits mantle much of the valley floors, as for example in Wright Valley (Hall et al. 1993). Such deposits range from spreads of till, to finer gravels and glacio-lacustrine or glacio-marine deposits. Arcuate moraine ridges border the lower portions of local glaciers both in the mountains and in the case of the lobes on the main valley sides. Also lateral moraines upslope of the margins of outlets such as Taylor and Mackay glaciers show that they have been thicker and more extended in the past than at present.

The landscape is marked in detail by a wealth of weathering forms. Till sheets are characterised by networks of tundra polygons, with the edges marked by depressions (Fig. 13.5). Apparently solid erratic boulders when viewed from one side are often found on the other side to be hollowed out by tafoni (Fig. 13.6). Such forms are better developed at low altitudes and near the coast. Sandstone cliffs are pitted and certain

Fig. 13.3 View inland showing the main escarpment and the outlying inselbergs of the Olympus Range. The landscape is reminiscent of parts of mid-western America and South Africa (Photo G. Denton)

lithologies undercut to depths of 4 m. Solution hollows, millimetres to centimetres across, pit the surfaces of dolerite, even at high altitudes. White salt deposits underlie many surface stones. On the floors of valleys at high altitudes individual surface stones of till and regolith are shaped into pyramid-shaped ventifacts. Sorted ripples, ~1 m across and several metres long, consist of debris less than a few cm in diameter and lie athwart the dominant wind direction. Sand dunes accumulate in depressions and in lower Victoria Valley.

13.4 Evolution

The origin and landscape significance of many of the above landforms have been the subject of much debate (Selby 1971). Indeed the fluvial versus glacial origin of the landscape has been debated since the first observations of the expeditions of Scott and Shackleton in the first years of the twentieth century (Taylor 1914). What follows is a synthesis which owes much to improvements in dating. Thermochronology has shown that the Dry Valleys landscape is typical of a passive continental margin. Techniques such as argon–argon analysis and cosmogenic isotope analysis have revealed that weathering rates in the dry polar climate have been exceptionally slow for millions of years; indeed, some of the regolith and the slopes on which it lies date back at least 15 million years and even to the onset of glaciation 34 million years ago.

The presence of a series of planation surfaces and escarpments rising from the coast and incised by river valleys issuing from local topographic highs is typical of a passive rifted margin (Fig. 13.7). Rifting exposes a new base level which releases a pulse of erosion as a result of steeper river gradients. Indeed a numerical simulation of the coupled erosion and tectonic processes simulates the topography of the Dry Valleys in remarkable detail (Beaumont et al. 2000; Jamieson and Sugden 2008). Apatite-fission-track analysis and the upwarping of the basement rocks suggests a wedge

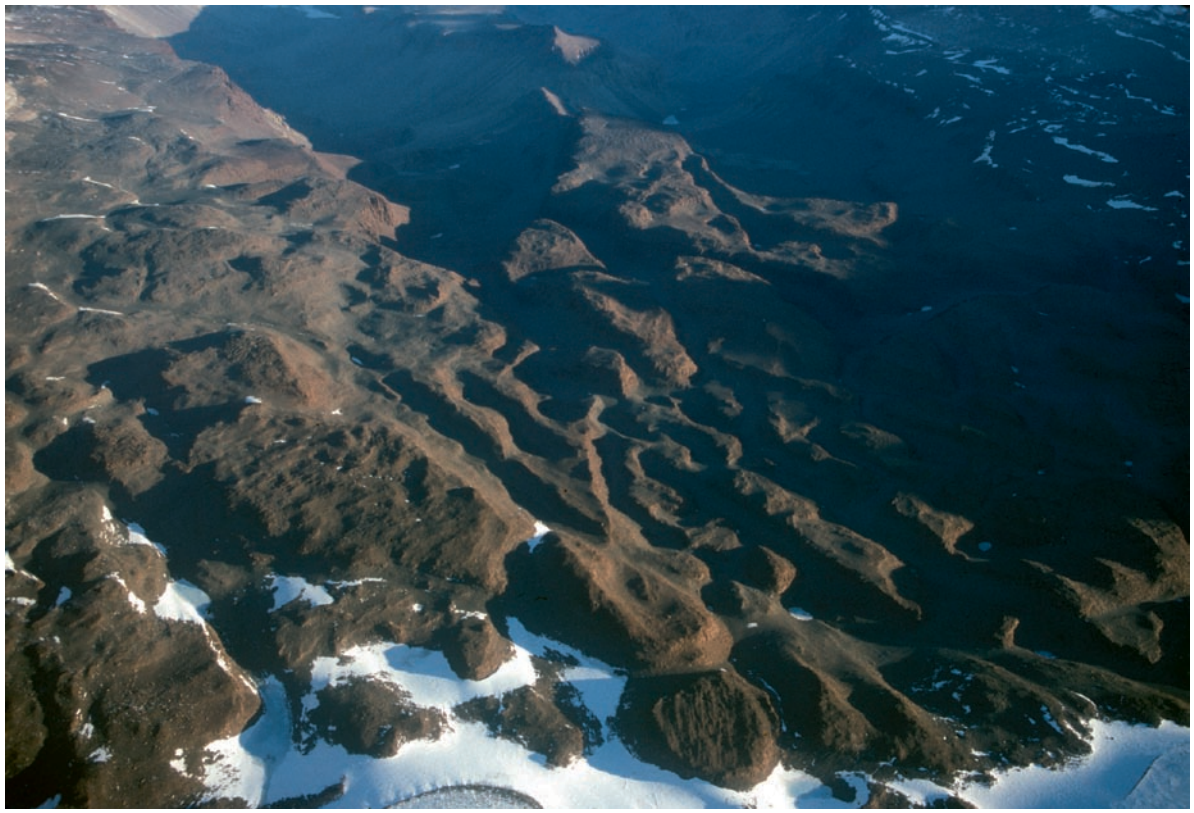

Fig. 13.4 Part of the Labyrinth channel system at the head of Wright Valley, the result of outburst floods beneath a former ice stream (Photo D.E. Sugden)

of rock 4–6 km thick at the coast, declining to 1 km inland beyond the escarpments, has been removed (Fitzgerald 1992). The main phase of denudation began ~55 million years ago and probably was largely complete by 40 million years ago, with the main valleys conformable with sea level at their mouths.

The onset of glaciation has been controversial mainly because of uncertainty about the age of the oldest till deposits in the area. This locally derived deposit, the Sirius Group, centred on the mountain summits, represents glaciers advancing into beech scrub in a Patagonian-type climate. Initial dating on the basis of marine diatoms to the Pliocene implied a mainly post-Pliocene evolution of the landscape (Van der Wateren et al. 1999). However, offshore drilling at Cape Roberts (Naish et al. 2001), coupled with the results of terrestrial argon–argon dating now demonstrate a pre-mid-Miocene age for the till and probably an Oligocene age of 34 million years.

One important development has been the dating of the overriding ice sheet to the mid-Miocene, ~14 million years ago. The expansion, which extended to the outer edge of the continental shelf, is younger than tills containing argon–argon dates on volcanic ash-falls of 14.8 million years, since the ice has moulded the underlying deposit. And yet it is older than 13.6 million years, since ashes of this age are preserved on bedforms created by the overriding ice (Marchant et al. 1993). Such an age is confirmed by the argon–argon age of volcanic cones erupted onto glacially scoured surfaces and on volcanic ash trapped in the meltwater channels of the Labyrinth (Lewis et al. 2006); it is also confirmed by ^{3}He ages of dolerite clasts deposited by the outburst floods (Margerison et al. 2005). What is interesting is that this mid-Miocene age correlates with marine evidence of a sharp cooling at the time (Shevenell et al. 2004; Sugden and Denton 2004), and with seismic and drilling evidence of the subsequent retreat of the ice sheet as it withdrew from the offshore continental shelf around 13.6 million years ago (Anderson 1999). An exciting implication for geomorphologists is that the Labyrinth is one of the routes by which a large sub-glacial lake drained catastrophically,

Fig. 13.5 Tundra polygons in till, McKelvey Valley, adjacent to the Olympus Range. Snowfall picks out the depressions in the polygons, which measure several metres across (Photo D.E. Sugden)

perhaps on several occasions; ice-sheet modelling shows that the main candidate upstream could well have been Lake Vostok.

Geomorphological evidence of weathering rates suggests that the climate of the last 13.6 million years has been stable and remained dry and cold throughout. The important implication is that the ice sheet that controls the climate has also been present throughout. The evidence of low weathering rates is borne out by cosmogenic analysis of surface clasts and bedrock (Brook et al. 1995). Summerfield et al. (1999) used cosmogenic ^{21}Ne in quartz to show that rates of denudation were 0.25–1 m per 1 million years on lower valley slopes and less than 0.16 m per 1 million years at high elevation sites, rates that have persisted for millions of years. These low rates, comparable with other hyper-arid deserts, reflect the slow rate of salt weathering and deflation, especially at drier, higher altitudes. Another constraint on rates of denudation can be related to the lack of water-related forms at all but low altitudes, as for example near lake Vanda (Fig. 13.2); indeed, allowing for lapse rate changes with altitude, the low-altitude distribution of the water-cut gullies in the Dry Valleys and their absence at high altitudes restricts any climatic warming to less than ~3°C. Finally, buried glacier ice has survived beneath 60 cm of regolith in Beacon Valley for at least 8 million years (Sugden et al. 1995a). Such an age attribution has been controversial since it implies unusually low rates of sublimation of ice. However, recent modelling of vapour flow in the regolith of Beacon Valley, based on instrumental measurements, suggests that the ice could have survived permanently under mean summer temperatures only 4° lower than present (Kowalewski et al. 2006). The latter figure is a reasonable long-term approximation for the Dry Valleys, bearing in mind lower average global temperatures in the Pleistocene and the late Miocene. Thus there is every reason to believe in the great age of the buried ice in Beacon Valley. It follows that the climate must have remained cold and dry for millions of years.

There is evidence of some small changes in climate and glacier extent during the Pliocene and Pleistocene which have left their mark in the Dry Valleys. One can predict that a slight climatic warming, such as occurred

Fig. 13.6 Tafoni on a boulder in Bull Pass on the southern flank of Wright Valley (Photo D.E. Sugden)

globally in the Pliocene, would lead to an increase in snowfall and glacier thickness and extent in Antarctica. This is because the warmer atmosphere can hold more moisture, but temperatures are still sufficiently low to prevent significant melting. Cosmogenic and argon–argon analyses suggest that Taylor Glacier did indeed thicken and expand down-valley in the Pliocene about 3–4 million years ago (Marchant et al. 1994).

In the Pleistocene, environmental changes affected the landscape of the Dry Valleys in response to the lowering of global sea level caused by ice-sheet growth in the Northern Hemisphere. The main change was the grounding and thickening of the Ross Ice Shelf as it flowed towards the outer edge of the offshore continental shelf. The effect in the Dry Valleys was to block the valleys at their seaward end and to discharge meltwater into ice-dammed lakes that expanded in their lower reaches. The lake in lower Taylor Valley saw the encroaching ice pushing lake ice onshore and depositing fine material on the lake floor and larger fragments on the lake shore. It is this unusual lake conveyor process that explains the complexity of the deposits in Taylor and Victoria valleys (Hall et al. 2002). In a sense the saline lakes of the inner Dry Valleys are the concentrated remains of former large Pleistocene lakes. In Victoria Valley, remnants of Pleistocene lake ice are still preserved beneath superficial deposits. An accompanying effect of the grounding of ice in the Ross Sea was the thickening of outlet glaciers at the coast. Mackay and Ferrar glaciers mimicked many outlet glaciers in the Transantarctic Mountains by thickening most near the coast as they merged with the grounded ice shelf and less so up glacier.

The initial thinning of the grounded Ross Ice Shelf has been dated by deltas associated with the moraine and ice dammed lakes and began later than 12,000 years ago. The first open water at the Dry Valleys' coast is indicated by the age of raised beaches forming around 6,600 years ago (Hall et al. 2004).

13.5 Conclusion

The Dry Valleys are unique in Antarctica for their large extent of ice-free ground. But perhaps their true significance is that their landforms open a direct window into

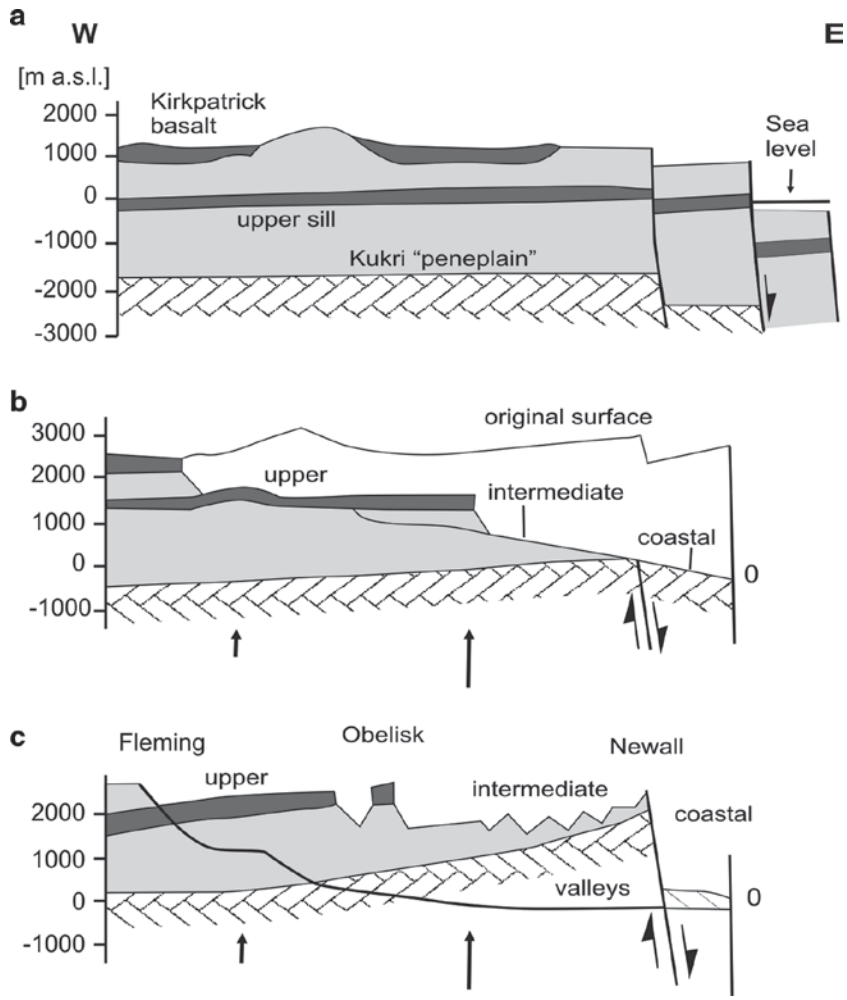

Fig. 13.7 Empirical model of the evolution of the Dry Valleys, showing the wedge of rock removed by denudation of the passive continental margin (Sugden et al. 1995b). The landscape at (**a**) the time of initial rifting, (**b**) following the pulse of denudation which began ~55 million years ago and (**c**) at the beginning of glaciation. *Arrows* denote rock uplift or subsidence. The transect is composite and in the latitude of Mt. Newall. The originally horizontal Kukri 'peneplain', cut in basement rocks, is warped upwards near the coast as a result of denudation

the Antarctic landscape of the Miocene and even the Oligocene. In this desert landscape one can recognise the ancient but classic signs of the fluvial erosion of a passive continental margin. Superimposed on this is the world's longest history of glacial modification and preservation, bequeathing such world gems as the Labyrinth and the oldest glacier ice in the world. Subsequently, since the mid-Miocene, we see processes that operate in the world's coldest hyper-arid desert. Intriguingly, the climate and processes of the higher parts of the Dry Valleys overlap with conditions on Mars. The Dry Valleys may yet have an additional and influential role in helping us to understand extra-terrestrial geomorphology.

The Author

David Sugden is Professor of Geography at School of GeoSciences, University of Edinburgh. He has published nine books, including *Glaciers and Landscape* with Brian John, and over 100 papers in international journals. He has several honours, including the Linton Award from the British Society for Geomorphology, Vega Medal (Sweden), Polar Medal (UK) and Mungo Park Medal (RSGS). He has worked in Antarctica on 14 occasions, including several seasons working in the McMurdo Dry Valleys with George Denton and David Marchant on projects supported by the US Antarctic Research Program and the UK Natural Environment Research Council.

References

Anderson J (1999) Antarctic marine geology. Cambridge University Press, Cambridge

Baker VR (1978) Paleohydraulics and hydrodynamics of Scabland floods. In: Baker VR, Nummedal D (eds) The channelled Scabland. NASA, Washington, DC, pp 59–79

Beaumont C, Kooi H, Willett S (2000) Coupled tectonic-surface process models with applications to rifted margins and collisional orogens. In: Summerfield MA (ed) Geomorphology and global tectonics. Wiley, Chichester, UK, pp 29–55

Brook EJ, Brown ET, Kurz MD, Ackert RP, Raisbeck GM, Yiou F (1995) Constraints on age, erosion and uplift of Neogene glacial deposits in the Trasantarctic Mountains determined from in situ cosmogenic ^{10}Be and ^{26}Al. Geology 23:1063–1066

Denton GH, Sugden DE (2005) Meltwater features that suggest Miocene ice-sheet overriding of the Transantarctic Mountains in Victoria Land, Antarctica. Geogr Ann 87A:67–85

Fitzgerald PG (1992) The Transantarctic Mountains of southern Victoria land: the application of fission track analysis to a rift shoulder uplift. Tectonics 11:634–662

Hall BL, Denton GH, Lux DR, Bockheim JG (1993) Late Tertiary Antarctic paleoclimate and ice-sheet dynamics inferred from surficial deposits in Wright Valley. Geogr Ann 75A:239–267

Hall BL, Denton GH, Overturf B, Hendy CH (2002) Glacial Lake Victoria, a high-level Antarctic lake inferred from lacustrine deposits in Victoria Valley. J Quat Sci 17:697–706

Hall BL, Baroni C, Denton GH (2004) Holocene relative sea-level history of the southern Victoria Land coast, Antarctica. Global Planet Change 42:241–263

Jamieson SSR, Sugden DE (2008) Landscape evolution of Antarctica. In: Cooper AK and the 10th ISAES team (eds) Antarctica: a keystone in a changing world. National Academies Press, Washington, DC and USGS, pp 39–54

Kerr A, Sugden DE, Summerfield MA (2000) Linking tectonics and landscape development in a passive margin setting: the Transantarctic Mountains. In: Summerfield MA (ed) Geomorphology and global tectonics. Wiley, Chichester, UK, pp 303–319

Kowalewski DE, Marchant DR, Levy JS, Head JW (2006) Quantifying low rates of summertime sublimation for buried glacier ice in Beacon Valley, Antarctica. Antarctic Sci 18:421–428

Lewis AR, Marchant DR, Kowalewski DE, Baldwin SL, Webb LE (2006) The age and origin of the Labyrinth, western Dry valleys, Antarctica: evidence for extensive middle Miocene subglacial floods and freshwater discharge to the Southern Ocean. Geology 34:513–516

Marchant DR, Denton GH, Sugden DE, Swisher CCIII (1993) Miocene glacial stratigraphy and landscape evolution of the western Asgard Range, Antarctica. Geogr Ann 75A:303–330

Marchant DR, Denton GH, Bockheim JG, Wilson SC, Kerr AR (1994) Quaternary ice-level changes in upper Taylor Glacier, Antarctica: implications for paleoclimate and and ice-sheet dynamics. Boreas 25:29–43

Margerison HR, Phillips WM, Stuart FM, Sugden DE (2005) Cosmogenic ^{3}He concentrations in ancient flood deposits from the Coombs Hills, northern Dry Valleys, East Antarctica: interpreting exposure ages and erosion rates. Earth Planet Sci Lett 230:163–175

Naish TR and 32 others (2001) Orbitally induced oscillations in the East Antarctic ice sheet at the Oligocene/Miocene boundary. Nature 413:719–723

Selby MJ (1971) Slopes and their development in an ice-free, arid area of Antarctica. Geogr Ann 53A:235–245

Shevenell AE, Kennett JP, Lea DW (2004) Middle Miocene Southern Ocean cooling and Antarctic cryosphere expansion. Science 305:1766–1770

Sugden DE, Denton GH (2004) Cenozoic landscape evolution of the Convoy Range to Mackay Glacier area, Transantarctic Mountains: onshore to offshore synthesis. Geol Soc Am Bull 116:840–857

Sugden DE, Marchant DR, Potter N Jr, Souchez RA, Denton GH, Swisher CC, Tison J-L (1995a) Preservation of Miocene glacier ice in East Antarctica. Nature 376:412–414

Sugden DE, Denton GH, Marchant DR (1995b) Landscape evolution of the Dry Valleys: Tectonic implications. J Geophys Res 100((B7)):9949–9967

Summerfield MA, Sugden DE, Denton GH, Marchant DR, Cockburn HAP, Stuart FM (1999) Cosmogenic isotope data support previous evidence of extremely low rates of denudation in the Dry Valleys region, southern Victoria Land. Geol Soc London Spec Publ 162:255–267

Taylor G (1914) Physiography and glacial geology of east Antarctica. Geogr J 44:365–382, 452–467, 553–571

Van der Wateren FM, Dunai TJ, Van Balen RT, Klas W, Verbers ALLM, Passchier S, Herpers U (1999) Contrasting Neogene denudation histories of different structural regions in the Transantarctic Mountains rift flank constrained by cosmogenic isotope measurements. Global Planet Change 23:145–172

Chapter 14
Drakensberg Escarpment: Mountains of Geomorphic Diversity

Stefan Grab

Abstract This chapter describes the diversity of geomorphological phenomena along the Drakensberg escarpment, which is the highest section along the Great Escarpment of southern Africa. The Drakensberg escarpment provides one of the most scenically impressive continuous rockwalls in the world, extending almost 300 km and reaching vertical heights of over 600 m. A summary is presented on the early and more recent views of landscape evolution that produced the Great Escarpment. Weathering phenomena, slope forms, mass movement and soil erosion are prominent features of the lower-lying sandstone formations, whilst most geomorphological research focusing on the basaltic escarpment summit area has endeavoured to unravel the late Quaternary periglacial and glacial geomorphic history.

Keywords Drakensberg escarpment • geomorphic diversity • southern Africa

14.1 Introduction

Great escarpments forming major scarps of several 100 m in height and hundreds to thousands of kilometres in length may be found near passive continental margins, such as those along eastern Brazil (Serra do Mar), western India (Western Ghats) – presented elsewhere in this volume, eastern Australia (Great Escarpment) and southern Africa (Drakensberg) (Fig. 14.1). Such escarpments are usually associated with an inland plateau and deeply dissected coastal platform, which are remnants of the old plateau surface. Great escarpments are thus mega-scale erosional landforms, hosting some of the world's most dramatic scenery and highest waterfalls. Several great escarpments are also associated with flood basalt volcanism such as the Deccan Traps (India), Simien mountains (Ethiopia) and Drakensberg.

The geomorphology of great escarpments is controlled by exceptionally steep gradients (frequently near 90°) and rock walls extending several hundred metres in height. Consequently, great escarpments are associated with complex micro-climates, controlled by steep lapse rates, weather system blocking effects and associated orographic uplift. This, together with a sometimes equally variable lithological composition, provides for a diverse geomorphic setting.

The geomorphology of the Drakensberg is varied owing to the considerable geological and climatological differences between the lower altitude sandstone regions and higher altitude basalt outcrops. Areas above 2,800 m a.s.l. host landscape components that are typical to 'alpine' or 'periglacial' environments, where cold temperatures, ice and snow are important controlling factors (Fig. 14.2). The steep slopes and deep valleys to the east of the Great Escarpment, associated with a high annual precipitation, produce substantial hydraulic gradients along fluvial channels and on slopes, thus providing for a diverse landscape which hosts a wide assortment of erosional, mass movement and depositional features.

14.2 Geographical Setting

The Drakensberg escarpment extends about 962 km from Polokwane in Limpopo Province to Elliot in the Eastern Cape Province (Fig. 14.1). The highest section of the Drakensberg forms a natural border between eastern Lesotho and KwaZulu-Natal Province in South Africa, where it extends about 280 km and attains an

P. Migoń (ed.), *Geomorphological Landscapes of the World*,
DOI 10.1007/978-90-481-3055-9_14,

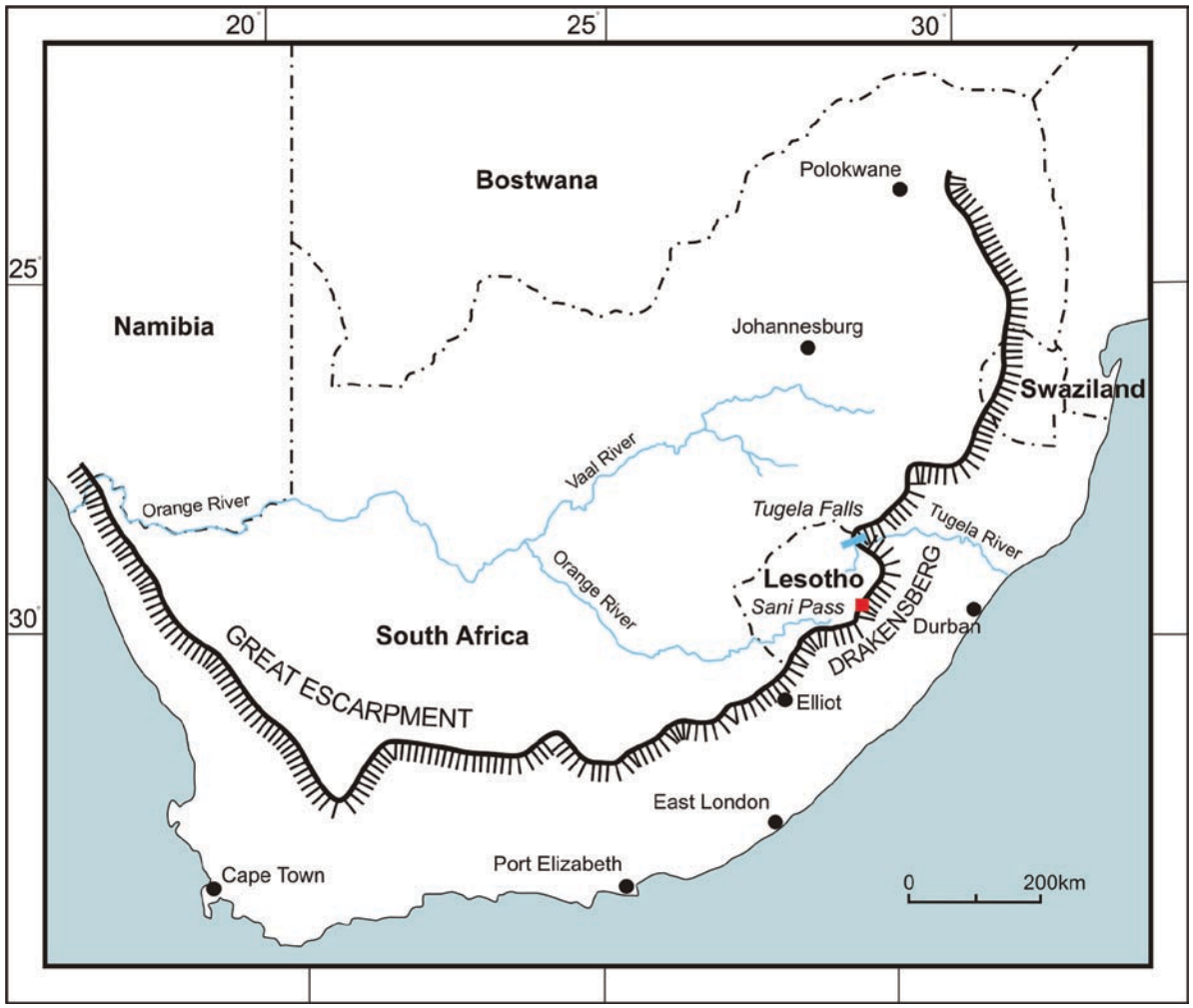

Fig. 14.1 Map showing the Great Escarpment and locality of the Drakensberg in southern Africa

average altitude of almost 3,000 m (max. at Thabana-Ntlenyana; 3,482 m a.s.l.) (Fig. 14.3). The Drakensberg-Maluti Transfrontier Park and World Heritage Site is located within this highest section of the Great Escarpment, which separates the interior plateau to the west from the coastal plain to the east (Fig. 14.2).

The climate of the Drakensberg escarpment and adjoining foothills is characterized by significant diurnal and seasonal temperature fluctuations which exercise considerable control on contemporary geomorphic processes. Annual temperature extremes may vary from 35°C in the foothills to −21°C on the high summits. The high escarpment above 3,000 m a.s.l. has a typically alpine climate of cool (av. 11°C) summers and cold winters (av. 0°C). Ground freezing occurs on about 200 days per annum and is usually accompanied by the formation of needle ice. Precipitation along the escarpment typically exceeds 1,000 mm per annum, but is mostly restricted to the summer months (70%). Only about 10% of annual precipitation falls during winter, thus limiting snowfall to about eight events per annum along the high escarpment.

The Drakensberg vegetation has been classified according to three climax communities ranging from the foothills to the escarpment summit; namely *Podocarpus Latifolius* forest (1,300–1,800 m, montane belt), *Passerina-Philippia-Widringtonia* shrubs (1,800–2,900 m, subalpine belt) and *Erica-Helichrysum* heath (above 2,900 m, alpine belt) (Killick 1963).

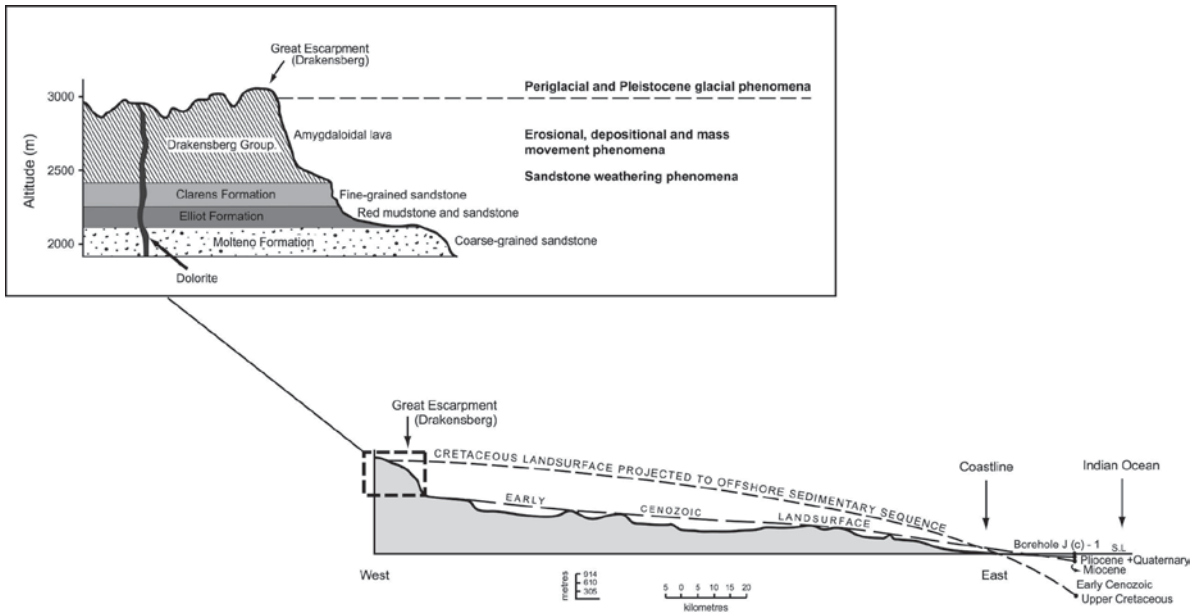

Fig. 14.2 Denudational and sedimentational relations to the east of the Great Drakensberg Escarpment, from the Cretaceous until the Miocene (Modified from King 1982). The inset shows the typical geological and geomorphological succession along the Great Escarpment (Modified from Pickles 1985)

14.3 Long-Term Landscape Evolution

The Drakensberg escarpment is located within the ancient Great Karoo Basin, a large shallow basin that formed the locus for the deposition of continental shelf sediments from over 200 million years ago (Partridge and Maud 2000). This inter-continental basin spanned beyond the present margins of the African subcontinent, when Antarctica, Africa, Madagascar, India, Australia and South America formed the super-continent of Gondwanaland. During the prolonged period of sedimentation, which totalled 7,000 m in places (Partridge and Maud 2000), climate changed from glacial conditions during the Permian (Dwyka tillite) through temperate to desert conditions when wind-blown sand deposits represented the final stage of sedimentation to form the Lower Jurassic aeolian strata of the Clarens Formation (Fig. 14.2). The basin sediments formed near horizontal, conformably bedded sedimentary formations. As Gondwanaland began to break up through rifting, the first extensive basaltic lava outpourings started during the early Jurassic, forming the Drakensberg volcanic group. At this stage the geological succession of the future Drakensberg had been completed, consisting of the Stormberg Group sedimentary sequences at lower elevations and capped by the Drakensberg Group basaltic series (Fig. 14.2). The Stormberg Group comprises the Molteno, Elliot, and Clarens Formations; these display a considerable variety of sedimentary rock types ranging from mudstones to coarse conglomeratic sandstones. Although sills and dykes of fine-grained dolerite have intruded various components of the Karoo Supergroup, these become increasingly scarce when moving up the stratigraphic sequence.

Much controversy has surrounded the interpretation of how the southern African landscape has evolved since the fragmentation of Gondwanaland (see Partridge and Maud 1987; 2000; Fleming et al. 1999; Brown et al. 2000). The dominant geomorphological structure of southern Africa is the Great Escarpment, which was first explained by Suess (1904) as being the result of uplift along a major fault. Subsequent work abandoned the fault hypothesis, rather suggesting an erosional origin (e.g. Penck 1908; King 1944). With time, several 'erosion surfaces' had been identified and these are thought to be the result of successive phases of erosion which were initiated by continental uplift at various times since the break-up of Gondwanaland.

Monocyclic and polycyclic stages of uplift were suggested to have taken place along faults, or alternatively,

Fig. 14.3 The foothills with solifluction lobes in the foreground (2,500 m a.s.l) and the Great Escarpment of the Drakensberg (over 3,000 m a.s.l.) in the background (Photo S. Grab)

to have caused a major monoclinal structure. King (1944) considered the erosion surfaces at different elevations as of the same age due to tectonic uplift. This view was later abandoned, when the main Drakensberg scarp was envisaged as a divide between the early Tertiary planation and the Gondwana/post-Gondwana land surfaces (King and King 1959) (Fig. 14.2). King and King (1959) believed that the regularity of erosion surfaces suggests a cyclic process within the Quaternary; this included uplift of land and extensive warping accompanied by strong seaward tilting, thereby raising the early Tertiary landscape and initiating the incision of river courses. Major upwarping during the late Miocene is believed to have contributed to considerable gully development and gorge incision along the Great Escarpment (King and King 1959). Some of the headwaters to the west of the escarpment, such as those near Sani Pass, have broad gentle valleys, which were considered to be the second erosion surface of 'Kretacic cycle' (King 1976).

King estimated an elevation of only 600 m for the present-day Lesotho highlands at the time Gondwanaland broke up and suggested that the Great Escarpment resulted from a major uplift in the Middle Cretaceous. However, according to Partridge and Maud (1987), the Lesotho highlands had a pre-rifting elevation of about 2,400 m, which was due, in part, to uplift along the rift system at the time of continental separation. At the time of rifting, the escarpment apparently featured as a substantial scarp along the continental margin (Partridge and Maud 2000). Since the Cretaceous, the Great Escarpment is said to have gradually eroded inland from the coast, such that about 300 m has been vertically removed and is now situated 50 to 200 km inland from the coast (Partridge and Maud 1987; 2000). The most rapid retreat is thought to have taken place during the early Cretaceous when elevations were high and the climate humid and tropical, consequently initiating rapid weathering and a dense, well-integrated fluvial erosion system (Dunlevey et al. 1993; Partridge 1998;

Partridge and Maud 2000). These authors further suggest that as the Great Escarpment receded, it left a gently sloping erosional bench across the coastal hinterland (Fig. 14.2). Subsequent uplift during the early Miocene and late Pliocene increased stream incision and produced the dissected topography that is so characteristic to many areas of KwaZulu-Natal, of which the foothill zone of the Drakensberg is a good example.

Most past models on southern African landscape evolution relied substantially on the characteristics of weathered deposits and the correlation of erosion surface remnants for their geochronological reconstruction (Fleming et al. 1999). More recent studies have used *in-situ*-produced cosmogenic isotopes (Fleming et al. 1999) and apatite fission-track data (Brown et al. 2000) to provide an improved palaeo-denudation chronology for portions of the southern African escarpment. The cosmogenic isotope data suggest a long-term escarpment retreat rate of 50–95 m Ma^{-1} (i.e. <10 km since continental break-up *c.* 135 Ma ago) and an average summit denudation rate of 6 m Ma^{-1} (Fleming et al. 1999), whilst the fission-track data indicate a major post-rifting denudational phase across the South Atlantic margins of Africa (Brown et al. 2000). Findings such as these challenge the long-standing previous views for the long-term survival of erosion cycle surfaces and original escarpment locality close to the continental edge immediately following Gondwana break-up.

14.4 Landforms

14.4.1 Weathering Phenomena

The Molteno, Elliot and Clarens Formation sandstones display an impressive assortment of macro- and micro-scale landforms that can be attributed to the combined action of weathering and erosion. Macro-scale phenomena include rock arches, caverns, buttes and 'mushroom' -shaped rock exposures, whilst the rock surfaces frequently display polygonal fracture patterns, fluted bedrock, and a variety of erosional (solutional) notches including pits and tafoni (Figs. 14.4 and 14.5).

Fig. 14.4 Weathering (solution) hollows ('rock doughnuts') within Clarens Formation sandstones below the escarpment (Photo S. Grab)

Fig. 14.5 The 'Golden Gate' consisting of Elliot (lower reddish unit) and Clarens (upper yellowish unit) sandstones, below the escarpment (Photo S. Grab)

Weathering is causing the deterioration of San ('Bushman') rock art located on rock overhangs, in particular where moisture is able to penetrate into the rock (Meiklejohn 1997). The weathering processes operating on the sandstone include thermal stress fatigue, salt crystallization, hydration and dehydration of rock minerals, hydrolysis, and chemical alteration (Meiklejohn 1997). Hall et al. (2007) have suggested that thermal variations between pigmented and adjacent paint-free surfaces may induce stresses that could contribute to the deterioration of the art.

The basalt along the high escarpment hosts less diverse surface morphologies but typically displays concentric exfoliation structures which contribute to the development of corestones in saprolite. Given the harsh alpine climate, the basalt is subjected to substantial near-surface thermal gradients (14°C/5 mm), whilst summit interfluves and south-facing slopes are likely to undergo cryogenic fracturing where and when moisture is available (Grab 2007a; b). Weathering processes provide relatively small (<20 cm *a*-axis) angular, platy clast shapes which accumulate along summit interfluves; these eventually become translocated downslope through fluvial or solifluction processes (Fig. 14.6).

14.4.2 Slope Forms

Bedrock slope forms in the Drakensberg are primarily controlled by the overall rock mass strength (RMS) (Moon and Selby 1983; Moon and Munro-Perry 1988). Although Moon and Selby (1983) ascribe the steeply inclined escarpment surfaces to high RMS ratings (67–86, according to Selby's [1980] RMS technique) and relatively uniform strength characteristics of basalt, Grab et al. (2005) demonstrated considerable spatial variabilities in the RMS characteristics of basaltic slopes along the high escarpment zone. In fact, most basaltic scarp faces fell outside the strength equilibrium

Fig. 14.6 A stone-banked lobe on a high escarpment interfluve (3,400 m a.s.l.) (Photo S. Grab)

envelope, with over-steepened slope angles relative to their mass strength (Grab et al. 2005). The distinct basalt-terraces at high altitudes correspond to different phases of lava outpourings and are thus primarily lithologically controlled (Grab et al. 2005). The lower sandstone units also host variable slope forms; these include steep slopes associated with high RMS values of between 75 to 91, quasi-rectilinear slopes inclined at angles lower than could be supported by the high-strength rocks on which they occur, and 'caves' (recessed surfaces) where the RMS is considerably lower due to siltstone outcrops or high joint densities (Moon and Selby 1983; Moon and Munro-Perry 1988). Whilst there is little contemporary talus material accumulation below basalt cliffs, suggesting slow cliff recession, the frequent occurrence of 'gentle' (30–35°) rectilinear slopes below steeper sandstone cliffs apparently indicates that valley sideslopes develop through a process of 'slope replacement' (Moon and Munro-Perry 1988).

14.4.3 Mass Movement and Erosion

The slopes immediately east of the Drakensberg Escarpment provide a high energy environment, as is evidenced by thousands of Holocene rockfalls and landslides (Fig. 14.7). A comparison of mass movement scars from the earliest available photographs (1949) to those taken more recently, has highlighted the slow natural recovery rate of such scars. Given the steep hydraulic gradients, natural sub-surface soil pipes are common to the lower Drakensberg slopes where they eventually develop into gullies once the roofs collapse. Gullies are also becoming more prominent in the high alpine wetlands of eastern Lesotho where they have eroded through alternating layers of sediment and peat. The high occurrence of needle ice on stream banks and gully sidewalls during winter nights weakens the soil structure and contributes to bank collapse and sediment loss in the high Drakensberg. Slopes above c 2,000 m

Fig. 14.7 Shallow landslides involving slope covers are common on the steep slopes below the main escarpment (Photo S. Grab)

a.s.l. are also susceptible to 'turf exfoliation', which is a denudation process destroying vegetation cover by removing the soil exposed along small soil terraces. A variety of synergistically operating factors are responsible for such turf exfoliation on the higher slopes of the Drakensberg; these include needle ice, burrowing ice rats (*Otomys Sloggetti*), grazing livestock, water flow, rain splash and deflation (Grab 2002a). Wind erosion is particularly prominent on the high plateau where wind speeds of over 120 km/h regularly occur.

The Drakensberg Escarpment forms the watershed for two of southern Africa's largest drainage basins, namely that for the Orange River flowing westwards into the Atlantic Ocean, and secondly that for the Tugela River flowing eastwards into the Indian Ocean (Fig. 14.1). Spectacular waterfalls, of which some are amongst the highest in the world (e.g. the Tugela Falls is the highest cascade of waterfalls in the world, totalling 947 m in five cascades), occur along the main Drakensberg scarp face and contribute toward the gradual retreat of the Great Escarpment. The eastward draining rivers have eroded deep valley systems, particularly where meeting the sandstone outcrops. The immense energy of these fluvial systems is evident from the large basalt boulder deposits located up to 10 km downstream from the basalt outcrops. As slope gradients are reduced eastward, so the channels gradually widen and begin to meander as lateral erosion becomes more prominent.

14.4.4 Periglacial and Glacial Landforms

The high Drakensberg Escarpment region hosts a wide variety of fossil and active periglacial landforms. Although lithology is a primary factor controlling macro-topographic features such as asymmetric valleys and slope terraces (resembling cryoplanation terraces), cryogenic processes are likely to have contributed to such landscape features through much of the Cenozoic.

Earth hummocks (thufurs) are common to the alpine wetlands, averaging 20 cm in height and 50 cm in

diameter. These actively forming cryogenic mounds have an important function to regulate and direct water flow through the wetland systems. Contemporary miniature (<12 cm in diameter) sorted soil stripes, circles, and polygons, characterized by finer-grained centres and courser-grained perimeters, develop where adequate moisture is available during the winter months. Somewhat larger stone-banked lobes (Fig. 14.6) and solifluction lobes (Fig. 14.3) are only marginally active and thus likely to have formed during cooler Holocene Neoglacial episodes.

Some high summit interfluves above 3,400 m a.s.l. provide rare sightings of large (>1 m diameter) sorted circles, whilst many south-facing slopes have block-streams of several 100 m in length. Although these landforms have not been dated, they are thought to originate from the Late Pleistocene and could be indicative of deep seasonal frost or permafrost (Grab 2002b). Recently discovered glacial moraine along some of the high (>3,100 m) escarpment riverheads and south-facing slopes in the southern Drakensberg have been dated to the Last Glacial Maximum and provide evidence for limited niche/cirque glaciation (Mills and Grab 2005).

14.5 Conclusions

The Drakensberg escarpment provides one of the most scenically impressive continuous basaltic rockwalls in the world, extending almost 300 km and reaching vertical heights of over 600 m. In addition, the Drakensberg offers an unrivalled regional diversity and abundance of smaller-scale active and relict geomorphic phenomena over relatively short distances, thus creating much aesthetic appeal to tourists. Whilst contemporary weathering processes are slowly removing the legacy left behind by the San rock painters, a host of landforms continue to provide a natural archival treasure of information on past environmental conditions along the Great Escarpment.

The Author

Stefan Grab is Professor in Geomorphology in the School of Geography, Archaeology and Environmental Studies, University of the Witwatersrand, South Africa. His research focuses mostly on broadening the understanding of African alpine geomorphic and climatic systems, both past and present. He has published over 50 peer-reviewed scientific articles in books and journals.

References

Brown RW, Gallagher K, Gleadow AJW, Summerfield MA (2000) Morphotectonic evolution of the South Atlantic margins of Africa and South America. In: Summerfield MA (ed) Geomorphology and global tectonics. Wiley, Chichester, UK, pp 255–281

Dunlevey JN, Ramluckan VR, Mitchell AA (1993) Secondary mineral zonation in the Drakensberg Basalt Formation, South Africa. S Afr J Geol 96:216–220

Fleming A, Summerfield MA, Stone JO, Fifield LK, Cresswell RG (1999) Denudation rates for the southern Drakensberg escarpment, SE Africa, derived from in-situ-produced cosmogenic ^{36}Cl: initial results. J Geol Soc London 156:209–212

Grab S (2002a) Turf exfoliation in the high Drakensberg, southern Africa. Geogr Ann 84A:39–50

Grab S (2002b) Characteristics and palaeoenvironmental significance of relict sorted patterned ground, Drakensberg plateau, southern Africa. Quat Sci Rev 21:1729–1744

Grab S (2007a) Near-surface rockwall temperatures in high Drakensberg basalt: spatio-temporal differences and possible implications for weathering. Z Geomorph NF 51(Suppl 1): 103–113

Grab S (2007b) Rock-surface temperatures of basalt in the Drakensberg alpine environment, Lesotho. Geogr Ann 89A:185–193

Grab S, van Zyl C, Mulder N (2005) Controls on basalt terrace formation in the eastern Lesotho highlands. Geomorphology 67:473–485

Hall K, Meiklejohn I, Arocena J (2007) The thermal responses of rock art pigments: implications for rock art weathering in southern Africa. Geomorphology 91:132–145

Killick DJB (1963) An account of the plant ecology of the Cathedral Peak area of the Natal Drakensberg. Bot Surv S Afr Mem 34:1–178

King LC (1944) Geomorphology of the Natal Drakensberg. Trans Geol Soc S Afr 47:255–282

King LC (1976) Planation remnants upon high lands. Z Geomorph NF 20:133–148

King LC (1982) The natal monocline. University of Natal Press, Pietermaritzburg, South Africa

King LC, King LA (1959) A reappraisal of the Natal monocline. S Afr Geogr J 41:15–30

Meiklejohn KI (1997) The role of moisture in the weathering of the Clarens Formation of the KwaZulu-Natal Drakensberg: implications for the preservation of indigenous rock art. S Afr Geogr J 79:199–206

Mills CS, Grab SW (2005) Debris ridges along the southern Drakensberg escarpment as evidence for Quaternary glaciation in southern Africa. Quat Int 129:61–73

Moon BP, Munro-Perry PM (1988) Slope development on the Clarens Sandstone Formation in the northeastern Orange Free State. S Afr Geogr J 70:57–68

Moon BP, Selby MJ (1983) Rock mass strength and scarp forms in southern Africa. Geogr Ann 65A:135–145

Partridge TC (1998) Of diamonds, dinosaurs and diastrophism: 150 million years of landscape evolution in southern Africa. S Afr J Geol 101:167–184

Partridge TC, Maud RR (1987) Geomorphic evolution of southern Africa since the Mesozoic. S Afr J Geol 90:179–208

Partridge TC, Maud RR (2000) Macro-scale geomorphic evolution of southern Africa. In: Partridge TC, Maud RR (eds) The Cenozoic of Southern Africa. Oxford University Press, Oxford, pp 3–18

Penck A (1908) Der Drakensberg und der Quathlambabruch. Sitzung der Kaiserlich Preussischen Akademischen Wissenschaften 11:235–237

Pickles J (1985) Landscape appreciation and preferences in the Natal Drakensberg. Natal Town and Regional Planning Commission Supplementary Report 17

Selby MJ (1980) A rock mass strength classification for geomorphic purposes: with tests from Antarctica and New Zealand. Z Geomorph NF 24:31–51

Suess E (1904) The face of the earth. Clarendon, Oxford

Chapter 15
Victoria Falls: Mosi-oa-Tunya – The Smoke That Thunders

Andy Moore and Fenton (Woody) Cotterill

Abstract Victoria Falls are located on the Zambezi, southern Africa's largest river. In full flood with a maximum vertical drop of 108 m, and length of 1,700 m, they form the world's largest sheet of falling water. The Falls demarcate two sections of the Zambezi of contrasting geomorphology: the low gradient, broad channel of the Upper Zambezi and the steep gradient, narrowly incised downstream Batoka gorges, ~100 km in length. The Victoria Falls represent the modern position of a west-migrating knickpoint that incised the lower gorges into Jurassic (Karoo-age) basalts that form the bedrock. Evolution of the Falls and lower Gorges was accompanied by deposition of Late Cenozoic sediments of the Victoria Falls Formation (VFF), which preserve a remarkable assemblage of hominin artefacts. This archaeological record provides a unique context to decipher how the Batoka gorges evolved through the Pleistocene; two contrasting estimates, obtained from these hominin artefacts, constrain estimates of headward erosion rates, westward, to between 0.042–0.052 m/year and 0.067–0.080 m/year. This faster rate means that headward erosion has incised 20 km of gorges below the Falls in 300–250 ka. The present position of the Victoria Falls reflects the culmination of evolutionary events initiated by diversion of drainage off the Kalahari plateau into the mid-Zambezi river that occupies a deep graben.

Keywords Basalt • Batoka gorges • drainage evolution • hominin evolution • Kalahari Plateau • knickpoint retreat • Zambezi River

15.1 Introduction

The Victoria Falls, or Mosi-oa-Tunya (The Smoke That Thunders), as they are known by their more descriptive vernacular name (Fig. 15.1) are located on the Zambezi, southern Africa's largest river (Fig. 15.2). With a length of 1,700 m and maximum vertical drop of 108 m, they form the world's largest sheet of falling water when in full flood. Their breathtaking beauty moved David Livingstone to write that "scenes so lovely must have been gazed upon by angels in their flight," and earned their designation as a UNESCO World Heritage Site in 1989.

The Victoria Falls demarcate two sections of the Zambezi with markedly contrasting geomorphologic characteristics, designated the upper- and mid-Zambezi, respectively (Wellington 1955). Upstream, the river flows in a low gradient, broad channel, which exceeds 2 km width in places. Below the Falls, the gradient is markedly steeper (Fig. 15.3), and the river is constrained by a series of narrow gorges, some 100 km in total length (Fig. 15.4). Downstream of these gorges, the Zambezi widens into the broad valley known as the Gwembe Trough, in which Lake Kariba is impounded.

Stone artefacts in river terrace gravels, along the Zambezi valley, testify to a lengthy and near continuous period of occupation by a succession of hominin cultures, extending back to the Early Pleistocene and possibly late Pliocene (Clark 1950). These stone implements present earth scientists with a remarkable geochronological resource, because they constrain ages of sediments, and so provide a time frame for elucidating

P. Migoń (ed.), *Geomorphological Landscapes of the World*,
DOI 10.1007/978-90-481-3055-9_15,

Fig. 15.1 Aerial view of the Victoria Falls and upper gorges, looking west. The former river banks prior to incision of the gorges is marked by the low scarp above the pale-hued, gently sloping surface that bounds the gorges (Photo R. Watts)

the evolution of the Falls and the downstream gorges. The story they tell us is, in turn, intrinsically linked with geomorphological events that changed surrounding landscapes across Africa through the Plio-Pleistocene.

15.2 Geographic Setting

The Victoria Falls are located on the section of the Zambezi that forms the international boundary separating Zambia and Zimbabwe (Fig. 15.2). Access is by good road, rail and air links to the town of Victoria Falls on the Zimbabwe side of the Zambezi, and Livingstone on the Zambian side. The area experiences summer rainfall (mainly during the months of November to March), with an average annual precipitation of 600 mm, which supports a broad-leaved savannah tree and shrub plant community. Nonetheless, peak river flow across the Falls occurs in April, controlled primarily by the input from the higher rainfall area (~1,600 mm per annum) in the Zambezi's headwaters in Angola and northern Zambia on the Southern Equatorial Divide – the watershed with the Congo River basin.

15.3 Landforms and Geology

15.3.1 The Zambezi River Above Victoria Falls

Figure 15.4 illustrates the stretch of the River immediately above and below the Victoria Falls where Jurassic (Karoo-age) basalts form the bedrock. The broad channel of the Upper Zambezi is broken by numerous islands, which increase in number with proximity to the Falls. The sedimentary sequence which overlies the basalts along the margins of the Zambezi is collectively referred to as the Victoria Falls Formation (VFF) and is summarized in Table 15.1 and Fig. 15.5. The detailed knowledge of

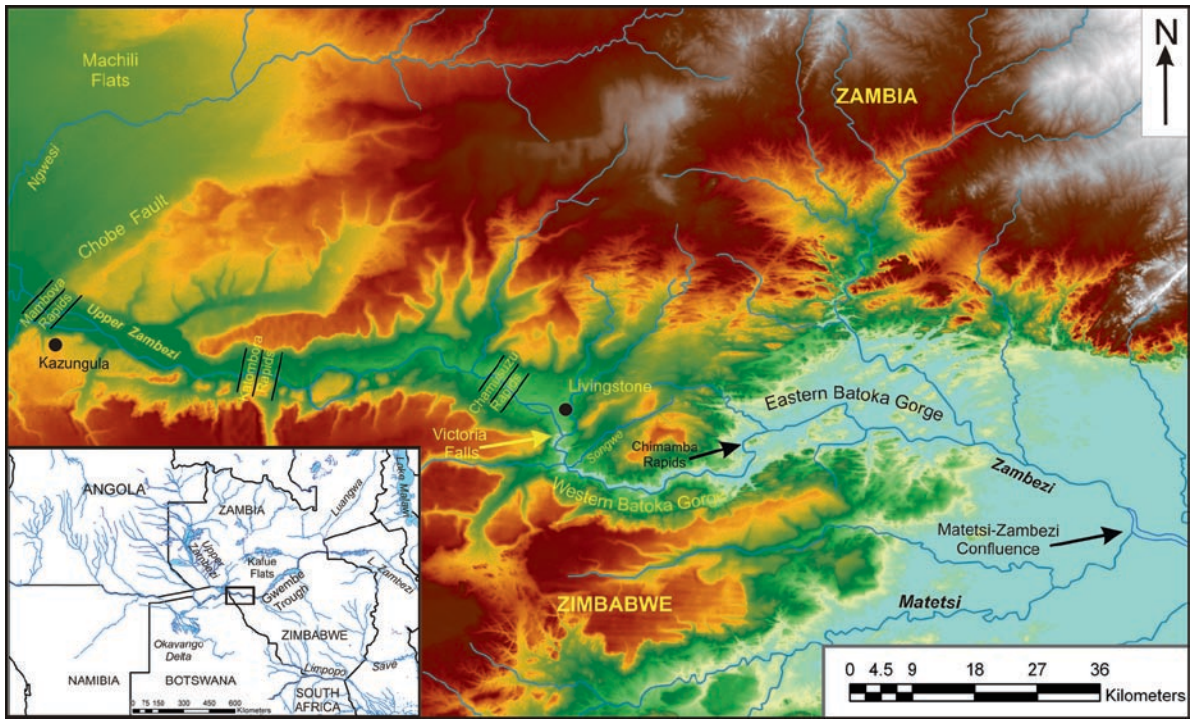

Fig. 15.2 The situation, in south-central Africa, of the Batoka gorge incised by the Zambezi River, in which the Victoria Falls represents the extant position of westward knickpoint migration of the Zambezi River. The ~100 km Batoka Gorge is situated between the Victoria Falls and the Matetsi-Zambezi confluence. Principal rapids upstream of Victoria Falls are labelled. In a continental context, the Batoka Gorge represents a site of significant incision into the eastern margin of the Kalahari plateau. It testifies to the evolution of a widening exorheic drainage net through sequential piracies of endorheic rivers draining the Kalahari plateau

the geology and geomorphology of country surrounding the Victoria Falls is a testament to the thorough research by geologist F. Dixey and archaeologist, J. D. Clark. They elucidated the stratigraphy of Zambezi sediments formed through the late Cenozoic in relation to ongoing occupancy of the valley by hominins. Their research entailed extensive field mapping in tandem with detailed excavations of representative sediments (Clark 1950; Dixey 1950). These descriptions remain an invaluable legacy to current researchers which can be judged by the fact that Clark's (1950) detailed study underwrites the present work in significant respects.

The river is bounded by a low (15–45 m) scarp, at a distance of about 5–6 km from the main channel, which marks the junction with the surrounding low-relief basalt plain, which is ascribed to the African Erosion Surface (Lister 1987; Moore et al. 2009). The basalt bedrock at the crest of this scarp is capped by a silicified limestone, designated The Chalcedony Beds (Dixey 1950; Fig. 15.5). The age of this unit is not well-constrained, but its origin may be linked to the development of the widespread African Surface (Lister 1987; Moore et al. 2009). The Chalcedony is overlain by a coarse sandstone, often silicified, that is known as the Pipe Sandstone. The Pipe Sandstone is in turn overlain by beds of red Kalahari sand, of variable thickness, interpreted to be of aeolian origin, and termed Kalahari Sand I (KS I) (Dixey 1950).

A series of abandoned river terraces have been recognized between the valley scarps and the modern channel of the Zambezi. The Upper Terrace is capped by two gravel benches separated in height by about 6 m altitude. Their modern association with the Zambezi varies, depending on local bedrock; so they extend up to 15 m vertically above the river, but some deposits are preserved at the present river level on ledges of the basalt bedrock. These upper terraces are referred to as Older Gravels I (OG I) (at the higher elevation) and Old Gravels II (at the lower level) respectively. Relict patches of KS I overlie these two gravel units.

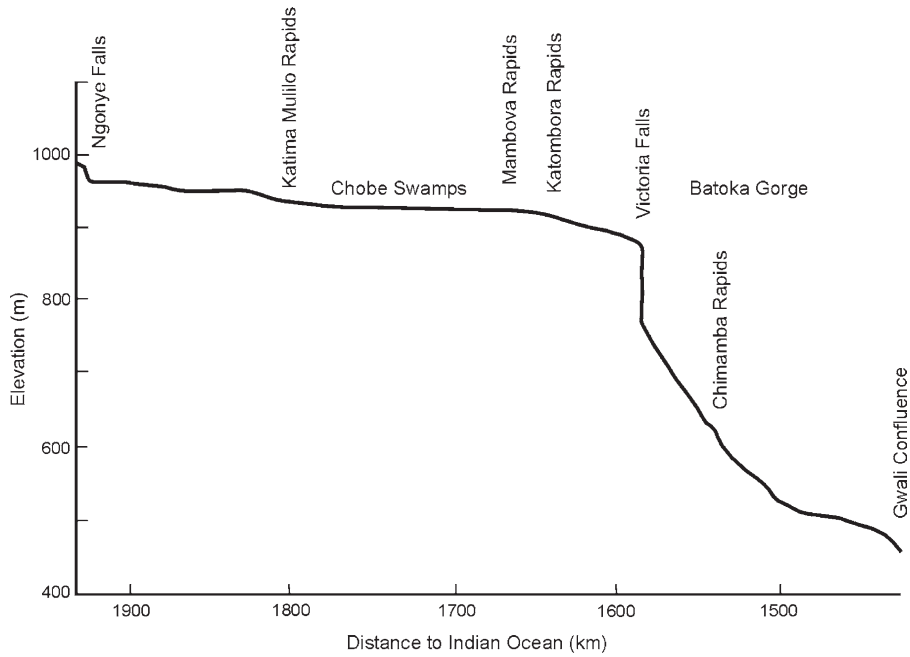

Fig. 15.3 Profile of the Upper Zambezi River, between N'gonye Falls and the Gwayi confluence, to show the radical changes in gradient along the Batoka Gorge, compared to the senile profile of the river where it crosses the Okavango Graben (Modified from Moore et al. 2007)

Their upper surfaces are cemented by a pedogenic ferricrete (termed Ferricrete I), inferred to have formed at the base of the KS I (Fig. 15.5). The higher gravels (OG I) contain Early Stone Age (ESA) Acheulian stone artefacts, and more rarely, rolled older Oldowan tools. The oldest stone artefacts preserved in the lower gravel unit (OG II) are attributed to the middle to late ESA, and also include Sangoan tools of the early, or pre-Middle Stone Age (MSA). The ferricrete cementing the upper surface of the Older Gravels entombs early MSA Sangoan picks and flakes, which are interpreted to have accumulated on the surface of the gravels prior to deposition of the KS I and induration by Ferricrete I (Clark 1950).

Younger Gravels and alluvial sands have accumulated on a Middle Terrace, at an elevation less than 10 m above the modern river. In parts, these are overlain by reworked Kalahari Sand (KS II). Lupemban (MSA) artefacts are preserved in these Younger Gravels and also the upper levels of KS 1, while KS 2 contains only later MSA artefacts, provisionally assigned to the Tshangulan culture. Below the Middle Terrace, the river is bounded by reworked aeolian sands and calcareous sandy alluvium (Dixey 1950). The most recent hominin living sites were attributed to the LSA, and these were on the calcareous sandy alluvium (Clark 1950).

The two deposits of Kalahari sands (KS I and KS II) testify to distinct episodes of regional aridity centred on the Mega-Kalahari sand sea. KS I and the basal pedogenetic ferricrete reflect a break in river flow of at least 140,000 years, which is designated the VFF unconformity (Cotterill 2006; Cotterill and Moore in review). Archaeological artefacts associated with these two sand beds allow us to constrain deposition of these Kalahari sands to within respective Marine Oxygen Isotope Stages (Cotterill and Moore in review), reliably documented in palaeo-climate archives (EPICA 2004; Lisiecki and Raymo 2006). The association of Tshangulan artefacts with KS II delimits its deposition within MIS 4 (71–57 ka[1]), in agreement with reliable U-series dates (Deacon 2001) that constrain the contemporaneous Howieson's Poort industry in South Africa. The age of KS I is more difficult to establish precisely, because the tenure of the early MSA Sangoan industry is not well-constrained. Nevertheless, available evidence allows us to constrain KS I to within MIS 12 or, less likely, MIS 14: between 474–427 ka or 568–528 ka, respectively (Cotterill and Moore in review).

[1]ka stands for 1,000 years

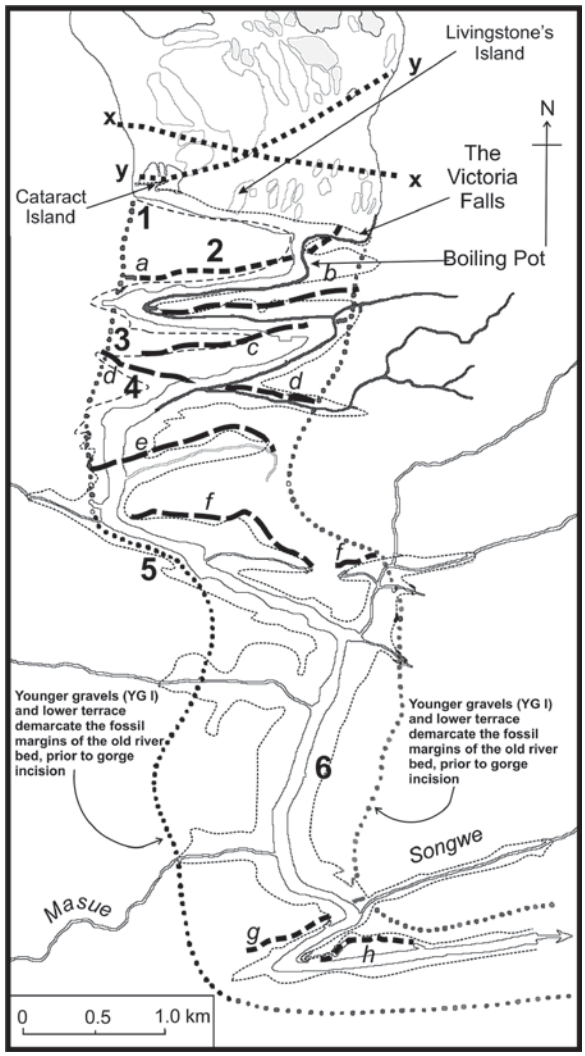

Fig. 15.4 The Victoria Falls and Gorges, modified from Wellington (1955: Fig. 86, 393), with numbers of gorges labelled one to six and past positions of the waterfalls labelled *a–h* (dashed lines). The edges of the Batoka Gorge approximated by fine dashed lines. The bold dotted lines *x–x* and *y–y* denotes where the next lines of future falls could develop (Bond 1976)

Table 15.1 Summary of the stratigraphy of the Victoria Falls Formation (VFF)

10. Aeolian sand and alluvium (LSA)
9. Redistributed Kalahari Sand (KS II) (Tshangulan)
8. Younger Gravels I (Lupemban)
7. Kalahari Sand I (KS I) (Lupemban)
6. Ferricrete I
---------- (Sangoan accumulated on Old Gravels)
5. Old Gravels II (OG II) (Mid- to Late-ESA and Sangoan)
4. Old Gravels I (OG I) (Rolled Oldowan and Acheulian)
----
3. Pipe sandstone
----
2. Silicified limestone or "Chalcedony"
---------- Marked Unconformity
1. Karoo Basalt

Dashed lines denote significant erosional gaps

15.3.2 Zambezi Below Victoria Falls

At the Victoria Falls, the Zambezi plunges in a single drop into a narrow cleft, some 60–120 m wide, known as First Gorge, which varies from 80 m in depth at the western end, to 108 m in the centre. During peak flood, the wall of water forming the Falls is divided by two islands (Cataract Island near the western end, and Livingstone Island near the centre), but more islands emerge during periods of low flood (Clark 1950; Bond 1976). The walls of the gorge are built up of six thick, dark, fine-grained basalt lava units exhibiting a strong vertical jointing. These are separated by amygdaloidal basalts that weather to a purple-red colour, which represent the contacts (tops and bottoms) of individual lava flows (Fig. 15.6). A fine example of the amygdaloidal basalt variety is seen on the path from Victoria Falls Hotel to the Falls (Bond 1976).

The river exits the First Gorge near the eastern end via a narrow, north–south outlet known as the Boiling Pot. Thereafter, it follows a series of gorges, generally oriented just south of either east–west or west–east, some linked by south-flowing channels. These have been incised into a continuation of the broad valley in which the Zambezi flows above the Falls and are known, in a downstream direction to the confluence with the east bank Songwe tributary, as the Second to Sixth Gorges (Fig. 15.4). The amygdaloidal basalt is less resistant to erosion than the fine-grained massive variety, and in the lower gorges, can be recognized by breaks in the steepness of the walls, marked by lines of trees (Fig. 15.6).

Immediately downstream of the Songwe, the river swings sharply to the east into the Batoka Gorge, which maintains this general direction for some 90 km thereafter. It narrows some 30 km downstream at the Chimamba rapids, where there is a drop of some 6–7 m. It is here that when:

> one stands on the brink of the lower cataract and sees the whole volume of the great Zambezi converging into a single pass only 50 to 60 feet in width, shuddering, and

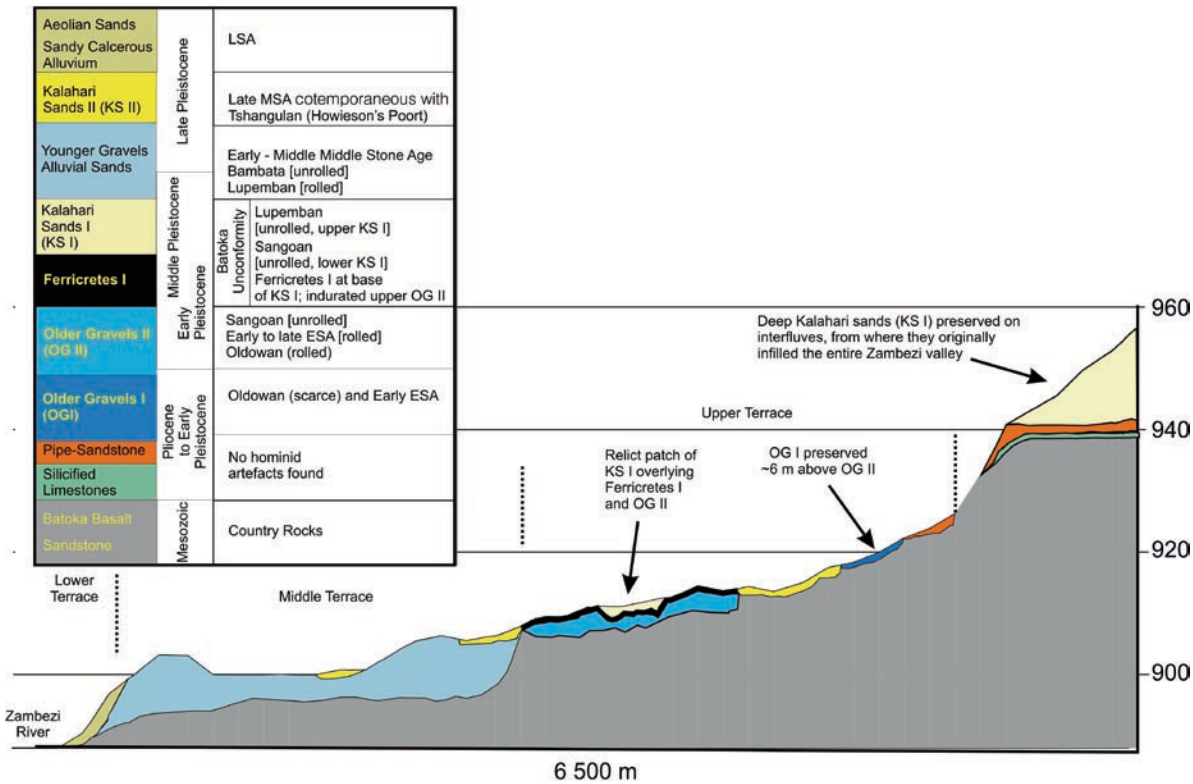

Fig. 15.5 Schematic transect of the three principal terraces within the wide valley of the Upper Zambezi River (only north bank depicted) above Victoria Falls, to illustrate stratigraphic relationships among alluvial and aeolian sediments. The Chalcedony beds interface with overlying Pipe Sandstone. Both sediments overlie the Batoka basalts, in parts, predating the river gravels. Stone Age artefacts preserved in their respective sediments are listed in the legend. In this region of the river, YG I is confined to the Middle Terrace, with Older Gravels II (OG II), capped by Ferricretes I and KS I, confined to the Upper Terrace. The Batoka Unconformity represents a break in alluvial deposition, when KS I covered the entire valley, but was subsequently eroded. Deposition of Kalahari Sands II (KS II) is inferred to have occurred between 71–57 ka in Marine Isotope Stage (MIS) 4. Vertical axis is exaggerated (not to scale) and distances and heights are approximate estimates (Compiled from illustrations and descriptions in Clark 1950 ; Dixey 1950)

> then plunging for 20 feet in a massive curve that seems in its impact visibly to tear the grim basaltic rocks asunder, one learns better than from the feathery spray-fans of the Victoria Falls what force there is in the river, and one wonders no longer at the profundity of the gorge! (Lamplugh 1907: 151).

The Chimamba Rapids demarcate a sharp break in the geomorphological unity of the Batoka Gorge, because downstream the Zambezi widens markedly, with decreasing gradient (Figs. 15.2 and 15.3). This break represented by the Chimamba Rapids is designated the Batoka Discordance (Cotterill 2006; Cotterill and Moore in review).

15.4 Evolution of the Victoria Falls and Lower Gorges

The northern banks of the gorges below the Falls, in particularly the upper ones, show evidence of water wear, and it was realized at an early stage that these mark former positions of the Falls (e.g., Wellington 1955). It is generally accepted that there are at least six abandoned former lines of falls (shown by dashed lines as *a–f*, Fig. 15.4). Wellington (1955) presented evidence for two further former fall lines (*g*, *h*) near the Songwe confluence.

Fig. 15.6 View of the Second and Third Gorges, looking east. Note the massive lava flows forming the walls of the gorges, separated by breaks in slope, which reflect amygdaloidal basalt, representing the upper and lower brecciated sections of successive lava flows. This brecciated basalt is frequently an aquifer, reflected by the vegetation that has colonized these sections of the basalt succession (Photo R. Watts)

The easterly oriented gorges are clearly structurally controlled, and aligned along either readily eroded faults with vertical throws of approximately 50 m (second and fifth Gorges), or prominent joints associated with shatter zones (Wellington 1955; Bond 1976). At each earlier position of the Falls, erosion would selectively incise the next line of weakness, upstream, and thus establish it as a new fall line; whereafter the earlier line was abandoned. A less prominent and probably more resistant set of north–south joints controls the south-flowing sections of the river below the Falls. The steep-sided Batoka Gorge would similarly have been incised by headward erosion, presumably also exploiting a line of structural weakness. If so, the advancing Batoka Gorge knickpoint may not have always presented a cascade as dramatic as the modern Falls, capped by their armour of massive basalt.

There are a number of pointers to the future evolution of the Falls. Immediately upstream of the Falls are two structural lines (*x*–*x* and *y*–*y*) that are readily identified from aerial photographs (Fig. 15.4). The lip of the modern Falls is lowest at the Devil's Cataract, between the western river bank and Cataract island, which carries the greatest concentration of water during flood. This may, therefore, mark the beginning of a north–south gorge, linking to structural line *x*–*x*, where the next fall line could develop. However, a deep, narrow cleft on Cataract Island is aligned with the second line of weakness (*y*–*y*). This cleft does not normally carry a great volume of water, but there is a strong flow in times of flood, when the river's erosive power is greatest. The alternative possibility is that over time, more rapid erosion along the line of weakness reflected by the Cataract Island cleft will progressively capture the flow from the

Devil's cataract, leading to development of a new fall line following *y–y* (Bond 1976; Fig. 15.4).

This discussion of the evolution of the Victoria Falls has still to answer the question as to what factors *initiated* the development of such a dramatic knickpoint in the interior of the African continent. Two contrasting models have been proposed. The first interprets the Falls in terms of a headward-migrating knickpoint, reflecting the youngest (Plio-Pleistocene) cycle of erosion, initiated by uplift of the coastal plain (King 1963). However, several lines of evidence point to an alternative explanation – that the Upper Zambezi was captured by a headwater tributary of the middle Zambezi relatively recently in the late Cenozoic (e.g., Du Toit 1933; Bond 1976; Moore and Larkin 2001). The rapid headward erosion of the Batoka and higher gorges would have been initiated by the marked lowering in base level of the Upper Zambezi following this capture. A system of major NE–SW faults traverses the bed of the Zambezi for over 160 km upstream of Victoria Falls. These represent the southwest extension of the East African Rift System (EARS) that initiated the development of the Okavango Graben, which includes the Machili Flats as part of the graben floor (Fig. 15.2). The gradient of the river shows distinct changes along this faulted section, especially where it crosses this shallow rift valley (Dixey 1950; Nugent 1990). Thereafter it steepens at the Mambova Rapids immediately downstream of the Graben (Figs. 15.2 and 15.3), plausibly reflecting uplift of the eastern rift shoulder. This uplift may have been responsible for triggering or accelerating aggressive headward erosion of a north bank tributary of the mid-Zambezi, which ultimately captured the modern upper sections of the river.

An important, additional, question pertains to what caused the break in geomorphological unity of the Batoka Gorge at the Chimamba rapids (the Batoka Discordance). This has been interpreted to reflect a period when the river ceased to flow, after the Zambezi had attained its modern topology (Derricourt 1976; Moore and Larkin 2001; Cotterill 2006; Moore et al. 2007), as a result of deflection of the upper Zambezi into a major inland lake in northern Botswana (Palaeo-lake Makgadikgadi) following uplift across the line of the river along the Chobe Fault – part of the Okavango Rift system (Fig. 15.2). A ferricrete on the bed of the Zambezi immediately above Victoria Falls may testify to the period when the flow from the upper reaches of the river was cut off. Flow was restored once the Zambezi again breached the barrier presented by the Chobe fault, whereafter the river incised the western Batoka and upper gorges.

15.5 Time Frame for Evolution of the Victoria Falls and Lower Gorges

It was realized by Lamplugh as early as 1907 that the sediments of the VFF, with their preserved hominin stone artefacts, offer a time frame for dating of the evolution of the gorges below Victoria Falls. More recently, available evidence was summarized by Derricourt (1976), but now we know that his reasoning and calculations were based on heavily underestimated ages of the different Stone Age cultures. The recent progress achieved in dating the MSA (McBrearty and Brooks 2000) has underpinned a reappraisal of the archaeological record, which in turn allows us to re-evaluate the antiquity of the Victoria Falls and its gorges.[2]

Scattered deposits of KS II cap gently sloping terraces above the western Batoka Gorge (upstream of the Chimamba Rapids), and extend upstream to the beginning of the fourth Gorge. At the time this unit was deposited, it would have been eroded by the broad river that occupied the higher sections of the valley. It follows that the Victoria Falls regressed 2.96 km from the end of third Gorge to the present position subsequent to the deposit of the KS II with its Tshangulan artefacts. Similarly, the Younger Gravels (YG I), with their Lupemban artefacts form a distinct terrace above the Gorges for a distance of 20 km below the modern Falls.

Limits of 71–57 ka for the Tshangulan culture (preserved in KS II) indicate headward erosion rates of 0.042–0.052 m/year for incision of the 2.96 km from the end of the third Gorge to the present position of the waterfall. In contrast, the age of 300–250 ka bracketing the Lupemban industry, associated with YG I, constrains rates of headward erosion to incise the 20 km below the falls at 0.067–0.080 m/year – almost double the estimated erosion rate based on the Tshangulan constraint (Table 15.2). The reason for the disparity

[2]Complete reference to archaeological work which allowed for this re-evaluation can be found in Cotterill (2006) and Cotterill and Moore (in review).

Table 15.2 Estimates of erosion rates of lower gorges and estimated time taken to erode the gorges

Estimates of erosion rates of Lower Gorges				
Section of gorge used for erosion rate estimate	*Distance eroded (km)*	*Stone Age culture constraining erosion rate*	*Age bracket of culture*	*Estimated erosion rate (m/year)*
Modern Falls to end of Third Gorge	2.96	Tshangulan	71–57 ka	0.042–0.052
20 km downstream of modern Falls	20	Lupemban	300–250 ka	0.067–0.080
Estimated time taken to erode the gorges				
Section of gorge	*Distance (km)*	*Stone Age culture constraining erosion rate*	*Estimated erosion rate (m/year)*	*Time required for erosion*
Victoria Falls to Chimamba Rapids	40.71	Tshangulan[1] Lupemban	0.042–0.052 0.067–0.080	970–783 ka 608–509 ka
Age limits for erosion of W Gorges assuming VFF Unconformity = 140 ka			0.042–0.080	1100–649 ka[a]
Age limits for erosion of Eastern Batoka Gorge (below Chimamba Rapids)	60	Tshangulan Lupemban	0.042–0.052 0.067–0.080	1.43–1.15 ma 0.90–0.75 ma
Time for erosion of entire Batoka Gorge excluding time gap represented by the Batoka Discordance	100.71	Tshangulan Lupemban	0.042–0.052 0.067–0.080	2.54–2.07 ma 1.65–1.40 ma
Time bracket for erosion of entire Batoka Gorge excluding time gap represented by the Batoka Discordance	100.71		0.042–0.080	2.54–1.40 ma[b]

[a](970 + 140) to (509 + 140) ka

[b](0.970 + 1.429 + 0.14) ma to (0.529 + 0.750 + 0.14) ma

[1]This Late MSA Industry is provisionally called Tshangulan subject to new research

between these estimates is not clear, and difficult to elucidate in light of current knowledge. It most likely reflects an underestimate age of the Lupemban, which points to a corresponding overestimate of erosion rate. It is nonetheless likely that flow rates, and thus the rate of gorge incision, decreased between Lupemban and Tshangulan times as a consequence of the severance of tributaries of the upper Zambezi by river capture. This can be attributed to severance of a former Kafue – Upper Zambezi link (Moore and Larkin 2001), resulting in the formation of Palaeo-Lake Patrick, which inundated an area of ~17 000 km^2 in the vicinity of the present day Kafue Flats (Fig. 15.2, Inset). The tenure of this lake has been dated from the mid-Pleistocene to approximately 300 ka, when the Upper Kafue was captured by a tributary of the mid-Zambezi (Simms 2000). The formation of Palaeo-Lake Patrick accounts for the loss of a significant east bank tributary of the Upper Zambezi (Cotterill 2006), with concomitant loss of erosive power.

The Chimamba rapids are considered to mark a significant break in the erosion of the Batoka Gorge, when the Zambezi was diverted into northern Botswana (Moore and Larkin 2001) – a hydrological input prerequisite to maintain the 945 m lake level of Palaeo-Lake Makgadikgadi (Grove 1969). Based on the two estimates of erosion rates, the time taken to erode the 41.71 km from the Chimamba Rapids to the modern Falls is bracketed between 970–783 ka (slower Tshangulan constraint) and 634–529 ka (faster Lupemban constraint) (Table 15.2). This excludes the minimum 140 ka break represented by the VFF unconformity. Thus, the minimum age constraint (529 + 140 = 669 ka), which brackets erosion of the western Batoka Gorge, reflects the most recent time that the Zambezi could have maintained the 945 m lake level of Palaeo-Lake Makgadikgadi in northern Botswana. This is consistent with the presence of an ESA factory site on the lake floor at an elevation of 936 m (McFarlane and Segadika 2001).

At present there are no reliable, independent constraints on the time frame for erosion of the eastern Batoka Gorge. While Older Gravels have been recorded in the lower reaches, it has not yet been firmly established whether these include OG I and OG II, or only the older unit. Based on the Lupemban and Tshangulan erosion rates, the time for incision of the 60 km of the eastern Batoka Gorge is bracketed between 900–750 ka and 1.43–1.15 ma[3] respectively. The total time indicated for erosion of the eastern and western sections of the gorge is therefore bracketed at 1.67–1.42 ma (faster rate of erosion) and 2.54–2.08 ma (slower erosion rate) (Table 15.2).

Nevertheless, the date for the commencement of the erosion of the Batoka Gorge (which equates to when the upper Zambezi was captured by the mid-Zambezi) is clouded by two uncertainties. Firstly, the timing of the break in erosion represented by the Chimamba Discordance is not yet well-constrained. Secondly, the Batoka Gorge widens markedly and decreases in gradient below the Chimamba rapids. Both these signatures preserved along the Zambezi's channel point to erosion of the Eastern Batoka gorge by a much larger flow than that which incised the western section upstream. This invokes the link to the upper Zambezi's catchment of a much larger river, which was plausibly the Palaeo-Chambeshi, with its headwaters in Katanga and northeast Zambia. It is interesting to speculate that erosion by such an enhanced flow would have been even faster than the estimates based on the Lupemban constraints (Cotterill 2006; Cotterill and Moore in review).

15.6 Summary

The modern physiographic context of the Victoria Falls reflects the culmination of events initiated by piracy of the Upper Zambezi by a mid-Zambezi headwater. In their context of conjoining the two segments of the Zambezi river of disparate origins, the Victoria Falls highlights the preservation of several, interlinked suites of evidence, which provide unprecedented insights into landscape evolution through the Plio-Pleistocene. These events have been driven by tectonic activity along the southwest extension of the African Rift System. The landforms created by eroding and aggrading agencies of the Zambezi River preserve a remarkable legacy of hominin artefacts. This archaeological record provides a unique framework to decipher how the Batoka gorges evolved through the Pleistocene. More detailed mapping and characterization of the stone artefact assemblages in the Old Gravels, which extend along the lower reaches of the Batoka Gorge, will undoubtedly refine our understanding of the evolution of the Victoria Falls. Nevertheless, the detailed knowledge we have been able to summarize for the origin of the Victoria Falls and the spectacular Batoka gorges is a testament to the careful mapping and attention to detail of a remarkable group of scientists. They blazed the trail in elucidating how geological events forged the Victoria Falls, through the period when our hominin ancestors populated the Zambezi valley.

The Authors

Andy Moore (Ph.D., University of Cape Town, South Africa) is a kimberlite (diamond) exploration geologist, and has initiated and managed prospecting programmes in Botswana, Zimbabwe, Namibia, South Africa and Madagascar. He is currently Vice President (Exploration, Diamonds) of African Queen Mines, listed on the Toronto Venture Exchange, and also an Honorary Research Associate of the Geology Department of Rhodes University, Grahamstown, South Africa. He has published 30 peer-reviewed papers covering kimberlite petrology and mineralogy, as well as large-scale processes responsible for the geomorphic evolution of southern Africa. A recent focus, together with Dr. Fenton (Woody) Cotterill, investigates the links between landscape development and the evolution of plant and animal species.

Fenton (Woody) Cotterill (Ph.D., University of Stellenbosch, South Africa) is a research fellow in the Africa Earth Observatory Network (AEON) at the University of Cape Town, where his interests centre on the evolution of Africa's biodiversity and landscapes, employing molecular genetic studies of indicator species to elucidate how landscapes have reacted to tectonism. From 1992 to 2003 he was Curator of Mammalogy, Natural History Museum of Zimbabwe, Bulawayo. His doctorate examined how the evolution of lechwe antelopes has interfaced with palaeo-drainage

[3] ma stands for 1,000,000 years

dynamics across central Africa. Taxonomic research, focused primarily on Africa's Chiroptera and Bovidae, includes the description of three new species of mammals. He has published over 40 publications spanning a range of interests. These include the epistemology interlinking natural science collections, biodiversity science and environmental conservation; biogeography and systematics of vertebrates; and impacts of geomorphological evolution on biodiversity dynamics.

Acknowledgments This essay owes an immense debt to several great scientists, whose dedicated research in southern Africa bequeathed a legacy of meticulous field data and profound insights. Geologists G. W. Lamplugh, A. L. du Toit, H. B. Maufe, A. J. C. Molyneux and J. H. Wellington, together with archaeologists A. L. Armstrong and N. Jones, laid the foundations on which Geoffroy Bond, Frank Dixey and Desmond Clark deciphered a most remarkable narrative of late Cenozoic evolution. We are grateful to Professor Hilary Deacon for his insightful comments on the archaeological aspects of this research. We thank Shearwater and Roy Watts for permission to use Figs. 15.1 and 15.6. All errors in interpretation remain our own. This is AEON publication No. 0061.

References

Bond G (1976) The geology and formation of the Victoria Falls. In: Phillipson DW (ed) Mosi-ou-Tunya: A handbook to the Victoria Falls region. Longmans, London, pp 19–27

Clark JD (ed) (1950) The Stone Age cultures of Northern Rhodesia. South African Archaeological Society, Cape Town

Cotterill FPD (2006) The evolutionary history and taxonomy of the *Kobus leche* species complex of south-central Africa in the context of palaeo-drainage dynamics. Ph.D. thesis, University of Stellenbosch, Stellenbosch

Cotterill FPD, Moore AE (in review) Late Cenozoic paleo-drainage dynamics on the Kalahari plateau: lakes, endorheic deltas, shifting river topologies, and the paleoecology of High Africa

Deacon HJ (2001) Modern human emergence: An African archaeological perspective. In: Tobias PV, Raath MA, Maggi-Cecchi J, Doyle GA (eds) Humanity from African Naissance to coming millennia – Colloquia in human biology and Palaeoanthropology. Florence University Press, Florence, pp 217–226

Derricourt RM (1976) Retrogression rate of the Victoria Falls and the Batoka Gorge. Nature 264:23–25

Dixey F (1950) Geology. In: Clark JD (ed) The Stone Age Cultures of Northern Rhodesia. South African Archaeological Society, Cape Town, pp 9–29

Du Toit AL (1933) Crustal movement as a factor in the geographical evolution of South Africa. S Afr Geogr J 16:4–20

EPICA (2004) Eight glacial cycles from an Antarctic ice core. Nature 429:623–628

Grove AT (1969) Landforms and climatic change in the Kalahari and Ngamiland. Geogr J 135:191–212

King LC (1963) The South African scenery. Oliver & Boyd, London

Lamplugh GW (1907) The geology of the Zambezi basin around the Batoka Gorge (Rhodesia). Quart J Geol Soc 63:162–216

Lisiecki LE, Raymo ME (2006) Plio-Pleistocene climate evolution: Trends and transitions in glacial cycle dynamics. Quat Sci Rev 26:56–69

Lister LA (1987) The erosion surfaces of Zimbabwe. Zimbabwe Geol Survey Bull 90:163

McBrearty S, Brooks AS (2000) The revolution that wasn't: A new interpretation of the origin of modern human behaviour. J Human Evol 39:453–563

McFarlane MJ, Segadika P (2001) Archaeological evidence for the reassessment of the ages of the Makgadigadi. Botswana Notes and Records 33:83–90

Moore AE, Larkin PA (2001) Drainage evolution in south-central Africa since the breakup of Gondwana. S Afr J Geol 104:47–68

Moore AE, Cotterill FPD, Main MPL, Williams HB (2007) The Zambezi River. In: Gupta A (ed) Large rivers: Geomorphology and management. Wiley, New York, pp 311–332

Moore AE, Cotterill FPD, Broderick TG, Plowes D (2009) Landscape evolution in Zimbabwe from the Permian to present, with implications for kimberlite prospecting. S Afr J Geol 112:65–86

Nugent C (1990) The Zambezi River: Tectonism, climatic change and drainage evolution. Palaeogeogr, Palaeoclimatol, Palaeoecol 78:55–69

Simms R (2000) Appendix 7. Preliminary report on the sediments of Lake Patrick. In: Barham L (ed) The middle Stone Age of Zambia, South Central Africa. Western Academic and Specialist Press, Bristol, pp 275–280

Wellington JH (1955) Southern Africa: A geographical study, vol 1: Physical Geography. Cambridge University Press, Cambridge

Chapter 16
Spitzkoppe: The World of Granite Landforms

Piotr Migoń

Abstract The granite inselberg of Spitzkoppe in west-central Namibia is one of the most impressive landforms of this type on Earth. It combines domical and conical shapes, depending on the angle of view, and its origin derives from differential weathering of two different granite complexes of Precambrian and Cretaceous age, respectively. Huge rock slope failures are the principal means of hillslope evolution. Low granite elevations around Spitzkoppe host a diverse assemblage of minor features such as boulder fields, weathering pits, and tafoni. Pediments are perfectly developed around larger residuals. Circumstantial evidence exists that the tall inselbergs of the Central Namib Desert may have been in existence for a few tens million of years at least.

Keywords Granite landforms • inselbergs • Namib Desert • weathering

16.1 Introduction

If there is a single landform that might typify the landscape of Africa, then this would be an isolated bare rock hill or mountain rising from the vast plains. Hills of this sort struck an early German explorer of East Africa, Walter Bornhardt, so much that he invented a special term and called them *inselbergs*, literally meaning "island hills" (Hövermann 1978b; Thomas 1978). Of course, inselbergs are not endemic to Africa and there are splendid examples of similar landforms from other continents (Twidale 1982; Migoń 2006). One of these, Uluru (Ayers Rock) in Australia, is presented elsewhere in this volume.

Inselbergs vary in terms of lithology, dimensions, height, and shape, but have a few characteristics in common. First, as the name implies, they stand in isolation and are surrounded by a flat or gently rolling topography. Second, the topographic boundary between the hillslope and the plain around is fairly abrupt. Third, inselbergs are residual landforms due to wearing down of the surrounding terrain. Hence, volcanic cones and up-faulted blocks are traditionally not regarded as members of the inselberg family.

The vast majority of inselbergs is built by strong and resistant rock, and very often this rock is granite (Twidale 1982). However, granite has many faces. Variable mineralogical composition, differences in average size of crystals, and contrasting spacing of joints are among factors which account for the great diversity in character within the granite group (Migoń 2006). This diversity has enormous geomorphological consequences. In granite terrains weathering and denudation act highly selectively, accounting for the variety of landforms of all sizes. The area around the majestic inselberg of Spitzkoppe in Namibia (Fig. 16.1) provides one of the most splendid examples of granite landscapes in the world, the clarity of which is enhanced by the harsh arid environment.

16.2 Geographical Setting

Spitzkoppe is located in the west-central part of Namibia, at the eastern fringe of the Namib Desert and in the front of the Great Escarpment (Fig. 16.2). The nearest town is Usakos, some 45 km to the ESE, from which the Spitzkoppe area can be easily reached by a gravel road. The climate is arid, with mean annual precipitation between 80 and 100 mm, mainly from January to April. Mean maximum temperatures range between about 24°C in July and 32°C in January

P. Migoń (ed.), *Geomorphological Landscapes of the World*,
DOI 10.1007/978-90-481-3055-9_16,

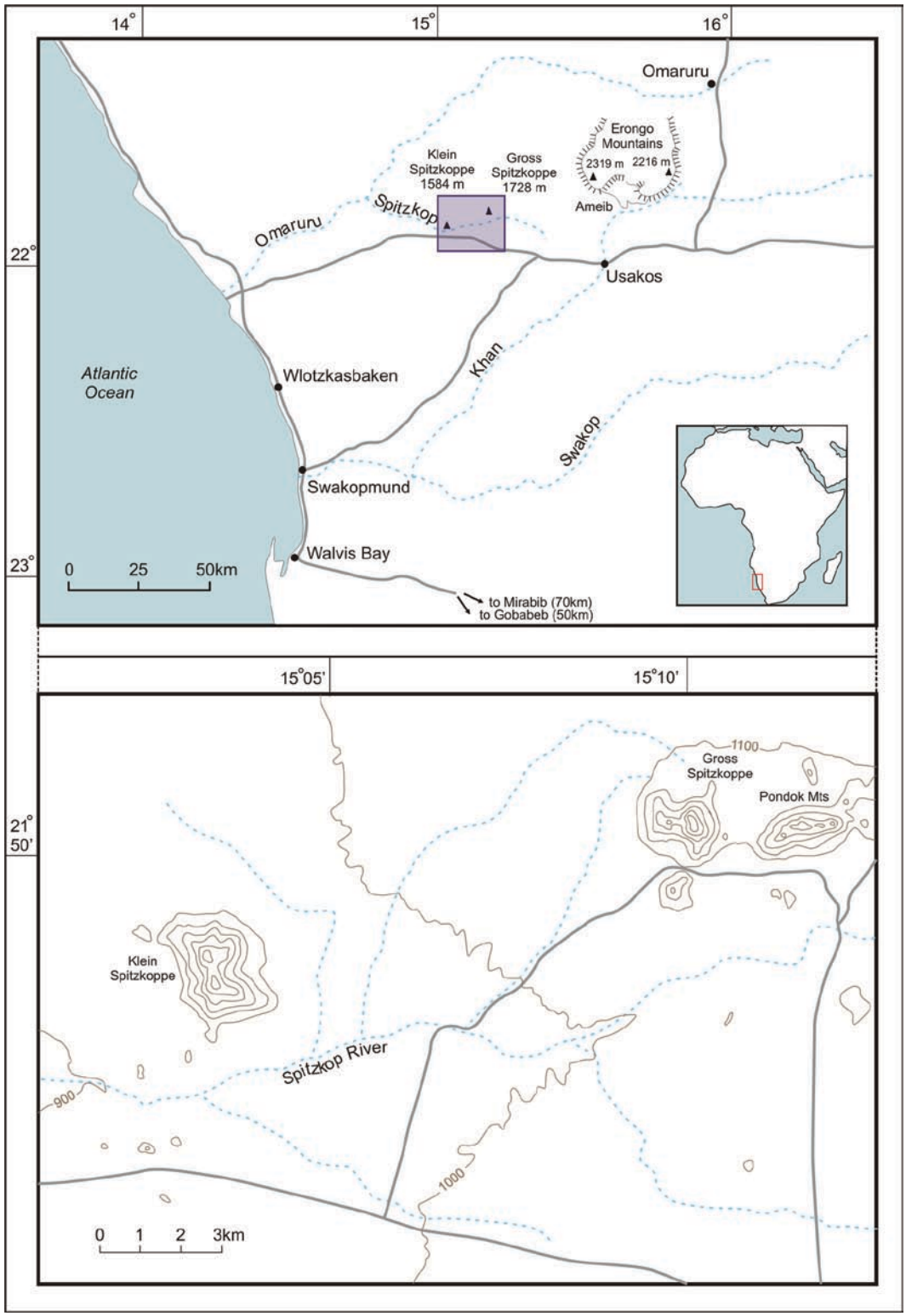

Fig. 16.1 Location map (*top*) and topography of the Namib Desert in the vicinity of Spitzkoppe (*bottom*)

Fig. 16.2 General view of Spitzkoppe, seen from the north-east (Photo P. Migoń)

(Jacobson et al. 1995). Vegetation is sparse, but acacia trees are fairly common along the watercourses and occasional trees and thorny bushes grow between the smooth faces of granite domes.

The Namib Desert around Spitzkoppe is developed as a gravel plain, characterized by a thin veneer of material transported by ephemeral streams and flash floods, resting on a truncated bedrock surface. In contrast to the southern part of the desert, no aeolian landforms or deposits are present.

Spiztkoppe is one of the tallest, if not *the* tallest inselberg on Earth. Its summit rises to 1,728 m a.s.l. and overlooks the adjacent plains by 600 m. Looking from the south, the main mountain shows a distinctive conical shape, hence its colloquial name of the "Matterhorn of Africa."

16.3 Landforms

16.3.1 Inselbergs

Spitzkoppe is actually not a single inselberg, but a group of hills of complex morphology (Selby 1982). It consists of two major hills, the big dome of Gross Spitzkoppe and the multi-domed ridge of the Pondok Mountains, separated by a 100 m wide pass (Fig. 16.1). The domes of Pondok attain 1,350–1,630 m a.s.l. Surrounding the main mountain masses are about a dozen of lower hills, from a few tens to about 100 m high.

Granite domes are very peculiar landforms, made distinctive by their pronounced convex shape and steep slopes. The origin of dome forms is not yet fully

understood, but they are probably derived from very massive compartments within an intrusion, saved from significant fracturing due to their location away from the main crustal discontinuities until erosion brings them near the topographic surface. Then, the ubiquitous mechanism of stress release begins to operate and the development of surface-parallel discontinuities is initiated. The newly produced joints tend to run parallel to themselves, dividing the rock mass into sheets of different thicknesses, hence their name of *sheeting joints*. The smooth rock faces of Spitzkoppe follow the steeply dipping sheeting joints and are an excellent illustration of an adjustment of form to structure (Selby 1982).

The inselbergs of the Spitzkoppe group are structural landforms, meaning that the principal control on their location and form is exerted by geology. First, they have developed within the younger granites of the Cretaceous Intrusive Complex, whereas the older Salem Granite, dated to the turn of the Palaeozoic, underlies the extensive plains around. Thus, there is a close association between lithological units and landforms. Second, Cretaceous granites are particularly suited to the formation of inselbergs as they rank among very resistant rocks. They are very rich in potassium, with a K_2O content in excess of 6%, mechanically strong, and poorly jointed, with major fractures spaced as much as more than 10 m apart in many places (Selby 1982; Migoń and Goudie 2003). Third, there is a clear relationship between the location of individual hills and the density of fracturing. The main body of Gross Spitzkoppe is built of a highly massive granite, whereas its east-facing lower slope has developed across a more densely jointed compartment, with dominant N–S trending fractures. In the eastern part of the Pondok Mountains a large enclosed basin underlain by jointed granite, the so-called Bushman's Paradise, occurs amidst the domes. The high degree of structural control on the granite landscape is not surprising, as similar relationships have been demonstrated in many localities worldwide (Twidale 1982; Migoń 2006), but the arid environment of Spitzkoppe makes them particularly easy to appreciate.

16.3.2 Minor Weathering Landforms

Granite outcrops in the Spitzkoppe area abound in minor landforms, superimposed on the domes, rock slopes, and big boulders. Here, the whole variety of weathering features can be found, including weathering pits and pans, tafoni (large-scale caverns incised into near-vertical rock surfaces), rills and fluted surfaces, case-hardened crusts and rock arches. They deserve special attention for two reasons, their diversity over a relatively compact area and their dimensions. A literature survey (Goudie and Migoń 1997; Migoń and Goudie 2003) has revealed that pits and tafoni in the Spitzkoppe massif belong to the biggest in the world.

Weathering pits are closed or partially open hollows on level rock surfaces, with a circular or elliptical ground plan, steep to vertical sides and flat floors (Fig. 16.3). Many are more than 2 m across, and diameters in excess of 5 m are not uncommon. Most pits are rather shallow, less than 0.5 m deep. On certain outcrops they occur in amazing abundance, covering up to one-third of the total rock surface and being connected by rills and channels. The occurrence of huge pits is intriguing, particularly if one realizes that standing water – by many claimed essential for pit enlargement – is very scarce in this marginal desert environment. Likewise, closed pits lacking products of rock disintegration are an enigma and the means of debris evacuation from the pits remain elusive. What is clear, however, is that the development of pits plays an important part in the reduction of granite elevations, particularly of those within the pediments (Goudie and Migoń 1997).

Likewise, tafoni attain imposing dimensions in the Spitzkoppe group. They are up to 12 m across, 4 m deep inside the rock face, and up to 3–4 m high (Fig. 16.4). Their inner sides are extensively flaked and the floors are covered by weathering debris, which attests to ongoing development. Tafoni occur within isolated boulders as well. The talus-mantled lower slopes of Gross Spitzkoppe provide many examples of hollowed boulders, where only the outer crusted surface is present, whilst the interior is a huge void up to 2.5 m high.

Further features of selective granite weathering are rock arches and overhangs. Both are controlled by structure, having developed along subhorizontal sheeting joints which focus weathering and groundwater sapping. The rock arch located south-east from Gross Spitzkoppe is about 4 m high and more than 15 m long. Among the overhangs, one in the Bushman's Paradise basin is probably the largest, more than 30 m long and up to 5 m high at the entrance. Inside, damaged relicts of indigenous rock art can be seen.

Fig. 16.3 A large weathering pit on a low residual hill next to Spitzkoppe. In the background is a sloping pediment with occasional rock outcrops (Photo P. Migoń)

Fig. 16.4 A huge tafone north of Spitzkoppe is an evidence of powerful selective weathering (Photo P. Migoń)

16.3.3 Pediments

Around the hills of Spitzkoppe extensive pediments have developed. These are rock-cut surfaces, sloping away from the inselbergs at a very low angle, typically less than 2° (Fig. 16.3). However, their geomorphology is fairly diverse in detail. Sections with exposed granite rock surfaces coexist with sedimentary veneers and patches of calcrete. There are frequent low elevations, from a mere 1–2 m to 10–15 m in height, many riddled with weathering pits. Less visible from the ground, but clear from a certain height is the drainage network comprising numerous shallow episodic channels. However, their floors are not incised, suggesting that the primary function of the channels is to carry sand and gravel brought in by sheet flow from the inter-channel surfaces.

16.4 Evolution

The evolution of the granite landscape of the Spitzkoppe inselbergs has been a complex and long-lasting process. The granite belongs to the family of Early Cretaceous (137–124 Ma ago) intrusions, associated with continental breakup and the development of the Tristan mantle plume (Milner et al. 1995). The intrusions were emplaced at depths of several km below the ground surface that existed at the time.

When the granites of Spitzkoppe were exposed to daylight is not known with precision, but the results of apatite fission-track analysis performed in the Namib Desert (Brown et al. 2000) and surface exposure dating from elsewhere in the Central Namib Desert (Cockburn et al. 1999) are helpful in this context. The mean denudation rate was high in the late Cretaceous/early Tertiary, and perhaps several kilometers of rock were lost, but then surface lowering proceeded at a lower rate, decreasing further since the Miocene. Cosmogenic isotope dating suggests that the mean denudation rate in the last 10 million years has been of the order of 5 m/1 million years. Hence, by simple extrapolation and assuming (unrealistically!) no denudation at the site of the future inselberg, 120 million years would be required to produce a 600 m high residual hill. Allowing for an increasing denudation rate prior to 10 million years ago, these rates indicate that the tops of the inselbergs may have been exposed as early as in the late Cretaceous, ~80–70 million years ago. Over time, their height increased as the surrounding terrain built of less resistant rock was worn down. Evidently, our inselbergs have a very long history and belong not only to the most spectacular landforms on Earth, but probably to the most persistent as well.

Fig. 16.5 Massive talus at the southern foot of Spitzkoppe indicates the role of catastrophic rock slope failures in the hillslope evolution of inselbergs (Photo P. Migoń)

As indicated above, an assumption that the inselbergs did not suffer from denudation throughout their existence is unrealistic. In fact, the geomorphology of the Spitzkoppe group shows clearly that their form was changing through time. The key evidence is the *talus*, which is a collective term to describe products of mass movement from the slopes that accumulate around the perimeter of the hills (Fig. 16.5). The nature of talus, along with features of rock slope morphology, provides an insight into how the inselbergs evolve. The sheer size of blocks building the talus, particularly at the south-western foot of Gross Spitzkoppe, shows that rock slopes fail catastrophically and large masses of rock are almost instantaneously delivered to the footslope. Depending on the angle of the failure plane and the slope steepness, massive rock falls, rock slides, and rock avalanches have occurred. The failure planes are typically sheeting joint surfaces. Further modifications of the dome form are experienced when inclined sheeting joints intersect vertical joints forming orthogonal sets (Selby 1982). Then the latter progressively open up, leading to the separation of joint blocks and destruction of the original dome. With time, a stepped rock slope profile develops, in equilibrium with the now reduced rock mass strength.

It remains to explain how the lowering of the terrain around the Spitzkoppe group has been accomplished. Inselbergs may evolve in more than one way, by either etching and stripping, or parallel scarp retreat, or mantle-controlled planation (Thomas 1978; Twidale 1982; Migoń 2006) and different models of origin have been applied to the Namibian examples. Hövermann (1978a) argued that deep chemical weathering was playing the major part and that the domes are the most resistant compartments excavated from the saprolite. However, Selby (1977, 1982) and Ollier (1978) pointed to the total absence of thick weathering mantles in the Namib. The long-lasting aridity, amplified after the establishment of the Benguela Current in the late Miocene (Goudie and Eckardt 1999), further renders the deep weathering and stripping hypothesis for Spitzkoppe rather improbable, although it may have played an auxiliary role in certain specific, more humid periods. On the other hand, there are evident contrasts between the strength of massive younger granites supporting the inselbergs and of densely fractured older granites

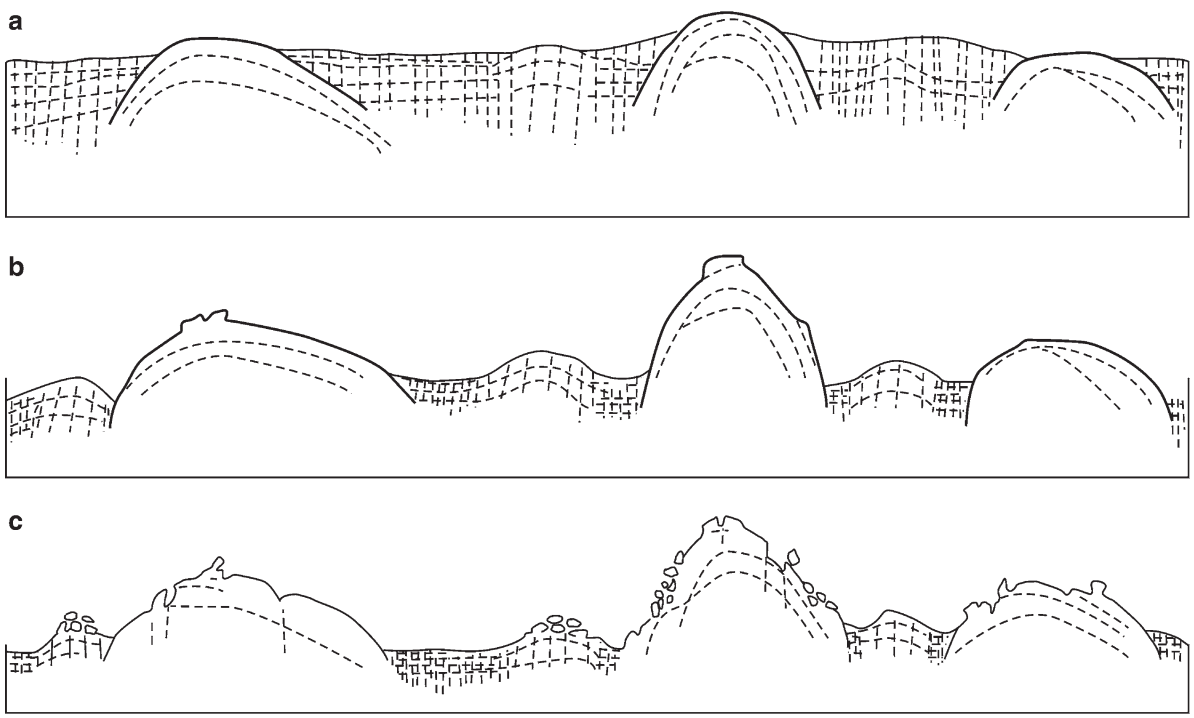

Fig. 16.6 Evolution and degradation of granite domed inselbergs in the Spitzkoppe area due to selective weathering of rock mass with different fracture patterns

under the plains. Therefore, Migoń and Goudie (2003) conclude that Spitzkoppe and the adjacent domes are subject to continuous exposure and adjustment to structure as the surrounding weaker rock is worn down, and that the massiveness of Mesozoic granite is fundamental to the survival of the inselbergs and to the increase of their relative relief over time (Fig. 16.6).

16.5 Conclusions

The granite landscape of the Spitzkoppe group is one of the best examples of its kind in the world. Its outstanding value stems from two circumstances. First, it is the size of individual landforms present here. The inselbergs are among the tallest known, the domes among the most massive, the weathering pits among the largest, and the tafoni among the deepest. Second, it is the geomorphological diversity. Examples of virtually any landforms described from granite terrains worldwide can be found here, in close coexistence. Structure-adjusted rock slopes, rockfall-derived talus mantles and pediments are all excellent textbook examples of these classic geomorphological features. In addition, Spitzkoppe has superlative scenic, aesthetic, and cultural value for the indigenous population. Clearly seen from more than 100 km distance, it is one of the greatest geomorphological landmarks of Africa.

The Author

Piotr Migoń is a Professor in the Department of Geography and Regional Development, University of Wroclaw, in Poland. His research concerns long-term landform evolution, rock geomorphology, mass movements, and conservation and promotion of geomorphological heritage. His previous publications include *Granite Landforms of the World* (2006), a number of entries to *Encyclopedia of Geomorphology* (2004) and more than 20 peer-reviewed papers. In 1997–2001 he served as Secretary General of the International Association of Geomorphologists and is now (2009–2013) one of IAG Vice-Presidents.

References

Brown RW, Gallagher K, Gleadow AJW, Summerfield MA (2000) Morphotectonic evolution of the South Atlantic margins of Africa and South America. In: Summerfield M (ed) Geomorphology and Global Tectonics. Wiley, Chichester, pp 255–281

Cockburn HAP, Seidl MA, Summerfield MA (1999) Quantifying denudation rates on inselbergs in the central Namib Desert using in situ-produced cosmogenic ^{10}Be and ^{26}Al. Geology 27:399–402

Goudie AS, Eckardt F (1999) The evolution of the morphological framework of the Central Namib Desert, Namibia, since the Early Cretaceous. Geogr Ann 81A:443–458

Goudie AS, Migoń P (1997) Weathering pits in the Spitzkoppe area, Central Namib Desert. Z Geomorph NF 41:417–444

Hövermann J (1978a) Formen und Formung in der Pränamib (Flächen-Namib). Z Geomorph NF 30(Suppl):55–73

Hövermann J (1978b) Untersuchungen und Darlegungen zum Inselbergproblem in der deutschen Literatur der 1. Hälfte des 20. Jahrhunderts. Z Geomorph NF 31(Suppl):64–78

Jacobson P, Jacobson KM, Seely MK (1995) Ephemeral rivers and their catchments: Sustaining people and development in western Namibia. Desert Research Foundation of Namibia, Windhoek

Migoń P (2006) Granite landscapes of the world. Oxford University Press, Oxford

Migoń P, Goudie AS (2003) Granite landforms of the Central Namib. Acta Univ Carolinae, Geogr 35(Suppl):17–38

Milner SC, Le Roex AP, O'Connor JM (1995) Age of Mesozoic igneous rocks in northwestern Namibia and their relationship to continental breakup. J Geol Soc London 152:97–104

Ollier CD (1978) Inselbergs of the Namib Desert. Process and history. Z Geomorph NF 31(Suppl):161–176

Selby MJ (1977) Bornhardts of the Namib Desert. Z Geomorph NF 21:1–13

Selby MJ (1982) Form and origin of some bornhardts of the Namib Desert. Z Geomorph NF 26:1–15

Thomas MF (1978) The study of Inselbergs. Z Geomorph NF 31(Suppl):1–41

Twidale CR (1982) Granite landforms. Elsevier, Amsterdam

Chapter 17
Namib Sand Sea: Large Dunes in an Ancient Desert

Andrew Goudie

Abstract The Namib Desert on the west coast of southern Africa is a very dry desert which is believed to be of considerable antiquity. It is underlain by a fossilized sand sea called the Tsondab Sandstone Formation. Modern dunes include barchans and transverse ridges at the coast and large linear and star dunes further inland. The sand, which is derived from the coast, rivers such as the Orange, and from weathering of bedrock, becomes progressively redder as one moves inland.

Keywords Barchans • linear dunes • Namib • star dunes

17.1 Introduction

Dunes are one of the world's most fascinating and aesthetically pleasing landform types. As Ralph Bagnold remarked in his classic 'Physics of Blown Sand and Desert Dunes' (Bagnold 1941: xxi):

> Here, instead of finding chaos and disorder, the observer never fails to be amazed by a simplicity of form, an exactitude of repetition and a geometric order unknown in nature on a scale larger than that of crystalline structure. In places vast accumulations of sand weighing millions of tons move inexorably, in regular formation, over the surface of the country, growing, retaining their shape, even breeding, in a manner which, by its grotesque imitation of life, is vaguely disturbing to an imaginative mind. Elsewhere the dunes are cut to another pattern – lined up in parallel ranges, peak following peak in regular succession like the teeth of a monstrous saw for scores, even hundreds of miles, without a break and without a change in direction, over a landscape so flat that their formation cannot be influenced by any local geographical features.

The development of these two types of dune, the rapidly moving mass and the linear ridge, are especially well-developed in the Namib as is another type, the star dune. Small mound-like dunes (shrub and coppice dunes) also accumulate around clumps of vegetation such as Nara melon plants (*Acanthosicyos horrida*).

Under strong wind conditions, sand grains are transported across desert surfaces. When the wind velocity exceeds the threshold velocity that is required to initiate sand grain movement, the grains begin to roll along the ground, but after a short distance this gives rise to a bounding or jumping action called saltation. Grains are taken up a small distance into the airstream and then fall back to the ground in a fairly flat trajectory. The descending grains dislodge further particles and thereby the process of saltation is maintained across country. Dunes form because saltating grains tend to accumulate preferentially on sand-covered areas rather than on adjoining sand-free surfaces. This seems to result from the check to a strong wind through intensified sand movement over a sand surface and from the lower rate of sand movement where saltating grains 'splash' into loose sand compared with firm ground. This means that a small sand accumulation gets bigger and turns into a dune. The precise form of such a dune will depend on such factors as the wind regime, the degree of vegetation cover, the amount of sand available, and the size of the grains involved.

17.2 The Environment

The Namib is one of the world's driest, oldest and most beautiful deserts. It extends for more than 2,000 km along the Atlantic coast of southern Africa from the Olifants River in South Africa itself to the Carunjamba River in Angola. On its inland side it is bounded by the Great Escarpment which forms the western edge of the

P. Migoń (ed.), *Geomorphological Landscapes of the World*,
DOI 10.1007/978-90-481-3055-9_17,

interior plateau and basin of southern Africa. Thus it forms a rather narrow strip some 120–200 km wide. Being on the west (and lee) side of the continent, in a zone of subsiding anticyclonic air, and bounded by the cool Benguela current offshore, the Namib is hyper-arid. Rainfall at the Namibian coastal resort of Swakopmund averages a mere 10–20 mm per annum, but increases towards the base of the Great Escarpment, where it may exceed 200 mm. The coastal Namib is also a foggy desert with fog on over 100 days in the year in the area around Swakopmund. This precipitates appreciable amounts of moisture (~34 mm/year at Swakopmund). Nonetheless, the vegetation cover is very sparse, and this means that desert winds are able to sweep unhindered across the surface, and to shape available sediments into a variety of sand dune types (Fig. 17.1). The desert has a number of sand seas (*ergs*) in which these dunes occur – in southern Angola is the Curosa-Bahia dos Tigres sand sea, in northern Namibia are the Cunene and Skeleton Coast sand seas, while in the south is the largest of them all – the Namib Sand Sea itself. Much of it is incorporated into the Namib Naukluft National Park.

17.3 The Birth of the Desert

The existence of arid conditions in the Namib must have been controlled to a considerable extent by seafloor spreading leading to the opening up of the seaways of the Southern Ocean as Africa and South America split apart in the late Jurassic and early Cretaceous around 130 million years ago. In addition, the movement of Antarctica to the South Pole, and the resulting initiation of the offshore, cold Benguela Current (Goudie and Eckardt 1999) were important. The precise date of the birth of this aridity in the Namib has, however, been a matter of some controversy though its great antiquity in comparison with many of the world's deserts seems clear. Ward et al. (1983) said (p. 182) that 'A review of the Late-Mesozoic-Cenozoic geology leads us to conclude that the Namib tract, which dates back to the Cretaceous, has not experienced climates significantly more humid than semi-arid for any length of time during the last 80 million years.' The cemented Tsondab Sandstone erg in the southern Namib dates from at least the Lower Miocene, and overlies wind-sculptured Late Proterozoic rocks (Senut et al. 1994).

The Tsondab Sandstone Formation is indeed a truly remarkable phenomenon. It is a red brown rock, up to 220 m thick, which underlies great tracts of the modern Namib Sand Sea and beyond (Ward 1988). Large parts of the Tsondab Sandstone are dune materials (Kocurek et al. 1999), though there are also materials that must have been laid down in salt lakes and in ephemeral rivers. The aeolian deposits appear to have formed under a similar wind regime to that of the present. They also contain the fossilized tracks of termites

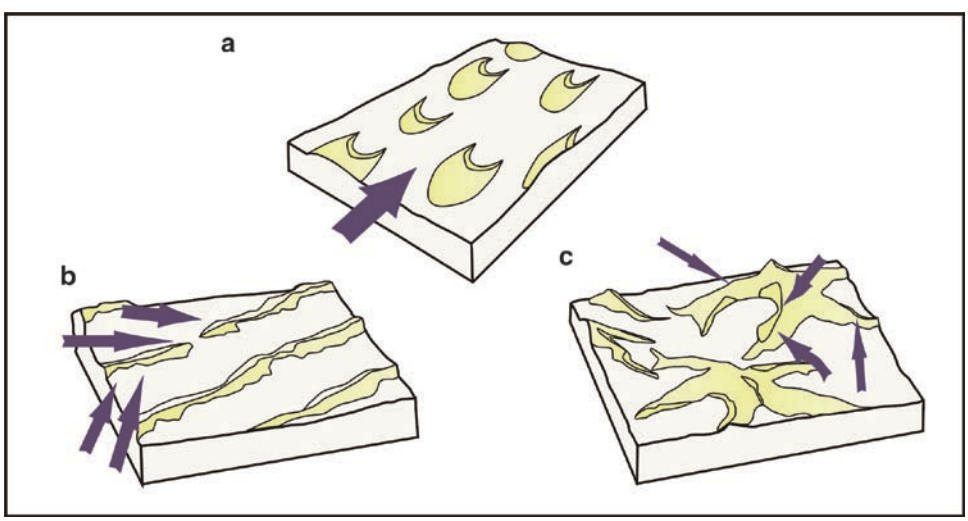

Fig. 17.1 The shape of three types of dune and the wind roses of the winds that have moulded them: (**a**) barchans, (**b**) linear dunes, (**c**) star dunes

and golden moles that live in the Namib today, together with lithified ostrich eggs.

17.4 The Modern Sand Sea

Overlying the Tsondab Sandstone Formation between Lüderitz and the Kuiseb River is the modern Namib Sand Sea (Lancaster 1989), an erg that covers some 34,000 km^2 (Fig. 17.2). At the coast crescentic dunes are dominant, including highly mobile barchans (Slattery 1990; Barnes 2001) (Fig. 17.3). Their horns point in the direction of movement, they have steep slopes (~32°) on their lee sides and gentler slopes (2–10°) on their windward (stoss) sides, they have an ellipsoidal shape in plan view, and have formed in response to the strong unidirectional (SSW) wind regimes that are prevalent in the coastal zone. These can be seen inland from Walvis Bay and in the vicinity of Lüderitz, where they often cross the railway and the main road respectively. They have encroached on the old mining town on Kolmanskop (Fig. 17.4). The barchan dunes of the Kuiseb Delta near Walvis Bay have average rates of movement of 12.4–14.6 m/year. Their mean height is about 8 m and the distance between their horns averages c 155 m. Where there is a large sand supply, the barchans sometimes coalesce to create transverse ridges. Elsewhere they may have the form of mega-barchans, with small features developed on a much larger crescentic base.

The heart of the sand sea is dominated by linear dunes (Fig. 17.5) that are associated with more bi-directional wind regimes (SSW–SW and NE–E). The

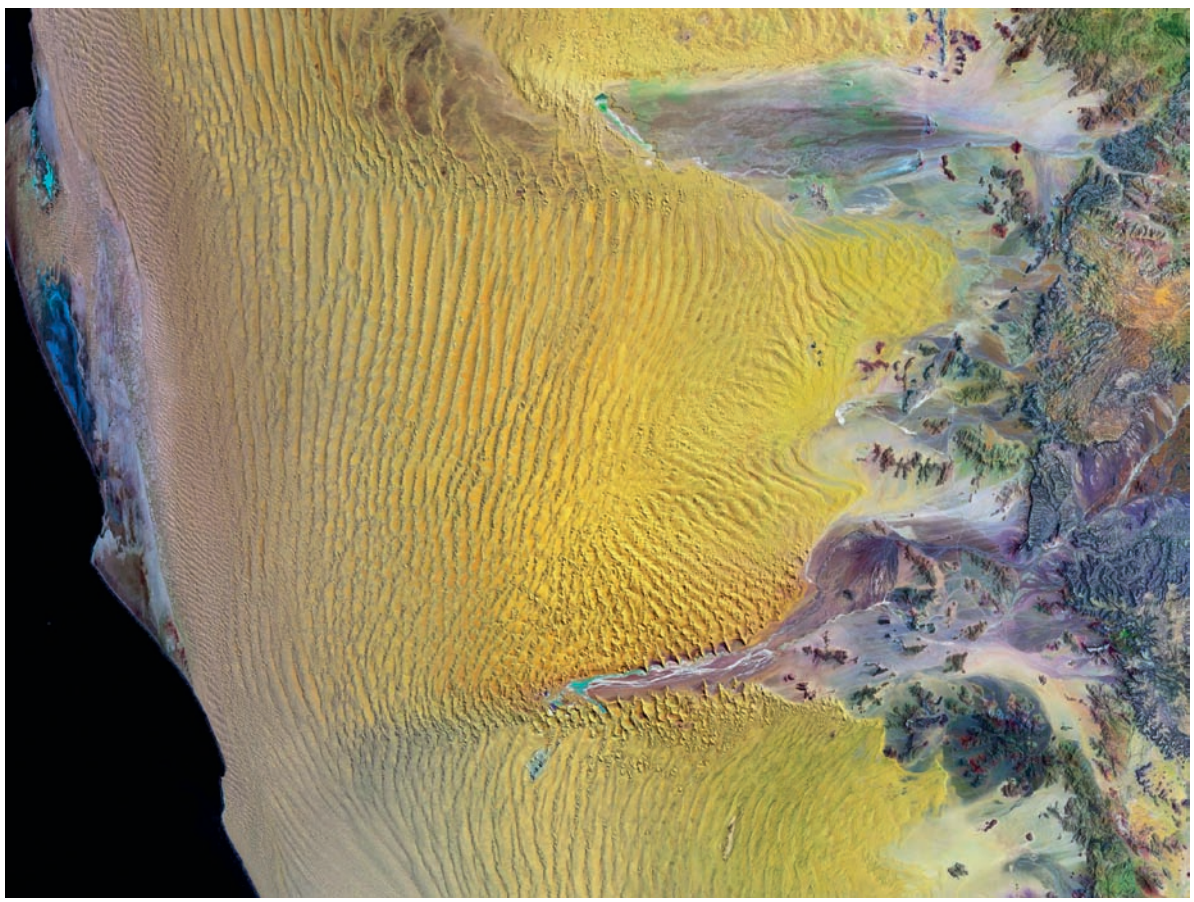

Fig. 17.2 Landsat 7 image of the central Namib Sand Sea, with the Atlantic Ocean to the west and the Great Escarpment to the east. Two ephemeral rivers occasionally flow into the eastern margin of the sand sea producing the Tsondab vlei (in the north) and the Sossus Vlei (in the middle) (Courtesy NASA)

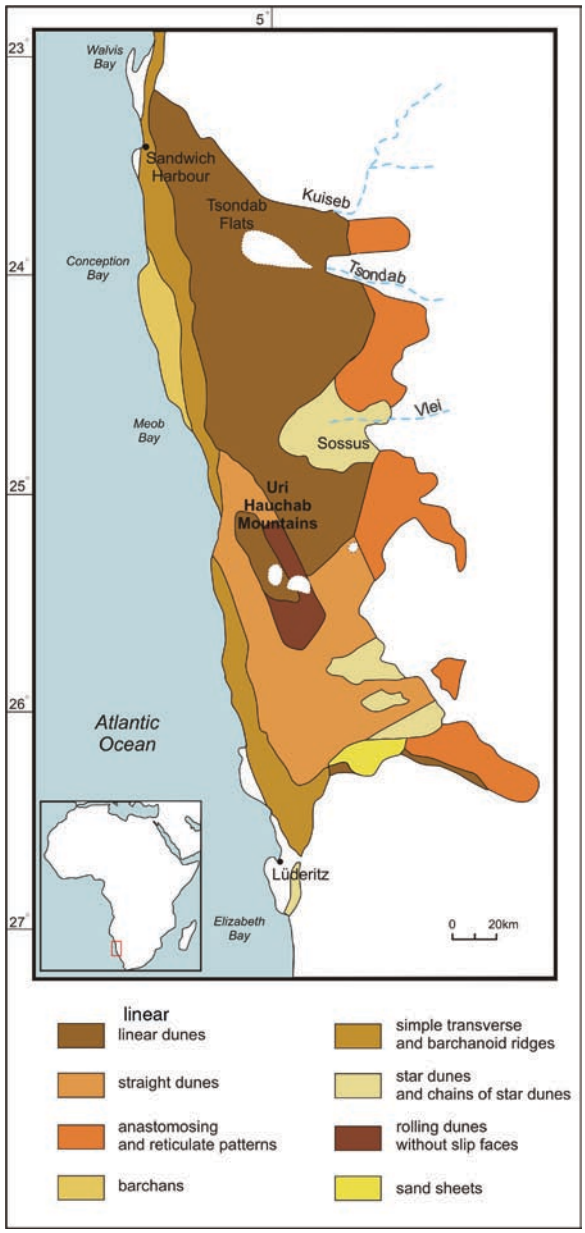

Fig. 17.3 Map of the main types of dunes in the Namib Sand Sea (Based on the work of N. Lancaster)

former winds blow inland from the South Atlantic Ocean and the latter sweep down the Great Escarpment from the interior. The dominant annual sand movement appears to be from the south. The spacing of the linear dunes varies through the sand sea. It is greatest in the central regions at 1,800–2,500 m, whereas in the southern parts these dunes are generally spaced at 1,500–2,000 m. The dunes are mostly between 6,000 and 900 m wide and between 50 and 150 m high. They are the dominant dune form in the sand sea. Changes in their form and the nature of wind flow over them over more than two decades have been described by Livingstone (2003). He found that the crests of the dunes move laterally back and forth in response to seasonal switching of wind direction, but return at the end of the year's cycle to their position at the beginning. This, says Livingstone, suggests that the dune is an equilibrium response to the wind regime and that there is no evidence of any lateral shifting of the dune. However, recent studies using Optically Stimulated Luminescence dating and ground Penetrating Radar (Bristow et al. 2007) have suggested that a few hundreds of metres of lateral migration have taken place in the last few thousands of years.

Star dunes, characterized by their pyramidal morphology and radiating sinuous arms, are associated with complex, multidirectional wind regimes (SW–WSW, NE–E and N) that occur along the sand sea's eastern margin, close to the Great Escarpment. The dunes are highest and most widely spaced in the central and some northern parts of the erg, with progressively lower and more closely spaced dunes towards the margins. Some of the star dunes, including those in proximity to the much visited Sossus Vlei, are well over 150 m high, and some may reach heights of 200–300 m, making them some of the largest dunes in the world, only exceeded perhaps by those of China's Badain Jaran Desert.

The sharply defined northern margin of the sand sea is formed by the Kuiseb River, for although this is only ephemeral, it flows sufficiently often and powerfully to prevent the dunes, driven by winds from the south, from moving further north, except in the immediate coastal fringe between Walvis Bay and Swakopmund. Further south, rivers deriving their flow from the mountains of the interior, such as the Tsauchab and the Tsondab Vleis, have entered the dune field and deposited light-coloured, horizontally laminated silts, but at the present time they do not have the power to reach the Atlantic. When conditions may have been moister in the past, these rivers may have extended further into the sand sea than they do today, depositing lake sediments (Teller and Lancaster 1986).

The sources for the sand that make up the sand sea are probably varied and could include eroded material from the older Tsondab Sandstone Formation (Besler and Marker 1979), weathering of extensive areas of

Fig. 17.4 Sand encroaching on the mining town of Kolmanskop, east of Luderitz (Photo A. Goudie)

Fig. 17.5 Linear dunes at Gobabeb in the north of the sand sea (Photo A. Goudie)

Fig. 17.6 Large linear dunes overlooking Sossus Vlei (Photo A. Goudie)

granites and Karoo sandstones, deflation of sand from river beds, and derivation from the Atlantic shoreline. Lancaster and Ollier (1983) believe that much of the sand may have been supplied by the Orange River to the coastal zone and then been blown inland.

The colour of the dune sand of the Namib shows clear spatial trends. In coastal areas dominated by crescentic dunes the sand is yellowish brown to light yellowish brown, whereas in eastern areas it becomes a very striking yellowish red, a shade that would not disgrace a ripe apricot (Fig. 17.6). Four main hypotheses have been suggested to account for the reddening of dunes as one progresses inland (Walden et al. 1996; Walden and White 1997). The first of these is that the increasing age of the sands inland allows greater time for weathering processes to develop the iron (haematite) coatings around quartz grains. The second is that in areas of active sand transport and high energy winds near the coast, coatings may be lost or fail to develop. The third is that different sand source materials occur in the coastal zone compared with inland. Finally, it may be that a regional climatic gradient with warmer and wetter conditions inland provides a control on the rates of weathering processes which generate the haematite coatings. On the basis of detailed analyses, Walden and White (1997) suggest that different sand source materials play a major role, but that so also do age and environmental gradients.

17.5 Conclusions

The dunes of the Namib Sand Sea are not only an example of the main forms of dunes that occur in the world's deserts, nor are they only some of the world's largest and most colourful. They are also home to a diverse and intriguing variety of animal life which has evolved remarkable adaptations to the aridity, stark temperature contrasts and instability of the dunes.

The Author

Professor **Andrew Goudie**, Master of St. Cross College in the University of Oxford, has worked in the Namib since 1967, and also in many of the world's other deserts. He has a particular interest in dunes, weathering, dust storms and

climatic change. He has been President of the International Association of Geomorphologists (2005–2009) and is author of *Great Warm Deserts of the World* (2002), as well as many other books and research papers.

References

Bagnold RA (1941) The physics of blown sand and desert dunes. Methuen, London

Barnes J (2001) Barchan dunes on the Kuiseb River delta, Namibia. S Afr J Geogr 83:283–292

Besler H, Marker ME (1979) Namib Sandstone: a distinct lithological unit. Trans Geol Soc S Afr 82:155–160

Bristow CS, Duller GAT, Lancaster N (2007) Age and dynamics of linear dunes in the Namib Desert. Geology 35:555–558

Goudie AS, Eckardt F (1999) The evolution of the morphological framework of the Central Namib Desert, Namibia, since the early cretaceous. Geogr Ann 81A:443–458

Kocurek G, Lancaster N, Carr M, Frank A (1999) Tertiary Tsondab Sandstone: Preliminary bedform reconstruction and comparison to modern Namib Sand Sea dunes. J Afr Earth Sci 29:629–42

Lancaster N (1989) The Namib Sand Sea. Balkema, Rotterdam

Lancaster N, Ollier CD (1983) Sources of sand for the Namib Sand Sea. Z Geomorph 45(Suppl):71–83

Livingstone I (2003) A twenty-one-year record of surface change on a Namib linear dune. Earth Surf Proc Landf 28:1025–1031

Senut B, Pickford M, Ward J (1994) Biostratigraphie de éolianites néogènes du Sud de la Sperrgebeit (Désert de Namib, Namibie). C R Acad Sci 318:1001–1007

Slattery MJ (1990) Barchan migration on the Kuiseb River Delta, Namibia. S Afr Geogr J 72:5–10

Teller JT, Lancaster N (1986) Lacustrine sediments at Narabeb in the Central Namib Desert, Namibia. Palaeogeo, Palaeoclimat, Palaeoe 56:177–195

Walden J, White K (1997) Investigation of the controls on dune colour in the Namib Sand Sea using mineral magnetic analyses. Earth Planet Sci Lett 152:187–201

Walden J, White K, Drake NA (1996) Controls on dune colour in the Namib Sand Sea: Preliminary results. J Afr Earth Sci 22:349–353

Ward JD (1988) Eolian, fluvial and pan (playa) facies of the Tertiary Tsondab Sandstone formation in the Central Namib Desert, Namibia. Sediment Geol 55:143–162

Ward JD, Seely MK, Lancaster N (1983) On the antiquity of the Namib. S Afr J Sci 79:175–183

Chapter 18
North-Eastern Niger: Sandstone Landscape of the Sahara

Detlef Busche

Abstract The landform history of the sandstone scarpland, inselberg and plains landscape of the greater Djado region, part of the presently hyper-arid central Sahara, in north-eastern Niger, begins with all-encompassing Paleogene etchplanation under humid-tropical conditions, followed by the almost compete stripping of the original soil cover and silcrete induration of the uniform etchplain during the Oligocene. Still under very humid conditions, deep-reaching karstification then penetrates silcrete, contemporaneous ferricrete and, above all, the saprolitic sandstones, also creating numerous poljes. Gradually decreasing humidity up to the end of the Neogene, resulting in increasingly restricted etchplanation, leads to the formation of scarplands, inselbergs, intra-plateau basins, pediments, and still sandstone-karst-related scarpfoot depressions. During a final relapse to quite humid conditions, landslide fringes form along all heterolithic escarpments at the onset of the Pleistocene, later on merely subject to fluvial dissection in the context of at least three phases of Quaternary pluvial river aggradation and terrace formation. A thorough reshaping of most of the region under Quaterary arid conditions is effected by more than one phase of aeolian corrasion, as part of the largest wind-corrasion landscape on Earth.

Keywords Aeolian corrasion • central Sahara • etchplanation • fossil landslides • sandstone karst • scarplands • silcrete

18.1 Geology, Setting and Climate

The Saharan desert of north-eastern Niger, consisting of the plateau and escarpment landscapes of Mangueni, Djado, Tchigai and Kaouar and the plains areas between them, at about 20–23°N and 12–16°E, is situated between the Murzuq Basin to the north and the Chad basin to the south (Fig. 18.1). It has been a region of terrestrial sedimentation ever since Cambrian times, preceded and interrupted by times of etchplanation, recorded first by the unconformity cutting across the Precambrian basement, followed by the next one separating tilted Cambro-Ordovician to Silurian and Carboniferous sandstones from the red silt and claystones of the Tilemsin beds (*Post-Tassilien* of the French literature), and finally by an unconformity cutting across all these rocks, preceding the last major phase of deposition, that of the Nubian/Messak Sandstone, *Grés de Nubie* or *Continental intercalaire*, mainly dated by its grading southward to the marine Upper Cretaceous (Faure 1966; Greigert and Pougnet 1967; Klitzsch and Baird 1969).

The geomorphic development of the region began with the removal, by etchplanation, of most of the Nubian Sandstone up to the Oligocene, with sediment transport southward to a swampy coastal plain where the partly ferruginous deposition of the *Continental Terminal* (Faure 1966) took place. Since then, gradual uplift has been up to 1,000 m a.s.l. in the north. The present landscape of plateaux, escarpments, inselbergs and foreland plains (Fig. 18.2) is the result, first, of increasingly selective etchplanation dismembering the initial etchplain, under humid conditions during the Neogene, and then of linear erosion and fluvial deposition alternating with times of aeolian corrasion under the mostly arid conditions of the Quaternary. Relative height differences are largely below 300 m.

The region, with not a single permanent weather station within it, is hyper-arid with annual rainfall of about 20 mm, falling as cyclonic winter rains in the north and monsoonal summer rains in the south. The direction of the predominant north-easterly trade wind is affected by the Tibesti Mts. to the east and appears to have been unchanged during the Quaternary, interrupted by occasional monsoonal SW winds in summer.

P. Migoń (ed.), *Geomorphological Landscapes of the World*,
DOI 10.1007/978-90-481-3055-9_18,

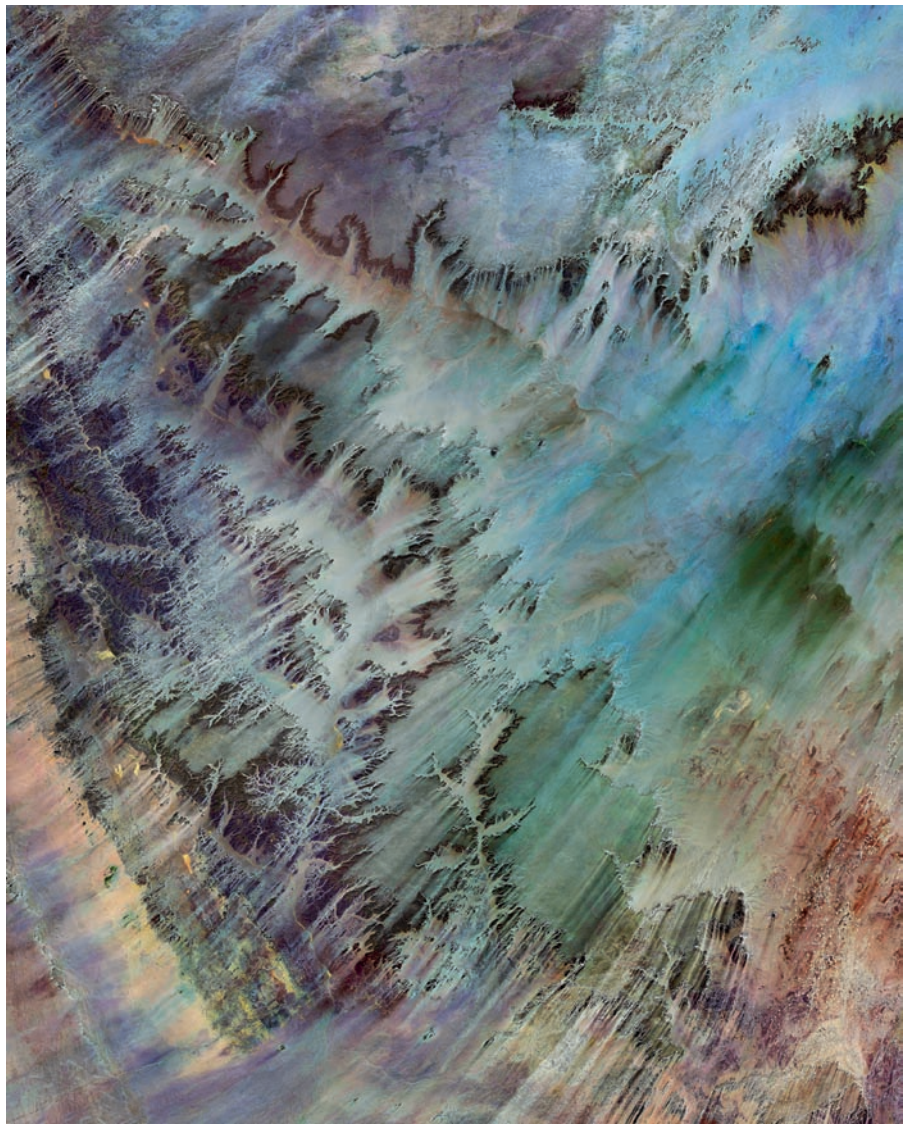

Fig. 18.1 Landsat satellite image of the Mangueni, Djado and Tchigai region of north-eastern Niger (for location see Fig. 18.2). It shows the plateau, scarpland and plains landscape, partly reshaped by aeolian corrasion during arid intervals of the Quaternary. Preserved from corrasion in the NE trade-wind direction are those plateau parts that lie within the wind-shadow of the Djebel Ati plateau, about 200 km to the north. All bedrock outcrops appear dark because of their coating by desert varnish (orthorectified Landsat ETM + mosaic, N33-20_ 2000, RGB 7-4-2, NASA, MrSid)

In the following sections, a brief outline of the landform history of the desert region will be given, largely representative of most of the central Sahara, a region once believed to have been an eternal core desert (e.g. Meckelein 1959), but indeed a landscape that owes its major traits to geomorphic processes at work in non-arid environments. The truly arid exception is its share of the largest wind-corrasion landscape on Earth, aside from the arid 'redecoration' of the landscape visible as many bare rock surfaces coated by brown – and frequently disintegrating – desert varnish, angular desert pavement on most plateau surfaces, and the thin veneer of wind-blown sand on the plains, with or without ripples and, in this part of the Sahara, only a small amount of sand dunes.[1]

[1] To overcome the page limit of the chapter, for further ev idence, details and photographs the reader is referred to Busche (1998) and Busche et al. (2005).

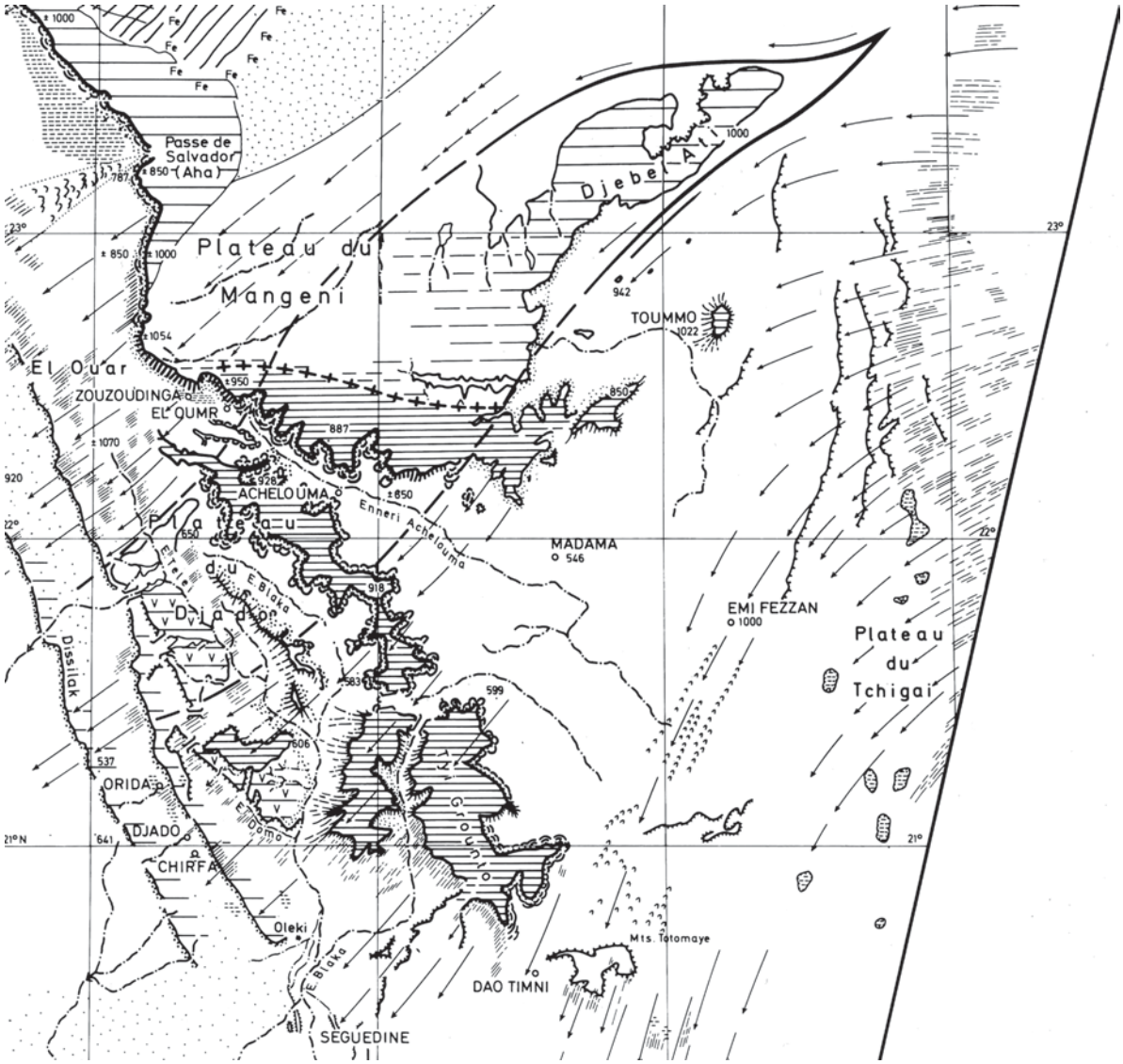

Fig. 18.2 Geomorphological map of north-eastern Niger. *Arrows* indicate wind direction derived from the stringers of aeolian sand and the orientation of sandstone yardangs shown as thin lines. The closely spaced horizontal hachure marks the areas of the very level Nubian sandstone plain with its silcrete cover pitted by sandstone karst depressions (cf. Fig. 18.3). Its northern boundary on the Plateau du Mangueni delineates low divide. The interrupted wavy line parallel to the escarpment rims marks the areas of Early Pleistocene landsliding. The forked thick line on both sides of Djebel Ati and its broken continuations to the south-west comprise the wind-shadow area. The ovals of the Tchigai region mark some of the sandstone karst poljes. The broken hachures in the Orida-Chirfa area mark the scarpfoot depressions. The areas left white stand for the more or less dissected etchplain and its continuations into the plateau region as intraplateau basins and plains (mapping D. Busche, cartography K. Wepler)

18.2 The Plateau Surface and Its Silcrete Cover

The pre-Oligocene removal of several 100 m of the Nubian sandstone – still largely preserved in the Messak plateau region farther to the northwest – was complete in much of the south-western Djado Plateau, re-exposing the level of the post-Tilemsin etchplain. Along the plateau rims of Mangueni, north of the broad ‘valley’ of Enneri Achelouma, and along the north-eastern parts of the Djado Plateau to the east and south, it has been worn down to a thickness of just a few

metres. The original land surface has been best preserved on the Plateau du Mangueni, surmounted by only a few low mesas farther to the north-west. Its most striking characteristic is its near-perfect flatness, which most likely is not original, but related to the development of a thin layer of silcrete on it (Busche 1983), so well-indurated that it was quarried for making hand axes in Palaeolithic times (Busche 1998).

From the as yet only known well-preserved complex *in situ* palaeo-latosol profile underneath a *Continental Terminal* iron crust on the Agadem plateau of south-eastern Niger (Busche 1998), from several sites of kaolinite and alunite as tropical weathering products (Faure 1966) and a few locations where the iron crust grades into silcrete, it can be inferred that a tropical soil cover of the land surface of the time was stripped at some time in the Oligocene, to be washed to the coastal plain in the south as clastics and in solution, to be deposited as the *Continental Terminal*. Much more ubiquitous evidence of the chemical deep weathering preceding the stripping is the groundwater-bleached saprolite, which at least in the area of the present high inselbergs of the Djado escarpment foreland reached more than 300 m below the level of the present plateau (Busche 1998).

Once stripped of its latosol cover, the land surface became indurated by the silcrete. The extreme flatness of the plateau may be explained by wash processes of shifting channels in the unconsolidated quartz sands produced by chemical weathering. Although a major climate change to most likely drier conditions must be assumed for the stripping, conditions must still have been humid-tropical, enough first for the export of iron in solution, and then for the solution, transport and deposition, by surface and groundwater, of vast amounts of silica, as silcrete is definitely not a product of arid conditions (Wopfner 1978; Busche 1983). Its present exposure on the plateau surface, frequently revealing a much cracked pillow structure, is due to the stripping of the Late Tertiary or younger soils above the silcrete in transition to phases of extreme aridity.

18.3 Sandstone Karst

A significant landform element of the silcrete surface, in particular in the Nubian Sandstone area, are often closely spaced, mostly circular, steep-walled basins a few metres deep, that show well as white specks on the 1:50,000 air photos of the 1950s from a thin sheet of whitish silt trapped in them, overlying a bright red pluvial soil of the Early Holocene. On the more dissected Palaeozoic-rock plateaux, an intricate system of partly sediment-filled, generally round tubes up to a few cm in diameter, and widened joints has been found (Fig. 18.3a). These and other features are conclusive evidence of an intensive former karstification of the carbonate-free sandstones (e.g. Busche and Erbe 1987; Busche and Sponholz 1992; Busche 1998).

On the Nubian Sandstone plateau the subterranean karst is only shallow, due to the underlying Tilemsin beds. From the bare inselberg flanks it appears, however, that the solution processes reached more than 300 m deep, below the foreland of the Djado escarpment. Subterranean karstification, with the whole range of joint-oriented tubular passages, dead ends, domes, vertical shafts and chambers more than 10 m high known from limestone karst (Fig. 18.3b) clearly post-dates saprolitization, but will not have been dependent on it as karst tubes also cut through massive silcrete and, farther south, through the *Continental Terminal* iron crusts, which gives a *terminus post quem* for its origin. Surficial karstification came to an end with the dissection of the original land surface. Lower levels merely cut across pre-existing karst tubes.

The most impressive superficial sandstone karst landforms are steep-walled poljes of subterranean drainage, up to several km in diameter and up to a few tens of metres deep, with about 20 of them within a 60 × 60 km part of the Tchigai Plateau. The largest one, Logozonou, is 10 × 5 km across. Smaller and shallower, but almost adjacent, are the iron crust poljes on the Termit Plateau to the south, and the Kaouar Plateau, SE of Séguedine, has completely been transformed to thousands of dune-sand-filled solution pits up to more than 100 m in diameter (Fig. 18.4) (Busche 1998). Evidently warm and wet conditions still – or again – must have prevailed in the central Sahara to permit such morphologically significant silica solution.

18.4 Shape and Development of Escarpments and Intra-plateau Basins

A significant change of environmental conditions led to the transformation of a continuous etchplain to a

Fig. 18.3 Examples of sandstone karst. (**a**) Vertical karst tubes close to the rim of the Dissilak escarpment, partly filled with aeolian sand and cutting across mechanically very hard silcrete. Creation by turbulently rushing water – instead of slow circulation of chemically aggressive groundwater – is unlikely, as there was no higher hinterland at the time of formation. Its abrupt beginning on the rock surface is circumstantial evidence that there was a soil cover at the time of formation, and that the silcrete was part of the soil profile. (**b**) Karst-riddled inselberg. Each of the shadows on its steep slope marks a karst vessel cut off in the process of etchplain lowering and relative 'growth' of the inselberg. The high portal at the foot is also an opening of a large cave system (Photos D. Busche)

scarpland landscape, as in other parts of the Sahara as well. Two types of escarpments have developed (Busche 1998): the heterolithic one, with a free face above a straight to slightly concave slope of Tilemsin beds or saprolitized basement, and the homolithic one, all in sandstone, with a stepped profile of treads and risers in varying numbers, often only preserved as small ledges, and also on escarpment back slopes. At the Djado escarpment, the broader treads are dotted with small, tower-like inselbergs (Busche 1998). In the foreland of both types of escarpments occasionally concave lower slope segments have been preserved.

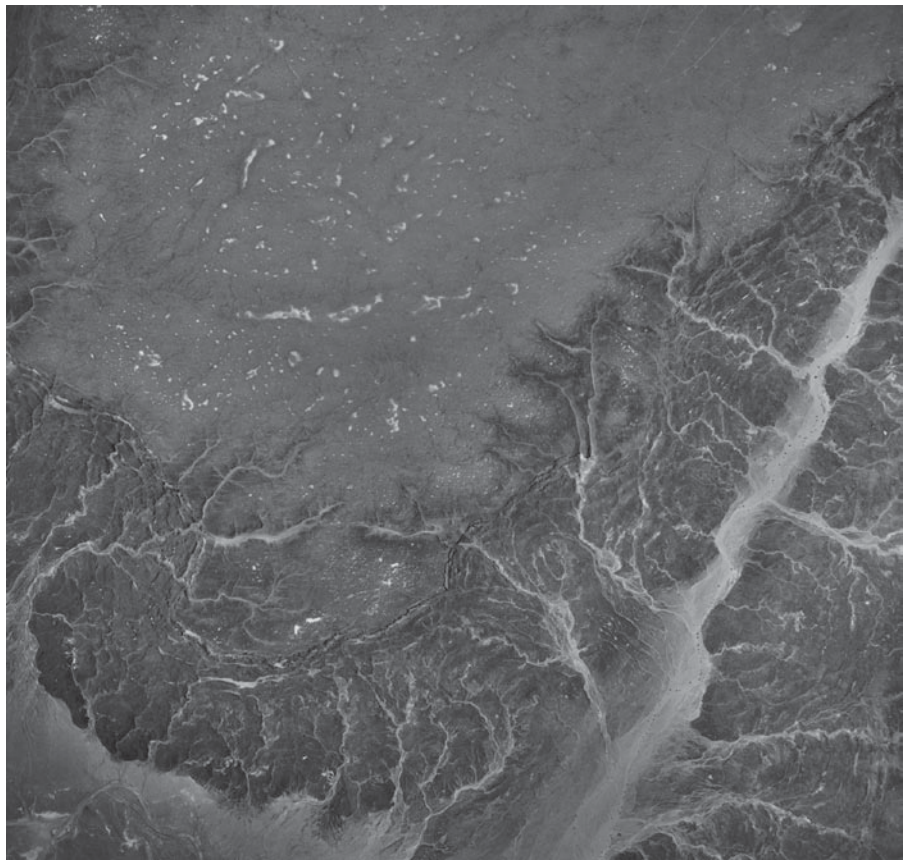

Fig. 18.4 Vertical aerial photograph of a section of the south rim of the Plateau du Mangueni. The almost perfectly level plateau is part of the Oligocene etchplain, with white specks denoting sandstone karst depressions, filled with pluvial red soil overlain by a thin whitish silt cover. The broad landslide fringe over a vertical distance of about 100 m shows the typical fluvial dissection by run-off from the plateau rim (Photo IGN Paris, NF 33-XIII, 195)

Often misinterpreted as evidence of slope retreat, they are indeed the relics of progressive frontslope steepening, once the present foreland level had been reached by etchplanation (cf. Grunert and Busche 1980). A trait also common to both types of escarpment is the mostly semi-circular embayments opening to the plateau rim, only a few metres below the plateau, and like it, irrespective of rock structure and faults (*Plateaurandbucht*, Busche et al. 2005).

The stepped profile of homolithic escarpments itself is irreconcilable with the still frequently assumed concept of slope retreat (Busche et al. 2005) Another argument for both escarpment types is that the regional divide strictly follows the plateau rim, with the fingertip channels draining the plateau surface originating right behind it, with no sign of beheading. An exception is the south rim of the Plateau du Mangueni, where the extremely shallow divide lies at some distance to the north, but the south-facing valleys dissecting the plateau rim are again no argument in favour of slope retreat. As the Enneri Achelouma separating it from the Djado Plateau to the south widens from barely 1 km to more than 50 km towards the plain of Madama, any slope retreat from an assumed incised valley would have had to proceed at vastly different speeds despite uniform environmental conditions within the area at any given time.

The onset of scarp formation and the reason for its permanent position is best seen along the heterolithic Dissilak and Mangueni escarpments. In cross section, the blunted tip of a wedge of the capping sandstone marks the approximate line where, on the original surface, the slightly tilted sandstone beds lay in contact with the underlying softer rocks. With a climatically

induced decreasing intensity of chemical weathering, denudational wash processes could proceed on the softer rocks only, thereby lowering them and initiating vertical escarpment growth. As for the homolithic escarpments, a slight asymmetry in a shallow divide, frequently preserved as the *walm* of German scarpland terminology, would have favoured one side by additional run-off for continued etchplanation. In both cases, the shallow plateau-rim embayments thus represent the first step of escarpment growth (Busche 1998; Busche et al. 2005).

The stepped escarpments are understood to be the result of the interplay of continued tectonic updoming and decreasing humidity from the time of Miocene sandstone karstification to the onset of arid conditions in the Plio-Pleistocene transition. Following the concept of differential erosion (e.g. Bremer 1980; Büdel 1982) or *érosion différentielle* of the French literature, whenever a threshold in climatically induced chemical weathering was crossed, surface wash would become less effective in certain parts, which would then drop out of the planation system. If such an area lay at the foot of the then still lower escarpment, a new tread would come into existence; if farther away, it would be a new inselberg (Fig. 18.5). Similarly, the small inselbergs on the broader treads of the Djado escarpment would have been initiated as shield inselbergs in the course of continuing foreland etchplanation, growing until their surrounding plain dropped out of the planation process. In contrast, the tallest inselbergs of the Djado foreland, around 300 m high, must have originated as shield inselbergs right at the beginning of scarpland formation. Along the heterolithic escarpment sections, the low resistance of the slope rocks largely precluded the formation of any steps by a continuous adaptation of the convex–concave profiles to further foreland lowering.

On the rear side, as in all escarpment regions of the world, in more resistant rocks, there was either valley incision or, just as important and best developed in the Palaeozoic sandstone parts of the Djado Plateau region, the formation of intramontane (Büdel 1982), or more

Fig. 18.5 View from the top of the much-dissected Djado escarpment to the west, across one of the broader treads lowered below the irregular remains of a higher etchplanation level to the scarpfoot depression of Orida in the foreland. The inselberg, Emi Wongan, close to 300 m high, rises from the floor of the sandstone karst depression, several tens of metres below the end-of-Tertiary Ténéré etchplain level at the horizon (Photo D. Busche)

precisely in this type of landscape, intra-plateau basins or plains, exorheïc equivalents to the Tchigai poljes, best seen in the Enneri Blaka system. In Quaternary times, their floors were modified by river activity in their deepest parts, whereas their rims became fringed by alluvial fans.

Whereas etchplanation had been nearly ubiquitous in the Palaeogene, post-Oligocene climate changes leading to gradually less aggressive chemical weathering led to progressively restricted etchplanation, by intensity and area. The outcome was the present pattern of plateaux, escarpments, inselbergs and foreland plains.

18.5 The Plio-/Pleistocene Transition

In striking contrast to the perfectly level silcrete plateau, the lowest and last etchplain level, as of the Ténéré to the west, is a gently undulating sequence of former wash divides and depressions (cf. Büdel 1982), long since stripped of its original soils. On it, with the major change to the Pleistocene climate regime, there was a complete shift from etchplanation to linear erosion, to the *grand creusement des vallées* of the French Saharan literature (e.g. Faure 1966; Rognon 1967), though only moderate in the study region in reaction to only moderately continuing uplift.

Before that, in the final phase of etchplanation, supplemental run-off from the escarpments obviously reduced planation to their immediate forelands, resulting in escarpment-parallel low depressions of subsequent drainage, the former etchplain parts being transformed to more steeply inclined pediments (Busche 1976). Following their dissection, they later became blanketed by several generations of alluvial fans (Busche et al. 2005). A comparable development modified the floors of the intra-plateau basins.

18.6 Endorheïc Scarpfoot Depressions and Their Karst-Riddled Inselbergs

The dissection of the pediments along the Djado and Kaouar escarpment resulted – as has frequently been the case – in the erosion of a shallow trough originally drained parallel to the foot of the escarpments (the *Subsequenzfurche* of German terminology). Following that phase, there was obviously still enough moisture available from the run-off of the escarpment front slopes to further deepen sections of the troughs to endorheïc scarpfoot depressions (*Stufenfußdepressionen*, Busche and Sponholz 1992), several tens of metres deep and several km long. They are not deflation hollows, as one might assume in a presently hyper-arid environment, lying at nearly right angles to the trade wind and in the wind-shadow of the escarpments. Belonging to a former aeolian regime are a few narrow, wind-oriented basins within the sediment-fill of the Kaouar depression presently occupied by artesian lakes.

Conclusive evidence for a solutional origin comes from the scarpfoot depressions below the Djado escarpment, where several of the tall inselbergs are located close to their deepest parts, fringed by a narrow dissected pediment. With no difference in their flanks above and below the level of the depression rim, the process of relative inselberg ‘growth’ must have continued during the deepening of the depressions.

18.7 Heterolithic Escarpments and Large-Scale Fossil Landslides

Aside from the almost complete absence of soils softening their contours, the principal shape of the homolithic escarpments is still that of the late Neogene. The case of the heterolithic escarpment sections is different. Wherever the silty to clayey Tilemsin beds cropped out at the escarpment slopes, similar to the situation at all other Saharan escarpments, they became part of the largest fossil landslide regions on Earth, with a fringe, at least several 100 m to as much as 3 km wide, following the ground plan of the plateau rims (Grunert and Busche 1980; Busche 1998; 2001). Wherever the sandstone cap was thick and stable enough at the plateau rim, a sequence of often more than ten rotational slide-segments moved towards the foreland. Where it was too thin, as along much of the Mangueni Plateau, the landsliding took place as vast mudflows. Its fringe has more of a highly irregular mudflow appearance (Fig. 18.6), with isolated blocks of the caprock sandstone floating on the highly disturbed silts and clays.

Fig. 18.6 Early Pleistocene mudflow-type landslide fringe, with some rotational slide segments to the left, below the silcrete-armoured, near-horizontal Oligo-Miocene level of the Plateau du Mangueni (Photo D. Busche)

The landslides overlie dissected pediments, pre-date the oldest river terraces and thus must have originated during the Early Pleistocene. Since then only secondary sliding on segment walls has taken place, related to the considerable fluvial dissection of the fringe that has locally exposed the contortions of the Tilemsin beds, obviously totally soaked and highly mobile during landsliding. Landsliding appears to have been preceded by a time of dissection and steepening of the originally sigmoid slope profiles in adaptation to an increasingly arid regime, which also shaped the free face – the trademark of arid escarpments.

With a final return to extreme rainfalls and the soaking of the Tilemsin beds, slope failure was unavoidable. Rainfalls must have been so high or persistent, that even a south-eastern outlier of the Djado Plateau, barely 100 m high and not much larger than a soccer field, received so much direct rainfall that sliding took place along all its sides.

18.8 Quaternary River Terraces

As the emphasis of this chapter is on the sandstone elements of the landscape, only passing reference will be made to the river terraces representing repeated pluvial phases of the Quaternary (cf. Busche 1998). The presumably oldest one has only been preserved as a thin veneer of perfectly rounded vein-quartz and silicified sandstone pebbles on the vast rock fan of Enneri Blaka, partly iron-cemented along former shallow thalwegs. Possibly the next younger terrace, dubbed the pre-Acheul terrace because of the many artefacts of the Palaeolithic that are spread on its surface, consists of mostly quite well-rounded boulders and very coarse gravel that, in such a saprolitic environment, can only be corestones derived from the late Neogene chemical weathering of the silcrete. This is also the terrace that blankets the toes of the landslides in Enneri Achelouma.

There is only one more coarse-grained terrace, the lower terrace, roughly dated as pre-Neolithic by the artefacts found within the hamada of its surface – certainly degradational and not the one on which the people lived. The dissected alluvial fans of the broader valley sections, with their hamada surface, grade into this terrace. Its deposition was preceded by the large-scale removal of the predominantly silty middle terrace that, in analogy to other parts of the central Sahara, should mainly have been deposited, mostly in a swampy environment, between 10,000 and 7,000 years ago, largely simultaneous with the diatomitic lake deposits which are found primarily to the south of the Djado region (cf. Baumhauer et al. 2009), but also in lower-lying sandstone karst depressions of the Tchigai and the foreland of the Mangueni escarpment.

The depositional periods certainly were pluvial ones. It should be noted, though, that also the periods of their dissection must have been quite humid at times, with enough force of the water for sediment removal from areas where before lesser transport energy had caused deposition. During the erosion of the middle terrace, catastrophic floods even moved blocks of several tonnes' weight (Busche 1998). The present fluvial activity of the region is so low that most valley floors carry at least a veneer of aeolian sand.

18.9 The Aeolian Reshaping of Sandstone Landforms

From the satellite image of Fig. 18.1 one gets the impression of a landscape of largely aeolian dynamics. The highly reflective sand sheet blanketing much of the terrain is mostly only a few cm thick, though, and sand dunes are scarce within the region. It is the streamlined pattern of bedrock yardangs (Fig. 18.7), though, that shows this to be part of the largest region of aeolian corrasion in the world (Mainguet 1968; Busche and Stengel 1993; Busche 1998; Busche et al. 2005). The pattern reflects the deflection of the north-easterly trade around the obstacle of the Tibesti Mountains to the east.

Fig. 18.7 Low whaleback aeolian-corrasion ridges (rock yardangs) on the Tchigai plateau; present and former wind direction from the left. The dark brown desert varnish typically incorporating a possibly joint-controlled crack pattern, is evidence that the *crêtes et couloirs* assemblage is a palaeo-landform of times of higher wind-erosion intensity than today (Photo D. Busche 1990)

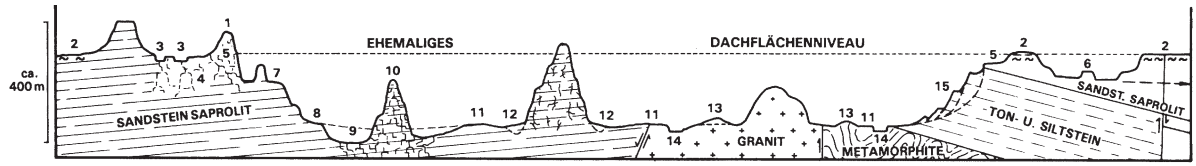

Fig. 18.8 Landform history of the Djado-Mangueni region of NE Niger, from the Oligo-Miocene original land surface and Mio-Pliocene time of increasingly restricted etchplanation and scarpland formation to the fluvially dissected Plio-Pleistocene Ténéré etchplain level. Not included is the Pleistocene aeolian corrasion (cf. Fig. 18.1) (Modified from Busche 1998: 43)

1. Inselberg of the original etchplain in typical plateau-rim position
2. Plateau sections of the original land surface with its silcrete cap post-dating the stripping of its humid-tropical soil cover
3. Sandstone karst solution hollows and basins in Palaeozoic sandstone; not shown but also existing on the Nubian Sandstone plateau (far right)
4. Underground sandstone karst tubes and caves of only partly known extent within the saprolitc sandstones
5. Plateau-rim embayment, relics of incipient foreland deepening and scarp formation
6. Intra-plateau basin at an intermediate level, drained by a valley; deeper basins and larger intra-plateau plains have been lowered to the Ténéré level
7. Broader intermediate level (tread) of the stepped homolithic escarpment, the top of the small inselberg on it marking a former etchplanation level
8. Cut-off pediment; dissected pediments also occur underneath the toe of the landslide fringe (between 14 and 15)
9. Scarpfoot depression
10. Karst-riddled inselberg of Palaeozoic sandstone within a scarpfoot depression
11. Ténéré or Madama etchplain level of end-of-Neogene age
12. Moat resulting from preferred (Late Neogene) chemical weathering due to higher water supply from slope run -off
13. Stripped shield inselberg
14. Valley of Early Pleistocene incision (*grand creusement des vallées*) with Quaternary pluvial terraces
15. Rotational landslide fringe on a heterolithic escarpment of Permian Tilemsin silt- and claystones underlying a wedge of Nubian Sandstone

The dark colour of the corrasion-shaped rocks, due to their coating of dark-brown desert varnish, indicates, though, that the whole pattern is ancient, dating back to times of the Quaternary of much higher wind speeds and greater availability of sand, the latter fluvially reworked from the vast resource of the saprolitic, easily disintegrating sandstones. During present-day sandstorms, only the lower flanks and heads of the sandstone yardangs are being undercut, creating a picture of aeolian corrasion landforms in destruction, whereas in the past inselbergs more than 100 m high were completely streamlined by corrasion. Miniature corrasion features on soft claystones today are at the mm-scale, whereas their older equivalents, only preserved on hard silcrete or iron crusts, are flutes up to several decimeters (dm) long. The latter will also be found on escarpments or basin rims of the region where today there is no more drifting sand. On soft rocks, some corrasion also takes place from monsoonal, south-westerly sand-storms today, and again such sand winds were much stronger in the past and also sculpted silcrete surfaces. As yet, there is no conclusive evidence as to the number of corrasive periods, though from the presence of wind-eroded landslides it can be reasoned that aeolian corrasion post-dates them.

The major and really remarkable aeolian impact on the region has been the almost complete removal, in other parts the complete reshaping, of pre-aeolian landforms to a rock-yardang landscape (of *crêtes et couloirs* of the French literature, e.g. Mainguet 1968). This shows best by comparing, on the satellite image (Fig. 18.1), those parts of the Djado Plateau where the fluvial pattern has been fully preserved, to those on both sides of it where it, and even the escarpment itself, has been almost completely erased. Just as striking is the difference between the dark, almost sand-free parts of the landslide fringe of the Mangueni plateau and the corrasive landforms to the east and west. The pre-aeolian landforms in between were preserved because they lie in the wind-shadow of the Jabal Ati Plateau about 200 km to the north, which was just high enough to split and laterally compress the sand-blasting trade-wind currents to both sides of an elongated triangle.

18.10 Conclusion

Unravelling the landform history of the greater Djado region of the central Sahara (Fig. 18.8), one of the truly hyper-arid regions of the earth, it appears that only the youngest – Quaternary – part of it, possibly not much more than one out of about 60 or more million years of

geomorphic sculpture, has been arid, and even that only in between pluvials, that at worst will have been semi-arid. The wind-abraded parts of the landscape are evidence, though, that there have been times of much more extreme desert conditions – not necessarily drier, but with much stronger and/or more frequent sand storms than today. By comparison to other parts of the desert, it can be summarized that the landform history outlined here is typical of most of at least the central Sahara.

The Author

Detlef Busche is a retired physical geographer of the Department of Geography of the University of Wuerzburg, Germany. In geomorphology, he has mostly worked in the arid regions of Iran, Namibia, the south-western United States and, primarily, in the central Sahara, with emphasis on the Pre-Quaternary and Quaternary landform history of those regions. Much of his Saharan research has been compiled from numerous papers in *Die zentrale Sahara* (1998); his general approach to geomorphology may be found in the pictorial geomorphology book by Busche, Kempf and Stengel (2005) *Landschaftsformen der Erde. Bildatlas der Geomorphologie*. Detlef Busche is one of the editors of *Zeitschrift für Geomorphologie* and is or was on the editorial board of several other journals.

References

Baumhauer R, Brauneck B, Sponholz B, Schulz E, Faran Maiga O, Sani I, Pomel S (2009) Holocene palaeoenvironmental changes in the central Sahara inferred from the Seggedim scarpfoot depression (NE Niger). Palaeoecology of Africa 29 (in press)

Bremer H (1980) Landform development in the humid tropics. German geomorphological research. Z Geomorph NF, Suppl 36:162–175

Büdel J (1982) Climatic geomorphology. Princeton University Press, Princeton, NJ

Busche D (1976) Pediments and Climate. Palaeoecology of Africa 9:20–24

Busche D (1983) Silcrete in der zentralen Sahara (Murzuk-Becken, Djado-Plateau und Kaouar; Süd-Libyen und Nord-Niger). Z Geomorph NF, Suppl 48:35–49

Busche D (1998) Die zentrale Sahara: Oberflächenformen im Wandel. Justus-Perthes-Verlag, Gotha, Germany

Busche D (2001) Early Quaternary landslides of the Sahara and their significance for geomorphic and climatic history. J Arid Environ 49:429–448

Busche D, Erbe W (1987) Silicate karst landforms of the southern Sahara (northeastern Niger and southern Libya). Z Geomorph NF, Suppl 64:55–72

Busche D, Sponholz B (1992) Morphological and micromorphological aspects of the sandstone karst of eastern Niger. Z Geomorph NF, Suppl 85:1–18

Busche D, Stengel I (1993) Rezente und vorzeitliche äolische Abtragung in der Sahara von Ostniger. Petermanns Geogr Mitt 137:195–218

Busche D, Kempf J, Stengel I (2005) Landschaftsformen der Erde. Bildatlas der Geomorphologie. Primus Verag, Darmstadt, Germany

Faure H (1966) Reconnaissance géologique des formations sédimentaires post-palaeozoiques du Niger oriental. Mém BRGM 47

Greigert J, Pougnet R (1967) Essai de désription des formations géologiques de la République du Niger. Mém BRGM 48

Grunert J, Busche D (1980) Large-scale fossil landslides at the Msak Mallat and Hamdat Manghini escarpment. In: Salem JM, Busrewil MT (eds) Geology of Libya, 2nd symposium on the geology of Libya, Tripoli, 1978, vol III. Academic, London, pp 849–860

Klitzsch E, Baird DW (1969) Stratigraphy and palaeohydrology of the Germa (Jarma) area, southwestern Libya. In: Kanes WH (ed) Geology, archaeology and prehistory of the southwestern Fezzan, Libya. Petroleum Exploration Society of Libya, 11th Annual Field Conference, pp 67–82

Mainguet M (1968) Le Borkou: aspects d'un modelé éolien. Ann Géogr 77:296–322

Meckelein W (1959) Forschungen in der zentralen Sahara. I: Klimamorphologie. Westermann, Braunschweig, Germany

Rognon P (1967) Le massif de l'Atakor et ses bordures (Sahara central). Centre de Recherches sur les Zones Arides, sér. géol., CNRS, Paris

Wopfner H (1978) Silcretes of northern South Australia and adjacent regions. In: Langford Smith T (ed) Silcrete in Australia. Department of Geography, University of New England, Armidale, Australia, pp 93–142

Chapter 19
Afar Triangle: Rift Valleys and Volcanoes over Plate Divergence

Tony Waltham

Abstract The barren deserts of the Afar Triangle constitute a basaltic ocean-floor terrain on a divergent plate boundary that is above sea level because it lies over a hot spot. Grabens and rift valleys including the Danakil Depression exhibit active normal faulting. Active dyke emplacement is indicated by heat loss from the Erta Ale lava lake. Both these processes accommodate the crustal extension, and excess magma input creates scattered volcanic eruptions.

Keywords Danakil • dyke • extension • graben • rift • volcano

19.1 Introduction

The Afar Triangle is a barren lowland bounded by the Red Sea and the two blocks of Ethiopian Highlands (themselves separated by the Rift Valley). Riven by the desert furnace, that is, the Danakil Depression, its terrain is a casebook of tectonic geomorphology. Plate divergence is at its most obvious where the Red Sea has opened, and is still opening, between the Arabian and African plates. The African plate is breaking apart along the well-known East African Rifts, separating the Somalian plate from the main continental block (often known as the Nubian plate in the north).

These three divergent boundaries have a triple junction at the Afar. The Triangle is the one place where the coastlines and plateau margins cannot be fitted neatly back into their pre-divergent entity – because the locally excessive constructive process of basalt generation has created anew the youthful lowland that is the Afar.

19.2 Afar Terrain

'Hostile environment' is a term tailor-made for the awful, hot, barren desert of the Afar (Fig. 19.1). Just one river enters it, and none leaves it. A few salt lakes contain almost the only water not yet lost to solar evaporation. Daily temperatures are 30–40°C in the cool of winter; summer regularly sees shade temperatures of 50°C on the floor of the Danakil Depression – and there is no shade. The permanent inhabitants of the desert are the various Afar tribes, renowned for their fierce and justifiable protection of scant water resources. They range across land that is now divided between Ethiopia, Eritrea and Djibouti, and are joined by migrants and refugees who gather to work in very hard conditions extracting the salt from the Danakil floor. The Afar's desert environment may be truly hostile, but its minimal weathering and negligible vegetation mean that the geology and geomorphology are beautifully clear to see (Waltham 2005).

The dominant rocks within the Triangle are flood basalts. Most of these formed within the depression, after the first rift had been lowered between the marginal faults; the oldest of these overlie red beds and date from about 24 million years ago. Locally, these lavas have a total thickness of 4,000 m. Volcanism is still active, and the more recent lavas form shield volcanoes in the northern Afar. Subsiding rifts have filled with basin sediments that are contemporary with the volcanics; these consist mainly of fine clastic sediments and evaporite sequences inter-bedded and surrounded by marginal wedges of scree. Both west and south of the Afar, the Ethiopian Highlands, with a mean altitude of 3,000 m, have cores of Precambrian metamorphics and granites, much of them capped by sandstones, limestones or alkaline basalts. East of the Afar, the Danakil micro-plate is a

P. Migoń (ed.), *Geomorphological Landscapes of the World*,
DOI 10.1007/978-90-481-3055-9_19,

Fig. 19.1 Bare rock, long fault scarps and sediment basins characterise the Afar desert, with a few acacia trees providing the only signs of life in a harsh environment (Photo T. Waltham)

fragment of continental crust, isolated within the oceanic rift zone that locally braids to underlie both the Red Sea and the Danakil Depression (Fig. 19.2). Its basement rocks form the Danakil Alps, whose peaks catch rainfall from the east to support ragged forests – and shelter the Danakil Desert in a deep rain shadow.

The largest single feature of the Afar is the Danakil Depression, which descends to 126 m below sea level over the line of current plate divergence, and would be larger except that half its floor is occupied by shield volcanoes. It is a classic rift valley, but both its margins are formed by wide zones of normal faults that are eroded into massive mountain slopes and lack dramatic individual scarps. South of the Depression, the rift breaks into many smaller rifts that indicate the complexity of the plate deformation when viewed in detail.

19.3 Rift Valleys of Djibouti

The dominant landforms of the Djibouti sector are four great rift valleys that parallel the Afar axis and are the most dramatic consequence of its extension tectonics (Fig. 19.3). Their marginal faults create spectacular scarps that have degraded to stable profiles while building their ramparts of scree. Subsidiary scarps along some parts show rotational movement of down-faulted wedges over curved fault planes. Their rims are little eroded, but their floors are covered by playa silts and salt pans. These are true rift valleys, nearly as deep and as steep as the graben structures that define them.

Deepest and most active of the rift valleys is that containing Lake Asal and the marine bay of Ghoubet. It is nearly 70 km long and 15–20 km wide, with cliffs rising 600 m along its southern fault boundary. The sea in Ghoubet is over 200 m deep, and the surface of Lake Asal fluctuates at around 155 m below sea level. Lake Asal lies over sediments up to 200 m deep, has thick beds of late Holocene gypsum exposed around its shores, and there is salt precipitation on its marginal flats, as its main recharge is by seawater infiltration through the porous basalts. The rift valley around Asal would be occupied by the sea, were it not for Ardoukoba, a zone of young volcanic rocks draped over minor fault blocks that stand inside the rift. These include the basalt lavas extruded in 1978 from numerous fissures and vents (Fig. 19.4), along with scattered hornitos and a large spatter ring that grew in the brief climax of that eruption.

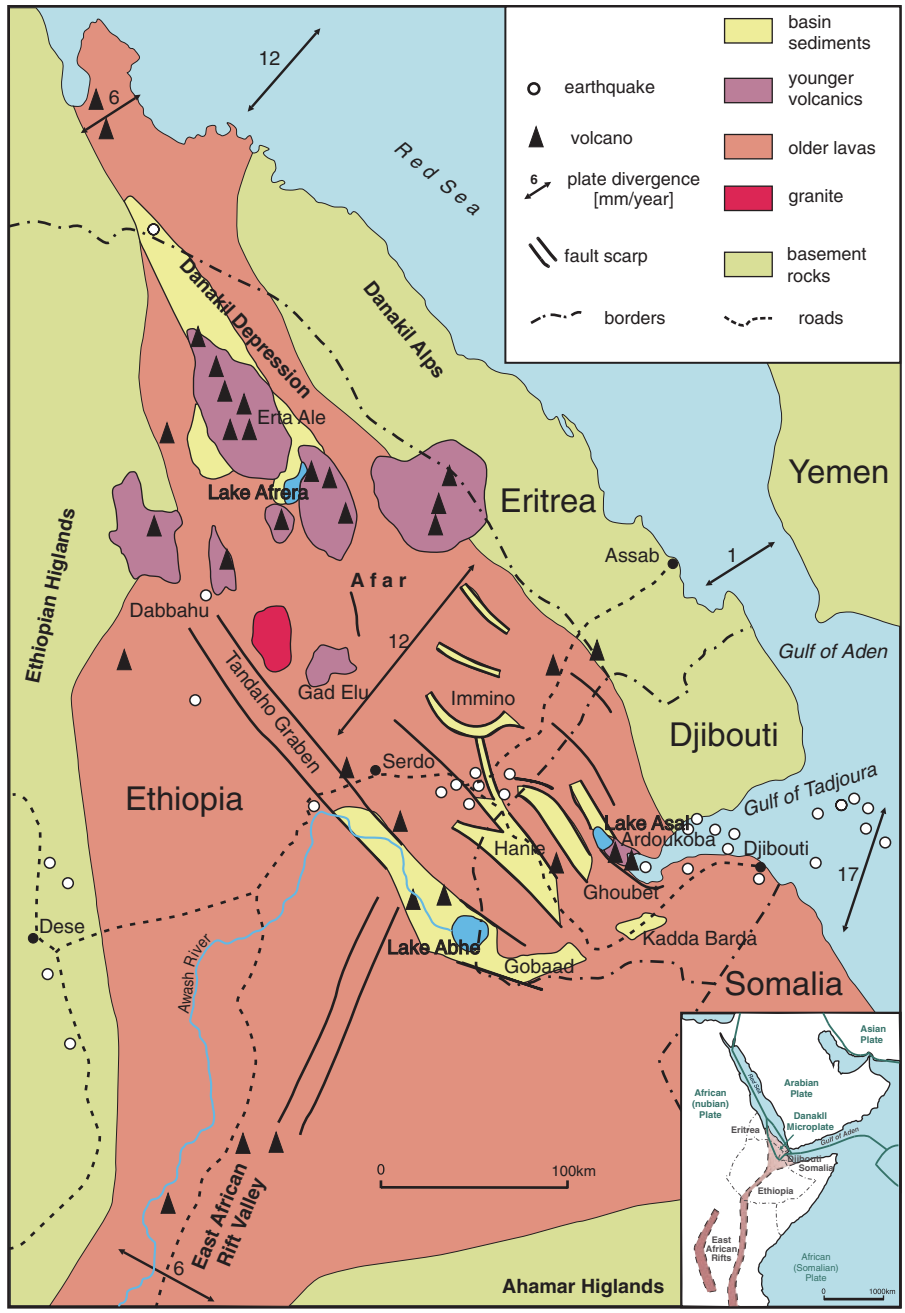

Fig. 19.2 Outline map of the Afar Triangle, with the main features of its geology and geomorphology. The basement massifs consist of older rocks with or without a variable cover of Tertiary basalts

The most southerly rift valley houses Lake Abhe on the Ethiopia–Djibouti border. It has been largely filled by sediments carried in by the River Awash, so that the lake lies more than 200 m above sea level and is now only 15 m deep. The site is best known for its hundreds of splendid travertine towers. Each tower was formed where a carbonate-saturated, geothermal spring emerged in the contemporary lake floor and deposited the calcite due to reaction with lake water. The towers are spread over an area of about 2,000 × 500 m, and individual towers are up to 60 m tall, some with steaming vents high on their sides; lake levels were last at their crests about 1,000 years ago.

Fig. 19.3 The Dobi, a northern branch of the Hanle valley that reaches into Ethiopia, a splendid rift valley with degraded marginal fault scarps on each side of a basin of sediments that sits on the graben floor (Photo T. Waltham)

Fig. 19.4 Basalts that were formed in the Ardoukoba event of 1978, in the Asal-Ghoubet rift valley. A short-lived fissure eruption produced lavas at various points along a fault line opened in tension, and a hornito on the ridge marks the line of a second, parallel fissure (Photo T. Waltham)

The distribution of earthquakes over the last 50 years falls into distinct zones that indicate the currently active areas of faulting within the Afar (only major epicentres are marked on Fig. 19.2). The main seismic zone passes westwards along the Gulf of Tadjoura, then curves northward through the Djibouti grabens to merge with a zone along the western margin of the Danakil Depression which acts as a single large graben.

19.4 Danakil Depression

At the northern end of the Afar Triangle, the Danakil Depression is a massive rift valley between the fault scarps of the Ethiopian Highlands and the Danakil Alps. It is also a true rift valley, created by a graben with down-faulted bedrock. Cut off from the sea since the Pleistocene, it has lost its water to desert evaporation

and is dry down to Lake Dalol, 126 m below sea level. Lake Afrera is a second salt lake, with its surface at −118 m. Between the two lakes, the multiple shield volcano of Erta Ale occupies much of the depression floor.

Away from the lava flows, the Danakil is floored by playa flats of silts and evaporites. Littoral and reef marine limestones of mid-Pleistocene age (200–80 ka)[1] survive in places around the margins of the Depression, remnants of its occupation by an arm of the Red Sea until 65,000 years ago. Reefs now lie at altitudes of −30 to +90 m, with individual shoreline beds changing levels by tens of metres, indicating the complex and locally variable rates of subsidence within the graben. Evaporites are over 1,000 m thick beneath the floor of the Dalol basin, and date from the same period before the Danakil Gulf was finally isolated from the Red Sea.

The surrounds of Lake Dalol are noted for their hot mineral springs and fumaroles that have created crystal pools, micro-terraces, miniature hornitos and colourful structures in sulphur, halite and other minerals. Afrera is a less spectacular lake, but is also fed by geothermal springs, and its brines are now exploited by extensive salt pans, where precipitation is very rapid in the hot dry desert.

19.5 Volcanoes of Danakil

Of the 34 volcanoes listed within the Afar Triangle, five have recorded activity within historical time. The largest and most frequently eruptive is Erta Ale, rising from the floor of the Ethiopian sector of the Danakil Depression. It is a classic shield volcano with gentle slopes of basaltic pahoehoe and aa lavas, numerous small hornitos and almost no tephra. It is markedly elliptical in shape, because both the central vents and the main parasitic vents lie over a major fissure zone along the axis of the Danakil. Its perimeter is more than 100 m below sea level within the depression, and its summit rises to 613 m above sea level (Barberi and Varet 1970; Yirgu et al. 2006).

The crest of Erta Ale is marked by an elliptical caldera 1,700 m long and 600 m wide, inclined to the south and with marginal walls about 20 m high except at its two ends. A large northern crater and a smaller central crater, both lie within the caldera. Recent extrusions of basalt have emerged from both craters and from fissures on the caldera margin faults. Consequently, the entire caldera floor is formed of fresh pahoehoe. Most of this dates from 1974, though there have been minor vent overflows since 1997.

Many years ago, the northern crater of Erta Ale was the dominant vent, containing a lava lake that was variably 100–300 m across. At times the lake surface was 150 m below the rim, but at other times it overflowed, until it cooled enough to crust over and become inactive, probably early in 1975. Soon afterwards, it suffered a major drain-back of magma; this left a deep crater that has since been partially refilled with collapsed wall debris and some fresh lava, including a very large central hornito. It is still unstable, with a number of pit craters and highly productive sulphurous fissure fumaroles around its rim.

Erta Ale is unique in that it has contained lava lakes that, between them, have been persistently active for at least 100 years (Fig. 19.5). The currently active lake lies within the central vent, which is a spectacular pit crater, developed by collapse when magma pressure declined beneath it. Only 60 m across when first recorded in 1968, it is now 150 m across, and about 80 m deep. A lava lake normally covers all or part of its floor, and has periodically overflowed. The lava has a temperature of about 1,200°C, while the rafts of chilled crust that cover most of its lake surface are at about 500°C.

Dabbahu is a small stratovolcano closer to the western margin of the Danakil. A Plinian eruption in September 2005 lasted over 3 days, when a fissure vent along its northern flank produced silicic ashfall and a small pumice dome. This localised explosive activity appears to have been a consequence of rising basaltic magma encountering a small silicic reservoir at shallow depth.

19.6 Evolution

Current rates of relative movement of the plates that are diverging beneath the Afar have now been determined by satellite radar interferometry of the ground surface distortion (Fig. 19.2). They match well earlier data from repeated geodetic surveys and also geological

[1]ka stands for 1,000 years

Fig. 19.5 The lava lake in the central crater of Erta Ale, when it was reduced to about 30 m in diameter during a period of low heat flow in the early 2000s (Photo T. Waltham)

evidence based on accurate dating over the last few million years. Total divergence of the Arabian plate from the African plates is 17–19 mm/year, but only about 12–13 mm/year are represented by expansion within the Afar, west of the Danakil micro-plate. The plate divergence is largely accommodated by dyke emplacement and normal faulting, while magmatic inflation, distributed ground extension, fissure opening and earthquake activity add to the extensional processes that are all so well-demonstrated in the Afar (Fig. 19.6).

Normal faulting is the second major component of crustal expansion, and its activity in the Afar is indicated both by seismic events and by the presence of the great rift valleys formed along actively subsiding grabens. There is now a wealth of data on tectonic extension and graben subsidence across the normal faults of the Asal-Ghoubet rift valley (Abdallah et al. 1979; Ruegg et al. 1979; Vigny et al. 2007; Doubre and Peltzer 2007). Graben subsidence has the floor of the rift valley subsiding relative to the adjacent highlands at a rate currently around 7 mm/year. This is distributed across a number of faults within the overall graben structure. At outcrop, each of these faults is steeply inclined, but relationships between the horizontal and vertical components of displacement indicate that the faults curve to dips of 45° or less at depth.

Long-term creep and subsidence of the grabens is interrupted by intervals of more rapid movement. The 1978 event at Asal saw 2 m of ground extension that was accommodated by the brief volcanic eruptions, by dyke emplacement at depth and by around 1 m of graben subsidence. Surface expression of that fault movement is still visible along the eastern margin of the graben where screes resting on the rift valley floor subsided to expose a fresh band of their headwall fault scarp (Fig. 19.7). The 2005 event at Dabbahu was dominated by dyke emplacement, but produced nearly 2 m of subsidence within the narrow central rift across the volcano. Lacking comparable shock movements, the area around Lake Dalol recorded 40 mm/year of subsidence through the mid-1990s (Amelung et al. 2000).

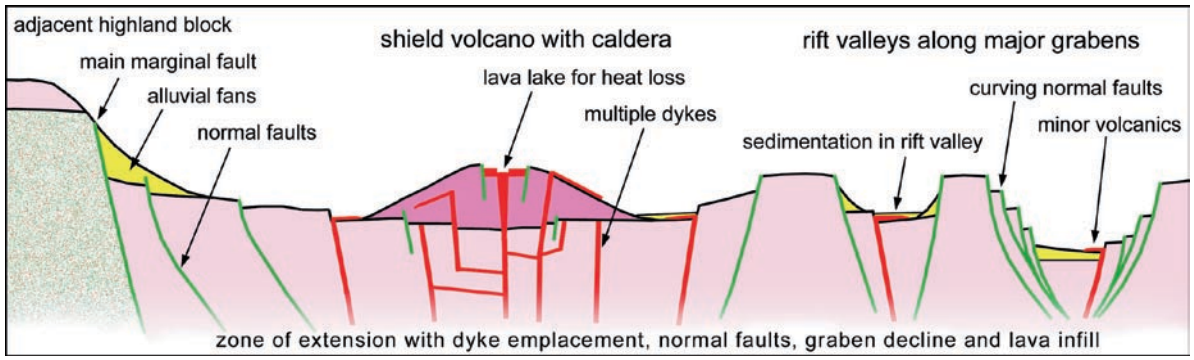

Fig. 19.6 Diagrammatic and greatly simplified profile to show the main features of ground extension in the Afar, incorporating features of both the Erta Ale volcano in the Danakil Depression and the main grabens in the Djibouti sector

Fig. 19.7 A minor fault inside a graben has created a slice of fresh fault scarp along the crest of screes that subsided on the down-faulted block, within the Asal-Ghoubet rift valley (Photo T. Waltham)

All these patterns of graben subsidence due to ground extension are superimposed on a broader profile of uplift due to magmatic inflation. Centred on the Asal rift valley, an elongate dome 40 km wide is currently rising at about 8 mm/year, slightly faster than the graben is subsiding within it. Further north, beneath the Danakil Depression, a higher rate of magma injection diminishes the graben activity and increases the volcanic activity. The continuing survival of Erta Ale's lava lake relies on a substantial heat supply to match its thermal loss into the atmosphere (Oppenheimer and Francis 1998). This heat supply is from rising magma that is feeding a zone of active emplacement of dykes and sills. Within the immediate vicinity of the volcano, these intrusions currently fill new fissures to keep pace with the plate divergence, so that they largely prevent further fault-related subsidence in the Erta Ale sector of the main graben.

A more detailed record of dyke emplacement has been obtained from modelling the 2005 event at the Dabbahu volcano with data gathered from radar interferometry and seismic records (Wright et al. 2006). This suggests that about 2.5 km^3 of basaltic magma was injected into a dyke that developed over a length of 60 km; it had a mean width of 3.5 m to match the crustal opening. While the dyke reached a depth of about 7 km, none of its basaltic magma reached the surface. This contrasts the 1978 Ardoukoba event where lava did emerge from short lengths of open fissure, even though the ground extension and mean dyke width were nearer 2 m. It appears that about one-fifth of the Dabbahu dyke material was derived from magma chambers beneath the Dabbahu and Gabho volcanic edifices, as indicated by broad areas of contemporary ground subsidence; the other 2 km^3 was primary magma that rose from greater depths. This dyke emplacement all occurred within about 1 week.

A longer record of ground movement is provided by the fragmented horsts that now lie between the grabens of inland Djibouti. Rotation of the Danakil microplate has dragged their northern ends eastwards, while their southern ends have been held firm against the Somalian plate, to create a pattern of 'bookshelf faulting', where the sub-parallel blocks have each rotated clockwise (Tapponier et al. 1990). Palaeomagnetic orientations of the Pleistocene lavas have shown that adjacent blocks have rotated by different amounts (up to 11° in 1.8 million years), with the slack taken by differential opening of the intervening grabens (Acton et al. 2000). Deconstruction of the graben movements indicates an unbroken tectonic unit at the start of the Pleistocene. Movements have evolved over time, and the most active zone was originally the Lake Abhe graben, but is now the Asal-Ghoubet graben.

19.7 Conclusions

Though the Afar is a segment of crust that has subsided between the diverging plates of Africa and Arabia, it is essentially an ocean-floor environment that is rising due to magmatic inflation over a mantle plume. Continuing extension is accommodated by dyke emplacement and normal faulting. While dyking is dominant at depth, curved fault planes account for most of the movement at and near the ground surface. The landscape is therefore dominated by series of conspicuous and active fault scarps except where greater rates of magma injection create active volcanic edifices. The combination of well-developed rift valleys and fresh volcanic features makes the Afar the world's finest example of a landscape developed over a zone of crustal extension.

The Author

Dr **Tony Waltham** recently retired from many years as a university lecturer in engineering geology in Nottingham, UK. His main research interest was in karst and specifically in engineering problems of construction on cavernous ground. Author of the popular textbook *Foundations of Engineering Geology*, and of many other books, he has travelled widely, mainly to areas with great caves or active volcanoes.

References

Abdallah A, Courtillot V, Kasser M, le Dain A, Lépine JC, Robineau B, Ruegg JC, Tapponnier P, Tarantola A (1979) Relevance of Afar seismicity and volcanism to the mechanics of accreting plate boundaries. Nature 282:17–23

Acton GD, Tessama A, Jackson M, Bilham R (2000) The tectonic and geomagnetic significance of paleomagnetic observations from volcanic rocks from central Afar, Africa. Earth Planet Sci Lett 180:225–241

Amelung F, Oppenheimer C, Segall P, Zebker H (2000) Ground deformation near Gada Ale volcano, Afar, observed by radar interferometry. Geophys Res Lett 27:3093–3096

Barberi F, Varet J (1970) The Erte Ale volcanic range. Bull Volcanol 34:848–917

Doubre C, Peltzer G (2007) Fluid-controlled faulting process in the Asal Rift, Djibouti, from 8-year radar interferometry observations. Geology 35:69–72

Oppenheimer C, Francis P (1998) Implications of longeval lava lakes for geomorphological and plutonic processes at Erte Ale volcano, Afar. J Volcanol Geotherm Res 80:101–111

Ruegg JC, Lépine JC, Tarantola A, Kasser M (1979) Geodetic measurements of rifting associated with a seismovolcanic crisis in Afar. Geophys Res Lett 6:817–820

Tapponier P, Armijo R, Manighetti I, Coutrillot V (1990) Bookshelf faulting and horizontal block rotations between overlapping rifts in southern Afar. Geophys Res Lett 17:1–4

Vigny C, de Chabalier J, Ruegg JC, Huchon P, Feig KL, Cattin R, Asfaw L, Kanbari K (2007) 25 years of geodetic measurements along the Tadjoura-Asal rift system, Djibouti, East Africa. J Geophys Res 112:B06410. doi:10.1029/2004JB003230

Waltham T (2005) Extension tectonics in the Afar Triangle. Geol Today 21:101–107

Wright TJ, Ebinger CJ, Biggs J, Ayele A, Yirgu G, Keer D, Stork A (2006) Magma-maintained rift segmentation at continental rupture in the 2005 Afar dyking episode. Nature 442:291–294

Yirgu G, Ebinger CJ, Maguire PKH (eds) (2006) The Afar Volcanic Province within the East African Rift System. Geol Soc Lond Spec Publ 259

Chapter 20
Dolomites: The Spectacular Landscape of the 'Pale Mountains'

Mauro Soldati

Abstract The geomorphological features of the Italian Dolomites are shown, with special emphasis on the aspects that make this mountain region unique from both the scenic and scientific viewpoint. The Dolomites are characterised by outstanding light-coloured dolomite cliffs, shaped in the form of platforms, towers, peaks and pinnacles, which overlie gentle slopes made up of dark clayey and volcanoclastic rocks. The geological factors which have influenced the origin of a wide variety of landforms, in terms of rock and tectonic control, and the geomorphological processes which have acted during the Quaternary, are discussed. Furthermore, the most significant structural, glacial, periglacial, karst and gravity-induced landforms of the Dolomites are presented, making it clear that this region can be considered a geoheritage open-air laboratory.

Keywords Dolomites • geoheritage • Italy • mountain geomorphology

20.1 Introduction

The superb landscape of the Dolomites is the result of geomorphological processes acting in a geological context that is certainly unusual when compared with the rest of the Alps and many other mountain chains of the world. The main distinguishing geological feature is given by the presence of rocks with very different geomechanical behaviour. As a result, spectacular light-coloured dolomite cliffs ('Pale Mountains', as they used to be called), shaped as platforms, towers, peaks and pinnacles, stand above gentle slopes often made up of dark clayey and volcanoclastic rocks, offering a unique landscape to the visitors. The spatial distribution of rocks with different erodibility, the intense tectonic fracturing, as well as the complex Quaternary evolution characterised by a series of glaciations, have determined a variety of landforms, which makes the Dolomites a unique place in the world, from both the scientific and aesthetic viewpoint.

The Dolomites are named after Déodat de Dolomieu (1750–1801), a French nobleman and scientist who found, during his travel to Rome in 1789, a 'strange calcareous stone horizontally stratified' in the Isarco Valley that did not react with acids. Chemical tests, carried out on his request by Nicolas de Saussure, showed that the rock was made of a yet unknown mineral, the calcium magnesium carbonate, which was then named after de Dolomieu. Since then the term 'dolomite' has been attributed to the mineral/rock itself, as well as to the entire region of Italy where its outcrops are so peculiar. Relevant scientific observations were carried out by outstanding cultural figures of the nineteenth century, such as Leopold von Buch and his scholar Alexander von Humboldt, who also paid attention to the beauty of the landscape. Because of the latter, not only scientists but even artists, writers and poets, especially from England and Germany, were attracted by the Dolomites. Among others, during their travels to Italy to visit places of classical and Renaissance heritage, Albrecht Dürer (in 1494) and Johan Wolfgang von Goethe (in 1786) experienced the fascinating Dolomite landscapes and left paintings and writings related to them.

20.2 Geographical Setting

The Dolomites are located in northern Italy, in the south-eastern sector of the Alpine chain (barycentre

P. Migoń (ed.), *Geomorphological Landscapes of the World*,
DOI 10.1007/978-90-481-3055-9_20,

latitude of 46°25'N and longitude 12°00'E). They lie in the regions of Trentino Alto Adige, Veneto and Friuli Venezia Giulia and occupy an area of over 9,000 km^2. Conventionally they are bounded by the Pusteria valley (to the north), the Piave valley (to the east), the Sugana Valley (to the south) and by the Isarco and Adige valleys (to the west). Nevertheless, dolomite mountain groups can be found outside this territory (e.g. Dolomiti di Brenta, west of the River Adige). The main mountain groups are Croda Rossa (3,139 m), Tofàne (3,243 m), Cristallo (3,216 m), Antelào-Sorapìs (3,263–3,205 m), Catinaccio (3,004 m), Sassolungo (3,181 m), Sella (3,151 m), Marmolada (3,342 m) – this being the highest, Civetta (3,218 m) and Pale di San Martino (3,193 m).

From the climatic standpoint the Dolomites are quite varied owing to their wide altitude range (1,200–3,200 m a.s.l.). The area has an Alpine climate, characterised by cold winters and mild summers. Precipitation patterns are typical of the Alpine climate, too: late springtime and summer are the rainiest periods, with a peak in July. A secondary precipitation maximum occurs in November, following the prolonged autumn rains. Permanent snowfall in the valley bottom normally begins in December and lasts until April. On the highest peaks this period usually lasts a couple of months longer. The average snow thickness is 50–100 cm. The annual average temperature is around 6°C. In summer, temperature ranges from more than 25°C during the day to 7°C during the night.

20.3 Geological Features

From the geological viewpoint, the Dolomites belong to the Southern Alps, a segment of the African continental margin. The stratigraphic sequence thus consists of a Permo-Mesozoic sedimentary succession, unconformably covering a Hercynian crystalline basement (Fig. 20.1) (Bosellini 1996; Bosellini et al. 2003). The outcropping rocks are mainly of sedimentary origin and were deposited in a warm tropical sea during the middle Triassic (e.g. Sciliar Dolomite) and in a vast tidal flat during the late Triassic (e.g. Dolomia Principale/*Hauptdolomit*). During the middle Triassic (Ladinian) the region experienced intense volcanic activity that enabled huge masses of lava to flow into the sea, partly filling the deep-water basins separating the reefs. In the late Triassic (Norian), the most famous and spectacular geological formation of the Dolomites

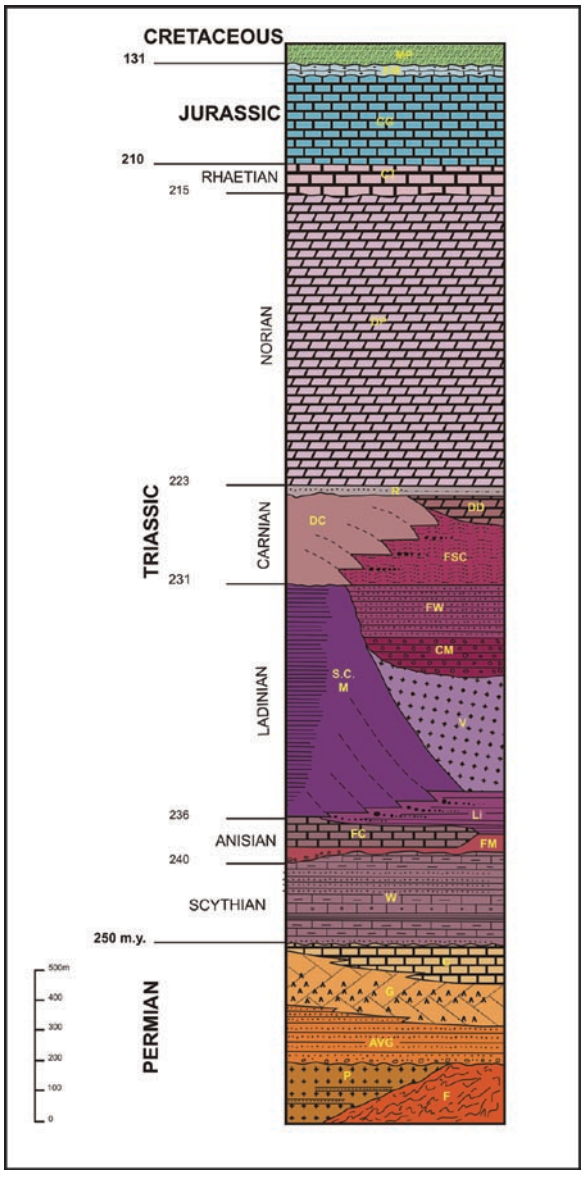

Fig. 20.1 Stratigraphic sequence of the Dolomites. Explanation: F, Crystalline Basement; P, volcanic rocks ('porphyries'); AVG, Arenarie di Val Gardena; g + c, Bellerophon Formation; W, Werfen Formation; FM, Moena Formation; FC, Contrin Formation; Li, Livinallongo Formation; V, volcanic rocks; M, Marmolada Limestone; SC, Sciliar Dolomite; CM, Marmolada Conglomerate; FW, Wengen Formation; FSC, S. Cassiano Formation; DC, Dolomia Cassiana; DD, Dürrenstein Dolomite; R, Raibl Formation; DP, Dolomia Principale; CT, Dachstein Limestone; CG, Calcari Grigi; AM, Ammonitico Rosso; MP, Puez Marls (After Panizza and Spampani 1988, modified)

was formed, the Dolomia Principale, that consists of white and light grey cyclic dolomites (up to 1,000 m thick) containing stromatolithes and fossils, such as the well known *Megalodon sp*. The famous mountains surrounding Cortina d'Ampezzo (e.g. Tofàne, Cristallo, Cinque Torri) and the Badia valley (e.g. upper part of Sella Group, Cunturines), the Tre Cime di Lavaredo and the lower part of Pelmo and Civetta near Alleghe are all made up of Dolomia Principale. At the very end of the Triassic (Rethian) and during the Jurassic and early Cretaceous, the sea became deeper and well-stratified calcareous rocks were formed, which make up the youngest marine sediments, locally outcropping in the region above the dolomites.

In the late Cretaceous, following the collision between the African and European plates, the mountain building started; it continued throughout the Cainozoic and is still ongoing (Doglioni 1987). The succession was intensely deformed, faulted and uplifted in the frame of two main Alpine tectonic phases: the mesoalpine phase during the Eocene-Oligocene, when the Dolomites were still below the sea level, and the neoalpine phase which showed the maximum intensity in the late Miocene. The effects of mountain-building process on the Dolomites were not the same everywhere, though. In fact, the Western Dolomites, due to the underlying thick and rigid Permian volcanic rocks, were uplifted as a quite undeformed block. The Eastern Dolomites instead, not underlain by similar rigid bedrock, were intensely compressed and folded. This has certainly played an important role in the Quaternary evolution of the region.

20.4 Landforms

The morphological features presently observed in the Dolomite landscape are the result of the geomorphological processes that acted during the Quaternary, particularly since the Last Glacial Maximum (LGM). However, it is now clear that the complex geological history of the region cannot be ignored if one intends to understand how landforms were modelled. The effects of Pleistocene glaciations (at least four major ones) have also to be taken into account, as well as the climate changes occurring during the Holocene. Varied morphostructural and morphoclimatic conditions in space and time have determined a significant variety of landforms (Carton and Soldati 1993; Gianolla et al. 2008) that are described below with reference to the relevant morphogenetic factors (Fig. 20.2).

20.4.1 Structural Landforms

The structural control on landform development, in terms of outcropping rock types and effects of tectonics, has been particularly high in the Dolomites. Folding, faulting and overthrusting of thick piles of sediments are clearly legible in the landscape. Tectonic discontinuities have often determined the direction of valleys, as in the case of the Funès, Tires and Marebbe valleys, and saddles as in the case of Falzarego Pass. Furthermore, the varied sedimentation (in space and time) together with the recurrent magmatic activity led to the presence of vertical and lateral contact between rocks showing different mechanical behaviour, which has controlled landscape evolution in terms of selective erosion. Morphoselective features can be observed where Ladinian carbonate formations are cut through by volcanic dykes (e.g. Latemar Group). Another typical example is given by the 'cengia', a lower inclined belt of pelitic rocks (generally covered by scree) that is typical where the Raibl Formation is interposed between Dolomia Cassiana and Dolomia Principale, like at the Sella Group (Fig. 20.3). However, all over the Dolomites strong morphological contrasts can be observed on slopes where dolomite rocks overlie more erodible clastic formations. This is the case of the steep-sided groups of Tofàne, Cristallo, Sorapìs and Antelào at Cortina d'Ampezzo. Also the location of some saddles is linked to the presence of more erodible rocks, like at Gardena, Sella, Pordoi and Campolongo passes, which are shaped on rocks that are clearly weaker than the surrounding dolomites. Furthermore, also where the effects of tectonics were more intense, morphoselective processes have been favoured leading to the origin of the spectacular peaks, towers and crests for which the Dolomites are undoubtedly well known (Fig. 20.3).

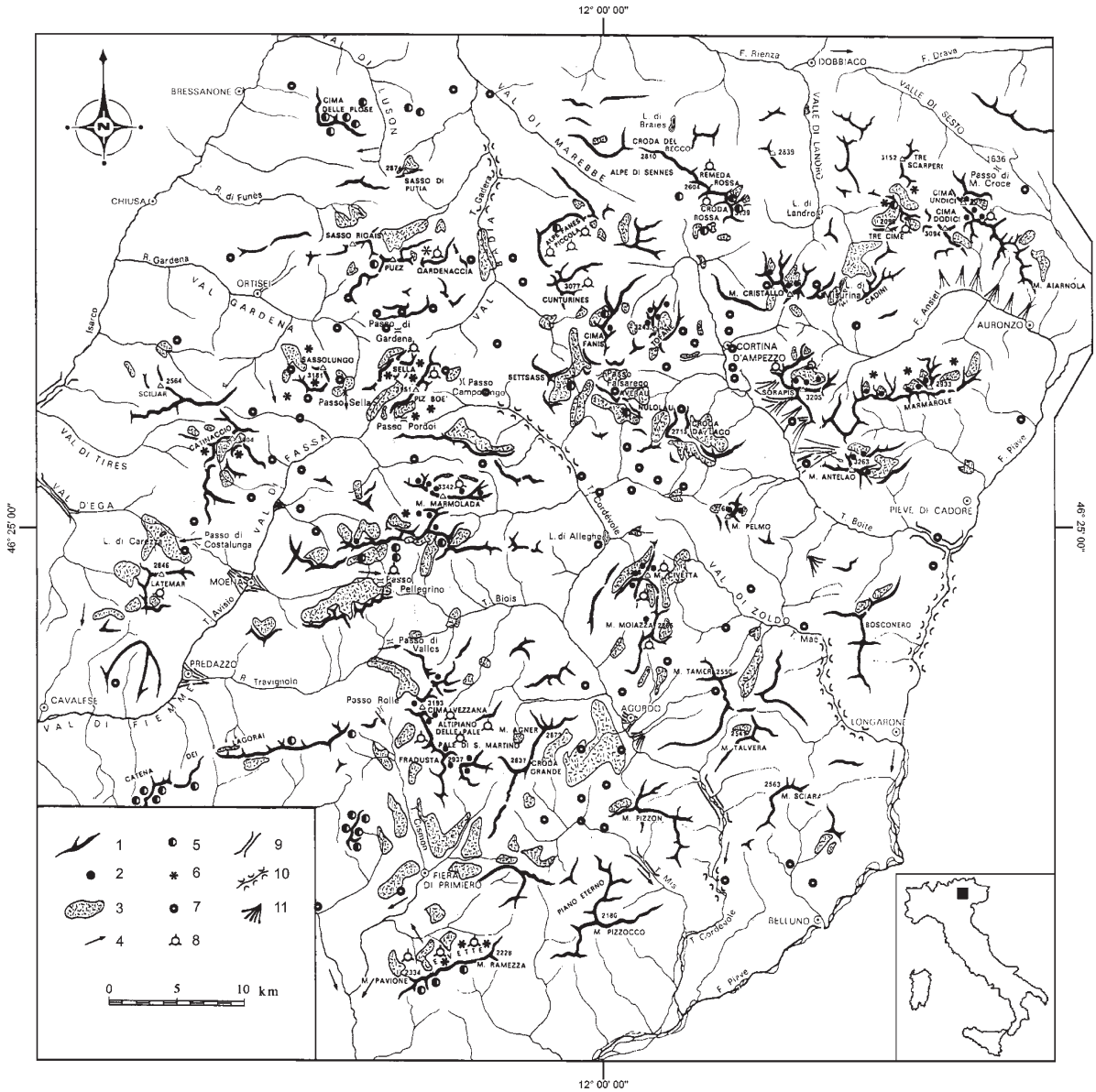

Fig. 20.2 Geomorphological schematic map of the Dolomites. Explanation: 1 – mountain crests, 2 – glaciers, 3 – main areas of glacial deposition, 4 – movement direction of Pleistocene glaciers, 5 – relict rock glaciers, 6 – significant cryonival landforms (e.g. protalus ramparts, patterned grounds), 7 – main landslides, 8 – areas intensely affected by karst processes, 9 – troughs, 10 – deeply eroded fluvial valleys, 11 – talus cones and alluvial fans (After Carton and Soldati 1993, modified)

20.4.2 Glacial Landforms

During the Pleistocene, glaciers repeatedly occupied valleys of the Dolomites and left evident traces of their presence (Fig. 20.4). However, at present there is no clear evidence of glacial landforms older than from the last glaciation and datable with certainty. The oldest observed glacial landforms are almost exclusively attributed to LGM. During this period, ice masses reached considerable thickness (up to 1,500 m) in all the Dolomite valleys with only the highest peaks and plateaux remaining uncovered. Ice masses flowed over the present Dolomite passes, which became transfluence saddles, the highest of which are Sella (2,244 m),

Fig. 20.3 The Val di Mesdì ('Midday Valley'), a deep incision in the dolomites of the Sella Group (Alta Badia Valley) in correspondence of a N–S normal fault. The down-cutting of the valley took place along the more jointed, and thus more erodible, portion of the mountain group. A typical 'cengia' made up of debris cones is clearly seen (Photo M. Soldati)

Pordoi (2,239 m), Gardena (2,121 m) and Falzarego passes (2,105 m). The most evident traces left by glacial morphogenesis can be attributed to the subsequent melting phases, which occurred intermittently and discontinuously as already outlined by Brückner (1909). Glacier retreat exposed various erosional landforms, such as cirques, steps, hanging valleys and U-shaped valleys, whose degree of conservation is mainly related to bedrock erodibility. Glacial cirques are scattered almost everywhere, especially near the valley heads. The cirques vary from semi-circular to elongated shapes and are either isolated, arranged in groups or in a step-like morphology. The flanked glacier cirques present in the Marmarole Group, as well as the isolated Croda Rossa cirque are worthy of note for their spectacular shape. Glacial deposits from the retreat phases of the LGM are quite frequent in the Dolomites (Castiglioni 1964). They can be found mainly in sequences of frontal ridges. They normally present a rounded and not very prominent topographic profile, especially in comparison with the moraines deposited during the Little Ice Age. Stadial moraines enclose the lakes of Misurina (Cristallo Group), Carezza (Latemar Group) and San Pellegrino.

Landforms related to recent or present-day glacier activity occur too, even if existing glaciers are very small, except for the Marmolada one, the largest in the Dolomites. This glacier presently extends over an area of about 2 km^2, being approximately 2 km wide and 1 km long. In recent years it has shown significant

Fig. 20.4 The Vallunga ('Long Valley') carved by glaciers in dolomite rocks. The scree slopes and debris cones are locally affected by spectacular debris flows. In the background the Gardena Valley (Photo M. Soldati)

retreat, up to more than 600 m for the main front of the glacier. The present limited development of glaciers in the Dolomites is mainly due to the Alps' decrease in mean altitude from west to east, with the resulting reduction of surfaces lying within the altimetric intervals with favourable climatic conditions for the formation and maintenance of glaciers. The Dolomites have in fact a relatively low mean altitude for glaciation. Moreover, although numerous peaks rise to above 3,000 m, their very steep sides are an unfavourable element for inception of glaciation.

20.4.3 Periglacial Landforms

A great variety of periglacial landforms characterises the Dolomite landscape (Carton and Pelfini 1988). Talus cones and scree slopes are very common and sometimes spectacular features (see Fig. 20.3). Frost-shattering processes have provided abundant debris accumulations (Soldati 1989). The extension, inclination and particle-size distribution of these landforms depend very much on the physical and mechanical properties of the rock types in the source areas and on the density and distribution of tectonic joints. Talus cones and scree slopes are often characterised by the presence of snow avalanche and debris flow tracks. Avalanches in some cases may threaten roads, villages, woods and crops, thus creating conditions of geomorphological risk. Other widespread periglacial landforms are protalus ramparts, which make up elongated ridges parallel to the slopes fed by debris falling from rock walls and sliding on snow patches. Rock glaciers can also be found, though they are not typical landforms in this mountain environment. They show the

classic shape of flows elevated over the surrounding terrain. They play an important role in climatic and palaeoclimatic reconstructions, since they mark the lower limit of the discontinuous mountain permafrost. A comparison with other sectors of the Alpine chain reveals an almost complete absence of active forms, nearly all of them being relict. The most spectacular rock glacier is found at San Pellegrino Pass; it consists of a tongue with convoluted troughs which attains the length of some 1,200 m. Patterned ground due to discontinuous frost action and/or snow is locally observed at high altitudes on plateau areas, like on the Sella and Catinaccio groups. Gelifluction processes also give rise to evident morphological features (scars, lobes, small flows, etc.), especially on slopes consisting of volcanoclastic and clayey formations. Several examples can be seen in the high Cordevole Valley between Arabba and Pordoi Pass.

20.4.4 Karst Landforms

Karst processes in the Dolomites are strictly related to structural and morphological conditions. Karst phenomena basically take place in the higher parts of the valleys and are mainly located in the high carbonate massifs (1,200–3,000 m a.s.l.), which rest on formations with little or no tendency to undergo karst processes (Bini et al. 1998). Among the carbonate formations of the Dolomites, the Marmolada Limestone, Calcari Grigi, Sciliar Dolomite and Dolomia Principale are more sensitive to karst processes. The most typical karst landforms in the Dolomites are large glacio-karst depressions, blind valleys, fluvio-karst dry valleys, dolines and karst features favoured by melt water of ancient glaciers (Nicod 1976). Undoubtedly, glacio-karst depressions are the largest and most characteristic forms (length: 500–1,500 m; depth: 20–60 m).

20.4.5 Gravity-Induced Landforms and Slope Evolution

Landslides are widespread in the Dolomites. They include mass movements of different type and size which occurred from the Lateglacial to date. The frequency and magnitude of gravitational phenomena is proved to be very high in the last Post-glacial period when slopes no longer supported by ice masses were affected by many large-scale landslides. Several landslides have been recently dated in the area of Cortina d'Ampezzo and in the Badia Valley. The analysis of the dated landslides has allowed for correlation between enhanced landslide activity and climate changes in the study areas (Panizza et al. 1996; Soldati et al. 2004; 2006). The first phase of marked slope instability is observed in the Preboreal and Boreal (about 11,500 to 8,500 cal BP[1]) and included both large translational rock slides, which affected the dolomite slopes following the withdrawal of the LGM glaciers, and complex movements (rotational slides and flows) which affected the underlying pelitic formations, probably favoured by high groundwater levels due to increase of precipitation and/or permafrost melting. A second concentration of landslide events took place during the Subboreal (about 5,800 to 2,000 cal BP), when mainly rotational slides and/or flows occurred. In the light of the data collected, the events dated may be considered reactivations of older landforms, linked to the phase of precipitation increase that has been documented in other European mountain regions during this mid-Holocene period.

Slope evolution was also influenced by non-climatic factors, in particular geological ones. First of all the spatial distribution of bedrock with different mechanical characteristics must be taken into account. In particular, the overlap of rigid and resistant rocks (dolomites, limestones, etc.), showing a brittle behaviour, over weaker rocks characterised by ductile behaviour (marls, clays etc.) has certainly conditioned landform development and slope evolution. This kind of geological setting, which is typical of the area of Cortina d'Ampezzo and of the valleys around the Sella Group, has controlled the geomorphological evolution of various parts of the Dolomites. Deep-seated gravitational slope deformations have been also favoured by this setting: sackung and lateral spreads have been recognised (Pasuto et al. 1997), e.g. at Cortina d'Ampezzo (Fig. 20.5).

At present, the most frequent types of landslides occurring in the Dolomites are: (1) rock falls, that seem to be favoured by global warming that accelerates permafrost melting; (2) earth flows, involving the clayey

[1] BP stands for 'before present', where 'present' is arbitrarily taken as 1950. 'cal' means that radiometric C^{14} ages have been calibrated and are expressed as calendar years.

Fig. 20.5 Lateral spreading phenomena at Cinque Torri near the Falzarego Pass (Cortina d'Ampezzo area), where the Dolomia Principale overlies the Raibl Formation (Photo M. Soldati)

material at the lower parts of the slopes, and (3) debris flows, generally affecting the scree slopes at the foot of dolomite cliffs during the episodes of short and intense summer precipitation. Needless to say that these slope movements may pose hazard issues, generally faced by the local communities by means of detailed risk plans.

20.5 Conclusions

The high variety of rocks and landforms, which makes the region a topical example of geodiversity (Panizza 2009), the verticality and monumentality of its features, as well as the contrasting and ever-changing colours of the mountains and meadows render the scenery of the Dolomites outstanding scientific and aesthetic value. From the geomorphological viewpoint, the Dolomites can be considered without a doubt as a high-altitude geoheritage field laboratory, where research, education and geotourism certainly find a privileged setting (Panizza and Piacente 2009).

For this reason, the Italian Dolomites have been recently recognised by UNESCO as a World Heritage property (Sevilla, Spain, June 2009). The nomination was promoted by the local territorial administrations and supported by a multi-disciplinary board of scientists (Gianolla et al. 2008). Naturally, the World Heritage Site status will certainly be a guarantee for long-term conservation and protection of this region and for an even wider recognition of its scientific and scenic relevance.

The Author

Mauro Soldati is Professor of Geomorphology at the Department of Earth Sciences of the University of

Modena and Reggio Emilia, Italy. His research deals with geomorphology and slope instability, with special emphasis on landslides and climatic change, as well as on landslide hazard assessment. He is a member of the Executive Committee of the International Association of Geomorphologists and has served the association as Training Officer since 2001. He is a member of the Editorial Board of the *Geomorphology* and has been guest-editor of a few special issues of the journal dealing with landslides. He has also contributed to the *Encyclopedia of Geomorphology* published in 2004.

References

Bini A, Meneghel M, Sauro U (1998) Karst geomorphology of the Altopiani Ampezzani. Z Geomorph NF, Suppl 109:1–21

Bosellini A (1996) Geologia delle Dolomiti. Athesia, Bolzano, Italy

Bosellini A, Gianolla P, Stefani M (2003) Geology of the Dolomites. Episodes 26:181–185

Brückner E (1909) Die venezianischen Gletscher. In: Penck A, Brückner E (eds) Die Alpen im Eiszeitalter. Tauchnitz, Leipzig, Germany, pp 954–1042

Carton A, Pelfini M (1988) Forme del paesaggio d'alta montagna. Zanichelli, Bologna, Italy

Carton A, Soldati M (1993) Geomorphological features of the Dolomites (Italy). In: Panizza M, Soldati M, Barani D (eds) First European intensive course on applied geomorphology – Proceedings, Istituto di Geologia – Università degli Studi di Modena, pp 13–29

Castiglioni GB (1964) Sul morenico stadiale delle Dolomiti. Mem Ist Geol Min Univ di Padova 24:1–16

Doglioni C (1987) Tectonics of the Dolomites (Italy). J Struct Geol 9:181–193

Gianolla P, Panizza M, Micheletti C, Viola F (eds) (2008) Nomination of the Dolomites for inscription on the World Natural Heritage List UNESCO – Nomination document. Provincia di Belluno, Provincia Autonoma di Bolzano – Bozen, Provincia di Pordenone, Provincia Autonoma di Trento, Provincia di Udine

Nicod J (1976) Les Dolomites de la Brenta (Italie). Karst hautalpin typique et le problème des cuvettes glaciokarstiques. Z Geomorph NF, Suppl 26:35–57

Panizza M (2009) The geomorphodiversity of the Dolomites (Italy): A key of geoheritage assessment. Geoheritage 1:33–42

Panizza M, Piacente S (2009) Cultural geomorphology and geodiversity. In: Reynard E, Coratza P, Regolini-Bissig G (eds) Geomorphosites. Verlag Dr. Freidrich Pfeil, Munich, Germany, pp 37–50

Panizza M, Spampani M (eds) (1988) Introduzione all'ambiente naturale e Itinerario n. 1 Passo Giau - Mondeval – Croda da Lago - Cortina. Edizioni Dolomiti, San Vito di Cadore – Belluno

Panizza M, Pasuto A, Silvano S, Soldati M (1996) Temporal occurrence and activity of landslides in the area of Cortina d'Ampezzo (Dolomites, Italy). Geomorphology 15:311–326

Pasuto A, Silvano S, Soldati M (1997) Deformazioni gravitative profonde di versante e frane: casi di studio nella Valle del Boite (Dolomiti, Italia). Geogr Fis Dinam Quat 20: 107–111

Soldati M (1989) Studio sul crioclastismo dell'alta Valle di S. Pellegrino (Dolomiti): indagini sul terreno e sperimentazioni in laboratorio. Il Quaternario – Italian J Quat Sci 2(1):79–98

Soldati M, Corsini A, Pasuto A (2004) Landslides and climate change in the Italian Dolomites since the Lateglacial. Catena 55:141–161

Soldati M et al (2006) Geomorphological evolution of slopes and climate changes in northern Italy during the Late Quaternary: spatial and temporal distribution of landslides and landscape sensitivity implications. Geogr Fis Dinam Quat 29:165–183

Chapter 21
Saxon-Bohemian Switzerland: Sandstone Rock Cities and Fascination in a Romantic Landscape

Václav Cílek

Abstract Central European sandstone landscapes have developed within a large geological unit known as the Bohemian Creataceous Basin. In ground plan it forms a west–east elongated platform of marine, estuarine and lacustrine sediments that reach 600–1,000 m in thickness and date back to the Late Cretaceous (Lower Cenomanian to Santonian). There are at least ten major sandstone districts scattered over the area which are protected as national parks, landscape protected areas and national reserves due to the scenic beauty of the sandstone relief. However, the largest and most important sandstone area of the whole of Europe – Saxon-Bohemian Switzerland – represents a historical and cultural phenomenon as well, due to the number of archaeological sites, medieval castles, folk architecture and one of the first cradles of European romanticism.

Keywords Geodiversity • landscape evolution • romanticism • sandstone formations

21.1 Introduction – Cradle of Continental Romanticism

One of the major European rivers – Elbe (Labe in Czech) – drains almost the entire area of the Czech Republic, mostly flowing across a flat land. However, north of Litoměřice in northern Bohemia it enters a large, in some place a monumental valley, or even a canyon up to 500 m deep. Passing through the so-called Porta Bohemica it begins to cut down into the neovolcanic rocks of the Middle Bohemian Mountains, and then a sandstone area on the boundary between Bohemia and Saxony of Germany. This area is known under several names, as the Elbe Sandstones when the whole sandstone terrain is dealt with, or as the Saxon-Bohemian Switzerland, when we talk specifically about the dissected mountainous core zone. Germans in the north call this land the Saxon Switzerland, while Czechs in the south prefer the name of Bohemian Switzerland. However, the area extends on both sides of the border as a twin national park. Hence the overall name of Saxon-Bohemian Switzerland is the most appropriate.

The sandstone landscape is multi-storeyed. The deeply incised Elbe valley and a number of its smaller, often deeply incised tributaries form the lowermost geomorphological storey. Then the terrain rises to agricultural and forested plateaux, located some 200 m above the Elbe. They are flanked by sandstone formations on the hillslopes and divided by smaller canyons. The highest storey is formed either by flat sandstone table mountains (mesas) or by conical basaltic hills. The geodiversity of relief, soils and microclimatic features provides the basis for abrupt changes of vegetation, whereas harmonious agricultural land may change within a few metres into rocky wilderness.

Rarely does any other area of Central Europe combine so many spectacular geomorphological features and cultural memory (Schama 1995). Since the intensive salt trade of prehistoric times up to the military Prussian campaigns of the eighteenth to nineteenth centuries, the Elbe River has provided a communication axis through which not only goods circulated but religious and cultural ideas as well. The river being a convenient waterway, and the vicinity of the flourishing Dresden court, led as early as in the last third of the eighteenth century and the beginning of the nineteenth century to the organization of aristocratic travel expeditions into the sandstone wilderness. These trips lasted several days. Parties slept in simple huts or under rock alcoves and participated in various activities,

P. Migoń (ed.), *Geomorphological Landscapes of the World*,
DOI 10.1007/978-90-481-3055-9_21,

from hunting to even landscape paintings and writing of poems influenced by company and landscape. The travelogues used as guide books were copied and professional artists created etchings and lithographs of the most important natural monuments. The aristocratic example was later followed by the upper and middle classes until it reached an almost mass level at the end of the nineteenth century. Therefore, we view this area as one of the most important continental cradles of romanticism, landscape transcendentalism and tourism. Caspar David Friedrich (1774–1840) and Carl Gustav Carus (1789–1869) painted there some of the most metaphysically sublime icons of early romanticism (Richter 1991; Wächter and Böhnert 1999).

Today, the area is one of the most heavily visited, featuring some of the iconic landscape images of the Czech Republic and Germany, such as the rock arch of Pravčická brána or the precipitous valley sides of the Elbe at Bastei. But it is also extremely interesting geomorphologically, presenting an unrivalled diversity of landforms at all scales and offering insights into how the spectacular rock cities evolve over time.

21.2 Location

The Saxon-Bohemian Switzerland area is located at the German–Czech border, extending on both banks of the Elbe River, north of the Czech town of Děčín and south of the German town of Pirna (Fig. 21.1a). Both towns are known as 'gates' to the area. The distance from Prague is 110 km, whereas Dresden – one of the major German cities – is only 50 km away. The main European railway line between Prague and Berlin passes through the Elbe canyon and the river itself is an important international waterway. The sandstone area covers ~700 km², with the lowest point at the river at 125 m a.s.l. and the maximum altitude of 726 m at Děčínský Sněžník Hill, close to Děčín.

21.3 Sandstone Landscapes of Central Europe

Central European sandstone landscapes have developed within a large geological unit known as the Bohemian Creataceous Basin (Fig. 21.1b). The basin is located between Moravia and Poland in the east, Prague in the south, Saxony in the north and Western Bohemia in the west (Rast 1959; Mikuláš et al. 2007; Valečka 1997). In ground plan it forms a west–east elongated platform of marine, estuarine and lacustrine sediments that reach 600–1,000 m in thickness and date back to the Upper Cretaceous (Lower Cenomanian to Santonian, 98–85 millions year ago). Since the Cretaceous basin suffered rather limited deformation later, the attitude of the strata is generally horizontal.

There are at least ten major sandstone districts scattered over the area which are protected as national parks, landscape protected areas and national reserves due to the scenic beauty of the sandstone relief. The most rewarding for an educated visitor are the sandstone districts of Góry Stołowe in Poland, the Teplice-Adršpach area in NE Bohemia, Český ráj (Bohemian Paradise) – a European Geopark since 2005, and Kokořínsko in northern Bohemia. Collectively, they represent a full spectrum of sandstone landscapes, from rather shallow canyons and box valleys in the vicinity of Prague, through to complex, tectonically influenced rock cities of Český ráj and finally to recently uplifted plateaux and dissected margins of the Teplice-Adršpach area and Góry Stołowe in adjacent Poland. However, many less known places contain significant specific features, both, natural, such as concentric ironstone forms or calcareous marshes, and cultural, including archaeological localities, folk Baroque reliefs and statues, underground quarries or medieval castles.

Notwithstanding all this, the Saxon-Bohemian Switzerland occupies a special position within the Bohemian Creataceous Basin. It represents the largest, highest and wildest 'end member' of the whole succession of sandstone landscapes.

21.4 Geomorphological Diversity

From the geomorphological point of view there does not exist one single characteristic landform assemblage of Saxon-Bohemian Switzerland. Instead, several distinctive environments occur and these can be described as follows:

– The major river gorge of Elbe River. Within the sandstone area it is almost 40 km long and typically 200–300 m deep. It reaches its deepest section right at the international border, where continuous lines

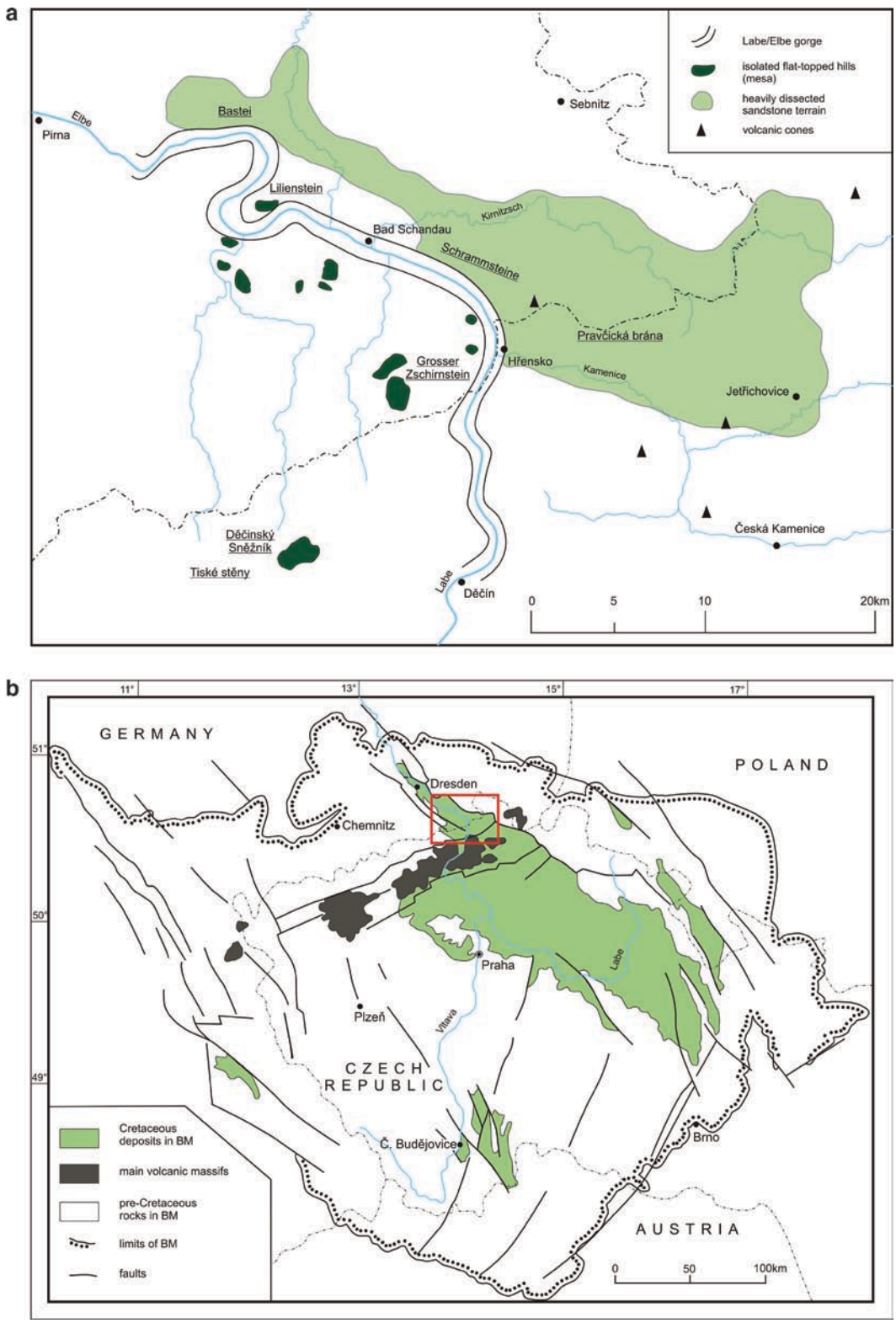

Fig. 21.1 (**a**) Saxon-Bohemian Switzerland and the Elbe gorge, with location of key localities mentioned in the text. (**b**) Extent of the Cretaceous Bohemian Basin. Red rectangle indicates the position of the part (**a**) of the figure (BM means Bohemian Massif)

of vertical cliffs and extensive talus deposits below form a canyon valley. Some of the most famous views of the valley are from the upper rim of the valley sides north of Děčín and from the top of a sandstone mesa at Lilienstein, west of Bad Schandau.

– Narrow, cold gorges of tributary valleys such as Kamenice or Kirnitsch/Křinice and smaller streams. These are sometimes only a few metres wide at the bottom and more than 100 m deep, with vertical or stepped canyon walls (Fig. 21.2). Humidity, microclimate inversion and lack of light lead to the development of rich 'moss gardens,' with up to 28 described fern species.
– Rock cities such as Jetřichovice or Tiské stěny in Bohemia or the Schrammstein range in Germany, developed as dissected margins of hills and plateaux, with a multitude of isolated rock towers and pillars. In addition, bedding caves and rock shelters are common. The largest natural arch of Central Europe, Pravčická brána (Pravčice Gate), is 16 m high and 26 m wide (Fig. 21.3). It is located within a spur radiating from the high, long escarpment of Pastýřské stěny and can be easily reached by one of most popular walking trails in the area.
– Table mountains or mesas are located mostly on the German side (Königstein, Lilienstein, Grosser und Kleiner Zschirnstein), although the highest and largest mesa of Děčínský Sněžník (726 m) is in the Czech Republic. They are characteristically flat-topped and bounded by steep rock slopes, often sculpted into a series of spurs and pillars. Their relative height is from a few tens to almost 200 m. They rise above a high-level planar surface which represents a relict of the shallow- and wide-end Neogene Elbe River (Fig. 21.4), deeply incised by the present-day valley as a consequence of young tectonic movements in the last 800,000 years or so (Záruba et al. 1977).

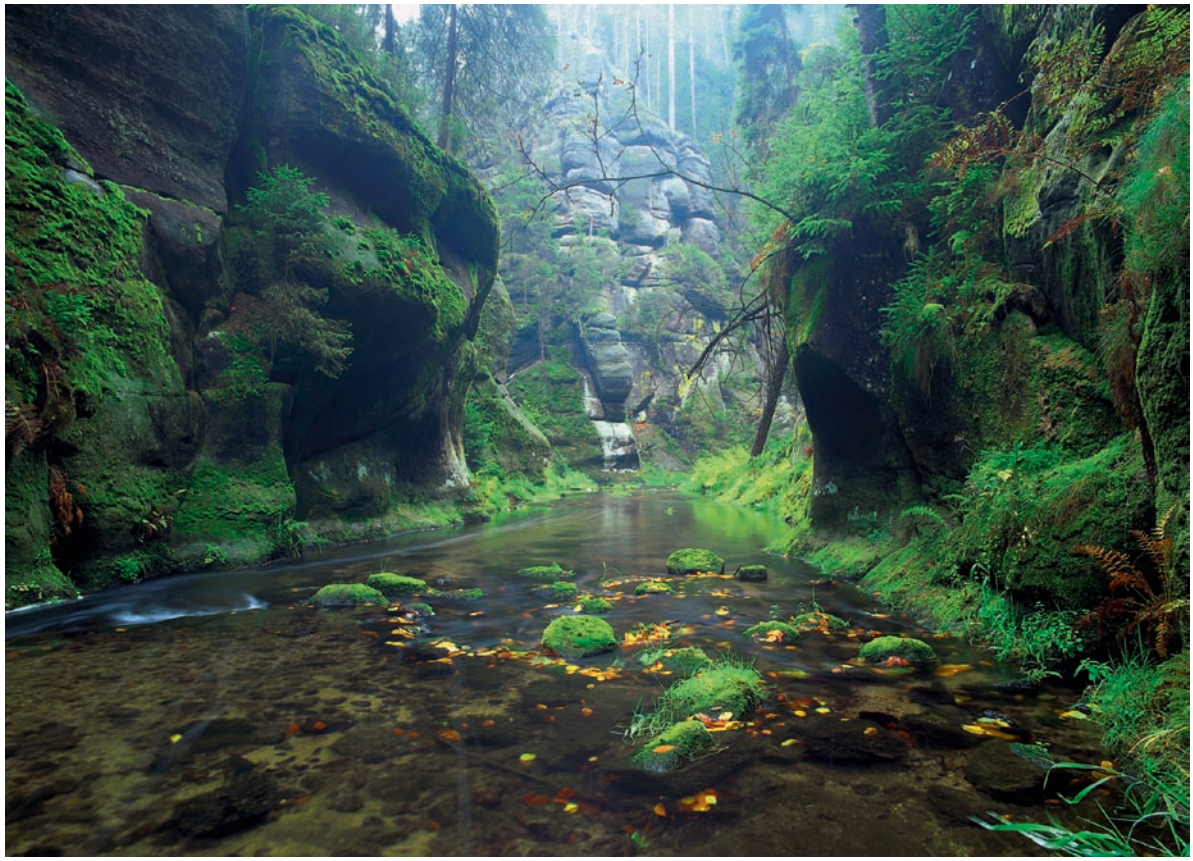

Fig. 21.2 The permanently humid and cold sandstone gorge of Křinice which separates Saxon and Bohemian part of the Saxon-Bohemian Switzerland (Photo V. Sojka)

Fig. 21.3 Pravčická brána – one of landmarks of the Saxon-Bohemian Switzerland (Photo V. Sojka)

Apart from the major landforms, minor relief features have generated considerable interest. One of the most notable features of all Central European sandstone areas is the abundant presence of well-developed microforms that are usually referred to collectively as honeycombs, but a detailed research resulted in description and classification of at least 60 different forms (Adamovič et al. 2009). Many of them develop under the protection of canopy forest on vertical or overhanging rock walls. The majority of microforms results from interaction of the lithology with bio-erosion, salt weathering and surface hardening.

The area is also known for numerous caves of non-solutional origin. On the slopes of Děčínský Sněžník mesa, large fissure caves up to 200 m long and 20 m high have originated as the result of gravitational movements. They were filled with ascending hydrothermal waters that almost completely covered cave walls with fluorite crystals 1–2 cm big. The caves were discovered during fluorite mining and remain preserved.

Two distinctive but interconnected models of sandstone landscape evolution can be applied to the Saxon-Bohemian Switzerland. The ‘classic’ model considers surface erosion triggered by, and associated with, the incision of the Elbe river consequent to surface uplift as the main agent responsible for creating large-scale erosional features (see Young and Young 1992). However, some medium- and small-scale forms cannot be explained as the result of lithological differences exploited by erosion only, but processes of hot fluid circulation, case hardening, bio-erosion and salt weather-

Fig. 21.4 View towards the mesas and buttes of the Saxon table mountains. Note the numerous karren on exposed sandstone surfaces in the foreground (Photo V. Sojka)

ing must be taken into account. Some of these processes, for instance cementation hardening of rock surfaces along tectonic faults, took place during the pre-Quaternary times, under the water-table level. Other examples of sandstone forms that originated below Quaternary sediments are dome-shaped structures. Thus some forms were created but others exhumed and modified by erosion (see Twidale 2002).

21.5 Rock Cities: The Star Attraction

The most distinctive landforms in the Saxon-Bohemian Switzerland are the so-called rock cities or castellated sandstone landform assemblages, although they occur elsewhere within the Bohemian Cretaceous Basin as well. They can be defined as complex labyrinthine structures, in which vertical sandstone cliffs are separated by tectonically conditioned linear depressions resembling the streets or, more commonly, the narrow lanes of medieval cities. There are notable differences between the top surfaces of the rock cities, which are dry and covered by thin soils, and the widened fissures which are typically humid, cold and have a thick sedimentary infill of slope sediments. The flora, fauna, land use and thus history are fully dependent on these sharp boundaries.

Although each rock city in the Bohemian Cretaceous Basin is different in detail, we can simplify their geology and geomorphology to an almost uniform scheme. At least 90% of them are developed in massive, thickly bedded quartz sandstones of Cenomanian to Coniacian, but mostly Turonian age, which were deposited in the shallow-shelf marine environment in a time span of some 12 millions years. The whole complex was originally about 1 km thick, but due to the later uplift and erosion it was reduced to 200–600 m.

The necessary component and a prerequisite of the development of sandstone rock cities is the presence of a dense network of tectonic discontinuities (Fig. 21.5). While the valleys are usually developed along regionally important, first- or second-order faults, the rock cities were eroded along a detailed tectonic grid, where the rectangular or polygonal pattern is repeated every 10–30 m.

The long-term evolution of rock cities may be divided into four phases:

- *Preparatory phase.* The sandstone massif of the future rock city is below the groundwater level. The circulation of fluids is taking place not only through the pores, but along tectonic fissures and in their vicinity as well. It may be observed in certain places that the sandstones are softened within a zone 0.5–4 m wide along tiny vertical fissures by fluid circulation and hence, viable to selective erosion. Some of the fissures are covered by ferruginous crusts or even chalcedony veinlets. Therefore, their distant Cainozoic age should be expected.
- *Initial phase.* The sandstone massif appears above the erosional base due to uplift and/or downcutting. The already softened sandstone is removed by erosion and vertical fissures are exposed. The freeze–thaw cycles of the Ice Ages seem to have played an extremely important role, resulting in microgelivation of the moister/more porous parts of the sandstone bed.
- *Mature phase.* No important uplift and erosion is taking place anymore, but the exposed surfaces are

Fig. 21.5 Pravčický důl (Pravčice Gorge) in winter, showing the close correspondence between joints, faults and landforms (Photo V. Sojka)

being modelled by weathering processes. These are mostly associated with capillary rise of water that activates both destructive and protective processes. Biological erosion and salt weathering are the most important destructive processes, while surface hardening caused mostly by free silica impregnation of the surface parts helps to produce surface stability. Isolated sandstone towers are in many cases relict features, protected by surface hardening. The other important process is the origin of exfoliation or desquamation scales. These are typically 20–80 cm wide layers parallel to surface that tend to detach and fall down. Some of the overhanging rock surfaces and natural arches are due to these processes. Solid blocks of fallen sandstones, when buried in loose and moderately humid sediment at the cliff base, rapidly disintegrate into sand, often in a few thousand years. Then, even an episodic stream is capable of easily eroding the sandy sediments and contributes to the origin of unusually large, mostly dry valleys. The spring meltwaters of Ice Ages may have been responsible for this process.

– *Senile phase.* Slope processes, creep and cambering, rock slope collapses and continuous action of salt and biological weathering characterize this stage, resulting in the origin of flat or gently undulating sandstone plateaus, above which residual hills and towers, often in the form of inselbergs, can be found.

Thus, the sandstone relief of the castellated rock formations represents an outcome of some very old (mid-Cainozoic?) and extremely young (Holocene) processes, acting in separate phases, that are now unified in appearance by the intricate interactions between weathering and surface hardening.

21.6 Conclusions

The area of Saxon-Bohemian Switzerland represents the largest and best-developed sandstone relief in the whole of Europe and is one of very few places where a major river breaks through a sandstone plateau. This combination of mountains and the river makes the natural scenery balanced and rich. Mesolithic rock shelters, archaeological sites of many prehistoric cultures, more than 50 medieval rock castles, folk architecture, prime tourist routes and monuments generate a stark contrast – that of closely coexisting wilderness and cultivated land. The boundary between Saxony (Germany, Prussia) and Bohemia is not only a frontier of two nations who for centuries lived or fought together, but sometimes of a passionate interface between Catholicism and Protestantism.

While almost every year there appears a new monograph on karst landforms, globally no less important sandstone landforms are usually covered by local periodicals only. Sandstone relief, particularly if compared with karst, is often undervalued as ‘pseudokarst.’ However, even a casual observer will notice that sandstone forms are not poor copies of karst, but constitute an independent and very different geomorphological world. For this reason more than a decade ago we replaced the term ‘pseudokarst’ with ‘sandstone phenomenon’ (see Härtel et al. 2007). This can be defined as the set or collection of interacting biotic and abiotic components of a natural system, conditioned by the specific relief of rock cities and allied landscapes in the Bohemian Cretaceous Basin (possibly also elsewhere), and closely associated with prehistoric to modern land use. The meso- and microrelief of castellated rocks is influenced by a number of factors such as frost weathering, bio-erosion, capillary water rise, etc. Two important but antagonistic processes, surface hardening caused mostly by silica impregnation and salt weathering enhanced by anthropogenic input via acid rains, play an important role in small-scale relief formation. However, the major features reflect lithological control and the tectonic environment, developing largely through gravitational processes.

It is almost impossible to explain in a few pages how deeply has been the local sandstone landscape felt, studied and depicted in hundreds of paintings, illustrations, poems and travelogues for almost two centuries. Yet the extremely strong landscape commitment becomes obvious, when one starts reading innumerable scientific and popular accounts of the different aspects of sandstone landscapes on both sides of the Czech/German border. The Saxon-Bohemian Switzerland therefore represents both a natural park, where the sandstone formations along the deep Elbe canyon reach their most majestic and completely developed image in the whole Bohemian Cretaceous Basin, if not Europe, and at the same time a sublime, romantic and transcendental land.

The Author

Václav Cílek is Quaternary geologist who works in Institute of Geology AS CR and teaches at several universities including Academy of Fine Arts. His principal field of interest is Holocene, landscape development and the ways former civilizations interacted with their environment. He is author of almost 250 scientific papers, number of essays and he is author or co-author of 30 books.

References

Adamovič J, Mikuláš R, Cílek V (2009, in print) The atlas of sandstone forms. Academia, Praha

Härtel H, Cílek V, Herben T, Jackson A, Williams R (eds) (2007) Sandstone landscapes. Academia, Praha

Mikuláš R, Adamovič J, Härtel H, Benda P, Trýzna M, Kučerová L (2007) Elbe sandstones. In: Härtel H, Cílek V, Herben T, Jackson A, Williams R (eds) (2007) Sandstone landscapes. Academia, Praha, pp. 326–328

Rast H (1959) Geologischer Führer durch das Elbsandsteingebirge. Bergakademie Freiberg, Fernstudium, Freiberg

Richter F (1991) Wanderungen in Elbsandsteine. Verlag J, Berg, München

Schama S (1995) Landscape and memory. Fontana Books/ Alfred A. Knopf, New York.

Twidale CR (2002) The two stage concept of landform and landscape development involving etching: Origin, development and implication of an idea. Earth Sci Rev 57:37–74

Valečka J (ed) (1997) The Bohemian Switzerland. Geology and Nature. Geological map 1:25,000 with explanations. Czech Geological Survey, Praha

Wächter A, Böhnert W (eds) (1999) Sächsische Schweiz. Landeskundliche Abhandlung. Natur-Mensch-Kultur. Sächsisches Staatsministerium für Umwelt und Landesentwicklung, Dresden

Young RW, Young ARM (1992) Sandstone landforms. Springer, Berlin

Záruba Q, Bucha V, Ložek V (1977) Significance of the Vltava terrace system for Quaternary chronostratigraphy. Rozpravy ČSAV, Řada mat. a fyz. Věd. 87(4):1–88. Academia, Praha

Chapter 22
The Dorset and East Devon Coast: England's Geomorphological World Heritage Site

Denys Brunsden and Richard Edmonds

Abstract The Jurassic Coast is England's only natural World Heritage Site. It documents 190 million years of Earth history over almost the whole of the Mesozoic Period. It includes world famous fossil localities where many of the first discoveries were made for science. It is also a classical coastal geomorphological laboratory. There is an ever-changing display of cliffs, landslides, estuaries and beaches of extraordinary pedagogic value for the study and teaching of the relationships between rocks, relief and episodic processes. It is a dynamic example of change at the ocean, atmosphere, and land interface. It is now the leading demonstration site for World Heritage management, science art and education.

Keywords Dorset and East Devon • geomorphological processes • Mesozoic • Natural World Heritage

22.1 Introduction

The Dorset and East Devon Coast (Fig. 22.1), sometimes called "The Jurassic Coast" is one of the most significant Earth science sites in the world. The geological exposures display a near continuous, accessible sedimentary succession that documents 190 million years of Earth history over almost the entire Mesozoic Period. It includes many fossil localities with superbly preserved remains, many unique, often where the first discoveries were made for science. The eastward dip of the rocks into the Wessex Basin means that a "walk along the coast" is a walk through "deep time" (Fig. 22.2). It is also a walk through the evolution of species. Recognized since the earliest days of geological science, it has been a birthplace of ideas for nearly 300 years (Dorset County Council et al. 2000).

The coast also portrays an exceptional range of classical coastal geomorphological features. These are arranged in such a beautiful, ever-changing display of cliffs, landslides and beaches that some of the world's most prominent artists and literary giants have here been inspired to greatness by the beauty and pattern of the geomorphology. John Constable, Joseph Turner, Jane Austen, Thomas Hardy, John Keats and John Fowles have all described the landforms that are the basis of England's only Natural World Heritage Site (Dorset County Council et al. 2000).

22.2 Geographical Setting

The Jurassic Coast, 155 km long, is located in southwest England (Fig. 22.1) between Exmouth and Studland Bay. The whole of the coast is accessible to the public by road, footpaths and "Gateway towns." The climate is temperate with mean annual temperatures close to 11° (7.8°–13.9°), mean annual precipitation of 750 mm distributed throughout the year, eight frost days and 1,768 h of sunshine.

The most important geomorphological controls are the geological setting, the variable but strong marine energy and the precipitation regime, especially the sequences of years with above average precipitation. These define the dynamic erosion, sediment transfer and beach accumulation units (Brunsden and Goudie 1997; Goudie and Brunsden 1997).

P. Migoń (ed.), *Geomorphological Landscapes of the World*,
DOI 10.1007/978-90-481-3055-9_22,

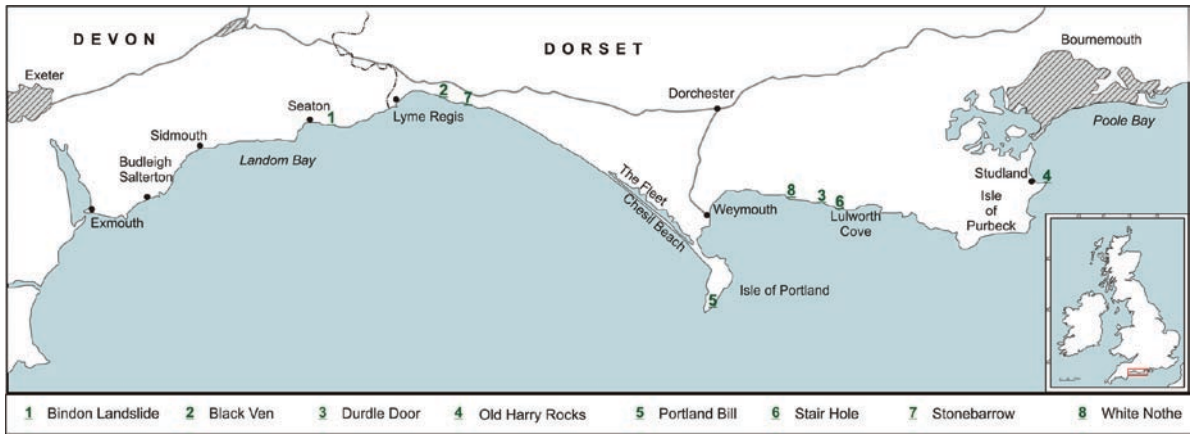

Fig. 22.1 The location of the Dorset and East Devon Coast World Heritage Site and main sites mentioned in the text

22.3 Geology and Its Control on Geomorphology

The remarkable geological succession and structure underpin the whole character of the coast. The Mesozoic sediments (251–66 Ma[1]) are largely undeformed and represent a remarkable range of past environments that formed in the Wessex Basin, one of the best known Mesozoic-early Cainozoic intra-plate sedimentary basins in Europe. In general, the strata dip gently to the east. The oldest rocks (Triassic, 251–190 Ma) outcrop in the west, with progressively younger Jurassic (199–146 Ma) and Cretaceous (146–66 Ma) sediments outcropping to the east. The Upper Cretaceous then unconformably steps back to the west to cover the whole succession in cap rocks of sands and Chalk of variable type and age.

The Triassic succession (Edwards 2008) consists of ~1,100 m of continental, terrestrial red-beds culminating in shallow marine facies. Consisting of the weathered products of the Variscan Mountains, the rocks are mainly pebble beds, alluvial fan deposits, sand dunes and playa basin deposits. The beds are coherent, strong and permeable. They form vertical cliffs sometimes 200 m high (Fig. 22.3). The quartzite clasts from the Budleigh Salterton Pebble Beds, when supplied to the coast, form one of the most durable beach pebbles in Europe and contribute to extensive fringing and barrier beaches. To the east the presence of marine clays at the bottom of the cliffs form the basis of the landforms of the Undercliffs Landslide Nature Reserve

The Jurassic rocks provide one of the finest marine sequences in the world. (Calloman and Cope 1995; House 1989). Only three of the 74 Jurassic ammonite zones are missing. The succession records six major cycles of sea-level change and this yields repeated rhythms of clay, sandstone and limestone.

From a geomorphological point of view this provides countless varying landslide scenarios (Fig. 22.4). Almost every cliff is formed by permeable beds overlying silty clay, clay or bedded mudrock formations. The overlying beds vary from sandstone to hard, jointed limestones. The resultant slope failure mechanisms include rock falls, topples, sags, rotational slides, translational failures, mudslides and true clay-rich debris flows.

The Cretaceous rocks include all stages of the Period except the last. The Purbeck Formation at the late Jurassic–early Cretaceous transition is one of the finest terrestrial sequences of this age in the world. It contains remarkable footprints, fossil soils, fossil forest and fossil sabkha and sedimentary details. The Wealden Group is the most complete sequence in north-west Europe. The most important structural feature is the spectacular unconformity documenting the worldwide Lower Cretaceous marine transgression.

Once again, this provides the setting for a wide range of coastal cliffs, landslides and Quaternary slope deposits. Most importantly, the Upper Greensand and the Chalk contain huge quantities of chert and flint which mantle many of the valley-side slopes and formed aprons at the base of the abandoned sea cliffs

[1]"Ma" stands for "million years ago"

Fig. 22.2 The limestones, clays and shales of Kimmeridgian age exposed at Encombe Bay, Dorset. The rocks of the Jurassic Coast dip gently to the east, steadily exposing younger and younger rocks (Photo R. Edmonds)

Fig. 22.3 Examples of the vertical cliffs developed in the well-drained Triassic sandstones at Orcombe point, East Devon (Photo R. Edmonds)

Fig. 22.4 Perhaps the most dramatic features and events are provided by the landslides of the Jurassic coast. A succession of permeable cap rocks overlying clays, shales and sandstones give an extraordinary sequence of landslide types. Featured are mass movements at Burton Hive on Chesil Beach developed in Bridport Sands (**a**); the Spittles, Lyme Regis, developed in lower Lias clays (**b**); and Stonebarrow Hill, Charmouth, where Upper Greensand overlies Lower Lias (**c**) (Photos R. Edmonds)

and landslides during the last glaciation. These gravels are also a primary source for the barrier beaches which dominate the coast, each with an enclosed salt marsh or estuary. The most important is Chesil Beach and the Fleet lagoon (Fig. 22.5).

22.4 Marine Influences

The second major control is the highly dynamic marine environment, open to the full force of the dominant W–SW winds crossing the Atlantic. Occasionally a storm that tracks and keeps pace with the swell generated in the west produces very long wave length, 8 m high waves with a period of 8 s that cause massive change of the coast. The typical wave character, however, is 1–5 m height with a 3–6 s period. The significant wave height is 4.5 m. Easterlies are of shorter fetch but powerful. The orientation of the coast relative to these energy sources is important. In general, there is a development of asymmetrical bays behind the successive headlands at all scales (Fig. 22.6). Wave diffraction around the headlands generates a typical shelter, drift-oriented and swell-oriented beach system

Fig. 22.5 Chesil Beach and the fleet (Photo P. Sills)

that determines sediment storage as well as cliff erosion patterns and rates.

Although the climate of the south-west of England is temperate, it is subject to the short-term extremes and sequences of the North Atlantic Oscillation. These oscillations between the easterly and westerly regimes dominate the present sediment flux directions of the coastline and longer-term variations in wind direction. On a millennial timescale the "Glacial" or "Little Ice Age" times were dominated by easterlies and the drift was mainly towards the west. Thus pebbles from Budleigh Salterton are found as far west as Slapton in South Devon. During much of the Holocene and the recent times, however, the coast has evolved with a strong westerly component. The beaches grew across the rivers towards the east and the small asymmetrical bays were created much as we see them today.

Superimposed on this regime and causing variation in the sediment supply are the wet periods of duration ranging from decades to hundreds of years. At these times the cliff and landslide systems become very active. The frequency of large slope failures increases and the main "formative" events occur. The 1835–1840 period was important in East Devon. The 1926–1929 wet years caused landsliding along the whole coast and the 1958–1959, 1976–1979, 1986, 1996–1999, 2002–2006 events were very significant for landsliding in the Jurassic rocks of Lyme Regis (Brunsden 1996).

Fig. 22.6 The asymmetrical bays of Lyme Regis. Such bays are typical of the south coast of England caused by diffraction of the dominant south-west waves around headlands and harbor walls. Understanding of these parabolic bays is essential for erosion control. The Spittles and Black Ven landslides are in the background (Photo copyright Dorset County Council)

22.5 Landforms

The Dorset and East Devon Coast includes superlative examples of geomorphological features that commonly occur on coastlines throughout the world. The importance, however, lies in the classic textbook exemplars that occur in close proximity and in the natural relationships that exist between materials, processes and forms. It is the wealth of landforms, developed in response to the varied geology, high energy and climatic variation that gives the site its intrinsic value and distinctive value and beauty. This superlative natural laboratory is famous for its mass movement systems, the development of a unique barrier beach and lagoon of Chesil Beach (Fig. 22.8); classic examples of coastal cliff evolution through time and space at Ladram Bay, Durdle Door and Old Harry Rocks (Fig. 22.7) (May and Hansom 2003). The textbook relationship between rock structure and form is only bettered on the Dalmatian Coast of Croatia.

22.5.1 Cliffs

Over 80% of its length the East Devon and Dorset coast is composed of cliffs developed in mudstones, sandstones, and limestones. Although much of the coast is characterized by steep, vertical cliffs descending precipitously into the sea, there are also the classical sites of Ladram Bay and Old Harry rocks where the development of stacks and bays have become textbook examples (Fig. 22.7). The beautiful coastal barriers, coves and rock arches such as Durdle Door and Stair Hole are also much beloved memories of school fieldtrips (Goudie and Brunsden 1997; May and Hansom 2003). The cliffs of East Devon have been well-studied for rock fall and mudslide processes and many new events, influenced by sea-level rise and beach diminution are now being documented (Gallois 2007).

22.5.2 Landslides

Due to the lithological variation, the Lower Cretaceous unconformity which brings permeable rocks into a cap rock position; the continuous renewal of erosion at the base of the sea cliffs and climatic variation, this coast portrays a comprehensive range of slope failures from rotational landslides to mudslides, topples, sags, and translational failures (Brunsden 1996). Many are the of late glacial origin, others date from Holocene or prehistoric times. The most famous occurred in the Little

Fig. 22.8 The Bindon landslide of Christmas Eve 1839 – shown here in contemporary print by Daniel Dunster (1840) – was probably the first landslide to be fully described in a scientific memoir. It is an enormous block slide which failed on the Triassic Murcia Mudstones and is composed mainly of Upper Greensand, which may have liquefied, and the Chalk which was strong enough to allow the development of a spectacular graben and many detached pillars

Ice Age, have eye-witness accounts or provide the subject of ongoing research.

The most significant is the Bindon landslide between Axmouth and Lyme Regis in 1839 (Fig. 22.8). This massive landslide created a 6.5 ha translational block, known as Goat Island, isolated from its back scar by a 30 m deep, 1.5 km long "chasm" or graben. This is probably the first landslide to be described in the scientific literature and it has a wonderful textual account and illustrative portfolio (Coneybeare et al. 1840; Pitts 1981; Pitts and Brunsden 1987).

Other classic sites are Black Ven, a large well-monitored and imaged mudslide system; Stonebarrow Hill which demonstrates time-dependent slope regression and energy diffusion models; the topples and translational slides of Portland Island with their relationships with periglacial and human activity; the spectacular, unstudied slides at White Nothe, St Adhelm's Head, Chapman's Pool and Swanage. These slides are a rich source of interest for geomorphologists, geologists and ecologists and a feast for the "eye" for the general public. The slide at King's Weir, Portland (1694) is the first known landslide to have been caused by human activity (for full references see Brunsden and Goudie 1997; Goudie and Brunsden 1997).

22.5.3 Beaches

This coast provides well-documented scenarios of beach formation and evolution during a post-glacial sea-level rise encountering a retreating coastline of varying resistance (May 2008). The shoreline during the Holocene period consisted of a "great beach" derived from the periglacial products of cliff degradation and sediment supplied by the rivers and strewn across the emergent sea floor during the last glacial period. In the post-glacial and Holocene this "beach" was steadily driven on shore in front of the rising sea. Eventually the sea began to re-excavate the, now degraded, pre-glacial cliffs to develop the current pattern of headlands and asymmetrical bay beaches.

The river mouths were crossed by high barrier beaches composed of flint, chert and quartzite pebbles derived from the degraded cliffs. Each barrier enclosed an estuary, salt marsh or lagoon (Fig. 22.5). During the late Holocene these slowly diminished in area as the beaches were driven onshore and drifted along the exposed shore so that the organic deposits eventually emerged on the seaward side to create an unstable foundation to the current storm beaches. It is now a regular occurrence to find blocks of peat thrown up onto the seaward face of

Fig. 22.7 The Jurassic Coast has classical development of arches and sea stacks. The most famous are Bat's Head (**a**) and Old Harry Rocks (**d**) in the Chalk; Durdle Door (**b**) in the Purbeck and Portland Stone limestones and the stacks of Ladram Bay (**c**) in Triassic sandstones (Photos R. Edmonds)

Chesil during storms. Every river mouth now has remnant salt marshes (often covered with tourist car parks!). Chesil and Radipole (Weymouth) have spectacular marshes and Nature Reserves.

Two large sediment accumulations are of international importance. The cliffs at Budleigh Salterton contain quartzite pebbles that are quite unique and therefore diagnostic of their source and transport history. These mottled red-grey pebbles are found on every beach on the south coast of England, from Slapton Ley in Devon to Hastings, except behind the Isle of Wight. They also occur in the Portland and Chichester raised beaches (10–15 m OD) and to a depth of -30 m in offshore gravel banks. They are a marker of beach evolution and barrier rollover for a coastal distance of 200 km and a time span of over 20,000 years! A possible cause of this strange distribution is that the pebbles travelled along the shorelines of the "great beach" as it was being driven onshore and up the English Channel during the Holocene but this has never been verified by research.

The largest and best studied beach is Chesil (Fig. 22.5) (May and Hansom 2003). This coast is open to the maximum energy waves and storm swells that enter the English Channel. The beach is 28 km long and ranges in height from 5 to 15 m between West Bay and Portland. It is renowned for the type, volume and size-grading of its pebbles, with many early scientific studies speculating on the processes that might have created it. It is most likely that the distribution is a function of a complex interplay of longshore drift under both directional regimes; transport of storm driven sediment "waves" or "slugs" in different directions at different tide levels; transport events of varying duration according to storm strength; and sudden over wash into the Fleet lagoon when storm conditions allowed. Sea-level rise, increased storminess, subsidence and diminishing sediment supply are other factors still to be analyzed. Although well-studied for more than 150 years the truth about Chesil is still to be told. Fortunately the Channel Coast Observatory has established long-term monitoring networks, sophisticated

surveying and research programs that should begin to unravel the secrets of the beach.

Behind Chesil is Europe's largest coastal lagoon – the Fleet which varies from fresh water to brackish salt water from west to east. It is a survivor of the water trapped behind the incoming Holocene "great beach" and is also an ecological habitat of great significance for plant, fish and bird life. The sediments preserved in its sheltered waters provide information on the late Holocene sea levels, storm frequency, climate and vegetation change. It is thought that much of the history of environmental change for the English Channel might be preserved in its rich organic deposits. Cores from the latest boreholes have recovered freshwater peat, containing fossil crustacean and ostracods, dating from 4,000 to 5,000 years ago (May and Hansom 2003).

22.5.4 Raised Beaches

There are two famous Pleistocene raised beaches deposits at Portland Bill (Fig. 22.9). They provide an important representation of terrestrial and marine sedimentation back to ~200,000 years ago. The fossil fauna are the most diverse found in any British raised beach. The exposures are possibly the best location in the UK to investigate the relationship between the nearshore, beach, lagoon and hillslope processes of the Pleistocene. The beach also overlies curious polygonal structures in the Purbeck Beds variously attributed to rock blistering under the cold conditions of the Pleistocene Anglian glaciation or the development of gypsum polygons under terrestrial saline salt flat (sabkha) conditions (for references see Goudie and Brunsden 1997; May and Hansom 2003).

22.6 History of Study

There have been many critical contributions to the major formative debates in the early days of geomorphology. In the early eighteenth to nineteenth centuries Earth Science was the "Queen of Sciences" occupied with the central questions of "What the World had been?" and "How it should be understood?." On the Jurassic Coast two fundamental geomorphological questions were established. The main controversy of the time was between the "catastrophists" who believed in the reality of the creation, violent formative, biblical geomorphological events took place on a very short timescale and the "uniformitarianists and actualists" who believed in slow progressive change over long periods of time. The Uniformitarian belief was that the geological/geomorphological processes observed today were the same as in the past and that; therefore we could interpret landscape evolution in terms of observable processes.

Although the main proponents operated elsewhere, the Dorset and Devon coasts were used to debate and illustrate the problem (Dorset County Council et al. 2000). William Buckland used the valleys of the Axe, Sid, Lim and Char as evidence for the action of the retreating waters of Noah's Flood – "The Great Deluge," and both William Conybeare and Henry de la Beche made observations of the steady changes wrought by these rivers as they carried debris to the sea. The importance of the site was such that nearly all the great figures of nineteenth-century geology and geomorphology visited the site. Notable figures at this time were Mary Anning (1799–1847) who found the first plesiosaur, a new fossil fish, brittle stars, the first British pterosaur and several ichthyosaurs. She knew and worked with Sir Roderick Impey Murchison (1792–1871), President of both the Geological and Royal Geographical Societies and contemporaries, who visited Lyme Regis included Gideon Mantell (1790–1852), the discoverer of the Iguanodon, Professor John Stevens Henslow (1796–1861), Darwin's tutor, Sir Charles Lyell (1797–1875), the "father of geology," Professor Richard Owen (1804–1892), superintendent of the Natural History Museum and Louis Agassiz (1807–1873), the founder of modern glacial geomorphology. More than 5,000 publications document the science of the site which therefore provides a teaching, research and recreation site of immense interest for groups of all ages. It has a continuing importance for research and as a training ground for the oil industry interested in the rock succession as an exemplar for the North Sea. The list and activity continues to the present with countless field trips and the development of heritage centres, guide books, education and arts strategies and research programmes. The Site is looked after by the Dorset and East Devon World Heritage Site Team and Steering Committee and the Jurassic Coast Trust,

Fig. 22.9 The Portland Bill raised beach. The section shown has been dated at approximately 129,000 years ago (Photo R. Edmonds)

who manage this wonderful example of geomorphological conservation.

The Authors

Denys Brunsden is Emeritus Professor and Fellow of King's College, London. Founder President of the International Association of Geomorphologists, Past Vice-president of the Royal Geographical Society, President of the Geographical Association, Chairman of the British Geomorphological Research Group and the initiator of the Dorset and East Devon Coast World Heritage Site. He holds the William Smith and Glossup Medals of the Geological Society of London, the D. L. Linton Award; Honors of the Association of American Geographers, the Association of Polish Geomorphologists and the International Association of Geomorphologists. Author of 15 books and numerous academic papers he is now happily in retirement in Dorset, UK although he does do a bit here and there!

Richard Edmonds is the Geological Officer for the Dorset County Council, UK and the Dorset and East Devon Coast World Heritage Site. He is a prolific author of geological guides and Web sites and renowned for the innovative way in which he has stimulated public education in geology and geomorphology. He encourages the development of Heritage Centres and Codes of Practice for fossil collection. He is a central figure in coastal zone management of Earth heritage sites.

References

Brunsden D (1996) Landslides of the Dorset Coast: Some unresolved questions. The Scott Simpson lecture. Proceedings of the Ussher Society, vol 9, pp 1–11

Brunsden D, Goudie AS (1997) Classic landforms of the West Dorset Coast. The Geographical Association, Sheffield

Calloman JH, Cope JCW (1995) The Jurassic geology of Dorset. In: Taylor PD (ed) Field geology of the British Jurassic. Geological Society, London, pp 51–103

Coneybeare WD, Buckland W, Buckland M (1840) Ten plates comprising a plan, sections and views representing the changes produced on the coast of East Devon between Axmouth and Lyme Regis by the subsidence of the land and the elevation of the bottom of the sea, on 25th December 1839 and 3rd February 1840. John Murray, Albemarle Street, London

Dorset County Council, Devon County Council, Dorset Coast Forum (2000) Nomination of the Dorset and East Devon Coast for inclusion in the World Heritage List. Sillson Communications

Edwards RA (2008) The Red Coast revealed, Exmouth to Lyme Regis. Geology of the Jurassic Coast. The Jurassic Coast Trust, Coastal Publications, Wareham

Gallois RW (2007) Photographic feature: A recent landslide on the East Devon coast, UK. Quart J Eng Geol Hydrogeol 40:29–34

Goudie AS, Brunsden D (1997) Classic landforms of the East Dorset Coast. The Geographical Association, Sheffield

House M (1989) Geology of the Dorset Coast. The Geologists Association, Guide No. 22

May VJ (2008) Geomorphology of Dorset: A review. Proceedings of the Dorset Natural History Archaeological Society, vol 129, pp 149–162

May VJ, Hansom JD (2003) Coastal Geomorphology of Great Britain. Geological Conservation Review Series, Joint Nature Conservation Committee, Peterborough

Pitts J (1981) A historical survey of the landslides of the Axmouth-Lyme Regis Undercliffs, Devon. Proceedings of the Dorset Natural History Archaeological Society, vol 103, pp 101–105

Pitts J, Brunsden D (1987) A reconsideration of the Bindon landslide of 1839. Proceedings of the Geologists' Association, vol 98, pp 1–38

Chapter 23
Fjords of Norway: Complex Origin of a Scenic Landscape

Atle Nesje

Abstract Norway has been called the 'Land of fjords'. This is easily envisaged when studying a map or satellite image of Scandinavia. Norway is characterised by a rugged, highly dissected coast with numerous islands, skerries, sounds, and fjords. Along the Norwegian coast there are some 200 principal fjords. Norway has a passive-margin coast and the coastline of Norway spans 13° of latitude (58–71°N) and 26° of longitude (4.5–31°E). Geirangerfjorden and Nærøyfjorden in western Norway were included in the UNESCO World Heritage List in 2005. These fjords are some of the longest, deepest, narrowest, and most beautiful fjords and they are therefore considered to be the prime symbol of Norway, and among the most spectacular fjord landscapes anywhere in the world.

Keywords Fjords • Norway • landscape • glacial erosion

23.1 Introduction

Norway is sometimes called the 'Land of fjords'. It is easy to understand why when looking at a satellite image of Scandinavia with some 200 principal fjords along the Norwegian coast (Fig. 23.1). The western part of Fennoscandia is a rugged, highly dissected coast with numerous islands, skerries, sounds, and fjords, and this landscape is counted among the most scenic landscapes on Earth. The Norwegian coast is a passive-margin coast and the coastline of Norway spans 13° of latitude (58–71°N) and 26° of longitude (4.5–31°E) and is extraordinarily long. The coastal perimeter distance is 2,650 km, but a digital summation of 30 m linear intercepts gives a total shoreline distance of 83,281 km. A conventional, lower-resolution measurement yields a total coastline length of c 57,000 km (Corner 2005).

Geirangerfjorden (Fig. 23.2) and Nærøyfjorden (Fig. 23.3) in western Norway, areas of great natural beauty, found their place on the UNESCO World Heritage List on 14 July 2005 and encompass some of the longest, deepest, narrowest, and most beautiful fjords. The Natural Heritage area is made up of two separate sections, Geirangerfjorden and Nærøyfjorden and surrounding districts, with a total area of approximately 1,227 km^2, of which 107 km^2 is water. These fjords are considered to be the prime symbol of Norway, and among the most spectacular fjord landscapes anywhere in the world. It is therefore more than likely that the Norwegian word 'fjord' has become a part of international languages because of these pearls of nature. Etymologically, the Norse noun 'fjorðr' means a 'lake-like' water body used for passage and ferrying. The Scandinavian word 'fjord', Proto-Scandinavian ferþuz, is the origin for similar European words: Icelandic 'fjörður', Swedish 'fjärd' (for Baltic water bodies), English 'ford', Scottish 'firth', and is related to: Greek 'poros', Latin 'portus', and German 'Furt'.

The fjords rank amongst the most dramatic and spectacular landscapes around the globe. In the field of natural science, Geirangerfjorden and Nærøyfjorden are considered to be the classic definers of this type of landscape. The area is typified by a diversity of rich natural beauty, with great variations in altitude and the close proximity of mountains and the sea.

National Geographic Traveller Magazine voted the fjords in Norway "the best unspoiled travel destination in the world", and the respected American newspaper *Chicago Tribune* included Norway's fjords on its list of the "Seven Wonders of Nature". The fjords of western

P. Migoń (ed.), *Geomorphological Landscapes of the World*,
DOI 10.1007/978-90-481-3055-9_23,

Fig. 23.1 Satellite image of Scandinavia. S-Sognefjorden (NASA World Wind)

Fig. 23.2 Geirangerfjorden seen toward NW (Photo A. Nesje)

Fig. 23.3 Nærøyfjorden seen toward NE. Ferries for scale (Photo A. Nesje)

Table 23.1 The longest fjords in Norway and on Svalbard

	Name	Length (km)
Norwegian mainland		
1	Sognefjorden	204
2	Hardangerfjorden	179
3	Trondheimsfjorden	126
4	Porsangen	123
5	Storfjorden	110
6	Nordfjorden	106
7	Oslofjorden	100
8	Boknafjorden	96
Svalbard		
1	Wijdefjorden	108
2	Isfjorden	107
3	Van Mijenfjorden	83
4	Woodfjorden	64
5	Wahlenbergfjorden	46

Norway recently emerged as the winner in a survey of the most popular World Heritage sites in competition with other prestigious UNESCO sites.

In this chapter, the formation of fjords will be discussed, with special emphasis on the Norwegian fjords, and with a particular focus on Sognefjorden, the second longest fjord on Earth (Tables 23.1 and 23.2).

23.2 Fjords

A fjord is commonly defined as a deep, high-latitude estuary excavated or modified by glaciers (Syvitski and Shaw 1995). In Norway the term is applied generically and in name to several morphological features. Geomorphologically, the term refers to a relatively long, narrow, over-deepened, steep-sided, commonly winding arm of the sea incised into highland (e.g. Corner 2005 and references therein). Fjords are distinctive both because of their great depth, and because of the over-deepening of their inner and middle sections that are deeper than the mouth (Fig. 23.4). Sognefjorden in western Norway has a maximum water depth of 1,308 m (+ c 200 m of late-glacial and Holocene sediments above bedrock). Most fjords have a threshold at their mouth consisting of bedrock or

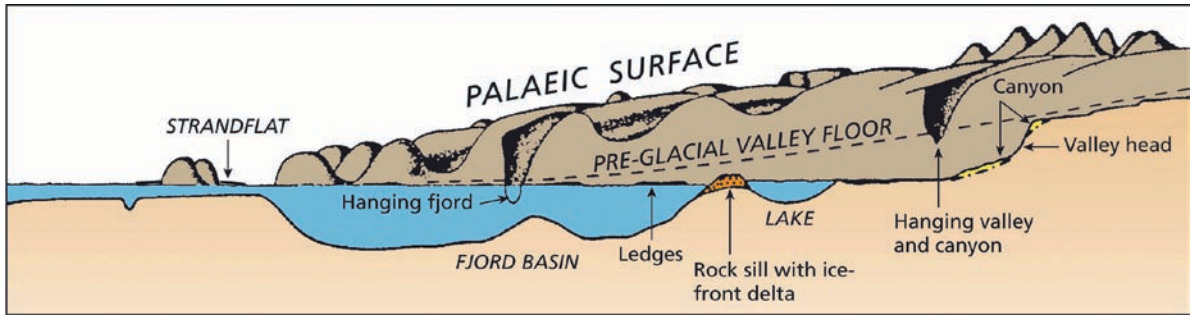

Fig. 23.4 Schematic longitudinal profile of a fjord landscape (Modified from Gjessing 1967)

associated with a terminal moraine. The shallow part at the seaward end of the fjord represents the spreading and thinning of ice as it is released from its narrow valley and spreads out over the lowland. Fjords are common along the coast of Norway, Greenland, Alaska, British Columbia, Chile, Antarctica, and New Zealand. The inner fjords are commonly narrow and deepen seaward as they are joined by tributary fjords. In the outer coastal parts the fjords typically broaden and diverge into interconnected sounds. Most fjords stop at a marked bedrock threshold, whereas a few extend onto the continental shelf.

23.3 Fjord Formation

Fjords commonly punctuate continental margins occupied by late Cainozoic ice sheets and they are several 100 m deep and extend many tens of kilometres inland. Ice sheets mainly drain through fjords and because rivers do not erode below sea level, the submarine part of the fjords must have been formed by glacial erosion. The origin and processes related to this feature have, however, been discussed for about 100 years and the problem is 'classic' in geomorphology (see Holtedahl 1967; 1975; Andersen and Nesje 1992; Nesje et al. 1992; Nesje and Sulebak 1994; Nesje and Whillans 1994 and references therein, Kessler et al. 2008). This debate has mainly focused on the 'classic' fjords and fjord lakes in Norway and Canada. Most authors agree that there has been a clear glacial-erosive influence on the fjords, but the importance of glacial activity relative to other processes, such as active tectonics (e.g. Gregory 1913), mass-wasting processes, and fluvial erosion (e.g. Troll 1957; Nesje and Whillans 1994), has not been unequivocally established.

The seeds of a fjord are laid when a glacier cuts a V-shaped fluvial valley or a U-shaped valley through abrasion of the surrounding bedrock. Many such valleys were formed during the Quaternary ice ages when the sea was at a much lower level than it is today. At the end of such a period, the climate warmed and glaciers retreated. Sea-level rise due to an influx of water from melting ice sheets and glaciers around the world (it rose ~120 m relative to sea level after the last ice age) caused inundation of the vacated valleys with seawater to form fjords.

In the fjord region of western Norway, geomorphological studies have been carried out by several authors. The earlier studies took little account of the bedrock geology. Ahlman (1919) favoured relatively modest glacial erosion, except for the over-deepening of the fjords. Gjessing (1967), on the other hand, suggested that glacial erosion was the most active process along the fjords and valleys. Holtedahl (1967; 1975) argued, based on observations along Hardangerfjorden, that glaciofluvial erosion played an important role in the fjord formation. Furthermore, he suggested that the confluence of tributary glaciers in the inner part of the fjords led to excavation of deep fjord basins. Near the coast, however, the glaciers spread out and the erosional capacity was strongly reduced, leaving behind bedrock thresholds. Nesje and Whillans (1994) suggested that V-shaped valleys and gullies along the sides of Sognefjorden were formed by fluvial and slope processes during interstadials/interglacials.

The inner ends of fjords and fjord valleys commonly end with thresholds or trough headwalls. Gjessing (1966) interpreted these as glacial rock steps (Fig. 23.4),

where the action of subglacial meltwater and later subaerial water cut waterfall notches. Gjessing (1966) argued that glaciers are necessary for fjord formation. The strongest indication for glacial erosion is the overdeepening of fjord floors well below present and past sea level and their outer rock threshold. Measured in volume eroded within a limited time span, an ice stream forming its own clearly defined drainage channel (fjord) is apparently one of the most significant erosive agents in operation on Earth.

Several authors have in recent years linked the upper terrestrial bedrock surface (the paléic surface, Fig. 23.4) to the history of offshore sedimentary basins (Doré 1992). Most of southern Norway was covered by Cretaceous sediments, which were stripped off during the following Cainozoic uplift caused by the opening of the Norwegian-Greenland Sea. The surface was exposed to weathering, mass wasting, and fluvial transport to the North Sea basins. Riis (1992) calculated the mean late Cainozoic onshore erosion to c 1,000 m just inside the coast of western Norway.

23.4 Sognefjorden

Sognefjorden is the second longest and deepest fjord on Earth (Table 23.2), but the longest deglaciated and inhabited one, penetrating 204 km inland from the western coast of southern Norway, just north of the city of Bergen (Fig. 23.1).

Three categories of bedrock dominate in the Sognefjord drainage basin (Sigmond et al. 1984). Solund in the western part (Fig. 23.5) consists of Devonian sandstones and conglomerates. The middle

Table 23.2 The longest and deepest fjords on Earth

The longest:
1. Scoresby Sound in Greenland – 350 km (220 miles)
2. Sognefjorden in Norway – 204 km (126 miles)
3. Hardangerfjorden in Norway – 179 km (111 miles)
The deepest:
1. Skelton Inlet in Antarctica – 1,933 m (6,342 ft)
2. Sognefjorden in Norway – ~1,308 m (4,291 ft)
3. Messier Channel in Chile, South America – 1,288 m (4,226 ft)

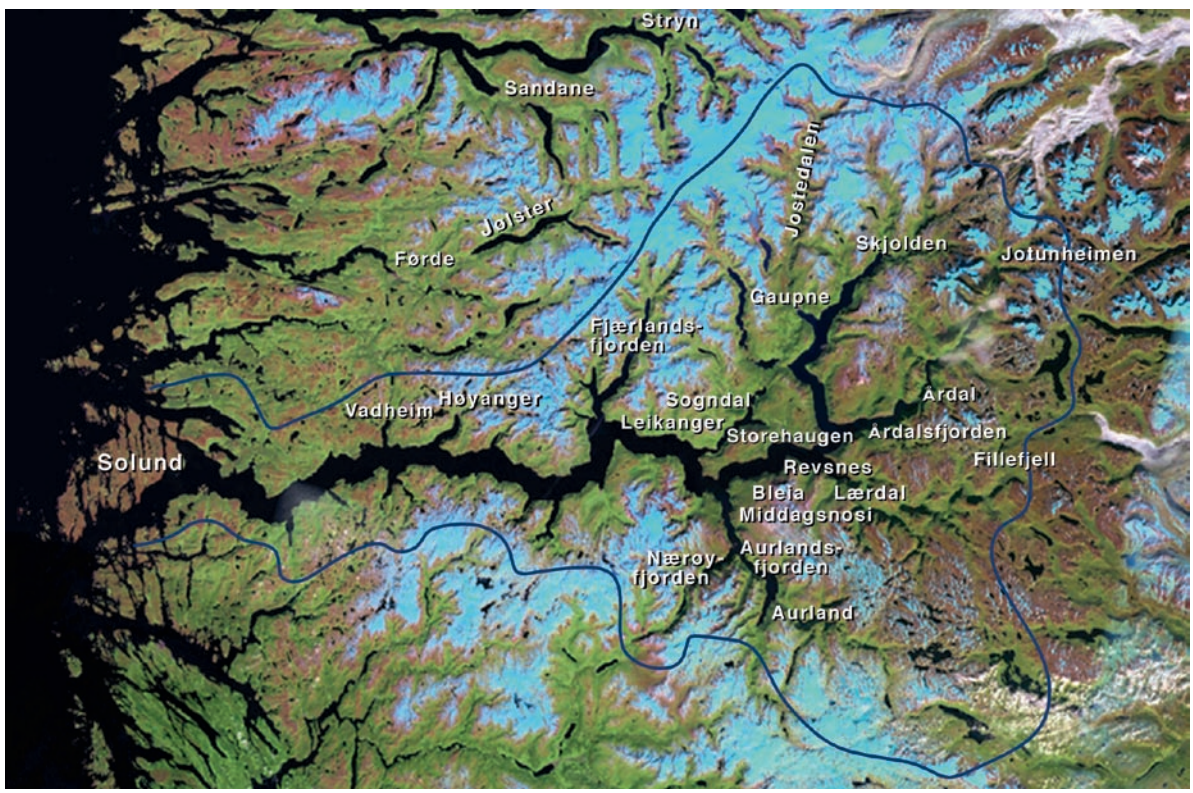

Fig. 23.5 The drainage area of Sognefjorden (satellite image: NASA World Wind) (Adapted from Nesje et al. 1992)

and western part of the Sognefjord drainage basin belongs to the west-Norwegian Precambrian gneiss complex with E–W and NE–SW trending structures. The eastern, inland portion of Sognefjorden consists of rocks of Caledonian (early Palaeozoic) age. The fjord branches are related to bedrock structures and some of the tributary fjords also follow the fold pattern.

The outer part of the Sognefjord drainage basin is relatively narrow (30–40 km) (Fig. 23.5). Most likely related to the width and bedrock structural factors in the inner parts of the Sognefjord drainage basin, there are seven main tributary fjords (Fjærlandsfjorden, Sogndalsfjorden, Lustrafjorden, Årdalsfjorden, Lærdalsfjorden, Aurlandsfjorden, Nærøyfjorden).

In the west the fjord starts at Solund. The main threshold is at 30 km along the profile (Fig. 23.6), with water depths on the order of 100–150 m. The bedrock threshold probably exists because of decreased erosion at the fjord mouth where ice diverged and thinned, and glacier velocity, or effective basal ice pressure, became reduced (Holtedahl 1967). The fjord becomes abruptly deeper eastward to reach a maximum water depth at Vadheim of 1,308 m below the present sea level. The fjord is relatively flat-bottomed between 50 and 180 km. Most of the tributary fjords 'hang' above the main fjord.

The mountains along the sides of Sognefjorden gradually increase in elevation eastward from about 500 m a.s.l. in the coastal region to about 2,200 m a.s.l. in Jotunheimen (Fig. 23.6). The average relief along the fjord is approximately 2,000 m, with the largest relief (c. 2,850 m) at Bleia (152 km inland). Between about 45 and 170 km inland approximately 50% of the total relief is below the threshold at the fjord mouth and 60% below the present sea level.

Transverse profiles of the fjord show a marked break in slope angle (Fig. 23.7) and this was used to elucidate the geomorphic history of Sognefjorden. During the Mesozoic and early Cainozoic, the landscape of Norway was eroded to a smooth and undulating surface called the paléic (= 'old') surface close to sea level at that time (Gjessing 1967). During the early Cainozoic, the crust was lifted asymmetrically, with the highest uplift along the central mountain range in Scandinavia, associated with the opening of the Nordic Seas. This old erosion surface is easily observed along Sognefjorden as numerous broadly concordant sum-

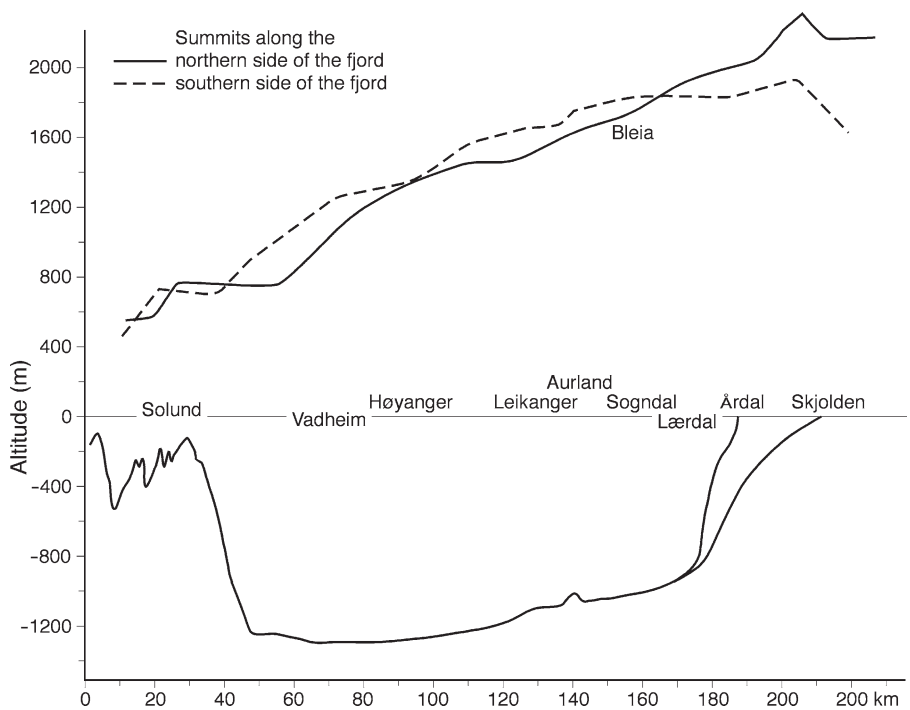

Fig. 23.6 Longitudinal profile of Sognefjorden with maximum summit levels along both sides of the fjord (Adapted from Nesje et al. 1992)

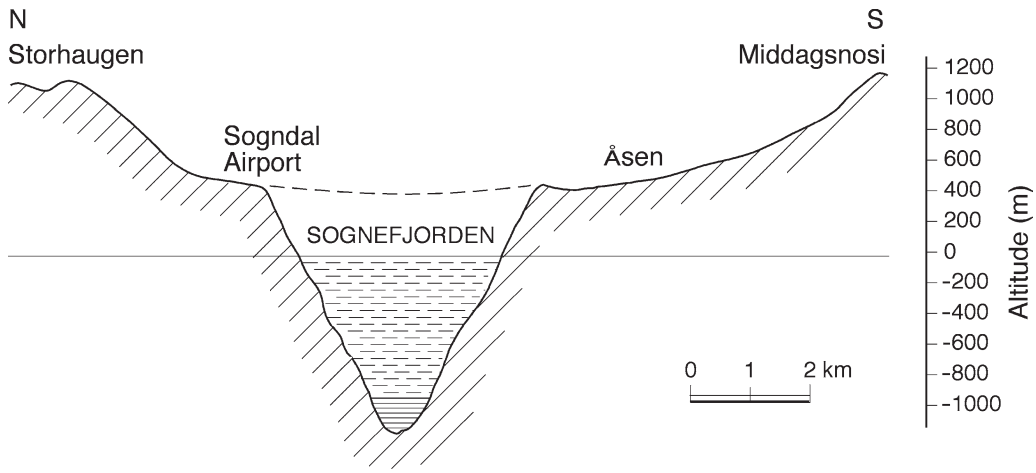

Fig. 23.7 Transverse profile of Sognefjorden south of Sogndal (see Fig. 23.5 for location; at 160 km in Fig. 23.6) (Adapted from Nesje et al. 1992)

Fig. 23.8 Remnants of the preglacial plateau landscape at both sides of Aurlandsfjorden and vertical gorges along the NE part of the fjord (for location, see Fig. 23.5) (Photo E.A. Vikesland)

mits and plateaux (Fig. 23.8). During and after the land uplift, river valleys were formed in the paléic landscape that forms the basis for the reconstruction of the preglacial land surface (Fig. 23.9). The occurrence of a low-gradient valley system >500 m above the present sea level is envisaged, with a wide eastern basin and a

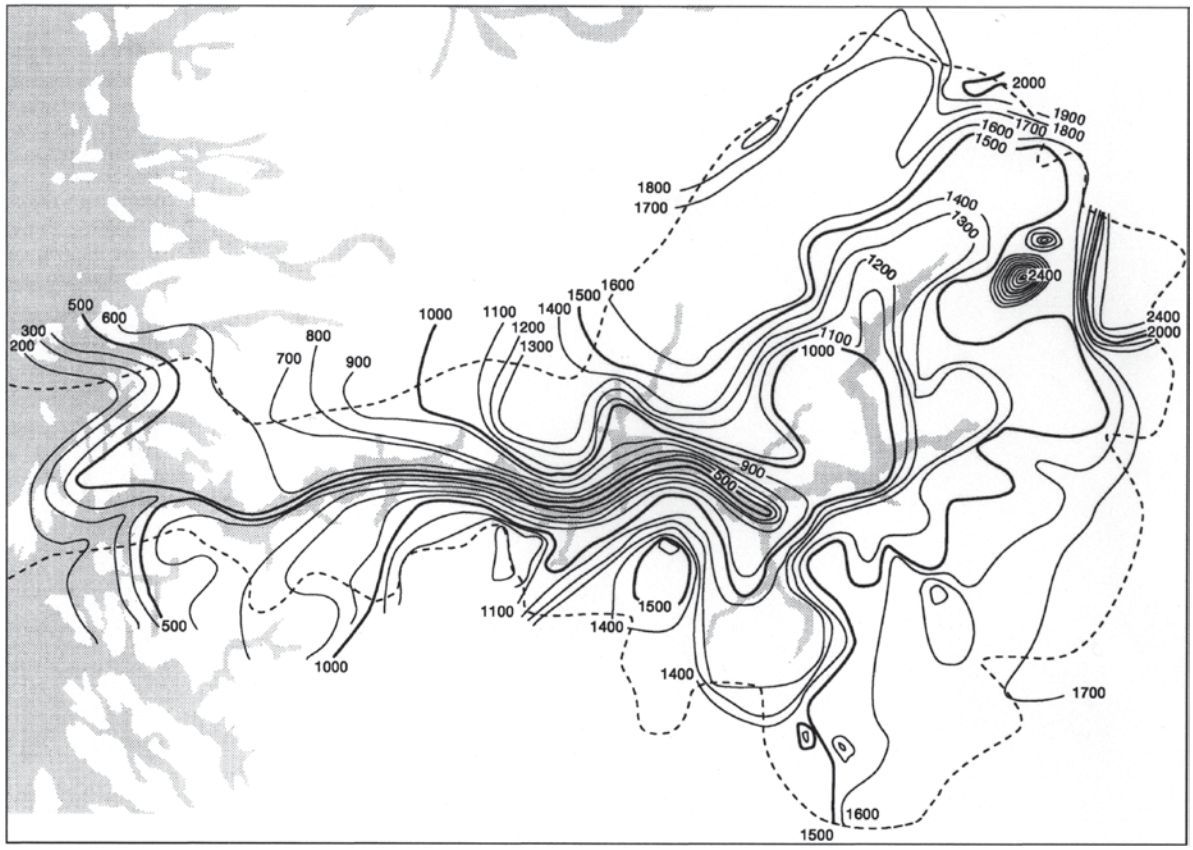

Fig. 23.9 Reconstruction of the preglacial landscape in the Sognefjord drainage basin (Adapted from Nesje and Whillans 1994)

narrow western part, similar to the modern shape. Commonly the fjord sides above the sea level are less steep than the submarine part. This is most likely due to subaerial weathering, denudation, and mass wasting processes. Almost all the regolith has been removed from this surface. However, some of the preglacial land surface escaped glacial erosion.

In the coastal part of Sognefjorden, an undulating rock surface close to the modern sea level exists, belonging to the Norwegian strandflat. The latter is a composite feature, broadly planar and parallel to the coastline, most likely formed by a combination of wave action, subaerial denudation, frost wedging, and glacial erosion.

The fjord walls along Sognefjorden are dissected by minor V-shaped valleys and gorges (Fig. 23.8). Based on their form and size, Nesje and Whillans (1994) suggested that these must have formed by fluvial downslope action and rock fall, rock-avalanche and colluvial transfer, not only during the present interglacial (Holocene), but also during previous interglacials/interstadials. They indicate that such processes have been active during interglacials/interstadials despite the glacial influence in the fjord landscape. So, how could glaciers, on the one hand, carve out deep fjords, and on the other, not erase the gullies and deeper V-shaped valleys formed during previous interstadials/interglacials? In the present interglacial, the most important means of downslope movement are rockfalls, rock and snow avalanches, debris flows, and slope wash. These processes have formed avalanche alluvial fans along the valley sides and on the fjord bottom. This material is removed during glaciations by glaciers and ice streams (Fig. 23.10). Thus, the long-term evolution of Sognefjord, summarized diagrammatically by Nesje and Whillans (1994) (Fig. 23.11) involved four major phases: (1) Erosion and denudation during the Mesozoic and early Cainozoic, forming the preglacial surface close to sea level at that time;

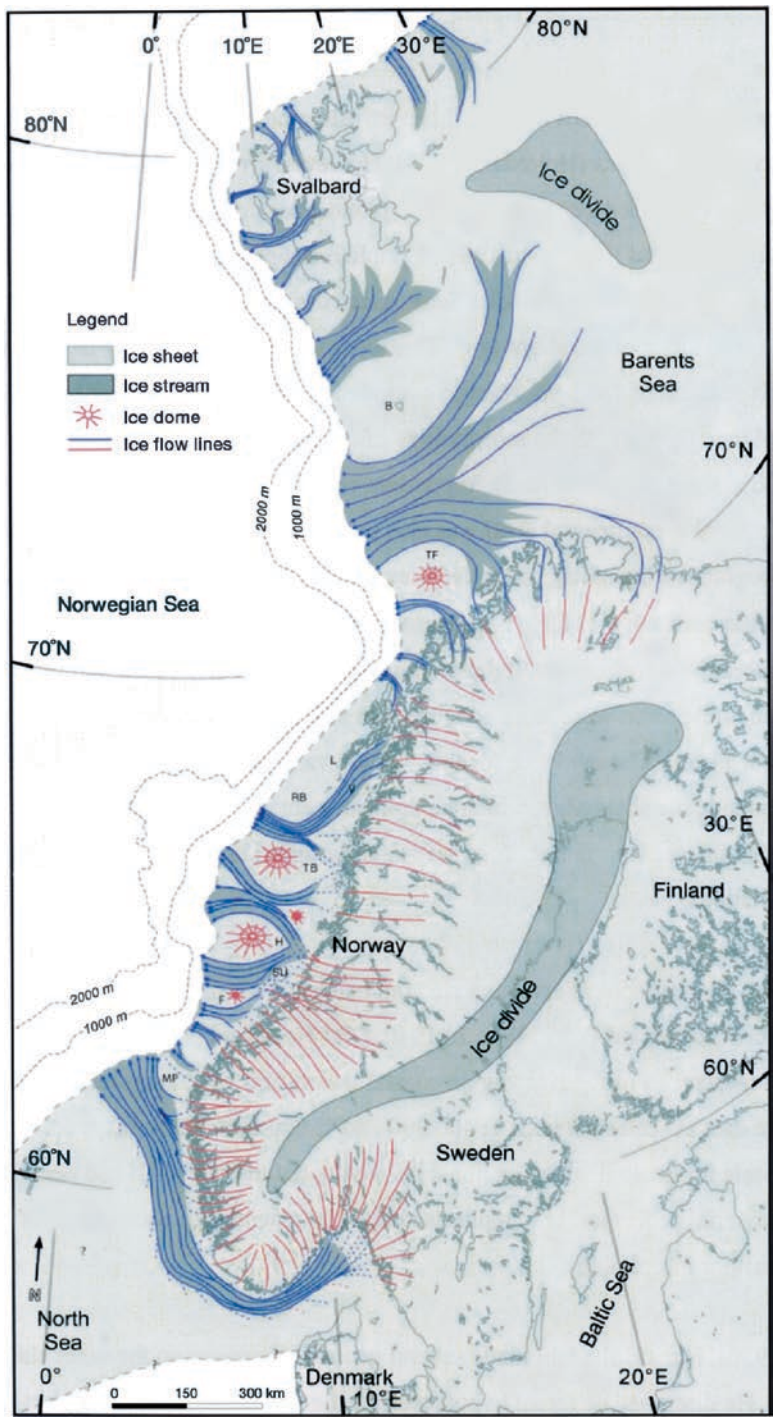

Fig. 23.10 Location of Late Quaternary ice streams along the coast of western Scandinavia (Adapted from Ottesen et al. 2005)

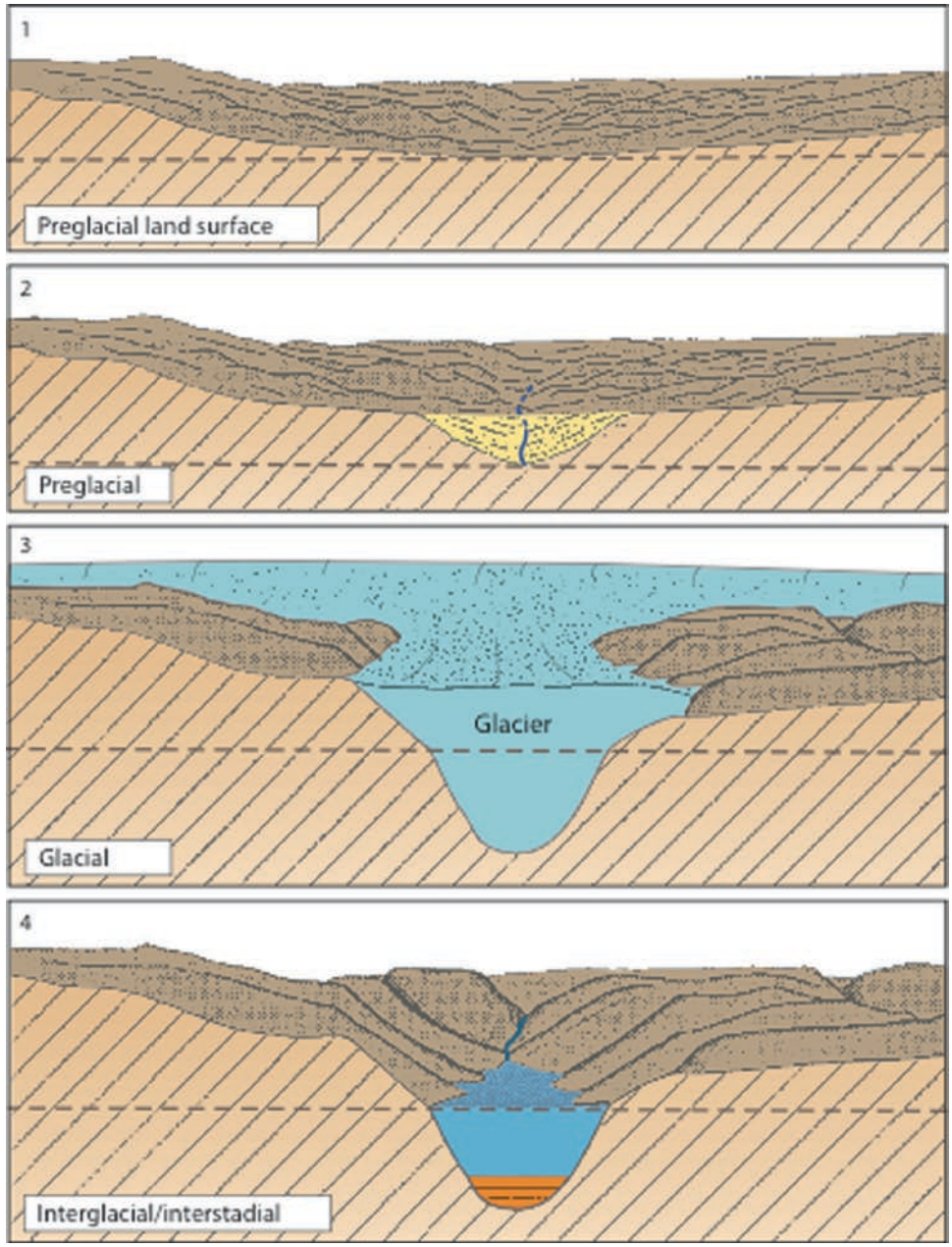

Fig. 23.11 Proposed history for the formation of Sognefjorden (adapted from Nesje and Whillans 1994). The horizontal dotted lines indicate the erosional basis

(2) Land uplift during the Cainozoic; (3) Successive Quaternary glaciations, and (4) Subaerial processes during Quaternary interglacials and interstadials.

The volume difference between the preglacial and present landscape in the Sognefjord drainage basin has been calculated to 5,400 km^3 (Nesje and Sulebak 1994). This volume of 5,400 km^3 eroded bedrock distributed over the Sognefjord drainage basin (12,518 km^2) yields an average vertical erosion in the Sognefjord drainage basin of 440 m. Supposing that the large-scale glacial erosion started at 2.57 million years ago, based on the first appearance of ice-rafted detritus in the Nordic Seas (Jansen and Sjøholm 1991), the average erosion rate was 17 cm/1,000 years (0.17 mm/year).

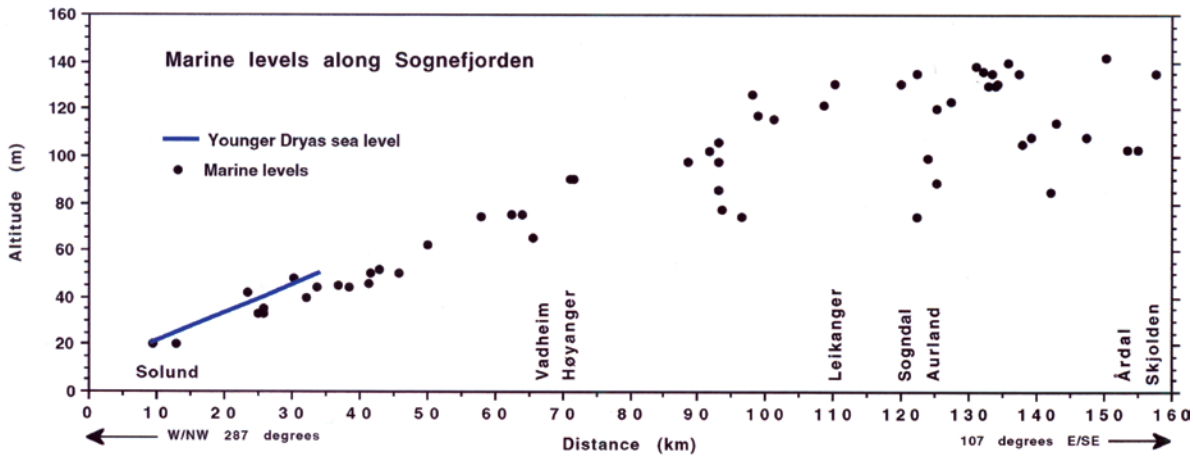

Fig. 23.12 Marine levels along Sognefjorden. The profile is oriented 107°E-SE/287°W-NW, perpendicular to the Younger Dryas isobases at the coast. The Younger Dryas sea level in the outer fjord region is from Aarseth and Mangerud (1974). The data have been collected by Eivind Sønstegaard at Sogn og Fjordane Regional College, Sogndal, and the author from different sources and field observations. For locations, see Fig. 23.5

Supposing further that glacial erosion was active in a period of 1 million years during the last 2.57 million years, the average glacial erosion rate in the Sognefjord drainage basin was about 40 cm/1,000 years (0.4 mm/year), close to erosion rates below modern glaciers. A mean maximum glacial erosion rate calculated for the region of maximum relief along Sognefjorden is estimated as 4.75 mm/year.

During the Late Cainozoic glaciations, Scandinavia was depressed isostatically. During deglaciation periods the land mass lifted isostatically relative to the sea level. Figure 23.12 shows marine levels (MLs) formed immediately after the Late Weichselian and early Holocene deglaciation of Sognefjorden. The MLs in the outer fjord region (between Solund and Høyanger) form apparently a straight line (gradient of ~ 1.2 m/km), indicating that they were formed more or less simultaneously immediately after the Younger Dryas. In the inner Sognefjord region, however, lower (and younger) marine levels were formed when the different tributary fjords and valleys were deglaciated, most likely during the Early Holocene.

23.5 Conclusions

Fjords are located along continental margins occupied by late Cainozoic ice sheets. Fjords are commonly several 100 m deep and may extend many tens of kilometers inland. Ice sheets mainly drain through fjords. Because rivers do not erode below sea level, the submarine part of the fjords must have been formed by glacial erosion. A fjord is considered a long, narrow estuary with steep sides, made when an over-deepened glacial valley was flooded by the sea.

The western part of Fennoscandia has a rugged, highly dissected coast with numerous islands, skerries, sounds, and fjords. Norway is therefore sometimes called the 'Land of fjords'. This landscape is considered among the most scenic landscapes on Earth. Geirangerfjorden and Nærøyfjorden in western Norway therefore found their place on the UNESCO World Heritage List on 14th July 2005.

During the Mesozoic and early Cainozoic, the Norwegian landscape was eroded to an undulating surface called the paléic (='old') surface developed at sea level at that time. During the early Cainozoic, the crust was lifted asymmetrically. The highest uplift was along the central mountain range in Scandinavia, associated with the opening of the Nordic Seas. The paléic surface can be observed along Sognefjorden as summits and plateaus. River valleys were formed in the paléic landscape during and after the land uplift. The summits, plateaus, and preglacial river valleys form the basis for the reconstruction of the preglacial land surface.

The volume difference between the preglacial and present landscape in the Sognefjord drainage basin has

been calculated to 5,400 km^3, yielding an average vertical erosion in the Sognefjord drainage basin of 440 m.

The Author

Atle Nesje is Professor at Department of Earth Science, University of Bergen and affiliated professor at the Bjerknes Centre for Climate Research in Bergen. His research concerns Quaternary geology, physical geography, glaciology, glacial history, paleoclimatology, geomorphology, and lake sediments. He has published 106 papers in international peer-reviewed scientific journals, 2 books, 22 book chapters, 47 popular science articles, and presented 174 conference papers. He has been involved in a number of national and international research projects and is an Associate Editor of *The Holocene*.

Acknowledgments I thank Eivind Sønstegaard for providing marine-limit data along Sognefjorden and Jane Ellingsen for preparing the figures. This is publication no. A 200 from the Bjerknes Centre for Climate Research.

References

Aarseth I, Mangerud J (1974) Younger Dryas end moraines between Hardangerfjorden and Sognefjorden, Western Norway. Boreas 3:3–22

Andersen BG, Nesje A (1992) Quantification of Late Cenozoic glacial erosion in a fjord landscape. Sver Geol Undersök Ca 81:15–20

Corner G (2005) Atlantic coast and fjords. In: Seppälä M (ed) The physical geography of Fennoscandia. Oxford University Press, Oxford, pp 203–228

Doré AG (1992) The base tertiary surface of southern Norway and the North Sea. Norsk Geol Tidsskr 72:259–265

Gjessing J (1966) Some effects of ice erosion on the development of Norwegian valleys and fjords. Norsk Geogr Tidsskr 20:273–299

Gjessing J (1967) Norway's paléic surface. Norsk Geogr Tidsskr 21:69–132

Gregory JW (1913) The nature and origin of Fjords. John Murray, London

Holtedahl H (1967) Notes on the formation of fjords and fjord valleys. Geogr Ann 49A:188–203

Holtedahl H (1975) The geology of Hardangerfjord. Norges geol undersøk 323:1–87

Jansen E, Sjøholm J (1991) Reconstruction of glaciation over the past 6 Myr from ice-borne deposits in the Norwegian Sea. Nature 349:600–603

Kessler MA, Anderson RS, Briner JP (2008) Fjord insertion into continental margins driven by topographic steering of ice. Nature Geoscience. doi:10.1038/ngeo201: 1-5

Nesje A, Sulebak J (1994) Quantification of late Cenozoic erosion and denudation in the Sognefjord drainage basin, western Norway. Norsk Geogr Tidsskr 48:85–92

Nesje A, Whillans IM (1994) Erosion of Sognefjord. Geomorphology 9:33–45

Nesje A, Dahl SO, Valen V, Øvstedal J (1992) Quaternary erosion in the Sognefjord drainage basin, western Norway. Geomorphology 5:511–520

Ottesen D, Dowdswell JA, Rise L (2005) Submarine landforms and the reconstruction of fast-flowing ice streams within a large Quaternary ice sheet: The 2500-km-long Norwegian-Svalbard margin (57°-80°N). Geol Soc Amer Bull 117:1033–1050

Riis F (1992) Dating and measuring of erosion, uplift and subsidence in Norway and the Norwegian shelf in glacial periods. Norsk Geol Tidsskr 72:325–331

Sigmond EMO, Gustavson M, Roberts D (1984) Bedrock Geology Map over Norway. Scale 1:1 Million. Geological Survey of Norway

Syvitski JPM, Shaw J (1995) Sedimentology and geomorphology of fjords. In: Perillo GME (ed) Geomorphology and sedimentology of estuaries. Developments of Sedimentology, vol 53. Elsevier, Amsterdam, pp 111–178

Troll C (1957) Tiefenerosion, Seitenerosion und Akkumulation der Fluesse im fluvioglazialen und periglazialen Bereich. Petermanns Geogr Mitt Erg 262:213–226

Chapter 24
Iceland: Glaciers and Volcanoes in the North Atlantic

W. Brian Whalley

Abstract This chapter provides an overview of the geology and geomorphology of Iceland. The position of Iceland on the Mid-Atlantic Ridge determines the volcanic geomorphology including shield volcanoes, lava flows, and the distinctive "moberg" mountains resulting from subglacial eruptions. The maritime location gives rise to large glacier systems in the mountains of the southeast of the island with much smaller valley glaciers in the drier north. The complex coastline shows steep cliffs, especially in lava flows, but large and complex spit–barrier beach systems occur, particularly in the southeast.

Keywords Basalt • coasts • glaciers • Iceland • Mid-Atlantic Ridge • mountains • slopes • volcanoes • weathering

24.1 Introduction

In few other places do geomorphology and geology link to produce varied and spectacular scenery as closely as in Iceland and where they are intermingled with its existence, culture, and economy. Iceland has surprisingly diverse landforms although there are clearly some that cannot be found by virtue of its brief geological history and geographical location. This chapter provides an overview of Iceland's geomorphology within the most important geological setting and introduces some landforms and features that are well exemplified. In particular, the interplay between volcanic rocks, volcanoes and geothermal activity, water, and ice are at the center of much of Iceland's geomorphology (Thorarinsson et al. 1959).

24.2 Geographical and Geological Setting

Iceland is an island of some 100,000 km^2 in the middle of the North Atlantic between Greenland and Norway (Fig. 24.1). It is almost all south of the Arctic circle with its southernmost limits (the Vestmann Islands; Vestmannaeyjar) at 63°28′ and between 13°30′ and 24°30′W. Iceland sits astride the North Atlantic Ridge system, the Reykjanes Ridge from which it has been developing over the later Cenozoic era (Fig. 24.2). As such, the main rocks are lavas (of various types), intrusive igneous rocks, and sedimentary rocks. For the most part, the Neogene-Quaternary basalts provide the most spectacular scenery. The Quaternary sediments are particularly associated with glaciation and associated processes (Einarsson 1994). The prevailing winds are moist and, with winters providing several months with snow, glaciers are present on the highest ground. These include Vatnajökull, covering about 8,000 km^2 and highest point Öræfajökull (2,110 m) at its southern extent. There is a decrease in precipitation northwards and glaciers in the north are small valley and have only small corrie glaciers at the present day and parts of the island's interior have a mean annual precipitation less than 600 mm.

24.3 Rift Spreading, Volcanic Rocks and Lavas

The Neogene Lava Province of the North Atlantic includes flows in Northern Ireland, Scotland, Faeroe Islands, Greenland, and Baffin Island. They were formed by seafloor spreading associated with the separation of

P. Migoń (ed.), *Geomorphological Landscapes of the World*,
DOI 10.1007/978-90-481-3055-9_24,

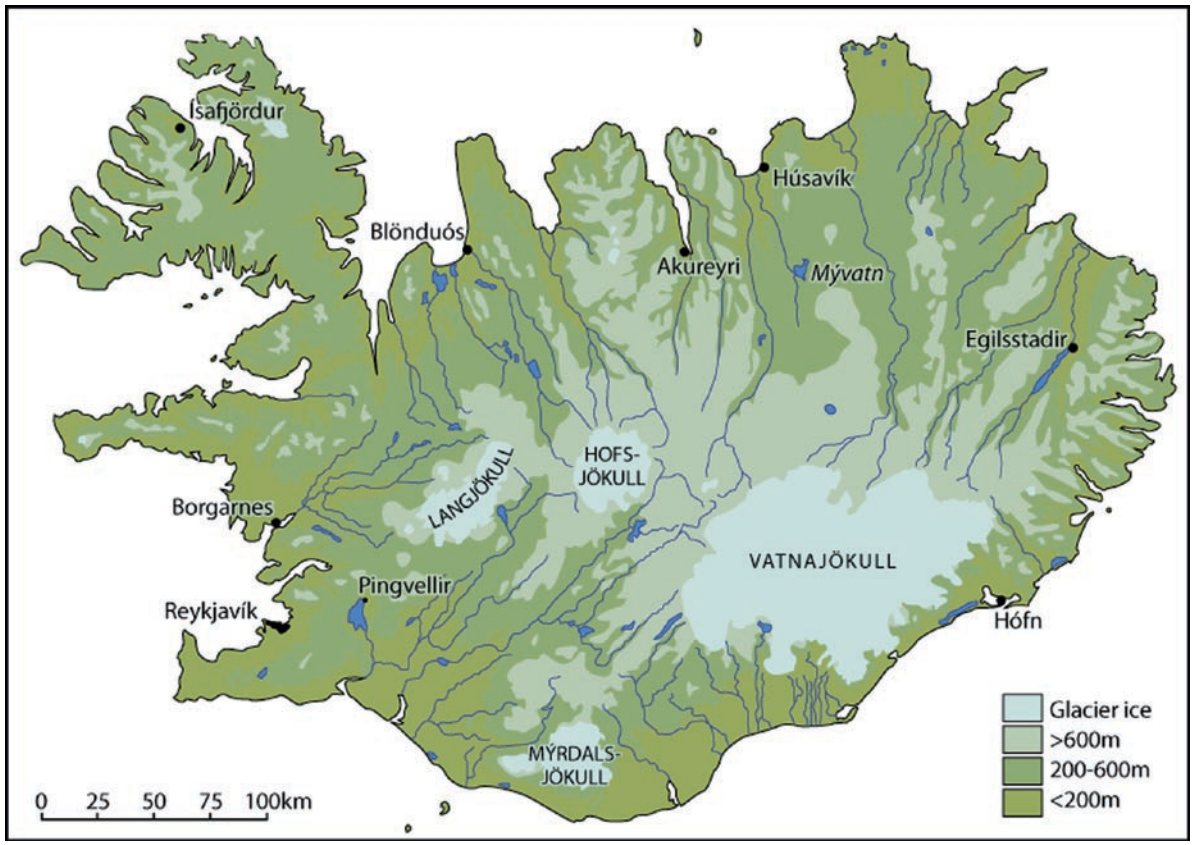

Fig. 24.1 Topographic map of Iceland

European and Atlantic plates (Fig. 24.2). In Iceland, these lavas are found on the western and eastern margins of the island separated by the inverted Y shape of the main rifting zones astride the Mid-Atlantic Ridge (Fig. 24.3). Within the flow areas lie shield (early Holocene) and central volcanoes (no longer active). Central volcanoes are generally buried below the lava pile of flood eruptions. Occasional Holocene volcanic activity has occurred through the lavas. The most catastrophic of these were the Laki fissure eruptions of 1783–1784. Laki is near Kirkjubæjarklaustur in the Skaftafell National Park (Fig. 24.2). The fissure was about 25 km long, with different sections erupting at different times. Although lava was erupted (estimated 15 km^3), tephra also was emitted (0.9 km^3), some of this being blown to the British Isles (giving the "sand summer" of 1783). Emitted gases killed both crops and animals and produced deaths by starvation in Iceland (estimated as 10,000 people, about 20% of the whole). Gases were also directed over the British Isles and continental Europe with resultant mortality recorded in several cities. Lava fissure eruptions are rather rare, but some occurred in 1975–1984 in the Krafla area near Mývatn.

Non-fissure eruptions also occur from time to time, most notably Hekla (the earliest recorded in 1104, but most recently in 2000) and Katla (notably 1755, last in 1918), while Askja had a major eruption in 1875 after a long dormant period. The well-known off-shore eruption was that of Surtsey in 1964. It was once considered that Icelandic volcanoes were active if they had erupted after the "Settlement" (Landnám, year 874) but in 1973 Eldfjell in the Vestmannaeyjar erupted, although the previous eruption was thought to be some 5,000 years before. The definition has now been changed so that any volcano that has erupted in the last 10,000 years is considered "active."

Some 90% of all igneous rocks in Iceland are basalts, but other rock types include ignimbrites (welded tuffs), rhyolites, and gabbros. Postglacially erupted magma gives two main types of basalt, tholeiitic (alkaline-poor), and alkaline series. Olivine tholeiite is

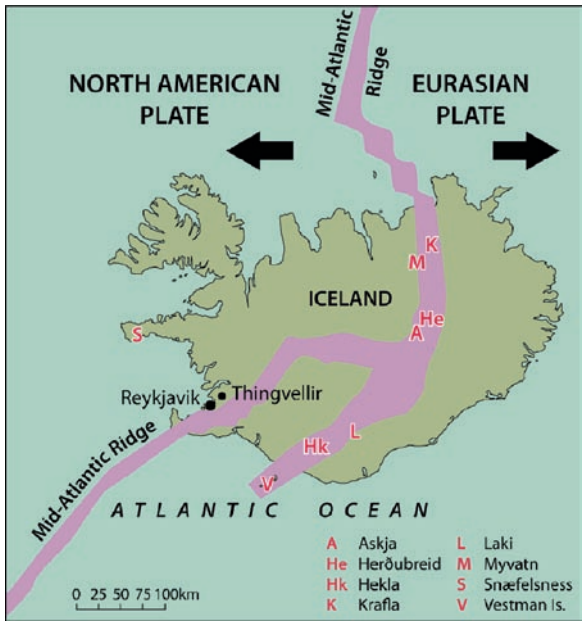

Fig. 24.2 Schematic map of Iceland showing the Mid-Atlantic Ridge and some of the major volcanic locations mentioned in the text

generally associated with shield volcano eruptions. Dykes (sills are rare) of various compositions are very common and may be of several kilometers length. Some dykes or sets of dykes can be distinctive landforms because of their length and thickness. Unsurprisingly, they are frequently aligned parallel to the rifting direction in the country.

24.4 Volcanic Landforms

Without delving too deeply into igneous petrology and volcanology we can recognize several geomorphological forms (Thorarinsson et al. 1959; Einarsson 1994). The greatest areal extent of volcanic activity is not a prominent peak but the areas of flood basalts (hraun) that cover much of the island. Stratovolcanoes (composite, of lava and tephra) can be seen in roughly circular form as Snaefellsjökull in western Iceland and in elongate form as Hekla. Shield volcanoes are built of flood basalts and the best example is Skjaldbreiður ("broad shield," Fig. 24.4) near Iceland's

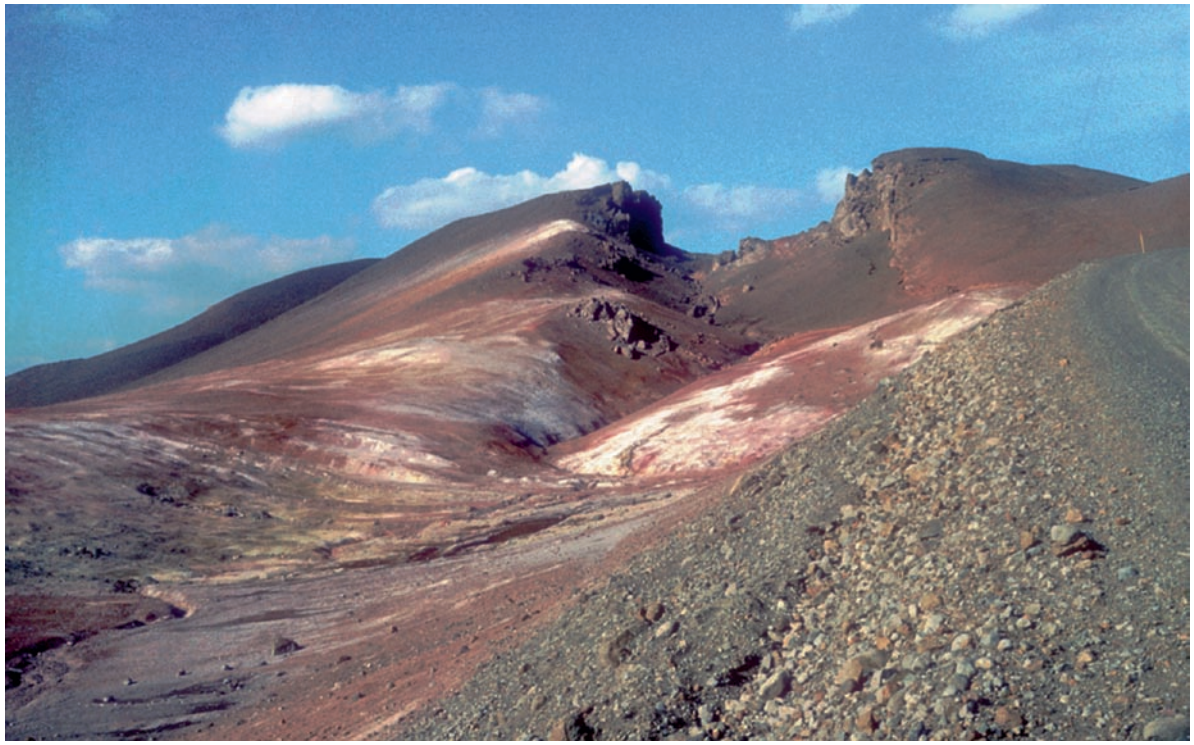

Fig. 24.3 Ridge spreading center, Námafjall, Mývatn area. The bright colors are due to geothermal alteration of minerals (Photo W.B. Whalley)

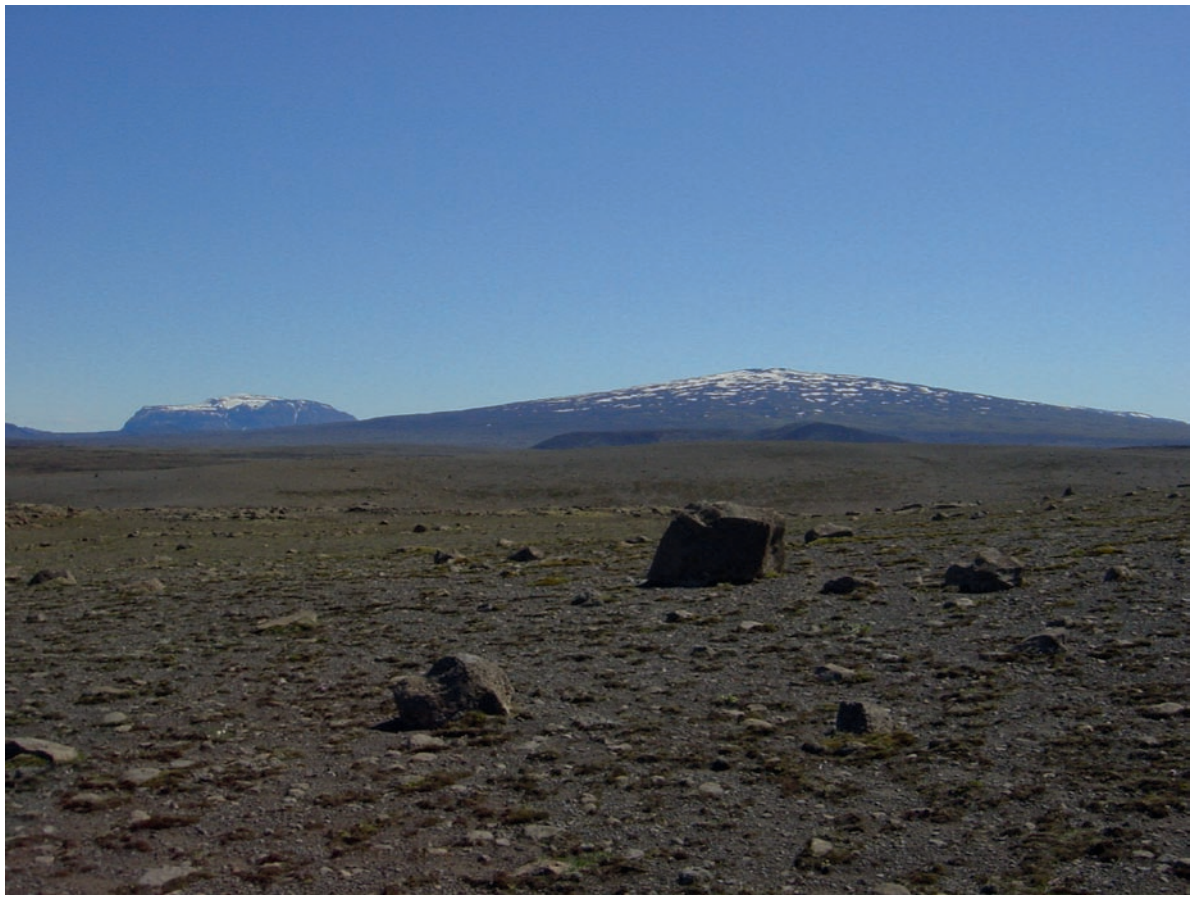

Fig. 24.4 The shield volcano Skaldbreiður, with Hlöðufell left in distance (Photo courtesy G.R. Douglas)

largest lake, Ţingvallavatn. It reaches 1,060 m, some 800 m above the surrounding lavafields and has a crater. Surtsey can be considered as a small shield volcano. Skjaldbreiður is a little north east of Ţingvellir (Thingvellir) where the original Icelandic parliament (Althing) was founded in 1930. The location shows distortion and rifting of the lavas from the shield volcano with the lineation of rifting parallel to the rifting of the Mid-Atlantic Ridge arm.

Tephra cones and craters also occur in Iceland, sometimes individual or elongate along a fissure line. An explosive crater is Graenavatn near Krýsuvík on the Reykjanes peninsula, some 30 km southwest of Reykjavik. One of the best examples is Ludent in the Mývatn area near Hlíđarfjall, a rhyolite mountain and the Hverfjall crater. The Mývatn area provides good examples of active minor volcanic landforms such as mud pools, fumaroles, and in the same area Dimmuborgir has lava pillars and drained lava tubes in the Younger Laxa lava.

One rather special geomorphic and volcano type is Móberg Mountains (Fig. 24.5). Móberg ("brown rock") is a distinctive rock type, not only because of its color, but also due to its subglacial formation. It is an altered subglacially injected ash (hyaloclastite) associated with altered glass (palagonite), hence these are termed palagonite tuffs or breccia. The distinctive table-top mountain landform (stapi) is associated with these subglacial eruptions; Móberg Mountains are no longer volcanically active in Iceland. They have flattened tops and steep, free-face profiles, and talus slopes below and result from eruptions below Late Pleistocene ice sheets. As such, they are rather rare in the world but others occur in British Columbia and the USA. (The name "tuya" is sometimes applied to the Canadian examples, after Tuya Bute, but the term is not Icelandic.) A good

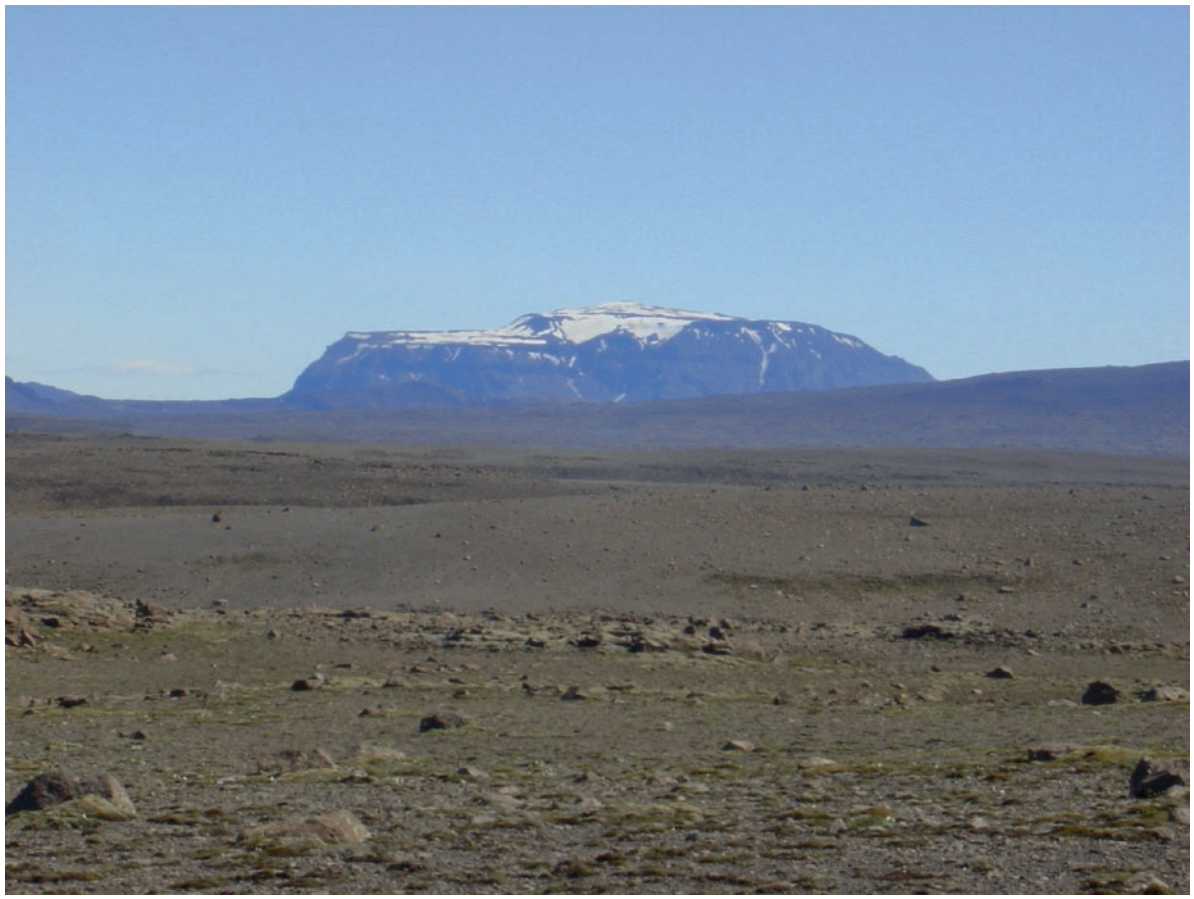

Fig. 24.5 Moberg mountain, Hlöðufell, with a typical lava desert in the foreground (Photo courtesy G.R. Douglas)

example is Herðubreið in the interior lava fields to the north of Vatnajökull. Some móberg ridges form strong lineaments rather than table-topped mountains.

24.5 Glacial Geomorphology

24.5.1 Glaciers of Southeast Iceland and Their Associated Landforms

Glaciers (Icelandic, jökull) are a notable part of the Icelandic scenery, especially in the southeast (Fig. 24.6) although various sizes of ice body occur, precipitation being modulated by altitude and latitude. The largest glacier, Vatnajökull (8,300 km^2), with its many distributory glaciers presents an imposing view from the Ring Road in the south of Iceland although northerly outlets are more difficult to reach. Vatnajökull has been depth profiled by ice radar for temperate glaciers (largely developed in Iceland) and is generally 600–800 m thick and up to about 1,000 m height at Skeiðararjökull near Grímsvötn (Björnsson 2003). Ice from the main cap is distributed radially by subglacial valleys cut into bedrock. The main southern outlet of Vatnajökull, Breiðamerkurjökull, has been used as a site for several investigations of moraine formation (e.g., Kruger 1993). Maps have been made of sections of Breiðamerkurjökull and the associated sandur (glacial outwash plains; plural: sandar) (Evans and Twigg 2002). These show a wide variety of glacial and glacio-fluvial landforms (Fig. 24.7), as well as changes that have occurred over the years (Evans et al. 1999). Other (wet-based) outlet glaciers Skeiðararjökull, Falljökull (of Öraefajökull), and Sollheimerjökull (of Mýrdalsjökull) have been used as geomorphological

Fig. 24.6 Kötlujökull outlet of Myrdalsjökull, with moraine ridges around and the sea beyond Myrdalssandur, South Iceland (Photo W.B. Whalley)

investigation areas over the years. Mainly, these investigations have been used as a means of providing present-day analogues for past glacial events and landforms. Some of the glaciers in Iceland are known to surge or produce surge-like behavior. A good example is Brurajökull (NE Vatnajökull), which shows "concertina eskers" surged 8 km over the winter of 1963–1964 culminating in a snout movement of some 25 m in a day. It is known to have surged in 1750, 1810, and 1890. The large frontal moraines of this glacier were produced during this last advance. Structures in sediments at Eyjabakkajökull are thought to be due to glacier surging (Sharp 1985). Other outlet glaciers known to have surged include Dyngjujökull (1934, 1951), Tungnárjökull (1945), and Siðujökull (1994).

There are other major glaciers in southeast Iceland as well as Vatnajökull; Langjökull (950 km^2, Fig. 24.8), Hofsjökull (900 km^2), and Mýrdalsjökull (600 km^2). Drangajökull (150 km^2) in northwest Iceland has decayed and thinned rapidly from its Little Ice Age maximum. This is also true of the small ice cap to the south of Langjökull known as Ok.

24.5.2 Jökulhlaups

A distinctive aspect of present-day Iceland glaciology is the proximity of large ice bodies and volcanic activity. Ice is melted and the water produced is stored at the base of the glacier system until the pressure exerted cannot be sustained by the glacier and water escapes down the pressure gradient (Björnsson 2003). Once initiated the outburst continues until all the water has escaped. The name jökulhlaup has traditionally been given to these events. The Icelandic word "hlaup" means to leap or run and probably refers to the glacier characteristic of producing a mini-surge before the main discharge, the glacier essentially having high sliding activity. Other terms used for these events are "self-dumping lakes" and "glacier lake outburst flood" (GLOF). Jökulhlaups are found coming from several glaciers with Vatnajökull or Mýrdalsjökull as their source. The most famous jökulhlaups are those from Grímsvötn and Katla. Peak discharges for the latter may be as high as 200,000 m^3 s^{-1}. Grímsvötn has filled and emptied at relatively regular periods of 4–5 years, although less regularly of recent years. The tractive effort available in such floods is seen in the movement of large boulders (Magilligan et al. 2002) or the removal of road bridges but damage is by no means always a consequence of a jökulhlaup.

24.5.3 Glaciers and Rock Glaciers in Tröllaskagi, North of Iceland

Tröllaskagi, the mountainous area to the west of Akureyri, has a few isolated peaks, such as Kerling (1,536 m), with radiating glaciers but is predominantly a lava pile plateau (>900 m) with corrie glaciers and cut by deep valleys (Fig. 24.9). Most glaciers are less than 1 km long due to the south–north

Fig. 24.7 Complex moraine ridge systems at the snout of Fjallsjökull (*right*) with buried ice mounds beyond, Õræfajökull (Photo W.B. Whalley)

Fig. 24.8 South-flowing outlet glaciers from Langjökull, west-central Iceland; lava desert in foreground (Photo W.B. Whalley)

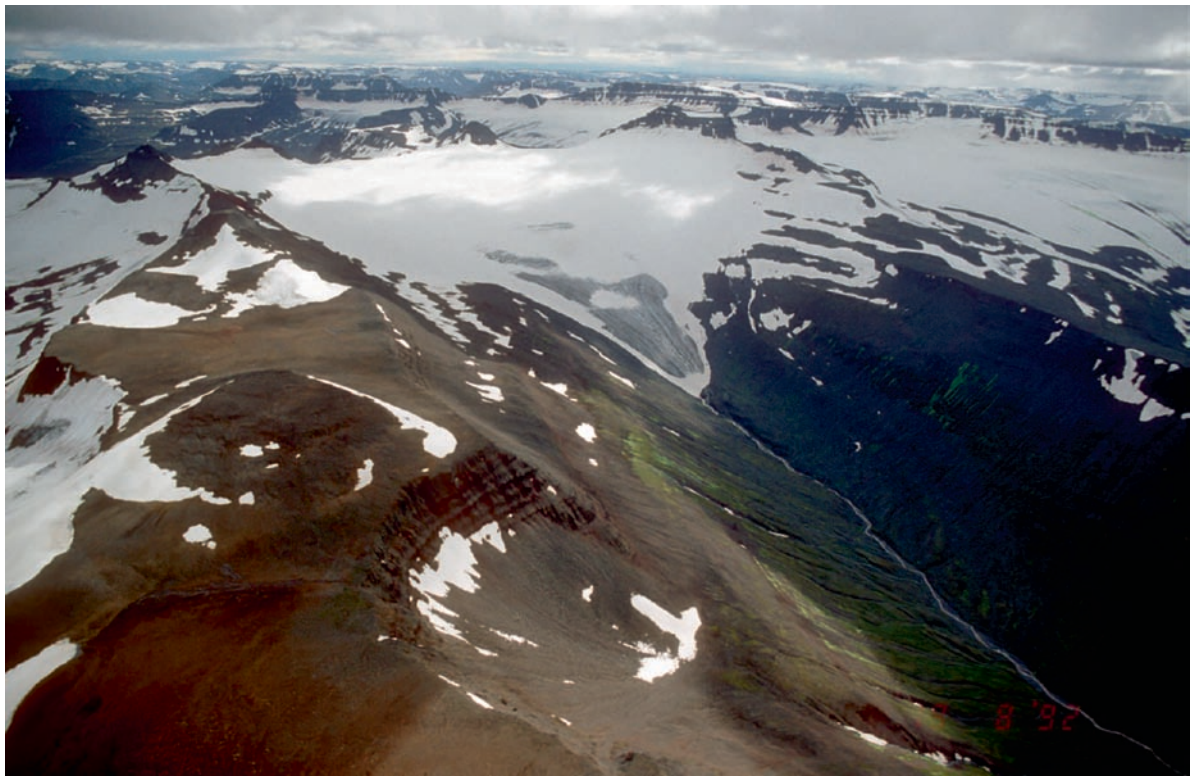

Fig. 24.9 Dissected plateaux and glaciers in Tröllaskagi, North Iceland; one of the longer glaciers, Bægisarjökull, is in the center (Photo W.B. Whalley)

precipitation gradient. Glaciers may have eroded these valleys, but it is not known what weathering and fluvial activity preceded the onset of glaciation or whether they are remnants of more extensive ice sheet.

Rock glaciers were discovered in Iceland in the 1970s, rather surprisingly as it was generally considered that these forms were only found in dry continental areas and not in wet, temperate glacial conditions. This reasoning followed from the model of rock glacier formation due to permafrost activity. Ice-rich weathered rock debris is thought to creep and produce the characteristic flow-structures of rock glaciers and low velocities (generally <1 ma^{-1}). However, glacier ice exists in several rock glacier features in Tröllaskagi (North central Iceland) that are below expected permafrost limits. The "glacier model" of rock glacier formation explains that glacier ice, seen in the corries (cirques) can become covered by rock debris of sufficient thickness to preserve the ice by cutting ablation down to a few percent of the uncovered rate (Whalley and Azizi 2003). Thus, a glacier wanes slowly under its cover and thins but the velocity falls as a consequence.

24.6 Periglacial and Permafrost Activity and Associated (Sorted Ground) Landforms

The lava fields (hraun, Fig. 24.5) are generally sparsely vegetated, even at low latitudes, so permafrost is thought to exist only where there is a thick enough soil but with thin vegetation in the drier interior, altitudes above about 500 m, and where snowfall comes late enough to allow ground freezing to take place and be preserved year on year. There are no major features attributed to permafrost activity other than where ice is found in flattened domes known as palsa, which contain lenses of ice. These features are found in palsa bogs in the interior, especially north of Langjökull. Needle ice can often occur in soils and sorting of soils

to give frost heaving forms such as sorted stone circles a meter or so in diameter can be found in flat places bare of soils. Where the ground is steeper they occur as sorted stone stripes. Sorted stone circles are common on the high plateaux of Tröllaskagi where winds keep snow cover to a minimum. At lower ground, thick soils with vegetation form thufur, grassy hummocks, formed during seasonal freezing periods. They can probably exist for many years and require only occasional freezing periods to reactivate and grow.

Although not specifically periglacial, it is worth mentioning that there are considerable soil erosional problems in Iceland. This is due to the presence of loess or sand blown sediments, often due to deforestation or overgrazing during the "Settlement" (Landnam) phase of Icelandic history. It has been suggested that up to half of the soil removal of Iceland has been anthropogenically triggered. Actual erosion is, for the most, part by strong winds. Tephrochronology has been particularly important in establishing the extent and degree of erosion (Dugmore and Buckland 1991). Like strong winds removing and redepositing soils, concentrated runoff also leads to soil removal and sandy desert conditions are found in the relatively dry interior (Arnalds et al. 2001).

24.7 Coastal Perimeter

With such a long perimeter, approximately 5,000 km, indented by fjords and bays, Iceland has a very varied coastline. Of particular note are the places where glacial sedimentary outwash comes to the coast. The outwash plains (sandar) of outlet glaciers of Vatnajökull are especially significant. The coast between Ingólfshöfði and Hvalnes, has several high, wide coast-aligned barrier beaches. At Höfn, about two thirds along this stretch, the combined rivers from Hoffellsjökull and Fláajökull flow into a large lagoon (Hornafjörður) and are deflected to an outlet to the south of the town where there are recurved spits. The capital, Reykjavík, sits on a barrier beach with the lake (Tjörn) being the lagoon behind. Other towns, such as Akureyri, are also built on spits or barriers. Because the high ground of the lava piles and plateau comes so close to the sea in many places the cliff line of Iceland is often spectacular. The fjord areas around the east (Höfn to Egilstaðir) and the northwest (Ísafjörður) are especially notable. In some cases the rock (especially móberg) is relatively easy to erode. Sea-level changes have left an imprint on the coast of Iceland, and wave-cut platforms can be seen in many places as can wave-cut cliffs tens or even hundreds of meters high (often identified by the name bjarg). Land uplift has been rapid enough to provide good exposures of glacial or glaciomarine sediments in many places. Gilbert-type deltas show the sediment movement from glaciated valleys and provide good sources of gravel for building.

24.8 Landslides and Mass Movements

Mountains and plateau sides are steep in most places, generally cut into the lava piles. Because the flows are generally distinct and nearly horizontal, slopes are frequently stepped and may show distinctive red-brown intra-basaltic layers. In general, therefore, the rocks are friable and so rather prone to a variety of mass movements. Impressive scree round many mountain and cliff slopes show this propensity for block and stone fall. This is exacerbated by "freeze-thaw" and water pressure conditions, although the properties of the basalts make them liable to chemical weathering along the many joints, cracks, and microcracks. The rock glaciers of Tröllaskagi are related to this availability of rock debris, which covers small glaciers that are insufficiently thick to remove them. Especially in spring, numerous debris slides are produced by the generation of high pore water pressures in slopes. Slide tracks on screes or rocky slopes do not seem much when viewed from a distance, but from close at hand boulders a meter or more in size mixed with finer material and water show considerable present-day activity! Some villages situated on the coastal strip between the steep rock walls and the sea are prone to damage by rockfalls, debris slides, and avalanches. In some cases, earthworks have had to be built to protect buildings as villages have expanded away from the coast.

On large scale, hundred of thousands or millions of cubic meters, are rockslides (berghlaup, Fig. 24.10). Many of these have been mapped and categorized by Olafur Jonsson (Whalley et al. 1983). Their location is often at ridge end and might be related to glacial trimming. However, other falls occur mid-ridge and all are probably related to groundwater conditions in the Postglacial, when many were formed. In bulk, basalt

Fig. 24.10 Berghlaup in basalt pile, Tröllaskagi, North Iceland. The scar is very distinctive for mid- and ridge-end locations (Photo W.B. Whalley)

piles are rather friable, so once a rockslide is initiated there tends to be a collapse and slump of the cliff rather than producing an airborne flow. In some cases, berghlaup have been misinterpreted as rock glaciers but identification of a tell-tale scar above shows the true origin.

24.9 Rivers and Lakes

Because of the high precipitation and snow/glacier melt, many rivers, especially in spring and early summer, are formidable undertakings for crossing, even by four-wheel drive vehicles. The rivers on the outwash plains of southern Iceland are particularly difficult to cross because of their wide, braided nature. The ring road was only fully completed in 1974 with bridges over the Skeiđará across the Skeiđarásandur to the south west of Öræfajökull. However, this was destroyed by a jökulhlaup in 1996. Rivers across the sandur in southern Iceland, which drain Vatnajökull are relatively short and, for the most part, flow across the extensive outwash plains of glacial sediments as the glacier termini are near sea level. Those rivers draining the north side across the interior plains are longer and drop much more in altitude. The longest river is the Jökulsá á Fjöllum and it cuts its way through the lava piles with a notable waterfall, Dettifoss, some way north of the ring road in the Jökulsá National Park. Other waterfalls, such as Gullfoss, Gođafoss, and Selfoss (Jökulsá á Fjöllum), are more easily seen from roads where they cut through lava piles. The Hvitá canyon, for example, is some 3 km long and was cut through the lavas during the Postglacial. Ţingvallavatn is the largest lake in Iceland and sits in the lava field of the south west. Mývatn ("Midge lake") is in the north in an area of active volcanic activity near to the village of Reykjahlið. The whole area is sometimes called Mývatn and includes the volcanic area, within which the lake was formed, and Late Glacial moraines.

24.10 Concluding Remarks

The necessarily brief review of the main aspects of the geomorphology of Iceland shows its diversity and complexity that is found in few areas of the world in such a small area. Glaciers and their sediments react with coastal process to produce barrier beaches and the juxtaposition of volcanic activity with glaciers giving Möberg Mountains in the past and jökulhlaups today is very special. If jökulhlaups and volcanic activity can be destructive, then glacial and volcanic sediments can be used for constructional purposes. Electricity is produced from hydroelectric and geothermal sources and geothermal hot water is supplied to Reykjavík and Akureyri while volcanic ash is used to make insulating building materials. Geology and geomorphology find practical applications in this unique island.

24.10.1 Visiting Iceland

Although geomorphologists may have a particular reasons for visiting Iceland, it would be something of a missed opportunity not to look at the wide variety of landforms and associated geology. This section provides a brief suggestion about the places to visit in a restricted time. Also the sites mentioned above the following include some important geomorphological locations together with those that produce spectacular scenery created by the geology and geomorphology. Car hire is expensive and the best way to travel is to use the circum-Iceland buses. These cover half the island in a day going both clockwise and anti-clockwise around the main bulk of the country. Buses also go to other coastal locations and internal air flights can also be made to remote areas such as Isafjörður in the northwest fjords. Tour buses may also be taken to the interior and specific locations such as Geysir and Ţingvellir. The circum-Iceland bus that follows Route 1 (Hringvegur) follows the rough perimeters of Iceland for about 1,340 km. Buses can be halted if you want to visit particular localities (although only stops for sightseeing at particular locations). However, you may break your journey anywhere and pick up the next bus, for example, Reykjahlið for the Mývatn area.

The Author

Brian Whalley teaches and researches at the Queen's University of Belfast where he is a Professor of Geomorphology. His main research areas lie in the behavior of small glaciers and rock glaciers, as well as in weathering studies. He has been Chair of the British Society for Geomorphology (formerly the British Geomorphological Research Group). In addition to his geomorphological and sedimentological research, he has an interest in teaching methods and e-learning and was awarded a UK National Teaching Fellowship in 2008.

References

Arnalds O, Gisladottir FO, Sigurjonsson H (2001) Sandy deserts of Iceland: an overview. J Arid Environ 47:359–371

Björnsson H (2003) Subglacial lakes and jökulhlaups in Iceland. Global Planet Change 35:255–271

Dugmore A, Buckland PC (1991) Tephrochronology and late Holocene soil erosion in South Iceland. In: Maizels JK, Caseldine C (eds) Environmental change in Iceland: past and present. Kluwer, Dordrecht, pp 147–159

Einarsson T (1994) Geology of Iceland: rocks and landscape. Mal og Menning, Reykjavík, Iceland

Evans DJA, Twigg D (2002) The active temperate glacial landsystem: a model based on Breiđamerkurjökull and Fjallsjökull, Iceland. Quat Sci Rev 21:2143–2177

Evans DJA, Lemmen DS, Rea BR (1999) Glacial landsystems of the southwest Laurentide Ice Sheet: modern Icelandic analogues. J Quat Sci 14:673–691

Kruger J (1993) Moraine-ridge formation along a stationary ice front in Iceland. Boreas 22:101–109

Magilligan FJ, Gomez B, Mertes LAK, Smith LC, Smith ND, Finnegan D, Garvin JB (2002) Geomorphic effectiveness, sandur development, and the pattern of landscape response during jökulhlaups: Skeiđararsandur, southeastern Iceland. Geomorphology 44:95–113

Sharp MJ (1985) "Crevasse-fill" ridges – a landform type characteristic of surging glaciers? Geogr Ann 67A:213–230

Thorarinsson S, Einarsson T, Kjartansson G (1959) On the geology and geomorphology of Iceland. Geogr Ann 41A:135–169

Whalley WB, Azizi F (2003) Rock glaciers and protalus landforms: analogous forms and ice sources on Earth and Mars. J Geophys Res Planets 108:8032. doi:10.1029/2002JE001864

Whalley WB, Douglas GR, Jonsson A (1983) The magnitude and frequency of large rockslides in Iceland in the postglacial. Geogr Ann 65A:99–110

Chapter 25
The Dead Sea Graben: Geomorphology of the Lowest Spot on Earth

Dan Bowman

Abstract The Dead Sea is a hypersaline, dense terminal lake, lying 422 m below sea level in the lowest continental depression on the Earth. The rift margins bear a rich record of lake terraces and additional markers of regressive beach lines. A successi on of telescopic alluvial fans progrades toward the lake, partly deeply dissected. Mount Sedom is an exposed head of an active, rising salt diapir, with a developed karst system. The young motions along the Dead Sea transform are indicated by a wide range of morphological field evidences, including spectacular soft sediment deformations. Nowadays the Dead Sea level is rapidly declining, making the area a unique natural field laboratory for studying, in real time, the processes of channel entrenchment and cross-sectional shape evolution.

Keywords Alluvial fans • base level • Dead Sea • lake terraces • morphotectonics • salt diapir

25.1 Introduction

The area around the Dead Sea in the Middle East is an extraordinary spot by global standards. The level of the Dead Sea Lake lies 422 m below sea level and is the lowest continental depression on the Earth. It has been mentioned in the story of Sodom, Gomorrah, and Jericho in the Old Testament (Neev and Emery 1995) and is described in the monograph of Neev and Emery (1967) and in the collections edited by Niemi et al. (1997) and Enzel et al. (2006).

The Dead Sea depression includes the southern Jordan Valley to the north of the lake and the northern Arava to its south (Fig. 25.1). The area is located between two broadly parallel, steep margins with imposing rock scarps. The main rift margin is on the eastern side, composed of the elevated mountains of Moab and Edom. The Dead Sea depression is a fault-bounded graben of the pull-apart, rhomb-shaped type. It is an intracontinental plate boundary (Fig. 25.2) between Arabia and the Israel plus Sinai subplates (Garfunkel 1981), part of the oceanic opening of the spreading Red Sea. The Dead Sea depression is controlled by horizontal, strike-slip faults, indicating a plate movement, which transfers the Arabia plate northwards, pushing it toward the Taurus collision zone in East Anatolia, Turkey. This left-lateral fault zone is named the Dead Sea Transform Fault and includes the famous 105 km of cumulative displacement (Freund et al. 1970).

Being located in the rain shadow of the Jerusalem-Hebron mountains (Fig. 25.2), the Dead Sea area is extremely arid with 50–100 mm mean annual precipitation. Drainage basins west of the rift reach up to 800–1,000 m a.s.l., with mean annual precipitation exceeding 600 mm. Mean temperatures at the Dead Sea range from 15°C in winter to 35°C in summer, whereas surface soil temperatures may reach over 50°C in summer. The mean annual evaporation rate from the Dead Sea ranges from 1.1 to 1.2 m and the annual humidity is 45–50%. Hydrological data show that the percentage of bedload in the wadis of the Dead Sea area and in the Arava is very high, amounting to 12–63%. Suspended matter also is very high, composing 3–5% of the flowing medium of big floods. However, in spite of the imposing work done during short flood events, the long-term mean annual load yield is low due to the long recurrence intervals of the ephemeral flash floods, which are of peaky hydrographs and last for very short periods, leaving the drainage system dry for more than 99% of the year. The therapeutic brines, hot springs, extremely hot climate, and clear weather make the Dead Sea area, in addition to its special morphological setting, a unique tourist target.

P. Migoń (ed.), *Geomorphological Landscapes of the World*,
DOI 10.1007/978-90-481-3055-9_25,

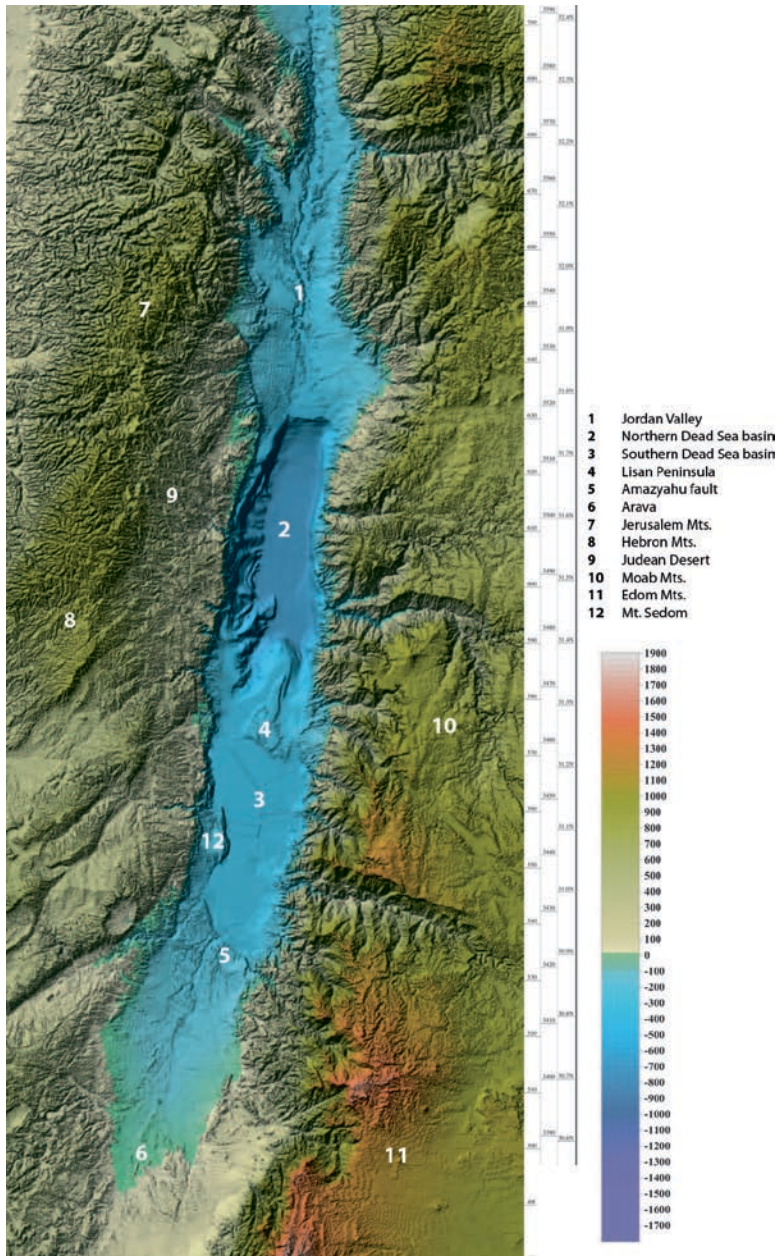

Fig. 25.1 Digital hypsometric colored and shaded relief map of the Dead Sea area and its surroundings by J.K. Hall and R. Calvo

25.2 Evolutionary History

25.2.1 The Lisan Stage

In the late Neogene the rift became a marine gulf. The maximum thickness of its fill reaches 10 km, consisting of both clastic sediments and evaporites. This thick sequence is known as the Dead Sea Group and contains a great volume of brines (Zak 1980). Since its continental enclosure, the Dead Sea basin was occupied by terminal lakes (Ben-Avraham 1997). The last large lake, the precursor of the Dead Sea, was the Late Pleistocene Lake Lisan, existing during the last glacial period, from 70,000 to 14,000 years ago (Schramm et al. 2000). Its salinity ranged up to 15% and the lake stretched, at its peak level, along 240 km, from the Sea of Galilee in the north to the northern Arava in the south. Lake Lisan deposited its typical Lisan marl (Fig. 25.3) and inundated the lower segments of the canyons, which drain

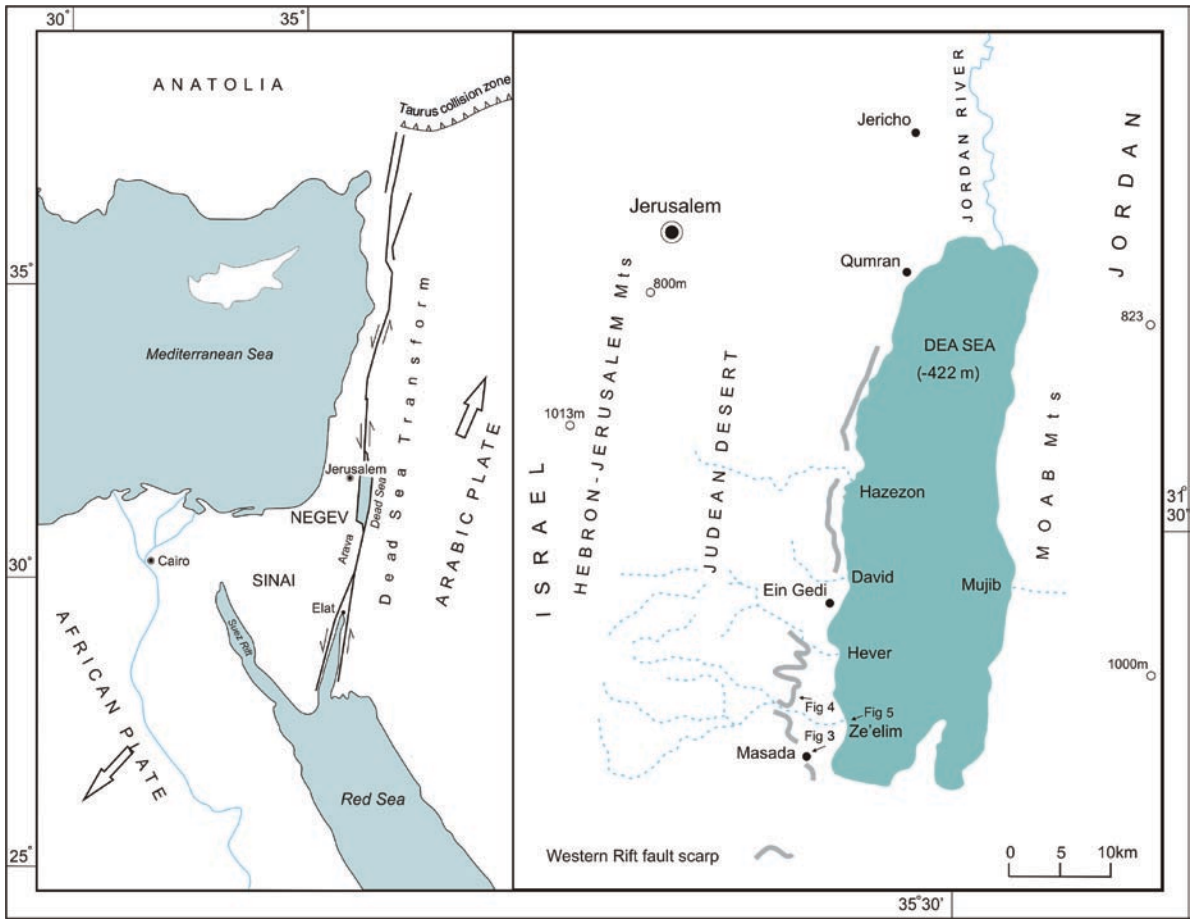

Fig. 25.2 Tectonic setting of the Dead Sea Transform (*left*) and location map of the Dead Sea area and its surroundings (*right*)

to the rift. Lake Lisan level fluctuated between 340 m and ~150 m below mean sea level and its peak stage is inferred from relict beach ridges in the northern Arava and from emerged terraces along the eastern Jordanian side (Abu Ghazleh and Kempe 2009).

Following the retreat of Lake Lisan, fluvial incision into the exposed unconsolidated lacustrine deposits resulted in the formation of spectacular badlands (Fig. 25.3). The Jordan River along the rift axis is a Holocene Post-Lisan meandering river, entrenched into the Lisan marl and flanked by badlands.

25.2.2 The Dead Sea Stage

The Dead Sea, the successor of Lake Lisan, is a hypersaline, dense (1.23 g/cc) lake, 76 km long and up to 17 km wide. It serves as a terminal lake for a 43,000 km^2 drainage system, spanning from southern Lebanon to the hyperarid Negev desert and the Sinai Peninsula (Fig. 25.2). The lake is saturated in halite and enriched in calcium, magnesium, potassium, and bromide. With its 340 g/l total dissolved solids it is the most saline lake on the Earth, showing about ten times the salinity of sea water.

Today, the Dead Sea occupies only its northern basin, 45 × 16 km, with the deepest floor at 700–730 m below sea level. Its shallow southern basin (Fig. 25.1, no. 3), with its floor at 411 m below sea level, is nowadays used as evaporation pans. The western shore of the Dead Sea is rich in ground water occurrences (Mazor 1997), several of which are fresh water springs. Some springs have compositional similarities to the Dead Sea water. In some cases mixing of the Dead Sea waters with freshwaters has been suggested. The springs change their location in response to the lake level drop.

Fig. 25.3 A view toward the western faulted escarpment of the rift, built of Cenomanian – Turonian sedimentary rocks, across the badlands developed in the Lisan Marl. The horst of Masada is seen in the background (Photo D. Bowman)

Sinkholes, which can reach 20 m in depth have formed in groups along the narrow coast of the lake (Closson 2005; Yechieli et al. 2006). The appearance rate of the sinkholes has risen dramatically since 1997, totalling over 1,500 along the western coast. Their formation results from the fall of the ground water table, following the lake level drop. This allowed dissolution of salt wedges below surface by ground water, which is undersaturated in respect to halite. The caves that formed led to the collapse of the overburden, thus causing a severe environmental hazard along the lake coast.

The Dead Sea level was 388.4 m below sea level in 1896, the highest lake level stand in the last 4,000 years. At the beginning of the twentieth century the lake level stood at −392 m. In 2008, the lake level had dropped to −422 m. The negative water balance of the Dead Sea during the twentieth century and its ever-shrinking areal extent is mainly due to the increased diversion of water from the Dead Sea drainage basin for watering in Jordan and Israel. This has caused reduction of the natural inflow from $1{,}100 \times 10^6$ m^3/year to 210×10^6 m^3/year since the 1960s. In addition, an amount of water responsible for 40% of the lake level drop is pumped from the Northern Basin into the evaporation pans in the south by both Israel and Jordan.

A large number of ancient sites have been found around the Dead Sea, the earliest dating back from the Epipaleolith, 12,000–10,000 years ago, excavated in old Jericho. Masada on the western fault scarp (Figs. 25.2 and 25.3) was captured by Jewish rebels and finally fell into the hands of the Romans in 73 CE bringing to a close the great Jewish rebellion against Rome. The deep gorges along the rift borderline and their caves made the Dead Sea area an ideal environment for seeking isolation. In Qumran on the northwestern side of the Dead Sea (Fig. 25.2), the Judean sect of Essenes settled in the second to the first century BC. In the nearby caves, the famous Dead Sea scrolls have been discovered, making among the most important archeological treasures ever found in the Holy Land.

25.3 The Sedimentary Fingerprints

The shrinkage of Lake Lisan and later of the Dead Sea exposed parts of their soft and unconsolidated bed sediments to entrenchment by ephemeral streams (wadis) sourced from outside the rift, where annual precipitation exceeds 600 mm. This entrenchment provides

notorious exposures of sedimentary successions with their architectural details. The intensive fluctuations of the lakes are revealed by facies migrations and cyclic interfingering sequences of lacustrine, shallow nearshore, beach, alluvial, and talus deposits. High palaeo-lake stands are often shown by lacustrine laminae or raised terraces, whereas the regressive low stands are demonstrated by major unconformities. The recognition and identification of the facies within the sequence stratigraphy and the determination of elevations and ages are instrumental in reconstructing the lake level curve (Bartov et al. 2002) as a tool for evaluating the paleo-hydrological/climatological fluctuations in the region.

Typical sedimentary facies exposed in the soft and unconsolidated deposits and encountered in boreholes include:

- Lacustrine low energy facies – consisting of finely laminated "Lisan marl," including alternating datable aragonite and detritus of fine lamina.
- Beach and shallow nearshore lacustrine facies – shown by symmetric ripples, micro cross-bedding, aragonite coating of pebbles, driftwood, pebbly washover ridges, and steeply dipping backsets.
- High-energy alluvial fan-delta facies – characterized by high-angle (20°–30°) foresets of the Gilbert type.

25.4 Alluvial Fans and Raised Beaches

At the outlets of wadis along the fault-generated escarpment of the rift, Holocene successions of alluvial fans were formed. Sub-lacustrine fans were deposited into Lake Lisan at its highest stand. In the second stage, following the retreat of the lake, a process of fan-head trenching commenced and a succession of telescopic, non-deltaic alluvial fans prograded over the newly exposed land. In Nahal Ze'elim, a terrace-like multicyclic sequence of 15 telescopic alluvial fans has formed according to this scenario. The fans became entrenched, controlled by normal downcutting flood episodes, which are an integral part of the fluvial behavior.

The fossil fan deltas that are exposed along the shoreline were deposited during a former higher stand of the Dead Sea and are typified by steeply inclined foresets of Gilbert type. Active fan deltas have become reestablished nowadays along the receding shore of the Dead Sea.

The last drop of the Lake Lisan level and subsequently that of the Dead Sea left its legacy in the form of regressive shorelines, seen as a succession of raised beaches. During stillstands within the shrinkage of Lake Lisan, a sequence of 28 lake terraces, composed of wave-cut treads and risers, was formed and is excellently preserved up to now (Fig. 25.4) along the western side of the Dead Sea as well as along the eastern Jordanian slopes (Abu Ghazleh and Kempe 2009). The rift margins bear a rich record of additional markers of regressive beach lines. It includes linear swash bars, beach ridges composed of well sorted and rounded disc-shaped gravel showing backsets and foresets, tar deposits, beach rock, abandoned coastal cliffs, and gravel coated by aragonite crust.

25.5 Salt Karst of Mount Sedom

A considerable sequence of bedded salt extends in depth, over the entire width of the Southern Dead Sea basin (Al-Zoubi et al. 2002) and includes the Lisan Peninsula (Fig. 25.1, no. 4). Mount Sedom (Fig. 25.1, no. 12) is an exposed head of an active, rising salt diapir, 11 km long, ascending ~260 m above the Dead Sea level after piercing the overlying formations. The mass of the diapir consists mostly of highly soluble Pliocene-Pleistocene, marine origin rock salt, composed mainly of halite (NaCl) and of gypsum, anhydrite, dolomite, marl, chalk, shale, and sandstone that were deposited during the Pliocene transgression in a marine embayment, which extended from the Mediterranean to the Dead Sea Transform depression. The estimated uplift rate of the Mount Sedom is up to 9 mm/year (Frumkin 1996).

Rock salt is rarely exposed on the surface of the earth. Its high solubility (360 g/l at 20°C) and the aggressiveness of rain water permit total dissolution of rock salt exposures, except for extreme arid conditions, which inhibit complete destruction.

Runoff on Mount Sedom, which develops only after high-intensity short rains, is captured into stream sinks, which divert channels via vertical shafts, up to 60 m deep, into the rock salt where the

Fig. 25.4 Excellently preserved Lisan Lake terraces, composed of wave-cut treads and risers

flow continues in steep conduits and sub-horizontal canyon passages. Part of the cave system is active today and part of it is abandoned, hanging over the modern channels. Some cave passages make tributaries that join to form an integrated underground network cave system, which reappears at the surface to drain subaerially toward the lake. Other cave systems may have no outlets and terminate in chambers, where water is ponded and form temporary lakes that loose water slowly.

Over 20 km of enterable cave passages have been surveyed in Mount Sedom. The oldest cave in the Mount Sedom karst system was dated to ~7,000 years before present. Downcutting rates in limestone caves range from 0.05 to 0.8 mm/year, but in Mount Sedom the rates rise to 4–25 mm/year. These rates are of the fastest encountered in nature. However, entering the cave system of Mount Sedom is very dangerous and strictly forbidden.

25.6 Tectonic Geomorphology

The continuing motions along the transform make the Dead Sea area very active seismically. In the last 1,000 years the Dead Sea transform experienced six destructive earthquakes of magnitude 5.8–6.2. The

strongest and most destructive earthquake in the twentieth century was the 1927 earthquake. Its instrumentally determined epicenter was in the northern Dead Sea basin. Young motions are indicated by a spectacularly wide range of morphological field evidence, including fault scarps and small grabens up to 40 m wide. Trenching has exposed Lisan and post-Lisan compressive structures, including folds, flexures, and reverse faults younger than 4,000 years. A faulted fan surface and free face facets along tectonic scarps have also been reported. Linear fault scarps transverse the graben and divide the rift into segments, the Amaziahu fault escarpment being a spectacular surface example of such a sharp intra-basinal morphotectonic border line (Fig. 25.1, no. 5).

Spectacular soft sediment deformations of the load-structure type have also been observed. The structures, which have been formed by fluidization of loose, metastable lake bed sediments, triggered by earthquake shaking, are shown by isolated ball and pillow structures and have the potential of chronological benchmarking by radiocarbon dating (Bowman et al. 2001). Seismically deformed sediments (seismites) of broken lacustrine laminae, in direct association with fault ruptures or widespread, are defined as "mixed layers" and reveal the recurrence intervals of large clustered earthquakes (Marco et al. 1996). Dating enables one to relate the deformed sediments to reported historical earthquakes. A good agreement between the two can be found by correlating the time width of a ^{14}C dated seismite to historically known seismite within the relevant time range. For example, the seismite horizon dated for 40 BC–AD 70 can be correlated to one of the historically reported earthquakes of 31 BC or AD 30, 33, and 48.

25.7 Drainage Response to Base Level Fall

The Dead Sea level is experiencing a rapid and continuous decline by more than 1 m/year. Following the continuous Dead Sea level drop the streams are in a prolonged incisional "relaxation period." The overall incision rates range between 0.4 and 0.8 m/year, suggesting that the area is morphologically extremely out of equilibrium. The desert streams that drain to the Dead Sea are not controlled by longitudinal concavity-forming factors as downstream-fining of grain size or downstream increase in sediment and water discharge. Many wadis (Nahal) as Nahal Hazezon, Nahal David, and Nahal Hever (Fig. 25.2) display, very close to the lake, convex or linear longitudinal profiles. This convexity seems inherited from the initial convex morphology of the fan deltas, and is also due to the ongoing base level fall.

The prevailing soft and unconsolidated sediments make the Dead Sea area a unique natural field laboratory for studying, in real time, the process of channel network development (Fig. 25.5) and channel cross-sectional shape evolution. The entren-ched channels demonstrate initial widening and formation of a trapezoidal cross section, indicating that the drainage system is beyond the initial net vertical incision response and has started widening. However, the evolutionary phase of intensive widening, infilling, and formation of a sedimentary storage is not demonstrated yet. The continuous and enhanced rate of base level lowering entraps the drainage systems mainly in the vertical incisional mode, preventing the evolutionary progress toward a wider, graded cross-sectional shape.

25.8 Summary

The margins of the Dead Sea are a unique morphological field laboratory in extreme arid conditions, with a high preservation potential, subjected to frequent flash floods. The lake-level fluctuations have left a rich inventory of datable raised shorelines and formed a rich sequence of interfingering environments. Abundant morpho-sedimentary evidence points to Holocene and recent tectonics. Base level fall triggers the response of the drainage systems, which demonstrate, in real time, channel shape evolution processes, including deposition, entrenchment, and progradation of alluvial fans. The excellent exposures in the soft sedimentary substrate reveal the sedimentary fingerprints of the evolution. All this, combined with scenic landscape and relatively easy access, make the Dead Sea area one of the most interesting places for a geomorphologist to visit.

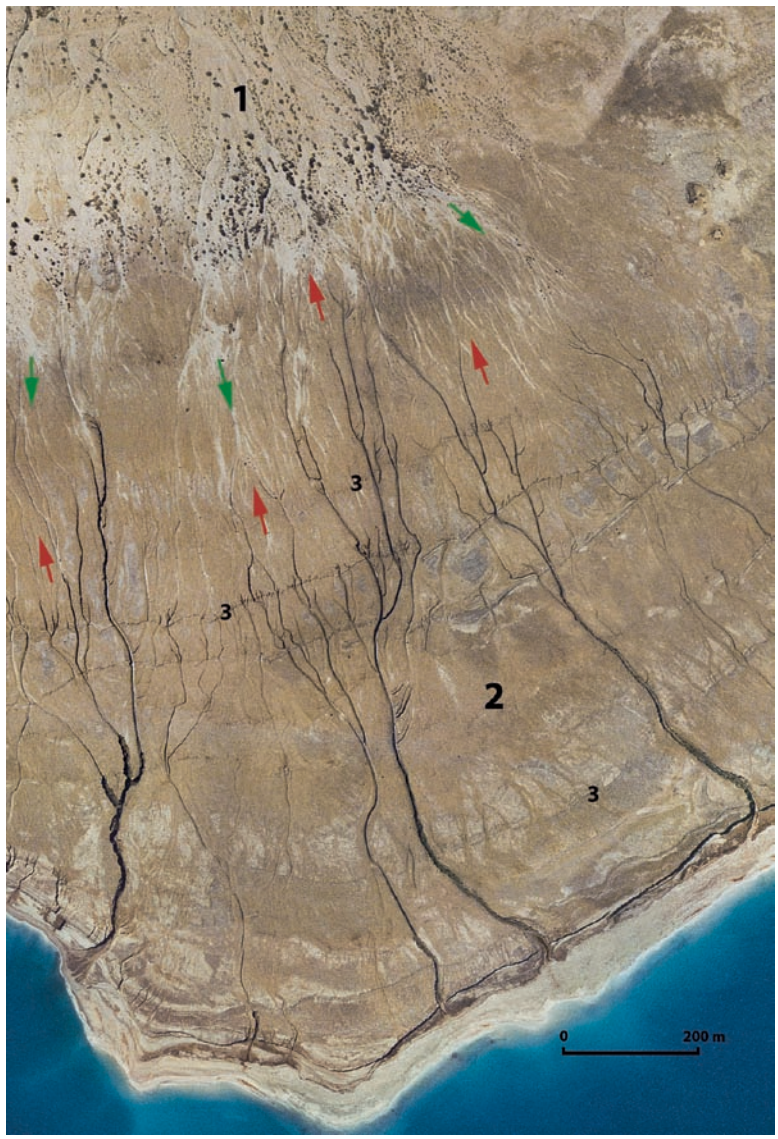

Fig. 25.5 The retreating Dead Sea in front of Nahal (wadi) Ze'elim. (1) An active propagating alluvial fan (*green arrows*), (2) recently exposed lake bed with headward entrenching channels (*red arrows*), triggered by the lowering base level, and (3) abandoned shorelines of the Dead Sea

The Author

Dan Bowman is a Professor Emeritus in the Department of Geography and Environmental Development, Ben-Gurion University of the Negev, Beer Sheva, Israel. His research focuses on coastal processes, alluvial fans, and geomorphological imprints of neotectonics in a wide range of geographical settings

References

Abu Ghazleh Sh, Kempe S (2009) Geomorphology of Lake Lisan terraces along the eastern coast of the Dead Sea, Jordan. Geomorphology 108:246–263

Al-Zoubi A, Shulmanh H, Ben-Avraham Z (2002) Seismic reflection profiles across the southern Dead Sea basin. Tectonophysics 346:61–69

Bartov Y, Stein M, Enzel Y, Agnon A, Reches Z (2002) Lake levels and sequence stratigraphy of Lake Lisan, the Late Pleistocene precursor of the Dead Sea. Quat Res 57:9–21

Ben-Avraham Z (1997) Geophysical framework of the Dead Sea: Structure and tectonics. In: Niemi TM, Ben-Avraham Z, Gat JR (eds) The Dead Sea, the lake and its setting. Oxford University Press, Oxford, pp 22–35

Bowman D, Bruins HJ, van der Plicht J (2001) Load structure seismites in the Dead Sea Area, Israel: chronological benchmarking with ^{14}C dating. Radiocarbon 43:1383–1390

Closson D (2005) Structural control of sinkholes and subsidence hazard along the Jordanian Dead Sea coast. Env Geol 47:290–301

Enzel Y, Agnon A, Stein M (eds) (2006) New frontiers in Dead Sea Paleoenvironmental research. Geol Soc Am Spec Pap 401

Freund R, Garfunkel Z, Zak I, Goldberg M, Weissbrod T, Derin B (1970) The shear along the Dead Sea rift. Philos Trans Roy Soc Lond 267:107–130

Frumkin A (1996) Uplift rate relative to base level of a salt diapir (Dead Sea, Israel) as indicated by cave levels. In: Alsop I, Blundell D, Davidson I (eds) Salt Tectonics. Geol Soc Spec Publ 100:41–47

Garfunkel Z (1981) Internal structure of the Dead Sea leaky transform (rift) in relation to plate kinematics. Tectonophysics 80:81–108

Marco S, Stein M, Agnon A, Ron H (1996) Longterm earthquake clustering: a 50, 000 year palaeoseismic record in the Dead Sea Graben. J Geophys Res 101:6179–6192

Mazor E (1997) Groundwaters along the Western Dead Sea shores. In: Niemi TM, Ben-Avraham Z, Gat JR (eds) The Dead Sea, the lake and its setting. Oxford University Press, Oxford, pp 265–276

Neev D, Emery KO (1967) The Dead Sea: depositional processes and environments of evaporites. Geol Surv Israel Bull 4:1–147

Neev D, Emery KO (1995) The destruction of Sodom, Gomorrah and Jericho. Geological, climatological and archaeological background. Oxford University Press, New York

Niemi TM, Ben-Avraham Z, Gat JR (eds) (1997) The Dead Sea, the lake and its setting. Oxford University Press, Oxford

Schramm A, Stein M, Goldstein SL (2000) Calibration of the 14 C time scale to >40 ka by 234U–230Th dating of Lake Lisan sediments (last glacial Dead Sea). Earth Planet Sci Lett 175:27–40

Yechieli Y, Abelson M, Bein A, Crouvi O, Shtivelman V (2006) Sinkholes "swarms" along the Dead Sea Coast: Reflection of disturbance of lake and adjacent ground water systems. Geol Soc Am Bull 118:1075–1087

Zak I (1980) The geochemical evolution of the Dead Sea. In: Coogan AH, Hauber L (eds) Fifth symposium on salt, Cleveland, Ohio. Northern Geol Soc 1:181–184

Chapter 26
The Western Ghat: The Great Escarpment of India

Vishwas S. Kale

Abstract The Western Ghat Escarpment is one of the classic examples of passive margin great escarpments in the world. The Western Ghat zone is an area of spectacular scenery, rugged terrain, deep valleys, impressive waterfalls, and dense forest teeming with wildlife. The ~1-km high wall is an assemblage of valley heads and spurs. Other associated landforms are plateau outliers, deep gorges, beheaded plateau valleys, and laterite plateaux or tablelands. There are many instances of stream piracy in the Ghat zone. The Ghat is the fountainhead of many large, east-flowing rivers and numerous short, swift, coastward-flowing rivers. Most workers believe that the Western Ghat Escarpment was initiated as a rifted margin at the time of eruption of the Deccan basalts in late Cretaceous. Although it is generally agreed that the escarpment has receded inland, there are differences of opinion about the mode and rate of recession.

Keywords Beheaded valleys • Deccan basalts • gorges • great escarpment • monsoon • outliers • scarp recession • Western Ghat

26.1 Introduction

Great escarpments are fundamental topographic features of many passive continental margins or Atlantic-type margins, which are trailing edges of tectonic plates. Escarpments are precipitous hillslopes of substantial length. Typical great escarpments occur in South Africa (Drakensberg), southeastern Australia, eastern Brazil (Serra do Mar), Namibia, and India (Western Ghat). All but a few passive margin great escarpments exhibit certain common characteristics (Ollier 2004): (a) they are several hundreds or thousands of kilometers long and over a kilometer high, (b) they show remarkable continuity and linearity despite structural variations, (c) they run roughly parallel to the coast and separate a high inland plateau from a coastal lowland or plain, and (d) they display erosional and youthful characteristics.

One of the most spectacular great escarpments is present along the western passive continental margin of India (Fig. 26.1). This very prominent physiographic feature runs almost parallel to the Arabian Sea coast and is known as the *Sahyadri* (Sanskrit for "benevolent mountain") alias Western Ghat (*ghat* = broad flight of steps leading to a river). In terms of size, stature, and grandeur it is second only to the lofty Himalayan Mountains in the Indian subcontinent. The Western Ghat is a textbook example of a great escarpment because it displays all the typical morphological features of passive margin escarpments, especially in the northern part, where it is developed in the Deccan flood basalts (Fig. 26.2a). Not surprisingly, this gigantic landform has been the subject for exploration and research for over a century (Gunnell and Radhakrishna 2001).

26.2 The Great Escarpment of India

Similar to other passive margins, the western coastal margin of India displays three prominent landscape features (Fig. 26.2c): an elevated inland plateau (the Deccan Plateau), a long, coast-parallel, high-relief, and seaward-facing escarpment (the *Sahyadri* or the Western Ghat), and a dissected coastal lowland (known as *Konkan* in the north and *Malabar* in the south).

Even a cursory glance at the physiographic map or satellite image of south Asia would reveal two most striking characteristics of the India's great escarpment:

P. Migoń (ed.), *Geomorphological Landscapes of the World*,
DOI 10.1007/978-90-481-3055-9_26,

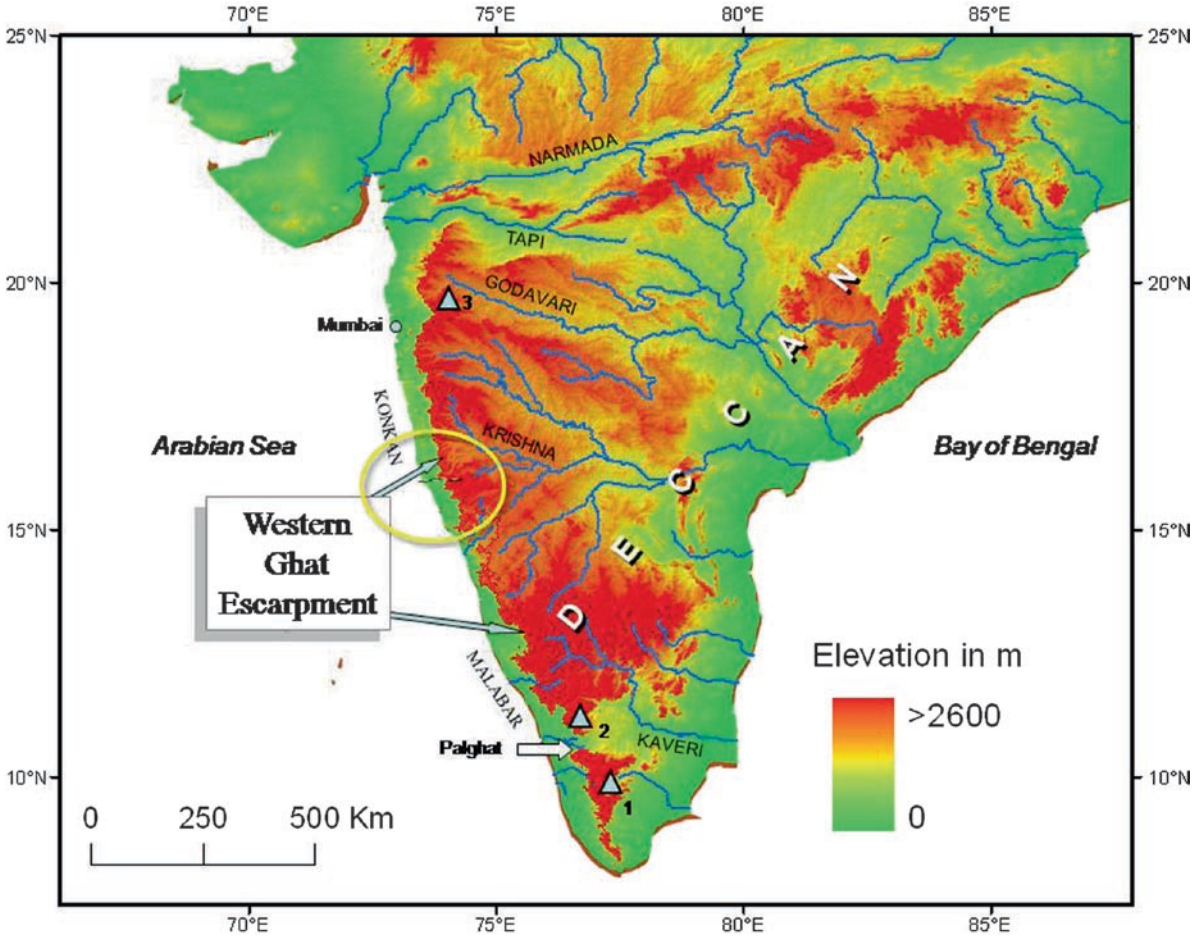

Fig. 26.1 Geographical setting of the Western Ghat. The dashed line south of Mumbai represents approximately the southern boundary of the Deccan basalt province. 1 – Anai Mudi peak (2,695 m), 2 – Doda Betta peak (2,637 m), 3 – Kalsubai peak (1,646 m) (Image based on GTOPO30 DEM data)

its remarkable linearity and extraordinary continuity. The escarpment runs for over 1,600 km along the western margin but displays only marginal changes in its configuration and morphology, despite significant lithological and structural variations (Fig. 26.1). The topographic feature is cut across Cretaceous-Eocene Deccan flood basalts in the north (roughly north of 16°N latitude) and the Pre-Cambrian gneisses, granites, and charnockites in the south.

The Ghat summit is not uniform in elevation, but is featured by high peaks and gaps. The peaks attain their greatest height in the southern segment. Some of the important high peaks are: Anai Mudi (2,695 m), Doda Betta (2,637 m), and Kalsubai (1,646 m) (Fig. 26.1). The last is the highest peak in the Deccan basalt province (DBP) (Fig. 26.2b). Interestingly, these high peaks are not coincident with the Ghat crest, but lie slightly eastward of the scarp. Occasionally, laterite plateaux or tablelands occur on the Ghat summit. One of the best examples is the Mahabaleshwar Plateau (Fig. 26.2b), which at ~1,400 m a.s.l. is a popular tourist destination during the hot Indian summer. The "swales" or gaps (referred as the *ghat*; hence the name Western Ghat) are often truncated valley heads on the Ghat edge (Kale and Subbarao 2004). Some of the major and well-known gaps are: the Palghat, Thal Ghat, Malshej Ghat, and Bor Ghat (Figs. 26.1 and 26.2b). Palghat is the most prominent gap (~15 km wide) in the Western Ghat Escarpment, where the elevation drops below 200 m a.s.l. A good number of these gaps

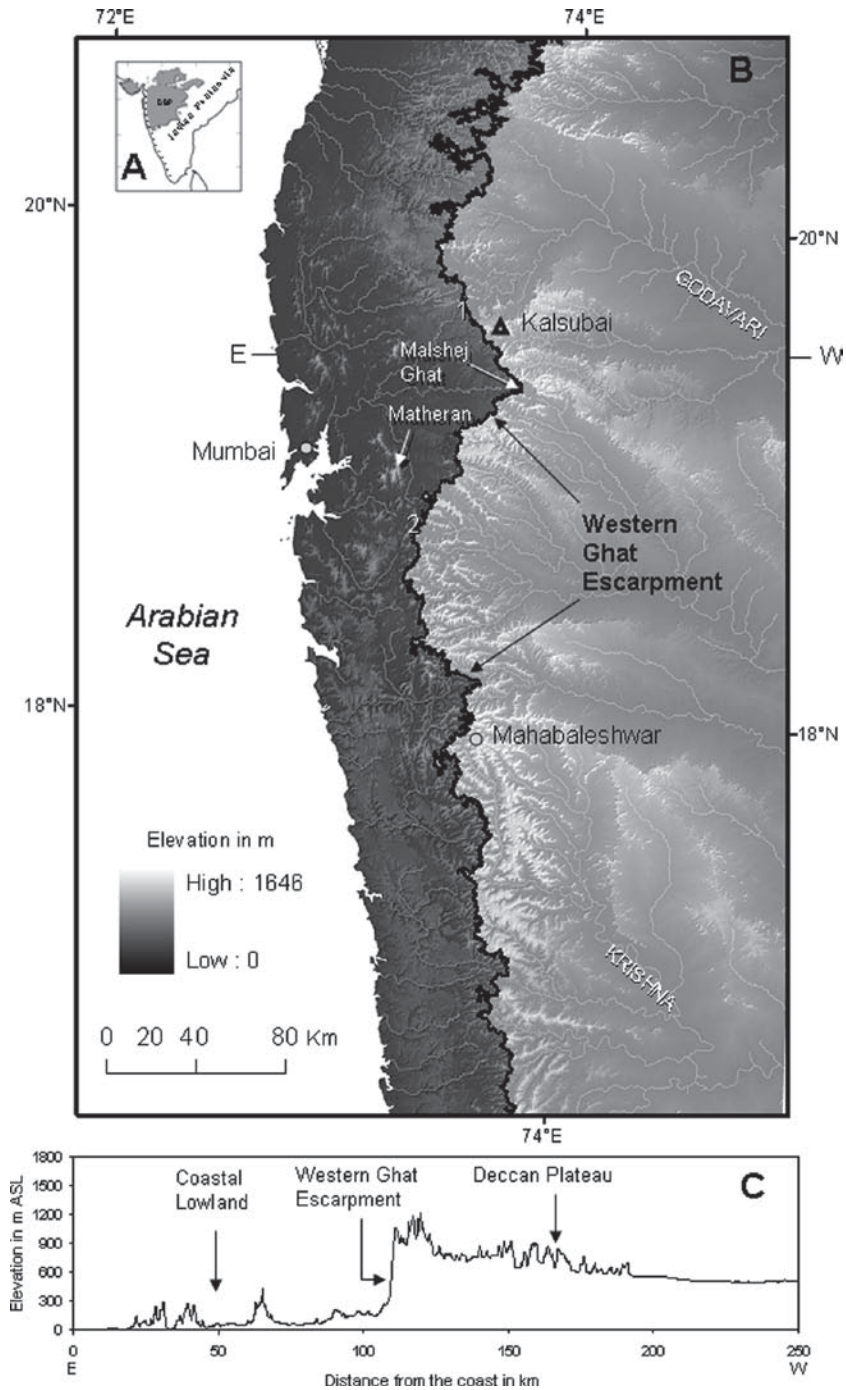

Fig. 26.2 (**a**) Geographical extent of the Deccan basalt province (DBP); (**b**) shaded relief image of the western DBP. The 600-m contour along the Ghat escarpment is shown by dark line. 1 – Thal Ghat; 2 – Bor Ghat; (**c**) cross profile (E–W) across the western margin in the DBP showing the three major topographic features (The image and the profile generated from SRTM-DEM data)

or passes used to be ancient trade routes, and even today carry highways and railways, which connect the coastal towns with the plateau towns.

The orographic effect of the ~1-km high Western Ghat Escarpment is primarily responsible for dramatic differences in monsoon precipitation (June to

September), and consequently in the natural vegetation and land use on either side of the scarp. The physical barrier intercepts the moisture-bearing southwest monsoon winds. As a result, a zone of high rainfall (2,000–6,000 mm) exists on the seaward-facing flank and a zone of pronounced rainshadow effect (600–1,000 mm) characterizes the leeward side. Due to large topographic and climatic diversity, there is a steep environmental gradient toward the east as well as toward the west. Consequently, the Ghat zone (~25 km belt around the scarp) is a home to countless varieties of endemic species and has been recognized as one of the world's major terrestrial biodiversity hot spots.

The great wall of the Western Ghat is a shoulder-type escarpment (Matmon et al. 2002) because the top of the escarpment essentially coincides with the main drainage divide of the Indian Peninsula. It is the fountainhead of many large, east-flowing rivers and numerous short, swift, coastward-flowing rivers. The principal east-flowing rivers are the Godavari, the Krishna, and the Kaveri (Fig. 26.1). These rivers together drain an area of over half-a-million square kilometers. The rivers originate within a few tens of kilometers from the Arabian Sea, but prefer to travel for over 800–1,400 km to debouch into the Bay of Bengal on the other side of the peninsula.

26.2.1 The Scarp in the Deccan Basalt Province

The great escarpment is remarkably straight and bold in the basaltic terrane (Fig. 26.2b) unlike in the southern Precambrian segment, where it loses its distinctiveness to some extent and is more convoluted. Within the DBP, the nearly 800-km long, imposing wall of the Western Ghat lies about 40–120 km (average 60 km) inland from the Arabian Sea coast and forms the western edge of the northern Deccan Plateau (known as *desh*). There is only one major embayment in this part, the Malshej Ghat, where the escarpment has receded significantly inland (Fig. 26.2b).

The Ghat zone is an area of spectacular scenery (Fig. 26.3), rugged relief, sheer cliffs, deep valleys, and dense forest. The height of the escarpment top in the basaltic terrane significantly varies (~600–1,400 m a.s.l.), but the average elevation is around 900 m. The scarp face is remarkably steep and high, particularly to the south of 20°N latitude. North of this latitude the face has a stepped appearance (Fig. 26.2b). Topographic analysis using data extracted from SRTM-DEM indicates that the relative relief along the escarpment ranges between ~200 and 1,100 m. The average slope of the Western Ghat scarp is close to 19°, but in places,

Fig. 26.3 Western Ghat Escarpment in horizontally bedded Deccan basalt flows at Mahabaleshwar (see Fig. 26.2 for location) (Reproduced from Kale and Subbarao 2004. With permission)

the scarp slopes exceed 30°. Due to the rugged terrain, high altitude, cooler climate, and breathtaking views, the Western Ghat zone is dotted with popular tourist resorts, medieval forts, and ancient temples.

26.3 Escarpment-Related Landforms

The Western Ghat Escarpment takes many interesting forms along its length. Although the escarpment sinuosity in the DBP is remarkably low (Kale and Shejwalkar 2007), the seaward face is not like a high, fortification wall, but exhibits an assemblage of valley heads and offshoots or spurs (Fig. 26.4). The escarpment is broken by deep, narrow notches developed by the steeper, west-draining streams, separated by short, sharp-ridged spurs (Fig. 26.3). Often a cataract is located at the reentrant head. The length of the spurs or offshoots seldom exceeds 5 km (Kale and Subbarao 2004). Other associated landforms are outliers, gorges, and beheaded valleys.

26.3.1 Plateau Outliers

Plateau outliers are prominent escarpment-related features and are a typical expression of the escarpment recession. Outliers are detached masses of the main plateau and are separated from the main escarpment face by narrow deep valleys. During the process of retreat of an escarpment, the promontories are often converted into outliers due to headward erosion by tributary streams. There are quite a few examples of outliers along the Western Ghat Escarpment (Dikshit 1981). Some of the outliers have been completely detached from the main plateau (Deccan Plateau), but some are still partly attached. Matheran (Fig. 26.2b) is one such completely detached outlier, which is one of the most popular tourist hill stations (resorts) near Mumbai (formerly Bombay). Patches of laterite occur on the summit at Matheran. Laterite is a common weathering product in tropical areas, which is enriched in iron and forms by intensive and prolonged weathering of the underlying rocks. The indurated or hardened iron-rich crust (also called duricrust) protects the

Fig. 26.4 Forms of the Great Escarpment of India in the Deccan basalt province. The photograph shows short razor-edged offshoots or spurs separated by narrow reentrants (Reproduced from Kale and Subbarao 2004. With permission)

underlying rocks from erosion, and gives rises to the characteristic plateau and mesa topography, as exhibited at Mahabaleshwar-Panchgani.

26.3.2 Beheaded Plateau Valleys

Another remarkable and conspicuous feature of the Western Ghat scarp is the occurrence of unusually wide (~1–6 km) gaps right on the top of the escarpment. These are beheaded plateau valleys, truncated not by faulting or river capture, but by the eastward recession of the Western Ghat scarp (Radhakrishna 1993). As the escarpment migrates inland, the headwaters of the east-flowing plateau rivers are consumed leading to the development of beheaded valleys (Kale and Subbarao 2004). In most cases, the rivers occupying the beheaded valleys become underfit because of loss of headwater area. Many plateau rivers in the DBP show evidence of such beheading and underfit nature. The most impressive example is seen at Malshej Ghat (Fig. 26.5).

26.3.3 Gorges and Stream Piracy

Deep gorges, with cataracts at the head, abound in the Western Ghat zone. Gorges are narrow, deep valleys with steep walls. They occur where valley deepening by vertical erosion significantly outpaces valley widening. Many of the high-gradient, seaward-draining rivers have developed such gorges by incision and headward retreat into the escarpment front. In general, the gorges are longer in the southern Pre-Cambrian segment, where some of the coastal rivers have penetrated far into the plateau. Along the Ghat scarp, gorges are one of the fundamental geomorphic landforms associated with coastal streams that have captured and gained more drainage area over the plateau by stream piracy.

The phenomenon of stream piracy is common in the Western Ghat zone due to the higher erosional potential of the rivers flowing down the escarpment face. There are many examples of elbow bends; one of the most commonly cited types of geomorphic evidence of stream piracy. Numerous instances of river captures

Fig. 26.5 Beheaded valley of the Pushpavati River at Malshej Ghat. The sharp top-edge of the escarpment is clearly seen in the foreground. See Fig 26.2b for location of Malshej Ghat (Reproduced from Deodhar and Kale 1998. With permission)

can be found all along the Western Ghat edge, particularly in the southern Pre-Cambrian terrane. One of the classical examples is that of the Sharavati River near Gersoppa (14.22°N and 74.81°E). It displays all the associated features – barbed drainage pattern, an elbow, a narrow steep gorge, and a major waterfall at the head of the gorge (Radhakrishna 1993). The 253-m waterfall, known as the Gersoppa or Jog Falls, is the highest waterfall in India in terms of its vertical drop.

26.4 Formation of the Western Ghat Escarpment

The exact mode of origin of the Western Ghat Escarpment has not yet been fully understood and explained. The scarp was previously thought to be an enormous, abandoned sea cliff by some and a gigantic fault scarp by others (Dikshit 1981; Gunnell and Radhakrishna 2001). In recent years, due to its remarkable similarity with the great escarpments along other passive margins, the great escarpment of India has been presumed to be the result of rift-flank uplift, long distance parallel slope retreat, and divide migration (Fig. 26.6a). It is now believed that the Western Ghat Escarpment was initiated as a continental edge as a consequence of rifting and separation of the Seychelles microcontinent at the time of the eruption of the Deccan basalts in late Cretaceous, and the present scarp is the product of long-distance parallel retreat of the rifted margin (Widdowson 1997). An alternative explanation is that an asymmetric divide was created along the western margin because of warping of the preexisting surface (Fig. 26.6b). The west-facing steeper slope was aggressively eroded and dissected by the seaward-flowing streams. Rapid incision and headward erosion along the seaward-facing flank created deep valleys and gorges, which eventually coalesced to give rise to a single, continuous escarpment (Ollier 2004; Kale and Shejwalkar 2007).

Although it is generally agreed that the present face of the great escarpment is formed erosionally and that the escarpment has receded inland, there are differences of opinion about how and at what rate the ~1,600-km long escarpment has migrated inland. Some workers have inferred substantially high rates of scarp retreat (1–3 km/1 million years) and long-distance (by 180–200 km) parallel slope retreat (Widdowson 1997). However, recent thermochronologic and cosmogenic isotope data indicate slow rates of scarp retreat along passive margins and no significant change in location

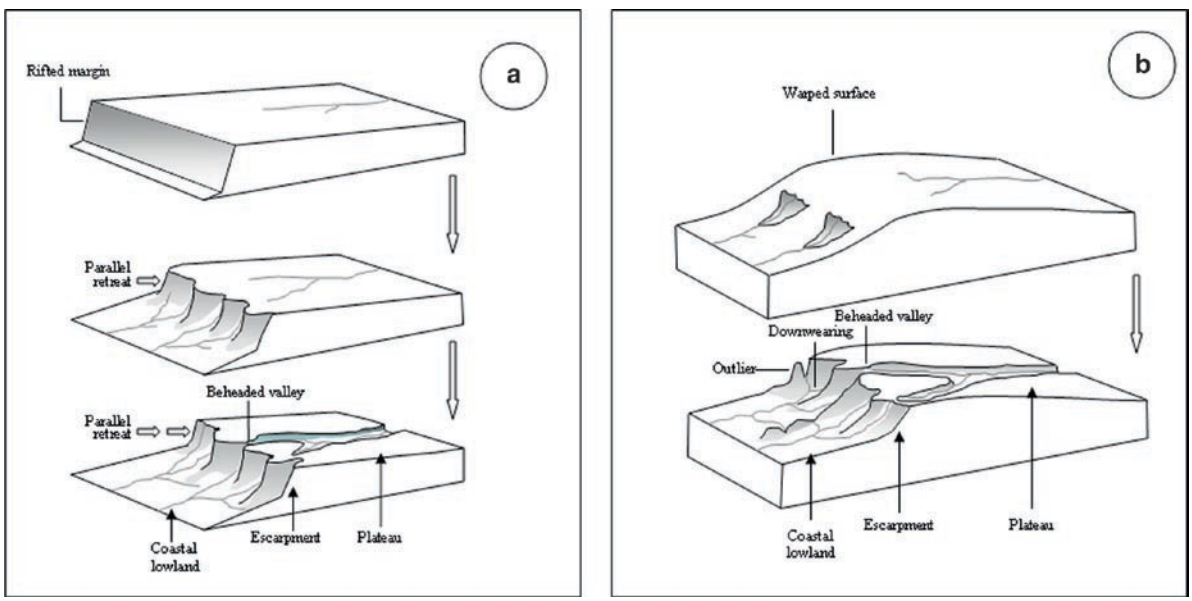

Fig. 26.6 Simplified diagrams showing the two main models of escarpment evolution along passive margins. (**a**) Parallel slope retreat of rifted margin; (**b**) warping and degradation or downwearing of asymmetric divide. Refer text for details

over time (Matmon et al. 2002). Further, these and other data do not support the concept of long-distance parallel scarp retreat (Matmon et al. 2002). The alternative model that places greater emphasis on degradation or downwearing of the plateau margin has also not been well established.

Geomorphologically, there are three essential conditions that create the Western Ghat-type escarpment: high divide elevation, divide asymmetry, and headward erosion of rivers of the coastal plain. The asymmetry of the divide, whether created by rifting or warping, favors the steep stream heads to breach the divide. The seaward-draining streams, because of their greater erosional potential, rapidly elongate headward, leading to the formation of embayments and the recession of the seaward-facing front of the divide (escarpment) inland. The offshoots or spurs, jutting out of the escarpment, are subsequently eroded by the tributary streams draining roughly orthogonal to the principal coastal streams (Kale and Shejwalkar 2007). In some cases, the headward erosion by escarpment-parallel tributary streams may lead to the cutting away of a part of the escarpment, creating an island or outlier. As the escarpment migrates inland, the headwaters of the plateau rivers are consumed, leading to the development of beheaded or truncated valleys. In the process, the plateau rivers loose headwater area and become misfit or underfit.

If the plateau drainage network orientation is favorable, the breaching of the divide (escarpment) by coastward-flowing streams may also lead to the seizure of the waters of the opposing, more gently sloped plateau streams, leading to river piracy as well as the destruction and lowering of the drainage divide.

26.5 Conclusions

The Western Ghat Escarpment is one of the classic examples of passive margin great escarpments in the world. Apart from the gigantic escarpment, the western margin of India displays all the typical morphological features associated with trailing edges of tectonic plates. Due to its high mean elevation and copious monsoon rainfall, the scarp zone is an area of spectacular scenery, rugged terrain, precipitous slopes, deep valleys, impressive waterfalls, and dense forests teeming with wildlife.

In the Indian context, the Western Ghat is a vital element of the physical as well as the cultural landscape for several reasons. Geomorphologically, the gigantic landform is second only to the great Himalayan Mountains in terms of dimension and grandeur. It is the longest continuous topographic feature outside the Himalayan region. Climatologically, this prominent feature plays a significant role in the spatial distribution of monsoon rainfall over the Indian Peninsula. Hydrologically, its significance lies in the fact that it is the fountainhead of many great Indian rivers and numerous small coastal rivers. Environmentally, due to its great topographic and climatic diversity, it comprises a rich and unique assemblage of flora and fauna. Not surprisingly, this outstanding landform is known as *Sahyadri*, the benevolent mountain.

The Author

Vishwas Kale is a Professor in the Department of Geography, University of Pune, India. His research interests include palaeohydrology, fluvial and flood geomorphology, Quaternary geomorphology, and landscape evolution. He has over two dozen research papers in peer-reviewed international journals such as *Nature*, *Geomorphology*, *Catena*, *Quaternary Science Reviews*, *Climate Change* etc.

References

Deodhar LA, Kale VS (1998) Downstream adjustments in allochthonous rivers: Western Deccan Trap upland region, India. In: Miller AJ, Gupta A (eds) Varieties of Fluvial forms. Wiley, New York, pp 295–315

Dikshit KR (1981) The Western Ghats: a geomorphic overview. In: Singh LR (ed) New Perspective in Geography. Thinkers Library, Allahabad, India, pp 1–25

Gunnell Y, Radhakrishna BP (eds) (2001) Sahyadri, The Great Escarpment of the Indian subcontinent. Geol Soc India, Mem 47, Bangalore, India

Kale VS, Subbarao KV (2004) Some observations on the recession of the Western Ghat escarpment in the Deccan Trap region, India: Based on geomorphological evidence. Trans Japanese Geomorph Union 25:231–245

Kale VS, Shejwalkar N (2007) Western Ghat escarpment evolution in the Deccan basalt province: Geomorphic observations based on DEM analysis. J Geol Soc India 70:459–473

Matmon A, Bierman P, Enzel Y (2002) Pattern and tempo of great escarpment erosion. Geology 30:1135–1138

Ollier CD (2004) Passive margin. In: Goudie AS (ed) Encyclopedia of Geomorphology. Routledge, London, pp 762–765

Radhakrishna BP (1993) Neogene uplift and geomorphic rejuvenation of the Indian Peninsula. Current Sci 64:787–793

Widdowson M (1997) Tertiary palaeosurfaces of the SW Deccan, Western India: Implications for passive margin uplift. In: Widdowson M (ed) Palaeosurfaces: recognition, reconstruction and palaeoenvironment interpretation. Geol Soc Spec Publ, London, 120:221–248

Chapter 27
The Pokhara Valley: A Product of a Natural Catastrophe

Monique Fort

Abstract The Pokhara valley in the central part of Nepal is one of the few Himalayan intramontane valleys that permits one to decipher the way the landforms of the world's highest mountain range evolve. The valley is attractive to tourists for the scenic majesty of its glaciated mountains, gorges, caves, and lakes, the formation of which results from a complex yet recent and dramatic evolution of the valley. For a long time, most of the inhabitants believed that the valley originated from the drying up of a huge lake similar to those of the Kathmandu and Kashmir valleys. Careful observations of the sediments filling the basin indicate that the Pokhara valley was affected by a giant, catastrophic debris flow five centuries ago. It is an emblematic site, where the steepness of the still rising front of the very Himalaya ("the abode of snow") is maintained by sporadic collapses of the mountain walls controlled by a combination of both glacial and seismo-tectonic dynamics.

Keywords Debris flows • glaciation • Himalaya • mountain building

27.1 Introduction

The Pokhara valley at the foot of the Annapurna Himal presents one of the sharpest contrasts in relief in the world. Located in the central part of Nepal, it stands out as a distinctive feature of the Himalayan landscape. It is an abnormally broad plain with an area of ~125 km^2, and confined by hills ranging from 1,200 to 3,000 m in elevation. Towering above it to the north is the Annapurna Himal (8,091 m), only 35 km as the crow flies from Pokhara town (800 m a.s.l.). It is drained by the Seti Khola (khola meaning "river" in Nepali language) and its tributaries, originating from the glacial cirque of Sabche, surrounded from west to east by the peaks of Macchapuchare (6,993 m), Annapurna III (7,555 m), and Annapurna IV (7,525 m). Well known for the outstanding scenic majesty of these "snowy mountains" ("Himal" in Nepali), the Pokhara valley is also attractive to tourists for its gorges, caves, and lakes, the formation of which results from the complex yet recent and dramatic evolution of the valley.

In fact, for a long time, the formation of the Pokhara valley was a mystery. Inhabitants were struck by the very many large rocks found in the upstream part of the valley, and had their own explanation of these features, referring to legends involving the action of God. Most of them believed that the Pokhara valley originated from the drying up of a huge lake similar to those of the Kathmandu and Kashmir valleys (Hagen 1961). Careful observations of the sediments filling the valley, together with a better understanding of the geomorphological processes in action, have led to new interpretations involving the very recent evolution of the glaciated mountain front of the Annapurna Range. This makes the Pokhara valley one of the few Himalayan basins that permits one to decipher the way the landforms of the world's highest mountain range evolve and explains why this particular part of the Himalaya has been selected for this volume.

27.2 Geographical and Geological Setting

The Pokhara valley is located in the midland region (or Pahar zone) of the Himalayan Range, a low-lying belt, which is sandwiched between the Lesser Himalaya (or Mahabharat Range) in the south and the

P. Migoń (ed.), *Geomorphological Landscapes of the World*,
DOI 10.1007/978-90-481-3055-9_27,

Great (or Higher) Himalaya to the north. It belongs to a series of intermontane basins, the formation of which is closely related to the formation of the Himalayas as a whole.

The Himalayan Arc results from the collision between the Asian and Indian plates, which occurred about 50–45 million years ago. The compressional motion between the two plates has been, and continues to be, accommodated by slip on a suite of major thrust faults, connected at depth along a major detachment plane. The extreme elevations were acquired by stacking of crust units in a continuing continental subduction régime. The Himalayan Range is still rising at a rate estimated to be between several millimeters per year to more than 1 cm/year. The collision process created a series of elongated, more or less parallel and asymmetrical ridges, developed to the north of the Indo-Gangetic plains as a fold-and-thrust belt (Lesser Himalaya), which controls the drainage pattern.

To the north, the steep barrier of the Greater Himalaya reaches more than 8,000 m above sea level (Fig. 27.1). It represents a more than 10 km thick thrust unit made of crystalline, gneissic rocks, bounded at depth by the Main Central Thrust, and overtopped by sedimentary rocks, mostly limestones, that now underlie the Himalayan peaks. It separates two very contrasted terrains: the humid, tropical, monsoon-influenced Indian subcontinent and the cold, arid, and rugged Tibetan and Central Asian High Plateaus. Nowhere in the Himalayan Range is this bioclimatic gradient greater than along the Annapurna Range, north of Pokhara.

The Pahar zone has developed between the Lesser and the Higher Himalayas, and may locally widen in the form of intermontane depressions such as the Pokhara, Kathmandu, or Kashmir valleys. They correspond to large confluences of river valleys and/or to fluvio-lacustrine basins, developed on the back of thrust units of the Lesser Himalaya. They were initiated by tectonic damming as a result of a relatively faster uplift rate in the Lesser Himalaya than along the Pahar, transitional zone.

In contrast to the flat, perched, lacustrine basins of the Kashmir and Kathmandu valleys (Burbank and Raynolds 1984), the Pokhara valley floor is characterized by an extensive, gravel-covered surface, the formation of which has been influenced by a long period of fluvial modeling and dissection, and was the

Fig. 27.1 Northern part of the Pokhara valley, developed at the foot of the High Himalayan Front, dominated by Macchapuchare (6,993 m), Gangapurna (7,454 m), Annapurna III (7,555 m), Annapurna IV (7,524 m), Annapurna II (7,937 m), and Lamjung Himal (6,983 m), from left to right. The Seti Khola, in the foreground, issues from deep gorges cut below the glaciated cirque of Sabche. The river is responsible for the accumulation of the indurated Gaunda conglomerates, which underlie the two highest and very flat terrace levels, for the catastrophic accumulation of Pokhara gravels, deposited about 500 years ago, and for their recent dissection into several (here at least five) strath terraces (Photo M. Fort)

locus for catastrophic events and processes developed in relation to the proximity of the steep Main Central Thrust Front (Fort 1987).

27.3 Landforms and Landform Diversity

Besides magnificent mountain views, the Pokhara basin is characterized by several specific landforms. Firstly, the wide, flat morphology of the Pokhara "plain" is striking, a view reinforced by the sharp contact between the plain and the surrounding hills. The plain slopes to the south; the general longitudinal gradient varies from 32‰ upstream to 9‰ downstream. The plain also slopes laterally from a central axis, a feature that has caused diversions of the tributary streams. The surface of the plain displays a braided-channel morphology (Fig. 27.2). These characteristics are those of a large alluvial outwash fan. In fact, this plain is underlain by the so-called Pokhara gravels (Gurung 1970), excavated by the present Seti Khola River, hence providing numerous sections that permit one to analyze and interpret the nature of the gravels and their mode of deposition.

Another distinctive landform of the Pokhara valley is the dramatic set of terraces shaped by the Seti Khola and its tributaries by both vertical incision and lateral erosion (Fig. 27.1). The number of terraces increases downstream, whereas their relative height above the Seti thalweg increases upstream, from 60 to 50 m in the south to >100 m to the north. Most of the terrace levels are unpaired, a feature distinctive of meandering streams and rapid incision, this last statement being reinforced by the fresh appearance of the topographic surface and the absence of soil developed on terrace surfaces.

The canyons of the Seti Khola and its tributaries are among the most intriguing features of the valley (Fig. 27.3). Interrupting the long sections of terraces, they occur along limited reaches, a few hundred meters to 1 km long, and are deeply (up to 50 m) entrenched into a material made of gravels and boulders, cemented together into a hard conglomeratic bedrock with a rich limestone matrix, locally known as "gaunda" (Hormann 1974). These gorges are locally so narrow that only the sound of water can be heard; in some cases the stream has even disappeared in underground tunnels. One of these canyons is crossed by the Mahendra Pul (bridge), along the main Kathmandu road before entering the old bazaar of the city. These gorges are often associated with potholes and caves, such as the Mahendra and Chamere caves, close to Batulechaur village, the Jogi cave in Balam Hill, or the Gupteshwor and Davis falls caverns in

Fig. 27.2 Surface, braided morphology of the Pokhara gravels, as highlighted by the rice-fields pattern, east of Pokhara airport (Photo M. Fort)

Fig. 27.3 Major terrace levels south of Pokhara valley, underlain by the Pokhara gravels. They have buried the older, indurated "gaunda" conglomerates, which are exhumed by the recent erosion of the Seti River, as observed in the foreground, where potholes and small canyons have developed (Photo M. Fort)

Chorepatan, south of the Phewa lake: there, the Pardi River disappears into a tunnel, 200 m long, with a natural bridge on which the Sidartha highway passes. The development of these karst-like features provides additional evidence for the combined action of water dissolving the limestone and abrading the conglomerates.

The last feature that makes Pokhara famous is the many lakes ("tal" in Nepali) that are found along the edges of the valley (Fig. 27.4). Most of them (Dipang, Maidi, Khalte, Kamalpokhari, and Gunde lakes) have virtually disappeared due to siltation. The lakes Rupa, Begnas, and Phewa are larger, and their sinuous shorelines clearly suggest that they are drowned valleys (Gurung 1970). Close to Pokhara city, the largest of them, the Phewa Tal, is an important tourist attraction, with its waters reflecting the entire Annapurna Himalayan peaks during clear days. The occurrence of these lakes in juxtaposition with the gravelly plain of Pokhara reflects their origin, as a response to the deposition of the Pokhara gravels.

27.4 The Pokhara Gravels

The Pokhara gravels (Gurung 1970; Yamanaka et al. 1982) are the main component of the basin fill: their top layer underlies the geomorphological surface upon which Pokhara town has been built. They extend from Bharabhure at the mouth of the Seti Khola gorge, downstream to Dhoban, at the foot of the Mahabharat Lekh. The total thickness of their accumulation decreases downstream, from an average thickness of over 100 m to about 60 m, although local variations are observed depending on the buried topography. The sections, well visible from along the Prithvi Narayan Road across the Seti valley or its tributaries such as the Bijaypur, reveal the main characteristics of the Pokhara gravels and their modes of deposition.

The Pokhara gravels consist of a rapid succession of beds, decimeters or meters in thickness, with flat basal contacts (Fort and Freytet 1979). The material is mainly composed of layered, sub-angular to sub-rounded, mostly calcareous gravels, centimeters to decimeters in size, embedded in a muddy, calcareous matrix present in variable proportions (Fig. 27.5). Blocks of a meter or more in size – mostly gneisses (Higher Himalaya) or quartzites (Lesser Himalaya) – can also be found randomly within the whole accumulation package. Blocks of exceptional size, such as the Bhimsen Kali Boulder (32 m in diameter) visible on the University campus of Pokhara (Fig. 27.6), are restricted to the top-most layers where they are distributed upon the surface of the Pokhara plain. All these sedimentological characteristics indicate that the Pokhara formation is an alluvial

Fig. 27.4 The Phewa Lake, seen from the west, with the Pokhara valley in the background. This lake is a remnant of a drowned valley dammed downstream by the catastrophic deposition of the Pokhara gravels. This lake, like many others located along the edges of the Pokhara valley, is nowadays subjected to intense siltation by tributary streams (Photo M. Fort)

Fig. 27.5 A 25-m high section of the Pokhara gravels. Noticeable are the flat beds that include random occurrences of big boulders. This accumulation typically exhibits irregular alternations of debris-flow and mud-flow layers (Photo M. Fort)

fan deposit, transported alternately by muddy flows, debris flows, and torrential discharge (Fort 1987). The occurrence of the largest boulders in the final stage of deposition can be explained as a sorting phenomenon distinctive of the dense, debris laden, muddy flow of the Pokhara discharge.

This discharge was first considered to be a product of glacio-fluvial outwash (Gurung 1970; Hormann 1974;

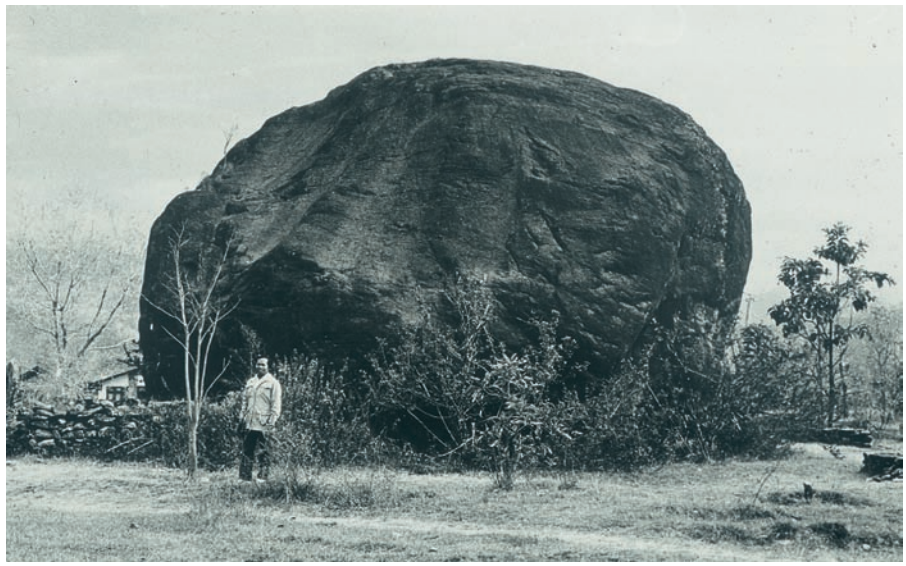

Fig. 27.6 The famous Bhim Kali boulder, 3,000 t large, preserved on the Pokhara University campus. A local legend tells that this rock was thrown down from Machapucchare Peak by the powerful hero Bhim. In fact, it represents the final stage of Pokhara gravels deposition, and was brought by a competent, highly muddy flow nourished by coarse debris detached from the High Himalayan Front. Most of these boulders have nowadays disappeared as they have been quarried (Photo M. Fort)

Fort and Freytet 1979), because most of the clasts are limestones derived from the glaciated cliffs of the Annapurna Range. However, the gneissic nature of the largest boulders indicates that materials derived from the adjacent valley walls located between the glacial cirques and the Pokhara plain were also incorporated by this massive discharge. Moreover, the volume of Pokhara gravels (estimated as >4 km^3; Fort 1987) and their dating between 400 and 1,100 ^{14}C years (Yamanaka et al. 1982; Fort 1987) suggest the occurrence of a short-lasting, historical event that led to the rapid filling of the Pokhara valley by a giant debris flow and to the damming, and hence flooding of the adjacent valleys. The present lakes are the relicts of this exceptional event.

Among the various origins and formation conditions that can explain this sudden, huge supply of both water and debris, it seems that ice and rock avalanches and/or landslide-dammed lake outbursts are capable of liberating the greatest volumes of water and debris simultaneously, in such a catastrophic way. Hence, these processes are the most likely causes of the exceptional Pokhara gravel discharge. The sources of the debris are the very steep slopes of the south face of Annapurna III and IV (Fig. 27.7). The triggering factor of an event of such a magnitude has probably to be related to a tectonic-induced instability, i.e., to an earthquake, the only mechanism capable of bringing instantaneously a slope into disequilibrium and setting into motion so huge a quantity of ice and rock material (Fort 1987).

27.5 Evolutionary History

The Pokhara gravels have buried an irregular topography, which includes the relicts of former stages of Pokhara valley evolution. The evolutionary history of the valley can be summarized as follows.

The formation of the intermontane basin is the result of a long-lasting process. As already pointed out, the basin belongs to the Pahar belt, which is rising at a slower rate than the Mahabharat Lekh (Lesser Himalaya) to the south and the Higher Range to the north. More specifically, it is situated along an anticlinal

Fig. 27.7 Close-up view of the northern part of the Pokhara valley, Seti Khola gorge, and the upper glaciated cirque of Sabche. The terraces developed on the foreground are underlain by the Pokhara gravels. Upstream the Seti gorge, entrenched within the High Himalayan gneisses, is particularly narrow and steep. It channelized the giant, catastrophic debris flow of Pokhara gravels, originated from the southwest face of Annapurna IV (Photo M. Fort)

structure, mostly carved out into schists with intercalations of quartzite and dolomitic limestone bands. The distinctive z-shape of the basin and of the Seti Khola course and its tributaries, together with the arrangement of the surrounding hills, may be interpreted as the superficial expression of deformation – namely fault scarps – induced by the oblique, northward convergence of the Sub-Himalaya underthrusting the Lesser Himalaya.

The present, large-scale morphology of the valley is the result of a complex alternation of aggradational and erosional stages, developed under a tropical, seasonally contrasted climate. In fact, the Pokhara valley has experienced several stages of dissection, separated by brief, yet intense periods of aggradation (Fig. 27.8). A few patches of perched calcareous breccia, like those preserved along the Sarankot ridge, represent early remnants of slope deposits, spread over an aggradational pediment, presently reduced to sharp, karstic ridges modeled into towers by the dissolution of carbonates. After a period of basin dissection to a depth of 50 m or more, perched weathered gravels provide evidence of a previous Seti Khola course. Another period of dissection also followed which, in the central part of the basin, penetrated lower than the present level of the Seti Khola river bed (Fig. 27.9).

This evolution was interrupted by the deposition of the "gaunda" (or "Gachok") conglomerates that are the first extensive deposits in the Pokhara valley. They underlie the prominent terrace benches of the northern part of the valley, near Lachok and Gachok villages (Fig. 27.8). Their well-rounded gravels and sand grains, dominated by limestone, are derived from the south-facing, upper cliffs of the Annapurna Himal. They were until recently considered to be glacio-fluvial outwash deposited by the melting of ice after the last glaciation, but are now explained by similar, catastrophic processes as were involved in the formation of the Pokhara gravels. After their deposition and lithification, these conglomerates were dissected to form a stepped topography of fluvial terraces, well preserved north of the valley, upstream of the Mardi Khola confluence, whereas to the center and south of the valley, they disappear under the Pokhara gravels.

The more recent and rapid deposition of the Pokhara gravels has resulted in burial of the former topography, disorganization of the entire drainage system of the valley, and creation of the peripheral lakes. Soon after, the Seti Khola started incising its bed again to readjust its longitudinal profile to the base level of the Mahabharat Range. In the central part of the valley, the new Seti course, superimposed on the Pokhara gravels, locally cut through the hard "gaunda" conglomerates (present beneath the Pokhara gravels), so that it prevented the river to widen its beds, thus leading to the formation of canyons instead (Fig. 27.4). Elsewhere, the presence of the loose Pokhara gravels favored the shift of the Seti River and the subsequent development of unpaired flights of terraces (Fig. 27.10).

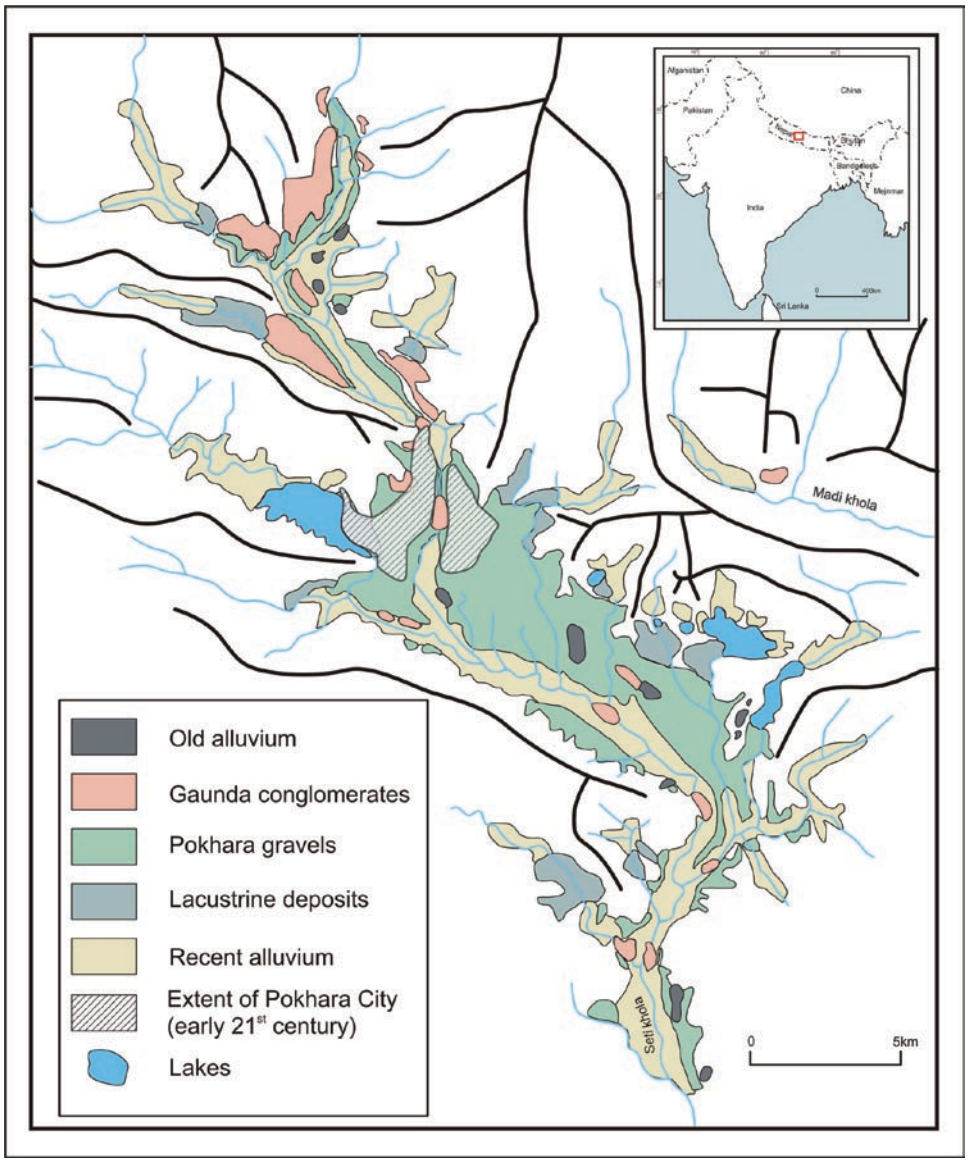

Fig. 27.8 Map of the major deposits of the Pokhara valley. The catastrophic accumulation of the Pokhara gravels buried a dissected topography carved into the older "gaunda" conglomerates. Since the giant debris flow, the Seti River cut through the Pokhara infill, and found locally the "gaunda" conglomerates beneath, so it was forced to incise deep canyons

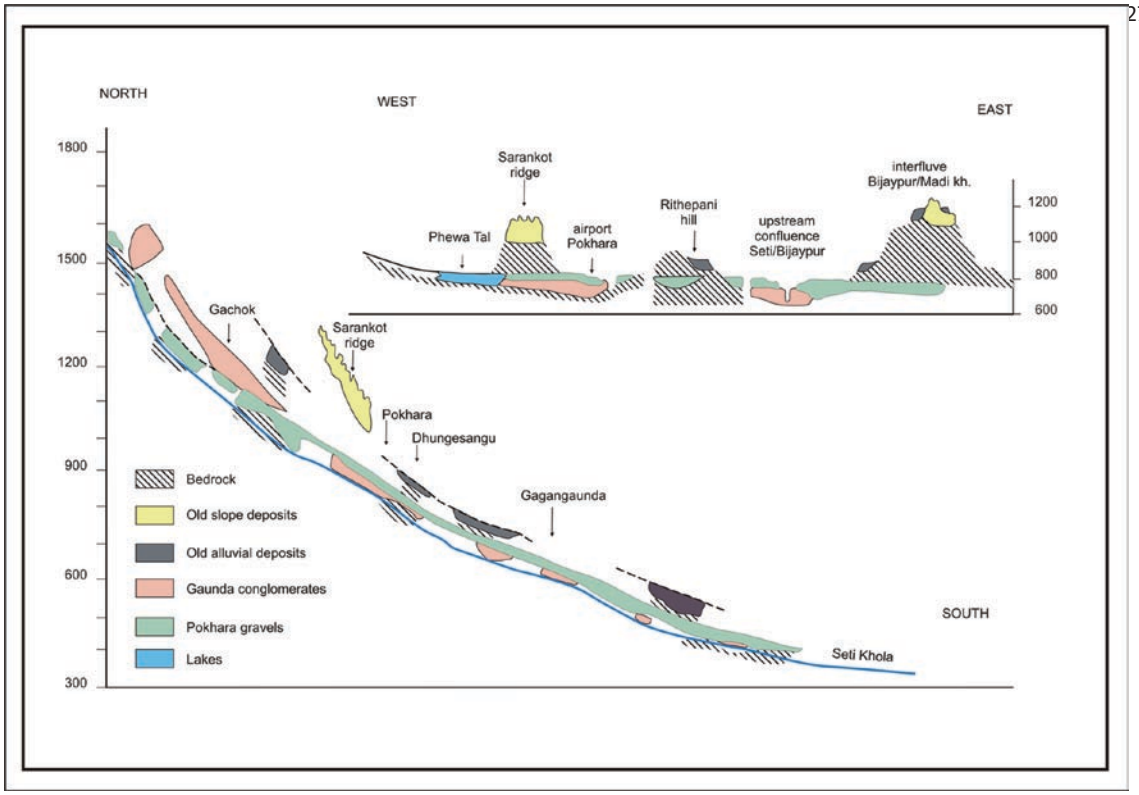

Fig. 27.9 Cross section and altitudinal distribution of the various formations deposited in the Pokhara valley in the last 100,000 years. To the north of the valley, the oldest perched slope deposits (limestone breccia), the old, deeply weathered alluvium and the Gaunda-Gachok formations are stepped above the most recent Pokhara gravels filling, whereas in the center of the valley, the Pokhara gravels have buried the Gaunda-Gachok conglomerates. This particular setting clearly indicates the rising of the High Himalayan Front relative to the basin

Fig. 27.10 Since the deposition of the Pokhara giant debris flow, the Seti Khola started incising its bed again at a rate varying between 20 cm/year upstream and about 10 cm/year downstream of the basin. Locally, the presence of loose Pokhara gravels favored the shift of the Seti River and the development of many, unpaired terraces (Photo M. Fort)

27.6 Conclusions

The catastrophic episode of the Pokhara debris-flow aggradation serves as a model for the geomorphic evolution of the High Himalayan Front (Fort 1987; Fort and Peulvast 1995). It shows how a huge mass of debris almost instantaneously delivered from the front may temporarily be stored in an intramontane basin of the Pahar before transit to the Himalayan foothills. It also demonstrates how the steepness of the still rising front of the very Himalaya ("the abode of snow") is maintained by sporadic processes of collapse of the mountain walls involving a combination of both glacial and seismo-tectonic factors. This makes the basins and the valley trenched across the High Himalayan Front, the areas most prone to unpredictable, catastrophic geomorphological hazards, and creates a permanent, low-recurrence, but significant threat for the growing population living in these valleys.

The Author

Monique Fort is a Professor of Geomorphology and Environmental Sciences, Natural Hazards and Risks, in the Department of Geography of Paris Diderot – Paris 7 University. She worked extensively in various high mountains of the world (Alps, Central Asia, and Himalaya). Her research interests evolved from the relations of landforms with respect to geological structures, then to glacial and climatic fluctuations, and palaeoenvironmental reconstructions. Ongoing field work includes studies on current instabilities and natural hazards (large-scale landslides, catastrophic floods) in the Himalayas and Pamir mountains, floods impacts, and their prevention in various parts of France. She published more than 50 peer-reviewed papers. She was the Vice President of the International Association of Geomorphologists (2005–2009), and member of the Commission on Mountain Response to Global Change of the International Geographical Union (2008–2012).

References

Burbank DW, Raynolds GH (1984) Sequential Late Cenozoic chronologic and stratigraphic development of the Kashmir inter-montane basin, northwestern Himalayan foredeep. Nature 311:114–118

Fort M (1987) Sporadic morphogenesis in a continental subduction setting. Z Geomorph NF, Suppl 63:9–36

Fort M, Freytet P (1979) L'évolution sédimentaire récente du basin intramontagnard de Pokhara (Himalaya, centre-ouest Népal). CR Acad Sci Paris 289(D):1195–1198

Fort M, Peulvast J-P (1995) Catastrophic mass-movement and morphogenesis in the peri-tibetan ranges, examples from West Kunlun, East Pamir and Ladakh. In: Slaymaker O (ed) Steepland geomorphology. Wiley, Chichester, pp 171–198

Gurung HB (1970) Geomorphology of Pokhara Valley. Himalayan Rev 2–3:29–49

Hagen T (1961) Nepal, the Kingdom in the Himalayas. Revised and updated with Deepak Thapa 1999. Himal Books, Kathmandu, Nepal

Hormann K (1974) Die Terrassen an der Seti khola. Ein Beitrag zur Quartären Morphogenese in Zentral Nepal. Erdkunde 28(3):161–176

Yamanaka H, Yoshida M, Arita K (1982) Terrace landforms and Quaternary deposits around the Pokhara valley, central Nepal. J Nepal Geol Soc 2(Sp. Issue):113–142

Chapter 28
The Loess Plateau of China: Aeolian Sedimentation and Fluvial Erosion, Both with Superlative Rates

Xiaoping Yang, Tao Liu, and Baoyin Yuan

Abstract Loess, draped over various types of bedrock landforms, is found in about 10% of the land surface on Earth. Among various loess landscapes in the world, the Loess Plateau of China, located in the middle reaches of the Yellow River, is the largest terrain of continuous and thickest loess sedimentation, offering probably the best terrestrial record for research on Quaternary palaeoclimatic changes. Prior to loess deposition, karst landforms formed in Cambrian and Ordovician carbonates, sandstone hills and basins were common in the area of the present-day Loess Plateau. The major components of contemporary relief are tablelands (Yuan), long ridges (Liang) and round hills (Mao), all named after local folks' language. Secondary erosion forms, such as gullies and dolines, have been impressively developed in the Loess Plateau, and their formation may have accompanied loess sedimentation for a long time, mostly in the Quaternary but occasionally much earlier. Erosion and collapse processes have been tremendously enhanced during historical times due to strong human impact.

Keywords China • gully erosion • human activity • loess • tableland

28.1 Introduction

Loess, composed mainly of windblown silt-sized particles, is a sedimentary deposit. It is draped over various kinds of bedrock landscapes, amounting to about 10% of the land surface on Earth (Liu 1985), concentrated in the temperate zones and on semi-arid desert margins. Loess deposits are characterized by their loose structure, high porosity, high concentration of calcium carbonate and relatively homogeneous composition. Vertical fissures typically develop in loess. Consequently, there are considerable similarities of landforms in the various areas covered by loess. For example, forms derived from the processes of collapse and subsidence are common in loess regions all over the world. The loess landscape is very prone to both water and wind erosion due to the silty nature of the deposit. Thus, the annual erosion rate may reach 5,000–15,000 t/km^2, and even 20,000 t/km^2 in the loess regions of northern China (Chen et al. 2007). A large proportion of this sediment is transported into the Yellow River (Huang He), causing the yellow colour of the river water. On average, the suspended sediment load, measured at the mouth of the Yellow River, is as high as 35 kg/m^3, with a maximum of 130 kg/m^3 (Jiang et al. 2007).

Loess landforms are various kinds of valleys and a range of denudational forms between these valleys. In many parts of the world loess is of Quaternary age. However, in western China its deposition had started by the Miocene, ca. 22 million years ago (Guo et al. 2002). Taking the Loess Plateau in China as an example, this chapter aims to introduce the landforms directly associated with the unique features of loess. The Loess Plateau is the largest area of continuous and thick loess sedimentation in the world. The landforms are controlled mainly by erosion accomplished by streams, sheet and underground flows and by slope processes.

28.2 Geographical Setting

The Loess Plateau is located in the middle reach of the Yellow River, between latitudes 35–41°N and longitudes 102–114°E (Fig. 28.1). Although the term 'Loess Plateau' is widely used, there are still different opinions on the

P. Migoń (ed.), *Geomorphological Landscapes of the World*,
DOI 10.1007/978-90-481-3055-9_28,

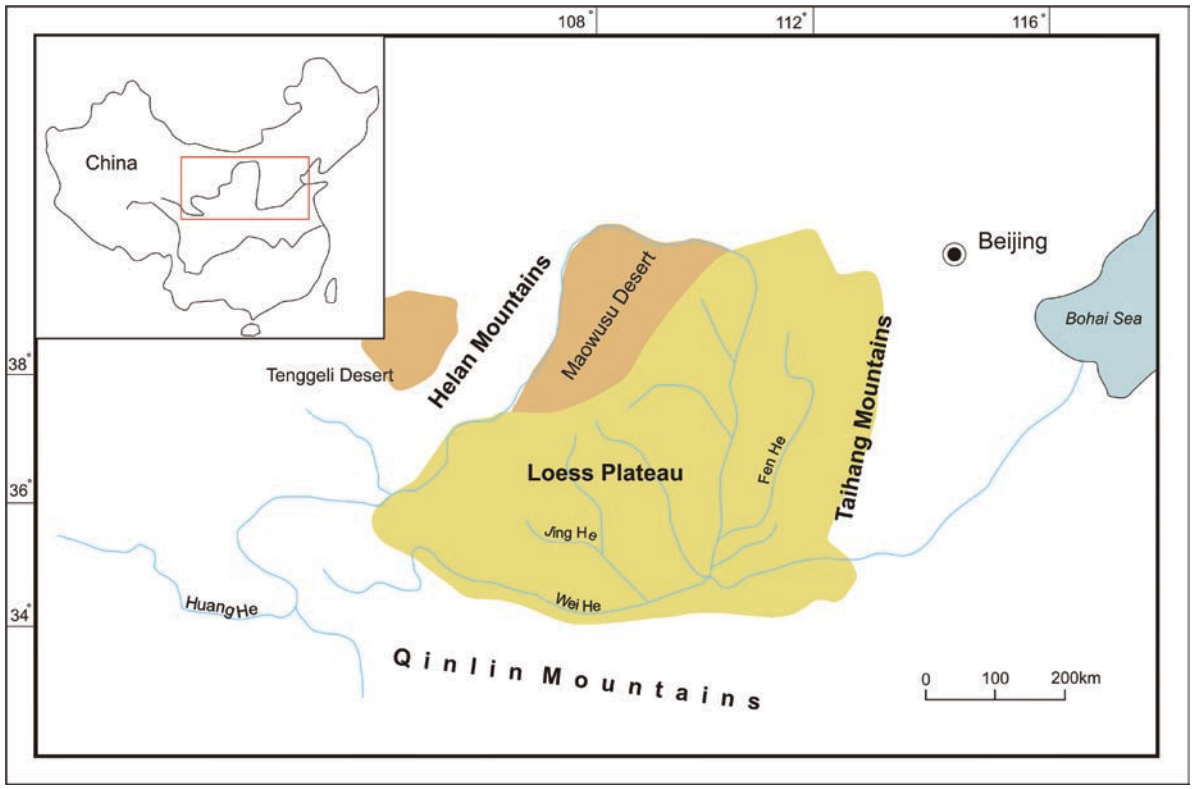

Fig. 28.1 Location of the Loess Plateau. The shadowed area indicates the Loess Plateau including the mountainous margins

boundaries of the Plateau among Chinese scholars. The key difference is whether to consider the mountainous areas on its margins as part of the Loess Plateau. Dependent on the definitions, the area of the Plateau varies accordingly.

The climate of the Loess Plateau is controlled by the East Asian monsoon system. It is characterized by hot summers and cold winters. The mean annual temperature decreases from 10°C to 6°C, and mean annual precipitation from 600 to 300 mm from south to north (Yang and Pretzsch 1999; Chen et al. 2007). The precipitation falls mainly in the summer months, often in a few heavy storms. Both arable land on steep slopes and gullies will be major sources of sediments because erosion can be extremely intensive during storms.

Although being economically backward at present, the Loess Plateau is considered to be the cradle of Chinese civilization, and has been intensively used for grain production over thousands of years. Continuous soil erosion has been imposing a tremendous challenge to social and economic development. Severe soil erosion is directly caused by destruction of the vegetation cover, but related to the loose structure of the sediment as well. To mitigate this environmental pressure, the Chinese government currently strives to reverse this trend by reducing agricultural cultivation and by planting trees and grasses. However, there is a controversy over whether the natural potential of the ecosystem is relatively dense forest or steppe.

28.3 Major Landforms

The large geomorphological subregions in the Loess Plateau are to a considerable degree influenced by the geological settings beneath the loess. Bedrock hills and mountains with a thin veil of loess are common in marginal areas. Typical large-scale landforms in the core areas of the Loess Plateau are, however, the *Yuan*, *Liang* and *Mao,* which are named after the local folks' language. As loess is very prone to erosion, various

types of erosion gullies occur on all kinds of slopes covered by loess. In addition, the process of underground subsidence takes place in the Loess Plateau, resulting in a number of distinctive landforms.

28.3.1 Yuan (Tableland)

Yuan means high tableland in Chinese, and it refers to a large remnant of a once continuous flat surface. There has been little erosion on the surface of *Yuan*. Normally, *Yuan* is based on old flat landforms such as basin bottoms where loess has accumulated to a thickness of over 100 m. Due to the flat basement, the strata of loess and palaeosols developed within it lie horizontally. As erosion proceeds, the large surface of *Yuan* will be destroyed and divided into small pieces. Interbedding of loess and paleosols of different ages is a significant stratigraphical feature of this landform. The loess – paleosol sequence in Luochuan, the centre of the Loess Plateau, is probably the best-known terrestrial record of Quaternary palaeoclimates in the world (Heller and Liu 1982).

28.3.2 Liang (Long Ridge)

Liang, meaning flat ridge in Chinese, refers to long ridges which can be several hundred metres to dozens of kilometres long but just dozens to hundreds of metres wide. The top of the ridge remains at a similar elevation and both sides could be as steep as 20° (Fig. 28.2). Dissection of a *Yuan* by erosion processes would produce numerous *Liangs*. However, most *Liangs* seem to be related to bedrock morphology. The gorges or valleys between the *Liangs* may have formed prior to loess sedimentation. The bedrock ridges, covered by loess, are often the basic structure of long, large *Liangs* in the Loess Plateau.

28.3.3 Mao (Round Hill)

Mao, meaning a round hill with a loess cap, can be generally described as a dome-shaped loess hill. The slopes around a *Mao* could be as steep as 20°. A *Liang* could be divided into a number of *Maos* due to intensive erosion.

Fig. 28.2 Three parallel *Liangs* (long ridges) dissected by gullies in the northern Loess Plateau. The top of *Liangs* is characterized by terraces of arable lands

28.4 Minor Landforms

28.4.1 Gullies

Rocks at Earth's surface are constantly being altered by water, air, changing temperatures, and other environmental factors. On a human timescale, typical rates of soil formation are very slow, because the formation of a single metre of soil depth requires a time span of 10,000–50,000 years. Soil erosion is the physical removal of soil particles by an agent such as stream, sheet flow or wind. In undisturbed conditions, soil erodes approximately as rapidly as it forms. Improper farming, livestock grazing and logging, however, can accelerate erosion. It is estimated that about 0.4 billion t of topsoil are formed annually on Earth by weathering, but 25 billion t are lost through erosion each year at the present time (Thompson and Turk 2005).

When it rains, three kinds of erosion may take place: sheet, rill and gully erosion. The former is caused by a sheet of water flowing across the sloping surface. A rill is an initial stage of linear erosion prior to gully development, often just a few centimetres deep and 10–15 cm wide, occurring mostly in the topsoil, while gullies incise into subsoil and even into parent rocks, reaching a depth of dozens of metres and a length of several kilometres. Rills can be formed in a single storm, but the formation of a gully needs a much longer period.

Although factors contributing to soil erosion may vary from region to region, the two most crucial ones are slope inclination and the amount of bare soil that is exposed on surface. The steeper the slope and lesser the amount of vegetation cover, the greater the soil erosion. Depending on local conditions, the depths and lengths of gullies vary considerably in the Loess Plateau. In the early stage of gully development in loess, the slopes of the gully are steep and the floor is very narrow. During later stages of its development the width increases and the slopes become less steep (Fig. 28.3). Rilling and gullying are the most evident processes of soil erosion in the Loess Plateau. In many cases land use practices have had great impact on the erosion rate and consequently on the formation and development of gullies. In the northern part of the Loess Plateau, where the soil erosion is particularly problematic, gully densities may reach 5–7 km/km^2 and gully heads may retreat backwards at an average rate of up to 10 m/year.

Fig. 28.3 Small gullies with almost vertical slopes in front and a large gully in the middle of the photo, northern Loess Plateau

28.4.2 Loess Doline

Due to underground erosion dolines often occur in the upper part of the slopes in the Loess Plateau (Fig. 28.4). Underground erosion is a physical process in loess areas, as the loess particles are carried away by underground flow, unlike in karst where the rocks are dissolved. In the headwater areas, the collapse of dolines is a common process of headwater erosion. Doline slopes can be vertical to relatively flat. Dolines with vertical slopes may reach a maximum depth of 20 m, others less than 10 m. Just like in karst areas, a series of dolines may be connected by underground channels.

28.4.3 Loess Column

As vertical fissures are well-developed in loess deposits, the processes of subsidence and collapse may cause some columns of the deposit to stand isolated above the ground. Such forms are commonly called loess columns.

28.5 Evolutionary History

The evolutionary history of the Loess Plateau can be divided into three different stages, i.e. the period of formation of bedrock landforms prior to loess sedimentation, the period of geomorphological evolution during loess sedimentation and the latest modification of the erosion landforms after loess sedimentation. Strictly speaking, loess sedimentation never stops; it is just a change of sedimentation rate. The loess in the Loess Plateau has originated from deserts in northwestern China (Derbyshire 1983; Liu 1985; Yang 2001). Its sedimentation rate, controlled by the global climate changes, has been much greater during glacials than during interglacials (Liu 1985). On the other hand, it is also to be expected that increased precipitation during the interglacials would enhance fluvial processes, causing an increase in incision.

In the core part of the Loess Plateau the loess has been deposited during the last 2.6 million years. Beneath the loess it is the red clay that was deposited between 7 and 2.6 million years ago (Ding et al. 2000). Various studies have shown that the red clay is of aeolian origin

Fig. 28.4 Loess dolines in the upper part of the slope, at the northern margin of the Loess Plateau. The red colour marks the bedrock (sandstone) landform upon which loess (light colour) has been deposited as a thick veil

too, transported probably by mid-latitude westerlies, whereas the loess was brought by the winter monsoon (e.g., Ding et al. 2000).

The key initial landforms that existed prior to aeolian sedimentation in the areas of the present Loess Plateau can be summarized as follows:

(1) Karst landforms formed in Cambrian and Ordovician carbonates. These palaeolandforms occur in the northern part of the Plateau. The carbonate outcrops are occasionally present.
(2) Hilly landscapes composed of sandstones and shales of Mesozoic age, present mainly in the marginal areas of the Loess Plateau (Fig. 28.4).
(3) Basins and slightly inclined plains. The palaeo-basins are the foundations of the large loess tablelands (*Yuan*). Indeed, the geological structure of the core areas of the Loess Plateau consists of basins rather than plateaux. The contemporary geomorphological character of the Plateau is due to the thick sediment of aeolian loess and red clay. The small tablelands in the eastern part of the Loess Plateau have developed on slightly inclined plains. The basements of the various loess tablelands would be different as well. The pre-Quaternary red clay occurs only occasionally. The ages of basement basins and plains are not identical. Therefore, only younger aeolian loess is present in the younger basins and plains.

In the Loess Plateau intensive incisions have taken place in the history of the loess sedimentation (Fig. 28.5). Loess has been deposited on various river terraces, with the younger loess being restricted to younger terraces. The older the terrace, the thicker is the loess. Therefore, the loess chronology is often used to date the ages of river terraces (e.g. Jiang et al. 2007). However, the causes of incision may vary, e.g. tectonic uplift, increase in precipitation and falling base level. During the Quaternary there has been clear regional differentiation in tectonic movements in the area of the Loess Plateau. For example, the southern margin of the Plateau, i.e., the graben of the Wei River, is continuously subsiding, whereas the northern margin is mainly subject to uplift. The Yellow River, as the largest river in northern China, acts as the base of erosion for the area of the Loess Plateau. The beginning of the full development of the Yellow River is still controversial and debated. The full development of the river means the process of incision would have cut through all the inland basins into which the river drained previously. The loess–paleosol sequence on the southeastern margin of the Loess Plateau suggests that the Yellow River was first formed at ~150,000 years ago (Jiang et al. 2007).

Many loess hills were formed while the loess was deposited on the hills built of basement rocks. However, some hilly loess landscapes are purely due to fluvial erosion. The forms of other present loess hills are probably inherited from the previous hilly forms caused by earlier erosion processes. This is quite common on the margins of the loess tablelands (*Yuan*). Intensive erosion should not be seen as a new phenomenon, associated with human activities in modern times. Also in the past, the loose structure and occurrence of vertical fissures increased the vulnerability of loess to water erosion, particularly when it rained heavily.

Various studies have demonstrated that erosion rates would be reduced if the land was to be kept as woodland/shrubland terrain rather than used for agricultural cultivation (e.g., Hessel et al. 2003). The historical literature tells that many parts of the Loess Plateau were covered by forest 2000 years ago. But forest almost disappeared from the flat areas and became degraded in mountainous terrains roughly in the period between the seventh and twelfth century AD. Dramatic destruction of natural vegetation has occurred during the last 400 years, when the population has increased rapidly in China, including the Loess Plateau (Shi 1985). Recent studies in a river basin in the northern part of the Loess Plateau confirmed that the average annual soil loss between 1981 and 1989 was very high, between 5,000 and 20,000 t/km^2, with a mean value of 14,460 t/km^2 (Fu et al. 2005). The direct cause of the increased soil erosion in the Loess Plateau has been deforestation accompanied by intensive cultivation, although the exact role of human activities in soil erosion is difficult to evaluate. To rehabilitate the ecological environment and to reduce soil erosion, China initiated the 'Grain for Green' project in the Loess Plateau during the past decade. Farmers were requested to plant trees and shrubs on the steep slopes of the Loess Plateau (Fig. 28.3) and have received grains and cash from the government as a return. There is no doubt that this measure will reduce soil erosion if it is sustained in the long term.

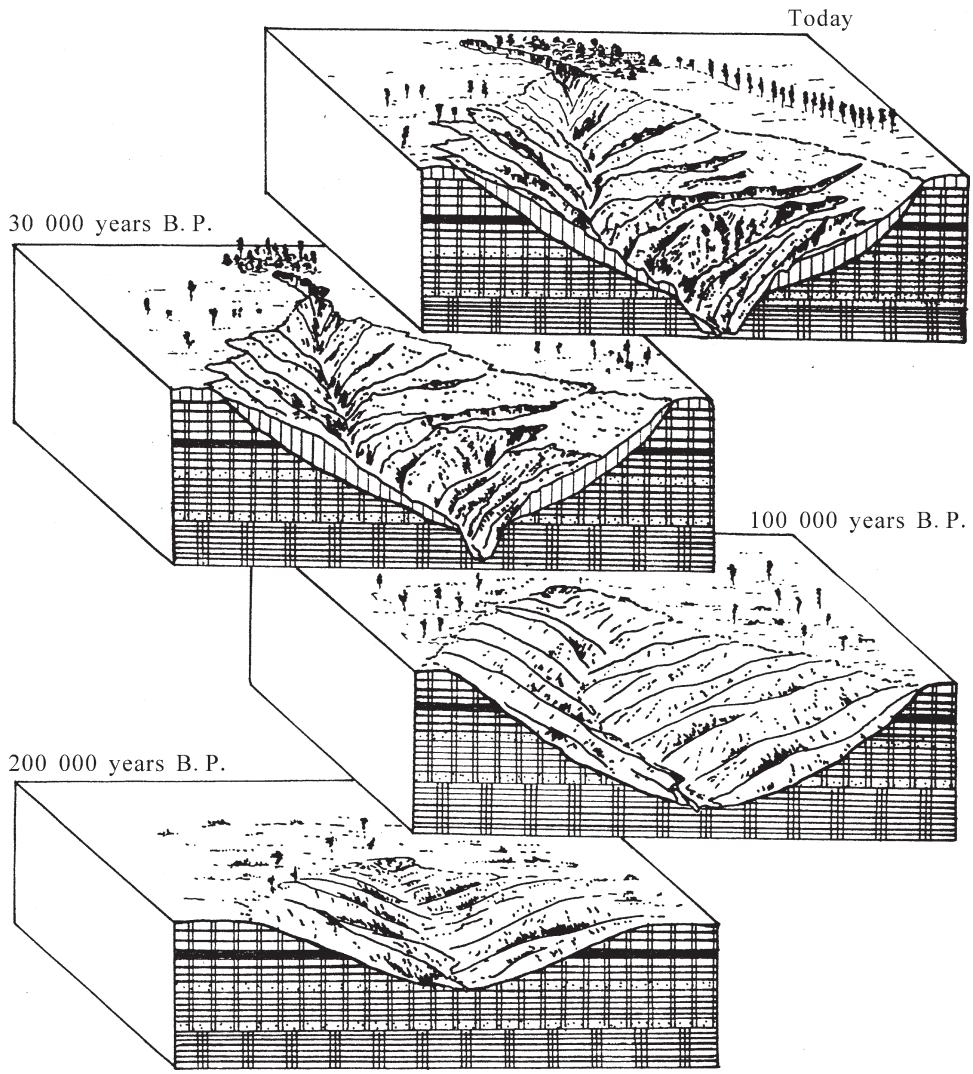

Fig. 28.5 Geomorphological changes of the central part of the Loess Plateau during the last 200,000 years. Reconstructed by Baoyin Yuan on the basis of palaeoclimatical data and loess – paleosol stratigraphy

28.6 Conclusions

Although the Loess Plateau was not glaciated during the Quaternary, its landforms are of quite young age. All were formed or modified during the latest period of Earth history. Even today water erosion may form impressive gullies in the Loess Plateau in a short period of time. The Loess Plateau has the thickest and largest cover of loess on Earth. The sedimentation of loess is closely related to climate changes on glacial – interglacial timescales. Therefore, the sedimentary sequence of the central Loess Plateau is probably the best terrestrial record on Earth for palaeoclimatic research. The strong winter monsoon has been the key agent bringing large quantities of dust from the desert regions to this area. The times of paleosol formation should represent periods with stronger fluvial processes. Older geological settings are often inherited by the loess landforms, showing the significant impacts of palaeo-landforms on the modern landscape. Strong erosion, which is associated with the basic lithological characteristics of loess and rainfall patterns in this environment (frequent storms), has been an important process in forming and modifying the loess landforms. As the cradle of Chinese civilization, the Loess Plateau has

experienced strong human influence during historical times. Therefore, the landforms in the Loess Plateau are among the most dynamic forms in the world. They are still experiencing considerable changes under different dynamics at the present day.

The Authors

Xiaoping Yang is Professor at the Institute of Geology and Geophysics, Chinese Academy of Sciences (CAS) and has been the chairman of the IAG Working Group on arid and semi-arid regions since 2001. His main research interests include dryland environments, specifically arid geomorphology and paleoclimatology during the Late Quaternary; global change and contemporary environmental issues such as desertification, particularly in northern China. He has published about 80 papers in international and Chinese journals and in abstract volumes of scientific conferences, has been on editorial boards of highly recognized research and review journals, and has served as a guest editor for dryland special issues of internationally reputable journals as well as co-author for the Chinese university textbook 'Physical Geography' (2005). He was awarded the Prize for Young Scientists in 2002 by Chinese Quaternary Association, COMLAND Award in 2007 by the International Geographical Union's Commission on Land Degradation and Desertfication, and Huang Jiqing (formerly written as Huang, T. K., one of the most important initiators of geological studies in China) Prize by Huang Jiqing Foundation in 2008.

Tao Liu is currently a graduate student for master's degree in Quaternary geology in the Institute of Geology and Geophysics, CAS.

Baoyin Yuan is Professor at the Institute of Geology and Geophysics, CAS. His main research interests include Quaternary geology and environmental changes in arid and semi-arid regions, particularly in the Loess Plateau of China. He has published over 100 papers in international and Chinese journals and edited or co-edited six books. He has been awarded various prizes over the years by Chinese scientific institutions.

Acknowledgements We would like to thank the Chinese Academy of Sciences (Grant no.: kzcx2-yw-119) and the National Natural Science Foundation of China (Grant no.: 40671020) for financial support.

References

Chen L, Wei W, Fu B, Lue Y (2007) Soil and water conservation on the Loess Plateau in China: Review and perspective. Prog Phys Geogr 31:389–403

Derbyshire E (1983) Origin and characteristics of some Chinese loess at two locations in China. In: Brookfield M, Ahlbrandt T (eds) Eolian sediments and processes. Elsevier, Amsterdam, pp 69–90

Ding Z, Rutter N, Sun J, Yang S, Liu T (2000) Re-arrangement of atmospheric circulation at about 2.6 Ma over northern China: evidence from grain size records of loess-palaeosol and red clay sequences. Quat Sci Rev 19:547–558

Fu B, Zhao W, Chen L, Zhang Q, Lue Y, Gulinck H, Poesen J (2005) Assessment of soil erosion at large watershed scale using RUSLE and GIS: A case study in the Loess Plateau of China. Land Degr Dev 16:73–85

Guo Z, Ruddiman W, Hao Q, Wu H, Qiao Y, Zhu R, Peng S, Wei J, Yuan B, Liu T (2002) Onset of Asian desertification by 22 myr ago inferred from loess deposits in China. Nature 416:159–163

Heller F, Liu T (1982) Magnetostratigraphical dating of loess deposits in China. Nature 300:431–433

Hessel R, Messing I, Chen L, Ritsema C, Stolte J (2003) Soil erosion simulations of land use scenarios for a small Loess Plateau catchment. Catena 54:289–302

Jiang F, Fu J, Wang S, Sun D, Zhao Z (2007) Formation of the Yellow River, inferred from loess – palaeosol sequence in Mangshan and lacustrine sediments in Sanmen Gorge, China. Quat Int 175:62–70

Liu T (1985) Loess and the environment. China Ocean Press, Beijing

Shi N (1985) Changes of forest and grassland in the Loess Plateau. Shaanxi People's Press, Xian (in Chinese)

Thompson G, Turk J (2005) Earth science and the environment, 3rd edn. Brooks/Cole, Belmont

Yang X (2001) Late quaternary evolution and Paleoclimates, Western Alashan Plateau, Inner Mongolia, China. Z Geomorph 45:1–16

Yang X, Pretzsch K (1999) Die chinesische Drei-Schlucten-Talsperre – ein Grossprojekt mit Kontroversen. Geoökodynamik 20:231–243

Chapter 29
Sanqingshan: The Incredible Granite Peaks of Eastern China

Michael F. Thomas

Abstract Sanqingshan and Huangshan, two areas of granite mountains in eastern China with World Heritage status, form iconic landscapes. Granites were intruded within a Palaeozoic orogenic zone during the Mesozoic and have been repeatedly uplifted to form striking mountain scenery. At Sanqingshan, a triangular pattern of faults delimits an area of towering rock pillars that rise above vertical cliffs of granite. These landscapes have strongly influenced Chinese classical painters and philosophers, and formerly held mystic importance in the Taoist religion. The so-called peak forests appear to reflect the chemical and erosive action of heavy monsoon rainfall acting on the dissected granite massif in a subtropical environment. The combination of rock type, tectonic history, and warm moist climate has created a spectacular relief rarely seen elsewhere.

Keywords Chinese mountains • granite weathering • iconic landscapes • rock pillars

29.1 Introduction

China possesses many iconic landscapes: from the 8,000 m peaks of the Himalayas, the great Tibetan Plateau in the southwest to the tower karst of Guilin in the far south, and the great deltaic plains of the Yangtse and Huang He (Yellow River) in the east. Perhaps less well known outside China are the spectacular granite mountains of eastern China, where two mountain parks are now recognized as World Heritage areas, not only for their unique landscapes, but also for their cultural and religious significance. These are Huangshan (Anhui Province, inscribed in 1990 for both its cultural and natural heritage) and Sanqingshan (Jiangxi Province, inscribed in 2008 for its natural heritage: superlative natural phenomena and exceptional natural beauty). This account is mainly concerned with the latter area.

The granites of Sanqingshan belong to an orogenic zone that marks the collision of Yangzi and South Chinese (Cathaysian) blocks in the Early Palaeozoic. Into the heart of these mountains granite intrusions were emplaced in the Jurassic and Cretaceous periods, and these have been exposed and sculptured during repeated episodes of uplift, from the Late Cretaceous throughout the Cainozoic. Their present-day mid-latitude (28°50′N–29°N) location is situated in a subtropical, wet monsoonal climate, receiving over 2,000 mm of rainfall annually.

Images of towering mountain peaks, often associated with isolated pine trees clinging to the mountain slopes, recur in Chinese painting across the centuries. Such images embody ancient religious and philosophic ideas: the mountains being the dwelling places of immortal beings and linking earth to heaven, while also offering refuges from a turbulent world and havens for contemplation. For nearly two millennia, Taoist priests have built temples in the mountains, and in dynastic China, the emperors commonly sought the blessing and advice of the priests, while artists often found inspiration in these remote and sacred places. Huangshan (Yellow Mountain) in particular has long been a place of pilgrimage and temples have been built among the peaks of both areas.

In the seventeenth century (Qing dynasty), Anhui Province emerged as a cultural center and landscape painters from this region (known as the Anhui School) visited many sacred mountains, which had previously been inaccessible. Hongren (1610–1664) was prominent in this school and took up residence in Huangshan, in the southwest of Anhui province. The area was

P. Migoń (ed.), *Geomorphological Landscapes of the World*,
DOI 10.1007/978-90-481-3055-9_29,

famous for its granite pinnacles that often appeared to emerge from the mists like islands in the sea. Hongren produced an "Album of scenes from Huangshan," which is now in the Beijing Palace Museum, and other artists were also inspired by this area (Cahill 1981).

In Jiangxi Province, some 150 km to the southwest of Huangshan, Sanqingshan is another, equally imposing massif, less well known only because of its location beyond Anhui, a former center of ancient Chinese culture and power. These two areas represent what can be regarded as "iconic landscapes," and idealized representations of their rock pinnacles and pine trees struggling for survival on vertical slopes are not only frequent in Chinese painting, but also often represented in the fantastic, sculpted shapes of Chinese classical gardens, such as those in the ancient city of Suzhou, near Shanghai. Miniature representations of these peaks were also created, frequently from jade.

So striking and unusual are these two areas that their landscapes deserve comparison with the famous granite mountains of Yosemite in the USA, and the Serra do Mar of eastern Brazil (which includes Rio de Janeiro, covered elsewhere in this book). Most other famous granite, and granite-gneiss, landscapes can be identified by their prominent granite domes and kopjes, such as the Spitzkoppe in Namibia. Others present an apparent confusion of smaller domes and rock boulders (*tors*), as in the Matopos Mountains of Zimbabwe and in Idaho and Wyoming, USA. Many famous granite landscapes occur in cratonic settings, but others form as syn- or post-orogenic intrusions in rising mountain chains and can emerge as towering massifs with complex morphology, as in the Guadalajara Mountains of central Spain and at Yosemite. The landscapes of Huangshan and Sanqingshan belong to this latter type of terrain, and have been subjected to repeated tectonism. They are characterized by a multitude of narrow pinnacles, which combine with massive vertical rock faces to present landscapes that are at once awe inspiring, yet delicate in their detail.

In this account the geological basis and geomorphological interpretation will be presented as a partial understanding of their scenic prominence.

29.2 Geology and Landforms

Huangshan and Sanqingshan are situated in a major NE–SW tectonic zone crossing southcentral China (Fig. 29.1a) and known as the Suzhou-Dexing Suture Zone, marking the collision of the Yangzi and Cathaysian palaeoplates in the Neoproterozoic (~850 Ma), resulting in their amalgamation in the Early Palaeozoic. Submergence beneath the Tethyan Ocean followed, to be interrupted by a Mesozoic intracontinental orogeny (Ziegler et al. 1996). This event led to melting of the crust to form syn-orogenic, Cretaceous "S" type granites followed, in an extensional post-orogenic phase, by the formation of (Yanshanian) "A" type granites. Both are represented in Sanqingshan, which forms part of the Huaiyu Mountain chain. The main batholith responsible for the landscape character at Sanqingshan is an "A-type, medium-coarse-grained, porphyroid biotite-moyite" (Guosheng 2006), which is ultra-acidic (77% SiO_2) with high potassium and low calcium content. The age of this intrusive phase is given as 123–115.6 million years ago (Early Cretaceous) (Guosheng 2006). The Huaiyu Mountain range was subjected to intensive block faulting from the Late Cretaceous through the Cainozoic, and Mountain Sanqingshan is defined by three major fracture zones, with a corresponding network of major joints (Fig. 29.1b). Guosheng (2006) refers to the history and impact of "uplift on uplift" on the landscape, which has led to bold, linear ranges and more than 23 deep gorges that fan out from south to north.

The landforms have, therefore, been influenced by repeated tectonism, and the morphology of individual massifs is strongly influenced by dominant vertical fractures, which subdivide the mountain areas into compartments of varying size (Fig. 29.2). This is typical of most granite plutons and their landscape expression, but these Chinese mountains are remarkable for the association of very high local relief with the survival of pillars of granite often less than 15 m in diameter, but more than 100 m in height. Summit elevations reach 1,816 m at Yujing Peak in Sanqingshan (1,820 m in Huangshan) and the mountains are more impressive for standing above a "sea" of forested hills of generally lower altitude and developed mainly on Palaeozoic clastic sediments. Often morning mists clothe these

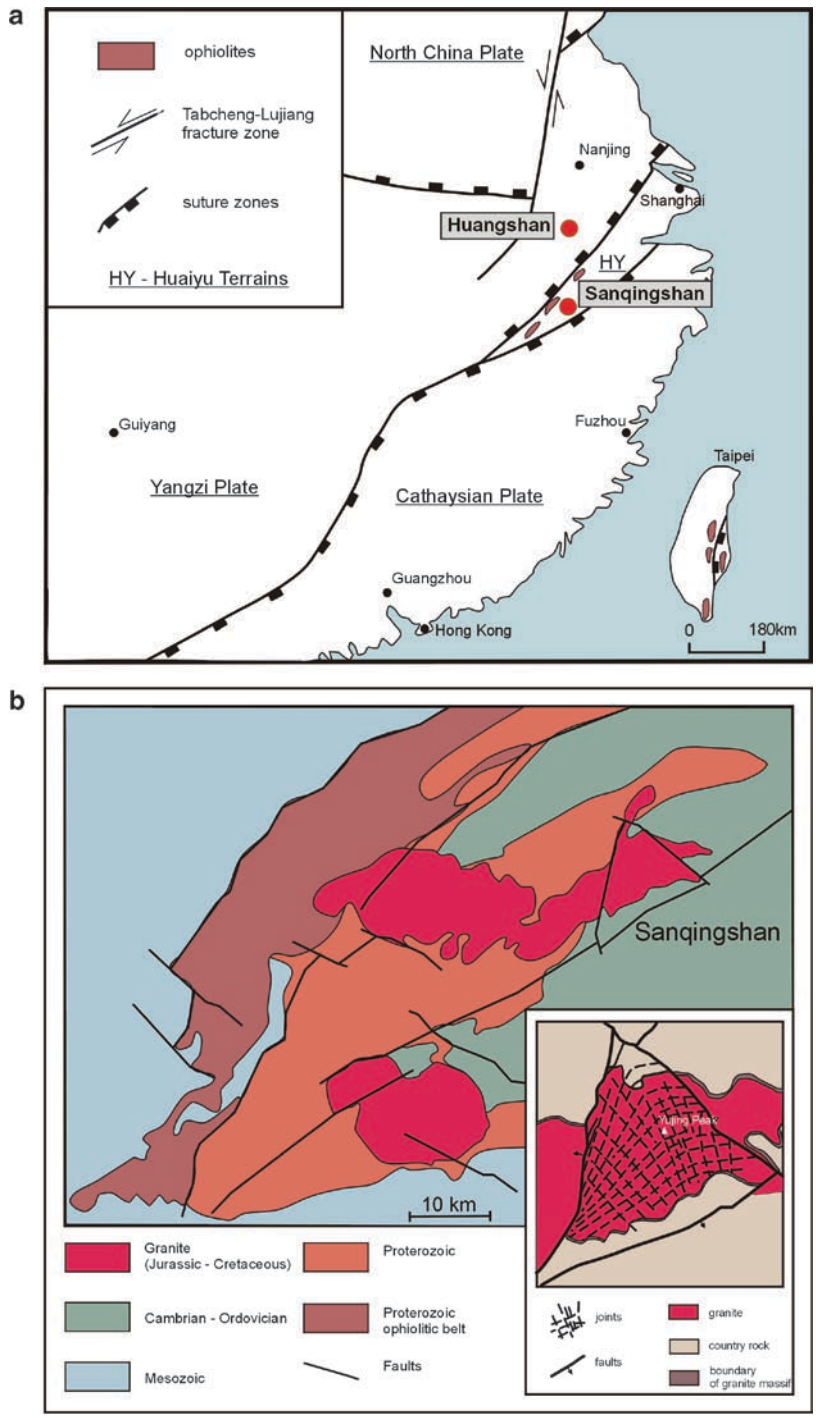

Fig. 29.1 Geology of Sanqingshan. (**a**) Location and geotectonic setting for Sanqingshan and Huangshan (After Guosheng 2006). (**b**) Outcrop geology in the wider vicinity of Sanqingshan. Inset shows the structure of the massif, with distribution of major faults and joints (After Guosheng 2006)

Fig. 29.2 High relief with formation of chasms and peaks is largely determined by strong vertical fractures (faults and joints). (**a**) Huangshan. (**b**) Summit relief on Mt. Yujing at Sanqingshan

lower hills and the granite peaks then rise, like fantastic islands from a sea of clouds. Hence Huangshan has often been called Huanghai (Yellow Sea).

Great rock walls (Fig. 29.3) form barriers to the inner mountain massif. Today these can be accessed by cable car, but in preindustrial times pilgrims climbed these hills and built thousands of rock steps, and even today many supplies are carried up these paths to hotels situated below the summits. In recent times vertiginous paths have been engineered around some of the most spectacular granite cliffs. Although massive rock faces exist, they are mainly found as buttresses around the margins of the granite intrusions, and the summits either culminate in piles of boulders or are part of what Chinese geologists refer to as "peak forests." These are comprised of numerous, closely spaced pillars of rock, and constitute a type of relief seldom encountered elsewhere (Figs. 29.4 and 29.5).

29.3 Origins of the Landforms

Although references have been made to the presence of possible glaciers, especially on Huangshan, during the ice-age maxima, the relief is essentially non-glacial, and there is no strong evidence for glacial modification, or indeed for subarctic conditions. The most striking impression is of the formation and survival of quite precarious peaked forms. Many of the summit blocks are etched by weathering pits. Evidence for granular weathering (*grus*) is found within small basins, located below the higher peaks and forming possible remnants of an elevated plateau above 1,200 m. But these features are few and limited in extent. Nonetheless, the process of differential denudation, which has given rise to this landscape, clearly involved chemical weathering processes, often operating on exposed and deeply fissured rocks. It would be premature

Fig. 29.3 The vertiginous "skywalk" offers a precarious access to the dramatic relief at Sanqingshan

to argue from the surviving morphology that excavation from a deep saprolite was fundamental to relief evolution. Although deep weathering profiles may have existed in the past, their traces have not been identified.

Nonetheless, although repeated uplifts have been a major feature of the geologic history, there has been adequate time during periods of crustal quiescence for weathering processes to play a significant role in shaping the landforms. In classical interpretations of granite weathering (Ruxton and Berry 1957) and in recent summaries (Twidale and Vidal Romani 2005; Migoń 2006) the advance of weathering into jointed granite is shown as limited to a few tens of meters, and joint blocks become progressively destroyed, leaving residual hills comprised of rounded boulders or slopes dominated by detached cores. Idealized profiles (Thomas 1994) always show a weathering sequence: the boulders becoming larger and more rectilinear with greater depth and grading eventually into fresh rock. Larger granite hills, perhaps hundreds of meters high are characteristically massive and usually domed, as in Yosemite (USA), around Rio de Janiero (Brazil), or they form part of complex mountain relief comprised of many intersecting rock surfaces, as in the Guadalajara Mountains (Spain). In most such instances major

Fig. 29.4 Granite landforms at Sanqingshan are dominated by high vertical pillars (termed "peak forests" by Guosheng 2006)

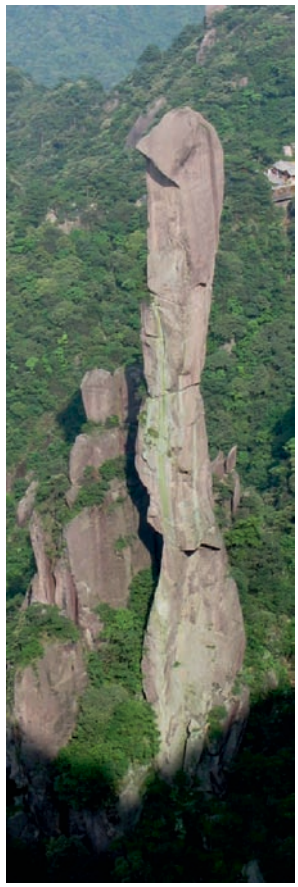

Fig. 29.5 Famous rock pillar at Sanqingshan, known as the "python" or "gigantic boa" (seen on the *left* of Fig. 29.4). It rises 128 m from a base at 1,250 m above sea level. Its width is only 7 m in places

vertical fractures in the granite are infrequent, perhaps hundreds of meters apart, and the relief is influenced mainly by the effects of lateral, inclined, and curvilinear joints (*sheeting*). But exceptions occur, and Twidale and Vidal Romani (2005) refer to large conical forms in Portugal and New Mexico, and to acicular (spine-like) towers strongly affected by frost, as at Cathedral Rocks in Yosemite.

Some granite massifs, however, are strongly influenced by vertical faulting. Barbier (1957) demonstrated this with regard to Pic Parana in southeastern Brazil (see Twidale and Vidal Romani 2005; Fig. 6.10), and a similar model was used to explain the Loma Mountains in Sierra Leone (Thomas 1995). The ancient granites involved in these movements subsequently formed large domes. The much younger (Mesozoic) intrusions in central China have also experienced repeated uplifts along major faults, but they are less massive and denudation has exploited frequent near-vertical joints to produce the distinctive forms that have created such a spectacular relief. Guosheng (2006) has demonstrated that Yujing Peak (1,816 m) is at the center of a triangular fault system (Fig. 29.1b). Within the massif a combination of strike-slip (extension-shear) faulting accompanied by rotation and subsequent uplift account for a fan-like pattern of deep vertical joints. Horizontal joints have remained subordinate, which accounts for the distinctive tower-like landforms, described by Guosheng (2006)) as a "peak forest."

Weathering processes have, therefore, had less opportunity to spread laterally, and less time to advance rock decay and produce saprolite. The heavy precipitation under tropical to subtropical conditions has clearly penetrated very deeply into vertical fractures, partially opened by the tensional forces acting on the rising granite blocks. The rarity of this type of development is implied by the absence of comparable examples in global surveys of granite landforms (Twidale and Vidal Romani 2005; Migoń 2006). One possible reason may be the fragility of very high, slender pillars of rock, which have been largely destroyed in the areas of extensive glaciation, and fail to survive among the ancient inselbergs of the former Gondwana continents. Thus deeply eroded, Mesozoic orogens, containing granite massifs at intermediate altitudes, where frost and ice are ineffective, and lying in wet tropical to subtropical, forested environments, are relatively few. The landscapes of Sanqingshan and Huangshan seem to represent a relief type that has not been specifically reported in the scientific literature.

The role of weathering penetration can be demonstrated from a few surviving sections in restricted areas of lower relief near the summits of Sanqingshan. These show the typical formation of granular weathering products, or *grus*, containing large corestones of relatively fresh rock (Fig. 29.6). The occurrence of this type of weathering in areas of high relief is not uncommon (Migoń and Thomas 2002) and the effectiveness of weathering during uplift and rapid denudation is not disputed. The existence of the corestone profiles at Sanqingshan demonstrates the survival of fragile regolith within fragments of a former elevated landsurface, now represented by restricted areas of gentle slopes, concentrated mainly around the Taoist temple, with its small lakes and gardens. The highest peaks at

Fig. 29.6 Exposure of sandy (grus) weathering and core boulders on an erosion bevel below the summits of Sanqingshan, showing that periods of deep weathering have occurred in this massif

Sanqingshan rise perhaps a further 400 m above this level, but the deepest gorges and most spectacular peak forests are found below it and, arguably, were formed by rapid dissection following a period of rapid uplift, probably during the Cainozoic.

Once steep, rocky relief in the jointed granite becomes established, vertical water flows within the rock mass and across exposed surfaces cause rock decay, and also remove the residual sands and clays that are the visible weathering products. The vertical development of the relief is then limited only by the rate of denudation and the potential for the rock pillars to collapse, which eventually appears inevitable. Interestingly, the distribution of this "peak forest" relief does not include the highest summits, many of which culminate in rounded cones. On Yujing Peak it is clear that some integrity remains in the rock mass, where several sheets of rock adjoin. A cluster of peaks at "Heavens gate" rise to between 1,500 and 1,600 m with a relative relief of over 300 m, and elsewhere single peaks with rock faces of more than 400 m relief are found. This means that many of the towering pillars of rock at Sanqingshan have their bases between 1,200 and 1,300 m above sea level, below which they often merge to form steep rock faces that fall away to lower elevations at the margins of the granite intrusions.

29.4 Landform Zones and Details

Guosheng (2006) has recognized several elevation zones with distinctive morphology: between 1,500 and 1,816 m are the highest peak clusters; from 1,000 to 1,500 m closely spaced peaks form walls, following the dominant (and earliest) fractures trending SW–NE and SE–NW; below 1,000 m cliffs and gorges mark a descent to surrounding hills and valleys below 500 m. A descriptive model, based on Yin Guosheng's work is shown in Fig. 29.7.

Many details of the granite landscape are intriguing, and indicative of the potency of monsoon rainfall. Frequently, the rock pinnacles have been weathered into slender finger tips, while pans and saddles (cuspate forms) have been sculpted on broader surfaces (Fig. 29.8a). But corestones and tors are also formed where sub-horizontal joints subdivide the rock sheets. It is tempting to see signs in these features that they may have been excavated from a former weathering cover (Fig. 29.6). The issue here is whether the undoubted rounding of joint blocks within a saprolite can be replicated by purely surface water flows. In many instances, it appears that the surface water regime is more likely to diversify the smooth rock surfaces, causing flutes and pits to form. Exposed blocks of granite appear to undergo progressive change toward needle-like forms. In Fig. 29.8a, the upper surface of the jointed granite block is being modified to form a saddle, with finger-tip protrusions at each side, while the vertical face is becoming faceted. The pale color of the rock surface indicates the pathways of torrential runoff during rainstorms, which are responsible for these changes. A later development of this process is shown in Fig. 29.8b, where the rock needle and saddle have become accentuated. Close examination of

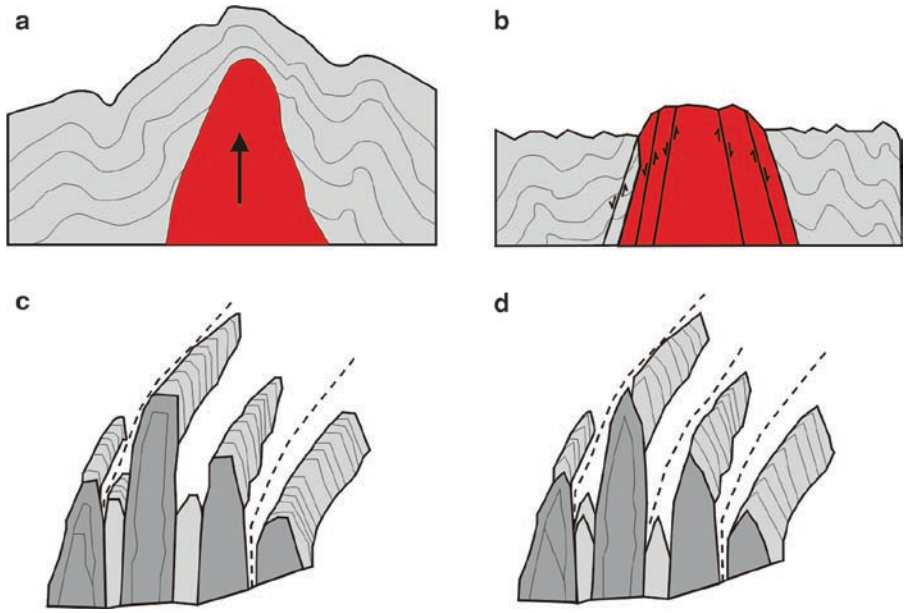

Fig. 29.7 Diagram showing the evolution of rock formations of Sanqingshan (After Guosheng 2006). A – granite intrusion into older Proterozoic – Palaeozoic rock formations, B – Neogene uplift along steeply dipping faults, C – separation of individual compartments, delineated by fracture zones, D – remodeling of angular blocks into cones and pillars

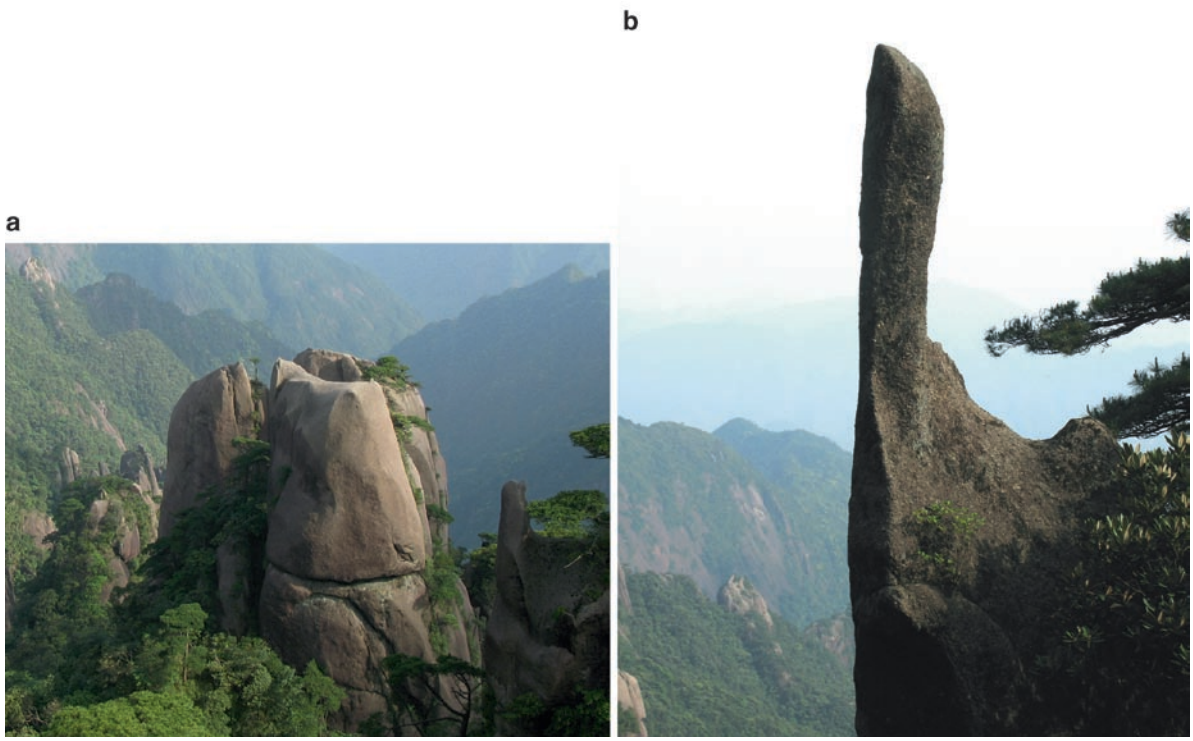

Fig. 29.8 Contemporary weathering at Sanqingshan. (**a**) Exposed blocks of jointed granite undergo weathering and erosion by monsoon rainfall. (**b**) Rock needle and saddle at Sanqingshan

distant forms in Fig. 29.2a shows a similar combination in Huangshan, and these features are common throughout both areas, although Huangshan exhibits both more angular and more conical forms.

29.5 Summary

Sanqingshan and Huangshan differ in their topographic expressions, but both belong to a class of granite landscape that is unusual, where closely fractured rock has been uplifted and dissected to create a precipitous relief in a largely frost-free environment. Rock slabs form great walls or cliffs in the midsections of the relief, but these are seldom found at the summit levels. Visitors can gain access to the higher levels by cable car and by ascending rock-hewn and concrete pathways, via thousands of steps and, at Sanqingshan a vertiginous skywalk (Fig. 29.3) rings the central ridge to offer astounding views of the unique scenery.

The Author

Mike Thomas has a doctorate in geomorphology from the University of London, and has lectured in geography at the Universities of Ibadan, Nigeria and St. Andrews, Scotland. He held the Chair of Environmental Science at the University of Stirling from 1980 to 2001, and is now a Professor Emeritus. He is a Fellow of the Geological Society of London and the Royal Society of Edinburgh. His publications include two books on geomorphology in the tropics and numerous papers on granite landform evolution and landscape response to climate change. He was presented with the Centenary Medal of the Royal Scottish Geographical Society in 2000, and the David Linton Award of the British Society for Geomorphology in 2001.

Acknowledgments My visit to Huangshan and Sanqingshan in 2007 was at the invitation of the Directors of the Management Committee of Sanqingshan National Park, Mr Liu Shuzong and Mr Yang Shaou. I would also like to thank Ms He Jian, who acted as translator and guide, and Dr Yin Guosheng, Senior Geologist and Deputy Director of Jiangxi Province Geological Survey, who provided much of the background geological mapping and interpretation. I am grateful to Professor Piotr Migoń, whose prior contacts with Sanqingshan made my visit possible and who jointly contributed to the fieldwork.

References

Barbier R (1957) Aménagements hydroélectriques dans le sud du Brésil. C R Bull Soc géol France 6:877–892

Cahill J (ed) (1981) Shadows of Mount Huang. University Arts Museum, Berkeley, CA

Guosheng Y (2006) Sections on geology. Mount Sanqingshan National Park. Ministry of Construction, People's Republic of China

Migoń P (2006) Granite Landscapes of the World. Oxford University Press, Oxford

Migoń P, Thomas MF (2002) Grus weathering mantles – problems of interpretation. Catena 49:5–24

Ruxton BP, Berry L (1957) Weathering of granite and associated erosional features in Hong Kong. Geol Soc Am Bull 68:1263–1292

Thomas MF (1994) Geomorphology in the Tropics. Wiley, Chichester

Thomas MF (1995) Models for landform development on passive margins. Some implications for relief development in glaciated areas. Geomorphology 12:3–15

Twidale CR, Vidal Romani JR (2005) Landforms and Geology of Granite Terrains. Balkema, Leiden

Ziegler AM, Rees AM, Rowley DB, Bekker A, Qing L, Hulver ML (1996) Mesozoic assembly of Asia: constraints from fossil floras, tectonics and palaeomagnetism. In: Yim A, Harrison M (eds) The tectonic evolution of Asia. Cambridge University Press, Cambridge, pp 371–400

Chapter 30
Guangxi Karst: The Fenglin and Fengcong Karst of Guilin and Yangshuo

Tony Waltham

Abstract The limestone karst of southern China is among the most extensive and spectacular in the world. Large blocks of fengcong karst consist of clustered conical hills with large caves draining beneath them and their intervening dolines. Isolated towers in the fenglin karst may evolve from the fengcong where input of allogenic sediments maintains alluviation of the base-level plain and hence permits undercutting of the limestone hills. This process appears to take more than 10 million years, and only occurs in areas of slow tectonic uplift.

Keywords Cave • fengcong • fenglin • Guangxi • karst • limestone

30.1 Introduction

Southern China consists of the world's largest area of mature limestone karst, which is perhaps the best known for the spectacular landscapes of limestone towers, most widely developed within the province of Guangxi. Most of the lowland karst is densely populated, with towns and villages, alongside rice paddies and market gardens, on almost every bit of alluviated ground that is near to flat. But it is also a hugely dramatic landscape with the limestone towers of the fenglin karst that feature so strongly in traditional Chinese art. Guilin (Fig. 30.1) is now a major tourist destination, and millions of visitors take the famous boat trip down the Li River (Li Jiang) from Guilin to Yangshuo every year – passing vistas that are classics of geomorphology.

30.2 Karst Terrains in the Guilin Basin

A succession of nearly 10,000 m of Devonian to Triassic carbonates lie at outcrop across around half the area of Guangxi, and erosional evolution of this huge mass of limestone has allowed development of what is arguably the world's finest karst terrain. Within this, the karst of the Guilin basin is formed in about 2,600 m of Devonian and Carboniferous limestones. These occupy a complex syncline between anticlinal mountains of Devonian sandstone, which are critically important in supplying allogenic drainage and sediment into the karst (Fig. 30.2). The limestones are pure, strong, and massively bedded, so are ideal for the development of cavernous karst.

Overlying the limestone around Guilin, scattered outliers of Cretaceous red beds lie at various elevations, resting unconformably on what appears to be the remnants of a pre-Cretaceous karst landscape (Zhu 1988). Their distribution is unrelated to the modern karst, which therefore dates them to no earlier than the Cenozoic. Notable among Pleistocene deposits in the karst are coarse and poorly sorted diamictons that appear as many low mounds on the dissolution plain. These have commonly been described as "boulder clays," which is very descriptive of their lithology, but is an inappropriate term when Pleistocene ice sheets never reached this far south in lowland China. Their origins, whether fluvial, glaciofluvial, or as mudflow deposits, remain controversial. Most of their cobbles are sandstone derived from the pre-Devonian outcrops in the adjacent hills; they generally have diameters of 10–30 cm, although boulders up to 1 m across are not rare.

P. Migoń (ed.), *Geomorphological Landscapes of the World*,
DOI 10.1007/978-90-481-3055-9_30,

Fig. 30.1 The northern suburbs of Guilin spread across the alluviated plain between the steep limestone hills of the fenglin karst (Photo T. Waltham)

Alluvial sediments form both floodplains and various terraces along the modern Li River and its tributaries. Most are well-sorted gravels covered by silty sand. The modern alluvium is mostly less than 10 m thick, but is thicker over buried dissolutional fissures. Recent drilling for new bridge sites along the Li River has revealed that there is usually a trough, 30–50 m deep, infilled by the Pleistocene diamicton beneath the Holocene alluvium (Yuan 2004). This trough may originate from erosion to lower sea levels during the Pleistocene ice ages, and may have influenced development of the karst that is now beneath the dissolutional plain.

Guilin's climate is humid tropical with a dry winter. Mean annual precipitation ranges from 2,000 mm at Guilin to 1,500 mm at Yangshuo, with 62% of the total falling in the rainy summer from April to August. Mean annual temperature is 18–19ºC.

The Li River forms the trunk drainage route with a mean flow of 215 m^3/s past Guilin; it defines local base level at 141 m at Guilin, descending to 103 m at Yangshuo. With the huge rise in tourism, groundwater abstraction from the karst has risen to around 150,000 m^3/day. New wells are now controlled by local environmental regulations. Karst collapses are frequent, and most are subsidence dolines within the alluvium induced by water table decline in areas of overpumping.

Show caves complement the major tourist appeal of the karst scenery. The abandoned chambers and galleries of Qixing Dong and Luti Dong, both near Guilin, are long-established, along with various culturally significant caves within the city. Guanyan is newly developed as a major show cave at Caoping, and there are smaller caves open to tourists around Yangshuo, where rock climbing on the limestone towers is also a popular new sporting attraction.

Mature tropical karst landscapes may be broadly divided into the two main types: fengcong and fenglin (Zhu 1988; 1991; 2005). In China, these are distinguished by either dolines or an alluviated plain between the hills, and not by the hill profile as in Western terminology. Fengcong karst has clustered limestone hills with intervening dolines; its name translates as peak cluster, and it may be known in the West as a variety of cone karst, though its profiles are much steeper than the often described cone karst of Gunung Sewu on Java (Lehmann 1936, Balazs 1973). Fenglin karst has isolated limestone hills rising from an alluviated karst plain; its name translates as peak forest, and it is popularly known in the West as tower karst. Each type accounts for about half the karst in this area, with fenglin dominant around Yangshuo and also south of Guilin, while fengcong dominates along the course of the Li River (Fig. 30.2).

Fig. 30.2 Outline map of the karst between Guilin and Yangshuo (above) and the location of Guilin karst within China (below)

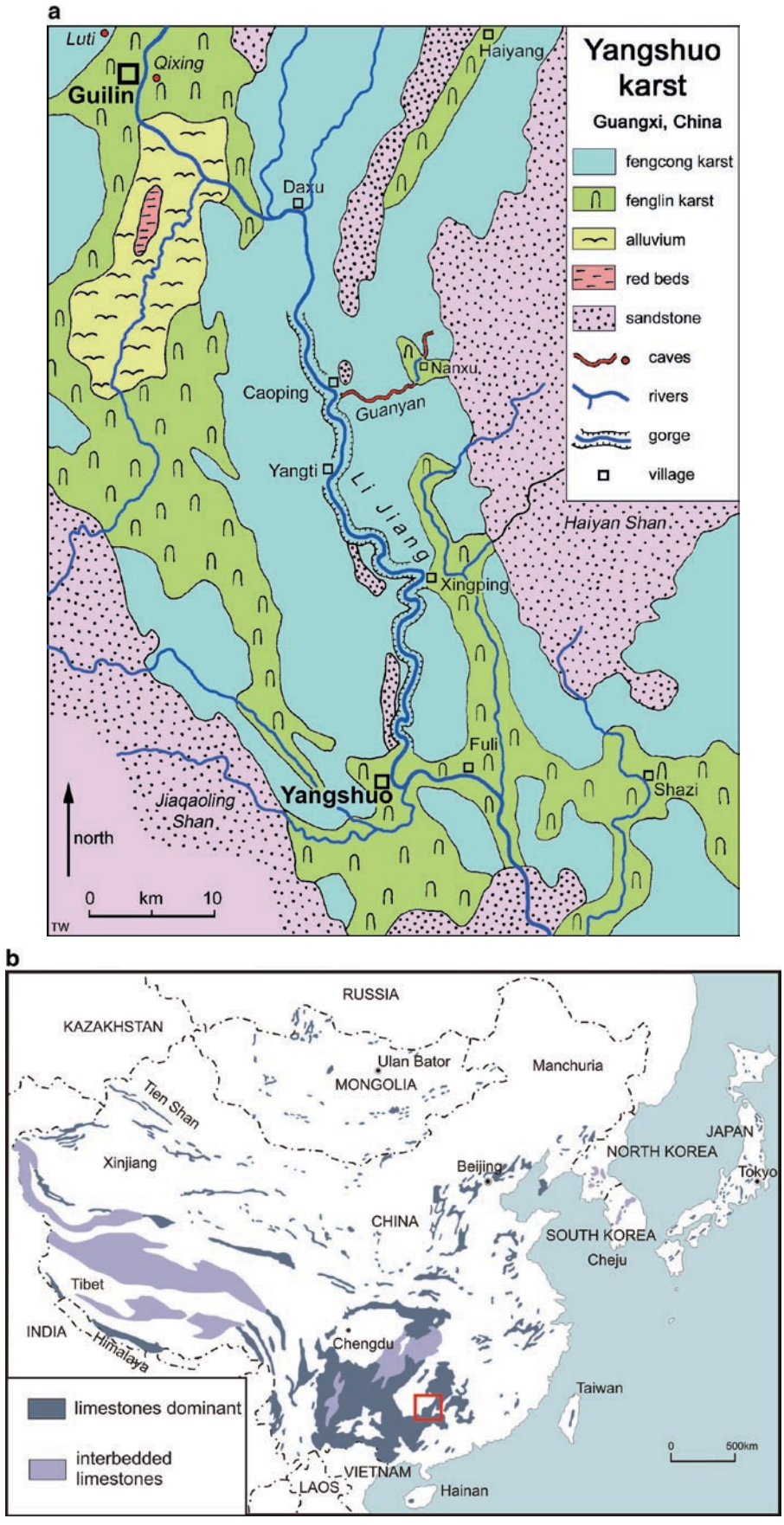
a
Luti
Qixing
Guilin
Haiyang
Daxu
Nanxu
Caoping
Guanyan
Yangti
Li Jiang
Haiyan Shan
Xingping
Fuli
Shazi
Yangshuo
Jiaqaoling Shan
north
0 km 10
TW
Yangshuo karst
Guangxi, China
fengcong karst
fenglin karst
alluvium
red beds
sandstone
caves
rivers
gorge
village
b
RUSSIA
KAZAKHSTAN
Ulan Bator
MONGOLIA
Manchuria
Tien Shan
Xinjiang
Beijing
JAPAN
NORTH KOREA
Tokyo
CHINA
SOUTH KOREA
Cheju
Tibet
INDIA
Himalaya
Chengdu
Taiwan
VIETNAM
LAOS
Hainan
0 500km
limestones dominant
interbedded limestones

Fig. 30.3 Limestone hills of the fengcong karst east of Caoping, and underlain by the Guanyan cave system; the alluvial flat in the foreground is a terrace of the Li River (Photo T. Waltham)

30.3 The Fengcong Karst and Its Caves

Fengcong is defined as a group of limestone hills with a common limestone base. Deep closed depressions lie between the peaks, so the integrated landscape is sometimes described as peak cluster depression karst. Some internal depressions are alluviated, but these are mainly those that are entered by sediment-laden allogenic streams. The fengcong forms large blocks of deeply dissected highland (Fig. 30.3). The largest block extends along the center of the basin, and is entrenched by the gorge of the Li River. This appears to be an inherited feature whose course was established early in the evolution of the terrain and has been maintained by the large allogenic flow of the Li. Local relief in the fengcong on each side of the Li River is typically 100–300 m, but rises to over 500 m in places. Hill profiles are mostly steep cones. Individual beds of strong limestone create cliffs that break these profiles, but there is a limit to how steep hill slopes can be when they continue down into conical dolines; vertical-sided towers cannot exist within fengcong karst.

With the intervening dolines reaching down to various levels that are mostly well above base level, fengcong has a deep vadose zone with considerable seasonal fluctuations in water table elevation (Zhu 2005). This allows the development of large and extensive cave systems. There are hundreds of caves within the fengcong karst. Most are not yet fully explored and mapped, but there are 23 known river caves each with a passage length of more than 1 km, along both sides of the Li River gorge.

The longest single series of caves is the Guanyan system between Nanxu and Caoping (Fig. 30.4). Its headwaters drain off the sandstones of Haiyan Shan and descend rapidly towards a graded profile, through the Xizhen caves and across the alluviated Nanxu basin. From there the route is underground through a sequence of large cave passages, broken only by one small surface basin, as far as the open resurgence cave on the bank of the Li River. Along much of the cave, the modern vadose canyon is entrenched in the floor of old, high-level, phreatic passages, though old and new passages separate in parts. A total length of over 14 km of cave passages has been mapped along this route (Waltham 1986), while a central flooded section remains unexplored through a phreatic loop. Flows range between 0.3 and 8.0 m^3/s, from a catchment of 80 km^2.

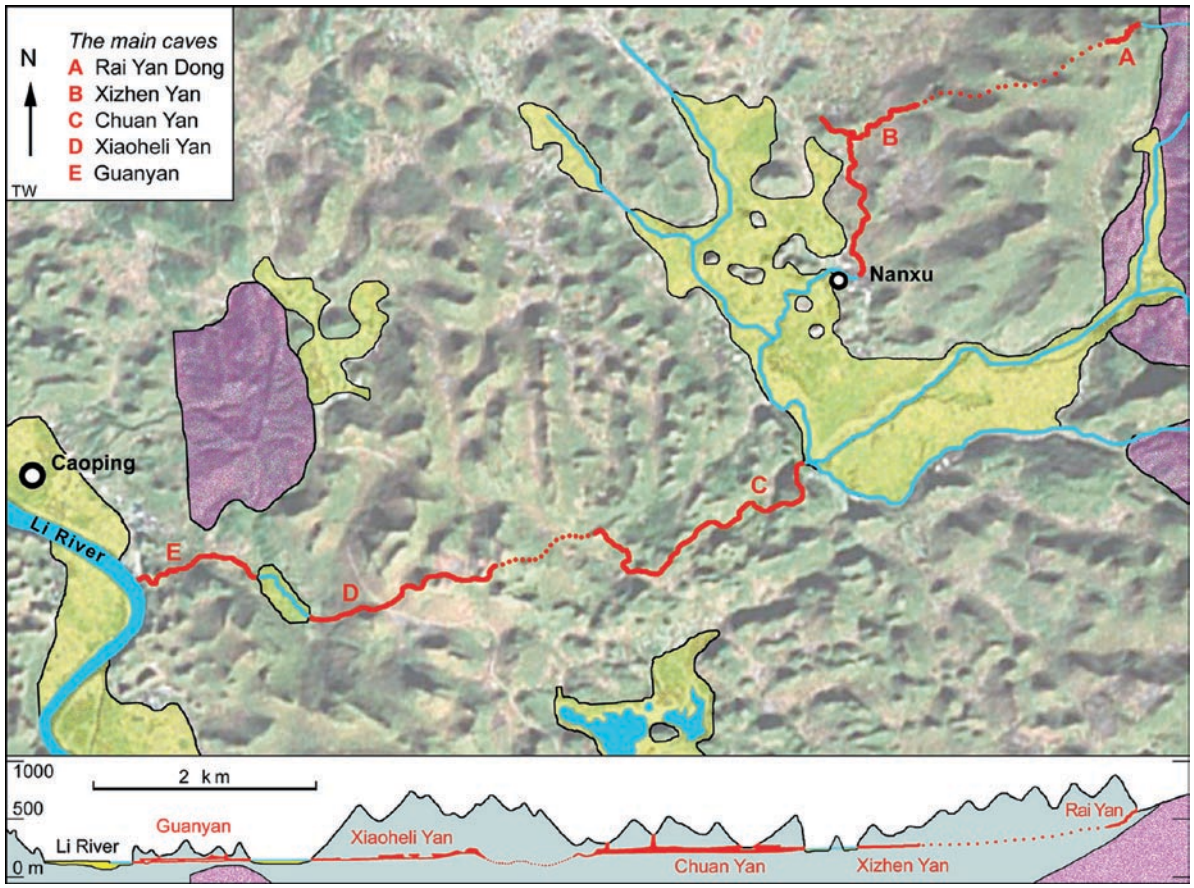

Fig. 30.4 The main line of the Guanyan cave system through the fengcong karst east of Caoping. The sandstone inliers are tinted purple and the main areas of alluvium are yellow. On the plan, only the main streamway is shown, and passage width is exaggerated for clarity; high-levels are included on the profile. Satellite imagery is from NASA, cave surveys, and geology are from China Caves Project (Waltham 1986)

It is significant that the cave route bears no relation to the fengcong surface topography (Fig. 30.4), but takes almost a direct line from the sandstone outcrop to the Li River. It now has a mature graded profile that hides most of the early stages of phreatic looping within the limestone. The cave passes beneath both hills and dolines, and locally breaks out into the floors or margins of some dolines (Fig. 30.5). There are some collapses of doline floors into the cave passage, but the limited local relief means that none of these is as large as the tiankengs (giant collapse dolines) elsewhere in the Guangxi karst (Zhu and Waltham 2005).

30.4 The Fenglin Karst of Yangshuo

Fenglin is defined as a landscape of limestone hills that are isolated from each other by a flat limestone surface that is generally covered by a thin layer of loose sediments. As the hills are usually surrounded by a plain, the integrated landscape may be called a peak forest plain. The hills may be steep-sided towers or lower conical hills, as its definition in China is based on the intervening flat plain, but the best known fenglin is the spectacular tower karst, especially that around Yangshuo (Fig. 30.6).

Fig. 30.5 The main passage of Chuan Yan, with daylight entering where its roof breaks into the floor of a doline within the fengcong karst (Photo A. Eavis)

Fig. 30.6 The classic fenglin karst east of Yangshuo, where limestone towers rise more than 200 m from the thinly alluviated karst plain (Photo T. Waltham)

Fig. 30.7 An almost perfect fenglin tower with vertical walls of limestone largely shrouded in vegetation, beside the Jingbao River on the outskirts of Yangshuo (Photo T. Waltham)

Within the karst of Guilin and Yangshuo, local relief (i.e., the height of the limestone towers) is generally around 30–80 m in the central part of the basin, but may be over 300 m in areas adjacent to the blocks of fengcong. Profiles of the individual peaks may be almost perfectly columnar where the limestone is gently dipping, and the fenglin around Yangshuo is the classic of its type with many towers having almost vertical sides (Fig. 30.7). Profiles tend towards asymmetrical cuestas where dips are steeper on the flanks of the syncline, notably to the west of Guilin. Towers may or may not have steep aprons of bedrock or talus around all or part of their bases, and there is almost every profile transitional to the steeper cones of the fengcong.

This is the type area of the Yangshuo type of tropical karst defined by Balazs (1973), with a base diameter of the tower being less than 1.5 times its height. Balazs used this ratio to distinguish the Yangshuo type towers from the other types of tropical karst hills – the Organos type mogotes of Cuba (ratio 1.5–3.0), the Sewu type hemispherical cones of Indonesian (ratio 3–8), and the Tual type of lower cones on some Indonesian islands (ratio >8). The contrasts in hill morphology are notably dependent on the limestone lithology. The Yangshuo towers are formed of strong and very massive limestone, while the hills of both Organos and Sewu are formed of weaker and more fractured limestones; the lowest cone profiles are formed on young reef limestones at Tual and are mimicked in thinly bedded dolomitic limestones elsewhere in Guangxi (though not in the Guilin basin). Geomorphological evolution also has an impact on the tower profiles in these different karst types, as there are other karsts in similar limestones with very different topographies, but the geological factors cannot be ignored.

In the fenglin karst, the deep vadose zone of the fengcong is replaced by a thin zone of seasonal fluctuation of the water table (Zhu 1988). Numerous foot caves within the fenglin towers are a significant component in the processes of lateral planation, slope undercutting, and cliff retreat. Long caves cannot fit inside the isolated towers, and while some extent of flooded caves must exist beneath the intervening karst plains, none has yet been explored and mapped. High-level caves lie abandoned within many of the towers, and these include old foot caves and also fragments of larger trunk passage that pre-date the modern landscapes.

30.5 Evolution of the Karst

The karst of Guangxi, and even just of the Guilin basin, is immensely complex and contains every variation in detail, including all intermediate morphologies between fenglin and fengcong and hill profiles between a cone and a tower.

Within the Guilin basin, there is no clearly recognizable pattern, either in plan view or in profile, in the distribution of fenglin and fengcong. Across the whole basin, the two types are very mixed in their lateral distribution. So it is possible that the fenglin and the fengcong are contemporary variants of the karst (Zhu 1991). With respect to all the Guangxi karst, there is considerable debate over the origins of fenglin, but it

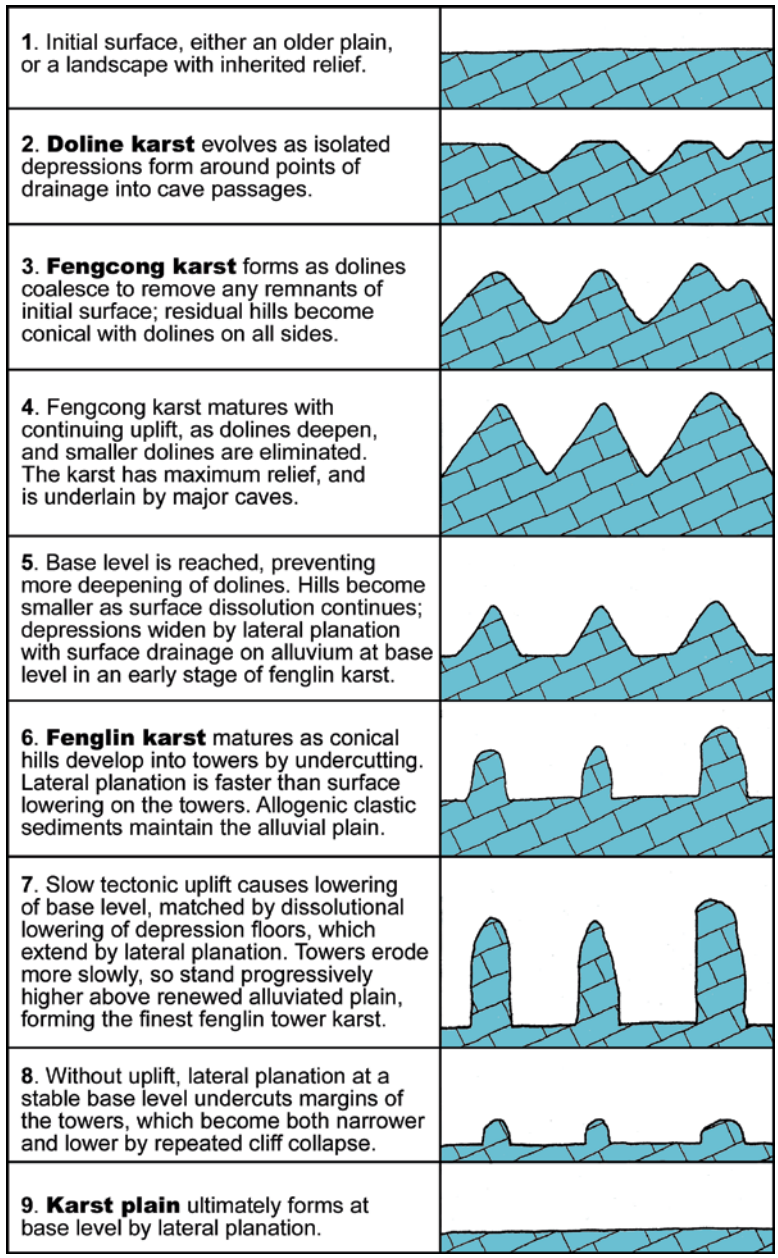

Fig. 30.8 A simplified sequence of stages in the development of fengcong and fenglin karst; details and critical factors are described in the text

appears that the more likely alternative is that fenglin evolves from fengcong, and this certainly seems to be applicable in the Guilin basin.

A greatly simplified evolutionary path for the fengcong and fenglin karst is summarized in Fig. 30.8. Whether starting from a newly exposed outcrop, from an uplifted karst plain, or from an inherited topography; a limestone terrain in a wet tropical environment first develops as a doline karst. This may then evolve into fengcong, as the dolines enlarge to occupy the whole land area, leaving only residual hills that assume conical profiles. With or without an early stage where valleys are entrenched before they break up into dolines, this process is recognized in cone karsts across the world.

Unless a thin limestone is totally removed, base level is ultimately reached, and lateral planation then proceeds to undercut, and reduce the residual hills. The isolated cones or small towers are fenglin in the Chinese sense of the word, and perhaps the best example is seen in the mogote karst of Cuba (Panoš and Štelcl 1968). Ultimately, the hills are removed (as evolution proceeds directly from stage 5 to 8 in Fig. 30.8).

The key factor for the development of mature fenglin karst, as in the Guilin basin, is slow and almost continuous tectonic uplift (Zhang 1980). Where dissolutional lowering of an established plain between the hills can keep pace with a declining water table, lateral planation erodes the bases of the towers faster than their upper surfaces that are reduced by direct rainfall. In effect the towers therefore grow, as the plain declines between them, and this is the key stage in the development of the tall fenglin tower karst of the Yangshuo area (as well as at other sites around Guilin and elsewhere in Guangxi). Important to continuation of the fluvial erosion and limestone planation is maintenance of the alluvial plain by continued replenishment of the clastic sediment from allogenic sources. In the Guilin basin, most of the fenglin stands in areas where streams from adjacent sandstone mountains provide this supply of clastic sediment into the karst (Yuan 1987). This excludes the course of the Li River, which carries little clastic material so far down its course and has simply entrenched its gorge through the main block of fengcong karst.

Development of the fenglin karst requires a delicate balance of processes, which is made possible in southern China by the humid tropical climate and tectonic uplift associated with the nearby Himalayas. With more rapid uplift, the water table may never reach the surface even in the wet seasons, so new dolines develop, and the karst ultimately reverts to fengcong. Too little uplift allows the karst to degrade into a karst plain. There is endless scope for interruptions and repetitions within the simplified sequence of Fig. 30.8, and these can account for a host of multiphase landscapes where fenglin is only one variant (Smart et al. 1986). Fenglin takes time to evolve, and this accounts for the juxtaposition of blocks of fengcong that have not yet reached the fenglin stage within the Guilin karst.

The last factor critical to the development of the mature fenglin of the Yangshuo area is an enormous thickness of limestone. The stages in Fig. 30.8 evolve only during overall surface lowering through perhaps 1,000 m or more of unbroken limestone. Guangxi has this thickness of limestone; its combination with the tectonic uplift, and with tropical weathering unbroken through the Pleistocene, leaves its fenglin karst unmatched in the world. Elsewhere, the only towers that approach the morphology of those in Guangxi are in the Phang Nga and Ha Long Bays of Southeast Asia, both of which have been modified by marine erosion.

An unresolved question concerns the age of the karst around Guilin and Yangshuo. Most of the caves are richly decorated with massive deposits of calcite, and stalagmite in the caves of Maomaotou Hill, in the suburbs of Guilin, has dates ranging from 41,000 to >350,000 years ago, with deposition in both warm and cold stages through the Pleistocene (Wang 1986). The karst is clearly much older. There is a range of data on rates of surface lowering in the Guilin basin. Zhang (1980) cites 80–120 mm/ka[1] based on dissolution measurements, Williams (1987) deduces a maximum rate of 23 mm/ka from palaeomagnetic studies of clays in tiered caves within a single tower near Guilin, Zhu (1988) cites around 100 mm/ka from data on fossils in the high-level caves, and Yuan (2004) cites 90 mm/ka from multiple studies. Lu (1986) estimates denudation rates at 100–300 mm/ka, and compares them to tectonic uplift rates of 50 mm/ka in the Pleistocene, increasing in the Holocene. Very approximate figures of 50–100 mm/ka for surface lowering, through somewhere in the order of 1,000 m of limestone, extend evolution of the karst to around 10–20 million years ago; these places origin well back into the Cenozoic, and appear to be a very reasonable concept until more precise chronological data is available.

30.6 Conclusions

The huge range of morphologies and the spectacular extreme variants make the karst of China, and particularly of Guangxi, the most important in the world. No study of karst, nor any concept of its development, can be complete without reference to the fenglin karst that is so magnificent in the area around Yangshuo. The fenglin appears to evolve under a very narrow suite of

[1] ka stands for 1,000 years

environmental factors, and this is what makes it so unusual and so special.

The Author

Dr **Tony Waltham** recently retired from many years as a university lecturer in engineering geology in Nottingham, UK. His main research interest was in karst and specifically in engineering problems of construction on cavernous ground. He is the author of the popular textbook *Foundations of Engineering Geology*, and of many other books. He has travelled widely, mainly to areas with great caves or active volcanoes.

References

Balazs D (1973) Relief types of tropical karst areas. In: Proceedings of Symposium on Karst-morphogenesis, International Geographical Union, European region conference, pp 16–32

Lehmann H (1936) Morphologische Studien auf Java. Geogr Abh 3(9):1–114

Lu Y (1986) Karst in China. Geological Publishing House, Beijing

Panoš V, Štelcl O (1968) Physiographic and geologic control in development of Cuban mogotes. Z Geomorph 12:117–173

Smart P, Waltham T, Yang M, Zhang Y (1986) Karst geomorphology of Western Guizhou, China. Trans British Cave Res Assoc 13:89–103

Waltham AC (ed) (1986) China Caves ’85. Royal Geographical Society, London

Wang X (1986) U-series age and oxygen carbon isotopic features of speleothems in Guilin. In: Proceedings of 9th International Speleological Congress, Spain, vol 1, pp 284–286

Williams PW (1987) Geomorphic inheritance and the development of tower karst. Earth Surf Process Landforms 12:453–465

Yuan D (1987) New observations on tower karst. In: Gardiner V (ed) International geomorphology. Wiley, New York, pp 1109–1123

Yuan D (2004) Yangshuo karst, China. In: Gunn J (ed) Encyclopedia of caves and karst science. Fitzroy Dearborn, New York, pp 781–783

Zhang Z (1980) Karst types in China. Geo J 4:541–570

Zhu X (1988) Guilin karst. Shanghai Scientific & Technical Publishers, Shanghai

Zhu X (1991) Tropic and subtropic karst. In: Yuan D (ed) Karst of China. Geological Publishing House, Beijing, pp 57–74

Zhu X (2005) Karst areas and karst types in China. Geogr Rdschau (International) 1(2):37–47

Zhu X, Waltham T (2005) Tiankengs: definition and description. Cave Karst Sci 32:75–79

Chapter 31
Mt. Fuji: The Beauty of a Symmetric Stratovolcano

Takashi Oguchi and Chiaki T. Oguchi

Abstract Mt. Fuji, the highest mountain in Japan, is internationally known for its attractive landscape, which resulted from the repeated basaltic eruptions near the junction of the four major tectonic plates since the Middle Pleistocene. Although Mt. Fuji has a relatively simple symmetrical shape, it consists of various geomorphological and geological components such as old buried volcanic bodies, deposits of huge sector collapses, craters on volcanic flanks, and some distinct valleys. Geomorphological and geological knowledge is important for providing strategies to cope with future possible volcanic hazards in and around Mt. Fuji.

Keywords Basalt • evolutionary history • Japan • stratovolcano

31.1 Introduction

Some stratovolcanoes such as Shishaldin in Alaska, Popocatépetl in Mexico, Mayon in the Philippines, and Fuji in Japan have tall, symmetric cones. As the beautiful shape of such cones can attract people's attention, they often become religious symbols, places of ancient tales, and objects of paintings and photographs. Mt. Fuji has been an important landmark for the people of Japan for both its attractive landscape as an isolated single mountain (Fig. 31.1) and its location close to the populated areas such as Tokyo. Mt. Fuji is also internationally known as a symbol of Japan and as a classic of volcanic geomorphology.

The tectonically active Japanese Islands have around 350 volcanoes of Quaternary age, of which about 100 have erupted at least once in the Holocene. Mt. Fuji is the largest of the Japanese volcanoes, characterized by a very rapid growth rate in the Holocene, although no eruption has taken place during the last 300 years. The magma produced to form Mt. Fuji is mostly basaltic, which is relatively rare among the mostly andesitic island arc lavas observed in Japan (Tsuya and Morimoto 1963). Such large composite stratovolcanoes made of basalt are also uncommon worldwide.

31.2 Geographical Setting

Mt. Fuji is located about 100 km west-southwest of Tokyo (Fig. 31.2), at the boundary of the Shizuoka and Yamanashi prefectures. It is the highest mountain in Japan at 3,776 m a.s.l., and its base is about 40–50 km in diameter (Fig. 31.3). The total volume of the volcano is about 500 km^3. The tectonic setting of Mt. Fuji is unique; it is close to the junction of four major plates (Eurasian, North American, Pacific, and Philippine Sea) and at the junction of three island arcs (Northeast Japan, Southwest Japan, and Izu-Ogasawara; Fig. 31.2). Abundant magma has been supplied under such an active tectonic environment to form the large volcanic body of Mt. Fuji. Although the subduction of the Pacific Plate is probably mainly responsible for magma production, as is the case of other volcanoes in the northeast to central Japan, the area around Mt. Fuji has been experiencing localized tension within the Philippine Sea plate, leading to repeated basaltic fissure eruptions (Aizawa et al. 2004).

The mean annual temperature at the summit of Mt. Fuji is −6.4°C, and the mean temperature of the hottest month (August) is 6.0°C, about 20°C lower than that in Tokyo. This condition accounts for the distribution of permafrost near the summit. Snowfall is possible throughout the year, though it mostly disappears from the ground surface during summer. The thickness of snow accumulation in winter and spring is up to 3 m in

P. Migoń (ed.), *Geomorphological Landscapes of the World*,
DOI 10.1007/978-90-481-3055-9_31,

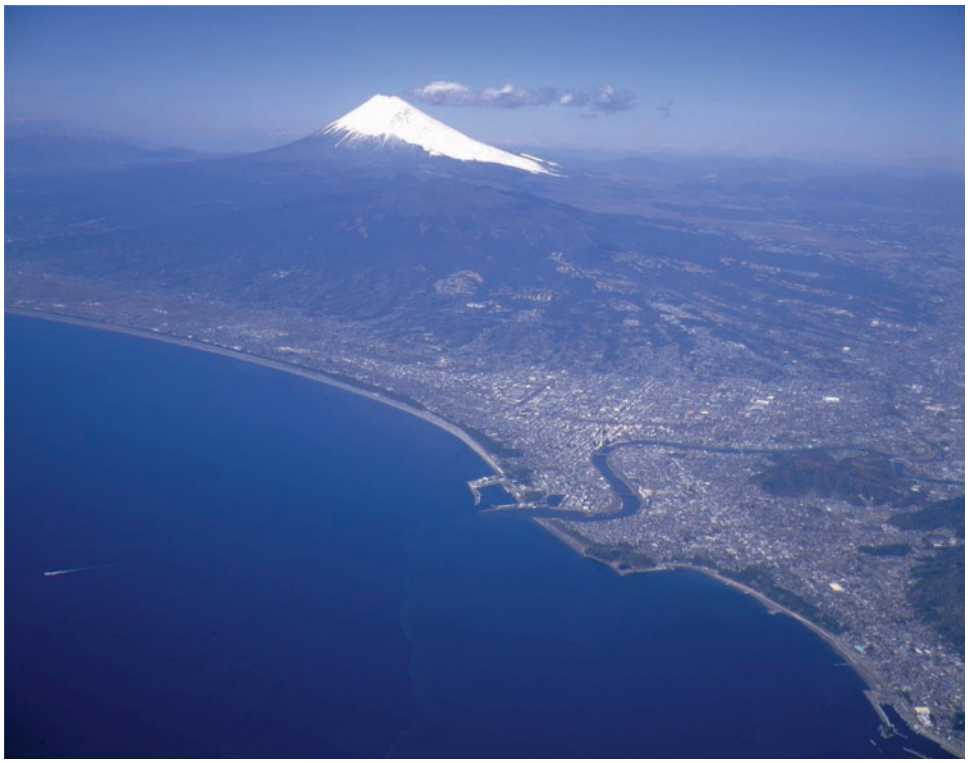

Fig. 31.1 Mt. Fuji (3,776 m a.s.l.) viewed from the southeast. Snow cover reaches the lower altitudes on the eastern flanks due to the snow transported by the westerlies. Upper rim of a large crater formed by the Hoei eruption in 1707 can be seen in the snow-covered area. The heavily dissected mountain in front of Mt. Fuji is Ashitaka Volcano (1,504 m a.s.l.) that formed in the Middle Pleistocene. The populated costal area in front of Ashitaka Volcano is Numazu City. Courtesy of Nakanihon Air Service Co. Ltd.

topographic depressions but less than 1 m on ridges because of snow dispersal by wind. A strong westerly wind prevails throughout the year, with wind speeds of 10 m/s or more recorded at the summit more than 300 days in a year. Many representative photographs of Mt. Fuji have been taken in spring or late autumn, when only the upper part of the mountain is covered with snow (Fig. 31.1). The vegetation distribution of Mt. Fuji mainly reflects the temperature gradients with height, although the effects of past volcanic activity on vegetation can be seen in places. Areas higher than 1,500 m a.s.l. are devoid of thick vegetation and are regarded as being a volcanic desert, whereas areas at lower elevations are dominated by pioneer forest (Ohsawa 1984).

31.3 Evolution

Although Mt. Fuji looks like a single isolated stratovolcano, it in fact consists of several volcanic bodies including some that have been buried (Fig. 31.4). Volcanic activity in the Fuji area began in the Middle Pleistocene (around 500,000 years ago). Early eruptions formed the pre-Komitake Volcano, whose existence was recently discovered through deep drilling (Aramaki et al. 2007). The center of this volcano was located about 7 km north of the current summit of Mt. Fuji. After the formation of the early volcano, there was a short break in the volcanic activity before subsequent eruptions, at nearly the same location, which formed the taller Komitake Volcano (Fig. 31.4). A part of this old volcano is exposed in the northern slope of Mt. Fuji, although most of it is buried under newer volcanics. Komitake Volcano finished forming around 100,000 years ago. Ashitaka Volcano, whose summit is located about 20 km southeast from the top of Mt. Fuji, was also active from 400,000 to 100,000 years ago. The dissected body of Ashitaka Volcano is mostly visible, with the exception of the northern area that has been buried below newer lava flows and sediments from Fuji Volcano (Figs. 31.1 and 31.3).

Eruptions near the present summit location of Mt. Fuji started about 100,000 years ago. The early Ko-Fuji (old-Fuji) volcanic body was created between

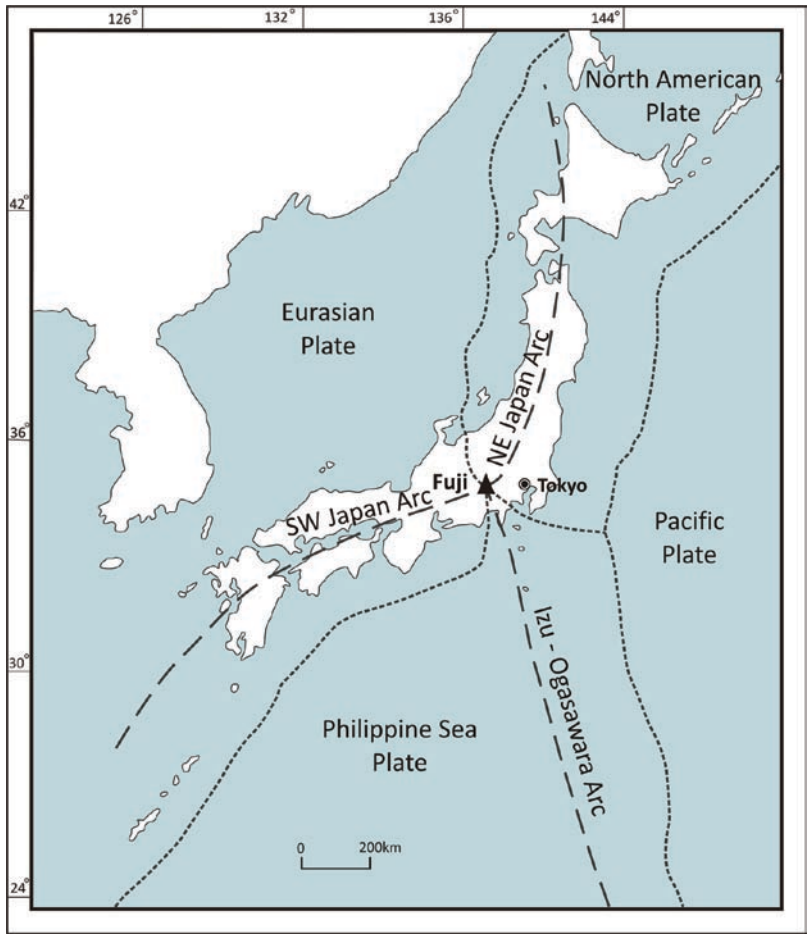

Fig. 31.2 Geographical setting of Mt. Fuji, close to the junction of four major tectonic plates and three island arcs

100,000 and 17,000 years ago, but is now mostly buried under newer volcanics. The height of Ko-Fuji Volcano reached nearly 3,000 m a.s.l. due to thick accumulations of mainly lava and scoria volcanics. Layers of volcanic ash from Ko-Fuji Volcano can be found in a wide area to the east of the volcano, including the Kanto Plain, because most of the ash was transported by the westerly winds. Ko-Fuji Volcano also experienced several catastrophic sector collapses with deep sliding surfaces (Inokuchi 1988), similar to the famous 1980 event of Mt. St. Helens, USA. These features illustrate the inherent instability of tall stratovolcanoes. The landslides supplied abundant debris-avalanche and mud-flow deposits to the piedmont areas. The last large landslide collapse occurred on the southwestern flank about 18,000 years ago (Aramaki et al. 2007). Lavas and debris-avalanche deposits from the sector collapses of Ko-Fuji Volcano can be observed in the western and eastern piedmont areas, not reached by younger lava flows and alluvial fan deposits.

Repeated eruptions around ~17,000 years ago belong to the Shin-Fuji (new-Fuji) geologic period. These supplied mostly lava, lapilli, and ash, and led to the taller, nearly symmetric volcanic body of Mt. Fuji as we see today (Aramaki et al. 2007). An enormous amount of lava (about 40 km^3) was erupted between 17,000 and 8,000 years ago. This was followed by a dormant period of about 1,000 years. Subsequent eruptions between 7,000 and 3,500 years ago led to lava flows from both the summit crater and fissures on flanks of the volcano. This was followed by repeated emission of scoria and pyroclastic flows from the summit crater between c 4,000 and 2,000 years ago (Yamamoto et al. 2005). Activity from the summit ceased

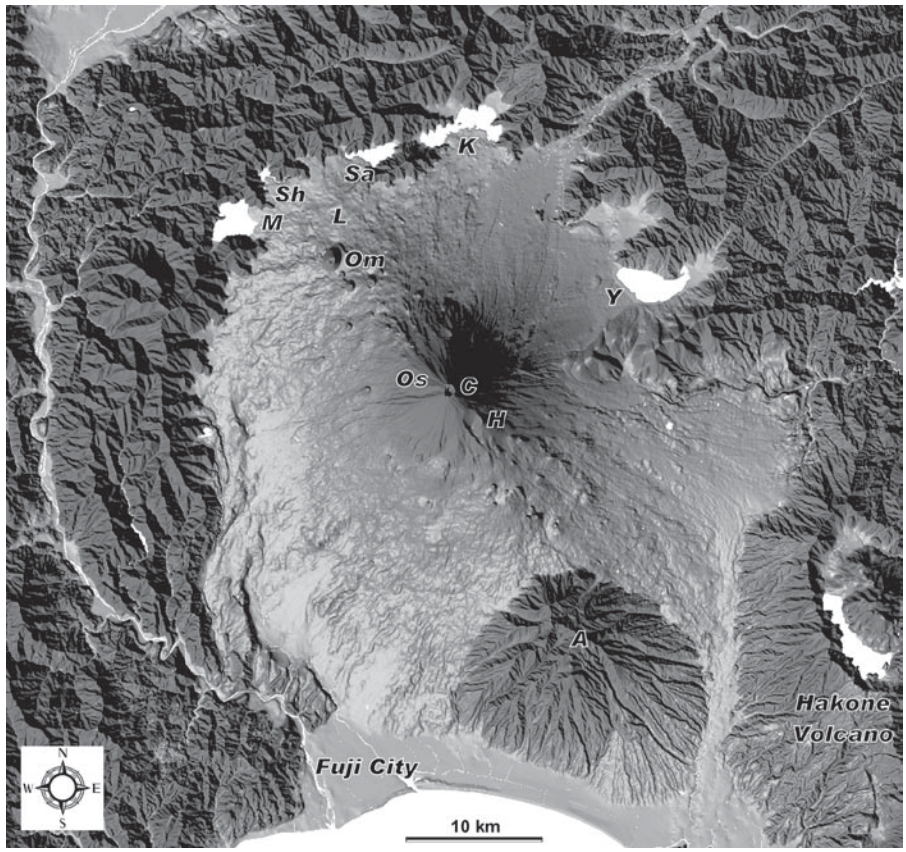

Fig. 31.3 Shaded-relief image of Mt. Fuji and surroundings, illuminated from the southwest. A – Ashitaka Volcano, C – Crater of Mt. Fuji, H – Hoei Crater formed in 1707, K – Kawaguchi Lake, L – Lava Flow of Aokigahara, M – Motosu Lake, Om – Omuro-Yama (cinder cone), Os – Osawa-Kuzure (landslide and valley), Sa – Sai Lake, Sh – Shoji Lake, Y – Yamanaka Lake

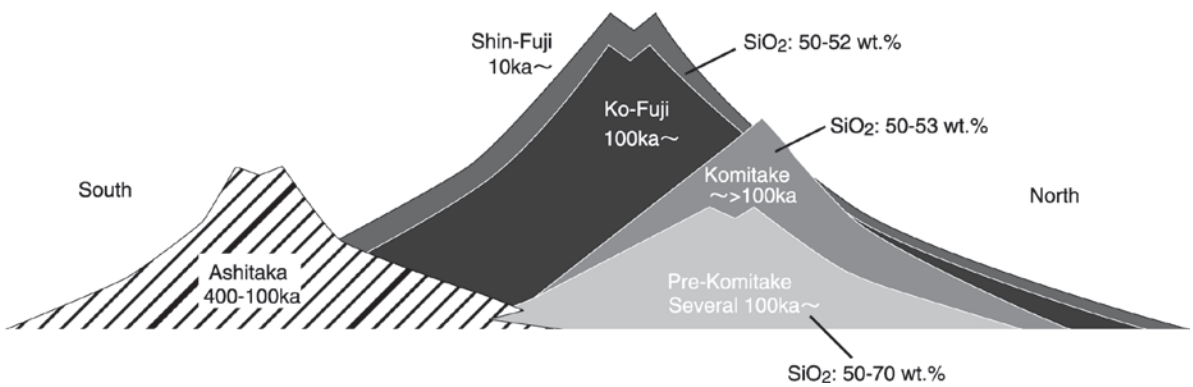

Fig. 31.4 Simplified geologic cross-section of Fuji and Ashitaka Volcanoes (After Aramaki et al. 2007)

after 2,000 years ago, although eruptions on the flanks continued in the form of parasitic cones, craters, and lava flows. The final eruption took place from craters on the southeastern flank in 1707. The event was relatively large (magma eruption volume of 0.7 km^3; Yoshimoto et al. 2004), producing abundant pumice and ash fall, particularly in the areas to the east of Mt. Fuji, including Tokyo. The resultant hazards, including secondary ones such as flooding from rapidly aggrading rivers, were recorded in many historical documents.

31.4 Landforms

31.4.1 Slopes

The slope angle of Mt. Fuji tends to increase with increasing altitude, and three zones can be differentiated in terms of average slope angle (Kato and Ikeda 1996). The highest zone, from near the summit to about 1.5–2 km from the crater rim, is characterized by slope angles between 31°–35°. This corresponds to the angle of repose of dry gravel and suggests that the gravitational fall of particles is the dominant geomorphic process here. Slopes immediately below this zone are 0.5–1 km in length and have lower angles of about 27°, although particle fall is still a dominant process. The surface deposits in this zone contain much more scoria, producing a lower angle of repose. The effects of running water become more evident in the lower zones, where slope angles gradually decrease from about 23° on the mid-flanks to less than 10° in the piedmont zones. Overall, the eastern flanks of the volcano are slightly gentler than the western flanks because the westerlies have transported more tephra onto the former sites. Such relatively minor differences in slope angle on the uppermost zone of the volcano have nevertheless influenced the presence or absence of pyroclastic flow deposits as they usually cannot rest on slopes steeper than 33° (Yamamoto et al. 2005).

31.4.2 Craters

The main crater at the summit of Mt. Fuji is about 780 m in diameter and 240 m in depth. Although the crater has been inactive for the last 2,000 years, no vegetation with the exception of moss has been established because of the location well above the forest limit and the effect of strong winds. Accumulated layers of volcanics forming the Shin-Fuji Volcano can be observed on the crater wall. The flat bottom of the crater is 100–130 m in diameter. Because of the water supply from melting snow and shallow underground permafrost, some wells and springs exist, even along the crater rim.

Another distinctive crater formed by the 1707 eruption is located on the southeast flank between ~2,400 and 3,100 m a.s.l (Figs. 31.1 and 31.3). It has a length of ~1,200 m and a width of ~900 m, looking like a deep landslide scar. Two small craters, formed during the same event, are located slightly below this large crater.

31.4.3 Lava Flows

Some of the lava flows from Mt. Fuji traveled long distances of up to 20 km, because of the low viscosity of basalt. The lavas are often associated with two types of micro-landforms: lava tubes/tunnels and lava tree molds (Miyamoto et al. 2003; Aramaki et al. 2007). More than 70 lava tunnels have been discovered, and many of them are characterized by low air temperatures, even in summer, when the remaining ice on the walls and floors of a tunnel has a cooling effect (Ohata et al. 1994). Thus, caving in these tunnels usually requires crampons. Small surface depressions also exist along some tunnels due to collapse of the tunnel roof. Lava tree molds form when lava flows through the forest. The standing or fallen trees caught in lava become burnt and disappear, leaving behind voids with shapes much like wells and small caves (Fig. 31.5). The distribution of tree molds around Mt. Fuji is one of the most extensive in the world.

31.4.4 Cinder Cones

The flanks of Mt. Fuji have more than 100 parasitic cinder cones formed by minor eruptions. The largest cone, Omuro-Yama, is located in the northwestern flank (Fig. 31.3). The cones are concentrated along two lines running through the summit from northwest to southeast and northeast to southwest, with the former having more cones, reflecting the principal direction of local tectonic stress. The relationship between the location and age of these cones indicates that the characteristics of tectonic stress changed with time during the Holocene (Aramaki et al. 2007).

31.4.5 Valleys and Landslides

Although the overall conical shape of Mt. Fuji is the dominant form, some valleys and gullies have developed, especially in the steep upper part of the mountain.

Fig. 31.5 Example of lava tree mold. Length of the folded scale is about 20 cm

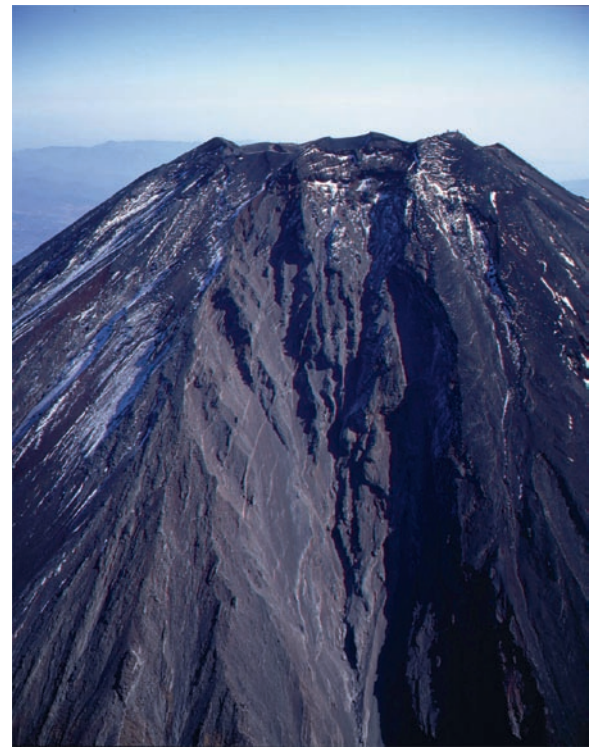

Fig. 31.6 Large landslide of Osawa-Kuzure on the western flank, immediately below the summit of Mt. Fuji. Courtesy of Nakanihon Air Service Co. Ltd.

The two most distinct valleys, with large landslides at their heads near the summit of the volcano, are Yoshida-Osawa on the northeastern flank and Osawa-Kuzure on the western flank. Osawa-Kuzure is the largest, with a maximum depth of ~200 m (Fig. 31.6) and mean annual sediment yield of ~1.6×10^5 m^3 (Aramaki et al. 2007). Dating of alluvial fan deposits below Osawa-Kuzure suggests that the large landslide in this valley started to form about 1,000 years ago (Tajima et al. 2006).

31.4.6 Lakes and Springs

The near-surface deposits of Shin-Fuji are mainly porous lava and ash, whereas the lower deposits of Ko-Fuji are less porous with more muddy components. Therefore, runoff from the slopes of Mt. Fuji tends to infiltrate and become confined within the Shin-Fuji deposits. In piedmont areas, this underground water flows out in many places to form ponds, streams, and even some large lakes. Isotopic compositions of ground water indicate that rainfall on the middle volcanic flanks, within altitudes from 1,100 to 2,700 m, is mainly responsible for the groundwater recharge of Mt. Fuji (Yasuhara et al. 1997).

The distribution of ponds and lakes at the foot of Mt. Fuji is partly a result of lava flows having entered into valleys and damming up rivers or separating existing water bodies. The Fuji Five Lakes (Kawaguchi, Motosu, Sai, Shoji, and Yamanaka) are a group of large lakes located on the northern foot at altitudes of ~1,000 m. The Aokigahara lava, which flowed down from a parasitic cone to the northern foot in AD 864 (Fig. 31.3), divided an existing large lake (Senoumi) into lakes Motosu and Sai. The lava also entered into Lake Shoji at the time. The water levels of these three lakes are almost identical and oscillate together, because of ground water interchange through the porous lava. Sediment cores taken from the bottoms of the lakes Kawaguchi, Yamanaka, and Motosu show that these lakes or their precursors already existed before the Holocene (Aramaki et al. 2007).

31.5 Conclusions

The symmetrical shape of Mt. Fuji may imply that its topography and history of formation are relatively simple. However, Mt. Fuji is composed of various geomorphological and geological components, and has had a complex evolutionary history since the Middle Pleistocene. Repeated basaltic eruptions, producing low-viscosity lava and abundant tephra, may account for the regular shape of the volcano as a whole despite its complex history.

Although Mt. Fuji has been dormant for about 300 years by now, a recent increase in volcanic earthquakes below the volcano has been reported (Nakamichi et al. 2004; Ukawa 2005). Future eruptions or large-scale erosion/deposition events such as a sector collapse may lead to serious hazards due to the high population densities in some piedmont areas of the mountain. Geomorphological and geological insights and knowledge about Mt. Fuji, including the characteristics of past hazardous events, are important for providing strategies to reduce the social impact of future events.

The Authors

Takashi Oguchi is a Professor at the Center for Spatial Information Science, the University of Tokyo, Japan. He received his Ph.D. in Geography from the University of Tokyo, and broadened his experience at the University of Arizona, Colorado State University, and the Centre for Ecology and Hydrology (UK). He has participated in research projects on fluvial/hillslope geomorphology, geomorphometry, geoarchaeology, water quality, and spatial databases. He has been one of the three editors-in-chief of *Geomorphology* (Elsevier) since 2003.

Chiaki T. Oguchi is an Associate Professor at the Geosphere Research Institute, Saitama University, Japan. She received her Ph.D. in Geoscience from the University of Tsukuba, Japan. Her research concerns rock weathering, including changes in various rock properties during long-term weathering and alteration, and salt weathering on rocks, bricks, and concretes. Her work has been published in international journals such as *Catena* and *Earth Surface Processes and Landforms*.

References

Aizawa K, Yoshimura R, Oshima N (2004) Splitting of the Philippine Sea Plate and a magma chamber beneath Mt. Fuji. Geophys Res Lett 31:L09603. doi:10.1029/2004GL019477

Aramaki S, Fujii T, Nakada S, Miyaji N (eds) (2007) Mt. Fuji. Yamanashi Institute of Environmental Sciences / The Volcanological Society of Japan, Japan (in Japanese, with English abstracts)

Inokuchi T (1988) Gigantic landslides and debris avalanches on volcanoes in Japan. In: Proceedings of the Kagoshima International Conference on Volcanoes, National Institute for Research Administration, Japan, pp 456–459.

Kato H, Ikeda H (1996) The cause of forming the slope at an angle of 27° in Yoshida-Osawa at Mt. Fuji. Bull Env Res Center, University of Tsukuba 21:41–50 (in Japanese)

Miyamoto H, Haruyama J, Rokugawa S, Onishi K, Toshioka T, Koshinuma J (2003) Acquisition of ground penetrating radar data to detect lava tubes: preliminary results on the Komoriana cave at Fuji volcano in Japan. Bull Eng Geol Env 62:281–288

Nakamichi H, Ukawa M, Sakai S (2004) Precise hypocenter locations of midcrustal low-frequency earthquakes beneath Mt. Fuji, Japan. Earth Planet Space 56:37–40

Ohata T, Furukawa T, Higuchi K (1994) Glacioclimatological study of perennial ice in the Fuji Ice Cave, Japan. Part 1. Seasonal variation and mechanism of maintenance. Arctic Alpine Res 26:227–237

Ohsawa M (1984) Differentiation of vegetation zones and species strategies in the subalpine region of Mt. Fuji. Plant Ecol 57:15–52

Tajima Y, Miyaji N, Inoue K (2006) History of the Kamiide Alluvial Fan formed by the products of the Younger Fuji Volcano. Quat Res (Tokyo) 45:287–301 (in Japanese with English abstract)

Tsuya H, Morimoto R (1963) Types of volcanic eruptions in Japan. Bull Volcanol 26:209–222

Ukawa M (2005) Deep low-frequency earthquake swarm in the mid crust beneath Mount Fuji (Japan) in 2000 and 2001. Bull Volcanol 68:47–56

Yamamoto T, Takada A, Ishizuka Y, Miyaji N, Tajima Y (2005) Basaltic pyroclastic flows of Fuji volcano, Japan: characteristics of the deposits and their origin. Bull Volcanol 67:622–633

Yasuhara M, Murai A, Kazahaya K (1997) Stable isotopic composition of groundwater from Mt. Yatsugatake and Mt. Fuji, Japan. IAHS Publ 244:335–344

Yoshimoto M, Fujii T, Kaneko T, Yasuda A, Nakada S (2004) Multiple magma reservoirs for the 1707 eruption of Fuji volcano, Japan. Proc Japan Acad, B 80:103–106

Chapter 32
Mulu: The World's Most Spectacular Tropical Karst

David Gillieson and Brian Clark

Abstract The Gunung Mulu karst of northern Sarawak hosts some of the longest caves in Southeast Asia. The majority of the cave passages in the Mulu karst are of phreatic origin and formed between sinks and springs as a series of loops crossing the bedding planes along which the passages formed. Water draining off the Mulu Sandstone also invaded the limestone down-dip, under a hydraulic gradient large enough to facilitate phreatic tubes rising up to 100 m to intersect other bedding planes. Rain falling directly on the limestone massifs has created vertical shafts and invasion vadose passages, which intersected the drained phreatic tubes, creating a three-dimensional array of cave passages. The drainage off the sandstone also migrated laterally along the contact with the limestone to produce a series of very large cavities, whose roof collapse produced a series of very large dolines or *tiankeng* (sky windows).

Keywords Caves • evolution • karst • Mulu • Sarawak • tropical

32.1 Introduction

Throughout Southeast Asia there are many outcrops of limestone, ranging in age from Cambrian to Quaternary, a span of about 500 million years. These areas contain some of the more extensive karst regions in the world (Gillieson 2005), with a total area of about 400,000 km^2. The imagination of travelers in this region has long been stimulated by the sight of cliffed limestone towers (Fig. 32.1) rising above forested plains and punctuated by gaping cave entrances and giant enclosed depressions (dolines). For a long time their inaccessibility combined with political restrictions limited scientific investigation, despite the early writings of Lehmann (1936), Verstappen (1960) and others.

To many, the global geomorphological potential of limestone solution is attained in the everwet, tropical karsts of the region. The extensive caves that underly the rugged limestone terrain are yielding diverse information on palaeoclimates (Cobb et al. 2007), and ecological studies are elucidating the rich biodiversity and complex relationships between biology and geomorphology (Gillieson 2005). One of the world's great tropical karst areas lies near the source of the Sungei (river) Tutoh in far northern Sarawak, Borneo. The Gunung Mulu National Park has been a World Heritage property since 2000 and the subject of scientific study since the pioneering work of Wilford (1964).

32.2 Geographical Setting

Mulu is located about 100 km east of Miri, a coastal city in northern Sarawak. The small town of Mulu is reached by daily air services from Miri and can also be reached by boats up the Baram and Tutoh rivers. Gunung Mulu National Park has an area of 90,000 ha and most visitors concentrate on the southernmost karst, accessible from the park headquarters adjacent to the town. Over 90% of the park remains unvisited and is in pristine condition (Gill 1999). The geology of the park has been the focus of much scientific study (Liechti et al. 1960; Wilford 1964; Webb 1982), revealing three main lithologies:

- The 5–6 km thick, slightly metamorphosed sandstone and shale of the Mulu Formation, of the Late Cretaceous – Eocene period
- The overlying shallow marine deposits of the Melinau Limestone of the Late Eocene – Early Miocene period
- The Setap Shales of the Middle Oligocene – Early Miocene period

The Mulu Formation shales and sandstones outcrop on the eastern side of the park as the ridges and summit of

P. Migoń (ed.), *Geomorphological Landscapes of the World*,
DOI 10.1007/978-90-481-3055-9_32,

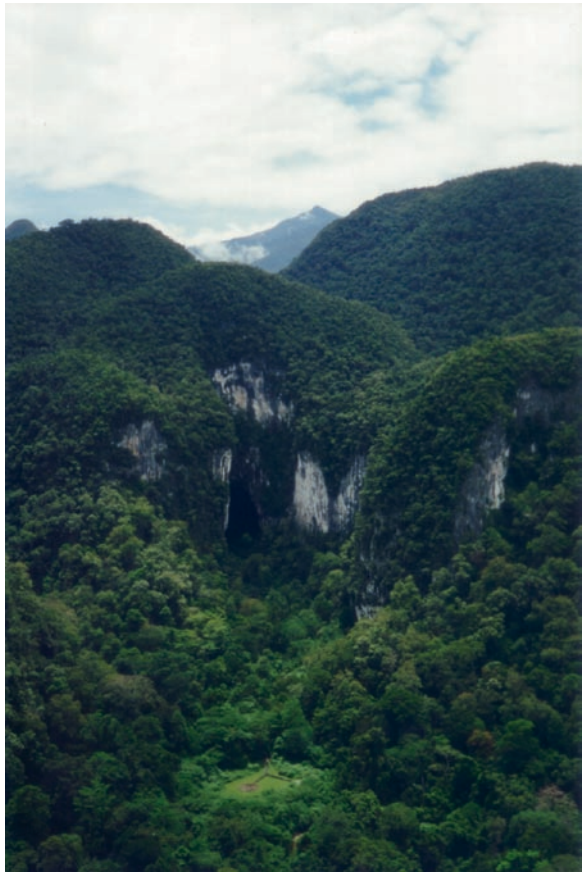

Fig. 32.1 Deer Cave entrance from helicopter (Photo D Gillieson)

Gunung Mulu, reaching an altitude of 2,377 m. The Melinau Limestone Formation of the Upper Eocene, Oligocene, and Lower Miocene ages, up to 1,500 m in thickness, overlies it and outcrops as a spectacular line of karst hills; it reaches a maximum altitude of 1,682 m at the summit of Gunung Api. The limestone formation has been dissected by deeply incised gorges dividing the limestones into four distinct blocks (Fig. 32.2). From south to north, the Southern Hills have been separated from Gunung Api by the Melinau Paku valley. The spectacular Melinau Gorge divides Gunung Api from Gunung Benarat, while the Medalam Gorge divides Gunung Benarat from Gunung Buda. The limestones are pure, massively bedded, dipping 80° to the northwest while faults and joints run northeasterly. The upper surface of the limestone massifs is spectacular and extremely rugged with pinnacle and arête morphology, deep gullies, and cliffs. There is a very strong control of jointing on these landforms. The Miocene Setap Shale Formation outcrops as a gentle line of hills on the western boundary of the park. Between the major limestone outcrop and the Setap Shales is a broad alluvial plain overlying the limestones, with Pleistocene terraces covered in *Karangas* peat swamp forest. The Sungei Melinau drains this plain and flows south into the Sungei Tutoh.

The climate of Gunung Mulu is equatorial perhumid, with a diurnal temperature range from around 22°C to 32°C. Humidity is high, usually around 90% in the early morning and decreasing to 60% in the afternoon. Annual rainfall is also high, from 4,400 to 6,800 mm. Sarawak experiences two relatively wetter monsoon seasons with intervening slightly drier periods.

32.3 Landforms

32.3.1 Limestone Hills and Towers

The massive Mulu Limestone forms almost vertical cliffs along the main rivers and in the gorges. These reach their maximum height of about 300 m in the Hidden Valley. This is the locus of most erosions with cliff-foot caves and undercutting enabling periodic collapse and large-scale sliding along the dominant joints, thus maintaining the verticality of the karst towers. Virtually all of the limestone walls have extensive deposits of secondary carbonates as tufas and outside stalactites. There is, however, no evidence of case-hardening of the limestone (Day 1980).

Numerous small outliers of Mulu Limestone occur on the floodplain of the Melinau River, emerging through the alluvium as at Bukit Berar and Bukit Pala near the Mulu Resort. At several places along the Melinau and the adjacent banks of the Tutoh, planed limestone surfaces with minor pinnacles are overlain by thick alluvium. Close to the southern end of the airport, quarrying has exposed a number of limestone mounds rising through the Setap Shales. These contain coral bioherms which may be in situ, and which are capped by a hard red carapace. This may be due to subaerial weathering and raises the possibility that some solutional sculpturing of the Mulu Limestone occurred prior to the deposition of the Setap Shales in the late Tertiary.

32.3.2 Gorges

Water draining the Mulu Formation sandstones and shales normally passes into streamsinks and caves on

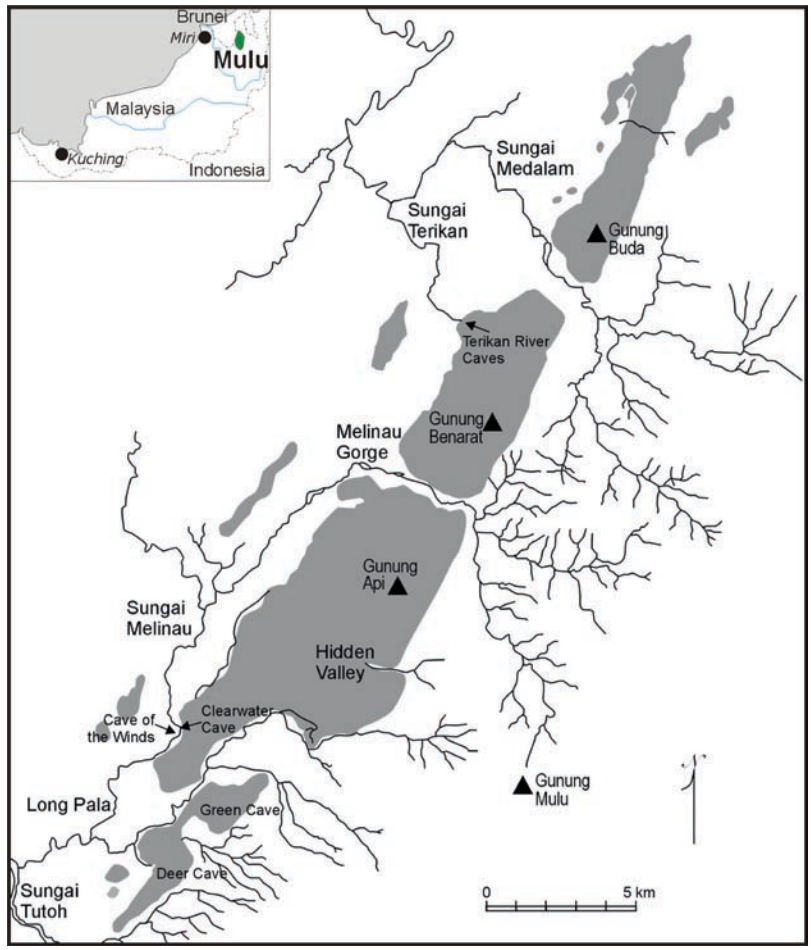

Fig. 32.2 Gunung Mulu National Park with limestone massifs (Inset of location in Southeast Asia)

reaching the limestone margins. The four massifs of Mulu Limestone are separated by deep, spectacular gorges through which the main rivers run. In all these cases there are zones of structural weakness which have been exploited by antecedent drainage on the reactivated Mulu uplift in the late Pliocene to Pleistocene. It is possible that some portions of the gorges are unroofed caves, for example, in the Melinau Gorge upstream of Camp Five. There is certainly a close association between the northernmost parts of the Clearwater Cave system (Blackrock, Whiterock, and Moon Caves) and the flanks of the gorge. Breached phreatic cave passages, such as Tiger Cave and Tiger Foot Cave, can be seen in the gorge walls. The steep gorge walls are maintained by undercutting during floods and subsequent collapse. The Melinau Paku valley is fed by a broad amphitheatre draining the Mulu Formation sandstone, and the wide valley is floored by alluvium. At its western end, the valley narrows significantly between Batu Panjang and the southern end of Gunung Api. It is possible that this represents a former cave, first unroofed as a tiankeng and then breached by the Melinau Paku stream.

Drainage along the strike is well developed in the headwaters of the Sungei Medalam east of Gunung Benarat, in the Melinau headwaters east of Gunung Api, and by both the Melinau Paku and the Sungei Langsat to the south. This strong structural control has implications for the location of stream sinks and the caves that they feed.

32.3.3 Dolines and Tiankeng

The upper surface of the limestone on all four massifs is dissected by deep closed depressions separated by asymmetric hills. Their morphology is evident on aerial photography, despite being covered in dense closed forest. The control of joints oriented along the strike is

obvious. Many of these depressions drain freely into underlying caves, though very few have been descended. The sides of the depressions are made up of vertical joint planes and steeply dipping bedding planes, with some overhangs due to cliff collapse.

A *tiankeng* (sky window) is a very large collapse doline that has evolved by roof collapse over a large cave chamber, whence a very large amount of breakdown debris has been removed by a large underground river (Zhu and Waltham 2006). Seventy-five have been recorded worldwide, with the majority being in China. Typically they are more than 100 m wide and deep, with a minimum volume of 1 million cubic meters. The most obvious example at Mulu is the Garden of Eden, a mega-doline about 1 km across that interrupts a very large, very old cave passage of which Deer and Green Caves are the remnants. The volume of the Garden of Eden is around 150 million cubic meters. Steep and vertical limestone cliffs, 150–300 m high, enclose one half of its perimeter (Fig. 32.3), while the other side of the doline is formed on slopes of shale and sandstone with waterfalls and streams draining them.

32.3.4 Pinnacles and Minor Solution Sculpture

The pinnacles on Gunung Api are visited by thousands each year, and have become an iconic feature of Mulu (Waltham 1995; Osmaston 1980). They are simply the most accessible of a wider array of pinnacle and arête karst (Williams 1971) at Mulu and in many other areas of tropical karst in Southeast Asia and Melanesia. The pinnacles are typically 20–30 m high and surrounded by closed depressions, which reflect the dominant control of jointing in the limestone. In most cases, the pinnacle fields are located close to the edges of major cliffs and faults. The intersections of conjugate joint sets at high density, coupled with another fracture set aligned with the bedding, create conditions of very high rainfall infiltration rates. Thus, water passes very rapidly underground to emerge as roof showers and rapid drips in many of the caves. Given the high rainfall, there is virtually no soil accumulation in the depressions. The depression bases are composed of a jumble of limestone blocks and deep fissures cloaked

Fig. 32.3 The interior of the Garden of Eden – a huge tiankeng in the eastern part of the limestone range (Photo P Migoń)

in moss, thick humus, and some herbs. The pinnacles are really a form of hyper-depression fields where the depression rims have lost their coherence, and the entire surface is covered in pinnacles and deep rifts.

The steep flanks of the pinnacles and the upper surfaces of most cliffs are drained by solution runnels (Wilford and Wall 1965), typically 10–20 cm wide and deep and up to 10–20 m long. Periodically down their length, there are small solution cups and pans, many with accumulations of leaf litter and humus. Small-scale solution rills (rillenkarren) are rare in this karst though common in temperate karst. A distinctive feature of most vertical surfaces are horizontal solution ripples, a form of microkarst (Wilford and Wall 1965). These gently undulating, rounded ridges, a few millimeters high, may relate to the dynamics of thin films of acidified water flowing down vertical rock surfaces. Light-oriented pinnacles (phytokarst) are well developed on the surface of limestone strata and boulders in cave entrances at Mulu, and may attain a length of 30 cm; the most easily accessible examples are at Clearwater Cave. These small-scale pinnacles are essentially erosional forms produced by the boring and solutional action of red and blue-green algae which colonize the rock surfaces (Bull and Laverty 1982).

32.3.5 Caves

The caves of the Gunung Mulu National Park are now world famous. Over 100 caves are now known with a total mapped length of over 330 km, ranging in altitude from local base level at 28–600 m a.s.l. (Brook et al. 1982). The caves are some of the largest to be found in the world, with 30–40 m diameter strike-orientated passages being common. They are amongst the finest examples of tropical river caves known, with well-developed flood incuts, extensive clastic sediment deposits, and circular or elliptical tubes linking different cave levels.

Deer Cave is one of the world's largest natural cave passages, measuring 120–150 m in diameter and 1,000 m in length (Fig. 32.4). It reveals evidence of faulting in its western wall and has thick coarse sediment accumulations throughout its kilometer length.

Fig. 32.4 Near-entrance part of the Deer Cave is nearly 100 m high and wide (Photo P Migoń)

A lower passage, Deer Water Cave, due to avulsion by sediment blockage, can be traversed at low water levels. Higher-level passages are visible in the roof and at several points local autogenic drainage has invaded the passage producing roof showers. The nearby Lang's Cave is a phreatic tube which may be genetically related to a major phase of sediment infilling. A higher-level and genetically related cave, Stone Horse, has sediment accumulations 50 m thick with imbricated and cemented gravels. These are exposed in massive pits in the floor of the passage. The levels of Stone Horse, upper Deer, and Green Caves are accordant at about 200 m altitude. The fossil tunnel of Green Cave has large floor pits consistent with those in Stone Horse Cave, and extends through the rim of the Garden of Eden *tiankeng* to a perched entrance to the north, overlooking the Melinau Paku valley. Solutional wall scallops indicate that the water flowed into the Garden of Eden, from a now-abandoned sink in the Paku valley.

Deer Cave leads into the Garden of Eden, a very large *tiankeng* formed on the junction of the Melinau limestone and Mulu sandstone and shale. The *tiankeng* formed by collapse and debris removal from a former section of the Deer–Green cave trunk passage. There is evidence to suggest that that the Sungei Lansat stream was also captured by the karst and aided this process; its underfit stream now flows to the south along the strike and joins the Sungei Tutoh. An analogous setting of similar size can be found at the huge Sarawak Chamber in Gua Nasib Bagus, which is floored by sandstone and bounded by faults (Gilli 1993). In time, it is likely that the Sarawak Chamber will also become a *tiankeng*.

Gua Nasib Bagus (Good Luck Cave) contains "Sarawak Chamber," the world's largest natural single chamber within a cave. The chamber measures 600 m long by 415 m wide and 80 m high, with a floor area of 162,700 m^2 and a volume of 12 million cubic meter, dwarfing any other chamber in the world so far discovered. The present entrance to Gua Nasib Bagus is a resurgence at grade with the first terrace of the Sungei Melinau Paku. An entrance lake leads to a kilometer of fine vadose canyon, which rises steeply at the end to a collapse leading into the Sarawak Chamber.

The Clearwater Cave System is presently 151 km in length, the longest cave so far discovered in Asia. It displays outstanding tubular passages and canyons developed at many levels (Fig. 32.5). The cave once captured all of the flow of the Melinau through streamsinks, and is now largely blocked. Dye tracing from

Fig. 32.5 Downstream passage in Clearwater Cave, looking out to entrance (Photo D Gillieson)

the Melinau Gorge proved a connection through to the Clearwater Cave resurgence, a linear distance of 12 km. The lowest level of the cave is a vadose canyon which carries a base flow of 0.1 m^3/s rising to 5 m^3/s in response to the afternoon rainstorms. The upstream sections of the cave contain canyons alternating with flooded loops. The highest levels of the cave are large tunnels oriented along the strike and formed on just a few bedding planes.

Gunung Benarat contains some very large caves, with 30 km of high-level ancient passages in Cobweb Cave and a sequence of more horizontal tunnels in Benarat caverns. The caves of Gunung Buda extend for at least 30 km and include some large chambers and phreatic ramps; in Gua Kulit Siput these attain an altitude of 470 m above the floodplain of the Medalam River.

32.4 Landscape Evolution

It is probable that there was some pre-existing relief on the Mulu Limestone at the time of deposition of the overlying Setap Shale, about 20 million years ago. This is evidenced by limestone pinnacles extending through the thinnest margins of the shale, resulting in an unconformity with a local relief of 5–10 m. Major uplift certainly occurred during the late Pliocene to Pleistocene, 5 to 2 million years before the present. This was accompanied by folding and faulting, producing a synclinal trough along which the Sungei Melinau runs today. The tension associated with this folding gave rise to the dense networks of conjugate joints that dissect the limestone and allow for rapid water infiltration. A fault runs along the western edge of the limestone massifs and another parallel fault is associated with Clearwater Cave. This uplift is also reflected in the wide range of cave passage levels in the karst.

The surface geomorphology and hydrology has been studied extensively (Day 1980; Rose 1984; Osmaston and Sweeting 1982; Walsh 1983). The Mulu karst has provided very significant information on the tectonic and climatic evolution of the island of Borneo. Large alluvial fans are evident, emerging from the Melinau Gorge and the Melinau Paku Valley, with remnants of early Pleistocene fans preserved as terrace gravels (Rose 1984). Fan aggradation is due to climatic control rather than tectonic influences. Increased rainfall during interglacials produced higher sediment loads, while relatively drier glacials with less sediment transport led to incision of the fans. This sequence of alluvial deposits thus provides an important record of glacial–interglacial cycles with which to interpret landform evolution.

The majority of cave passages in the Mulu karst are of phreatic origin. The phreatic tubes propagated between sinks and springs as a series of loops guided by major joints crossing the bedding planes along which the passages formed. The injection of large quantities of gravels and mud partially blocked most passages, allowing paragenetic solution development to bypass the down-loops while bedrock canyons were cut though the up-loops. Subsequent erosion of the sediments has revealed a depth of sediment fill at least 50 m thick in many locations. This can be easily seen in Lagang's Cave, as well as in Stone Horse and Clearwater.

The high-level passages of Clearwater Cave are tunnels developed along the strike, forming a vertical sequence developed on a few bedding planes. Water draining off the Mulu Sandstone invaded the limestone down-dip, under a hydraulic gradient large enough to facilitate phreatic tubes rising up to 100 m to intersect other bedding planes (Smart et al. 1985). These phreatic risers are now abandoned dry shafts and are amongst the largest of their kind in the world (Waltham 2004). There is some downstream vadose development, for example, the 30 m high canyon in Clearwater Cave, but wherever it is present, the original phreatic elements are clearly preserved as roof half-tubes.

As the overlying Setap Shale retreated westwards, due to the incision of the Melinau valley, more limestone was exposed. Autogenic drainage from rain falling on the limestone massif created vertical shafts and invasion vadose passages, which intersected the drained phreatic tubes, creating a three-dimensional array of cave passages (Fig. 32.6). There is thus an age sequence from east to west, rendered more complex by subsequent invasion of older passages when sediments blocked the lower cave conduits. The reversal of flow caused by this can be seen in several passages. This is a form of the channel avulsion seen in surface rivers (Gillieson 1986).

The stream sinks on the eastern side of the limestone massifs have also migrated over time, as alluvial fans formed in Mulu Sandstone sediments created a convex surface over which the surface streams moved. This process can be seen today in the Melinau Paku valley. Several caves show genetic relationships with

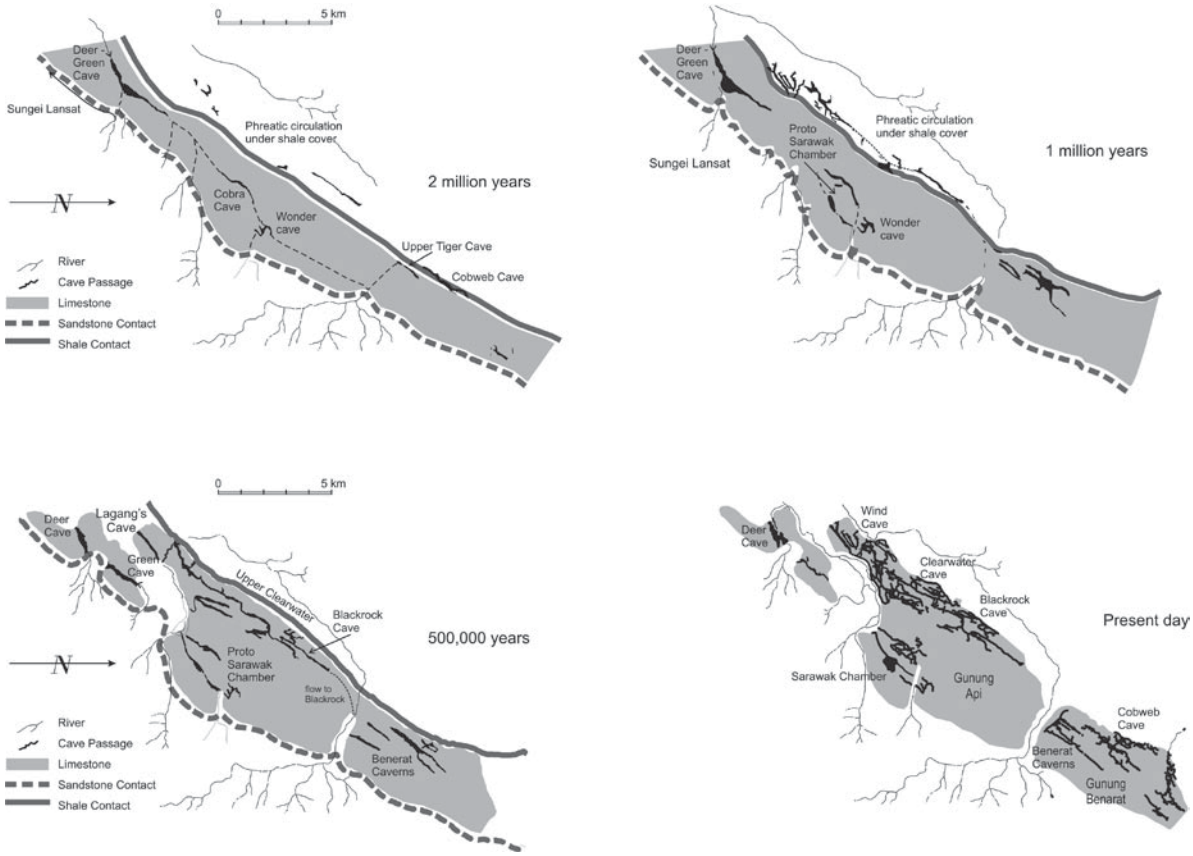

Fig. 32.6 Evolution of the Mulu karst (Greyscale, showing tiankengs and stream sinks, caves in black)

the headwards retreat and lateral shift of streamsinks along the flank of the Melinau Paku valley (Fig. 32.6). The youngest caves in the sequence are the active springs from Wind Cave and the downstream parts of Clearwater Cave (Fig. 32.5). Down valley, Racer Cave is a former spring with a series of sediment-filled chambers leading toward a former sink in the Paku valley. The furthest downstream, and potentially oldest, is Lagang's Cave. This cave has large phreatic tubes with roof pendants, abundant speleothems, and both finely laminated clays and gravels.

The cave sediment deposits are still intact at all altitude levels, affording the opportunity for important scientific investigations of climatic change (Farrant et al. 1995). These clays and gravels are therefore not subject to normal surface erosion processes but have been preserved in situ for millennia. Paleomagnetic dating revealed a Plio-Pleistocene uplift rate of 190 mm/1,000 years. Reversal of the earth's magnetic field, recorded in the sediments at 1.8 million years before present, indicates that the caves are at least 2 million years old, possibly as much as 3 million years.

Notches in the walls of the caves at various levels over a range of 300 m vertically can be correlated with interglacial periods (Farrant et al. 1995). Interglacial gravel aggradation created local base levels at which notches, typically 2 m high and 4–5 m deep, formed. Several of these can be traced over a distance of 2–3 km. At the lowest cave levels, at grade with the Melinau River, these dissolutional notches are forming today.

The evolution of Gua Nasib Bagus (Good Luck Cave) reveals further interactions between the drainage off the sandstone in Hidden Valley and the role of structural control in cave morphology. At the earliest times, the cave passage may have been a wide slot, cut by a large stream along the contact between sandstone and overlying limestone. This passage migrated laterally along the contact to produce an inclined cavity which

was subject to roof collapse to produce the present enormous chamber. Today the stream is confined to one side of the chamber and drains into a strike-oriented canyon, which feeds a spring at the level of the Melinau Paku floodplain. As indicated previously, the Garden of Eden *tiankeng* may have formed in a similar manner.

32.5 Conclusions

The Gunung Mulu National Park provides very significant tropical cave and karst features and ecosystems in a relatively undisturbed state, with effective management and training programs in place. It has universal significance in terms of its geology, geomorphology, and biology.

The karst mountains exhibit classical tropical karst features, pockmarked with dolines, closed depressions, valleys, and caves. In the southern hills, "The Garden of Eden" is a fine example of a *tiankeng*, being over 1 km in diameter. Hidden Valley on the east side of Gunung Api is a deeply incised closed valley with a misfit stream sinking in its bed. The Melinau, Melinau Paku, and Medalam Rivers have truncated the limestones, forming deeply incised gorges with towering 300 m high cliffs and remnants of high-level caves. Some of the world's finest examples of pinnacle karst can be found on the karst mountains of Gunung Benarat and Api.

The caves of Mulu are currently the longest in Southeast Asia and more will undoubtedly be found. The caves are predominately phreatic in origin but exhibit vadose, phreatic, and paragenetic profiles with some of the world's finest examples of phreatic pendants. The cave sediment deposits are still in place at all altitude levels, affording the opportunity for important scientific investigations of climatic change. Reversal of the earth's magnetic field, recorded in the sediments at 1.8 million years before present, indicates that the caves are at least 2 million years old, possibly as much as 3 million years. Notches in the walls of the caves at various levels can be correlated with interglacial periods. The caves and associated karsts are therefore of outstanding significance in recording the major changes in the earth's history, and have thus joined the rich array of karst sites inscribed on the World Heritage List.

The Authors

David Gillieson is Professor of Geography in the School of Earth & Environmental Sciences, James Cook University, Australia. His research concerns cave and karst landform evolution, especially tropical karst, and cave management. His previous publications include *Caves: Processes, Development, Management*, a number of entries to the *Encyclopaedia of Caves and Karst Science* and more than 120 peer-reviewed papers. He is a former Chair of the International Geographical Union Commission on Karst and a member of the IUCN-WCPA Taskforce on Caves and Karst.

Brian Clark was a manager of cave and karst–based national parks in Australia before becoming the park manager at Gunung Mulu National Park in 2002. He has collaborated in the publication of numerous articles on climate change and actively encourages research which supports the development of geodiversity conservation awareness programs. He is a life member of the Australasian Cave and Karst Management Association.

References

Brook DB, Eavis AJ, Lyon MK (1982) Caves of the limestone, Gunung Mulu National Park, Sarawak. Sarawak Mus J 51(1):95–120

Bull PA, Laverty M (1982) Observations on phytokarst. Z Geomorph NF 26:437–457

Cobb KM, Adkins JF, Partin JW, Clark B (2007) Regional-scale climate influences on temporal variations of rainwater and cave dripwater oxygen isotopes in northern Borneo. Earth Planet Sci Lett 263:207–220

Day MJ (1980) Landslides in the Gunung Mulu National Park. Geogr J 146:7–13

Farrant AR, Smart PL, Whitaker FF, Tarling DH (1995) Long-term Quaternary uplift rates inferred from limestone caves in Sarawak, Malaysia. Geology 23:357–360

Gill D (1999) Nomination of the Gunung Mulu National Park, Sarawak, Malaysia for World Heritage Listing, Report to UNESCO World Heritage Committee. Sarawak Forestry Department, Kuching

Gilli E (1993) Les grandes volumes souterrains du massif de Mulu (Borneo, Sarawak, Malaisie). Karstologia 22:1–14

Gillieson DS (1986) Cave sedimentation in the New Guinea Highlands. Earth Surf Proc Landf 11:533–543

Gillieson D (2005) Karst in Southeast Asia. In: Gupta A (ed) The physical geography of South East Asia. Oxford University Press, New York, pp 157–176

Lehmann H (1936) Morphologische Studien auf Java. Geogr Abh 3(9):1–114

Liechti P, Roe FN, Haile NS, Kirk HJV (1960) The geology of Sarawak, Brunei and the western part of North Borneo. Bull British Borneo Geol Surv 3

Osmaston HA (1980) Patterns in trees, rivers and rocks in the Mulu Park, Sarawak. Geogr J 146:33–50

Osmaston HA, Sweeting MM (1982) Geomorphology, Gunung Mulu National Park, Sarawak. Sarawak Mus J 51(1):75–94

Rose J (1984) Alluvial terraces of an equatorial river, Melinau drainage basin, Sarawak. Z Geomorph NF 28:155–177

Smart PL, Bull PA, Rose J, Laverty M, Noel M (1985) Surface and underground fluvial activity in the Gunung Mulu National Park, Sarawak: A palaeoclimatic interpretation. In: Douglas I, Spencer T (eds) Tropical Geomorphology and environmental change. George, Allen & Unwin, London, pp. 123–148

Verstappen HT (1960) Some observations on karst development in the Malay Archipelago. J Trop Geogr 14:1–10

Walsh RPD (1983) Hydrology and water chemistry of the Gunung Mulu National Park. Sarawak Mus J 30:121–180

Waltham AC (1995) The pinnacle karst of Gunung Api, Mulu. Cave Karst Sci 22(3):123–126

Waltham AC (2004) Mulu, Sarawak. In: Gunn J (ed) The Encyclopedia of Caves and Karst Science. Taylor and Francis/Routledge, New York, pp 531–533

Webb B (1982) The geology of the Melinau Limestone, Gunung Mulu National Park, Sarawak. Trans British Cave Res Assoc 9:94–99

Wilford GE (1964) The geology of Sarawak and Sabah Caves. Geol Surv Borneo Region, Malaysia, Bull 6:1–177

Wilford GE, Wall JRD (1965) Karst topography in Sarawak. J Trop Geogr 21:44–70

Williams PW (1971) Illustrating morphometric analysis of karst with examples from New Guinea. Z Geomorph NF 15:40–61

Zhu X, Waltham T (2006) Tiankeng: definition and description. Speleogenesis Evol Karst Aquifers 4(1):2–8

Chapter 33
Uluru (Ayers Rock) and Kata Tjuta (The Olgas): Inselbergs of Central Australia

C.R. Twidale

Abstract Uluru and Kata Tjuta are inselbergs standing in isolation in the desert plains of central Australia. Uluru is a beveled bornhardt shaped steeply dipping Cambrian arkose. Kata Tjuta is a complex of domes, each developed by fracture-controlled weathering and erosion of a mass of gently dipping conglomerate, also of Cambrian age. The sedimentary formations strike northwest to southeast and the compartments on which the residuals are formed were compressed as a result of either cross- or interference folding. They were exposed as low hills by the latest Cretaceous and possibly as early as the Triassic, since which time the detailed morphology of the forms shows that they have come to stand higher and higher in the relief as a result of the episodic lowering of the surrounding plains. Their persistence is attributed to reinforcement effects.

Keywords Bornhardts • episodic exposure • Mesozoic age • survival

33.1 Introduction

Although truly "a land of sweeping plains," there are few parts of Australia where the level and otherwise smooth horizon is not interrupted by an isolated distant hill or range. Of all such inselbergs, however, none are as well known as Uluru (Ayers Rock) and Kata Tjuta (The Olgas), which rise abruptly from the plains of the arid "red centre," and together constitute a UNESCO World Heritage site, established in 1987 (Figs. 33.1 and 33.2).[1] The two uplands have much in common. Both are shaped in fanglomerates of Cambrian age that originated in the piedmont of the precursors of the Petermann, Musgrave, and associated ranges (Wells et al. 1970; Sweet and Crick 1992). Both are bare, rocky, domical hills, one comprising a single bornhardt and the other comprising several bornhardts, each developed on a fracture-controlled block. Yet they differ in their detailed morphology. Minor features provide much of the evidence for the evolution of the gross landforms on which they occur, and as Uluru is the more complex, it is discussed first. Kata Tjuta is then considered in light of the conclusions that emerge from that analysis.

33.2 Uluru

33.2.1 Introduction

Uluru was sighted from afar by Giles in 1872 (Giles 1889) but was not explored until 1873, when Gosse became the first European to ascend the residual he named Ayers Rock (Gosse 1874). But the native Pitjanjara people had long been familiar with the site, which they knew as Uluru, for its water holes attracted frequent settlement. They believed the hill had been thrust up from the desert floor, and interpreted the various features on the hill in terms of Dreamtime animals, people, and events (e.g., Mountford 1965).

33.2.2 Geology and Topography

Uluru is lozenge-shaped in plan, steep-sided in profile, and with a beveled crest (Figs. 33.3 and 33.4). It stands 877 m a.s.l. and some 350 m above the adjacent plains.

[1]All photographs in this chapter were taken by the author

P. Migoń (ed.), *Geomorphological Landscapes of the World*,
DOI 10.1007/978-90-481-3055-9_33,

It is shaped by steeply dipping, northwest to southeast striking, arkosic sandstone, a facies of the Mt. Currie Conglomerate. As revealed in some shelters or cliff-foot caves, the feldspathic sandstone is greenish-grey in color, but most exposures carry a patina of finely divided feldspar coated with iron oxide (haematite/goethite) that is derived from the weathering of mica and epidote (both minor constituents of the arkose), and which imparts a bright rusty red color to the surface.

To the south of the inselberg the Cambrian strata are faulted and there the piedmont is underlain by a considerable thickness of unconsolidated sand over arkose (Fig. 33.1c). Elsewhere, however, the sand cover is only a few meters thick (Fig. 33.1b) and discontinuous, for

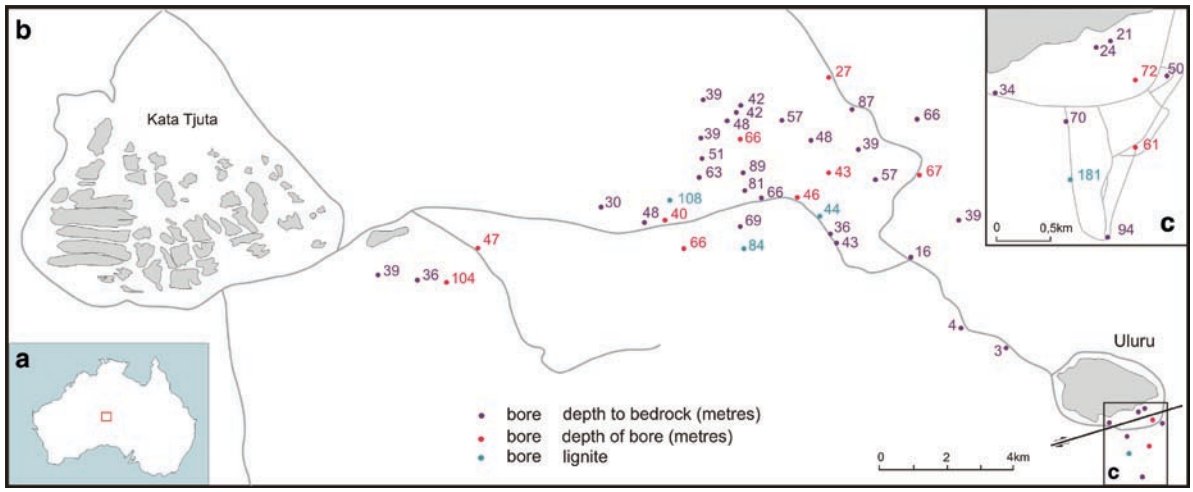

Fig. 33.1 (**a**) Location map, (**b**) Uluru and Kata Tjuta with depth to lithified Cambrian bedrock shown for the area between the two residuals, and (**c**) to the south of Uluru

Fig. 33.2 (**a**) Aerial view of Uluru from the southeast showing beveled crest and gaping-mouth caves located 35–60 m above plain bevel on southern face of the residual.

Fig. 33.2 (continued) (**b**) Pitted upper bevel of Uluru seen from the southeast, with three major valleys breaching southern face and steep northeastern bluff. (**c**) Aerial view of Kata Tjuta from the south. Note fracture-controlled clefts, basal caves, and the steepening and lighter color of the basal zone suggesting recent exposure

sandstone crops out in the northeastern piedmont and in low platforms located some 800 m from the southwestern corner of the inselberg (Figs. 33.3 and 33.4).

The beveled crest and the flanks of the residual are characterized by innumerable thin (~1 cm) plates of rock**,** and are in a few places scarred by lightning strikes. The northwestern flanks of the hill are ribbed, reflecting the northwest to southeast strike of the arkose. During and after heavy rains, streams run off the upland, causing waterfalls and potholes on its steep flanks. Rock basins or gnammas also are common on the summit (Fig. 33.2b).

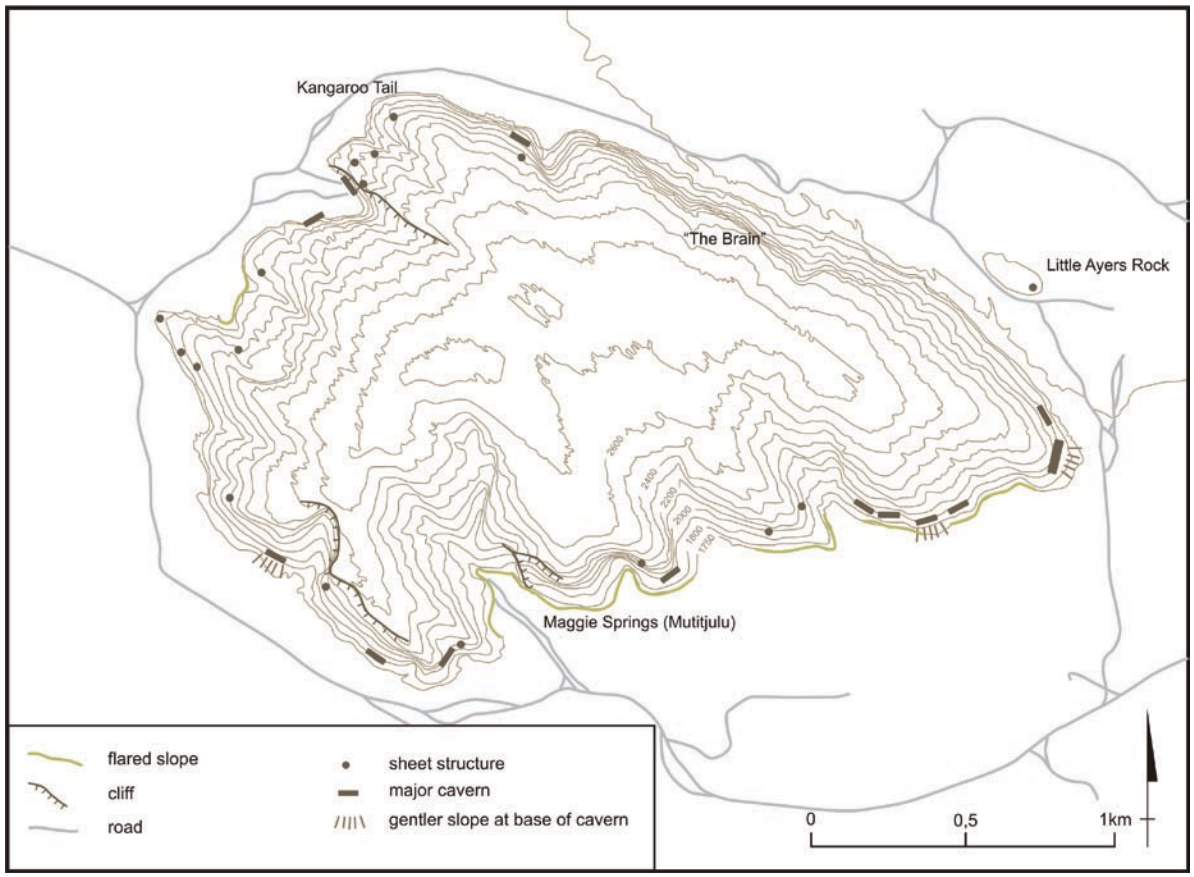

Fig. 33.3 Topographic Map of Uluru

"The Brain" and similar fretted areas on the northeastern face are due to the preferential weathering of steeply dipping strata (Fig. 33.5a), but the skull-like outline is fortuitous. The Kangaroo Tail (Fig. 33.5b) is a 2 m thick sheet structure located near the northwestern corner of the inselberg. Three major valleys breach the southern ramparts of the upland, but the most notable minor feature is the horizontal zone of large shelters or "gaping-mouth caves" situated between 35 and 60 m above the present plain (Figs. 33.2a and 33.5c). Sundry breaks of slope and associated tafoni occur at roughly the same 35 m level (Fig. 33.4). Concavities or flared slopes 4–5 m high occur at the base of the residual (Fig. 33.5d). Near Mutitjulu Water Hole the flares merge laterally with cliff-foot caves, in some of which triangular wedges and sheet fractures are exposed. In others alveoles and prongs resembling speleothems are developed but are caused by the preferential weathering of the bedding planes.

Flared slopes are also found elsewhere in the Uluru perimeter (e.g., adjacent to the Kangaroo Tail), but they are best and most numerous in the southern piedmont. The reason may be that whereas the piedmont on the other flanks is cut in bedrock, the southern aspect is shaded and also underlain by a considerable thickness of sand resting on the downfaulted arkose. The sand is permeable and retains the moisture essential for weathering: hence, the well-developed basal concavities.

33.2.3 Origin of Uluru

In an immediate sense the morphology of Uluru is most plausibly explained by successive phases of piedmont weathering and erosion. First, the prominent flared slopes found at various sites around the perimeter of Uluru, but especially on the southern flank, are

Fig. 33.4 Platform west of the beveled Uluru and the climbing track to the summit. Note break of slope below gaping-mouth cave, seen in profile at right (south) of residual and also near walk up

caused by moisture concentrated in the scarp-foot zone, creating a moat of weathered rock that undercuts the drier exposed slope above. Stripping of the detritus has revealed smooth concavities that are two-stage or etch forms (e.g., Twidale 1962). They indicate a recent lowering of the plains by some 5 m. The cliff-foot caves result from especially aggressive scarp-foot weathering and are interpreted as congeners of flares.

Second, the gaping-mouth caves are the equivalents of cliff-foot caves. Like the breaks of slope from steep to more gentle, they developed during a phase of weathering associated with a water table standing 35–60 m higher than the present plain and beneath a piedmont located around the present 610–640 m level, and marked by the shoulder between the crestal bevel and the bounding scarps. They imply an extended period of scarp-foot weathering and a regolith many scores of meters thick.

Thus, at least two phases of weathering and lowering are evidenced, suggesting that like many granite inselbergs, Uluru has been exposed episodically, and as a corollary, that the residual has increased in relief amplitude through time as a result of successive lowerings of the surrounding plains (Twidale and Bourne 1975; Twidale 1978; Bourne and Twidale 2000; Twidale and Vidal Romani 2005: 127 et seq.). Subsurface weathering prepared the country rock for erosion and made possible the lowering of the plains. It also etched into the lower margins of the basal slopes which were steepened, causing blocks and slabs perched on higher slopes to become unsupported and tumble to the piedmont. Stripping of the regolith from the summit bevel and from the developing flanks of the residual exposed gutters and basins that were initiated at the weathering front. It removed the regolithic sponge that retained moisture and rotted the bedrock, so that the rate of weathering was reduced and the residual thereby preserved.

This assemblage of forms has been interpreted in terms of past Cenozoic climates (Bremer 1965). The gross form of Uluru and the gutters have been construed as relic from a humid climatic phase or phases, whereas tafoni were taken to indicate a Mediterranean climate. The surficial scaling was associated with present aridity. Such constructions are worthy of consideration, for central Australia certainly experienced Cenozoic climatic changes (e.g., Williams et al. 1991). But any links between climate and specific landforms are complicated by structural influences, by the azonality imposed by subsurface initiation (etching), and by the ubiquity of water-related processes (e.g., Twidale and Lageat 1994). Climatic changes may have

Fig. 33.5 Minor landforms on Uluru. (**a**) The Brain with other weathered hollows near base of bluff. (**b**) The thick sheet structure known as the Kangaroo Tail. Note also flared slopes and cliff-foot caves. (**c**) Moderate foot slope associated with gaping-mouth caves with fretted bedrock. Note fallen blocks at the base of bedrock slope and sheet structure cutting across bedding. (**d**) Flared basal slope 4–5 m high in southern piedmont of Uluru. Similar features occur at other piedmont sites at Uluru but are most common on the southern flank

influenced the rate rather than the trend of landform evolution and in any event their effects are superimposed on forms generated during the episodic exposure of the residual.

However, though compatible with the field evidence, episodic exposure does not explain why Uluru is upstanding while similar strata all around have been weathered and eroded; though some 6,000 m thick, only about 2,500 m of the arkosic sandstone is exposed in Uluru. The bedrock extends well to the west and north and there is no suggestion that the Uluru strata are inherently more resistant than any others in the sequence. Nor can the persistence of Uluru be attributed to surficial silicic induration (e.g., King 1975). Ollier and Tuddenham (1961) suggested that Uluru is the last remnant surviving long-distance scarp retreat, but that accounts neither for the detailed field evidence which indicates the episodic lowering and steepening of the lower slopes of an original broad topographic rise nor for the persistence of the particular compartments of rock on which the residuals are developed.

The most likely explanation is based partly in the inherent resistance of the various facies of the Mt. Currie Conglomerate but specifically in the tectonic chronology of the region. In the Devonian, the strata were folded during localized northeast to southwest compression. This accounts for the steep dip of the strata and hence for a number of minor features, but it does not explain why the upland does not extend along the strike, in a northwest to southeast ridge coincident with the outcrop of the arkose.

The three most prominent inselbergs of this part of central Australia, Kata Tjuta, Uluru, and Mt. Conner (a mesa capped by massive sandstone preserved in a basin structure), stand in west-northwest to east-southeast alignment (Twidale 2007a: 108). This suggests either that they occur in a zone of north-northeast to south-southwest compression superimposed on the pre-existing northeast to southwest structural alignment, or that they have been compressed as a result of shearing along the east-northeast to west-southwest trending faults known to exist in the vicinity of Kata Tjuta and Uluru (Sweet and Crick 1992). Such shearing, considered with the evidence of episodic alternations of subsurface weathering and erosional exposure, can account for the preservation of the inselberg masses which can be envisaged projecting first into and then above a deep regolith. The compartments of rock were partly unconstrained, and the continued application of compressive stress – related to continued tectonism, of which there is ample evidence – can account for the sheet fractures like that expressed in the Kangaroo Tail, and for such associated features as triangular wedges (Twidale and Sved 1978; Twidale et al. 1996).

33.2.4 The Age of Uluru

The age of Uluru cannot directly be determined. Obviously the landform postdates the strata in which it is shaped and the Devonian orogeny. The broad shallow valley detected by drilling for water between Uluru and Kata Tjuta (Fig. 33.1b) also supplies relevant evidence. It is about 90 m deep and carries a sedimentary sequence including a basal lignite with plant fossils of Maastrichtian (latest Cretaceous, ~70 million years old) age (Harris and Twidale 1991), resting unconformably on the Cambrian country rock. The gentle eastern slope of this ancient valley plausibly can be projected into the summit bevel of Uluru, which probably then carried a regolith, and which by implication is of Maastrichtian age (Fig. 33.6). This is compatible with regional evidence.

Remnants of the epigene and the exhumed palaeosurfaces of the late Mesozoic ages are preserved in

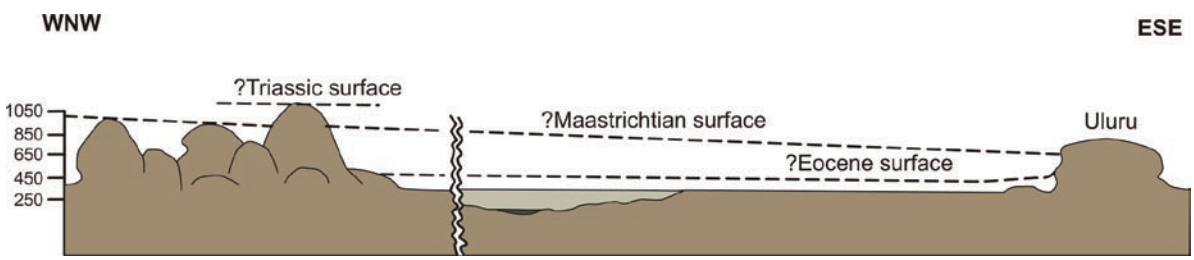

Fig. 33.6 Stages in the development of Uluru and Kata Tjuta. Heights in meters above sea level. Quaternary (4–5 m) surface not shown. Total length of section in field some 37 km, but 13 km of plain omitted where indicated

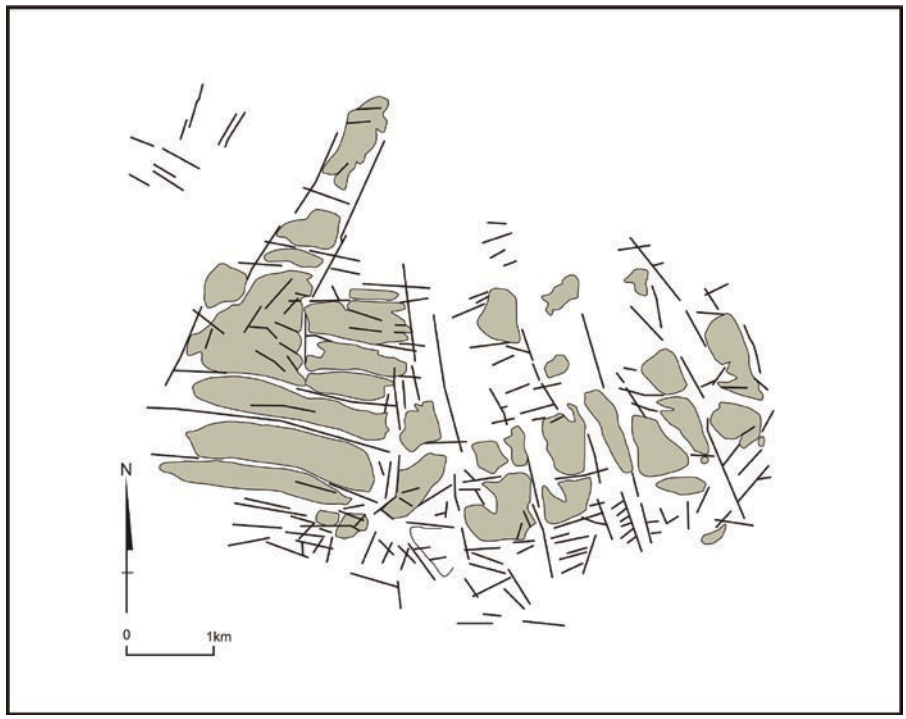

Fig. 33.7 Kata Tjuta, with domes shown in color, fractures by thick, black lines

uplands adjacent to the desert plains, in the Macdonnell and associated uplands to the north and northeast, and in various ranges to the south and southwest (e.g., Twidale 2007a). Furthermore, the widespread occurrence of a regolith capped by remnants of Eocene silcrete (Mabbutt 1965; Wopfner et al. 1974) on the present plains suggests that an ancestral Uluru – and Kata Tjuta – predate the Cenozoic. The gaping-mouth caves and associated breaks of slope may have been formed during the extended period of weathering associated with the siliceous duricrust, when Uluru was but a low rise. The basal flares and cliff-foot caves were shaped in a later and shorter phase of weathering and exposure.

The alternate phases of (piedmont) weathering and stream incision and associated planation implied by the episodic exposure of the inselberg can be attributed to base-level changes caused, first, by joggling of its constituent structural blocks during the northward drift of the continent that followed its separation from Antarctica; second, and later, to the spasmodic and continuing tectonic subsidence of the Lake Eyre depression (Wopfner and Twidale 1967); and third, to the climatic changes of the Quaternary (e.g., Williams et al. 1991).

33.3 Kata Tjuta

In contrast to the isolated single upland that is Uluru, Kata Tjuta consists of several domical towers, "giant pink cupolas and monstrous domes" (Giles 1889: I, 190–191), each developed on a fracture-defined block of Mt. Currie Conglomerate dipping southwest at angles of 10–20° (Figs. 33.2c and 33.7). The matrix of the conglomerate is siliceous and lacks feldspar. For this reason, the Kata Tjuta domes are more resistant and higher than Uluru, and though some are slightly beveled, no prominent summit surface is either developed or preserved.

The highest of the domes, Mt. Olga, stands about 1,069 m a.s.l., some 200 m higher than the crest of Uluru and some 600 m above the surrounding plains. Several others also surpass Uluru, but some stand at about 100 m above the plains and other low domes and platforms stand only 5–6 m higher than this datum (Twidale and Bourne 1978; Fig. 33.8).

The gentle but massive bedding of the conglomerate is evidenced in the towers. Some strata are well jointed and display a blocky pattern delineated by "chisel" marks (Fig. 33.8c). Tafoni or alcoves are developed in the "100 m" zone on the flanks of many

Fig. 33.8 Geomorphological features of Kata Tjuta. (**a**) Domes with "100 m" and "5 m" levels well displayed. (**b**) Domes with flares high on slope associated with 100 m level. (**c**) Domes with "chisel marks" on well-jointed stratum

Fig. 33.9 Kata Tjuta from the west with rock platforms in foreground and Uluru in distance

domes (Fig. 33.8b), and flared slopes occur at the bases of the hills which in many sectors are a lighter color than the rest of the domical surfaces, suggesting more recent exposure (Fig. 33.2c). Some towers rise from inclined bedrock slopes that are correlated with the flares that are developed at some sites, but most rear abruptly from bedrock plains and fracture-controlled valley floors or from flat plains carrying a regolithic veneer. Discontinuous conglomeratic platforms extend many kilometers to the west (Fig. 33.9).

The Kata Tjuta domes are most plausibly understood in terms of fracture-controlled subsurface weathering (cf. Falconer 1911: 246; Twidale and Vidal Romani 2005). The rounding of the residual remnants can be attributed to the preferential weathering of the corners and edges of angular blocks but the development of sheet fractures within sheared orthogonal blocks may also have contributed. Several domes stand about 100 m above the adjacent plains. Alcoves and flares on the steep sidewalls of these higher residuals, and correlated with the "gaping mouth" level at Uluru, stand as witness to a higher and older weathering surface. Other domes attest a plain level standing about 5 m higher than the present. It is evidenced by flared slopes, cliff-foot alcoves, and breaks of slope. Thus, as at Uluru, there may have been episodic exposure with alternations of weathering and erosion (Fig. 33.6).

Cross-folding and shearing again can be invoked in explanation of the various fracture patterns and the survival of the massif. Shearing may also be responsible for the splitting of many cobbles, and even small boulders contained within the conglomerate are split in such a way that the resultant plane faces of the hemispheres are flush with the surface of the slope. Ollier (1969: 17–18) suggested that this is caused by the differential insolational heating of the confined and unconfined parts of the cobbles. Evidence from other conglomeratic sites, however, suggests that shearing along sheeting planes, in places evidenced by slickensides and fault steps, may be responsible (Bourne and Twidale 2003).

33.4 Discussion and Conclusions

This interpretation implies that the higher domes of Kata Tjuta predate both the lower adjacent domes of Kata Tjuta and Uluru. If the age for the crest of Uluru deduced from the deposits preserved in the valley between Uluru and Kata Tjuta is valid, then the crests of the highest conglomeratic bornhardts, such as Mt. Olga, predate the latest Cretaceous and may compare to earlier Mesozoic forms recognized elsewhere in Australia (cf. Twidale 2007a).

The initiation of Uluru and Kata Tjuta is attributed to the compression associated with cross-folding, either simple or consequent on shear. The rock compartments are massive, with few open fractures. Water cannot readily penetrate into the rock mass. Only when and where the rocks below the surface were in contact with moisture were they susceptible to weathering and hence erosion. Once they stood in positive relief, Uluru and the Kata Tjuta domes shed water. Concatenation ensued involving unequal erosion and reinforcement (Twidale 2007b).

Though the main masses or compartments remained intact, the footslopes were weathered. When base level permitted they were lowered and steepened during successive alternations of weathering and erosion. In this way broad rises were converted to steep-sided inselbergs over a period of some 70 million years. Uluru and Kata Tjuta developed in similar ways and plausibly during the same time span.

The survival of the original low rises of the putative later Mesozoic age that became Uluru and Kata Tjuta is incompatible with conventional geomorphological theory, a major tenet of which is that the entire land surface has continually changed. Consequently, with the exception of some exhumed forms, landscapes must be youthful (see Twidale 2007a for references, evidence, and argument). Also, and unless tectonically renewed, the received wisdom is that relief amplitude tends to decrease, whereas the field evidence suggests that both inselbergs have increased in height relative to the adjacent plains over the past 70 million years or more.

Uluru and Kata Tjuta stand in isolation and rise abruptly from the desert plains of central Australia. They also stand sharply in denial of conventional geomorphological theory. The inselbergs not only have persisted as landscape features, but also have increased in relief amplitude through most of the Cenozoic, and possibly longer. One can but echo Gosse's declaration (Gosse 1874: 10) that: "[t]his rock [Uluru] appears more wonderful every time I look at it"; and extend the sentiment to include Kata Tjuta.

The Author

Rowl Twidale is a graduate of the University of Bristol and McGill University, Montreal. He was awarded an honorary doctorate in the University Complutense of Madrid in 1991. After service with CSIRO Land Research and Regional Survey, he joined the University of Adelaide, where he taught and carried out research from the late 1950s onwards. Although mainly concerned with Australian landscapes, he has worked on a variety of problems in other parts of the world. He remains particularly interested in granitic landforms, weathering, desert landscapes, planation surfaces, palaeoforms, the dating of landforms, and the history of ideas. He has published 15 books, the most recent being *Ancient Australian Landscapes* (2007), co-edited ten others, and has more than 350 papers in refereed journals. He has been a visiting professor at Rensselaer Polytechnic, UC Berkeley, UT Austin, Texas A and M, Western Cape, Coruña, Salamanca, and several other universities. Presently he holds an Honorary Visiting Research Fellowship in the University of Adelaide and a professorial appointment in the University of Coruña.

References

Bourne JA, Twidale CR (2000) Stepped inselbergs and their significance for general theories of landscape development. S Afr J Geol 103:105–119

Bourne JA, Twidale CR (2003) Geomorphological development of the Baxter Hills, a conglomeratic upland near Iron Knob, South Australia. Z Geomorph NF 47:351–371

Bremer H (1965) Ayers Rock, ein Beispiel für klimagenetische Morphologie. Z Geomorph NF 9:249–284

Falconer JD (1911) The geology and geography of Northern Nigeria. Macmillan, London

Giles E (1889) Australia twice traversed: The romance of exploration, 2 vols. Sampson/Low/Marston/Searle/Rivington, London

Gosse WC (1874) Report and diary of Mr W. C. Gosse's central and western exploring expedition, 1873. S Austr Parl Pap, 48

Harris WK, Twidale CR (1991) Revised age for Ayers Rock and The Olgas. Trans Roy Soc S Austr 115:109

King LC (1975) Bornhardt landforms and what they teach. Z Geomorph NF 19:299–318

Mabbutt JA (1965) The weathered land surface in central Australia. Z Geomorph NF 9:82–114

Mountford CP (1965) Ayers Rock: Its people, their beliefs, and their art. Angus and Robertson, Sydney

Ollier CD (1969) Weathering. Oliver and Boyd, Edinburgh

Ollier CD, Tuddenham WG (1961) Inselbergs of central Australia. Z Geomorph NF 5:257–276

Sweet IP, Crick IH (1992) Uluru and Kata Tjuta. A geological history. Australian Geological Survey Organisation, Canberra

Twidale CR (1962) Steepened margins of inselbergs from northwestern Eyre Peninsula, South Australia. Z Geomorph NF 6:51–69

Twidale CR (1978) On the origin of Ayers Rock, central Australia. Z Geomorph NF, 31(Suppl):177–206
Twidale CR (2007a) Ancient Australian landscapes. Rosenberg, Sydney
Twidale CR (2007b) Concatenation and resultant inequalities in denudation. Phys Geogr 28:50–75
Twidale CR, Bourne JA (1975) Episodic exposure of inselbergs. Geol Soc Amer Bull 86:1473–1481
Twidale CR, Bourne JA (1978) Bornhardts developed in sedimentary rocks, central Australia. S Afr Geogr 6:35–51
Twidale CR, Lageat Y (1994) Climatic geomorphology: A critique. Prog Phys Geogr 18:319–334
Twidale CR, Sved G (1978) Minor granite landforms associated with the release of compressive stress. Austr Geogrl Studies 16:161–174
Twidale CR, Vidal Romani JR (2005) Landforms and geology of granite terrains. Balkema, Leiden
Twidale CR, Vidal Romani JR, Campbell EM, Centeno JD (1996) Sheet fractures: Response to erosional offloading or to tectonic stress? Z Geomorph NF, 106(Suppl): 1–24
Wells AT, Forman DJ, Ranford LC, Cook PJ (1970) Geology of the Amadeus Basin, central Australia. Bur Min Res Geol Geophys Bull 100
Williams MAJ, De Deckker P, Kershaw AP (eds) (1991) The Cenozoic in Austalia; a re-appraisal of the evidence. Geol Soc Australia Spec Publ 18:99–118
Wopfner H, Callen R, Harris WK (1974) The lower Tertiary Eyre formation of the southwestern Great Artesian Basin. J Geol Soc Austr 21:17–51
Wopfner H, Twidale CR (1967) Geomorphological history of the Lake Eyre basin. In: Jennings JN, Mabbutt JA (eds) Landform studies from Australia and New Guinea. Australian National University Press, Canberra, pp 117–143

Chapter 34
Bungle Bungle: Tower Karst in Sandstone

Robert W. Young

Abstract Although the complex array of towers in the Bungle Bungle massif resembles the tower karst found in tropical limestone terrain, it has been eroded in quartz sandstone. Long-term leaching of silica by chemical weathering has produced a sandstone made up of highly etched and interlocking quartz grains with little intergranular cement. The resultant high compressive strength but low shearing and tensile strengths have maintained very steep slopes but have promoted intricate dissection of the massif. Topographic variation from rounded towers to joint-bounded pinnacles and sinuous ridges separating box valleys is due to variations in rock properties. The spectacular red and grey banding on rock faces is only a surface phenomenon on the intensely weathered sandstone, and results from deposition of iron and clay skins and the growth of cyanobacteria. The prominent pediment near the summit and the vast pediments surrounding much of the massif are erosional surfaces rather than stripped weathering fronts. Similar, though less spectacular, tower assemblages in sandstones occur elsewhere in tropical Australia and in the temperate southeastern part of the continent. As sandstone tower complexes also occur in other continents, it is now clear that long duration of weathering in quartz sandstone can produce landforms similar to those previously believed to be limited to limestone.

Keywords Arenization • rock strength • sandstone • silica leaching • tower karst

34.1 Introduction

Although quartz sandstone is one of the most chemically resistant rocks, some of the assemblages of landforms developed in it are remarkably similar to the karst topography developed in limestone. These include extensive systems of caves, such as those in the Roraima quartzites of Venezuela that are described elsewhere in this volume, and fields of towers that occur in environments as diverse as central Europe, southeastern China, and northern Australia. As the term karst has been regarded as synonymous with the topography developed mainly by solution in carbonate rocks, these landforms in sandstone have frequently been referred to as pseudo-karst. However, Jennings (1983) argued that they should rightfully be called karst because, although solution is not necessarily the dominant process, it is the critical process in their development. The extension of the term karst to sandstones and quartzites has gained widespread, though not complete, acceptance (Wray 1997).

The largest and most spectacular of the numerous tower landscapes developed in quartz sandstone in Australia is the Bungle Bungle Range, which is in Purnululu National Park, in the East Kimberley region (Fig. 34.1). The uniqueness of this amazingly intricate array of towers, with their tiger-stripe red and grey banding, was recognized internationally with the inclusion in 2003 of Purnululu National Park on the World Heritage List. Similar, though smaller, landforms occur in Mirima National Park (Hidden Valley) at Kununurra, and in Keep River National Park, 50 km east of Kununurra.

34.2 Geographical Setting

The Bungle Bungles lie in the Ord River catchment, about 300 km by road south of Kununurra, which is the largest town in the region (Fig. 34.1). There is good

P. Migoń (ed.), *Geomorphological Landscapes of the World*,
DOI 10.1007/978-90-481-3055-9_34,

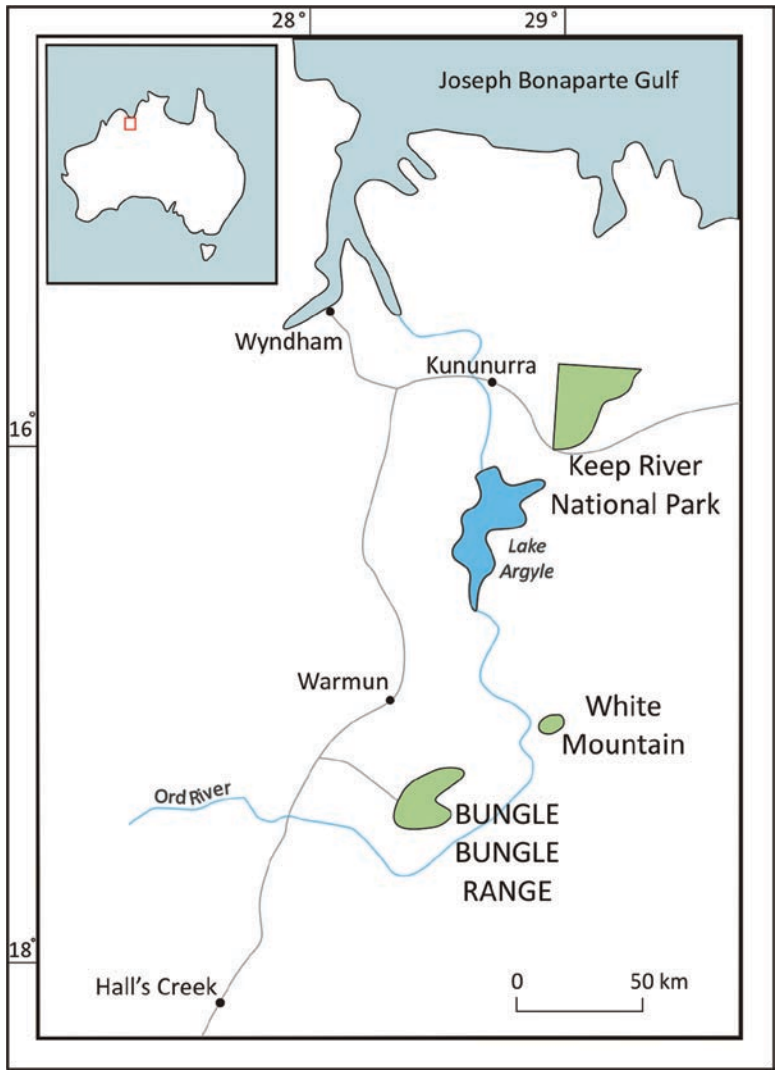

Fig. 34.1 The East Kimberley region showing the location of the Bungle Bungle Range

access during the dry season, but the landscape can really be appreciated only when seen from the air. The climate is tropical with a long dry season in autumn and winter. The average annual rainfall is about 650 mm, more than 80% of which falls between December and March. Average temperatures range from 29°C in July to 38°C in October. The vegetation is typically savanna, being mainly sparse woodland, dominated by *Eucalyptus brevifolia*, with large clumps of spinifex (*Triodia*) grass. Moister microclimates in sheltered gorges support galleries of palms (*Livistonia*), but much of the area supports only sparse shrubs and grasses, and many rocky slopes are almost bare.

The topography has been carved from fluvial sandstone and conglomerate deposited in the Ord Basin during Devonian times (Hoatson et al. 1997). The Boll Conglomerate outcrops in the northwestern part of the Bungle Bungles, and the Glass Hill Sandstone and Puralili Sandstone comprise the bulk of the range.

34.3 Landforms

34.3.1 Towers

Sandstone towers are best developed on the eastern and southern side of the range, where they occur in three main settings. Many isolated clusters of towers rise abruptly from the surrounding, extensive pediments. This pattern is repeated about 200 m higher, on the broad eastern summit of the range, where towers rise abruptly from an undulating surface; elsewhere, especially in the southwest, the summit consists mainly of broad, slightly convex platforms. The most numerous towers occur on the intricately dissected eastern margin of the range, where they form clustered arrays that rise toward the summit (Fig. 34.2). Although most of the towers have very steep foot slopes, they almost invariably have convex to ovoid crests. Both the intricacy of dissection and the general convexity of vertical form seem to be largely the product of two factors. First, the dominant process of disintegration on the flanks of the towers is the detachment of individual grains, rather than the collapse of large slabs of sandstone. Second, many of the small gullies dissecting the towers show remarkably little evidence of being controlled by joints. Indeed, the pattern of dissection seems almost chaotic over considerable areas.

34.3.2 Ridges and Box Valleys

Along the northeastern margin of the range, clusters of vertical towers give way to long and narrow ridges. Some of these very steep-sided ridges are straight, and coincide with case hardening along major joints. Others are remarkably sinuous, and appear to be the result of the growth of small valleys on both flanks of a ridge; the crests become increasingly sinuous as the valleys extend back into the sandstone until the ridge is breached (Fig. 34.3). These small valleys are up to several 100 m wide, and have flat or gently sloping bedrock floors. The junction between the floors and the ridge walls is generally very sharp, so imparting a pronounced box-like form to the valleys,

34.3.3 Joint-Bounded Pinnacles

In the central and western part of the range the assemblages of towers give way to a *ruiniforme* relief (cf. Mainguet 1972) of vertical, joint-bounded cliffs, pinnacles, and rock ribs (Fig. 34.4). The jointing control of erosion is particularly strong on the northern wall of the gorge of Piccaninny Creek, which is the main stream draining the range. The detachment of individual grains as the dominant process of disintegration is now

Fig. 34.2 Sandstone towers along Piccaninny Creek showing the characteristic convex summits, steep lower slopes, and prominent horizontal banding (photo RW Young)

Fig. 34.3 Narrow sandstone ridges rising from flat, streamless embayments on the eastern margin of the Bungle Bungle Range. Many of the straight ridges coincide with case hardened joints (photo RW Young)

Fig. 34.4 Vertical pinnacles with rounded crests in the upper part of the Piccaninny Creek gorge. Note the prominent joint control both of the alignment of the gorge and the cliffed faces of the pinnacles (photo RW Young)

replaced by the collapse of large slabs of sandstone from the cliffs, indicating an increasing resistance of the sandstone to erosion. In contrast to the flat-floored box valleys in the northeast, the valleys here have narrow floors, with numerous potholes and ribs carved in the friable sandstone by high summer discharges carrying coarse debris.

The northwestern flank of the range has been deeply dissected along mega-fractures, forming steep-sided canyons with convex upper slopes. Isolation by erosion of sections of the canyon walls has produced rounded dome-like pinnacles, similar to the *pitons émoussés* described from parts of Africa by Mainguet (1972). The change in morphology coincides largely with a facies change across the range from dominantly sandstone to dominantly conglomerate. The coarse pebbles and cobbles falling from the conglomerate form large mounds in many places at the base of the

cliffs. And the apparently greater permeability of the conglomerate has resulted in caves being formed near the base of some sections of the cliffs.

34.3.4 Pediments

The junction between the range, together with its outlying towers, and the surrounding pediments is invariably abrupt. But this is not a typical etch plain boundary between weathered and largely unweathered rocks, like that described from many parts of the tropics. To the contrary, drilling south of the range has shown that highly weathered sandstone extends to depths of at least 100 m below the pediment. This is a notable instance of pediment formation by scarp retreat, with stream dissection of the sandstone within the retreating margins of the range. The low gradient of the main pediments is apparently due to the dispersal of stream discharge, and of sheet flow of water running off the interfluves, onto the surrounding lowlands. The abrupt change from upland to pediments may be largely the result of the concentration of seepage through a permeable rock.

34.3.5 Surface Banding

The most visually striking feature of the Bungle Bungles is the amazingly regular, red and grey, horizontal banding that occurs on almost every outcrop (Fig. 34.2). The banding is clearly controlled by the bedding of the sandstone, but it is completely a surface phenomenon, for the sandstone beneath the skins is almost invariably white, though iron diffusion patterns can be seen in some outcrops. Some of the red skins have the metallic luster of desert varnish. Most of them, however, consist of well-crystallized kaolinite, with small amounts of iron and quartz (Young 1986). Although clay and iron mobilization from the sandstone may have been more rapid during more humid climates in the past, it is still active under the present seasonally arid conditions. The grey banding, which consists mainly of very thin layers of blue-green algae (*cyanobacteria*), occurs preferentially either on beds of sandstone with higher clay content that remain moist for longer (Hoatson et al. 1997), or on beds of greater permeability that maintain seepage for longer.

The skins stabilize the surface, but once they are broken, individual quartz grains are easily removed. The protective role of the skins is well illustrated by red clay skins that preserve aboriginal axe grooves on a disintegrating outcrop (Fig. 34.5). The breakdown of the skins may be partly the result of the differential dilation or expansion of the skins and the underlying sandstone during wetting and drying cycles, and especially during fire. But surface tensional stress alone may be sufficient to cause fracturing, especially as the skins become older (Young 1986; Young et al. 2009).

34.4 Evolution

The spectacular tower and ridge assemblages of the Bungle Bungles are essentially the product of the unusual mechanical properties of the sandstone. It is quite strong in compression, but weak in tension and shear (Young 1986, 1988). These properties are due to the almost complete absence of natural cement between the quartz grains. The interlocking of the closely packed grains imparts a uniaxial compressive strength of 35–50 MPa, but the lack of cement gives very low shearing and tensional strengths (<5 MPa), so that the rock shatters readily under a slight hammer blow, and blocks up to 5 cm thick can be crushed with a shearing motion of the fingers. Consequently the sandstone will stand in steep faces but is easily eroded. The very low tensional strength also imposes a severe limit on the size of overhanging slabs except, as in Cathedral Gorge, where the overhang forms an arch that transmits the load to the adjacent rock walls.

It has been suggested that this sandstone was never well cemented (Hoatson et al. 1997), but this hypothesis is difficult to reconcile with the apparent burial of the sandstone beneath several kilometers of younger sediment. Scanning Electron Microscope images (Young 1986; 1988) certainly demonstrated that, instead of consisting of rounded and uncemented quartz grains, the sandstones of the Bungle Bungles consist of extremely etched quartz grains with numerous remnants of extensive quartz overgrowths that testify to previous close bonding. Moreover, the etching was the result of a regional event that affected sandstones, ranging in age from Proterozoic to Palaeozoic,

Fig. 34.5 Aboriginal axe grooves preserved by clay and iron skins. Sand grains are easily detached from the very friable white sandstone where the skins are broken (photo RW Young)

over an area of at least 30,000 km^2 (Young 1988). The intensity of etching seems to have depended on the variability of the elimination of the primary porosity in the sandstones. The high degree of overgrowth development in most of the Proterozoic sandstones almost completely eliminated intergranular pathways through which corroding solutions could subsequently move, but preservation of such pathways in Palaeozoic sandstones resulted in the extensive corrosion even of those with abundant overgrowths. This was so in the eastern and southern parts of the Bungle Bungle massif, where virtually the entire sandstone was thoroughly etched and left as a mass of essentially cohesionless grains held together mainly by the compressive stress generated by their own weight. The increasing resistance of the sandstone toward the center of the range may be due to thermal effects of a postulated ancient meteor impact, vestiges of which seem to be preserved in the roughly circular fractures and quartz injection features of what is termed the Piccaninny Structure (Beere 1983).

Several hypotheses can be advanced to explain the intense leaching of silica. The first is diagenetic, and it attributes the leaching to the replacement of quartz by carbonate while the sediments were still deeply buried. However, as there is no sign here of typical carbonate replacement textures, the leaching was presumably due to deep subaerial weathering long after the development of the quartz overgrowths. Increased mobility of silica is generally attributed to the high acidity of solutions and abundance of organic molecules under humid tropical climates. As conditions in northern Australia were favorable for lateritic weathering, during much of Cainozoic times, the etching of quartz grains here can probably be attributed mainly to past tropical humid climates, or at least to climates with a very humid wet season. Nonetheless, chemical etching of quartz can also occur in relatively dry and alkaline conditions. It has long been known from laboratory studies that the solubility of silica is greatest when pH is high, and that the rate of silica dissolution is enhanced by high chloride concentrations (e.g. Yariv and Cross 1979). The occurrence of microscopic chloride crystals scattered across the surface of corroded quartz grains, and closely intermeshed with the tiny channels etched into the grains, indicates that this process is still operating here (Young 1988).

Outlining a chronology for the development of the tower assemblages is made difficult by the paucity of reliable dating of events in the region from the apparent end of sedimentation during the Permian, almost to the Pleistocene. As the Aptian (early Cretaceous) shoreline lies 100 km offshore in the Joseph Bonaparte Gulf (Veevers 1984), the entire region apparently has been above sea level, almost without interruption, since before the Cretaceous. The only evidence of later marine incursion is an estuarine outcrop of Miocene age in the White Mountain Formation of the central part of the Ord valley (Lloyd 1968). These estuarine sediments were subsequently uplifted by about 300 m

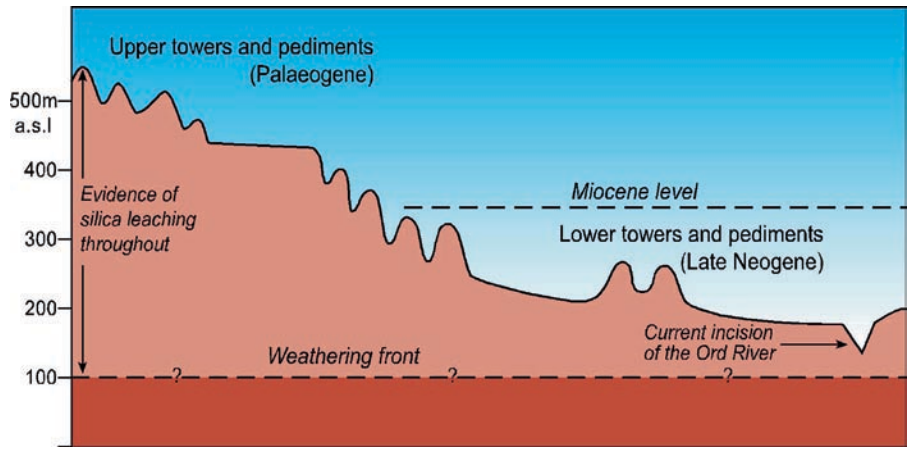

Fig. 34.6 Stages in the evolution of the tower assemblages. The summit towers and pediments probably date from the Palaeogene, and the lower towers and pediments from the Neogene. The Miocene level is projected from estuarine beds in the White Mountain Formation

(Veevers 1984). Nonetheless, the offshore record also shows that the last major input of non-marine sediment was in the Palaeocene and Eocene, and prior to that in the Jurassic (Veevers 1984).

The highest parts of the Kimberley region, that rise to elevations 300 m above the summit of the Bungle Bungle Range, probably date from late in the Mesozoic (Young 1992). The onset of regional weathering probably also dates from that time. The towers and pediments on the summit of the range can best be assigned to the Palaeogene because they are 150–250 m above the level of the Miocene beds in the White Mountain Formation (Fig. 34.6). They also lie above the extensive, but as yet undated, laterites of the southern part of the Kimberley region. The lower level of towers and pediments apparently postdate the Palaeogene as they lie below the elevation of the White Mountain Formation. But they too probably date well back into the Neogene because the modern channel of the Ord River has incised some 50 m below the base of the pediment.

34.5 Conclusions

Although not widely known until fairly recently, the Bungle Bungles have become recognized as one the most outstanding natural features in Australia. Indeed the combination of their size and intricacy, especially when viewed from the air, is unrivalled on this continent. It is, moreover, one of the most striking examples worldwide for the effects of intensive weathering of quartz. Recognition of the importance of this process prompts reassessment of the still widely held beliefs that tropical landscapes are predominantly the result of the formation and subsequent stripping of kaolinitic weathering profiles, and that tower karst is limited to carbonate rock (Young 1987).

The Author

Robert Young graduated from the University of Sydney, taught for 25 years at the University of Wollongong, Australia, and since retirement has continued research and writing. His research interests include long-term landscape evolution, weathering and soils, bedrock channels, history of geomorphology, coastal studies with special reference to tsunami, and sandstone landforms. He has published over 100 peer-reviewed papers, and with his wife Dr. Ann Young wrote *Sandstone Landforms* (1992; a new edition with R.A.L. Wray appeared in 2009), *Soils in the Australian Landscape* (2001), and two books titled *Understanding the Scenery* in national parks near Sydney (2006 and 2007).

References

Beere GM (1983) The Piccaninny Structure; a crypto-explosive feature in the Ord Basin, East Kimberley. Geol Surv Western Australia Record 1983/6

Hoatson DM and others (1997) Bungle Bungle Range, Purnululu National Park, Western Australia: a guide to the

rocks, landforms, plants, animals and human impact. Australian Geological Survey Organisation, Canberra

Jennings JN (1983) Sandstone pseudokarst or karst? In: Young RW, Nanson GC (eds) Aspects of Australian sandstone landscapes. Australian & New Zealand Geomorphology Group, Wollongong, pp 21–30

Lloyd AR (1968) Possible Miocene marine transgression in northern Australia. Bureau of Mineral Resources Australia Geol Geophys Bull 80:87–100

Mainguet M (1972) Le modelé des grès. Problèmes généraux. Institut Geographique National, Paris

Veevers JJ (1984) History of the Great Western Plateau. In: Veevers JJ (ed) Phanerozoic earth history of Australia. Clarendon, Oxford, pp 149–168

Wray RAL (1997) A global review of solutional weathering forms on quartz sandstones. Earth-Sci Rev 42:137–160

Yariv S, Cross H (1979) Geochemistry of colloid systems. Springer, Berlin

Young RW (1986) Tower karst in sandstone: Bungle Bungle massif, northwestern Australia. Z Geomorph 30: 189–202

Young RW (1987) Sandstone landforms of the tropical East Kimberley region, northwestern Australia. J Geol 95:205–218

Young RW (1988) Quartz etching and sandstone karst: examples from the East Kimberleys, northwestern Australia. Z Geomorph 32:409–423

Young RW (1992) Structural heritage and planation in the evolution of landforms in the East Kimberley. Austr J Earth Sci 39:141–151

Young RW, Wray RAL, Young ARM (2009) Sandstone landforms. Cambridge University Press, Cambridge

Chapter 35
Wellington's Tectonic Landscape: Astride a Plate Boundary

Michael J. Crozier and Nicholas J. Preston

Abstract The landscape of the Wellington Region is dominated by ongoing tectonic activity as the Pacific plate converges with and subducts beneath the continental Australian plate, at a rate of 40 mm per year. Within the last few million years, this activity has block-faulted, deformed, and uplifted a former erosion surface whose tilted remnants can be found at elevations ranging up to 1,000 m a.s.l. Relict marine benches and a series of raised beaches provide a record of sea-level change and coseismic uplift – the most spectacular being a series of five raised Holocene beach ridges. The amount of vertical uplift experienced by these individual beach ridges ranged between 3 and 9 m, during their respective initial uplift events. Fluvial modification of this landscape has been strongly influenced by fault movement, producing shutter ridges, faceted spurs, offset drainage patterns, while glacial cycles have seen the dominant subaerial processes shift between fluvial and periglacial regimes.

Keywords Erosion surface • faults • glacial cycles • New Zealand • raised beaches • tectonics

35.1 Introduction

> The site of the capital of New Zealand was chosen primarily because of the existence of a spacious harbour (Port Nicholson), with good anchorage for ships in a convenient part of the Dominion's land area. High hills almost completely surround the harbour, rising in general in steep slopes from the water's edge. A view from any prominent position in the hills around Port Nicholson discloses an elevated country stretching in all directions, broken by narrow valleys and deep ravines … one is struck by the general uniformity of height attained by the crests of the hills. Since this even skyline is quite independent of the structure of the country rocks (consisting of highly folded and shattered argillites and grauwackes) it apparently exhibits an elevated plain of erosion or peneplain. Following the peneplanation the land was elevated … the predominant line of faulting seems approximately to follow the western shore-line of the harbour... evidence of faulting is found in the fact that the small streams … do not enter the harbour at grade, as would be the case with normal drainage, but instead flow over the lower part of the fault scarp in abrupt waterfalls.

This description of the Wellington landscape was given by J.M. Bell in a paper read before the Wellington Philosophical Society in 1909, some 7 years prior to a visit to New Zealand by William Morris Davis and 13 years before Charles Cotton published his influential book *Geomorphology*. Although it is 100 years since it was given, it reveals a shrewd assessment of landform features and evolution and introduces a notion of cyclicity involving removal of landmass by erosion and subsequent tectonic uplift, as well as the Davisian concept of peneplanation that continues to be debated today.

Wellington is a city built on rugged and mountainous terrain located at the southern tip of New Zealand's North Island, adjacent to Cook Strait (Fig. 35.1). Its physiography can be attributed to its location astride the boundary between the Pacific and Australian tectonic plates which are converging obliquely at a rate of about 40 mm/year. In the region of the central and southern North Island, the oceanic Pacific plate is being subducted beneath the Australian plate, the leading edge of which has been folded, faulted, and upthrust to form the Mesozoic greywacke axial ranges of the North Island.

Seismic activity associated with plate convergence is common. Since the magnitude 8.2 earthquake of 1855 raised the land now occupied by the central business district by over 1.5 m, the region has experienced 15 earthquakes of magnitude 5 or greater, eight of

P. Migoń (ed.), *Geomorphological Landscapes of the World*,
DOI 10.1007/978-90-481-3055-9_35,

Fig. 35.1 The Wellington Peninsula defined by a strong linear feature (the Wellington Fault, running through the centre of the photograph) forming the western side of the harbor and confining the western side of the Hutt Valley. The finely dissected topography represents a faulted and uplifted erosion surface, now strongly degraded by fluvial erosion. The view is to the north. The Hutt Valley can be seen at the northern end of Wellington Harbour and Tongue Point in the central foreground (photo © Lloyd Homer, GNS Science)

which had shaking intensities greater than MM VII, causing damage to buildings and infrastructure.

While Wellington's contemporary climate is humid temperate, and supported a dense rainforest prior to European settlement, the landscape has been shaped by oscillation between colder and warmer periods. There is little evidence in the Wellington landscape of Pleistocene glaciation, although the climate of this period was clearly periglacial. With average temperatures some 2–5°C cooler than today, cryergic processes were dominant in the elevated parts of the landscape, supplying ample material for colluvial processes such as scree formation and solifluction. On gentler slopes, the bedrock is covered by a mantle of poorly sorted periglacial material, and in steeper terrain bedrock depressions have been filled with this material. On lee slopes that have remained stable throughout the Holocene, loess deposits can be found, derived from coastal plains to the northwest, formerly exposed during periods of lower sea level.

35.2 Evolution of the Primary Landscape Features

35.2.1 The Wellington Peneplain?

The degree of tectonic intra-formational deformation of the Mesozoic greywacke basement geology of the region together with the fact that there are no marine sediments of Cretaceous to late Neogene age within the Wellington area suggest that an ancient mountain range once existed in the region for a considerable period of time. Cotton's (1957) detailed mapping of contemporary landforms identified a summit accordance which, although deformed and tilted, he interpreted as representing remnants of a formerly extensive region-wide erosion surface. This surface, although currently existing at a range of altitudes, in Cotton's eyes conformed closely to the criteria required by Davis to constitute a peneplain. Cotton's landscape

interpretation had been strongly influenced by Davis' (1899) formulation of "The Geographical Cycle" or "Cycle of Normal Erosion," as it became known, where the end point of successive stages of down wearing was the terminal peneplain. Chorley et al. (1973) acknowledged the strong link between these two influential geomorphologists with the observation: "Davis also now found a prolific disciple in New Zealand where C.A. Cotton soon acquired an international reputation … a young New Zealander who after the death of the master took over his mantle and wore it with great distinction for several decades."

Davis' cycle has been strongly criticized and doubt has been cast as to whether peneplanation is a realistic concept (Chorley 1965). Nevertheless, the surface identified by Cotton is still considered an erosion surface of some sort; those not willing to accept its subaerial genesis have suggested an origin of marine planation instead (Begg and Mazengarb 1996). However, this alternative explanation, significantly, also requires the surface to have been at one time near sea level and thus reinforces its geomorphic significance as a "Key" surface (Cotton 1957). Cotton used the term "Key" or "K-surface," meaning it is the key to understanding rates of uplift and tectonic deformation in the region (Fig. 35.2). Remnants of the K-surface are commonly between 250–400 m a.s.l. around the city but are more eroded and less distinct as the topography increases in elevation towards the axial ranges. Unfortunately, with age estimates of between 4 and 0.4 million years (Ota et al. 1981; Begg and Mazengarb 1996), the surface is an imprecise datum for calculating uplift rates.

35.2.2 Development of the Tectonic Terrain

Since the region-wide erosion surface was formed, oblique subduction along the plate boundary has resulted in dextral (right-lateral) faulting producing fault bounded tilted blocks of hills, mountain ranges, fault angle basins, and associated downwarping and doming. The axis of topographic highs and lows, major fault lines, hills and bounding mountain ranges, as well as principal drainage lines are all parallel to the plate boundary with a southwest to northeast orientation (Fig. 35.3). Fault-bounded blocks, tens of square kilometers in extent, dip gently toward the west, bounded on the east by distinctive residual fault scarps, and separated from adjacent blocks by fault angle depressions. The relatively low-lying areas such as the main river valleys and harbor have accumulated sediment to

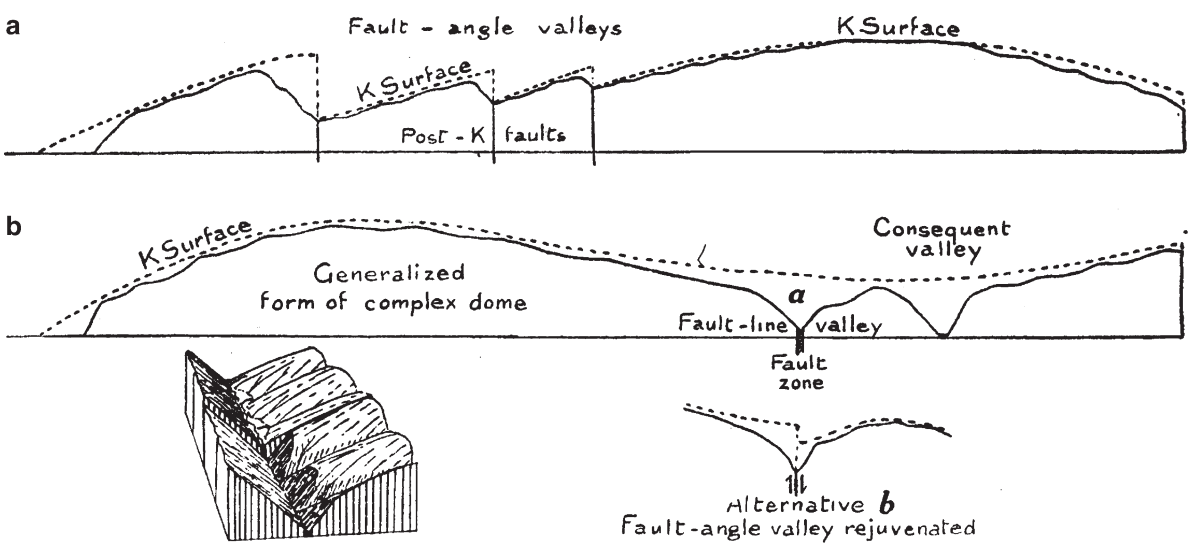

Fig. 35.2 An original sketch by Sir Charles Cotton showing "surface profiles of the western part of the Wellington Peninsula interpreted according to the development of relief by deformation of the K surface (uplifted peneplain). A: profile (WE) across the northern part of the peninsula; B: profile (WE) across the southern part of the peninsula. Block diagram: rejuvenation of a fault-angle valley" (Cotton 1957)

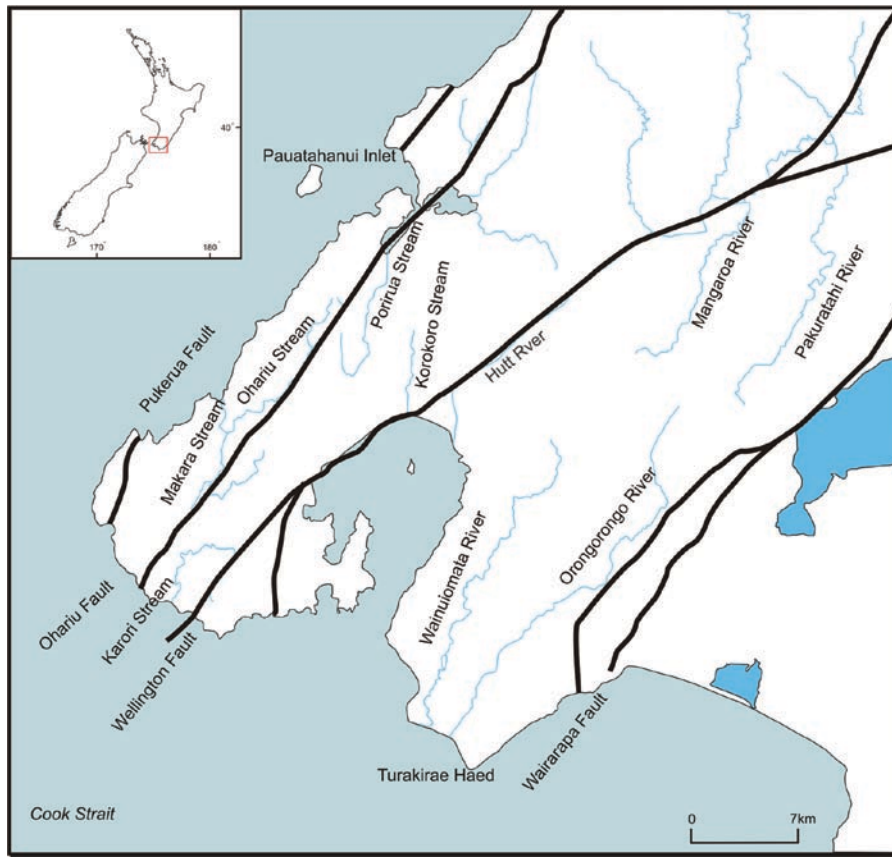

Fig. 35.3 Major faults and selected drainage lines of the Wellington Region. The onshore extent of the Pukerua Fault is shown. Turakirae Head and the Pauatahanui Inlet are indicated (After Stevens, 1974)

depths of up to 300 m dating from about 450,000 years ago, with pollen and other evidence indicating lowered temperatures over four glacial periods.

35.3 Modification of the Primary Features

35.3.1 Raised Beaches

Uplift has exposed secondary landforms such as wave-cut shore platforms around the Wellington landscape (Fig. 35.4). These can be correlated with known seismic events; the most evident in Wellington Harbour and on the south coast were raised as a result of the 1855 earthquake on the Wairarapa Fault. In this event, the ground surface along the Wairarapa Fault (Fig. 35.3) was displaced 2.7 m vertically and 13 m horizontally. A series of raised beaches at Turakirae Head provides evidence of past movement on this fault. These uplifted shorelines at Turakirae are amongst the best examples of such features in the world. Movement on the Wairarapa Fault, which runs to the immediate east of Turakirae Head, has a vertical component with uplift on the western side. Each uplift event raises the shoreline out of reach of marine processes, leaving raised shorelines. The vertical offset between raised shorelines enables an estimate of the uplift magnitude. A series of these raised shorelines, representing Holocene uplift events, are evident at Turakirae Head – one of the best such records in the world – and have been dated (McSaveney et al. 2006). The most recently formed elevated shoreline, which represents a maximum of 6.0 m uplift, was coincident with the magnitude 8.2 1855

Fig. 35.4 Wave-cut shore platforms on Wellington's south coast exposed by the 1855 earthquake (photo MJ Crozier)

earthquake. In order of increasing age, the remaining elevated beach ridges reveal maximum uplifts of 9.1 m (2,220 years BP[1]), 5.5 m (4,767 years BP), and 3.0 m (6,765 years BP). A fifth shoreline, which is now almost buried by colluvia, was raised some 9,000 years BP.

Older uplifted marine benches occur at various points along the south coast. For example, Tongue Point, which can be seen in the foreground of Fig. 35.1, exhibits an extremely well-defined sequence of uplifted marine terraces spanning the late Quaternary. The lower terrace (elevation: 23–46 m) is extensive and well preserved, and was cut by the sea during the last interglacial (Oxygen Isotope Stage 5). The higher terrace (76–91 m) is eroded and only remnants remain; it was cut by the sea during the penultimate interglacial (Oxygen Isotope Stage 7). A still higher, highly dissected terrace can be distinguished at 133 m. Terrace surfaces slope to seaward and elevation across the surfaces is uneven due to deformation which has therefore occurred subsequent to their formation. However, conforming to the regional pattern, these surfaces dip toward the west. A comparable sequence of uplifted marine terraces occurs further to the east, preserved between the mouths of the Wainuiomata and Orongorongo Rivers (Fig. 35.5).

35.3.2 Activity and Features of the Wellington Fault

The Wellington Fault (Figs. 35.1 and 35.3) is the dominant structural lineament in the Wellington region. Earthquakes associated with rupture on this fault have a characteristic magnitude of 7.5 and occur about once every 600 years, the last one having taken place between 350 and 500 years ago. The typical displacement on this fault during one such event is about 4 m horizontally and 1 m vertically. A number of distinctive features are manifest along the Wellington Fault. Uplifted Holocene terraces of the Hutt River have been offset by varying amounts at Harcourt Park where the course of the river is perpendicular to the fault. The extent of offset gives an indication of the rate of strike slip.

Where relict topography has been truncated by movement on the Wellington Fault, two characteristic landforms occur. Where truncation occurred close to the end of a spur or ridge, as along the western shore of

[1] BP = before present, where 'present' is considered as 1950

Fig. 35.5 Three flights of uplifted interglacial marine terraces at the mouth of the Orongorongo River (photo DW Mackenzie)

Wellington Harbour or in the lower parts of the Hutt Valley, the eastern (lower) section of the former spur/ridge has often been removed by erosion. This has left behind faceted spurs forming part of the fault scarp. Where erosion has not been as effective in removing material and both sides of the truncated feature remain, Cotton's (1951) "shutter ridges" can be seen. Both these features give a good indication of the fault trace location.

35.3.3 Drainage Pattern Control

Major drainage lines (e.g., Hutt, Orongorongo, Wainuiomata, Pakuratahi, and Ohariu) are oriented parallel to the strike of major faults. Some 4–6 million years ago, the ancestral Hutt River drained westward through what is now Pauatahanui Inlet (Stevens 1974), but with commencement of the current uplift phase, its course was diverted and it now drains southward through the Hutt Valley, following the trace of the Wellington Fault for much of its lower course. In its alluvial reaches, regional tilting pushes it to the western side of the lower and upper Hutt Valley.

Lateral movement on the Wellington Fault is evident in the abrupt lateral offset of streams as they cross the fault, and has resulted in the capture of a number of the area's principal drainage systems (Fig. 35.3). Small, ungraded streams occupy hanging valleys on the fault scarp and in some instances (e.g. Korokoro, Porirua) larger streams have eroded valleys along north–south trending splinter faults.

35.4 Landscape Modification of Slopes by Fluvial and Mass Movement Process

While the formation of primary and secondary landforms has been driven by tectonics and their geometry defined (and continually modified) by faulting, folding, uplift, and tilting, the resultant forms have been vigorously modified by fluvial and mass movement processes (Fig. 35.6). These processes have produced what Cotton (1912) describes as an extremely finely dissected relief (maximum drainage densities of 11 km/km^2 according to Eyles 1973), consisting of a network of swales and spurs, v-shaped valleys and ridges

Fig. 35.6 Ongoing modification of the uplifted landscape through mass movement (photo K Stent, *Sunday Star Times*, Fairfax)

that provide pathways for sediment and runoff from the major upstanding fault blocks. However, active development of that network has been successively interrupted by changes to the climatic regime during the course of the Pleistocene. The geomorphic development of relief has been determined by the contrasting processes associated with alternating climatically driven morphogenic regimes. Fluvial network development has been most active during interglacial regimes, where precipitation in the form of rain has occurred on slopes dominated by a dense temperate rainforest (tree limit of about 1,000 m a.s.l.), that has limited the supply of slope-derived sediment. First-order channels extended upslope as gully systems, increasing drainage density and enhancing the fine-textured relief. In contrast, during glacial periods, tree limits were reduced to around present sea level (Fleming 1970), and periglacial processes dominated, providing solifluction material and scree to the drainage network, filling in channels, reducing drainage density, mantling slopes with loess, and generally subduing the relief. In the current "interglacial," remnants of this subdued landscape which remain in upper catchments and buried channels (referred to by Cotton as "fossil gullies") are common. These infilled components of the drainage network are referred to as "zero-order basins," and they continue to act as subsurface drainage pathways and preferred sites for shallow landsliding (Crozier et al. 1990). However, in interglacials, as at present, the tendency is to evacuate sediment from zero-order basins, exhume formerly buried drainage channels, and generally change the periglacially subdued relief into a more emphatic and angular relief to establish what Cotton referred to as a "feral" landscape (specifically meaning, one that was once subdued but has returned to its wild state).

35.5 Conclusions

Existing astride an active compressional plate boundary, the Wellington landscape is active and young with only a few remnant forms attesting processes that existed earlier than the Pleistocene. Tectonic activity that drives and defines the primary landforms is continually taking place and continues to modify the landscape. Because of the high rates of plate convergence, the Wellington landscape exhibits some of the most extreme rates of fault displacement to be found anywhere in the world. The area provides textbook examples of fault scarps, spur-end facets, shutter ridges, knick point waterfalls, offset streams, displaced Quaternary and Holocene terraces, and series of raised marine abrasion platforms and raised beach ridges. Potential energy has been maintained by continual uplift, which ensures constant rainfall, steep slopes, landsliding, and rapid rates of runoff. While early Pleistocene glacials may have had little impact because the region's relief had not fully developed, the last glacial period has had a modifying effect on the finer features of the landscape. However, the region remains as one of the finest examples of the role of tectonics in landform control.

The Authors

Michael Crozier is a Professor of Geomorphology in the School of Geography, Environment and Earth Sciences, Victoria University of Wellington, New Zealand. His

research is focused on contemporary processes and instability in geomorphic systems, particularly landslides and natural hazards. He is the President of the International Association of Geomorphologists (2009–2013) and President of the New Zealand Geographical Society.

Nick Preston is a Lecturer in Physical Geography in the School of Geography, Environment and Earth Sciences, Victoria University of Wellington, New Zealand. His research concerns geomorphic responses to land-use change and connectivity within catchment systems, focusing on sediment transport, fluvial, and slope instability.

References

Begg JG, Mazengarb C (1996) Geology of the Wellington area. Institute of Geological and Nuclear Sciences Ltd, Lower Hutt, New Zealand

Bell JM (1909) The physiography of Wellington Harbour. Art LIV. Transactions of the New Zealand Institute XLII:534–540

Chorley RJ (1965) Re-evaluation of the geomorphic system of W. M. Davis. In: Chorley RJ, Haggett P (eds) Frontiers in geographical teaching. Methuen, London, pp 21–36

Chorley RJ, Beckinsale RP, Dunn RJ (1973) The history of the study of landforms or the development of geomorphology. Volume 2: The life and work of William Morris Davis. Methuen, London

Cotton CA (1912) Notes on Wellington physiography. Trans New Zealand Inst 44:245–265

Cotton CA (1951) Fault valleys and shutter ridges at Wellington. New Zealand Geogr 7(1):62–68

Cotton CA (1957) Tectonic features in a coastal setting at Wellington. Trans Royal Soc New Zealand 84(4):761–790

Crozier MJ, Vaughan EE, Tippett JM (1990) Relative instability of colluvium-filled bedrock depressions. Earth Surf Proc Landf 15:329–339

Davis WM (1899) The geographical cycle. Geogr J 14:481–504

Eyles RJ (1973) Drainage density representation on Wellington maps. J Hydrol (New Zealand) 12(1):19–31

Fleming CA (1970) Radiocarbon dating and pollen analysis from Otiran periglacial fans in western Wellington. Trans Royal Soc New Zealand (Earth Sci) 7(11):197–208

McSaveney MJ, Graham IJ, Begg JG, Beu AG, Hull AG, Kim K, Zobdervan A (2006) Late Holocene uplift of beach ridges at Turakirae Head, south Wellington coast, New Zealand. New Zealand J Geol Geophys 49:337–358

Ota Y, Williams DN, Berryman KR (1981) Late Quaternary map of New Zealand, 1:50000. Parts sheets Q27, R27 and R28 – Wellington, 1st edn. Department of Scientific and Industrial Research, Wellington

Stevens GR (1974) Rugged landscape. The geology of Central New Zealand. DSIR Publishing, Wellington

Chapter 36
Pacific Atolls: A World Apart

Patrick D. Nunn

Abstract Atolls are low islands made from biogenic detritus that are scattered across the low-latitude Pacific Ocean. Atolls mark places where reef-fringed volcanic islands were once emerging but then sank slowly allowing the reef to continue growing at the ocean surface, finally forming an atoll. Owing to their low elevation and mostly soft-sediment composition, atolls are among the most vulnerable island environments on Earth. Some may disappear during this century as a result of sea-level rise.

Keywords Atoll • coral reef • island • ocean • Pacific

36.1 Introduction

Continental dwellers are apt to think of the ocean as a destroyer, along the shores of which superficial structures last only a short time, and where organic life is generally subordinate to the power of the waves. Atolls seem to contradict both these assumptions for, not only are they massive biogenic structures sometimes hundreds of meters high, but the islands of superficial material that often develop on them may endure for thousands of years just a few meters above mean sea level.

An atoll is a ring of living coral reef, typically enclosing a lagoon that is much shallower than the ocean on the outside of the reef ring. This reef is commonly cut by one or more reef passages (known as *hoa* in the Pacific) through which water rushes as the tide rises and falls. On top of the reef, large waves have sometimes dumped piles of reef detritus that may come to form islands (known as *motu*) which develop a freshwater lens, become armored with beachrock and vegetated, and thus available to support human life.

There are around thousands of atolls in the world. From a Maldivian word, the English usage of "atoll" is imprecise, sometimes referring to the sub-circular ring of coral reef, sometimes to the islands built upon it, and sometimes to the whole package. Most atolls are found in the central Pacific – the island nations of Kiribati (most), Marshall Islands, Tokelau, and Tuvalu exclusively comprise atoll islands (Fig. 36.1).

When we see an atoll, it is difficult to readily apprehend its magnificence. We see a ring of reef, with its ocean edge marked by a line of breaking waves. On one side, the darker blue of the deep ocean, often marked by long-range swells; on the other side, the lighter aquamarine of the shallower lagoon, calmer waters understandably preferred by the islanders. And then running along the centers of the larger sections of the reef rim, especially on its windward side, you will see strips of dark green which are *motu* covered with forest, usually dominated by coconuts.

This sight may convey admiration that any such island could exist in the middle of the unforgiving ocean, and that people could successfully wrest a living from its apparently meager resources. But it is unlikely to inspire awe. For that, we need to see below the ocean surface and appreciate how the ring reef is simply the surface expression of a coral reef that extends downwards for hundred of meters until the point where it becomes attached to the submerged flanks of a sunken volcanic island. For thousands, maybe millions, of years before today, atolls in the world's oceans began life with the growth of a coral reef on the side of a volcanic island. As that island began to sink, the reef, its living veneer, unable to survive in deeper water, began to build itself upwards. And this is the remarkable thing about atolls – that truly, they may spend millions of years growing upwards in response to the downward movement of

P. Migoń (ed.), *Geomorphological Landscapes of the World*,
DOI 10.1007/978-90-481-3055-9_36,

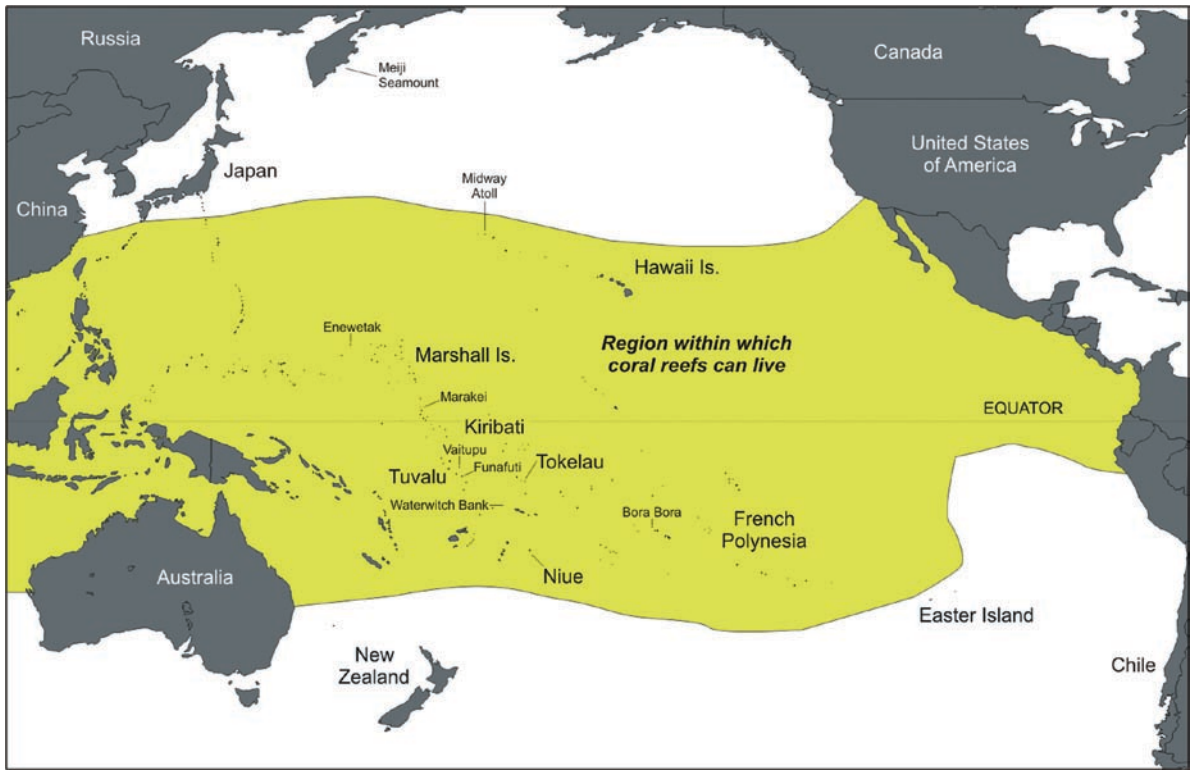

Fig. 36.1 Map of the Pacific Ocean showing the region, delimited by the 20°C isotherm, outside of which corals cannot grow and atolls cannot therefore form. All atolls and countries mentioned in the text are marked

their foundations. Atolls provide an extraordinary story about the tenacity of life. Reef corals have grown upwards, growing atop the remains of their ancestors, up and up, keeping their "heads" close to the surface so that they continue to receive enough sunlight to allow the photosynthesizing algae within them to keep producing the food they both need.

36.2 Origins of Atolls

Remarkable in many ways, Charles Darwin had read about atolls but in 1835, before he had ever seen one for himself, he worked out how they must form. His explanation – the so-called *Subsidence Theory of Atoll Formation* – has largely stood the test of time yet appears to have been founded upon a fallacy. Darwin outlined his theory as he wandered the coasts of Chile – devastated by a massive earthquake on 20 February of that year – and realized that this part of the Earth's crust rose every time there was such an event. If that happened, he reasoned, there must be sinking somewhere else (or subsidence), and what better evidence for that than atolls?

Darwin implied in his trailblazing 1842 book *The Structure and Distribution of Coral Reefs* that atolls existed in parts of the ocean basins that were sinking. In this he was wrong for while the island edifice that is capped by an atoll has by definition been sinking for a long time, this does not necessarily apply to the entire region within which the atoll is situated. Of course, Darwin could not have known everything that we know today, particularly the part that, because of the moving Earth's crust, islands are sometimes transported from places where the ocean floor is shallow to places where it is deeper and where, as a result, the islands may develop into atolls.

The subsidence theory of atoll formation simply says that a high volcanic island with a fringing coral reef may develop into a smaller volcanic island with a barrier reef simply as a result of island subsidence (Fig. 36.2). Further subsidence of the volcanic island may result in its complete submergence, but the reef

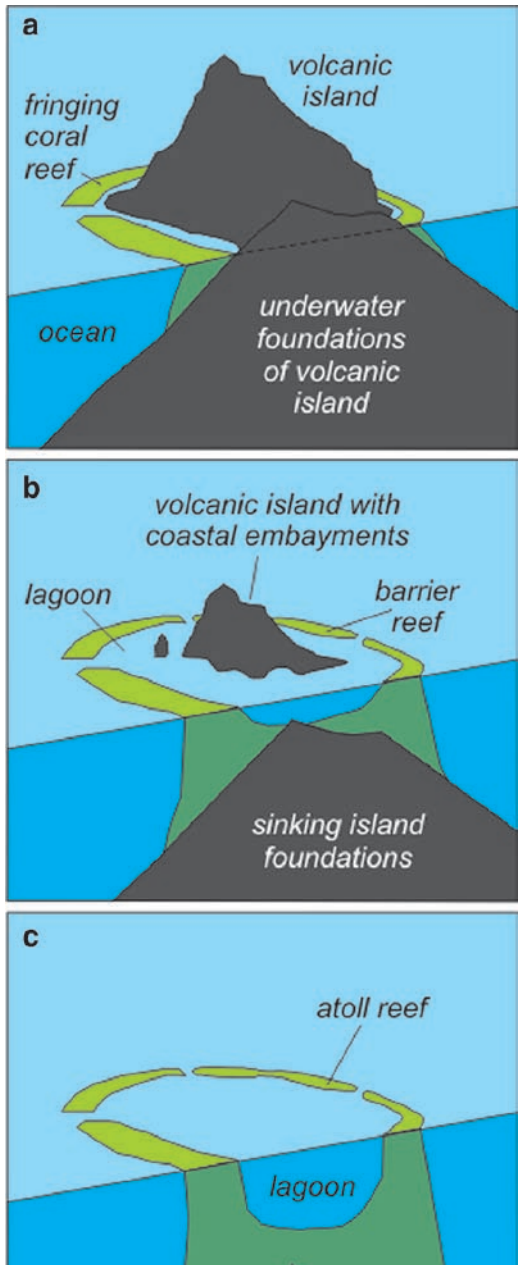

Fig. 36.2 The subsidence theory of atoll formation outlined by Charles Darwin in 1842 remains correct in its essentials today. Darwin envisaged a three-stage process as shown. (**a**) The process of atoll formation begins when a volcanic island in the coral seas, surrounded by a fringing reef growing upwards from shallow foundations, begins to sink; (**b**) Subsidence begins to drown the volcanic island, causing its shoreline to become embayed or scalloped. To stay alive, the coral reef will build itself upwards, which results in a fringing reef being transformed into a barrier reef, separated from the island's shoreline by a lagoon; (**c**) The process of atoll formation is complete when the volcanic island sinks completely below sea level. The coral reef has continued to build itself upwards so that a ring reef (or atoll reef) is formed, enclosing a lagoon

may continue growing upwards, thus forming an atoll – a ring reef surrounding a shallow lagoon.

Now Darwin did not know about the sea-level changes that have regularly affected the planet over the past few million years, and have periodically (at times of low sea level) converted atolls into high limestone islands before changing them back to atolls once again (as sea level rose again). But all that we have learned about atoll formation since Darwin wrote is essentially compatible with his prescient ideas.

The essential correctness of Darwin's idea that atolls were reefs that grew up from submerged volcanic foundations was suggested by the results of a landmark field study by Edgeworth David on Funafuti Atoll in Tuvalu in 1897 but not finally confirmed until drilling in the 1950s on Enewetak Atoll in the Marshall Islands prior to the commencement of nuclear testing hit the volcanic foundations of this ancient atoll.

As drilling techniques became more sophisticated, it became possible to interpret more about both atoll history and sea-level history from the nature of the thick sequences of fossil reef that underlie their surfaces. In particular, the presence of solution unconformities within these sequences allowed scientists to precisely reconstruct the times when atolls emerged (as sea level was falling) and were subsequently submerged. A good example comes from the drilling reported by Lincoln and Schlanger (1987) on Midway Atoll in the Hawaiian Islands which showed how a solution unconformity 169 m below the atoll surface had formed during a low stand of sea level about 7–8 million years ago when it dropped to 75–125 m below the present.

For the sake of completeness, it is also worth explaining that sometimes atolls do not survive for millions of years – as some undoubtedly do – and become "drowned atolls." Drowned atolls appear to have been those where coral reefs could not keep up (or catch up) with rising sea level at the end of an ice age. In such a situation, the reef ring would simply cease growing, and become a largely lifeless surface, typically tens of meters below the ocean surface, waiting for the onset of some future ice age during which sea-level fall could expose it and revive it once again (see Fig. 36.5b).

For the purposes of understanding the range of situations in which atolls can form, it is instructive to look at the Hawaiian-Emperor Island-Seamount Chain in the northeast Pacific (Fig. 36.3). This island chain

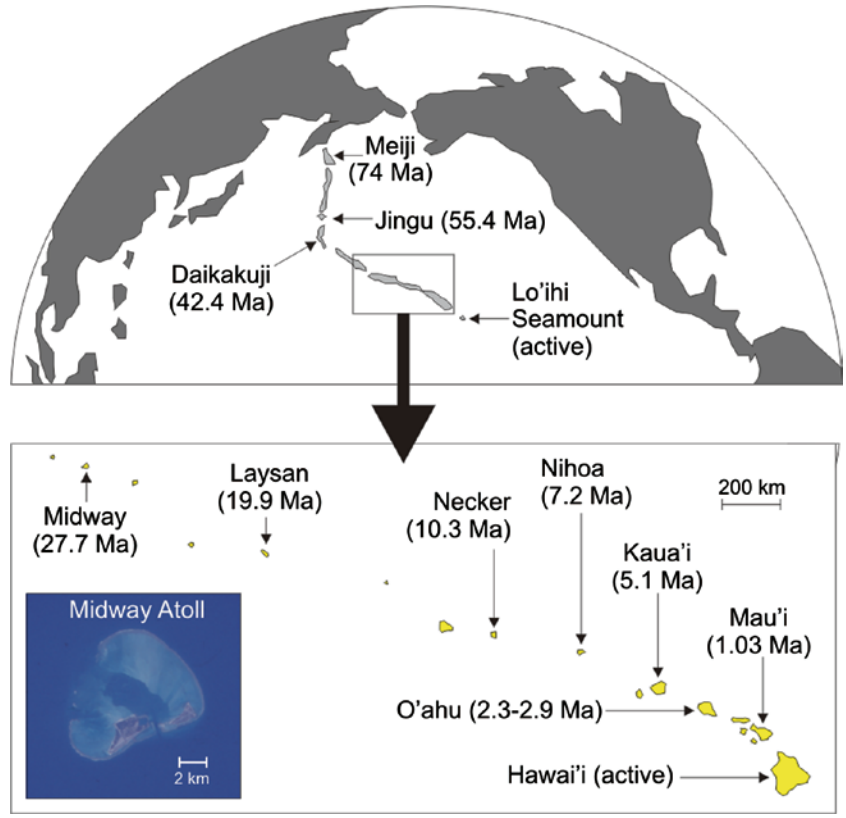

Fig. 36.3 Ages of the youngest dated eruptions of shield volcanoes along the Hawaii-Emperor island-atoll-seamount chain (dates in millions of years ago [Ma] from Duncan and Clague 1985). The upper map shows the location of the Hawaiian Ridge within the Pacific, and the lower map the geography of the younger, largely emerged part of the island chain. Aerial photo of Midway Atoll without annotations obtained from Image Science and Analysis Laboratory, NASA-Johnson Space Center

represents the movement of the Pacific Plate northwest across a fixed (island-forming) hotspot for at least the past 85 million years. After an island forms over the hotspot, it is carried away to the northwest and sinks. At one end of the chain lie the high volcanic islands, in places fringed with coral reefs. As you move northwest along the chain, the volcanic islands become lower (and smaller in size) and the reefs change from being fringing to barrier varieties. Eventually the volcanic islands disappear altogether, and only atolls mark the places where once they poked their heads above the ocean surface. But then as you move farther northwest, the ocean water becomes too cold for corals to survive so the reefs die and the atolls sink. The deepest atoll is Meiji Seamount, which lay over the hotspot 85 million years ago and is now several kilometers below the ocean surface.

Before we leave the subject of atoll origins altogether, we should note that in a few places atolls have been uplifted (usually because of crustal upbending) and their internal structures, obscured in most, are exposed. One of the best examples is Niue Island, central South Pacific, which has been uplifted by some 70 m. The former atoll reef now forms the highest part of the island (as the Mutalau Reef) and encloses the former lagoon, around 30 m lower. A staircase of emerged coral reefs around its fringes calibrates the gradual progress of island uplift (see Fig. 36.5c).

36.3 Atolls and Atoll Islands

Nothing that lives on an atoll can readily escape the influence of the ocean. Atoll reefs (and barrier reefs) are generally broader than fringing reefs and can be divided into zones of relative ocean influence. Their

Fig. 36.4 Marakei Atoll, Kiribati. Aerial photo without annotations obtained from Earth Sciences and Image Analysis Laboratory (www.reefbase.org)

outer parts – the forereef – experience the greatest influence and exhibit the greatest biodiversity. Both these tail off as you cross to the lagoon side of an atoll reef (Nunn 1994).

On the other hand, the sediment – itself mostly coral detritus from the underwater forereef slope – that is delivered by the waves to the outer parts of an atoll reef does not generally stay there. Commonly the waves pile the sediment up onto the reef and then – perhaps over a period of several years – move it gradually lagoonwards. The pace of sediment movement decreases across the reef (from outer to inner edge) so that sometimes on wide reefs the sediment near the inner edge may hardly ever be moved. This allows it to build up and, if it is not disturbed by the waves for a long time, it may develop natural armoring that allows it to grow into a true *motu*. This armoring may be simply from soil and vegetation, but the more effective types come from beachrock along its sandy shores or from phosphate rock, the latter sometimes produced when phosphate (from bird excrement) cements together the sand in the island's center.

Motu (atoll islands) rarely grow higher than 2–3 m above sea level, this being the maximum height to which waves can pile up reefal sediment in such locations. Such islands grow through the natural accretion of storm ridges. A good example was found after 1973 when Hurricane Bebe created a 18 km long rubble ridge along the eastern side of Funafuti Atoll in Tuvalu (Maragos et al. 1973). When it formed, the ridge was on the outer edge of the reef, in places several 100 m away from the main *motu* but subsequent monitoring showed it being moved by the waves progressively closer and eventually becoming incorporated into the existing *motu*. Surveys elsewhere in Tuvalu of the structure of *motu* showed that most had formed from a central sediment core surrounded by a number of accreted storm ridges of this kind (McLean and Hosking 1991).

It has become clear in recent years that the model of atoll *motu* growing by sediment accretion alone may be unduly simple as many *motu* have been found to have a solid core of emerged coral reef, formed when sea level was 1.5–2.0 m higher than today some 4,000–4,500 years ago. If you envisage the situation, as appears to have been obtained throughout the Central Pacific at this time, when sea level was rising and coral reefs were keeping pace with this, you can understand how coral reef was able to grow above the present sea level. In the past 4,000 years or so, there has been a net fall of sea level which left such reefs stranded above

the sea level: they emerged, sticking up above the ocean surface from the surrounding reef flat. These emerged reefs would have provided effective foci for sediment accumulation, and help explain both why large *motu* developed in so many places and how they managed to survive erosion for so long.

Particularly on atolls where the ring reef is comparatively narrow – maybe less than 50 m – the sediment that gets deposited on it may be washed quickly across into the lagoon. Sometimes the lagoon may become infilled as a result, as has happened on the island of Vaitupu in Tuvalu.

To understand how an atoll lagoon forms, it is helpful to think of an atoll as a bucket with a thick wall. Once sediment-laden water gets into that bucket, the sediment cannot escape, so it settles at the bottom of the bucket and gradually fills it up. It is the accumulation of sediment on the floors of atoll lagoons that largely explains why these are so shallow (typically 30–50 m deep) compared to the surrounding ocean. Shallow lagoons (or shallow parts of lagoons) can see smaller patches of coral reef developing. In those lagoons that are entirely enclosed by reef or where there may be only one small reef pass, the ocean level may be higher than the surrounding ocean.

While there is a lot of diversity in atoll form in the Pacific, many of the most common features are represented on Marakei Atoll in Kiribati (Fig. 36.4). First to note is the contrast between the depth of the lagoon compared to the surrounding ocean. On Marakei, there are only two exits (*hoa*) for water from the lagoon and these are narrow, meaning that water exchange is low and that the lagoon is only completely flushed on rare occasions, perhaps when the *hoa* are temporarily widened by storms. The forested *motu* of Marakei is almost continuous and are fringed by a reef slope visible in this aerial photograph to depths of around 25 m below sea level.

36.4 The Future of Atolls

Even though some have endured for tens of millions of years, many atolls are comparatively short-lived landforms compared to those of larger islands and continents. Figure 36.5 shows a pictorial representation of the beginning and some ends of atolls. In Fig. 36.5a, we see the typical beginning: a subsiding volcanic island surrounded by a *motu*-covered barrier reef that will slowly become an atoll reef. Basically atolls can cease to be atolls (in the strict sense) in two ways; either they go down or they go up. Figure 36.5b shows an atoll that has gone down, its shadowy form still discernible from space, while Fig. 36.5c shows an atoll that has gone up, and will continue to do so for another half a million years or so.

The immediate outlook for atolls is bleak, however much we hope it could be otherwise. Sea level is currently rising faster than it has been for millennia, and the very fabric of atoll *motu* is disappearing. Rising temperatures will see the widespread death of corals in the next few decades, with as yet uncertain implications for long-term reef ecology. Both issues are critically important to atoll dwellers, and to all who are curious about this most unusual landform type.

When we compare them to other types of oceanic island, atoll *motu* are ephemeral and transient. Most of them were formed only within the past few 1,000 years and have been inhabited by people for even fewer. So on the one hand, we should not be unduly surprised that atoll *motu* may disappear once more as a result of a comparatively minor climatic perturbation. On the other hand, we might justifiably regret that, after millennia of surviving in an extraordinarily invidious situation, atoll *motu* world over are now threatened with extinction. But one way or the other, it seems unlikely that most atoll *motu* can survive the projected sea-level changes of the twenty-first century; many will probably disappear by 2050.

To understand why, we need to look no further than the unconsolidated nature of the sediment that comprises atoll *motu*. Despite the armoring it has developed in places, this is most effective when the sea level is stationary, and not when it rises, as then the ocean can overtop the armor and excavate (and remove) the less resistant material within. And studies have shown that once the high-tide level exceeds that of the coral cores of atoll *motu*, the overlying cover of unconsolidated sediment will be rapidly eroded (Dickinson 1999).

This brings us to the issue of human survival on the atolls in the future. Many atolls are already experiencing the effects of overcrowding, problems to do with waste disposal and freshwater supply, for example, and issues of resource (particularly marine food) depletion that began long before the effects of global warming made themselves felt (Barnett and Adger 2003). Future temperature rise will exacerbate all these issues, as

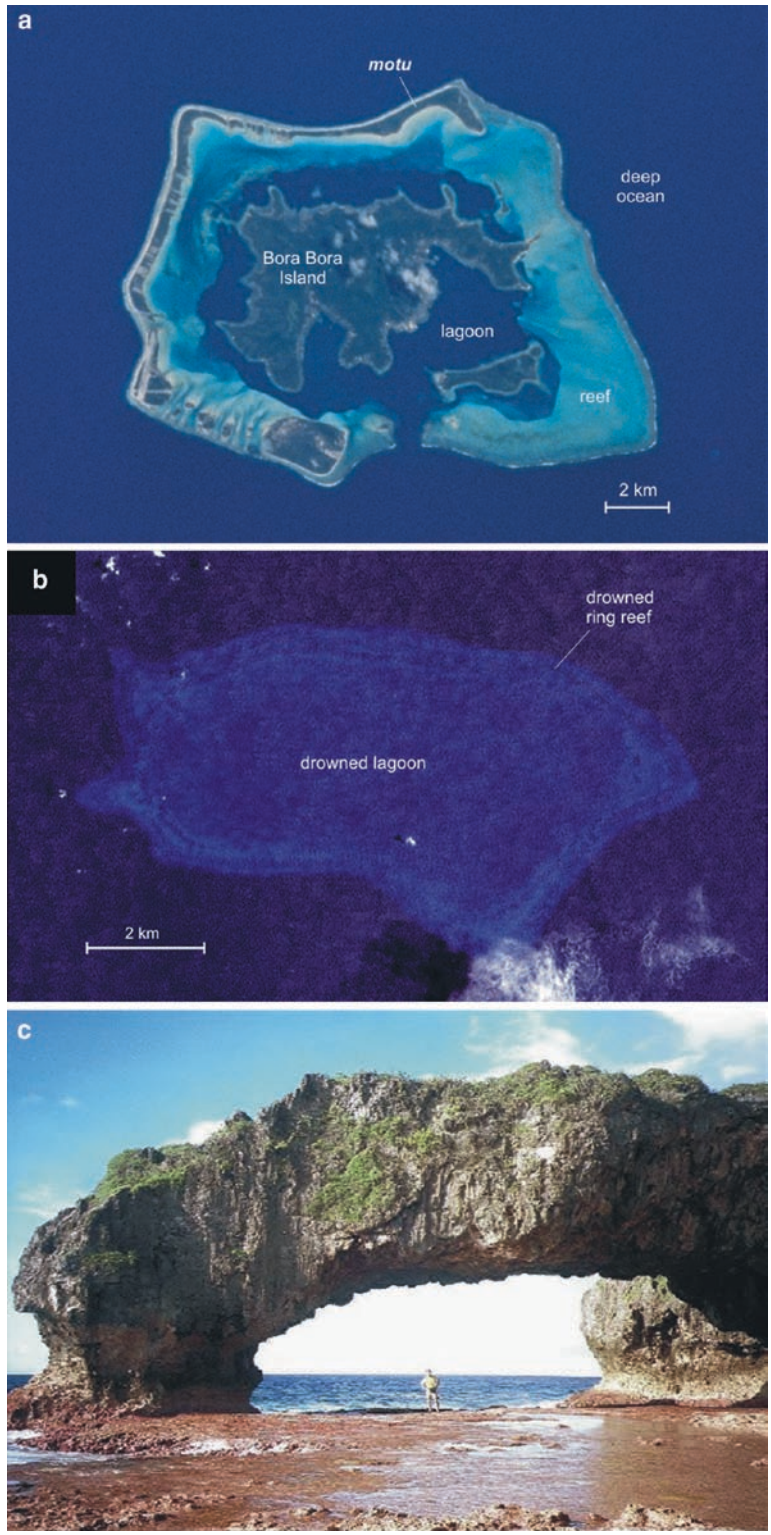

Fig. 36.5 The beginning and the ends of atolls. (**a**) The island of Bora Bora in French Polynesia is an atoll in the making. The high volcanic island shows signs of subsidence. Note particularly the shoreline embayments that are formed when the lower parts of radial river valleys are drowned. Also note how there is a barrier reef separated from the coast of the main island by a lagoon; such a reef is formed from a fringing reef by upgrowth on subsiding foundations. Eventually the volcanic part of Bora Bora will be submerged and all that will remain to mark the spot will be a ring reef, an atoll. Base photo without annotations obtained from Image Science and Analysis Laboratory, NASA-Johnson Space Center. (**b**) Some atolls may be drowned when sea level rises. In this remarkable photograph of Waterwitch Bank (12.536°S, 176.767°W), the surface of which lies 170 m below sea level, the outline of the former atoll can be seen clearly. Note that horizontal scale is approximate. Such photographs are obtained using sensors in low-earth orbit at optical wavelengths. Original photo from NASA, obtained and licenced through oceandots.com. (**c**) The island of Niue in the central South Pacific is a classic uplifted atoll. Within the past 600,000 years, it has been raised by about 70 m as a result of being carried up a crustal flexure on the Pacific Plate as it approaches the Tonga Trench. Uplift continues. This view of the Talava Arches on Niue's northwest coast shows the surface of the Last Interglacial coral reef 18 m above sea level

will sea-level rise, and it is unlikely that many people will be able to live as they do now on the remaining atoll *motu* at the start of the twenty-second century.

The Author

Patrick D. Nunn holds a personal chair in Oceanic Geoscience at the international University of the South Pacific, where he has taught and researched for a quarter of a century. He is the author of more than 175 peer-reviewed publications as well as several books including *Oceanic Islands* (Blackwell, 1994), *Environmental Change in the Pacific Basin* (Wiley, 1999), *Climate, Environment and Society in the Pacific During the Last Millennium* (Elsevier, 2007) and the popular *Vanished Islands and Hidden Continents of the Pacific* (University of Hawai'i Press, 2008). In March 2003, he was awarded the prestigious Gregory Medal of the Pacific Science Association for "outstanding service to science in the Pacific."

References

Barnett J, Adger WN (2003) Climate dangers and atoll countries. Climatic Change 61:321–337

Darwin CR (1842) The structure and distribution of coral reefs. Smith, Elder, London

Dickinson WR (1999) Holocene sea-level record on Funafuti and potential impact of global warming on central Pacific atolls. Quat Res 51:124–132

Duncan RA, Clague DA (1985) Pacific plate motions recorded by linear volcanic chains. In: Nairn AEM, Stehli FG, Uyeda S (eds) The Ocean Basins and Margins, Vol 7A, The Pacific. Plenum Press, New York, pp 89–121

Lincoln JM, Schlanger SO (1987) Miocene sea-level falls related to the geologic history of Midway atoll. Geology 15:454–457

Maragos JE, Baines GBK, Beveridge PJ (1973) Tropical cyclone Bebe creates a new land formation on Funafuti Atoll. Science 181:1161–1164

McLean RF, Hosking PL (1991) Geomorphology of reef islands and atoll motu in Tuvalu. South Pacific J Nat Sci 11:167–189

Nunn PD (1994) Oceanic islands. Blackwell, Oxford

Chapter 37
World Heritage and Geomorphology

Tim Badman

Abstract The 1972 UNESCO Convention Concerning the Protection of the World Cultural and Natural Heritage, generally called the World Heritage Convention, recognizes places (termed properties within the Convention) that are of "Outstanding Universal Value." The convention has a significant role in identifying and protecting properties with geomorphological values, and around 41% of the natural properties on the World Heritage List have been recognized for their geological values. A thematic approach has been proposed by IUCN, the advisers on natural heritage, to aid the identification and protection of World Heritage properties with earth science values.

Keywords Geoconservation • geoparks • IUCN • UNESCO • World Heritage

37.1 Introduction

The 1972 UNESCO Convention Concerning the Protection of the World Cultural and Natural Heritage (UNESCO 1972) generally called the World Heritage Convention recognizes places (termed properties within the Convention) that are of "Outstanding Universal Value." With 185 states that are signatories to the convention (as at April 2008) it enjoys almost complete recognition by the states that are members of UNESCO.

This critical term of "Outstanding Universal Value" is not formally defined in the convention. Instead this task is left to the World Heritage Committee, the governing body of the convention which governs through the *Operational Guidelines for the Implementation of the World Heritage Convention.* These guidelines are kept periodically updated and form the framework which the convention operates.[1] The definition provided for the term Outstanding Universal Value is as follows:[2]

> **49.** Outstanding Universal Value means cultural and/or natural significance which is so exceptional as to transcend national boundaries and to be of common importance for present and future generations of all humanity. As such, the permanent protection of this heritage is of the highest importance to the international community as a whole. The Committee defines the criteria for the inscription of properties on the World Heritage List.

The criteria noted in this paragraph are set out elsewhere in the Operational Guidelines, and include the following:

> **77.** The Committee considers a property as having Outstanding Universal Value (see paragraphs 49–53) if the property meets one or more of the following criteria. Nominated properties shall therefore:

(i) represent a masterpiece of human creative genius;
(ii) exhibit an important interchange of human values, over a span of time or within a cultural area of the world, on developments in architecture or technology, monumental arts, town-planning or landscape design;
(iii) bear a unique or at least exceptional testimony to a cultural tradition or to a civilization which is living or which has disappeared;
(iv) be an outstanding example of a type of building, architectural or technological ensemble or landscape which illustrates (a) significant stage(s) in human history;
(v) be an outstanding example of a traditional human settlement, land-use, or sea-use which is representative of a culture (or cultures), or human

[1]The latest version of the *Operational Guidelines* is available at whc.unesco.org/guidelines.
[2]See Paragraph 49 of the 2008 version of the *Operational Guidelines.*

P. Migoń (ed.), *Geomorphological Landscapes of the World*,
DOI 10.1007/978-90-481-3055-9_37,

interaction with the environment especially when it has become vulnerable under the impact of irreversible change;

(vi) be directly or tangibly associated with events or living traditions, with ideas, or with beliefs, with artistic and literary works of outstanding universal significance. (The Committee considers that this criterion should preferably be used in conjunction with other criteria);

(vii) contain superlative natural phenomena or areas of exceptional natural beauty and aesthetic importance;

(viii) be outstanding examples representing major stages of earth's history, including the record of life, significant on-going geological processes in the development of landforms, or significant geomorphic or physiographic features;

(ix) be outstanding examples representing significant on-going ecological and biological processes in the evolution and development of terrestrial, fresh water, coastal and marine ecosystems and communities of plants and animals;

(x) contain the most important and significant natural habitats for in-situ conservation of biological diversity, including those containing threatened species of Outstanding Universal Value from the point of view of science or conservation.

78. To be deemed of Outstanding Universal Value, a property must also meet the conditions of integrity and/or authenticity and must have an adequate protection and management system to ensure its safeguarding.

This qualification in paragraph 78 is a critical point; it is not enough for a property to display values of outstanding global importance, but to be accepted onto the World Heritage List, it must also meet other requirements. Integrity in this regard is defined as "a measure of the wholeness and intactness of the natural and/or cultural heritage and its attributes. Examining the conditions of integrity, therefore requires assessing the extent to which the property: (a) includes all elements necessary to express its Outstanding Universal Value; (b) is of adequate size to ensure the complete representation of the features and processes which convey the property's significance; and (c) suffers from adverse effects of development and/or neglect."[3]

37.2 The World Heritage List and Geomorphological Sites

As can be quickly seen from a review of the criteria listed above, geomorphological values are explicitly recognized as part of the framework of the World Heritage Convention, notably with the reference under criterion viii, alongside recognition of geological sites, but also implicitly within the definition of criterion vii, which also relates more broadly to the aesthetics of the natural world. Annex lists all of the 145 (figure at May 2008) properties (including seven transboundary/transnational properties) that have been inscribed under one or both of these criteria, and makes an assessment of those properties where geomorphological values are a significant basis for their inclusion on the World Heritage List. It appears that at least 82 properties can be considered to have been listed as being of Outstanding Universal Value for their geomorphological attributes, normally alongside other natural values. This amounts to 41% of all the natural and mixed properties included on the World Heritage List. This is a significant part of the World Heritage Estate. In addition to these World Heritage properties, it should also be noted that many other places that are listed for other natural values and some places listed for cultural values also possess significant geomorphological values, or are places where an understanding of geomorphology is fundamental to their effective management.

IUCN, the International Union for Conservation of Nature, is named within the World Heritage Convention as the advisory body on natural heritage to the World Heritage Committee. This reflects IUCN's instrumental role in the drafting of the convention (Batisse and Bolla 2005) and the significant reach of IUCN through its network of states and NGO members, and its expert commissions. IUCN has a good number of geographers and geologists within its ranks, but recognizes

[3]See paragraph 88 of the 2008 edition of the *Operational Guidelines*.

that these areas of natural science are not its heartland area of expertise. IUCN has therefore always sought advice on the application of the World Heritage Convention to earth science related sites from outside of these networks. This has involved, since 2006, the operation of formal cooperation agreements with the International Union for Geological Sciences, and the International Association of Geomorphologists in relation to the review of new nominations to the World Heritage List. IUCN is also receiving growing interest from its members in working more on geoconservation, and in 2008 the first motion specifically referring to geodiversity was passed by IUCN's quadrennial Congress.[4]

IUCN has focused on the application of criterion viii in relation to the recognition of geological and geomorphological phenomena and values within the World Heritage List (Dingwall et al. 2005). Noting that the diversity of geological and geomorphological phenomena that can be accommodated on the World Heritage List is considerable, IUCN has been working since 2005 within a thematic strategy to guide the work of states in recognizing geological and geomorphological heritage.

A key principle of this strategy is to recognize that other mechanisms than the World Heritage Convention will be required to recognize and protect the full scope of the world's geodiversity. The rationale for this position is that the World Heritage List is never likely to include many more than 150 sites of primary geological or geomorphological interest. The necessarily selective nature of World Heritage listing cannot, therefore, be regarded as adequate for recognizing the full range of globally significant geological sites.

National systems have the potential to recognize many sites of different characters and sizes that represent the earth heritage resources of that country. Many countries have national geoconservation programs and these cover a wide range of approaches to inventory and documentation of the diversity of geological and geomorphological phenomena.

IUCN also recognizes a critical relationship with the UNESCO Geoparks initiative, an ad hoc approach that is philosophically founded in the 1991 Digne "*Declaration of the Rights of Memory of the Earth.*"[5] Geoparks aim to be a global series of earth heritage sites intended to integrate the preservation of geological and geomorphological heritage and sustainable resource and economic development. In this respect Geoparks are considered to be in harmony with the objectives of biosphere reserves under the UNESCO Man and the Biosphere Program (MAB). They are also regarded as complementary to the World Heritage List, in providing an appropriate mechanism for recognizing internationally important sites identified from both national and international geological and geomorphological site inventories. The Geoparks program incorporates a highly innovative policy mandate in giving recognition to the interests of social advancement and economic resource development. The Geoparks program remains a UNESCO initiative rather than an officially adopted program, but is rapidly developing in several regions of the world.

The IUCN thematic study sets up a basic classification scheme to help logical decisions to be made in preparing nominations and within site evaluation. Any thematic classification must reflect the fact that the *World Heritage Convention* can only recognize a limited number of sites. The classification scheme used to assist in site selection and evaluation was designed to be broad and to not be over-elaborate. Thirteen major thematic areas are recommended as a broad conceptual framework for geological World Heritage (Table 37.1).

The adoption of a thematic approach does not imply equal representation on the World Heritage List of each theme. Nor does it automatically imply that sites of suitable quality will be found for each theme. Sites will be required to satisfy not only the conditions of Outstanding Universal Value, but also the requirements of integrity and management. Some themes may only be represented by very few sites, because even the best sites within a theme may not satisfy integrity/management criteria.

IUCN is developing a series of further studies to support the application of these different themes and to also suggest some of the key sites that could be considered to be gaps on the World Heritage List. These studies build on a number of previous studies which include reports on Wetland and Marine Systems (Thorsell et al. 1997), Mountains (Thorsell and Hamilton 2002), and Caves and Karst (Williams 2008).

[4]IUCN (2009). Resolutions and Recommendations. Gland, Switzerland: IUCN. The motion is number 4.040.

[5]See http://www.sgu.se/hotell/progeo/digne.html for the text of the Digne Declaration.

Table 37.1 IUCN's suggested thirteen themes for geological and geomorphological World Heritage

Theme	Brief summary of content
1. Tectonic and structural features	Elements of global-scale crustal dynamics including continental drift and seafloor spreading. Major crustal landforms and structural features at plate boundaries. Geosyncline/anticline development and erosion; rift-valley systems.
2. Volcanoes/volcanic systems	Major areas and types of volcanic origin and evolution. These may include examples of major features such as the "Pacific Ring of Fire" as a global-scale expression of volcanic activity and associated crustal movements.
3. Mountain systems	Major mountain zones and chains of the world.
4. Stratigraphic sites	Rock sequences that provide a record of key earth history events.
5. Fossil sites	The record of life on Earth represented within the fossil record (see also Wells, 1996).
6. Fluvial, lacustrine and deltaic systems	Land systems resulting from large-scale river erosion and drainage system development, lakes, wetlands and deltas.
7. Caves and karst systems	Subterranean hydrological processes and landforms, together with their surface expressions.
8. Coastal systems	The role of water at oceanic margins on large-scale erosional and depositional coasts and banks.
9. Reefs, atolls and oceanic islands	Geo-biological and/or volcanic features in oceanic areas or with oceanic influences.
10. Glaciers and ice caps	The significant role of ice in landform development in alpine and polar regions, including periglacial and nivation (snow) influences.
11. Ice Ages	Global patterns of continental icesheet expansion and recession, isostasy, sea-level changes, and associated biogeographic records.
12. Arid and semi-arid desert systems	Land systems and features reflecting the dominant role of wind (eolian processes) and intermittent fluvial action as agents of landform development and landscape evolution.
13. Meteorite impact	Physical evidence of meteorite impacts (astroblemes), and major changes that have resulted from them, such as extinctions.

37.2.1 Tectonic and Structural Features

No thematic study exists for this group of sites, whose values are primarily related to hard rock geology. IUCN considers that only a few places are likely to warrant inscription on the World Heritage List under this theme. The inscription of the Swiss Tectonic Arena Sardona, an area of Alpine geology including the iconic Glarus Overthrust, is seen as a significant advance in fulfilling the recognition of such properties on the World Heritage List. Another example of such an inscription is Macquarie Island (Australia) which was noted as an unique example of exposure of the ocean crust above the sea level and geological evidence for sea-floor spreading, and is an exposure of the oceanic plate boundary between the Pacific and Australian/Indian plates, exposed with active faults and ongoing tectonic movements. In other inscriptions, tectonic and structural features are present as one part of a broader set of values.

37.2.2 Volcanoes/Volcanic Systems

Volcanoes and volcanic sites are strongly represented on the World Heritage List, with at least 14 inscriptions that are directly based on the volcanic values displayed. Iconic volcanoes already inscribed on the World Heritage List include those of the Hawaii Volcanoes National Park (USA), the Aeolian Islands (Italy) – including Stromboli and Vulcano and Ujung Kulon National Park (Indonesia) – a site that includes Krakatoa. Recent additions include Teide National Park (Tenerife, Spain) and Jeju Island (Republic of Korea), which were both added to the World Heritage List in 2007. The numbers have grown sufficiently that in 2007 the World Heritage Committee requested that a thematic study to be prepared in view of the increasingly limited potential for further World Heritage volcanic properties. The study (Wood 2009) is expected to both confirm that the representation of volcanoes on the World Heritage List is very good, and that there remain

a few gaps that could be addressed. It will also provide guidance on what constitutes "integrity" and effective protection and management for a volcanic World Heritage property. A further excellent source of information regarding world volcanoes that IUCN has used repeatedly in its assessment of nominations related to volcanoes is the database of the Global Volcanism Program, based at the Smithsonian Institution.[6]

37.2.3 Mountain Systems

Mountain systems are also strongly represented on the World Heritage List, although many inscriptions relate to their biological values, rather than their geological values. Iconic sites include Sagarmatha National Park (Nepal) – which includes Mount Everest, Los Glaciares (Argentina), and several mountain sites across China. IUCN's thematic study from 1997 remains a key source of information on the remaining gaps that could be filled.

37.2.4 Stratigraphic Sites

Although sequences of geological strata form a part of many World Heritage properties, few if any have been identified expressly solely for their stratigraphic values, although these values are a key component of the inscriptions of the Grand Canyon (USA) and the Dorset and East Devon Coast (UK) and of other fossil site inscriptions. The International Geoscience Program of UNESCO (IGCP) includes the provision to identify global stratotypes through the designation of GSSPs. Given the specialized processes involved in such identification and the large number of very specific sites that will be thus located, the GSSP is considered to be a more effective means to recognize stratigraphic sites than inscription on the World Heritage List.

37.2.5 Fossil Sites

IUCN's thematic study of 1993 (Wells 1993) has provided a clear and consistent framework for the recognition of properties with significant fossil values on the World Heritage List. It provides both a strong conceptual model for the interpretation of Outstanding Universal Value within sites, and a ten-question checklist that has been used consistently to advise on comparative analysis. The inscription of Miguasha National Park (Canada) in 1999[7] is also a benchmark decision, setting a standard for the delivery for peer-reviewed studies to establish beyond reasonable doubt that the values can be accepted as being the most worthy of recognition through World Heritage Site status.

37.2.6 Fluvial, Lacustrine, and Deltaic Systems

IUCN's study of 2002, referred to above (Thorsell et al. 1997), provides guidance on this group of sites. As with a number of other geomorphological categories, actual inscriptions of fluvial, lacustrine, and deltaic sites are driven as much by considerations of biodiversity as for geomorphology. Iconic sites that are listed include Lake Baikal, and the gorges of the Three Parallel Rivers (China). Nevertheless there remain some key gaps identified from past studies within this theme such as the Lena Delta (Russia) and the Okavango (Botswana).

37.2.7 Caves and Karst Systems

As with volcanic properties, caves and karst sites are seen as relatively well represented on the World Heritage List, as they have been subject to much early attention by the member states of the World Heritage Committee. Iconic cave and karst sites included on the World Heritage List include Mammoth Cave National Park (USA), the drowned karst of Ha Long Bay (Viet Nam), and the South China Karst (China) – which includes a series of sites representing the best of this massive karst region. The Committee requested a theme study on the possible future scope of World Heritage karst listings, which was published in 2008 (Williams 2008). This study noted that the representation of karst values was indeed significant, and especially in relation

[6] See: http://www.volcano.si.edu/

[7] http://whc.unesco.org/en/list/686

to the inclusion of karst sites from temperate regions. It advised gaps that could be filled included the fuller recognition of the iconic Dinaric Karst, which is currently represented by a few sites but without a coordinated strategy, and the recognition of karst in permafrost areas, arid and semi-arid areas, and evaporitic karst. The most spectacular forms of pseudokarst could also be considered as a further gap.

37.2.8 Coastal Systems

IUCN's study of 1997 (Thorsell et al. 1997) provides guidance on the recognition of both coastal systems and also of the following category of reefs, atolls, and oceanic islands. Coastal systems are often also unlikely to be recognized solely for their geomorphological values, although a recent inscription of the West Norwegian Fjords (Norway) is one example where such an inscription was made, based on the classic display of fjord values.

37.2.9 Reefs, Atolls, and Oceanic Islands

There are many islands inscribed on the World Heritage List, and also a significant and growing number of inscriptions of reef areas. The Great Barrier Reef (Australia) is currently the largest inscribed World Heritage property. Almost without exception such inscriptions are made with reference to biodiversity values as the principal basis of nomination, and further thematic work is currently being commissioned in relation to the growing global recognition of Marine Protected Areas (Laffoley 2006). Better integration and consideration of geomorphological values to this program could be valuable.

37.2.10 Glaciers and Ice Caps

The recognition of glaciers within mountain systems is already a feature in many mountain system inscriptions, including that of the Swiss Alps Jungfrau Aletsch (Switzerland), where the size and speed of glacial processes was one significant factor in justifying this inscription. The inscriptions of Waterton Glacier International Peace Park (USA/Canada), a series of other Canadian protected areas, and Los Glaciares (Argentina) are other relevant examples. More recently there have been two significant Arctic inscriptions: Wrangel Island (Russia) and Ilulissat Icefjord (Greenland, Denmark). A thematic study on the Arctic and World Heritage is currently being launched by IUCN, following an international workshop on this subject (World Heritage Centre 2008) in 2007. Together with the IUCN thematic study on mountains, these will provide a framework for further development of ideas regarding the recognition of glaciers and ice caps on the World Heritage List. Antarctica currently lies outside the scope of consideration of the World Heritage Committee as the states do not hold territory there.

37.2.11 Ice Ages

Values related to Ice Ages are a feature of the inscription of a number of mountain landscapes, in relation to the display of glacial geomorphology; however, none of these properties is only listed for their Ice Age values. One property, however, is recognized solely for values related to Ice Ages: The High Coast / Kvarken Archipelago (Sweden/Finland) was inscribed (first the Swedish part and then an extension to Finland) as the classic example of eustacy, exemplified by dramatic evidence within protected areas in both countries. It is unlikely that there will be further inscriptions solely for ice age-related values on the World Heritage List.

37.2.12 Arid and Semi-Arid Desert Systems

In contrast to the possible "over-recognition" of volcanoes and karst, desert systems are seen as underrepresented on the World Heritage List. There are some inscriptions in drylands but for a variety of reasons rather few properties have been nominated in recent years. With this background IUCN commissioned a study of gaps that will be published during 2009 (Goudie and Seely 2009). This is expected to both analyze the current coverage of desert properties for landscape, geomorphology, and biodiversity values and also comment on future priorities.

37.2.13 Meteorite Impact

The representation of meteorite impact sites was considered during the evaluation of the Vredefort Dome World Heritage Site in 2005, which is the oldest and largest meteorite impact crater recorded on the Earth's surface. Given the relatively small number of such structures, and that Vredefort Dome is the largest, it is probably unlikely that further inscriptions would be supported.

37.3 Conclusion

The World Heritage List has recognized a significant number of places for their geomorphological and geological values, within the overall limit to the list set by the concept of Outstanding Universal Value. There nevertheless remain a number of gaps, and the development of a thematic approach to the future priorities of the World Heritage List is seen as one important means to begin to fill these. Although this chapter has focused on the parameters for selection, it is also essential to note that sites should also meet the conditions of integrity set for World Heritage properties, and be effectively protected and managed. The evaluation of this approach is greatly strengthened by the inputs of IUGS and of the International Association of Geomorphologists. IUCN welcomes feedback and ideas on how the World Heritage List can better recognize, better protect, and better celebrate the world's most important geomorphological sites.

The Author

Tim Badman joined IUCN as a special adviser, World Heritage in August 2007. He was previously based in Dorset County Council (UK) as environment policy manager. Between 2000 and 2006 he was the team leader of the Dorset and East Devon Coast World Heritage Site, a role which included the supervision of the nomination process which culminated in the inscription on the World Heritage List in 2001, and the subsequent development of the World Heritage program for this site. He has been a member of the IUCN World Commission on Protected Areas since 2002 and has served on IUCN's World Heritage Panel since 2003, carrying out a range of World Heritage evaluation missions and working as part of the IUCN delegation to the annual UNESCO World Heritage Committee. He is the focal point for IUCN's work on earth science within the World Heritage Convention and an adviser to UNESCO's Global Geoparks Network. Tim trained as a geologist and countryside manager in Southampton and Manchester (UK). Aside from World Heritage, his career has mainly focused on coastal zone management and on policy and management of protected landscapes/seascapes (IUCN Category V protected areas).

Acknowledgments The author wishes to acknowledge colleagues in the IUCN Program on Protected Areas, and the IUCN World Commission on Protected Areas in the development of the work on which this chapter is based, and the excellent Web site of the UNESCO World Heritage Centre (whc.unesco.org) which provides ready access to the case histories of all World Heritage properties currently inscribed on the World Heritage List. Thanks are expressed to Paul Dingwall of WCPA who originally conceived the framework of 13 themes, and Tony Weighell of the UK's Joint Nature Conservation Committee who worked in developing IUCN's thematic approach, and also to Dorset County Council who supported the production of this study. The chapter is partly based on a lecture to the Dorset Natural History and Archaeological Society in April 2009, and the author is grateful to Dr. Michael Le Bas of DNHAS for the invitation. Piotr Migoń is thanked for comments on an earlier draft of the manuscript.

References

Batisse M, Bolla G (2005) The invention of "World Heritage." History Papers, AAFU

Dingwall P, Weighell T, Badman T (2005) Geological world heritage: A global framework. IUCN, Gland, Switzerland

Goudie A, Seely M (2009) World heritage deserts. IUCN, Gland, Switzerland, in press

Laffoley D. d'A. (ed) (2006) The WCPA – Marine plan of action. Working together to secure a global, representative system of lasting networks of marine protected areas (consultation version). IUCN WCPA, Gland, Switzerland

Thorsell J, Ferster Levy R, Sigaty T (1997) A global overview of wetland and marine protected areas on the world heritage list. IUCN, Gland, Switzerland

Thorsell J, Hamilton L (2002) A global overview of mountain protected areas on the world heritage list. IUCN, Gland, Switzerland

UNESCO (1972) Convention concerning the protection of the world cultural and natural heritage. UNESCO, Paris

Wells RT (1993) Earth's geological history: A contextual framework for assessment of world heritage fossil site nominations. IUCN, Gland, Switzerland

Williams P (2008) World heritage caves and karst. IUCN, Gland, Switzerland

Wood C (2009) World heritage volcanoes. IUCN, Gland, Switzerland

World Heritage Centre (2008) World heritage and the Arctic. UNESCO, Paris, France

Annex

Properties listed under World Heritage critera *vii* and *viii*, and a provisional assessment of the properties that are recognised for their geomorphological values.

Note: the assessment of whether an inscription was made on the basis of geomorphological values requires some degree of interpretation. Properties listed for geological values (such as fossils and structural geology) are not marked as geomorphological inscriptions. For criterion *vii* the attempt has been made to identify where the superlative natural phenomena referred to are geomorphologically related, rather than major displays of ecological values.

Country/property	Criterion *vii*	Criterion *viii*	Geomorphological basis for Outstanding Universal Value?
Algeria			
Tassili n'Ajjer	**X**	**X**	Yes
Argentina			
Los Glaciares	**X**	**X**	Yes
Ischigualasto/Talampaya Natural Parks		**X**	
Iguazu National Park	**X**		Yes
Australia			
Great Barrier Reef		**X**	Yes
Kakadu National Park	**X**		Yes
Lord Howe Island Group	**X**		
Willandra Lakes Region		**X**	Yes
Tasmanian Wilderness	**X**	**X**	Yes
Gondwana Rainforests of Australia		**X**	Yes
Uluru-Kata Tjuta National Park	**X**	**X**	Yes
Wet Tropics of Queensland	**X**	**X**	Yes
Shark Bay, Western Australia	**X**	**X**	Yes
Fraser Island	**X**	**X**	Yes
Australian Fossil Mammal Sites (Riversleigh/Naracoorte)		**X**	
Heard and McDonald Islands		**X**	Yes
Macquarie Island	**X**	**X**	
Purnululu National Park	**X**	**X**	Yes
Belarus			
Belovezhskaya Pushcha/Białowieża Forest (transboundary with Poland)	**X**		
Belize			
Belize Barrier Reef Reserve System	**X**		Yes
Brazil			
Iguaçu National Park	**X**		Yes
Atlantic Forest South-East Reserves	**X**		
Pantanal Conservation Area	**X**		
Brazilian Atlantic Islands: Fernando de Noronha and Atol das Rocas Reserves	**X**		
Bulgaria			
Pirin National Park	**X**	**X**	Yes
Canada			
Nahanni National Park	**X**	**X**	Yes
Dinosaur Provincial Park	**X**	**X**	
Kluane/Wrangell-St Elias/Glacier Bay/Tatshenshini-Alsek (transboundary with USA)	**X**	**X**	Yes
Wood Buffalo National Park	**X**		
Canadian Rocky Mountain Parks	**X**	**X**	Yes
Gros Morne National Park	**X**	**X**	Yes

(continued)

(continued)

Country/property	Criterion *vii*	Criterion *viii*	Geomorphological basis for Outstanding Universal Value?
Miguasha National Park		**X**	
Joggins Fossil Cliffs		**X**	
Waterton Glacier International Peace Park (transboundary with USA)	**X**		Yes
China			
Mount Taishan	**X**		Yes
Mount Huangshan	**X**		Yes
Huanglong Scenic and Historic Interest Area	**X**		Yes
Jiuzhaigou Valley Scenic and Historic Interest Area	**X**		Yes
Wulingyuan Scenic and Historic Interest Area	**X**		Yes
Mount Wuyi	**X**		
Three Parallel Rivers of Yunnan Protected Areas	**X**	**X**	Yes
South China Karst	**X**	**X**	Yes
Mount Sanqingshan National Park	**X**		Yes
Colombia			
Malpelo Fauna and Flora Sanctuary	**X**		
Costa Rica			
Talamanca Range-La Amistad Reserves/La Amistad National Park (transboundary with Panama)		**X**	Yes
Côte d'Ivoire			
Taï National Park	**X**		
Croatia			
Plitvice Lakes National Park	**X**	**X**	Yes
Cuba			
Desembarco del Granma National Park	**X**	**X**	Yes
Democratic Republic of the Congo			
Garamba National Park	**X**		
Salonga National Park	**X**		
Virunga National Park	**X**	**X**	Yes
Denmark			
Ilulissat Icefjord	**X**	**X**	Yes
Dominica			
Morne Trois Pitons National Park		**X**	Yes
Ecuador			
Galápagos Islands	**X**	**X**	Yes
Sangay National Park	**X**	**X**	Yes
Egypt			
Wadi Al-Hitan (Whale Valley)		**X**	
Ethiopia			
Simien National Park	**X**		
Finland			
High Coast/Kvarken Archipelago (transnational serial property with Sweden)		**X**	Yes
France			
Gulf of Porto: Calanche of Piana, Gulf of Girolata, Scandola Reserve	**X**	**X**	Yes
Pyrénées - Mont Perdu (transboundary with Spain)	**X**	**X**	Yes
Lagoons of New Caledonia: Reef Diversity and Associated Ecosystems	**X**		Yes

(continued)

(continued)

Country/property	Criterion *vii*	Criterion *viii*	Geomorphological basis for Outstanding Universal Value?
Germany			
Messel Pit Fossil Site		**X**	
Greece			
Meteora	**X**		Yes
Mount Athos	**X**		
Honduras			
Río Plátano Biosphere Reserve		**X**	Yes
Hungary			
Caves of Aggtelek Karst and Slovak Karst (transboundary with Slovakia)		**X**	Yes
India			
Manas Wildlife Sanctuary	**X**		
Nanda Devi and Valley of Flowers National Parks	**X**		Yes
Indonesia			
Lorentz National Park		**X**	Yes
Komodo National Park	**X**		
Ujung Kulon National Park	**X**		Yes
Tropical Rainforest Heritage of Sumatra	**X**		
Italy			
Isole Eolie (Aeolian Islands)		**X**	Yes
Japan			
Yakushima	**X**		
Kenya			
Lake Turkana National Parks		**X**	Yes
Mount Kenya National Park/Natural Forest	**X**		
Korea, Republic of			
Jeju Volcanic Island and Lava Tubes	**X**	**X**	
Madagascar			
Tsingy de Bemaraha Strict Nature Reserve	**X**		Yes
Malawi			
Lake Malawi National Park	**X**		
Malaysia			
Gunung Mulu National Park	**X**	**X**	Yes
Mali			
Cliff of Bandiagara (Land of the Dogons)	**X**		Yes
Mexico			
Sian Ka'an	**X**		
Islands and Protected Areas of the Gulf of California	**X**	**X**	
Monarch Butterfly Biosphere Reserve	**X**		
Montenegro			
Durmitor National Park	**X**	**X**	Yes
Nepal			
Sagarmatha National Park	**X**	**X**	
Royal Chitwan National Park	**X**		
New Zealand			
Te Wahipounamu – South West New Zealand	**X**	**X**	Yes
Tongariro National Park	**X**	**X**	Yes

(continued)

(continued)

Country/property	Criterion *vii*	Criterion *viii*	Geomorphological basis for Outstanding Universal Value?
Niger			
Air and Ténéré Natural Reserves	**X**	**X**	
Norway			
West Norwegian Fjords – Geirangerfjord and Nærøyfjord	**X**	**X**	Yes
Panama			
Darien National Park	**X**		
Talamanca Range-La Amistad Reserves/La Amistad National Park (transboundary with Costa Rica)	**X**	**X**	Yes
Peru			
Huascarán National Park	**X**	**X**	Yes
Historic Sanctuary of Machu Picchu	**X**	**X**	
Río Abiseo National Park	**X**		
Philippines			
Tubbataha Reef Marine Park	**X**		
Puerto-Princesa Subterranean River National Park	**X**	**X**	
Poland			
Belovezhskaya Pushcha/Białowieża Forest (transboundary with Belarus)	**X**		
Romania			
Danube Delta	**X**	**X**	
Russian Federation			
Lake Baikal	**X**	**X**	Yes
Virgin Komi Forests	**X**		
Volcanoes of Kamchatka	**X**	**X**	Yes
Saint Lucia			
Pitons Management Area	**X**	**X**	
Senegal			
Djoudj National Bird Sanctuary	**X**		
Seychelles			
Aldabra Atoll	**X**		
Vallée de Mai Nature Reserve	**X**	**X**	
Slovakia			
Caves of Aggtelek Karst and Slovak Karst (transboundary with Hungary)		**X**	Yes
Slovenia			
Škocjan Caves	**X**	**X**	Yes
South Africa			
iSimangaliso Wetland Park	**X**		
uKhahlamba/Drakensberg Park	**X**	**X**	
Spain			
Garajonay National Park	**X**		
Doñana National Park	**X**		
Pyrénées - Mont Perdu (transboundary with France)	**X**	**X**	Yes
Teide National Park	**X**	**X**	Yes
Sweden			
Laponian Area	**X**	**X**	Yes
High Coast/Kvarken Archipelago (transnational serial property with Finland)		**X**	Yes

(continued)

(continued)

Country/property	Criterion *vii*	Criterion *viii*	Geomorphological basis for Outstanding Universal Value?
Switzerland			
Swiss Alps Jungfrau-Aletsch	**X**	**X**	Yes
Monte San Giorgio		**X**	
Swiss Tectonic Arena Sardona		**X**	
Tanzania, United Republic of			
Kilimanjaro National Park	**X**		Yes
Ngorongoro Conservation Area	**X**	**X**	Yes
Serengeti National Park	**X**		
Thailand			
Thungyai-Huai Kha Khaeng Wildlife Sanctuaries	**X**		
the Former Yugoslav Republic of Macedonia			
Natural and Cultural Heritage of the Ohrid region	**X**		
Turkey			
Göreme National Park and the Rock Sites of Cappadocia	**X**		Yes
Hierapolis-Pamukkale	**X**		Yes
Uganda			
Bwindi Impenetrable National Park	**X**		
Rwenzori Mountains National Park	**X**		
United Kingdom of Great Britain and Northern Ireland			
Giant's Causeway and Causeway Coast	**X**	**X**	Yes
Dorset and East Devon Coast		**X**	Yes
St Kilda	**X**		
Henderson Island	**X**		
Gough and Inaccessible Islands	**X**		
United States of America			
Yellowstone National Park	**X**	**X**	Yes
Everglades National Park		**X**	Yes
Grand Canyon National Park	**X**	**X**	Yes
Redwood National and State Parks	**X**		
Kluane/Wrangell-St Elias/Glacier Bay/Tatshenshini-Alsek (transboundary with Canada)	**X**	**X**	Yes
Mammoth Cave National Park	**X**	**X**	
Olympic National Park	**X**		
Great Smoky Mountains National Park	**X**	**X**	Yes
Yosemite National Park	**X**	**X**	Yes
Hawaii Volcanoes National Park		**X**	Yes
Carlsbad Caverns National Park	**X**	**X**	Yes
Waterton Glacier International Peace Park (transboundary with Canada)	**X**		Yes
Venezuela (Bolivarian Republic of)			
Canaima National Park	**X**	**X**	Yes
Viet Nam			
Ha Long Bay	**X**	**X**	Yes
Phong Nha-Ke Bang National Park		**X**	Yes
Zambia			
Mosi-oa-Tunya/Victoria Falls (transboundary with Zambia)	**X**	**X**	Yes
Zimbabwe			
Mosi-oa-Tunya/Victoria Falls (transboundary with Zimbabwe)	**X**	**X**	Yes
Mana Pools National Park, Sapi and Chewore Safari Areas	**X**		Yes

Index